UNIVERSITÉ DE TOURS

École Doctorale : Santé, Science Biologiques et Chimie du Vivant

UMR CNRS INRAE 7247 – Physiologie de la Reproduction et des Comportements

Thèse présentée par :

Anne-Charlotte Trouillet

soutenue le : **07 Décembre 2021**

Pour obtenir le grade de : **Docteur de l'Université de Tours**

Discipline - Spécialité : Sciences de la Vie et de la Santé

Rôle des mécanismes de signalisation olfactive impliquant $G\alpha_{i2}$ dans le contrôle des comportements socio-sexuels.

THÈSE dirigée par :

M. CHAMERO Pablo	Chargé de Recherches, HDR, INRAE Val de Loire, Nouzilly, France

RAPPORTEURS :

M. MARTINEZ-GARCIA Ferran	Professeur, Universitat Jaume I, Castelló, Espagne
M. ROTHERMEL Markus	Professeur, Stiftung Tierärztliche Hochschule, Hannover, Allemagne

JURY :

M. MARTINEZ-GARCIA Ferran	Professeur, Universitat Jaume I, Castelló, Espagne
M. ROTHERMEL Markus	Professeur, Stiftung Tierärztliche Hochschule, Hannover, Allemagne
Mme. BAKKER Julie	Directrice de Recherches, Université de Liège, Liège, Belgique
Mme. MIGAUD Martine	Directrice de Recherches, HDR, INRAE Val de Loire, Nouzilly, France
M. SURGET Alexandre	Maitre de Conférences, Université de Tours, Tours, France
M. CHAMERO Pablo	Chargé de Recherches, HDR, INRAE Val de Loire, Nouzilly, France

Le propre de la connaissance complexe, c'est qu'on ne peut pas éliminer l'incertitude.

Edgar Morin

Education isn't something you can finish.

Isaac Asimov

Note aux lecteurs :

Ce manuscrit de thèse a été pensé et écrit en anglais afin d'être accessible à l'ensemble de la communauté scientifique. Pour des raisons académiques, vous en trouverez une traduction française, mais ce n'est qu'une traduction.

Note to the readers:

This thesis manuscript was conceived and written in English in order to be accessible to the entire scientific community. For academic reasons, you will find a French translation, but it is just a translation.

Résumé en français

Chez la plupart des mammifères, le système olfactif régule les comportements socio-sexuels via la détection d'informations chimiques. Les neurones sensoriels du système olfactif détectent ces signaux par l'intermédiaire de récepteurs couplés aux protéines G, chacun étant exprimé par un seul ensemble de neurones. Les signaux olfactifs pertinents pour la communication sociale sont principalement détectés par l'organe voméronasal, dans lequel au moins deux populations de cellules réceptrices (les VSNs) détectent les phéromones par l'intermédiaire de deux familles de récepteurs couplés aux protéines G, les V1Rs et les V2Rs. Il a été proposé que la liaison d'un ligand à son récepteur, V1R ou V2R, active une protéine G correspondante, respectivement $G\alpha_{i2}$ et $G\alpha_{o}$. Les neurones exprimant la protéine $G\alpha_{o}$ détectent des peptides et des protéines modulant plusieurs comportements sociaux. Des études génétiques et comportementales sur la souris indiquent également un rôle potentiel des neurones exprimant $G\alpha_{i2}$ comme transducteurs de l'information olfactive et modulateurs de la physiologie et des comportements sexuels. Cependant, la contribution exacte de cette voie de signalisation reste largement méconnue. Par conséquent, l'objectif principal de ce projet est de déterminer comment les comportements socio-sexuels sont contrôlés par le système olfactif, en particulier par les neurones de l'organe voméronasal exprimant V1R-$G\alpha_{i2}$.

Pour répondre à cette question, nous avons utilisé le système Cre-lox pour ainsi générer une souris dans laquelle la délétion du gène codant pour $G\alpha_{i2}$ est limitée aux neurones sensoriels olfactifs. Tout d'abord, nous avons évalué le rôle fonctionnel de $G\alpha_{i2}$ dans le processus de transduction du signal via des techniques d'imagerie calcique sur cellules vivantes. Nous avons ainsi établi que $G\alpha_{i2}$ est nécessaire pour la détection des petites molécules organiques et des stéroïdes sulfatés. Ensuite, nous avons étudié le rôle des VSNs exprimant $G\alpha_{i2}$/V1Rs dans l'expression des comportements reproducteurs et sociaux. Nous avons testé les comportements sexuels, parentaux et agressifs de souris mâles et femelles déficientes pour $G\alpha_{i2}$ et identifié les régions du cerveau transformant l'information olfactive en décision comportementale. Nous avons observé une influence des VSNs exprimant $G\alpha_{i2}$ en fonction du sexe avec des effets spécifiques pour chaque comportement. Nous avons constaté que la délétion de $G\alpha_{i2}$ dans les VSNs joue un rôle central dans le comportement agressif des mâles en augmentant l'agression territoriale et en réduisant l'agression dirigée vers les nouveau-nés. Cependant, l'agressivité des femelles reste inchangée en l'absence de $G\alpha_{i2}$. Le comportement parental est également affecté par la délétion de $G\alpha_{i2}$ de façon différente chez chaque sexe, augmenté chez les mâles et inhibé chez les femelles. De plus, l'expérience sociale modifie l'implication de la signalisation voméronasale $G\alpha_{i2}$ dans le comportement sexuel des femelles, alors que chez les mâles, la délétion de $G\alpha_{i2}$ n'a aucun effet sur le comportement sexuel. Enfin, nous avons identifié un nouveau rôle pour les VSNs exprimant $G\alpha_{i2}$ dans les comportements d'aversion médiés par les signaux de prédateurs et de congénères malades.

Toutes les espèces intègrent continuellement des informations environnementales et adaptent leurs réponses en conséquence. Ce projet vise à mettre en lumière les mécanismes neuronaux qui sous-

tendent le traitement des signaux chimiques olfactifs, afin de comprendre comment les entrées olfactives périphériques interagissent avec les centres neuronaux qui contrôlent les réponses comportementales. La compréhension de ces mécanismes a une large portée et peut conduire à de nouvelles perspectives dans la compréhension des troubles du comportement et le développement de nouvelles stratégies d'élevage chez les animaux domestiques.

English abstract

In most mammals, the olfactory system drives socio-sexual behaviors through the detection of chemosensory information. Sensory neurons of the olfactory system detect these signals through dedicated G protein-coupled receptors, each expressed by a single ensemble of neurons. Chemosignals relevant for social communication are mainly sensed by the vomeronasal organ in which at least two populations of receptor cells detect pheromones through two families of G-protein-coupled receptors, V1Rs and V2Rs. The binding of ligands to the receptor (V1R or V2R) has been proposed to activate the corresponding G protein, $G\alpha_{i2}$ and $G\alpha_{o,}$ respectively. $G\alpha_{o}$-expressing neurons have been shown to detect peptides and proteins modulating several social behaviors. Genetic and behavioral studies on mice also point to a potential role of $G\alpha_{i2}$-expressing neurons as transducers of the olfactory information controlling reproductive physiology and behaviors. However, the exact contribution of this signaling pathway remains elusive. Therefore, the main goal of this project is to determine how socio-sexual behaviors are controlled by the olfactory system, particularly by the V1R-$G\alpha_{i2}$-expressing neurons of the vomeronasal organ.

To address this point, we used the Cre-lox system to generate a conditional knockout mouse in which the deletion of $G\alpha_{i2}$ gene is restricted to olfactory sensory neurons. First, we evaluated the functional role of $G\alpha_{i2}$ in the process of VSNs signal transduction using live-cell calcium imaging experiments. We first established that $G\alpha_{i2}$ is necessary for the detection of small organic molecules and sulfated steroids in V1Rs-expressing VSNs. Second, we investigated the role of $G\alpha_{i2}$/V1Rs-expressing VSNs in displaying reproductive and social behaviors. We tested sexual, parental, and aggressive behaviors of male and female mice deficient for $G\alpha_{i2}$ and identified brain regions transforming the olfactory information into a behavioral decision. We observed an influence of $G\alpha_{i2}$-expressing VSNs in a sex-dependent manner with distinctive traits for each behavior. We found that the deletion of $G\alpha_{i2}$ in VSNs played a central role in male aggressive behavior by increasing territorial aggression and reducing infant-directed aggression. However, female aggression remained unaltered in the absence of $G\alpha_{i2}$. Parenting was also differentially affected by $G\alpha_{i2}$ deletion in each sex, activated in males and inhibited in females. Further, social experience changed the implication of $G\alpha_{i2}$ vomeronasal signaling in female sexual behavior, while in males, $G\alpha_{i2}$-deletion had no effect on sexual behavior before or after experience. Last, we identified a new role of $G\alpha_{i2}$-expressing VSNs in avoidance behaviors mediated by predators and sick-conspecifics aversive olfactory cues.

All species continuously integrate environmental information and adapt their responses accordingly. This project aims to shed light on neural mechanisms underlying the processing of olfactory chemosignals in order to understand how peripheral olfactory inputs interact with neural centers controlling the behavioral responses. Understanding these mechanisms is of broad relevance and may lead to new insights in the comprehension of behavioral disorders and the development of new breeding strategies in domestic animals.

Remerciements

Thank you to the jury members, Markus Rothermel, Ferran Martinez-Garcia, Julie Bakker, Martine Migaud, and Alexandre Surget. I apologize for the size of this manuscript, I tried to stay brief but there are so many beautiful things to talk about!

Un immense merci à Pablo Chamero de m'avoir donné la possibilité de faire cette thèse, de m'avoir encadré tout du long et tant appris. Merci de m'avoir fait confiance pour mener à bien tout ce travail. Merci de m'avoir laissé proposer, tenter, rater, retenter pour des fois réussir ou encore rater. Merci d'avoir vu quand j'avais besoin d'aide, d'avoir su reprendre les rênes quand c'était nécessaire. Merci de m'avoir poussé à faire mieux et d'avoir toujours eu un moment à m'accorder. En resumen, gracias por todo, siempre te estaré agradecida.

Merci à Matthieu Keller de m'avoir accueilli dans le laboratoire et d'avoir toujours un œil sur le travail de chacun pour délivrer de judicieux conseils et répondre aux questions.

Un grand merci à tous les collègues qui ont, à un moment donné, partagé mon quotidien de travail. Particulièrement à Kevin qui supporte mes humeurs tous les jours (bien que niveau tête de cochon il ne se pose pas mal aussi) mais grâce à qui le quotidien est beaucoup moins morne. Merci pour toute ton aide et puis surtout de m'avoir emmené de temps en temps prendre le bon air frais auvergnat pour d'épiques parties de chasse aux campagnols ! Manon, pour tous ces quarts d'heure papote et toutes ces fois où tu m'as emmené à la bergerie pour que je puisse recevoir un peu d'amour caprin. David, pour toutes ces heures de covoit, de guinguette, de fin de journées au labo à discuter de science et autre. Morgane, grâce à toi aucun escape game ne me résiste. Chantal, pour toute l'aide au quotidien et les petites attentions gustatives. Maxime, parce que te regarder préparer tes manips ça vaut de l'or. Et aussi Didier, Philippe, et Arsène pour leurs conseils. Adrian, Anna, et Jon pour leur bonne humeur espagnole. Joran, parce que c'est tellement agréable d'être face à un étudiant qui a envie. Enfin, bienvenue à Mathilde et Elliott.

Merci à toutes les personnes avec qui j'ai interagit pendant ces 4 années à la PRC, qu'ils soient étudiants, administratifs, ou scientifiques.

Merci aux badistes de l'INRAE, je me traine quand même vachement moins sur un terrain, même si ça ne se voit pas tant que ça !

Merci aux filles de l'animalerie, Déborah Crespin, Aurelie Gasnier et Flora Martin pour le soin qu'elles apportent quotidiennement aux animaux. C'était toujours un plaisir de prendre un petit café ou simplement discuter quand j'en avais assez d'être toute seule dans la pénombre à regarder mes souris. D'ailleurs, merci à toutes ces souris, surtout à la seule qui a bien voulu pisser correctement lors de mes innombrables essais d'expériences de countermarking.

Thank you to Frank Zufall and Trese Leinders-Zufall for welcoming me in their lab, teaching me and giving me wise advices. Thanks also to the people from their lab, Gaby, Jan, Martina, Brett, Koike, Ana, Hui, Abhi, and Navin, for their warm welcome. A special thanks to Nawal, my trainee over there. Although it was shortened by the f*****g COVID, I enjoyed my stay among you and I hope to come back!

Je n'aurais pu accomplir tout ce travail sans toutes les personnes que j'ai rencontrées lors de mes précédentes expériences en laboratoire de recherche à Liège et Paris. Je suis reconnaissante à Julie Bakker et Sakina Mhaouty-Kodja de m'avoir offert ces expériences et enseigné ce qu'elles savent. Un merci particulier au Dr. Elodie Desroziers qui aura eu la lourde tâche de m'encadrer à mes débuts. Je garde de ces tranches de vie des souvenirs impérissables, notamment grâce à Maïna, Aurore, Vincent, Arnaud, Emma, et Raphaële. Merci à vous.

Merci Amandine d'écouter inlassablement mes misères et mes joies. 21 ans que ça dure. Merci à tous mes amis rencontrés dans le nord, à Liège, à Paris et à Tours. Il n'est pas toujours aisé de

vagabonder de ville en ville comme je l'ai fait. Merci à vous d'être là quand je suis de passage même s'ils s'espacent de plus en plus.

Une énorme reconnaissance à ma famille qui a désespéré jours après jours, années après années de me voir finir les études. Ce coup-ci je vous le jure c'est fini. Enfin, je crois. Ce qui est beau c'est que même si un jour je vous annonce que je recommence, je sais que vous serez là et que vous me soutiendrez. Merci, ça n'a pas de prix.

Enfin, que dire à celui qui, patiemment et quotidiennement, subit le fait que je rentre à des heures indues pour parfois directement me recoller à mon ordinateur ? Merci parait bien petit. À mon Julien, qui me soutient et me supporte avec patience tous les jours, merci du fond du cœur.

Ce que ces expériences m'auront apprises ? Surtout la persévérance. J'en ai vu réussir, j'en ai vu abandonner pour trouver l'épanouissement ailleurs. Peu importe ce que la suite augure, je ne regrette rien de tout ce parcours et je suis heureuse d'être où je suis aujourd'hui. À la fin de travail, il n'est qu'une question à laquelle je n'ai pas de réponse : est-ce que les dinosaures avaient un organe voméronasal ? Pourtant je suis une grande procrastinatrice, j'ai cherché la réponse, en vain. J'espère que ce n'est que le début d'une nouvelle période de ma vie consacrée encore à me poser des questions et chercher les réponses.

STATE OF THE ART 1

1 THE OLFACTORY SYSTEM 3

1.1 THE MAIN OLFACTORY SYSTEM 4
1.1.1 The main olfactory epithelium 4
1.1.2 Canonical olfactory sensory neurons 5
1.1.3 Non-canonical olfactory sensory neurons 7
1.1.3.1 TAARs-expressing OSNs 8
1.1.3.2 GC-D-expressing OSNs 8
1.1.3.3 TRPC-2-expressing OSNs 9
1.1.4 The main olfactory bulb 10
1.2 THE SEPTAL ORGAN OF MASERA 11
1.3 THE GRÜNEBERG GANGLION 12
1.4 THE ACCESSORY OLFACTORY SYSTEM 13
1.4.1 The vomeronasal organ 14
1.4.2 Vomeronasal signaling 15
1.4.2.1 V1Rs 16
1.4.2.2 V2Rs 17
1.4.2.3 VRs sensory cascade 18
1.4.2.4 FPRs 20
1.4.3 The accessory olfactory bulb 20
1.4.4 Vomeronasal ligands 22

2 VOMERONASAL CONTROL OF SOCIO-SEXUAL BEHAVIORS 24

2.1 SEXUAL BEHAVIORS 25
2.1.1 Male sexual behaviors 26
2.1.2 Female sexual behaviors 28
2.1.3 The curious case of sex preference in Trpc2$^{-/-}$ mice 30
2.2 AGGRESSIVE BEHAVIORS 31
2.2.1 Territorial aggression 32
2.2.2 Maternal aggression 33
2.2.3 Infanticide 33
2.3 PARENTAL BEHAVIORS 34
2.4 AVOIDANCE BEHAVIORS 35
2.4.1 Predator avoidance 36
2.4.2 Pathogen avoidance 37

3 NEURAL CONTROL OF SOCIO-SEXUAL BEHAVIORS 38

3.1 SEXUAL BEHAVIORS NEURAL CIRCUITRY 40
3.1.1 Sex coding of the vomeronasal inputs 40
3.1.2 Male mounting neural circuitry 41
3.1.3 Lordosis behavior neural circuitry 42
3.2 AGGRESSION NEURAL CIRCUITRY 43
3.3 PARENTING NEURAL CIRCUITRY 45
3.4 PREDATOR AND SICK CONSPECIFIC AVOIDANCE NEURAL CIRCUITRY 46

OBJECTIVES 51

RESULTS 55

1 $G\alpha_{i2}$ FUNCTION IN VSNS SIGNALING AND MALES' SOCIO-SEXUAL BEHAVIORS 55

1.1 INTRODUCTION 57
1.2 RESULTS 58

1.2.1 Conditional deletion of $G\alpha_{i2}$ in VSNs 58
1.2.2 $G\alpha_{i2}$ is required for sensory function of apical VSNs 59
1.2.3 Normal male sexual behavior in $G\alpha_{i2}$ mutants 60
1.2.4 Territorial aggression is enhanced in $G\alpha_{i2}$ mutant males 60
1.2.5 Increased brain activation to male intruder in $G\alpha_{i2}$ mutant males 60
1.2.6 Infant-directed aggression is diminished in $G\alpha_{i2}$ mutant males, but parental behavior is enhanced 60
1.3 DISCUSSION 62
1.4 METHODS 63
1.5 SUPPLEMENTARY INFORMATION 66

2 IMPACT OF $G\alpha_{i2}$ DELETION IN VSNS ON FEMALES' SOCIO-SEXUAL BEHAVIORS 85

2.1 INTRODUCTION 87
2.2 METHODS 88
2.3 RESULTS 90
2.3.1 Inactivation of the apical vomeronasal cell layer reduces pup retrieval in virgin females 90
2.3.2 Deletion of $G\alpha_{i2}$ does not affect maternal behavior in mothers 91
2.3.3 Incomplete sexual receptivity acquisition in $G\alpha_{i2}$ mutant females 92
2.3.4 Reduced cFos expression in the AOB and RP3V of $G\alpha_{i2}$ mutant females 94
2.3.5 $G\alpha_{i2}$ deletion has no impact on reproductive physiology 95
2.4 DISCUSSION 96

3 CONTROL OF AVOIDANCE BEHAVIORS BY APICAL VSNS 101

3.1 INTRODUCTION 101
3.2 METHODS 102
3.3 RESULTS 105
3.3.1 Apical VSNs mediate sick and predator avoidances 105
3.3.2 Sick and predator associated olfactory cues activate Gαi2 vomeronasal signaling pathway 107
3.3.3 Deletion of $G\alpha_{i2}$ reduces the detection of owl odors 108
3.3.4 $G\alpha_{i2}$ deletion does not specifically impact LPS-urine detection 109
3.4 DISCUSSION 110

DISCUSSION 115

1 A MODEL IS JUST A MODEL 115

2 THE USE OF TWO VOMERONASAL SYSTEMS IN MAMMALS 116

3 ONE PATHWAY, TWO SEXES, MANY EFFECTS 117

3.1 EXPERIENCED-DEPENDENT VOMERONASAL CONTROL OF SEXUAL BEHAVIORS 117
3.2 CONTEXTUAL REGULATION OF AGGRESSIVE BEHAVIORS 119
3.3 THE TRANSITION TO PARENTHOOD 120
3.3.1 $G\alpha_{i2}$ and the transition to fatherhood 120
3.3.2 $G\alpha_{i2}$ and the transition to motherhood 122

GENERAL CONCLUSION 127

BIBLIOGRAPHY 131

APPENDICES 157

Abbreviation List

2-PT: 2-propylthietane
ACIII: adenylyl cyclase III
ANO1/2: anoctamin channel 1/2
AOB: accessory olfactory bulb
AON: anterior olfactory nucleus
AOS: accessory olfactory system
AR: androgen receptor
Aro: aromatase
ATP: adenosine triphosphate
AVPV: anteroventral periventricular nucleus
BNSTp: posterior bed nucleus of the stria terminalis
Ca^{2+}: calcium cation
cAMP: cyclic adenosine-3', 5' monophosphate
c$G\alpha_o^{-/-}$ conditional $G\alpha_o$ KO
c$G\alpha_{i2}^{-/-}$ conditional $G\alpha_{i2}$ KO
cGMP: cyclic guanosine-3', 5' monophosphate
CNG: cyclic nucleotide-gated channel
CNGA2/A3/A4/B1: cyclic nucleotide-gated channel subunit A2/A3/A4/B1
CoA: cortical amygdala posterolateral/posteromedial
DAG: diacylglycerol
ECx: entorhinal cortex
ERα: estrogen receptor alpha
ESP: exocrine secreted protein
FPR: formyl peptide receptor
Fpr-rs1/2/3/4/6/7: formyl peptide receptor related sequence 1/2/3/4/6/7
GABA: gamma aminobutyric acid
GC-D/G: guanylyl-cylcase D/G
GCL: granule cell layer
GDP: guanosine diphosphate
GG: Grüneberg ganglion
GL: glomerular layer
GnRH: gonadotropin-releasing hormone
GPCR: G-protein coupled receptor
GTP: guanosine triphosphate
Gucy1B2: guanylyl cyclase 1B2
$G\alpha_{i2}$: G protein alpha i2 subunit
$G\alpha_o$: G protein alpha o subunit
$G\alpha_{olf}$: G protein alpha olfactory subunit
Gβ/γ: G protein beta/gamma
H2-Mv: major histocompatibility complex molecule
HPA: hypothalamo-pituitary-adrenal
HPG: hypothalamo-pituitary-gonadal
IP_3: inositol-1,4,5-trisphophate
Kiss: kisspeptine
KO: knock-out
LPS: lipopolysaccharides
MC: mitral cell
MCH-Ib: major histocompatibility complex Ib
MCL: mitral cell layer
MeApv/pd: medial amygdala posterodorsal/posteroventral
MOB: main olfactory bulb
MOE: main olfactory epithelium
MOR256-3: mouse olfactory receptor 256-3
MOS: main olfactory system
MPOA: medial preoptic area
MUP: major urinary protein
OB: olfactory bulb
OR: olfactory receptor
OS: olfactory system
OSN: olfactory sensory neuron
OT: olfactory tubercle
Oxt: oxytocin
PAG: periaqueductal grey area
PDE1C/4A: phosphodiesterase 1C/4A
PEA: 2-phenylethylamine
PiCx: piriform cortex
PIP_2: phosphatidylinositol-4,5-bisphosphate
PLCβ2: phospholipase isoform beta 2
PMv: ventral premammillary nucleus
PR: progesterone receptor
SBT: 2-sec-butyl-4,5-dihydrothiazole
SF1: steroidogenic factor 1
SO: septal organ
TAAR: trace amine-associated receptor
TC: tufted cell
TH: tyrosine hydroxylase
TLR-4: Toll-like receptor 4
TMT: 2,5-dihydro-2,4,5-trimethylthiazole
TRP: transient receptor potential
$Trpc2^{-/-}$: TRPC2 KO
TRPC2/6: transient receptor potential channel subfamily C member 2/6
TRPM4/5: transient receptor potential channel subfamily M member 4/5
USVs: ultrasonic vocalizations
V2R2: vomeronasal receptor type 2 family-C
VMHdm/vl: ventromedial hypothalamic nucleus dorsomedial/ventrolateral
VNE: vomeronasal sensory epithelium
VNO vomeronasal organ
VNOx: vomeronasal surgical ablation
VR1/2: vomeronasal receptor type I/II
VSN: vomeronasal sensory neuron

Figures and Tables List

Figure 1: Schematic organization of social interactions. 1

Figure 2: The olfactory system. 3

Figure 3: The main olfactory epithelium. 5

Figure 4: The canonical-OSNs pathway. 7

Figure 5: GC-D-expressing OSNs. 9

Figure 6: Trpc2-expressing OSNs. 9

Figure 7: organization of the main olfactory bulb. 10

Figure 8: The septal organ of Masera. 12

Figure 9: The Grüneberg ganglion. 13

Figure 10: Histology of the vomeronasal organ. 15

Figure 11: Organization of the vomeronasal epithelium and markers associated with VSNs population. 16

Figure 12: Basal VSNs. 18

Figure 13: Vomeronasal signaling pathway. 19

Figure 14: The accessory olfactory bulb. 21

Figure 15: Male sexual behavior sequence. 28

Figure 16: Aggressive behavior sequence. 31

Figure 17: Mechanism of neural sensory processing and integration to socio-behavioral decisions. 38

Figure 18: Neural structures involved in olfactory processing and behavioral responses. 39

Figure 19: Male sexual behavior neural circuit. 42

Figure 20: Female sexual behavior neural circuit. 43

Figure 21: Aggression neural circuit. 44

Figure 22: Disynaptic communication between the MeA and VMH. 44

Figure 23: Parenting neural circuit. 46

Figure 24: Predator avoidance neural circuit. 47

Figure 25: Expression of marker proteins in the VNO of $cG\alpha_{i2}^{+/-}$ and $cG\alpha_{i2}^{-/-}$ mice 58

Figure 26: Essential role of $G\alpha_{i2}$ in molecular sensing by apical VSNs 59

Figure 27: Loss of $G\alpha_{i2}$ enhances territorial aggression and increases activity in aggression-controlling brain centers 61

Figure 28: $cG\alpha_{i2}^{-/-}$ male mice show diminished infant-directed aggression but enhanced parental behavior 62

Figure 29: Relative to figure 25. Olfactory system organization and function in $cG\alpha_{i2}^{-/-}$ mice 70

Figure 30: Relative to figure 26. $G\alpha_{i2}$ role and molecular sensing 72

Figure 31: Normal sexual behavior and partner preference in $cG\alpha_{i2}^{-/-}$ males 75

Figure 32: Relative to figure 27 77

Figure 33: Relative to figure 28 79

Figure 34: Pup retrieval is altered in virgin $cG\alpha_{i2}^{-/-}$ females 91

Figure 35: Loss of $G\alpha_{i2}$ does not affect maternal behavior in lactating females 92

Figure 36: Incomplete sexual receptivity in $G\alpha_{i2}$ mutant females 93

Figure 37: Reduced neural activity in the AOB and RP3V of $G\alpha_{i2}$ mutant females 94

Figure 38: Model for the proposed control of pup retrieval and lordosis behaviors depending on social experience 96

Figure 39: Preparation of predator samples. 102
Figure 40: Predator avoidance in cG$\alpha_{i2}^{-/-}$ animals. 105
Figure 41: Sick-conspecific avoidance in cG$a_{i2}^{-/-}$ animals. 106
Figure 42: VNO and AOB activation after owl and LPS-urine exposures. 107
Figure 43: Specific reduction of VSNs activation by owl odors in the absence of Gα_{i2}. 109
Figure 44: Gα_{i2} deletion reduces VSNs responsiveness to sick and healthy LMW urine fractions. 110
Figure 45: Sexually dimorphic control of sociosexual behaviors by Gα_{i2}-expressing VSNs. 117
Figure 46: Proposed model of the vomeronasal control of female sexual receptivity. 118
Figure 47: Proposed model for the transition to infanticidal to paternal behaviors in male mouse. 122
Figure 48: Proposed model of the olfactory control of innate behaviors. 128

Table 1: Vomeronasal ligands, their receptors. 23
Table 2: Surgical VNO removal and genetic mutation effects on sexual behaviors. 25
Table 3: Antibodies used 81
Table 4: Primer sequences 82
Table 5: cG$\alpha_{i2}^{-/-}$ females show normal reproductive physiology 95

State of the art

Social behaviors are the backbone of every society. Individuals of a species interact to ensure their survival and that of their kind. Agonistic or antagonistic, social behaviors are innate, meaning they are produced without learning and consist of stereotypical sequences. Years of evolution have anchored innate social behaviors because of their contribution to the perpetuation of life, and they are found in most living species. Social interactions result from the integration of three components: multiple sensory modalities emitted by the protagonists, internal state information, and environmental/contextual cues (Figure 1). The correct interpretation of this delicate balance allows an individual to display an adapted behavioral response to each situation. Impaired systems for interpreting sensory information lead to inadequate expression of social behaviors, thus jeopardizing one's survival chances.

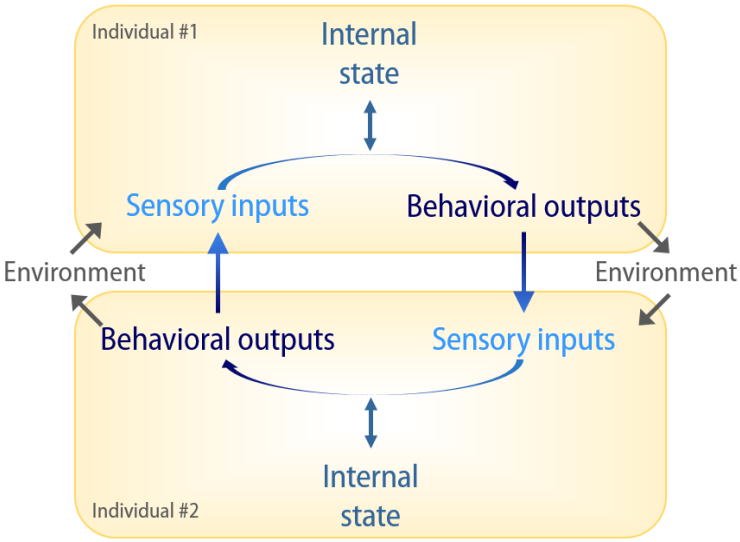

Figure 1: Schematic organization of social interactions. Sensory inputs from an individual and the environment are detected by another individual, interpreted regarding its internal state, and transformed into behavioral output. Then, this behavioral output and the environment are perceived as sensory inputs by the second individual. Figure adapted from Chen and Hong, 2018.

In many animals, olfactory cues prevail among the sensory information emitted and received. An odor is a complex mixture of monomolecular odorants carried in plumes. Among odorants, pheromones play a particular role in the regulation of social behaviors. P. Karlson and M. Lüscher defined the term pheromone as "*substances which are secreted to the outside by an individual and received by a second individual of the same species, in which they release a specific reaction, for example, a defined behavior or a developmental process*" (Karlson and Lüscher, 1959). Since then, the line between pheromone and odorant became blurred (Wyatt, 2017). A pheromone can act as such in one species but be received as a simple odorant in another, and vice-versa. Further, a pheromone is not necessarily odorous or volatile. Anecdotally, in the late 19th century, the physiologist E. Aronsohn bravely filled his nostrils with different diluted odorants, such as camphor or vanillin, therefore proving

that odors could be liquid (Keller, 2007). An optimal definition is still needed, and no consensus is established. More broadly, a pheromone could be defined as a molecule used for communication that carries information about the individual (e.g., species, sex, and age) even if it does not obviously elicit a behavioral or physiological change. Throughout this manuscript, the terms pheromone, chemosignal, and odorant will be used indiscriminately to evoke social odors.

Studying the olfactory control of innate social behaviors is a powerful tool to decipher brain circuits underlying these behaviors. The olfactory system presents a high molecular diversity, allowing us to modulate specific targets and decipher specific brain pathways associated with that target. Further, it provides insights into how the brain integrates information to ensure appropriate reactions. Compared to other sensory systems, the processing of olfactory information is not hierarchical. Coding probably occurs at the olfactory system level, and the information is then integrated and contextualized in higher brain regions. Olfactory circuits are highly streamlined, using a few synaptic connections to convert sensory inputs into behavioral outputs. Among the olfactory system, the vomeronasal organ (VNO) plays a central role in detecting social odors. Studies on the vomeronasal control of social behaviors lead to major advances in the comprehension of both olfactory control and neural processing of social behaviors (Chamero et al., 2012; Wyatt, 2013). However, questions remain about:

i- How chemosignals are perceived by the VNO and transformed into a nervous influx;
ii- Which chemosignals control the different socio-sexual behaviors;
iii- How chemosignals are integrated into brain circuits sustaining socio-sexual behaviors.

Here, I will first review the current knowledge about the organization of the olfactory system in rodents (my study model), focusing on the molecular aspects of the different sensory organs and their ligands. I will then describe the olfactory-driven behaviors and their control by the specific odorants and vomeronasal molecular pathways. In the final part of this introduction I will describe brain pathways sustaining innate socio-sexual behaviors and their regulation by the vomeronasal system.

1 The olfactory system

What is an odor? In 1963, J. Amoore exposed his stereospecific receptor theory, saying that the perceived odor of a chemical depends on its structure which is recognized by an adapted receptor (Amoore, 1963). The existence of a plethora of odorants therefore implies as many receptors matching them. Amoore's theory has been confirmed by the discovery of hundreds of receptors in the mammalian olfactory system. He also hypothesized that complex odors (such as almond, which has camphoraceous, floral, and pepperminty components) may result from chemicals having a structure matching several receptors. Indeed, in his view, a characteristic structure confers an odor. This also suggests that a receptor can detect related molecules. Although he clearly conceived the existence of specific receptors in the olfactory system, his conception of an odor was erroneous. The combination of several chemicals activating several receptors constitutes, in fact, what we call an odor. We know now that a chemical can bind different receptors, and a receptor accepts different ligands, allowing a myriad of combinations (Malnic et al., 1999).

Detecting and recognizing odorants requires a highly performant sense of smell. In most mammals, the olfactory system (OS) comprises millions of neurons distributed in anatomically and functionally distinct sensory organs in the nasal cavity. Since they are in close contact with the external world and undergo its aggressions, the olfactory neurons are permanently renewing from progenitor cells, making them a special class of neurons (Brann and Firestein, 2014). Each sensory organ differs from the others by its signal transduction mechanisms, the chemosensory cues it detects, and its axonal projection to the brain (Munger et al., 2009). Based on those criteria, four sensory organs are classically described in rodents: the main olfactory epithelium (MOE), the vomeronasal organ (VNO), the septal organ (SO), and the Grüneberg ganglion (GG) (Figure 2).

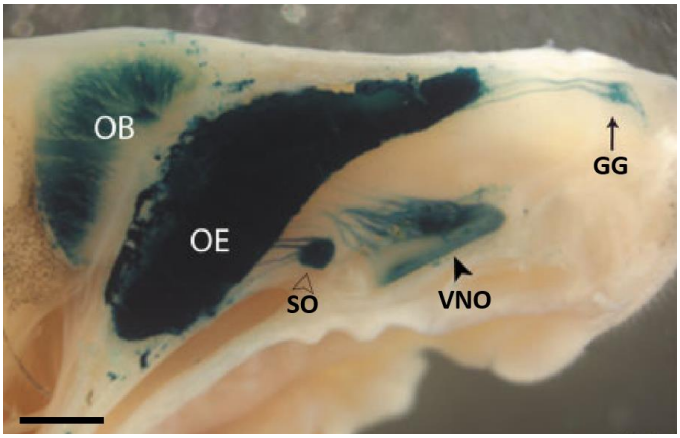

Figure 2: The olfactory system. Wholemount view of the nasal cavity of 7.5 day-old OMP:tau-LacZ transgenic mouse. Olfactory neurons are highlighted by LacZ staining. GG: Grüneberg ganglion; OE: olfactory epithelium; OB: olfactory bulb; SO: septal organ; VNO: vomeronasal organ. Scale bar, 500µm. Figure adapted from Storan and Key, 2006.

Olfactory neurons detect odorants by specialized receptors and largely obey the rule "one neuron – one receptor" (Serizawa et al., 2004). Thus, at each breath, the environment is sampled and receptors are activated. Olfactory neurons project their long axons through the nasal cavity to reach

their first cerebral relay, the olfactory bulb (OB). Then, the information is broadcasted to interconnected brain areas where it is integrated to produce an adapted response. Olfactory information coding process could be viewed as the real-time reading by the OB and the brain of the activated olfactory neurons map (Wachowiak and Shipley, 2006). This process is not yet clearly established.

Although the molecular function of the main olfactory epithelium is starting to be better documented, the other olfactory organs are less understood. Some markers and ligands have been described, but a lot of their function remains unclear. This first section will introduce the reader to the cellular and molecular function of the olfactory subsystems, a prerequisite for understanding how olfaction regulates socio-sexual behaviors.

1.1 The main olfactory system

By sniffing, animals collect odorants of their environment, scan them, determine which ones are relevant, and act upon them. The main olfactory system (MOS) could be seen as an ultra-wideband frequency detector. Indeed, it detects most odorants surrounding us and its impairment causes global anosmia that severely impacts social and non-social behaviors (Song and Leonard, 2005; Tirindelli et al., 2009). In humans, who rely mainly on the MOS, olfactory disorders impact the quality of life and are frequently associated with depressive states (Croy et al., 2014).

The MOS consists of: *i*- the main olfactory epithelium (MOE), where odorants are detected; *ii*- the main olfactory bulb (MOB), the first cerebral relay of the olfactory information; *iii*- the olfactory cortices, that receive direct or indirect information from the MOB (Munger et al., 2009). The MOS is the oldest component of the vertebrate olfactory system (Taniguchi et al., 2011). Shaped by years of evolution, it is heterogeneous and presents sensory particularities. Here, I will review the MOS organization in rodents.

1.1.1 The main olfactory epithelium

The main olfactory epithelium (MOE), the sensory organ of the MOS, is located in the roof of the posterior part of the nasal cavity and covers the nasal turbinates. It arises from the olfactory placode around embryonic day 9 in mice and shows the characteristics of an organized tissue at embryonic day 13 (Cuschieri and Bannister, 1975). The adult MOE is a pseudostratified epithelium composed of, basally to apically, three cell layers: basal stem cells (horizontal and globose basal cells), olfactory sensory neurons (mature and immature), and supporting cells (sustentacular cells) (Moulton and Beidler, 1967). It also comprises glands that secrete mucus to protect the cells and capture airborne odorants (Figure 3) (Moulton and Beidler, 1967).

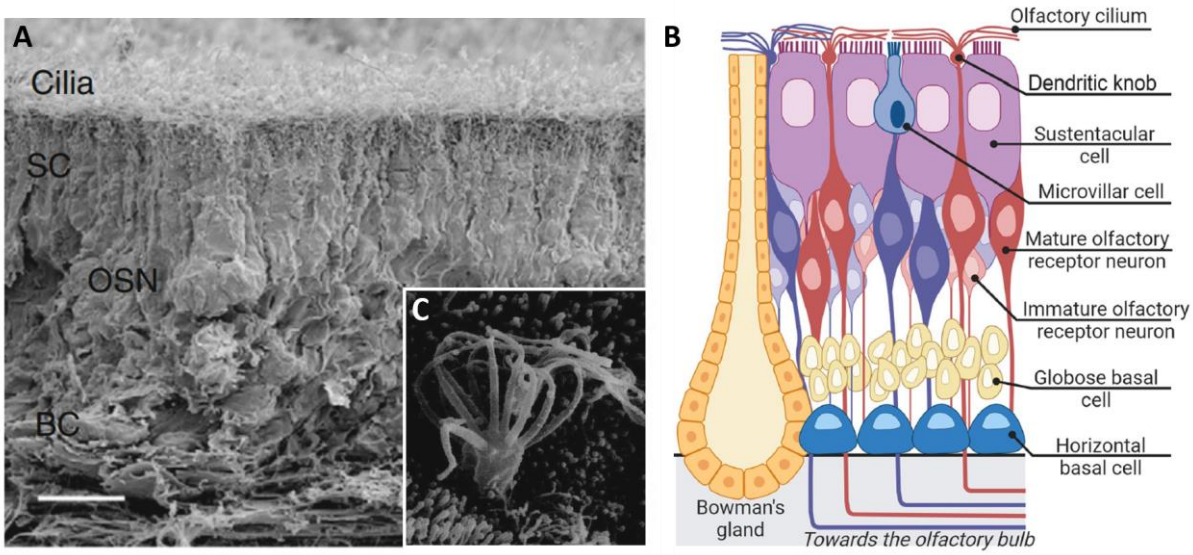

Figure 3: The main olfactory epithelium. A) Scanning electron micrograph of the side view of a mouse olfactory epithelium depicting the different cell layers. Zoom 1030x; scale bar, 10 µm. BC: basal cell; OSN; olfactory sensory neuron; SC: sustentacular cell. From McEwen et al., 2008. B) Schematic representation of the MOE cell layers. From Dibattista et al., 2021. C) Scanning electron micrograph of a human OSN dendritic knob emerging at the MOE surface. Zoom 18 525x. From Morrison and Costanzo, 1990.

Olfactory sensory neurons (OSNs) are bipolar, with a single dendrite and axon. The OSN axon is unmyelinated; it fasciculates with others to form the olfactory nerve and reach the olfactory bulb through the cribriform plate of the ethmoid bone. The dendrite extends to the epithelium surface and forms a terminal knob from which several cilia expand into the mucus to enlarge the receptive surface (Figure 3) (Mendoza, 1993). The cilia surface is covered by olfactory receptors (ORs) that bind odorants. It also contains all the proteins required to trigger the neuron's depolarization (Munger et al., 2009). OSNs form distinct subpopulations from their internal machinery and their localization. First, based on their molecular baggage, OSNs are classified as canonical or non-canonical (Munger et al., 2009). A detailed description of those signaling pathways is made hereafter. Second, a recent study showed that OSNs expressing a type of OR are not randomly scattered through the MOE (Zapiec and Mombaerts, 2020). They elegantly mapped the expression area of several ORs and defined overlapping zones, suggesting the existence of zonal distribution of OSNs types, each of which is restricted in its choice of ORs.

1.1.2 Canonical olfactory sensory neurons

The vast majority of OSNs in the MOE share common features and are categorized as classical or canonical OSNs. Among similarities, canonical OSNs detect odorant by specialized receptors: the ORs. L. Buck and R. Axel discovered the new multigene family coding for ORs in 1991 (Buck and Axel, 1991); a work rewarded by a Nobel Prize in 2004 that provided new leads into the logic of olfactory processing. Since then, we know that mammals express up to 1500 genes coding for ORs (Mombaerts, 2004). Up to date, the mouse ORs repertoire comprises 1141 protein-coding genes and

342 pseudogenes (Barnes et al., 2020). A wave of pseudogenization occured in the OR repertoire of primates to reach 50% of OR pseudogenes in humans (Gilad et al., 2004). This is consistent with a transition from a primary olfactory-based sensory perception to a vision-based one.

ORs belong to the superfamily of G-protein coupled receptors (GPCR), characterized by 7 transmembrane segments (Buck and Axel, 1991). Their number and shared features make the ORs a class of GPCR apart. ORs present several conserved amino acid small motifs in the transmembrane segments, a characteristic that has served to highlight them in the genome (Zhang and Firestein, 2002). Ligand binding occurs in the dedicated binding pocket formed by the hydrophobic parts of the transmembrane segments (Katada et al., 2005). High variability is found in these regions (Buck and Axel, 1991), allowing a wide spectrum of 3D-folding, needed to adapt to the variety of possible ligands. Interestingly, a single amino-acid modification can switch the specificity of a given OR (Katada et al., 2005).

The signaling pathway of canonical OSNs is composed of a variable element, the OR, that activates a unique molecular machinery (Figure 4). As GPCR, the primary effector of ORs activation is the triad of G protein subunits Gα/β/γ. ORs use a particular Gα subunit called $G\alpha_{olf}$ (Belluscio et al., 1998; Jones and Reed, 1989). OR binding to its ligand triggers guanosine triphosphate (GTP) hydrolysis into guanosine diphosphate (GDP) by the G proteins, releasing $G\alpha_{olf}$ from the triad. $G\alpha_{olf}$ then activates the calcium (Ca^{2+})-sensitive adenylyl cyclase III (ACIII), which converts adenosine triphosphate (ATP) into cyclic adenosine-3', 5' monophosphate (cAMP) (Bakalyar and Reed, 1990; Wong et al., 2000). The rise of cAMP concentration activates a cyclic nucleotide-gated channel (CNG), allowing intracellular Ca^{2+} rise and neuron depolarization (Brunet et al., 1996; Dhallan et al., 1990; Leinders-Zufall et al., 1997; Nakamura and Gold, 1987). Olfactory CNG is tetrameric and results from the association of 2 CNGA2 with one CNGA4 and one CNGB1 subunits (Bönigk et al., 1999; Bradley et al., 1994; Dhallan et al., 1990; Liman and Buck, 1994). CNGA2 is necessary for the channel formation and its loss causes anosmia (Brunet et al., 1996). The two other subunits modulate the channel sensitivity (Bradley et al., 1994; Liman and Buck, 1994; Lin et al., 2004; Michalakis et al., 2006; Munger et al., 2001).

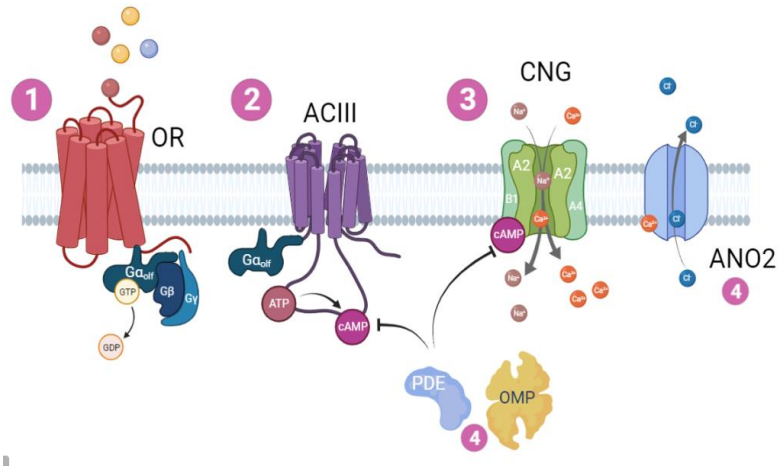

Figure 4: The canonical-OSNs pathway. ① *Step 1: odorant binding to the olfactory receptor (OR) activates GTP hydrolysis into GDP by the G protein complex.* ② *Step 2: $G\alpha_{olf}$ activates the adenylyl cyclase III (ACIII), which in turn transforms ATP into cAMP.* ③ *Step 3: cAMP activates the CNG channel, allowing Na+ and Ca^{2+} entrance.* ④ *Step 4: several intracellular proteins modulate the signal. The anoctamin 2 channel (ANO2) amplifies the depolarization by a Cl- current; phosphodiesterases (PDE) regulate cAMP levels; the olfactory marker protein (OMP) action is not clearly established (see for review Dibattista et al., 2021). This scheme is created in BioRender.com.*

After this primary signaling cascade, other effectors modulate the signal and regulate Ca^{2+} concentration to restore the neuron's firing potential. Many actors have been identified (see for review Neuhaus, 2020). Worth noticing, and relevant for this work, are: the Ca^{2+}-activated channel anoctamin-2 (ANO2) that amplifies the signal (Billig et al., 2011; Lowe and Gold, 1993; Stephan et al., 2009); the phosphodiesterases PDE1C and PDE4A that hydrolyze cAMP (Cygnar and Zhao, 2009); the olfactory marker protein (OMP), that modulate kinetics and termination of the signal (see for review Dibattista et al., 2021) (Figure 4). OMP, as suggested by its name, is a constitutive marker of olfactory neurons found in every sensory organ. Its precise function remains largely unknown, but thanks to its almost exclusive expression in olfactory neurons, it has been widely used to generate olfactory-restricted gene targeting in rodents (Li et al., 2004).

1.1.3 Non-canonical olfactory sensory neurons

It was long admitted that the cAMP signaling pathway was mandatory for olfactory sensing. Other pathways were theorized (Baker et al., 1999), and a study on a mouse model harboring a genetic deletion of the CNGA2 subunit revealed that a cAMP-independent pathway mediates the detection of some odorants (Lin et al., 2004). Since then, we know that OSNs using different receptor types or transduction proteins exist in the MOE. They are therefore referred to as non-canonical OSNs. Here, I will present three types of non-canonical OSNs for which the function is known and relevant to this work.

1.1.3.1 TAARs-expressing OSNs

Trace amine-associated receptors (TAARs) are a distinct family of GPCR expressed in various tissues (Borowsky et al., 2001; Bunzow et al., 2001). They became interesting for the olfactory world when 14 over the 15 TAAR mouse genes were shown to be expressed in the MOE (Liberles and Buck, 2006). TAARs-expressing and canonical OSNs share numerous similarities. TAARs are expressed only one at a time in mature OSNs (Pacifico et al., 2012); OSNs expressing a specific TAAR are localized within a limited spatial zone and project to dedicated glomeruli in the MOB (Pacifico et al., 2012); TAARs-expressing OSNs use the same key component for signal transduction (Liberles and Buck, 2006; Zhang et al., 2013).

While canonical OSNs detect a wide range of chemosignals, TAARs-expressing OSNs are tuned to biogenic amines detection (Liberles and Buck, 2006). Biogenic amines result from amino acid degradation and are therefore enriched in some body fluids such as urine. TAARs are not the only sensor for amines, but they tune the threshold sensitivity of OSNs to amines (Dewan et al., 2018). We can speculate that their fine detection ability could be evolutionary relevant, hence developing a parallel detection system.

1.1.3.2 GC-D-expressing OSNs

A subset of scattered OSNs does not use cAMP to support signal transduction. Guanylyl-cyclase (GC) receptors are one transmembrane segment receptors catalyzing GTP into cGMP upon activation (Kuhn, 2016). Several GC are expressed in diverse tissues, but GC-D expression seems mostly restricted to the MOE (Figure 5) (Fülle et al., 1995). GC-D-expressing OSNs lack key components of canonical OSNs odor transduction cascade and instead use the cyclic nucleotide-gated channel CNGA3 and the phosphodiesterase PDE2 (Juilfs et al., 1997; Meyer et al., 2000). Another specificity is their projection pattern in the MOB. GC-D-expressing OSNs project to several posterior interconnected ring-shaped glomeruli called the necklace glomeruli (Figure 5) (Juilfs et al., 1997).

GC-D remained an orphan receptor for a decade after its discovery. The hormone peptides guanylin and uroguanylin were the first ligands discovered (Leinders-Zufall et al., 2007). These are a byproduct of the digestive system and are naturally present in feces and urines. Later, Munger and colleagues showed that GC-D neurons also respond to the gas CS_2 in the context of food-odor preference (Munger et al., 2010). Mice can transmit the presence of a safe food source by their breath. The combination of CS_2 with the food odor in the breath is detected and learned by a congener, and, when confronted with the food odor, it can recall its safeness. Lastly, GC-D may respond to CO_2 variations around atmospheric levels, which could be a behavioral advantage to avoid unsafe environments (Hu et al., 2007).

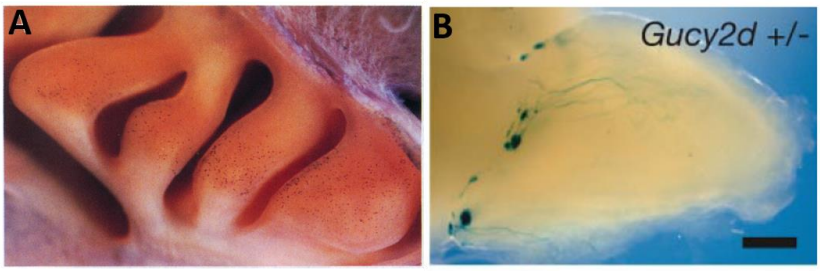

Figure 5: GC-D-expressing OSNs. A) In situ hybridization of GC-D mRNA in a wholemount MOE. From Fülle et al., 1995. B) Wholemount view of the olfactory bulb of a GC-D:LacZ transgenic mouse. GC-D positive axons, highlighted by LacZ staining, gathered into the necklace glomeruli. Scale bar, 500µm. From Leinders-Zufall et al., 2007.

1.1.3.3 TRPC-2-expressing OSNs

Transient receptor potential (TRP) channels are involved in a plethora of cell functions (Yildirim and Birnbaumer, 2007). TRPC2 is the primary cation channel expressed in the vomeronasal organ (Liman et al., 1999) (see section 1.4.2.3 for a detailed description) and was long thought to be restricted to this olfactory sensory organ. In 2014, M. Omura and P. Mombaerts highlighted MOE cells expressing TRPC2 and provided a detailed description of this new cell population (Omura and Mombaerts, 2014, 2015).

Based on other cellular markers, they determined two cell types (Figure 6): Type-A cells express CNGA2 and ACIII but are negatives for Gucy1B2 (another guanylyl cyclase); conversely, Type-B cells express CNGA2 and Gucy1b2 but are negatives for ACIII. Type-A cells function remains unknown, but they express some ORs and ACIII, suggesting a function similar to that of canonical OSNs (Omura and Mombaerts, 2014). Type-B cells are O_2 and H_2S gases sensors (Bleymehl et al., 2016; Koike et al., 2021). Interestingly, in Type-B cells, each cation channel (CNGA2 and TRPC2) is dedicated to one gas, and the sensing occurs at separate subcellular compartments (Figure 6) (Koike et al., 2021).

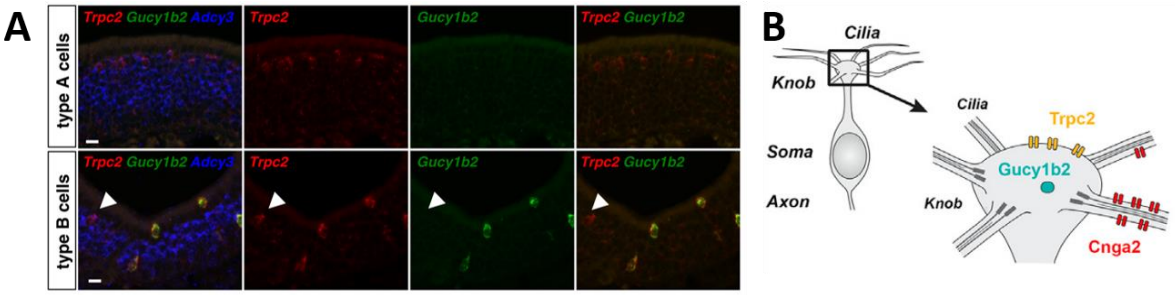

Figure 6: Trpc2-expressing OSNs. A) In situ hybridization of distinctive markers of Trpc2-expressing OSNs. Type-A cells are positive for Adcy3 (adenylyl cyclase III) but not Gucy1b2 (guanylyl cyclase 1b2), inversely for Type-2 cells. Arrowhead represents a Type-A cell in Type-B cells region. Scale bar, 10 µm. From Omura and Mombaerts, 2015. B) Schematic representation of Trpc2, Cnga2, and Gucy1b2 compartmentalized expression in the OSNs knob and cilia. From Koike et al., 2021.

1.1.4 The main olfactory bulb

OSNs axons reach the olfactory bulb (OB) to form their first relay in the central nervous system. The main olfactory bulb (MOB) is a subdivision of the OB that specifically receives inputs from the MOE. The MOB is a bean-shaped laminated structure with layers forming concentric circles (Figure 7). The glomeruli are devoid of cell bodies but contain one the highest density of synapses. Within glomeruli, OSNs axons contact dendrites of mitral and tufted cells (MCs and TCs) (Figure 7) (Pinching and Powell, 1971) by a glutamatergic synapse (Sassoè-Pognetto et al., 1993). Activated MCs and TCs then project to the olfactory cortices (Figure 7) (Haberly and Price, 1977). Intrinsic regulatory mechanisms involving other cell types exist within the MOB (see for review Ennis and Holy, 2015). Notably, a type of uncommon synapse exists within the MOB, the dendrodendritic synapse (Figure 7). It involves the granule cells, a peculiar type of axon-less interneuron whose dendrites contact dendrites of MCs and TCs. This interaction is reciprocal and is thought to modulate several aspects of the olfactory signal, such as synchronization or tuning specificity (see for review Shepherd et al., 2020).

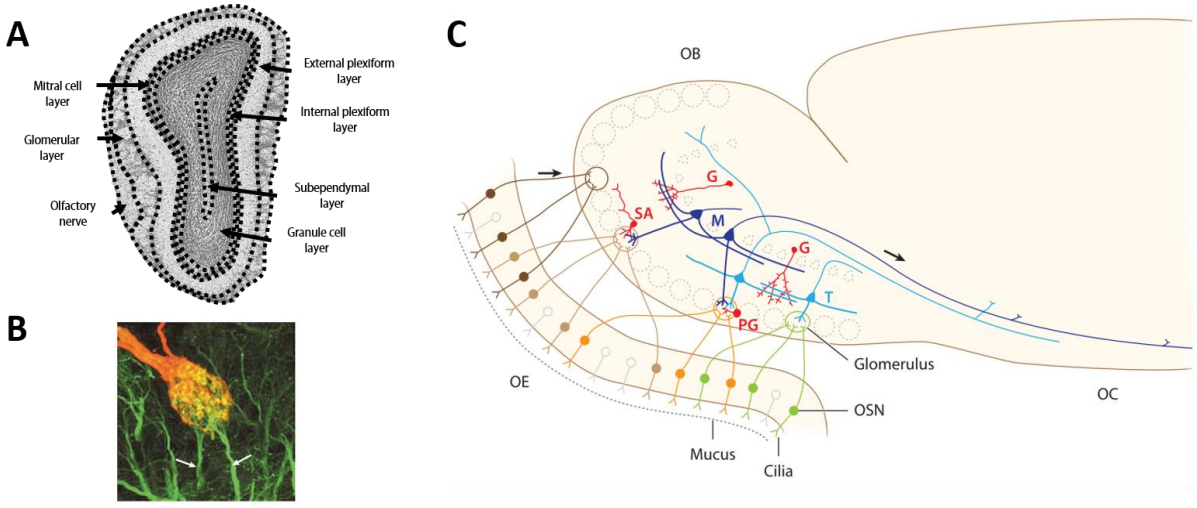

Figure 7: organization of the main olfactory bulb. A) Nissl stained coronal section of a mouse olfactory bulbs shows its laminar organization. Each layer is labeled. The image is from the Paxinos Mouse Brain Atlas. B) Fluorescent micrograph showing OSNs axons (red) forming a glomerulus. Mitral cells dendrites (green) contact OSNs axons within the glomerulus. From Belluscio et al., 2002. C) Schematic cellular organization of the MOB. OSNs expressing a similar OR project to the same glomerulus. Inside the glomerulus, mitral cells (M) and tufted cells (T), periglomerular cells (PG), and short axon cells (SA) contact OSNs axons. Granule cells (G) forms dendrodendritic synapses with the M and T cells. M and T cells project the olfactory cortices (OC). From Uchida et al., 2014.

OSNs do not randomly project to glomeruli. Like OSNs maps in MOE, it exists glomeruli maps in the MOB. One OSNs projects to one or two glomeruli, and one glomerulus receives input only from OSNs expressing the same OR (Ressler et al., 1994; Vassar et al., 1994). Interestingly, some glomeruli tuned for a given OR are mirroring, one located at the medial side of the MOB and the other laterally opposite (Ressler et al., 1994; Vassar et al., 1994). These two isofunctional glomeruli are interconnected (Belluscio et al., 2002), but the impact of this connection on odor decoding remains unknown. Several mechanisms ensure a correct targeting of the OSNs to the glomeruli. The presence

of the OR is mandatory. Indeed, mutation or deletion of an OR sequence causes the OSNs axon to wander in the OB (Wang et al., 1998). The identity of the OR, and therefore its place within the MOE, constrains its dorsoventral projection area (Takeuchi et al., 2010). cAMP signaling is also a key component of axonal targeting. Modulation of cAMP levels within the OSNs shifts the axonal projection sites along the anterior-posterior MOB axis by changing the expression of axon guidance molecules (Imai et al., 2006; Nakashima et al., 2013).

The olfactory information goes directly from the bulb to the olfactory cortices without a thalamic relay, emphasizing the particular place of olfactory information among the other sensory inputs. The MOB directly innervates the piriform cortex, the olfactory tubercle, the anterior olfactory nucleus, the cortical amygdala, and the entorhinal cortex (Tirindelli et al., 2009). Most of these cortical regions project back to the main olfactory bulb (Brunert and Rothermel, 2021) and other brain areas, including the thalamus, the hypothalamus, the hippocampus, and the limbic system (Tirindelli et al., 2009).

1.2 The septal organ of Masera

The septal organ (SO) is a small epithelium located near the base of the nasal septum (Figure 2 and 8) (Rodolfo-Masera, 1943). The vast majority of SO-neurons express ORs, proteins of the canonical-OSNs pathway, are OMP-positive, and project to the MOB (Ma et al., 2003; Tian and Ma, 2004). Interestingly, 50% of the neurons express the same OR, MOR256-3 (Figure 8), a broadly tuned OR, and only around 80 different ORs are found in the SO (Tian and Ma, 2004). Few cells nonetheless express the GC-D receptor and project to the necklace glomeruli (Figure 8) (Ma et al., 2003; Walz et al., 2007).

The SO epithelium organization overlaps with that of the MOE, suggesting a redundant function in the olfactory system. A study reported that SO-neurons are mechanical sensors, in addition to being odor sensors (Grosmaitre et al., 2007). They proposed two interesting hypotheses to this new function. First, during intense sniffing, the increased airflow pressure activates the mechanoreceptors in addition to the ORs. It might increase the probability of a neuron to fire in response to a weak olfactory stimulation. Based on the few ORs expressed in the SO, we can speculate that these might sense ethologically relevant cues, hence increasing the sensitivity of olfactory system to these odorants. Second, the coupling of mechanosensitivity with olfactory sensitivity may synchronize breathing and odor sensing to facilitate odor coding at the MOB level.

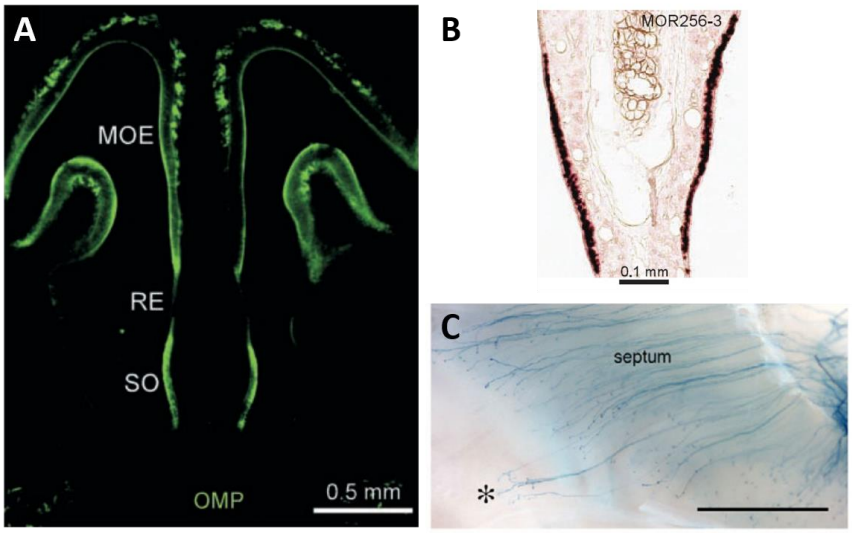

Figure 8: The septal organ of Masera. A) Visualisation of the olfactory marker protein (OMP) on a sagittal cut of a mouse snout. The septal organ (SO) is separated from the main olfactory epithelium (MOE) by the respiratory epithelium (RE). From Ma et al., 2003. B) In situ hybridization for MOR256-3 shows a strong expression through the SO. From Tian and Ma, 2004. C) Wholemount view of the septal area of a GC-D:tau-LacZ transgenic mouse. GC-D positive axons are highlighted by LacZ staining, and the asterisk shows axons emerging from the septal organ. Scale bar, 40 µm. From Walz et al., 2007.

1.3 The Grüneberg ganglion

In 1973, H. Grüneberg described a cell cluster residing in the most rostral region of the mouse nasal cavity (Figure 2 and 9) (Grüneberg, 1973). Several years later, several laboratories categorized it as an olfactory sensory organ and named it the Grüneberg ganglion (GG) (Fleischer et al., 2006; Fuss et al., 2005; Koos and Fraser, 2005; Roppolo et al., 2006; Storan and Key, 2006). The GG is not an epithelium. Rather, it comprises non-neuronal and OMP-positive neuronal cells, covered by a keratinized shell (Figure 9) (Brechbühl et al., 2008).

GG-neurons use a cGMP-dependent signaling pathway instead of the classical cAMP-dependent one of canonical OSNs. They employ the guanylyl-cyclase GC-G and the CNGA3 channel subunit to sense several kinds of chemicals (Figure 9) (Mamasuew et al., 2011). Like GC-D OSNs, GG-neurons project to several posterior interconnected ring-shaped glomeruli (Figure 9) (Fuss et al., 2005; Koos and Fraser, 2005). Other receptors have been described, some overlapping with the GC-G, which is an unusual scenario in the olfactory system (Figure 9) (see for review Fleischer, 2021).

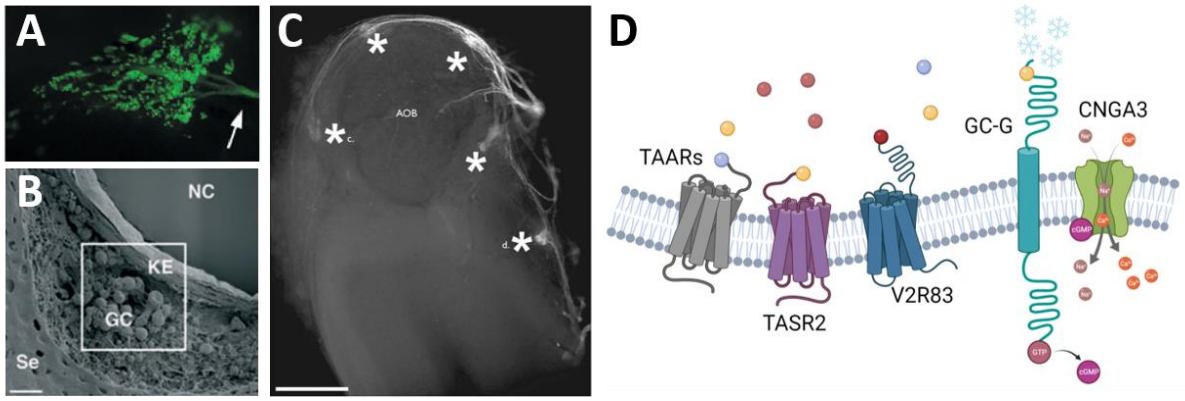

Figure 9: The Grüneberg ganglion. A) Wholemount view of the GG of an OMP-GFP mouse highlights GG-neurons. The arrow indicates GG-neurons axons that fasciculate to form a single nerve. From Fuss et al., 2005. B) Scanning electron micrograph of a GG coronal section. Scale bar, 20 µm. GC: GG cells; KE: keratinized epithelium; NC: nasal cavity; Se: septum. From Brechbühl et al., 2008. C) GG-neurons anterograde tracing to the posterior OB of a 7 day-old mouse. Asterisks show GG-innervated glomeruli. Scale bar 500 µm. From Koos and Fraser, 2005. D) Signaling pathways in GG-neurons. GG-neurons express the GC-G receptor that activates CNGA3 by hydrolyzing GTP into cGMP. Other receptors, like TAARs, TASR2, or V2R83, are expressed in GG-neurons. Cold (symbolized by snowflakes) can also activate GG-neurons, most probably through GC-G. This scheme is created on BioRender.com.

The GG is a dual sensory organ. On one side, it detects alarm pheromones and predator kairomones (Brechbühl et al., 2008, 2013; Chao et al., 2018; Mamasuew et al., 2011; Pérez-Gómez et al., 2015), which are also sensed by the MOE and VNO. Then, it was proposed that the GG do not participate in the discrimination of these odorants but rather send the alarm signal *per se* to induce adequate behavioral and physiological responses (e.g., cortisol secretion and freezing) (Fleischer, 2021). On the other side, coldness activates GG-neurons, especially in pups that are highly sensitive to cold temperatures (Mamasuew et al., 2008; Schmid et al., 2010). Interestingly, these two functions are intermingled. Warmth reduces GG-neuron responsiveness to odorants (Bumbalo et al., 2017). This could be ethologically relevant. Rodents are nocturnal animals. They explore their environment during the coldest period to find food and rest in warmth to sleep during the day. Having a higher sensitivity to danger only when needed could be advantageous to this species (Fleischer, 2021).

1.4 The accessory olfactory system

Besides the MOS, many mammals possess a secondary system, the accessory olfactory system (AOS), dedicated to socio-sexual communication (Munger et al., 2009). The AOS has long been associated with the detection of non-volatile pheromones, while the MOS was associated with environmentally volatile odorants. This strict functional segregation is no longer valid. We know now that both systems can detect volatile and non-volatile chemicals and that the pheromonal nature of odorants is not restricted to the initial pheromones definition made by Karlson and Lüscher (Brennan and Zufall, 2006). Despite this sensitivity overlap, the primary role of the AOS in chemical

communication is well established. Indeed, alteration of the AOS severely impairs the expression of innate socio-sexual behaviors (Mohrhardt et al., 2018).

The AOS consists of: *i*- the vomeronasal organ (VNO), where odorants are detected; *ii*- the accessory olfactory bulb (AOB), the first cerebral relay of the olfactory information; *iii*- the vomeronasal amygdala, that receives direct or indirect information from the AOB (Munger et al., 2009). Organization of the AOS as an independent system occurred with the development of lung respiratory in amphibians but did not persist in every taxon (Taniguchi et al., 2011). Among mammals, there is a heterogeneity in the expression of AOS molecular markers, and some do not possess a functional AOS, such as higher primates (including humans), cetaceans, and almost all bats (Tirindelli, 2021). Here, I will review the AOS organization in rodents.

1.4.1 The vomeronasal organ

In 1813, L. Jacobson described in detail a novel organ in the nose of domesticated animals that *"may be of assistance to the sense of smell"* (see the translation of Jacobson's seminal article in Trotier and Døving, 1998). It was later renamed *vomeronasal organ* due to its location at the vomer bone base. The VNO is a tubular structure surrounded by a cartilaginous cap that communicates with the nasal and oral cavities by the vomeronasal and nasopalatine ducts. On a coronal VNO section, distinct histological structures can be delineated (Figure 10): glands located dorsally along the nasal septum; the vomeronasal sensory epithelium (VNE) in crescent shape, medially; a large blood vessel surrounded by cavernous tissue, laterally. The VNO is blind-ended, and its lumen is full of mucus secreted by the dorsal glands. Odorant transfer to the VNO lumen occurs by an active pumping process triggered by sympathetic innervation (Meredith and O'Connell, 1979). Pumping can be induced during an olfactory investigation and activated by arousal, stress, or fear (Tirindelli, 2021).

The VNE derives from the olfactory placode around embryonic day 11 in mice and shows the characteristics of an organized tissue at embryonic day 13 (Cuschieri and Bannister, 1975). Interestingly, evidence suggests that the VNO is functional in utero although the complete development of the VNO is reached after birth (Pedersen et al., 1983). The VNE is composed of OMP-positive vomeronasal sensory neurons (VSNs), supporting cells, and stem cells (Figure 10). Unlike in the MOE, stem cells are not only basal but also form two neurogenic niches at the extremities of the VNE crescent (Figure 11) (Brann and Firestein, 2014).

VSNs are bipolar, with a single dendrite and axon (Figure 10). VSNs axon are unmyelinated, they fasciculate to form the vomeronasal nerve and reach the accessory olfactory bulb. The dendrite extends to the VNO lumen and forms a terminal knob from which several microvilli expand into the mucus to enlarge the receptive surface (Mendoza, 1993). Like cilia in OSNs, the microvilli contain all the molecular machinery necessary for the odorant transduction process (Munger et al., 2009).

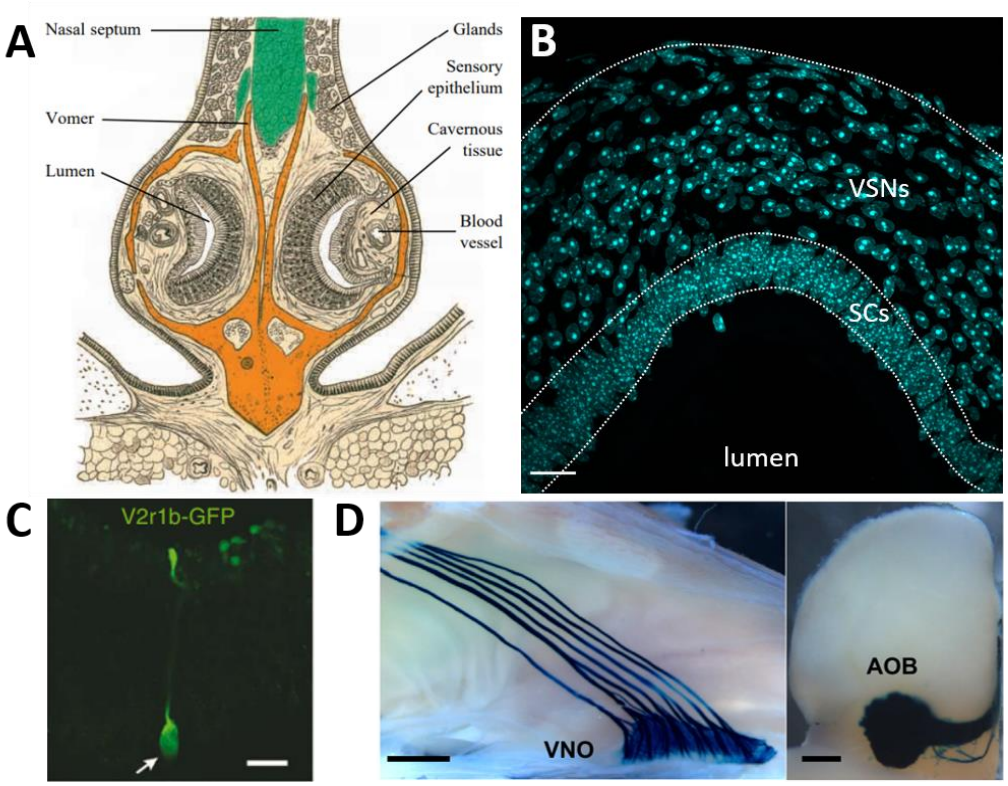

Figure 10: Histology of the vomeronasal organ. A) Schematic of a whole VNO coronal cut showing its different histologic structures. From Døving and Trotier, 1998 B) Dapi staining of the VNE. The supporting cells (SCs) are located apically at the lumen border. Scale bar, 20 µm. C) Visualization of a single VSNs. The arrow points to the cell body located in the VNE. The dendrite extends to the lumen border and forms a protruding knob. Scale bar, 10 µm. From Leinders-Zufall et al., 2009. D) Wholemount view of the VNO (left) and AOB (right) of a Trpc2-IRES-taulacZ mouse, highlighting VSNs axons projection to the AOB. Scale bar, 200 µm (left) and 50 µm (right). From Omura and Mombaerts, 2014.

1.4.2 Vomeronasal signaling

VNO signaling results from the activation of three GPCR types: Type-I and Type-II vomeronasal receptors, namely V1Rs and V2Rs, and formylated peptide receptors, FPRs (Munger et al., 2009). Additionally, some VSNs express an OR (Lévai et al., 2006; Nakahara et al., 2016). V1Rs- and V2Rs-expressing VSNs form non-overlapping populations within the VNE, each associated with specific molecular markers (Munger et al., 2009) (Figure 11). V1Rs are restricted to apical VSNs positive for the G protein subunit $G\alpha_{i2}$, the phosphodiesterase PDE4A, and the semaphorin neuropilin 2; conversely, V2Rs are restricted to basal VSNs positive for $G\alpha_o$ and β2-microglobulin (Ishii et al., 2003; Jia and Halpern, 1996; Lau and Cherry, 2000; Matsunami and Buck, 1997; Walz et al., 2002).

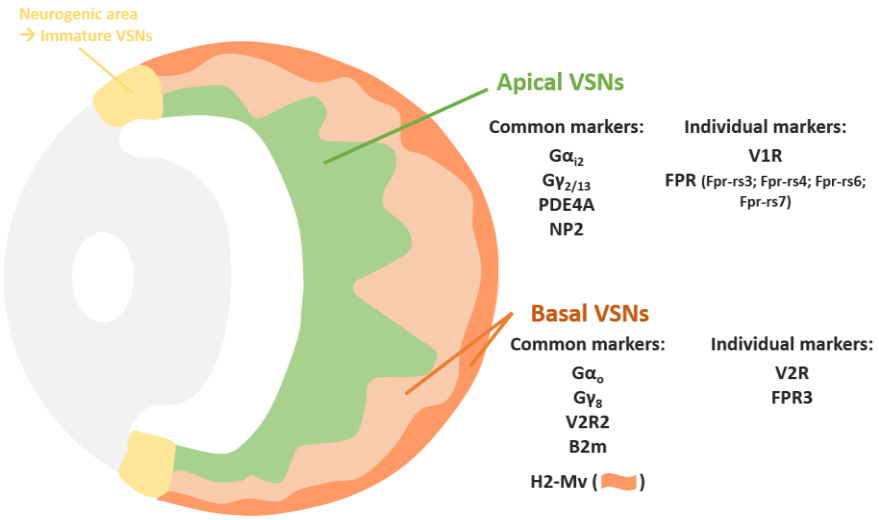

Figure 11: Organization of the vomeronasal epithelium and markers associated with VSNs population. Apical and basal VSNs populations each have specific markers (common markers), and individual neurons within each population express one receptor (individual markers). Note that basal VSNs are also divided into two segregated populations, the most basal one expressing H2-Mv (dark orange).

1.4.2.1 V1Rs

The V1Rs family was the first discovered in 1995 by screening genes library from individual VSNs (Dulac and Axel, 1995). Seven members were initially isolated and further analyses in mice led to a complete repertoire of 250 genes, including 150 coding genes, clustered in 12 families of 1 to 30 representatives (Boschat et al., 2002; Del Punta et al., 2000; Roppolo et al., 2007; Young et al., 2010). V1Rs repertoires are highly species-specific (Grus et al., 2005; Silva and Antunes, 2017; Young et al., 2010), even between closely related ones (Kurzweil et al., 2009), suggesting rapid and ethologically relevant adaptive changes in functional V1Rs. Interestingly, many mammals like goat, sheep and most domestic animals express V1Rs but not V2Rs (Silva and Antunes, 2017). Also, humans have several *V1R* pseudogenes and five *V1R-like* genes potentially coding for functional receptors (Rodriguez et al., 2002). This suggests distinctive origins for the two VRs families, with V1Rs expanding among mammals until the disappearance of a functional VNO in some branches.

V1Rs are co-expressed with the $G\alpha_{i2}$ protein, but no functional link between this G protein and the initiation of intracellular signaling has been proposed. Indirect evidence comes from the $G\alpha_{i2}$ global knockout mouse model ($G\alpha_{i2}^{-/-}$) in which exposure to soiled bedding fails to activate apical projection sites in the AOB (Norlin et al., 2003). Structurally, V1Rs possess a short extracellular region, suggesting that ligand binding occurs at the levels of the transmembrane domains (Del Punta et al., 2000). This also means that odorants detected should be at some degree hydrophobic to reach the binding pocket. Further studies confirmed this hypothesis. The first one to attribute a functional role to V1Rs results of the genetic inactivation of V1Rs clusters A and B (Del Punta et al., 2002). It revealed that V1Rs detect small organic volatile compounds, and several studies later added the sulfated steroids to the list (Boschat et al., 2002; Haga-Yamanaka et al., 2014; Nodari et al., 2008; Turaga and Holy,

2012). Recently, bile acids were also associated with V1Rs (Wong et al., 2020). In 2011, Isogai and colleagues mapped VSNs activation in mice after stimulation from hetero- or conspecifics cues (Isogai et al., 2011). It revealed that most V1Rs families detect chemical cues common to multiple species, suggesting that they may not encode information about the emitter identity but rather its physiological status.

1.4.2.2 V2Rs

Three groups simultaneously discovered the V2Rs in 1997 (Herrada and Dulac, 1997; Matsunami and Buck, 1997; Ryba and Tirindelli, 1997). Currently, the mouse V2Rs repertoire comprises 280 genes, including 120 coding genes, clustered in 4 families (A to D) of 1 to more than 100 members (Shi and Zhang, 2007; Yang et al., 2005; Young and Trask, 2007). V2Rs greatly extended in amphibians and reptiles but are largely absent in most mammals, except rodents, lagomorphs, some marsupials, platypus, and lower primates (Shi and Zhang, 2007; Young and Trask, 2007). This discrepancy between V1Rs and V2Rs repertoires among mammals suggests that rodents (and other taxa expressing V2Rs) may face a more complex pheromonal environment, hence maintaining a second VRs family.

V2R-expressing VSNs are the notable exception to the "one neuron-one receptor" rule that prevails among olfactory neurons (Rodriguez et al., 1999; Serizawa et al., 2004). The family-C V2Rs comprises seven highly homologous receptors (also called V2R2) of which at least one member is expressed simultaneously with V2Rs from A, B, or D families in every basal VSNs (Figure 12) (Belluscio et al., 1999; Martini et al., 2001; Silvotti et al., 2007, 2011). Some postulates that V2R2 may serve as chaperoning dimerization partner for V2R-subunits (Mohrhardt et al., 2018), as it is postulated for the constitutive Orco receptor in insects (Larsson et al., 2004).

V2Rs are co-expressed with the $G\alpha_o$ protein, which is required to trigger VSNs signaling after ligand detection (Chamero et al., 2011). V2Rs do not belong to the same GPCR family as ORs and V1Rs. Those are rhodopsin-like (class-A), whereas V2Rs are class-C ones, like the glutamate receptor, meaning they possess a long extracellular hydrophobic N-terminal domain (also called Venus Flytrap module) (Matsunami and Buck, 1997; Mombaerts, 2004). This structural conformation predicts that V2Rs should detect large molecules such as peptides and proteins. In 2003, the discovery of a second receptor class expressed in basal VSNs supported this theory (Ishii et al., 2003; Loconto et al., 2003). *H2-Mv* genes are coding for nonclassical class Ib MHC (a class of glycoproteins that bind extracellular proteins to present them to the immune system). Studies revealed that the most basal VSNs coexpress one of those *H2-Mv* genes with V2Rs (Figure 12) (Ishii and Mombaerts, 2008; Ishii et al., 2003; Loconto et al., 2003; Silvotti et al., 2007). Subsequently, Leinders-Zufall and colleagues showed that peptidic ligands for the MHC-Ib also serve as V2Rs ligands (Leinders-Zufall et al., 2004, 2009).

Further, they demonstrated that *H2-Mv* deletion decreases V2Rs sensitivity to their natural ligands, suggesting an interaction between them.

MHC-ligand peptides were the first class of V2Rs ligands identified. Then, other families of ligand were discovered, such as the major urinary proteins (MUPs), the exocrine secreted peptides (ESPs), and salivary peptides (Chamero et al., 2007, 2011; Dey and Matsunami, 2011; Haga et al., 2010; Isogai et al., 2018; Osakada et al., 2018; Stein et al., 2016). These secreted proteins carry robust information about the characteristics of their emitter (Ferrero and Liberles, 2010; Hurst and Beynon, 2004). Considering that basal VSNs can express three types of receptors simultaneously, V2R2, V2RA/B/D, and H2-Mv, this could allow them to encode a highly refined message. In their master analysis of VSNs activation, Isogai and colleagues found that individual V2Rs are mainly responsive to cues of a unique ethological context (i. e. from conspecific of from a particular other species) (Isogai et al., 2011). Consequently, V2Rs would be good candidates to encode information about the identity of the emitter.

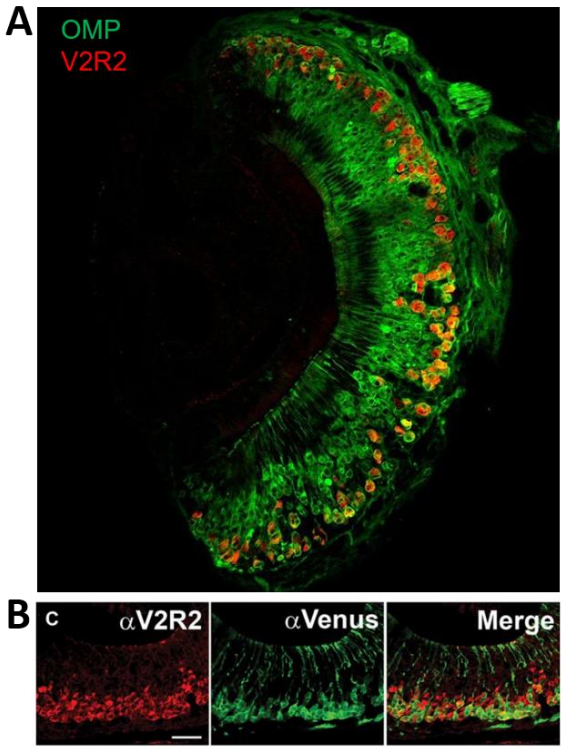

Figure 12: Basal VSNs. A) Immunostaining of a coronal VNE section. VSNs express OMP (green) and basal VSNs are highlighted by staining of the V2R2 family. B) Basal VSNs (expressing V2R2, in red) are segregated into two populations, the most basal ones expressing H2-Mv (revealed by the Venus transgene in a M10.2-Venus mouse). Scale bar 50 µm. From Ishii and Mombaerts, 2008.

1.4.2.3 VRs sensory cascade

As mentioned above, V1Rs and V2Rs respectively use $G\alpha_{i2}$ and $G\alpha_{o}$ as the primary G protein α-subunit (Chamero et al., 2011; Jia and Halpern, 1996; Norlin et al., 2003). The remaining intracellular signaling pathway is then common to the two VSNs population (Figure 13). Upon activation by a ligand, the Gα subunit hydrolyzes GTP into GDP and releases the Gβ/γ complex. Subsequent cellular

activation does not depend on a GDP-activated enzyme, like in the OSNs, but rather involves the Gβ/γ complex. Its nature varies in basal and apical VSNs (Sathyanesan et al., 2013), but it seems that the functional activity relies on the association of Gβ2/γ8 in basal (Montani et al., 2013; Rünnenburger et al., 2002; Ryba and Tirindelli, 1995) and Gβ2/γ2 or γ13 in apical VSNs (Liu et al., 2018; Rünnenburger et al., 2002). The different Gβ/γ complexes activate the phospholipase C (PLC) (Holy, 2000; Smrcka, 2008; Spehr et al., 2002), which in turn hydrolyzes the phosphatidylinositol-4,5-bisphosphate (PIP_2) into the second messengers diacylglycerol (DAG) and inositol-1,4,5-trisphosphate (IP_3). The functional role of the PLC isoform β2 (PLCβ2) has been attested in VSNs, but it does not count the majority of PLC isoforms expressed in the VNO, the remaining still lacking evidence for a functional role (Dey et al., 2015). Downstream to the PLC-dependent lipid turnover, IP_3 is not necessary for VR signaling (Chamero et al., 2017). Genetic deletion of type 3 IP_3 receptor modifies the initial current but does not prevent VSN depolarization, suggesting that it only participates in signal modulation. DAG activates TRPC2, a cationic channel member of the transient receptor potential (TRP) family, to trigger VSNs depolarization (Leinders-Zufall et al., 2021; Liman et al., 1999; Lucas et al., 2003). Secondary to TRPC2 activation, the induced Ca^{2+} influx activates the chloride channels anoctamin 1 (ANO1) to depolarize the cell further (Amjad et al., 2015; Münch et al., 2018; Yang and Delay, 2010).

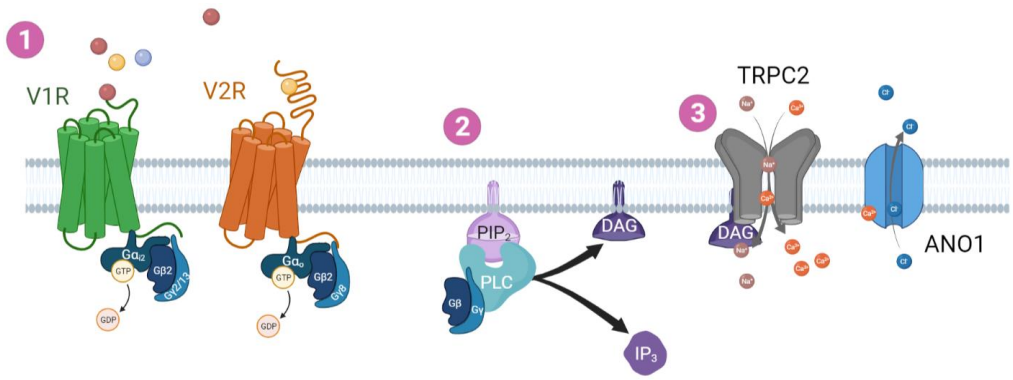

Figure 13: Vomeronasal signaling pathway. ① Step 1: odorant binding to the vomeronasal receptor (V1R, V2R) activates GTP hydrolysis into GDP by the G protein complex. ② Step 2: Gβ/γ complex activates the phospholipase C (PLC), which in turn hydrolyses phosphatidylinositol-4,5-bisphosphate (PIP_2) into the second messengers diacylglycerol (DAG) and inositol-1,4,5-trisphosphate (IP_3). ③ Step 3: DAG activates the TRPC2 channel, allowing Na+ and Ca^{2+} entrance. Intracellular Ca^{2+} then activates the anoctamin 1 channel (ANO1) to amplify the depolarization by a Cl- current. This scheme is created in BioRender.com.

Several studies show that some degree of VSN signaling can be achieved without TRPC2. The first clue came from a study showing *in vitro* that MHC binding peptides activate VSNs from TRPC2 knock-out mice (TRPC2-KO; $Trpc2^{-/-}$) (Kelliher et al., 2006). Other studies strengthened this hypothesis and highlighted the existence of other cation channels (Kim et al., 2012; Zhang et al., 2008, 2010). Some even showed that the chloride current by itself could trigger VSNs depolarization, probably since chloride concentration within the knob is quite high (Kim et al., 2011, 2015; Spehr et al., 2009). A question remains about the role of these TRPC2-independent pathways. Whether they

sustain the transmission of specific odorants, complement the electrical signal triggered by TRPC2, or simply take over TRCP2 function in its absence remains elusive.

1.4.2.4 FPRs

Apart from VRs, some VSNs express a third family of rhodopsin-like GPCR, the formyl peptide receptors (FPRs) (Liberles et al., 2009; Rivière et al., 2009). FPRs are expressed in numerous tissues and cell types of the immune system, where they participate in defense mechanisms against pathogens (Boillat et al., 2021). Most mammals possess two immune FPRs, but rodent FPR repertoire significantly expended, and mice possess seven genes coding FPRs. Two of them are orthologs of the immune FPRs (Fpr1 and Fpr-rs2), whereas the five others result from duplication of Fpr-rs2 (Dietschi et al., 2017; Gao et al., 1998; Wang and Ye, 2002). The role of these five additional FPRs (Fpr-rs1/3/4/6/7) remained elusive until two laboratories discovered that they were almost exclusively expressed in the VNO (Liberles et al., 2009; Rivière et al., 2009). The existence of vomeronasal-FPRs implies that rodents may smell pathogens. Another usage of such receptors would be assessing the microbiota of conspecifics (Boillat et al., 2021).

FPRs-expressing VSNs constitute 4% of total VSNs (Boillat et al., 2021) and observe the same "one neuron-one receptor" rule than most olfactory neurons (Bufe et al., 2019; Dietschi et al., 2013; Liberles et al., 2009; Rivière et al., 2009). Vomeronasal-FPRs are spatially segregated: FPR3 (Fpr-rs1) is restricted to $G\alpha_o$-expressing VSNs and the others to $G\alpha_{i2}$-expressing VSNs, suggesting that they derived from two independent genetic events (Dietschi et al., 2017; Liberles et al., 2009; Rivière et al., 2009). They are responsive to classical immune-FPRs ligands (Rivière et al., 2009), but *in vivo* confirmation has been brought only for FPR3 (Bufe et al., 2019). This latest study also demonstrated the requirement of $G\alpha_o$ and TRPC2 for *in vivo* FPR3 signaling. This suggests that vomeronasal-FPRs probably use the same intracellular pathway as VRs even if confirmation for apically localized FPRs is still needed.

1.4.3 The accessory olfactory bulb

VSNs axons reach the olfactory bulb (OB) to form their first relay in the central nervous system. The accessory olfactory bulb (AOB) is a dorsal subdivision of the OB that specifically receives inputs from the VNO. Like the MOB, the AOB is organized in different cell layers, although not concentric. Dorsally to ventrally, the glomerular layer (GL) receives VSNs axons within glomeruli; the mitral cell layer (MCL) contains interneurons transmitting VSNs information to the brain, and the granule cell layer (GCL) contains axon-less neurons doing dendrodendritic synapses with the mitral cells (MCs) (Figure 14) (Mohrhardt et al., 2018).

The GL-AOB retains the structural dichotomy observed in the VNO and V1Rs- and V2Rs-expressing VSNs target segregated regions of the GL-AOB along its rostro-caudal axis. Apical VSNs synapse into anterior glomeruli, and basal VSNs into posterior ones (Figure 14) (Belluscio et al., 1999; Ishii and Mombaerts, 2008; Jia and Halpern, 1997; Rodriguez et al., 1999). A study suggests a tripartite AOB-GL map, with the posterior part being further subdivided to organize inputs from *H2-Mv* positive or negative basal VSNs (Figure 14) (Ishii and Mombaerts, 2008).

AOB topographic segregation is not as strict as for the MOB. First, VSNs-axons can divide to innervate multiple glomeruli (up to 30) (Belluscio et al., 1999; Rodriguez et al., 1999). It has also been reported that some glomeruli, mainly the larger ones, receive inputs from different VRs-expressing VSNs, each being restricted to microdomains within the glomerulus (Belluscio et al., 1999). However, glomeruli receiving axons from VSNs expressing VRs of the same family (e.g., V1Rj or V2R1) are gathered in domains (Wagner et al., 2006) (Figure 14). In the MOB, MCs receive inputs in one glomerulus. On the contrary, AOB-MCs have branched dendrites that contact several glomeruli (Takami and Graziadei, 1991; Yonekura and Yokoi, 2008). They respect the AOB-GL rostrocaudal segregation, meaning that anterior MCs contact anterior glomeruli and vice-versa, but some cross-connectivity has nonetheless been reported (Yonekura and Yokoi, 2008). This organization argues for a direct computation and integration of the olfactory information in the AOB. This is consistent with the fact that AOB-MCs do not project into dedicated cortices but rather directly activate limbic and hypothalamic brain structures. These regions are large hubs for sensory information, hence the upstream information coding.

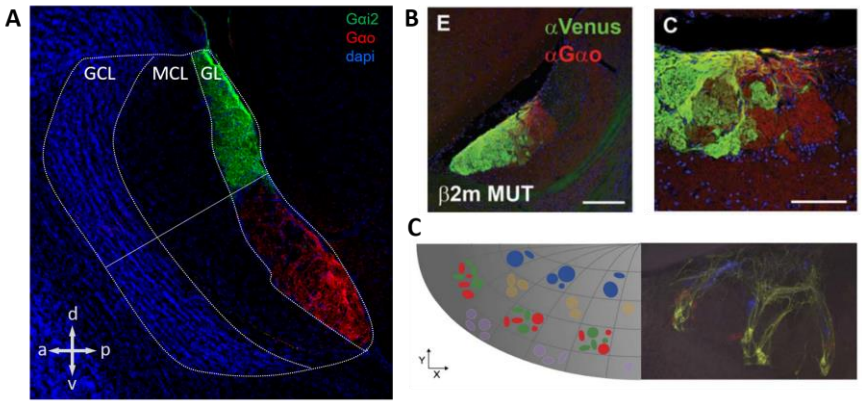

Figure 14: The accessory olfactory bulb. A) Sagittal cut of the AOB. Dapi staining (blue) allows the delimitation of different cellular layers (GL, MCL, GCL). The GL-AOB reflects the VNO topographic organization with $G\alpha_{i2}$ VSNs (green) projecting to the anterior GL and $G\alpha_o$ VSNs (red) to the posterior GL. B) The posterior GL is also subdivided, the most posterior part receiving inputs from H2-Mv-expressing VSNs (Shown here by the Venus transgene in a M10.2-Venus mouse). Scale bars, 200 µm (left) and 100 µm (right). From Ishii and Mombaerts, 2008. C) VSNs expressing receptors from the same family project to glomeruli gathered in domains. Right: schematic proposed organization. Left: Experimental tracing. Here, V1R-family A expressing VSNs, represented by red and yellow fibers (from respectively V1Ra1 and V1Ra3 positive VSNs) project to close ventral glomeruli, whereas V1R-family B expressing VSNs, represented here by blue fibers (from V1Rb1 positive VSNs) project to dorsal glomeruli. From Wagner et al., 2006.

1.4.4 Vomeronasal ligands

Among the hundreds of receptors expressed in the VNO, only a handful have been associated with their(s) ligand(s). Large-scale screening by in-situ hybridization or mRNA-sequencing (Isogai et al., 2011; Wong et al., 2020), KO-mouse models for VRs (Haga et al., 2010; Osakada et al., 2018), and genetic mouse models allowing fluorescent reporter in VSNs expressing a specific VR (Boschat et al., 2002; Haga-Yamanaka et al., 2014; Leinders-Zufall et al., 2009, 2014; Del Punta et al., 2002) allowed the identification of a few pairs. Such work is highly technic, time-consuming, and costly, thus unadapted to cover the large VR repertoire. The main constrain to deorphanize VRs is the lack of suitable *in vitro* models. Heterologous expression systems are complex to adapt for VR expression due to peculiar requirements for receptor docking to the membrane (Dey and Matsunami, 2011). Still, such systems exist and allowed the identification of additional vomeronasal ligands (Bufe et al., 2012, 2015, 2019; Dey and Matsunami, 2011; Stein et al., 2016). The Table 1 contains known pairs of VRs and ligands. Additionally, it lists vomeronasal ligands whose receptors are unknown and indicates if they activate a specific type of VSNs (e.g., $G\alpha_o$-expressing VSNs).

Some of the vomeronasal ligands act as pure pheromone, in line with the initial definition of Karlson and Lüscher (Karlson and Lüscher, 1959). A clear example is ESP22, a peptide secreted in tears of juvenile mice that inhibits the sexual behavior of adults (Ferrero et al., 2013; Osakada et al., 2018). Others have been linked to specific behaviors or physiological processes, but not strictly to a particular one. As mentioned in the general introduction, we have to rethink the definition of pheromone: a pheromone could be defined as a molecule used for communication that carries information about the individual. Each individual emits a combination of odorants, read by the others to adapt their behavior.

Now that the reader is kin with the rodent olfactory system, I will describe mouse socio-sexual behaviors and how the vomeronasal system controls them.

Deorphanized receptors

	receptor name	gene	ligand(s)	biological source	reference
V1Rs	V1Rb2	*Vmn1r49*	2-heptanone	urine	1
	V1Re2	*Vmn1r226*	sulfated corticosteroids	urine	2, 3
	V1Re6	*Vmn1r227*	sulfated corticosteroids	urine	2
	V1Rf3	*Vmn1r237*	sulfated estrogen		
	V1Rj2	*Vmn1r89*	sulfated androgens sulfated estrogens	urine	2, 3
	V1Rj3	*Vmn1r85*	sulfated estrogens	urine	3
	V1Rc28	*Vmn1r21*	deoxycholic acid	bile	4, 5
	V1Rc29	*Vmn1r16*	cholic acid		
	V1Rl1	*Vmn1r70*	lithocholic acid	bile	4
V2Rs	V2Rp5	*Vmn2r116*	ESP1	male tears	6
	V2Rp1	*Vmn2r112*	ESP5 ESP6	male tears	7
	V2Rp2	*Vmn2r111*	ESP5		
	V2Rp4	*Vmn2r115*	ESP22	juvenile tears	8
	n/a	*Vmn2r65*	submandibular gland protein C	female saliva	9
	n/a	*Vmn2r88*	haemoglobin	blood	9
	n/a	*Vmn2r28*	CRP1	rat tears	10
	n/a	*Vmn2r52*			
	V2R1b	*Vmn2r26*	MHC-proteins	urine	11
	V2Rf2	*Vmn2r81*	MHC-proteins formyl peptide	urine	12
FPRs	FRP3	*Frpr-rs1*	MgrB peptide W-peptide	bacteria	13, 14

Partially deorphanized receptors and unmatched ligands

VSNs marker	gene	ligand(s)	biological source	reference
V1Rc1 V1Rc30	*Vmn1r10* *Vmn1r9*		neonate	9
V1Re9 V1Re12	*Vmn1r69* *Vmn1r185*		female urine	3
V1Ra & V1Rb	*n/a*	n-pentylacetate isobutylamine 6-hydroxy-6-methyl-3-heptanone	urine	15
$G\alpha_o$	*Gnao*	MUPs MHC-proteins mitochondrial formyl-peptides LMW fraction	urine	16
		Feld4	cat fur	17
n/a	*n/a*	α/β-farnesene 2-*sec*-butyl-4,5-dihydrothiazole 2,5-dimethylpyrazine 2,3-dehydro-*exo*-brevicomin	urine	18
n/a	*n/a*	hexadecanol hexadecyl acetate	urine	19
n/a	*n/a*	sulfated androgens sulfated estrogens sulfated progestagens sulfated corticosteroids	urine	20, 21

Table 1: Vomeronasal ligands, their receptors. n/a: not applicable. [1] Boschat et al., 2002; [2] Isogai et al., 2011; [3] Haga-Yamanaka et al., 2014; [4] Doyle et al., 2016; [5] Wong et al., 2020; [6] Haga et al., 2010; [7] Dey and Matsunami, 2011; [8] Osakada et al., 2018; [9] Isogai et al., 2018; [10] Tsunoda et al., 2018; [11] Leinders-Zufall et al., 2009; [12] Leinders-Zufall et al., 2014; [13] Bufe et al., 2012; [14] Bufe et al., 2019; [15] Del Punta et al., 2002; [16] Chamero et al., 2011; [17] Pérez-Gómez et al., 2015; [18] Leinders-Zufall et al., 2000; [19] Liu et al., 2019; [20] Nodari et al., 2008; [21] Turaga and Holy, 2012

2 Vomeronasal control of socio-sexual behaviors

Individuals of a species interact to ensure their survival and that of their kind. What does survival depend on? Feeding, mating, raising offspring, defense, and danger avoidance are crucial, and all depend on olfactory cues detection and interpretation. Tinbergen theorized four ways to study behaviors: causation (how does it work), ontogeny (how is it implemented), function (what is its survival value), and evolution (how does it evolve) (Tinbergen, 1963). Here, we will mainly focus on the causation of social behaviors, especially their vomeronasal control and modulation.

Agonistic or antagonistic, social behaviors are innate, meaning they are produced without learning and consist of stereotypical sequences. However, innate is by no means static. Reproductive state, social experience, internal state, and environmental factors influence the decision of action and its realization. Patterns of social behavior are well-characterized, and their plasticity is under increasing scrutiny (Tan and Stowers, 2020; Wei et al., 2021). Further, social behaviors are highly sexually dimorphic. The emergence of sexual reproduction has led to the development of sex-specific behavioral responses adapted to the complementary role of each sex in perpetuating the species. This section will describe four categories of behavior: sexual, aggressive, parental, and avoidance behaviors.

Several models unraveled VNO implication in the control of social behaviors (Chamero et al., 2012). Before the explosion of genetic tools, surgical ablation of the VNO (the VNOx model) laid the groundwork for this research field (Wysocki and Lepri, 1991). Then, the genetic dissection of VNO-dependent behaviors began with the TRPC2-KO mouse ($Trpc2^{-/-}$), which induces vomeronasal anosmia (Leypold et al., 2002; Stowers et al., 2002). Finest dissection of vomeronasal pathways followed, with models of genetic ablation of intracellular messengers or VRs (Chamero et al., 2011; Haga et al., 2010; Isogai et al., 2018; Kim et al., 2012; Leinders-Zufall et al., 2014; Liu et al., 2018; Loconto et al., 2003; Montani et al., 2013; Münch et al., 2018; Norlin et al., 2003; Osakada et al., 2018; Del Punta et al., 2002). A huge step in the precise comprehension of vomeronasal function came from the OMP-driven deletion of $G\alpha_o$ ($cG\alpha_o^{-/-}$ mouse), the primary effector of V2Rs-positive VSNs (Chamero et al., 2011; Oboti et al., 2014; Pérez-Gómez et al., 2015). However, similar information concerning V1R/$G\alpha_{i2}$ VSNs is still lacking.

The VNO is a crucial actor of social behaviors, yet the implication of other olfactory sensory organs should not be undermined. Ablation of the MOS function induces global anosmia, rendering it difficult to determine its precise implication. Recent advances allowed partial MOS dysfunction, thus revealing its cooperation with the VNO to ensure complete behavioral responses (Kobayakawa et al., 2007; Matsuo et al., 2015). When relevant, I will mention the participation of non-vomeronasal pathways.

2.1 Sexual behaviors

Some would say that mating is The gold achievement of an animal's life. If not to perpetuate the species, why would one live for? Besides philosophical questioning it may raise, reproduction indeed takes a particular place in most animals' life, often impinging other activities. In extreme cases, reproduction becomes the one and only activity, like the giant peacock moth, which has no proboscis to feed itself and devotes its entire week of life to mating.

Rodent sexual behavior is composed of an appetitive phase, which englobes the detection, the approach and the investigation of the target, followed by a consummatory phase, the sexual act by itself (Figure 15) (Ball and Balthazart, 2008). The requirement of olfaction to detect and approach a potential mate makes perfect sense but is not limited to that. Rodents detect and track the olfactory signature of a congener. Once found, close nasal contacts allow them to determine if it is a suitable choice to mate with. Finally, some olfactory cues can stimulate sexual intercourse. The discrimination between a direct effect of olfactory cues on the consummatory phase and an indirect effect coming from a modification of the appetitive phase is not always easy (Baum and Kelliher, 2009). Specific behavioral testing paradigms exist for each phase, but their results should always be interpreted cautiously according to the overall behavioral sequence (Table 2).

		Olfactory sex discrimination			olfactory sex preference		USVs (to ♀)	urine marking (to ♀)	male sexual behavior						opposite sex mounting	female sexual behavior (lordosis)
		♂ vs ♀	♂ vs cast ♂	♀ vs ovx ♀	nonvolatiles	volatiles			latency to mount		mounting		ejaculation			
VNOx	♂	✓ 1, 2		✓ 1	✗ 1, 2		↘ 7, 8, 9	↘ 13	✓ 1	↘ 14	✓ 1	↘ 9, 14	✓ 1	↘ 14	✗ 1	
	♀	✓ 20	✓ 21		✗ 20, 22	✓ 20, 22									✗ 20	↘ 22
AOBx	♂	✓ 3		✓ 3			✗ 7		✓ 3		✓ 3		✓ 3			
	♀														✗ 20	
Trpc2$^{-/-}$	♂	✓ 4, 5				✗ 4, 5	✓ 10, 11		✓ 15		✓ 10, 15				✓ 10, 11, 15	↘ 24
	♀														✓ 11, 23	
cGao$^{-/-}$	♂		✓ 6						✓ 16		✓ 16				✗ 6	
	♀					✓ 16									✗ 16	✗ 16
ΔV1rabΔ$^{-/-}$	♂						✓ 12				↘ 12		↘ 12		✗ 12	
Gai2$^{-/-}$	♂										✓ 18				✗ 18	
SK3$^{-/-}$	♂								↘ 17		↘ 17				✗ 17	
GIRK1$^{-/-}$	♂								↘ 17		↘ 17				✗ 17	
β2m$^{-/-}$	♂														✗ 19	
H2Mv$^{-/-}$	♂															↘ 25

Table 2: Surgical VNO removal and genetic mutation effects on sexual behaviors. ✓ : no effect; ✗ : absence; ↘ : decrease. Numbers refer to research articles demonstrating the effect. [1] Pankevich, 2004; [2] Pankevich et al., 2006; [3] Jakupovic et al., 2008; [4] Beny and Kimchi, 2016; [5] Beny-Shefer et al., 2017; [6] Chamero et al., 2011; [7] Bean, 1982; [8] Wysocki et al., 1982; [9] Wysocki and Lepri, 1991; [10] Stowers et al., 2002; [11] Kimchi et al., 2007; [12] Del Punta et al., 2002; [13] Maruniak et al., 1986; [14] Clancy and Nobles, 1984; [15] Leypold et al., 2002; [16] Oboti et al., 2014; [17] Kim et al., 2012; [18] Norlin et al., 2003; [19] Loconto et al., 2003; [20] Martel and Baum, 2009; [21] Lloyd-Thomas and Keverne, 1982; [22] Keller et al., 2006; [23] Chalfin et al., 2014; [24] Fraser and Shah, 2014; [25] Leinders-Zufall et al., 2014.

2.1.1 Male sexual behaviors

Male mice have a high copulatory potential. They mate with every receptive female they encounter to disseminate their genetic background as much as possible. While exploring their territory, they have to detect the presence of a female and attract her by showing their reproductive fitness (Figure 15). Detection of a potential mate occurs mainly by analyzing urines and feces deposited by congeners. Therefore, mice need to discriminate the sex of the emitter. Intriguingly, nor VNO surgical ablation (VNOx model) neither AOB removal affects sex discrimination from urine in male mice (Jakupovic et al., 2008; Pankevich, 2004; Pankevich et al., 2006). Thus, the MOS is sufficient to promote sex discrimination. Rodents prefer to seek out and investigate odors from the opposite sex. AOS versus MOS implication of this phenomenon is nonetheless unclear. When not given access to the odorant source in a two-choices test (e.g., a urine filter paper), meaning that volatile components only are available, animals prefer opposite-sex cues, suggesting that the MOS can sustain alone sexual preference (Baum and Kelliher, 2009). When access to the odor source is granted, VNOx males fail to show a preference and investigate male and female odor equally (Pankevich, 2004; Pankevich et al., 2006). Similarly, a study showed that Trpc2$^{-/-}$ males olfactory preference is affected (Bayless et al., 2019). Sustaining the role of the VNO in sex discrimination and preference, a map of activated VSNs by male or female urines revealed the existence of VSNs tuned for each sex cue (Ben-Shaul et al., 2010; He et al., 2008). Thus, it emerges that the MOS and AOS may have complementary roles in inducing an olfactory sex preference: the MOS drives the initial attraction and discrimination; then, the AOS maintains the interest for opposite-sex cues (Baum and Kelliher, 2009).

Once a male has detected a female, he has to attract her, using courtship behaviors (Figure 15). First, males scatter small urine spots to show their presence (Reynolds, 1971). If the detected female passes by, she will follow the odor and find the male. Another fitness of urine marking is to present genetic and social status to the female. Indeed, urine contains molecules carrying individual information about its sender (Ferrero and Liberles, 2010; Hurst and Beynon, 2004). Early studies showed that VNOx males marked less than sham-operated ones in response to female urine stimulation (Labov and Wysocki, 1989; Maruniak et al., 1986). Thus, VNO-dependent stimuli may drive motivation to engage in courtship behaviors. Besides marking, males also emit ultrasonic vocalizations (USVs) to attract a female. Those can be triggered by female urine and are not emitted towards males. Like urine scent-marks, USVs are characteristic of an individual and serve for females' mate choice (Egnor and Seagraves, 2016). Early work also showed that VNO ablation reduces USVs emissions (Bean, 1982; Wysocki and Lepri, 1991). However, Trpc2$^{-/-}$ males maintain strong vocalizations (Kimchi et al., 2007; Stowers et al., 2002), questioning the validity of previous results. Partial ablation of the MOS function revealed that the MOS and AOS both participate in inducing USVs (Matsuo et al., 2015). It is possible that in the absence of TRPC2 signaling through development, the MOS provides sufficient input to generate USVs in Trpc2$^{-/-}$ mice.

Male sexual consummatory behavior starts when the male mounts a female. There follows a series of mounts with intromissions and vigorous pelvic thrusts, punctuated by anogenital grooming sessions to maintain the erection, finally reaching ejaculation (Figure 15). Early studies reported an effect of surgical VNO ablation on the motivation to start sexual intercourse (increased latency to mount) and on the sexual performance (reduced number of mount and increased latency to ejaculate) (Clancy and Nobles, 1984; Wysocki and Lepri, 1991). However, more recent investigations showed no effect of AOS impairment (Jakupovic et al., 2008; Pankevich, 2004). Such discrepancy could be explained by the experimental protocols used in each experiment. Older studies investigated the behavior over a limited period, too short to see every phase of the intercourse, whereas the most recent ones analyzed males' behavior until they reach ejaculation. Genetic modifications of VNO function also gave contradictory results. On the one hand, Trpc2$^{-/-}$, cG$\alpha_o^{-/-}$, and G$\alpha_{i2}^{-/-}$ males present similar behavior as their control littermates (Kimchi et al., 2007; Leypold et al., 2002; Norlin et al., 2003; Oboti et al., 2014; Stowers et al., 2002). On the other hand, deletion of a *V1R* genes cluster reduces the proportion of males mounting (Del Punta et al., 2002). This major discrepancy on V1Rs function may result from the G$\alpha_{i2}^{-/-}$ model of Norlin and colleagues, which induces a whole-body deletion of Gα_{i2}, and consequently, dysfunction of non-sensory cells such as brain neurons (Hamada et al., 2017; Rudolph et al., 1995). None of these studies analyzed the behavior over its entire sequence, from the first mount to ejaculation, which does not allow for any clear conclusions. Del Punta and colleagues reported that mutant males engaging in sexual intercourse displayed an equal level of sexual activity in terms of latencies and number of mounts. This statement suggests that the VNO may drive motivation to initiate sexual behavior, as it is suggested for courtship behaviors. Altogether, current knowledge does not point to a major role of the VNO in male sexual consummatory behavior. Nonetheless, better investigation of V1Rs/Gα_{i2} signaling is needed since available models give conflicting evidences (Norlin et al., 2003; Del Punta et al., 2002).

Although not controlling sexual behavior under basal conditions, VNO signaling can influence it. ESP22, a juvenile lachrymal peptide detected by V2Rp4, completely inhibits sexual behaviors of adults (Ferrero et al., 2013; Osakada et al., 2018). On the other side, exposure to sulfated estrogens, detected by V1Rj2 and V1Rj3, increases the mounting behavior of sexually naïve males (Haga-Yamanaka et al., 2014). Sexual behavior depends on prenatally organized brain pathways located at brain sites of sensory inputs convergence (Simerly, 2002). Thus, one might suppose that removing one of these sensory inputs, here the vomeronasal ones, is insufficient to abolish such an anchored behavior. Given the VNO place in pheromones transduction, it must participate in sexual behavior regulation. Results suggest it might be by motivating males to attract females actively and then maintaining motivation to engage in sexual intercourse. Laboratory experimental conditions may hide the natural role of VNO, and one could think that wild animals lacking a functional VNO would not reproduce efficiently.

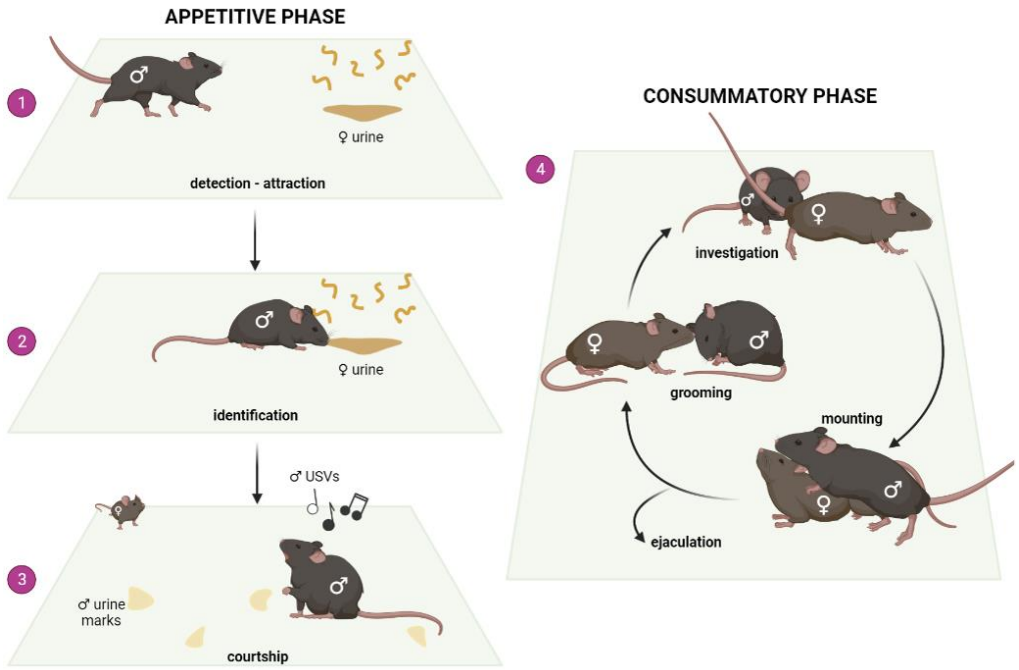

Figure 15: Male sexual behavior sequence. The male sexual behavior is composed of an appetitive phase (left) and a consummatory phase (right). ① The male detects the presence of a female and is attracted by her odor. ② Close olfactory investigation allows the identification of the odor sender characteristics. ③ The male starts a series of courtship behaviors to attract the female, such as scent marking and USVs. ④ The consummatory phase starts with the close olfactory investigation of the female; then follows a series of mounts with intromissions and vigorous pelvic thrusts facilitated by the female lordosis posture, punctuated by anogenital grooming sessions to maintain the erection, finally reaching ejaculation. This scheme is created in BioRender.com.

2.1.2 Female sexual behaviors

Female mouse sexual appetitive behaviors are different from those of males. While males can multiply partners, females have to choose the best one. First, female mating occurs during her ovulatory period, restricted to a dozen hours every four to five days. Second, females carry and raise pups until weaning, once again restricting mating possibilities. Consequently, females must select their partners to ensure a robust genetic background for their progeny (Trivers, 1972).

Females' ability to discriminate and show a preference for volatile olfactory cues from gonadally intact males is not impacted by VNO surgical or genetic (restricted to basal VSNs) ablation (Keller et al., 2006; Lloyd-Thomas and Keverne, 1982; Oboti et al., 2014). However, preference for gonadally intact male over castrated male or female non-volatile urinary odors is lost in VNOx females (Keller et al., 2006; Martínez-Ricós et al., 2008). Thus, like in males, the MOS and AOS may have complementary roles in inducing an olfactory sex preference (Baum and Kelliher, 2009). Indeed, a series of chemical attractants have been identified in male urine, some detected by both VSNs and OSNs (Ishii and Touhara, 2019; Novotny, 2003). Once detected, the evaluation of male urine allows the female to evaluate the fitness of the emitter. In a simplistic view, females seek a partner who is genetically rich and distant. Three families of peptides detected by the VNO could serve as such cues: the MHC-peptides, the MUPs, and the ESPs. Expression of each of these peptides is specific to the

genetics of the animals (Boehm and Zufall, 2006; Kimoto et al., 2007; Logan et al., 2008), and all are detected by basal VSNs (Chamero et al., 2011; Hattori et al., 2017; Leinders-Zufall et al., 2004).

MUPs are particularly interesting. First, their combination in urine carries individual information (Cheetham et al., 2007; Hurst et al., 2001; Kaur et al., 2014). Females assess the genetic heterozygosity of a potential partner, a marker of genetic diversity providing a benefit, through the sensing of its MUPs (Thom et al., 2008). Second, some isolated MUPs like the Darcin (MUP20) can induce female attraction (Roberts et al., 2010). MUPs are also carrier proteins, thus sequestrating attractant volatiles in urine to extend their longevity (Hurst et al., 1998; Kwak et al., 2012; Sharrow et al., 2009). Signaling through MUPs is, therefore, a powerful tool acting as an attractant and informant. Outside the female ovulatory period, such a message is irrelevant. An elegant study showed a mechanism to silence VSNs detecting MUPs outside the ovulatory period and therefore inhibit MUPs attractivity (Dey et al., 2015). High progesterone levels outside the ovulatory period inhibit PLCβ2 by phosphorylation, thus preventing VSNs activation by MUPs. This study shed new light on the plasticity potential of VNO signaling. Recently, Eckstein and colleagues highlighted the existence of another TRP channel in the VNO, TRPM4 (Eckstein et al., 2020). Interestingly, TRPM4 expression follows the female estrus cycle and is higher during the ovulatory period. No regulation of behavior or VSNs function has been associated with this channel. However, it would be an excellent candidate to reinforce relevant signals or silence irrelevant ones during the critical period of sexual receptivity.

In addition to being attracted to male scents, females express a specific behavior in response to male mounts during their ovulatory period, the lordosis behavior. The appellation lordosis comes from the posture adopted by females: they arch their backs, spread their legs, and lift their tails to facilitate male intromission (Figure 15). Lordosis response is triggered by male mounting but cannot be induced outside the ovulatory period (Bonthuis et al., 2010). The hormonal environment is critical for promoting lordosis behavior, but olfactory signals are just as important. Surgical or genetic ablation of the VNO diminished the expression of lordosis responses, even under controlled hormonal levels (Fraser and Shah, 2014; Hellier et al., 2018; Keller et al., 2006). Similarly, olfactory-restricted genetic invalidation of $G\alpha_o$ decreases female sexual receptivity (Oboti et al., 2014). Further, the lachrymal peptide ESP1 detected by V2Rp5 is able to promote lordosis response in sexually naïve females (Haga et al., 2010). In laboratory conditions, female mice predictably demonstrate a gradual enhancement of receptivity (Bonthuis et al., 2011; Thompson and Edwards, 1971). Interestingly, acute optogenetic inhibition of AOB mitral cells decreases lordosis responses of sexually experienced females to basal levels usually seen in sexually naïve females (McCarthy et al., 2017a), reinforcing the importance of vomeronasal signaling in sexual receptivity.

2.1.3 The curious case of sex preference in Trpc2$^{-/-}$ mice

The knock-out mouse model for TRPC2 (Trpc2$^{-/-}$) has been widely used to study the vomeronasal function, the regulation of socio-sexual behaviors, allowing great discoveries (Boillat et al., 2015; Ferrero et al., 2013; Haga et al., 2010; Hasen and Gammie, 2009; Kimchi et al., 2007; Leypold et al., 2002; Papes et al., 2010; Stowers et al., 2002; Wu et al., 2014). Seminal papers reported indiscriminate mounting behavior in Trpc2$^{-/-}$ males (Leypold et al., 2002; Stowers et al., 2002), and a later study showed a similar behavior in Trpc2$^{-/-}$ females (Kimchi et al., 2007). Additionally, both sexes' Trpc2$^{-/-}$ mice produce USVs towards male and female congeners (Kimchi et al., 2007; Stowers et al., 2002). This discovery led the authors to hypothesize that the VNO is essential for sex discrimination and ensures sex-specific behaviors. Quite exciting but questionable.

The first and foremost objection comes from studies on VNOx animals. The only study in which same-sex mounting behavior has been reported in VNOx mice is the same one showing it in Trpc2$^{-/-}$ mice (Kimchi et al., 2007). Moreover, transgenic mouse lines with a partial deficit in VNO signaling do not show indiscriminate mounting behavior (Table 2) (Chamero et al., 2011; Kim et al., 2012; Norlin et al., 2003; Oboti et al., 2014; Del Punta et al., 2002). Second, besides VSNs, TRPC2 expression is reported in OSNs (see section 1.1.3.3) and the developing nervous system (Boisseau et al., 2009; Elg et al., 2007). The Trpc2$^{-/-}$ model consists of a germline genetic deletion; consequently, MOE function is impacted, and brain development may be altered. Third, as mentioned in the description of vomeronasal signaling, TRPC2-independent mechanisms exist in VSNs (see section 1.4.2.3). Consequently, vomeronasal sensing may not be abolished entirely in Trpc2$^{-/-}$ mice. Lastly, Kimchi and colleagues stated that since Trpc2$^{-/-}$ females exhibit mounting behavior, functional neuronal circuits underlying this behavior exist in the female brain and are naturally repressed by vomeronasal inputs (Kimchi et al., 2007). This assumption contradicts the admitted role of prenatal hormonal environment organizing male sexual behavior brain circuits (Simerly, 2002). Further, studies show that neonatal or adult treatment with sex steroids can increase mounting behavior in female mice (Manning and McGill, 1974; Wu et al., 2009). This is particularly interesting since Trpc2$^{-/-}$ mice present high testosterone levels (Kimchi et al., 2007; Stowers et al., 2002) and one study manage to reproduce Trpc2$^{-/-}$ females phenotype by combining ovariectomy, testosterone supplementation, and VNO surgical ablation (Martel and Baum, 2009). For all that reasons, Trpc2$^{-/-}$ mice indiscriminate mounting behavior should not be seen as a strict reflection of the lack of VNO function.

Several labs observed the same behavior (Fraser and Shah, 2014; Haga et al., 2010; Kim et al., 2012; Leypold et al., 2002; Stowers et al., 2002). Further, Chalflin and coworkers backcrossed their Trpc2$^{-/-}$ laboratory mice into a wild mice strain (Chalfin et al., 2014). Wild and laboratory controls show different basal innate behaviors, but TRPC2 mutation induces the same effect on mounting behavior in both strains. Still remains the question of its explanation. Leypold and colleagues already emitted the possibility of displacement behavior (Leypold et al., 2002). Displacement reaction corresponds to the display of a particular behavior out of its context due to conflicting drives. Here,

because of the genetic origin of Trpc2$^{-/-}$ behavior, Yu proposed to speak instead of neomorphic behavior (Yu, 2015). One way to answer this issue would be to create alternative models of complete or partial vomeronasal dysfunction. An inducible Cre deletion of TRPC2 in adulthood would avoid potential developmental effects. Alternatively, an olfactory-restricted deletion of $G\alpha_{i2}$ would allow complementary information to match those of the c$G\alpha_{o}^{-/-}$ model. Lastly, the combined deletion of $G\alpha_{i2}$ and $G\alpha_{o}$ genes in olfactory neurons may represent a better model of VNO dysfunction.

2.2 Aggressive behaviors

Aggression can be, in fact, a defense mechanism. Defending a territory to keep access to food, mating partners, and protect progeny is crucial to individuals' survival. Aggressive behavior starts with an appetitive phase during which the resident investigates and intimidates the intruder, followed by a consummatory phase comprising a sequence of attacks (Figure 16). Aggression is costly; it demands a high energic investment and puts the aggressor at risk of being injured. On the other side, the decision to attack should be promptly taken when facing a potential threat. Thus, accurate olfactory detection and identification of potentially dangerous congeners are crucial.

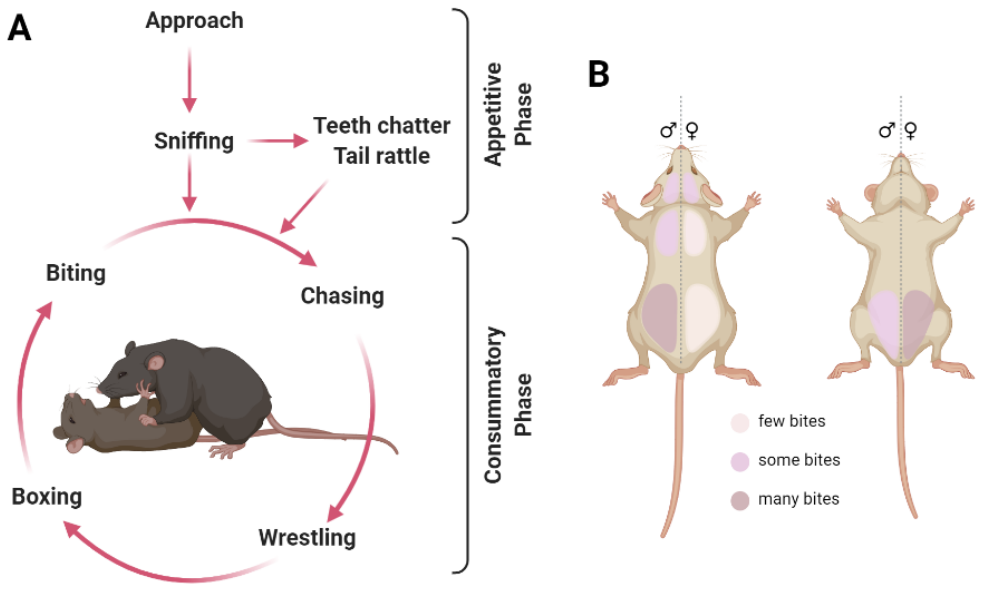

Figure 16: Aggressive behavior sequence. A) Aggression is composed of an appetitive phase (up) and a consummatory phase (down). During the appetitive phase, the resident approaches the intruder, investigates it to determine its nature, and intimidates it. Then follows a series of attacks composed of sequential chasing, wrestling, boxing, and biting events. B) Difference between males and females attack sites. Males provide many bites on the intruder's back, whereas females attack mostly the abdomen and the anogenital region. Adapted from Hashikawa et al., 2018. This scheme is created in BioRender.com.

2.2.1 Territorial aggression

In natural conditions, male mice reign over a territory and one or several females. In laboratory conditions, isolated males consider their cage as their territory, and intrusion triggers territorial responses. The most studied is offensive aggression. In a resident/intruder behavioral paradigm, the resident mouse (an isolated male) defends his territory by attacking intruders. Neither VNOx nor Trpc2$^{-/-}$ males exhibit aggression towards intruders, pointing to a major role of the VNO in the control of territorial aggression (Clancy and Nobles, 1984; Leypold et al., 2002; Maruniak et al., 1986; Stowers et al., 2002; Wysocki and Lepri, 1991). A later study showed that $G\alpha_o$-positive basal VSNs are essential to display aggressive behavior (Chamero et al., 2011).

Chemicals promoting aggression are secreted in the urine, and their production is androgen-dependent (Mugford and Nowell, 1970). Indeed, a castrated male intruder is not attacked, but swabbing its back with urine from a gonadally intact male restores the aggressive response of the resident. In urine, several low or high molecular weight (LMW, HMW) compounds can elicit attacks of similar intensity (Chamero et al., 2007, 2011; Kaur et al., 2014). MUPs are responsible for the HMW-fraction aggression activity. Swabbing the back of a castrated male with synthetic MUPs triggers an aggressive response, suggesting that MUPs act as pheromones by themselves (Chamero et al., 2007). Interestingly, c$G\alpha_o^{-/-}$ males fail to attack a castrated male intruder swabbed with LMW urine fraction (Chamero et al., 2011). Detection of several small volatiles molecules has been linked to apical VSNs, and $G\alpha_{i2}^{-/-}$ males show reduced aggressive behaviors (Leinders-Zufall et al., 2000; Norlin et al., 2003). Altogether, data suggest that both apical and basal VSNs may work in concert to promote aggression. $G\alpha_o$ seems a more critical factor to initiate the behavior but $G\alpha_{i2}$ function remains elusive.

Besides attacking, territorial males countermark urine spots of an intruder. Olfactory cues are sufficient to elicit urine countermarking (Desjardins et al., 1973; Rich and Hurst, 1999), and VNOx and Trpc2$^{-/-}$ males fail to countermark when exposed to male urine (Kaur et al., 2014; Maruniak et al., 1986; Wysocki and Lepri, 1991). Interestingly, isolated Trpc2$^{-/-}$ males countermark in the presence of an intruder (Leypold et al., 2002), indicating that non-olfactory cues are also used to induce countermarking. Group-housed males also use countermarking to assert their status within the group. Dominant males countermark whereas subordinates do not (Desjardins et al., 1973). Interestingly, when group-housed, each Trpc2$^{-/-}$ male continues to countermark, suggesting they fail to establish territorial dominance relationships since they do not display aggressive interactions (Leypold et al., 2002). However, no strict assessment of hierarchical dynamic within Trpc2$^{-/-}$ male groups exists. c$G\alpha_{i2}^{-/-}$ males are able to form stable groups (Pallé et al., 2020), suggesting that if disorganization of group hierarchy exists in Trpc2$^{-/-}$ males, it should result from the loss of basal VSNs function. Unfortunately, c$G\alpha_o^{-/-}$ group-housed males hierarchy has not been evaluated.

2.2.2 Maternal aggression

Laboratory female mice rarely exhibit aggressive behaviors, except when lactating. During the first week after parturition, females ardently defend their progeny. Compared to male territorial aggression, female maternal aggression is way more dangerous for the intruder since lactating females directly attack vulnerable regions of the intruder, like their abdomen or anogenital region (Figure 16) (Parmigiani et al., 1988; Unger et al., 2015). The display of maternal aggression is under a complex control of internal hormonal and sensory factors, but olfactory cues emitted by the intruder are crucial to trigger the behavioral response (Martín-Sánchez et al., 2015).

Again, vomeronasal olfactory inputs play an essential role in perceiving aggression-inducing cues. VNOx and Trpc2$^{-/-}$ lactating females do not attack an intruder (Bean and Wysocki, 1989; Hasen and Gammie, 2009; Kimchi et al., 2007; Leypold et al., 2002). The differential implication of basal and apical VSNs in this process is not clear. Chamero and colleagues showed that basal VSNs are essential since virtually none of cG$\alpha_o^{-/-}$ females attack an intruder (Chamero et al., 2011). Conversely, germline ablation of Gα_{i2} or deletion of one V1R gene cluster decreases maternal aggression (Norlin et al., 2003; Del Punta et al., 2002). Thus, both systems may cooperate to promote maternal aggression, and, like for territorial aggression, Gα_o-expressing VSNs seem more critical to initiate the behavior.

Less is known about chemicals inducing aggression in lactating females. Studies suggest that mothers are more likely to attack an intact male intruder than a castrated male or a female (Parmigiani et al., 1988; Rosenson and Asheroff, 1975). Lactating females attack a castrated male intruder swabbed with LMW or HMW urine fractions, suggesting once again that both fractions contain chemicals that promote aggression (Chamero et al., 2011). Interestingly, lack of aggressive response in cG$\alpha_o^{-/-}$ females is observed whatever the castrated intruder is swabbed with, sustaining a more important role of Gα_o to induce an aggressive response (Chamero et al., 2011). Up to date, only one pheromone has been tested for its potential to promote aggression in lactating females, Darcin (Martín-Sánchez et al., 2015), which elicits equivalent levels of aggression than intact male urine.

2.2.3 Infanticide

Infanticide behavior is a well-known but little-studied behavior mainly expressed by virgin male mice. Its evolutionary value is unclear, but some suggest that males benefit from killing unrelated young because they suppress parental investment in offspring they have not sired and restore mothers capacity to be impregnated (Labov et al., 1985; Vom Saal and Howard, 1982). The role of the VNO in infanticide was first demonstrated in rats (Mennella and Moltz, 1988). Later, it was also shown that VNOx and Trpc2$^{-/-}$ male mice do not kill alien pups (Nakahara et al., 2016; Tachikawa et al., 2013; Wu et al., 2014). Pup exposure activates anterior and posterior parts of the AOB, suggesting that basal and apical VSNs layers participate in pup-cues detection, although the activation was more important

in the anterior AOB (Tachikawa et al., 2013). The implication of each VSNs layer is unknown since infanticide behavior has not been tested in $cG\alpha_o^{-/-}$ and $G\alpha_{i2}^{-/-}$ mouse models.

Two studies investigated deeper the acute detection of pup olfactory cues. First, Nakahara and colleagues showed that the ectopic olfactory receptor Olfr692, one of the few ORs expressed in the VNO, specifically detects pup cues (Nakahara et al., 2016). They showed that extracting pup odor by incubation in buffer still induces Olfr692-positive VSNs activation. Interestingly, they found that pup exposure activates Olfr692 in males but not in females, pointing to a role of this receptor in infanticide. Unfortunately, they did not provide functional proof of this involvement. Second, Isogai and coworkers highlighted pup-activated VRs by an *in situ* hybridization-based screening (Isogai et al., 2018). They identified 5 VRs potentially activated by pup-cues: V1Rc1, V1Rc30, V2R88, V2R65, and V2R122/123. However, none of these receptors was exclusively activated by pup odors. They focused their attention on V2R65 and V2R88, to which they found a ligand, the submandibular gland protein C and hemoglobin, respectively. Genetic ablation of one of these 2 VRS slightly impacts infanticide. However, combined mutation significantly reduces infanticide. While writing this work, an ingenious study came out in which the pup volatolome was extracted and analyzed (Lacalle-Bergeron et al., 2021). Their data highlight 11 components whose concentration decreases after one week of age, thus potentially being pup-specific pheromones. A particular one, durene, is already known to be detected by the VNO and could be involved in triggering infanticide (Sam et al., 2001).

2.3 Parental behaviors

Parenting increases the likelihood of offspring survival. In rodents, several parental behavior patterns are described, including lactating, retrieving, crouching, grooming, nest building, and pup-defense. In mice, both mothers and fathers participate in this care, except lactation provided by females only. Multiple sensory modalities trigger parental response, and olfaction is one the most important in mice.

In females, we have seen in the previous section that pup defense (maternal aggression) relies on the vomeronasal organ; however, other parental behaviors instead depend mainly on the MOS signaling. Early studies showed no effect of VNO surgical ablation on offspring survival and mothers' interaction time with their pups (Bean and Wysocki, 1989; Lepri et al., 1985). In contrast, MOE chemical lesion impacts pup survival and reduces mothers' care (Seegal and Denenberg, 1974; Vandenbergh, 1973), and genetic ablation of OSNs signaling pathway reduces parental behaviors (Belluscio et al., 1998; Fraser and Shah, 2014; Wang and Storm, 2011). Yet, VNO implication in parental behaviors should not be overlooked. Pup exposure activates VSNs in virgin females and mothers (Isogai et al., 2018; Navarro-Moreno et al., 2020). Longitudinal evaluation of maternal behavior over 14 days revealed a progressive decreased investment of $Trpc2^{-/-}$ females toward their pups (Kimchi et al., 2007). This deficit may have been missed in VNOx females since testing only

occurred during the early postpartum period. One could hypothesize that the particular hormonal environment accompanying parturition hides the potential involvement of the VNO in parenting. Virgin females are naturally maternal and take care of an alien pup, but repeated pup-exposures increase the quality of care (e.g., shorter latency to retrieve) (Stolzenberg and Rissman, 2011). Further, this phenomenon is independent of female hormonal status (Stolzenberg and Rissman, 2011). Thus, pup-cues detection by the VNO may be involved in stimulating parental behavior outside the peripartum period, a phenomenon necessary for the maintenance of parenting.

Virgin male mice are infanticidal, but this behavior progressively disappears when cohabitating with pregnant females and fathers are parental (Vom Saal, 1985; Tachikawa et al., 2013). VNO activation by pup cues also diminishes over the time spent with a female and ceases in fathers (Nakahara et al., 2020; Tachikawa et al., 2013). One possibility is that the VNO undergoes a remodeling after mating, silencing its response to pup olfactory cues to inhibit infanticide behavior and promote parenting. Sustaining this hypothesis, $Trpc2^{-/-}$ virgin males are parental when exposed to an alien neonate (Wu et al., 2014). Unfortunately, no study investigated the vomeronasal control of mouse parental behaviors in fathers. Fathers become infanticide again after weaning of their pups (Vom Saal, 1985). Thus, parental behavior expression in male mice seems tightly controlled, maybe by exposure to a pregnant female. The exact process by which VNO sensitivity to pup cues is modified, as well as the extent of the modification, are still unknown. Mating induces oxytocin secretion (Waldherr and Neumann, 2007), and treatment with oxytocin inhibits VNO activation by pup cues (Nakahara et al., 2020). Thus, it has been proposed that oxytocin could be the messenger of a forthcoming progeny. By acting on VNO sensitivity, since VSNs express the oxytocin receptor (Nakahara et al., 2020), it can release parental behavior expression. However, a possibility exists that parental and infanticide behaviors are more than two faces of the same coin. Each may need its mechanism of activation-inhibition. Accordingly, a study showed that inhibition of histone deacetylation (unleashing the chromatin and promoting genetic expression) increased the expression of paternal behaviors in non-aggressive males without modifying the expression of infanticide in aggressive males (Mayer et al., 2019). However, nothing is known about potential vomeronasal cues stimulating paternal behaviors.

2.4 Avoidance behaviors

A major cost of social behaviors is the increased risk of exposure to dangers. Rodents are often prey, and rambling through their territory to find food or mate puts mice at risk of encountering predators. Another daily challenge is exposure to parasites and infection during social interactions with congeners. Social species have developed various behavioral mechanisms and responses to minimize their potential exposure to threats while maintaining their social activities. The olfactory system is also crucial in these processes by coding the valence of surrounding odors and thus tipping the balance towards attraction or aversion (Li and Liberles, 2015).

2.4.1 Predator avoidance

Preys and predators share their environment, and both liberate semiochemicals into it to communicate. During evolution, predator cues have been incorporated into preys' memory and naturally induce avoidance and defensive behaviors. These interspecific chemicals are referred to as kairomones. Several taxa highly predate mice, like carnivorous mammals (e.g., mustelids, felids, or canids), raptors (e.g., falcons and owl), reptiles, or spiders. Several behavioral patterns are associated with predator avoidance, such as risk assessment, freezing, foraging, or active escape, and all can be induced by exposition to the predator scent alone (Kavaliers and Choleris, 2001). Kairomones detection is not restricted to a single olfactory subsystem, but some appear dedicated to convey information limited to one class of predators (Pérez-Gómez et al., 2015; Takahashi, 2014).

Due to its involvement in pheromones sensing, the vomeronasal system was early thought to mediate kairomones detection. Indeed, VNOx mice do not avoid cat odor (Samuelsen and Meredith, 2009). Later, the VNO was also associated with rat and snake avoidance (Papes et al., 2010). Isogai and coworkers added birds of prey, mustelids, and other carnivorous to the list of predators detected by the VNO (Isogai et al., 2011). Interestingly, this study shows that VRs activated by one type of predator are clusterized, some predators even activating only basal or apical VSNs. In line with these results, ablation of $G\alpha_o$ basal VSNs function abolishes avoidance for cat fur odors (Pérez-Gómez et al., 2015).

Species-specific kairomones have been identified. Researchers looked toward MUPs, orthologues in predators, based on the pheromonal activity of this class of molecule. As a result, a rat MUP, MUP-Rn13, and a MUP-like lipocalin from cats, Feld4, were proven to act as kairomones and to drive avoidance through the VNO (Papes et al., 2010; Pérez-Gómez et al., 2015). Carnivorous mammals' urines are enriched in biogenic amines as a result of meat consumption. One, the 2-phenylethylamine (PEA), precisely activates TAAR4 and induces avoidance (Dewan et al., 2013; Ferrero et al., 2011). TAARs are mainly expressed in the MOE, some are found in the GG, but none are described in the VNO (**see section 1**). Nonetheless, carnivorous mammal urine activates the VNO, suggesting that several urine compounds may carry avoidance cues (Ben-Shaul et al., 2010; Isogai et al., 2011). Two volatile compounds, 2-propylthietane (2-PT) and 2,5-dihydro-2,4,5-trimethylthiazole (TMT), respectively found in stoat anal gland and fox feces, activate dedicated neurons in the GG and induce avoidance (Brechbühl et al., 2013; Pérez-Gómez et al., 2015). 2-PT has no other known detector, but TMT is also detected by the MOE but not the VNO (Kobayakawa et al., 2007; Papes et al., 2010; Saito et al., 2017).

After detecting a potential threat, rodents can warn their congener by secreting alarm pheromones (Rottman and Snowdown, 1972). Interestingly, some alarm pheromones, such as the 2-sec-butyl-4,5-dihydrothiazole (SBT), have structural similarities with predator kairomones and are detected by the GG and MOE (Brechbühl et al., 2008, 2013; Matsuo et al., 2015). Thus, generic

pathways for signaling danger may exist, although the routes for specific olfactory detection are not fully identified.

2.4.2 Pathogen avoidance

Wild animals are typically exposed to various pathogens, including bacteria, viruses, and helminths. To counteract this permanent threat, animals have evolved several defense mechanisms of avoidance, resistance, and tolerance to pathogens (Rivas et al., 2014). Mice are macrosmatic, they detect sickness in their congeners by smell and actively avoid them to prevent contagion (Kavaliers et al., 2005). Parasitized conspecifics recognition also intervenes in mate selection, as females prefer to copulate with healthy males (Kavaliers, 1995).

The VNO has been proposed to mediate sick conspecific recognition. Indeed, VNOx and Trpc2$^{-/-}$ mice do not avoid an LPS-treated one (Boillat et al., 2015). Bacterial lipopolysaccharides (LPS) injection is a standard protocol to induce a general inflammatory state, thus mimicking pathogen infection. VNOx males also lose their natural preference to mate with a healthy females when given the choice with an LPS-treated one (Kwon et al., 2021). Urine from LPS-treated animals is sufficient to induce avoidance (Boillat et al., 2015; Kwon et al., 2021), but urine modification by LPS treatment is unknown. Some LPS are directly excreted in urines (Kleine et al., 1985). LPS bind the Toll-like receptor 4 (TLR-4), whose mRNA has been detected after VSNs sequencing (Ibarra-Soria et al., 2014). Thus, direct sensing at the level of VSNs could occur. Two studies highlighted two distinct compounds of LPS-treated urine, the SBT and dimethyl sulfone (Millet et al., 2018, 2021). Surprisingly, SBT is present in mouse urine and has been proposed as an alarm pheromone (Brechbühl et al., 2013), and dimethyl sulfone is found in urines of different predators (Apps et al., 2012; Burger et al., 2006). This suggests that sickness could be detected through alarm pheromones or analogs to predator cues, implying that sick-conspecific and predator avoidance may result from similar processes.

The VNO express FPRs, natural receptors for bacterial peptides (Bufe and Zufall, 2016). Vomeronasal FPRs, except FPR3, do not respond to classical immune FPRs ligands, suggesting a neofunctionalization of these receptors (Bufe et al., 2012). Bufe and colleagues showed that FPR3, the only FPR expressed in basal VSNs (see section 1.4.2.4), has a high selectivity for the conserved bacterial virulence-associated proteins MgrB (Bufe et al., 2019). Further, adding MgrB peptide to female urine induces aversion and genetic deletion of FPR3 or $G\alpha_o$ suppresses it, suggesting that FPR3 is involved in pathogen avoidance. Interestingly, deletion of FPR3 does not abolish LPS-treated mouse avoidance. Investigation of apical FPRs implication in detecting LPS-urine or in sick conspecific avoidance would be of particular interest.

Now that the reader is kin with mouse socio-sexual behaviors and how the vomeronasal system controls them, I will describe the general neural pathway sustaining them.

3 Neural control of socio-sexual behaviors

The expression of an adapted behavioral reaction occurs after the neural integration of sensory information with social and internal states, triggering the decision of the motor action (Figure 17). This work focuses on olfactory sensory cues, but other sensory modalities (auditory, visual, and somatosensory) are also compiled. All this information is balanced with the animal's state. Particularly relevant for social behavior is the social experience, which hastens the decision process (e.g., a sexually experienced male starts sexual intercourse quicker). Additionally, the neuroendocrine status of the animal enhances or inhibits the expression of some behavioral responses (e.g., a female mates only during her ovulatory period).

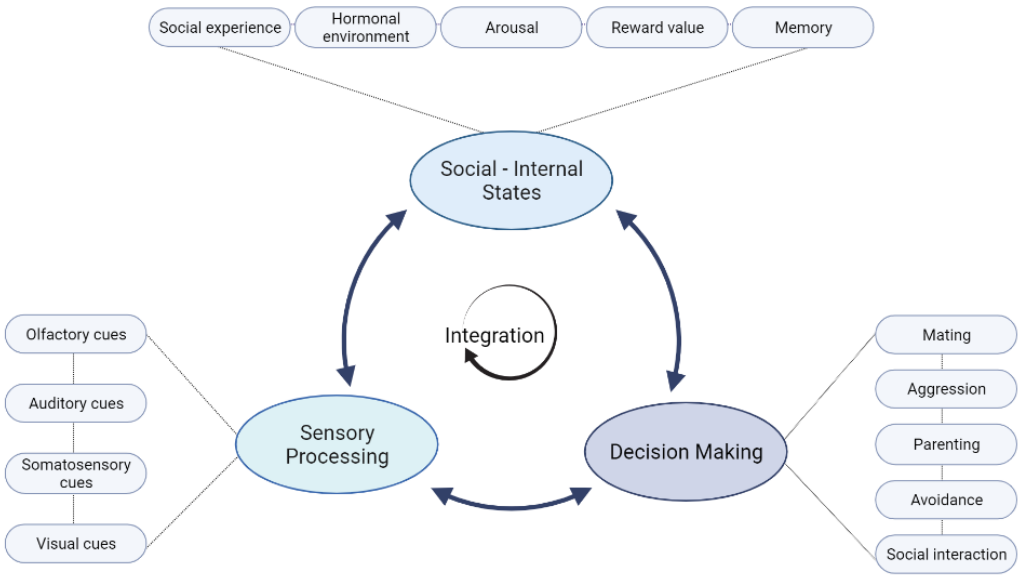

Figure 17: Mechanism of neural sensory processing and integration to socio-behavioral decisions. Adapted from Chen and Hong, 2018. *This scheme is created in BioRender.com.*

The MOB projects to the olfactory cortices, whereas the AOB sends information to the vomeronasal amygdala, which is composed of the posterior part of the bed nucleus of the stria terminalis (BNSTp), the medial amygdala (MeA), and the posteromedial cortical amygdala (CoApm) (Figure 18). The apparent segregation between the olfactory cortices and vomeronasal amygdala suggests differential information processing, but, like MOS and AOS cooperate to detect odorant and trigger behavioral responses, information they respectively carry are integrated together. Within the AOS, apical and basal VSNs projections are initially segregated. Apical VSNs project to the aAOB and then reach the BNSTp, CoApm, and MeA, while basal VSNs send their axons to the pAOB which is only connected with the CoApm and MeA (Gutiérrez-Castellanos et al., 2014; Mohedano-Moriano et al., 2007). These regions are nonetheless connected to each other. It is not known if the segregation of V1Rs/$G\alpha_{i2}$ and V2Rs/$G\alpha_{o}$ inputs is maintained once arriving in the vomeronasal amygdala.

However, information carried by V1Rs/$G\alpha_{i2}$ signaling pathway may undergo specific processing in the BNSTp, before being integrated with V2Rs/$G\alpha_o$ inputs in the MeA. The convergence site of MOS and AOS information is also unclear, but the MeA appears central since the posterolateral cortical amygdala (CoApl, part of the olfactory cortices) projects to the MeA (Canteras et al., 1992).

Socio-sexual behaviors are sexually dimorphic; consequently, sex dimorphisms exist among brain regions controlling them. Decades of rodent lesion and stimulation studies revealed a limited and overlapping set of hypothalamic and limbic brain regions controlling social behaviors (Figure 18). Among them, the MeA, BNST, medial preoptic area (MPOA), and ventromedial hypothalamic nucleus (VMH) are of particular interest. Within these nuclei, distinct cell populations control different aspects of socio-sexual behaviors (Wei et al., 2021). One major challenge to overcome is to assign a precise function to each of these nuclei and neuron populations in the interpretation – integration – decision loop (Figure 17). The vomeronasal inputs processing most probably occurs at the level of the medial amygdala (Raam and Hong, 2021) and integration of social and internal states can happen all along the circuit, from the VSNs (Dey et al., 2015; Oboti et al., 2015) to the brain (Wei et al., 2021). As for decision-making area, numerous studies show that stimulating one of the nuclei or neuron populations of a dedicated behavioral brain pathway, even those very upstream, can be sufficient to trigger the corresponding motor pattern (Raam and Hong, 2021). Here, I will focus on nuclei members of the vomeronasal amygdala and mention downstream areas when necessary.

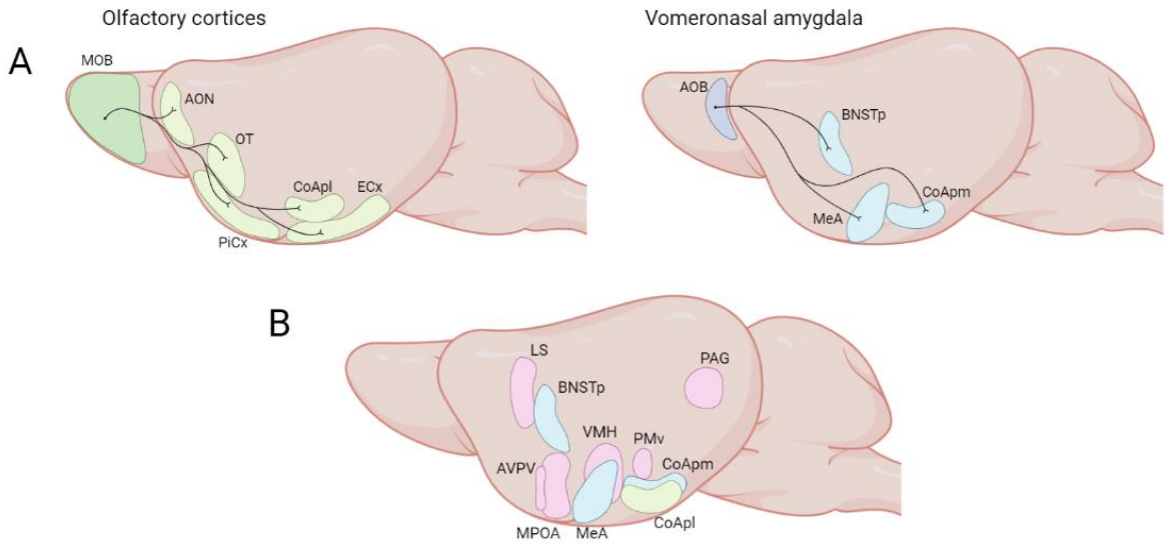

Figure 18: Neural structures involved in olfactory processing and behavioral responses. A) The MOB projects to the olfactory cortices (left), composed of the anterior olfactory nucleus (AON), olfactory tubercle (OT), piriform cortex (PiCx), posterolateral cortical amygdala (CoApl), and entorhinal cortex (ECx). The AOB projects to the vomeronasal amygdala (right), composed of the posterior part of the bed nucleus of the stria terminalis (BNSTp), medial amygdala (MeA), and posteromedial cortical amygdala (CoApm). B) Principal brain nuclei involved in the behavioral responses. Blue nuclei belong to the vomeronasal amygdala and green ones to the olfactory cortices. LS: lateral septum, AVPV: anteroventral periventricular nucleus, MPOA: medial preoptic area, VMH: ventromedial hypothalamic nucleus, PMv: ventral premammillary nucleus, PAG: periaqueductal grey area. This scheme is created in BioRender.com

3.1 Sexual behaviors neural circuitry

3.1.1 Sex coding of the vomeronasal inputs

Before engaging in social interaction, one must first determine the identity of the encountered, especially its sex, as it conditions the type of behavioral response to trigger (e.g., mating versus aggression). To understand how sensory information is integrated, it should be remembered that male and female brains are organized by sex steroids during development and maturation, thus allowing the adult expression of sexually dimorphic behaviors (Bakker, 2018). Briefly, the male brain undergoes masculinization during the perinatal testosterone surge, while the female brain is feminized during the peripubertal period by ovarian estrogens. Sex dimorphisms of brain nucleus size, neuropeptide expression, and connectivity are therefore permanently established. It should be mentioned that male and female VRs repertoires are relatively similar, besides few exception (Van der Linden et al., 2018). For example, female VNO is enriched in V2Rp5, the receptor for the lordosis-stimulating peptide ESP1, and male VNO contains more V1Rj2, the receptor for ovulation-induced urinary sulfated estrogens.

The response pattern of the message arriving at the AOB appear mostly similar in males and females (Ben-Shaul et al., 2010; Luo, 2003). If and how coding occurs at the AOB level is unclear, but AOB-MCL forms synchronous microcircuits, strongly suggesting a role in information processing (Tsitoura et al., 2020). Further, sex dimorphism in AOB function may exist since a recent study reported a male-specific top-down projection from the MeA to the AOB (Inbar et al., 2021). Whether or not this connection modulates the signal is unknown, but one can speculate that it shapes the information, then activating the circuit dedicated to the appropriate behavioral response.

Downstream to the AOB, the MeA largely received glutamatergic input from AOB-MCL (Mohedano-Moriano et al., 2007). The MeA is a heterogeneous structure with a tripartite organization: the anterior MeA (MeAa), posterodorsal MeA (MeApd), and posteroventral MeA (MeApv). MeApd and MeApv are further distinguishable by molecular markers: the MeApv contains mostly glutamatergic neurons, while most MeApd neurons are GABAergic and express the aromatase (Aro, the enzyme converting testosterone into estradiol), androgen and progesterone receptors (AR and PR) (Bian et al., 2008; Juntti et al., 2010; Keshavarzi et al., 2014; Wu et al., 2009; Yang et al., 2013). The MeA is also enriched in oxytocin-expressing neurons (Oxt), which were early shown to be required for social recognition (Choleris et al., 2007; Ferguson et al., 2001). Within the MeA, social stimulation induces neurons activation in a sex-specific manner (Bergan et al., 2014). Males activation-map is biased toward female cues, while females map is biased toward male cues. Further, the establishment of these maps is organized by neonatal sex-steroids and requires activation of MeApd neurons expressing Aro and Oxt in males only (Bergan et al., 2014; Yao et al., 2017). Thus, the MeA is probably an integrating center of sex-associated cues with their behavioral value. Interestingly, single-cell RNA sequencing of the MeApd did not reveal a sex dimorphism in cell populations expressing Aro or Oxt

(Chen et al., 2019). Thus, the differential activation of these neurons in males and females rather derives from differential intracellular physiological properties or wiring differences.

Social and sexual experience shapes the MeA activation map (Li et al., 2017). Sexually naïve males and females show similar patterns of activation, and differences arise after a sexual experience. The BNSTp also shows sex-specific activation after male or female stimulation, especially a higher activity in Aro-expressing neurons during female exposure in males (Bayless et al., 2019). However, contrary to the MeA, BNSTp activation is already sexually dimorphic in sexually naive animals. Bayless and coworkers proposed that the BNSTp neurons may encode the sex of a conspecific, whereas the MeA defines how to react to that sex, a process shaped by experience. Trpc2$^{-/-}$ males present similar activation of Aro-BNSTp neurons after male or female exposure, suggesting that vomeronasal inputs carry supplemental information defining the sex (Bayless et al., 2019). In their absence, equal activation of Aro-BNSTp neurons could result in indiscriminate mounting. The source of these vomeronasal inputs is unknown, but the BNSTp only receives direct information from the aAOB (Mohedano-Moriano et al., 2007), pointing to V1Rs/Gα_{i2} signaling as the mediator of sex-associated cues. BNSTp activation could also result from indirect vomeronasal inputs from both apical and basal VSNs transiting through the MeA.

3.1.2 Male mounting neural circuitry

We have seen that MeA and BNSTp, especially Aro-positive neurons, are necessary to strengthen females cues in male brains. Interestingly, ablation of BNSTp-Aro cells, but not MeApd-Aro ones, inhibits male sexual behavior (Bayless et al., 2019; Unger et al., 2015). The BNST is highly interconnected with the medial preoptic area (MPOA), a key structure in male sexual behavior (Hull and Dominguez, 2019). Sex steroids action in this structure is primordial to enable mounting (Sano et al., 2013; Wei et al., 2018), in addition to other neuropeptides (Hull and Dominguez, 2019). Of particular interest is the role of dopamine signaling. Sexual cues are highly rewarding, and structures associated with the reward system are connected to MPOA (Paredes, 2009). A recent study revealed that dopamine release within the MPOA primes males' interest to mate for several minutes (Zhang et al., 2021). The source of dopamine is tyrosine-hydroxylase (TH) neurons of the anteroventral periventricular nucleus (AVPV), a substructure of the preoptic area. The authors did not provide a link with the olfactory system, but males AVPV-TH neurons are activated by female cues, and not by male ones (Taziaux and Bakker, 2015), suggesting that this mechanism belongs to the process of transforming olfactory cues into a behavioral decision. The optogenetic stimulation of AOB-MCL neurons following a nasal contact with a female increases the occurrence of intromission (Kunkhyen et al., 2017), supporting the idea that vomeronasal cues are stimulating the sexual behavior neural circuitry. Other structures complete the circuitry, like the VMH and periaqueductal grey area (PAG). The Figure 19 shows a potential circuitry sustaining male sexual behavior proposed by Wei and colleagues (Wei et al., 2021).

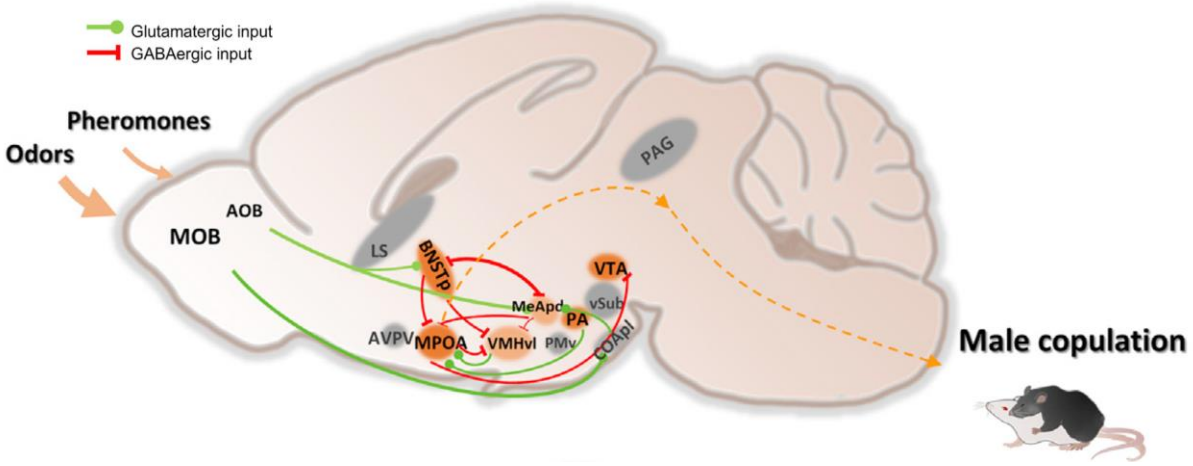

Figure 19: Male sexual behavior neural circuit. Solid lines denote known pathways that are involved in mediating the behavior. Dashed lines denote potential pathways to be explored further. Orange regions promote the behavior, light orange marks regions that play minor roles in the behavior, gray regions are not essential for the behaviors or have not yet been studied. Arrow size indicates the importance of the sensory input. Line width indicates connection strength. Not all known connections are shown. MOB/AOB, main/accessory olfactory bulb; AVPV, anteroventral periventricular nucleus; BNSTp, posterior part of the bed nucleus of the stria terminalis; CoApl, posterolateral cortical amygdala; LS, lateral septum; MeA, medial amygdala; MPOA, medial preoptic area; PA, posterior amygdala; PAG, periaqueductal gray; PMv, ventral premammillary nucleus; VMHvl, ventrolateral part of the ventromedial hypothalamus; vSUB, ventral subiculum; VTA: ventral tegmental area. From Wei et al., 2021.

3.1.3 Lordosis behavior neural circuitry

The lordosis reflex is triggered by somatosensory cues provided by the male during mounting, but olfactory cues are necessary to allow it (Keller et al., 2006). Ishii and coworkers drew a labeled line brain circuit supporting the enhancement of lordosis by stimulation with the ESP1 peptide (Ishii et al., 2017). Detection of ESP1 by V2Rp5-expressing VSNs activates glutamatergic neurons of the MeApv, followed by SF1-VMHdm (SF1, steroidogenic factor 1) neurons and ERα-PAG (ERα, estrogen receptor alpha) ones. ESP1 is only secreted by some mouse strains (Kimoto et al., 2007), and females exhibit lordosis during mounting by ESP1-deficient males. Thus, the brain circuit activated by ESP1 is not necessarily the circuit sustaining the initiation of the lordosis reflex. The reduction of the lordosis response in $cG\alpha_o^{-/-}$ females and after acute inhibition of AOB firing sustain the implication of vomeronasal inputs in the lordosis brain circuitry (McCarthy et al., 2017a; Oboti et al., 2014). Lesion or pharmacological inhibition of the MeA reduces lordosis behavior, even though those studies do not discriminate the participation of each MeA subdivision (DiBenedictis et al., 2012; McCarthy et al., 2017b). Recently, Johnson and colleagues point to GABAergic, but not glutamatergic, MeA neurons as mediator of the lordosis reflex (Johnson et al., 2021). The VMH can be subdivided in a posteroventral and a dorsomedial parts (VMHvl and VMHdm). Clear evidence shows that the VMHvl is also necessary for lordosis behavior (Bentefour and Bakker, 2021; Hashikawa et al., 2017; Micevych and Meisel, 2017; Yang et al., 2013). The Figure 20 shows a potential circuitry sustaining female sexual behavior proposed by Wei and colleagues (Wei et al., 2021).

The AVPV, more precisely Kisspeptin-AVPV neurons, are gatekeepers of the lordosis response (Hellier et al., 2018). Kisspeptin (Kiss) is a neuropeptide regulating the hypothalamic-pituitary-gonadal (HPG) axis by mediating sex steroids feedback on the hypothalamic GnRH (gonadotropin-releasing hormone) neurons (Oakley et al., 2009). Kiss-AVPV neurons are activated by males odors (Bakker et al., 2010), and their inhibition abolishes olfactory preference and lordosis behavior (Hellier et al., 2018). Further, a study revealed that the hormonal environment gated the AVPV function (Inoue et al., 2019). Estrogens increase the projections from the VMHvl to the AVPV. The authors did not analyze if VMH-innervated AVPV neurons express Kiss. Nonetheless, Kiss neurons appear as a perfect candidate to transform olfactory cues into a behavioral decision.

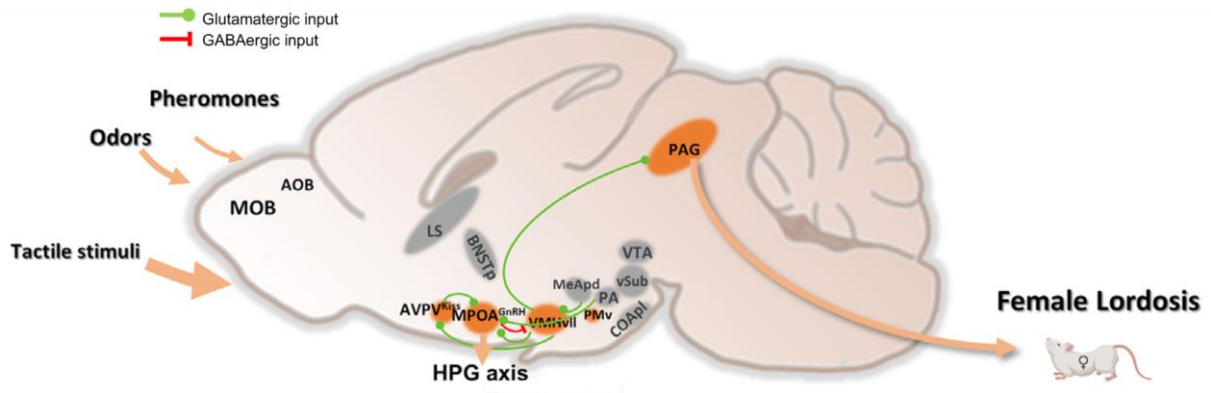

Figure 20: Female sexual behavior neural circuit. Orange regions promote the behavior, gray regions are not essential for the behaviors or have not yet been studied. Arrow size indicates the importance of the sensory input. Line width indicates connection strength. Not all known connections are shown. MOB/AOB, main/accessory olfactory bulb; AVPV, anteroventral periventricular nucleus; BNSTp, posterior part of the bed nucleus of the stria terminalis; CoApl, posterolateral cortical amygdala; LS, lateral septum; MeA, medial amygdala; MPOA, medial preoptic area; PA, posterior amygdala; PAG, periaqueductal gray; PMv, ventral premammillary nucleus; VMHvl, ventrolateral part of the ventromedial hypothalamus; vSUB, ventral subiculum; VTA: ventral tegmental area. From Wei et al., 2021.

3.2 Aggression neural circuitry

Aggressive behavior in males and females is qualitatively dimorphic and is expressed under different circumstances (see section2.2). However, it is controlled by vomeronasal signaling in both sexes and nearly all regions associated with male aggression are also involved in female aggression, pointing to a common aggression circuitry in some extent (Hashikawa et al., 2018). The Figure 21 shows a potential circuitry sustaining aggressive behavior proposed by Wei and colleagues (Wei et al., 2021).

GABA-MeApd neurons induces an aggressive response toward an adult intruder, regardless of sex or gonadal status (Hong et al., 2014). Surprisingly, it can be achieved only by a robust activation, whereas low activation of GABA-MeApd neurons resulting in mounting behavior. Similarly, low activity of GABA-MeApd neurons results in parenting in a male exposed to a neonate, while strong activity trigger infanticide in similar conditions (Chen et al., 2019). Thus, MeApd activity measurement

is already a proxy of the behavioral response. Whether vomeronasal signaling could increase activation of GABA-MeApd neurons to lead to aggressive behaviors is unknown.

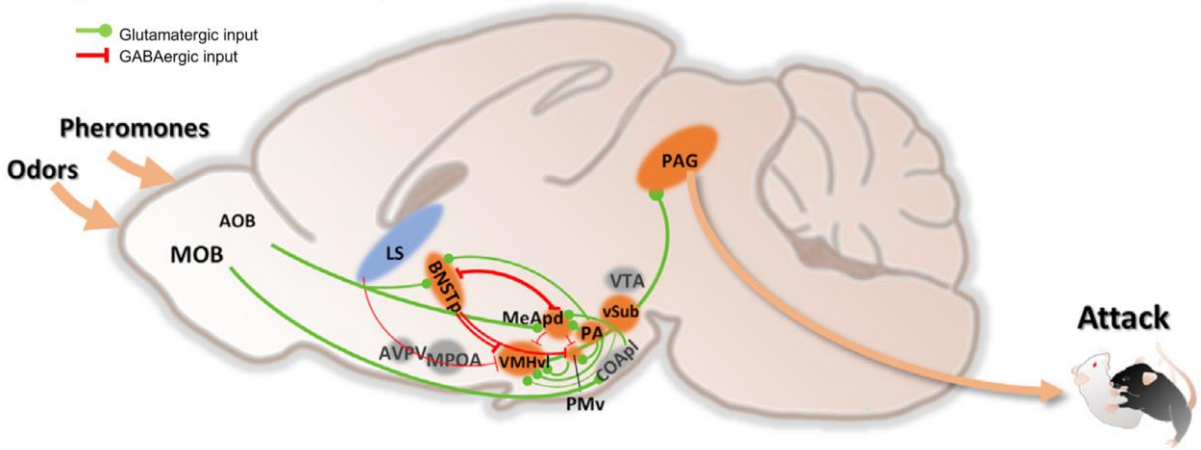

Figure 21: Aggression neural circuit. Blue regions suppress the behavior, whereas orange regions promote the behavior, gray regions are not essential for the behavior or have not yet been studied. Arrow size indicates the importance of the sensory input. Line width indicates connection strength. Not all known connections are shown. MOB/AOB, main/accessory olfactory bulb; AVPV, anteroventral periventricular nucleus; BNSTp, posterior part of the bed nucleus of the stria terminalis; CoApl, posterolateral cortical amygdala; LS, lateral septum; MeA, medial amygdala; MPOA, medial preoptic area; PA, posterior amygdala; PAG, periaqueductal gray; PMv, ventral premammillary nucleus; VMHvl, ventrolateral part of the ventromedial hypothalamus; vSUB, ventral subiculum; VTA: ventral tegmental area. From Wei et al., 2021.

The MeA project to the VMH, which is a crucial node for the expression of aggression (Canteras et al., 1995; Lin et al., 2011). How could inhibitory GABA-MeApd neurons promote VMH activation? Padilla and colleagues revealed a disynaptic pathway between the MeA, BNSTp, and VMH controlling aggression in the context of starving (Padilla et al., 2016). BNSTp neurons are mostly GABAergic, project to the VMH, and inhibition of Aro-BNSTp neurons (also GABAergic) impacts aggression (Bayless et al., 2019). Consequently, an inhibition-disinhibition circuit could transmit information from the MeApd to the VMH through the BNSTp (Figure 22).

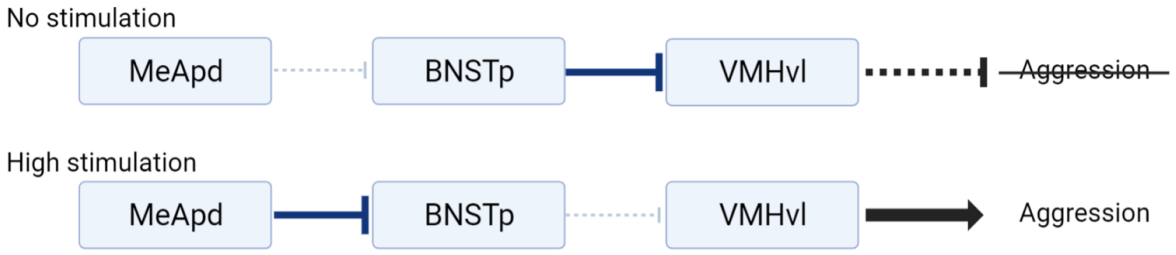

Figure 22: Disynaptic communication between the MeA and VMH. In the absence of stimulation, GABA-MeApd neurons are silent and the BNSTp inhibits the VMHvl, restraining the expression of aggression. During strong stimulation, GABA-MeApd neurons inhibit the BNSTp, releasing the inhibition of the BNSTp on the VMH and allowing the expression of aggression.

Sex steroids are permissive factors of aggression. Castrated males do not display territorial aggression, and AR, ERs, and Aro are found in many brain nuclei of the aggression circuitry (Hashikawa et al., 2018). Aromatase neurons are indeed strongly involved in aggressive behaviors (Bayless et al., 2019; Unger et al., 2015). In female rats, the rapid hormone levels fluctuation of estrus cycles does not induce aggressive reactions (De Jong et al., 2014). However, the transition to motherhood is accompanied by a major and long lasting change in hormonal environment. It induces a profound modification of female aggression: males become a threat instead of a mate. This change in behavioral significance is not yet explained. The female brain undergoes a remodeling around parturition, modifying cell activation (Moffitt et al., 2018) and gene expression (Abellán-Álvaro et al., 2021). Pregnancy also remodels the VNO by enhancing neurogenesis and modifying the VRs repertoire (Oboti et al., 2015). Both mechanisms probably act in concert to induce such a drastic change of behaviors.

3.3 Parenting neural circuitry

Vomeronasal signaling implication in parental behaviors is not clearly established (see section 2.3). However, studies on rat suggest that the MeA negatively regulates parenting (Numan and Woodside, 2010) and pup exposure induce cell activation in the MeA (Alsina-Llanes and Olazábal, 2020), suggesting that vomeronasal inputs may be integrated to the parenting neural circuitry. Early investigations on rats also revealed the central role of the MPOA in parental behaviors (Numan, 1974). The MPOA is a vast and heterogeneous structure highly activated during parenting in mice (Tsuneoka et al., 2013). The combination of anatomical and molecular markers allows the design of several subdivisions (Moffitt et al., 2018; Tsuneoka et al., 2013). However, it does not exist clear markers allowing strict discrimination. Genetic dissection of MPOA-cells driving parental behaviors highlighted ERα- and galanin-expressing neurons (Fang et al., 2018; Kohl et al., 2018; Wei et al., 2018; Wu et al., 2014). ERα-MPOA neurons are necessary for expressing parental and sexual behaviors (Ribeiro et al., 2012; Sano et al., 2013). However, sequential stimulation with a pup and an adult conspecifics activates distinct ERα-expressing neuronal populations (Wei et al., 2018). A subpopulation of ERα neurons express the neuropeptide galanin (Tsuneoka et al., 2017), but ablation of galanin-expressing neurons also abolishes sexual behavior (Wu et al., 2014). The Figure 23 shows a potential circuitry sustaining parental behaviors proposed by Wei and colleagues (Wei et al., 2021).

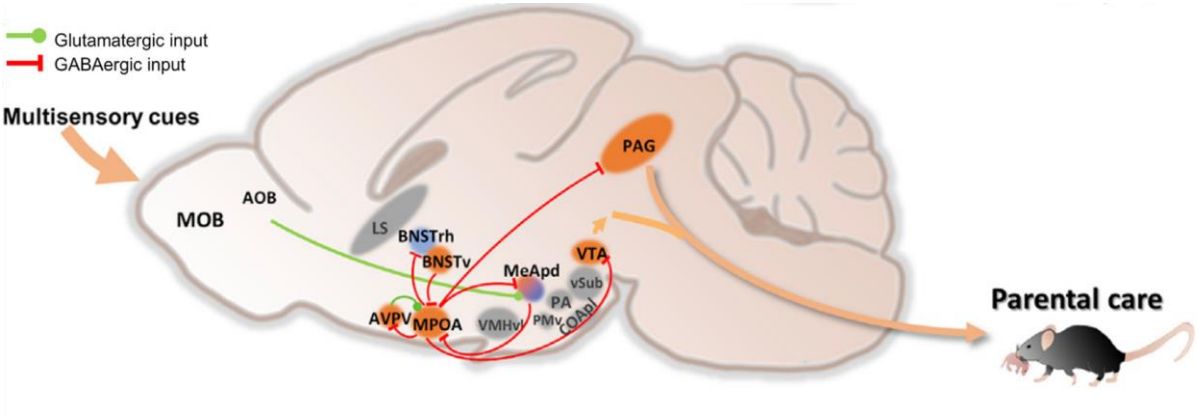

Figure 23: Parenting neural circuit. Blue regions suppress the behavior, whereas orange regions promote the behavior, gray regions are not essential for the behavior or have not yet been studied. Arrow size indicates the importance of the sensory input. Line width indicates connection strength. Not all known connections are shown. MOB/AOB, main/accessory olfactory bulb; AVPV, anteroventral periventricular nucleus; BNSTp, posterior part of the bed nucleus of the stria terminalis; CoApl, posterolateral cortical amygdala; LS, lateral septum; MeA, medial amygdala; MPOA, medial preoptic area; PA, posterior amygdala; PAG, periaqueductal gray; PMv, ventral premammillary nucleus; VMHvl, ventrolateral part of the ventromedial hypothalamus; vSUB, ventral subiculum; VTA: ventral tegmental area. From Wei et al., 2021.

Parenting seems tightly linked to infanticide. The brain circuit of infanticide is not elucidated, but the MeApd, BNSTp, MPOA, anterior hypothalamic and amygdalohippocampal areas seem to be involved (Autry et al., 2021; Chen et al., 2019; Sato et al., 2020; Tachikawa et al., 2013; Tsuneoka et al., 2013, 2015; Wu et al., 2014). In virgin animals, inhibition of infanticide brain nuclei stimulates parenting, and inversely, activation of parenting brain nuclei inhibits infanticide (Sato et al., 2020; Tsuneoka et al., 2013, 2015; Wu et al., 2014). A comparison of brain-activated regions between a lactating female and an infanticidal male shows a higher number of regions overactivated in males (Renier et al., 2016). However, whether this difference results from a lack of inhibition in the virgin brain or from a virgin-specific sensory activation is unclear. The VNO detects pup-cues in virgin males that can act as pro-infanticide cues (Isogai et al., 2018; Nakahara et al., 2020; Tachikawa et al., 2013). Chen and colleagues showed that high activation of GABA-MeApd neurons triggers infanticide in males, even in fathers (Chen et al., 2019). Interestingly, reducing the stimulation intensity of GABA-MeApd neurons made virgin males becoming parental. It is not known to what extent vomeronasal signaling may lead to this high MeApd activation. The balance between the activation of pro-parental and pro-infanticide circuits is far to be understood. Rigorous discrimination of sex and experience factors are lacking.

3.4 Predator and sick conspecific avoidance neural circuitry

Predator avoidance neural circuitry is tightly linked to those sustaining social behaviors. Both signals are processed by the olfactory system and converge to the same brain structures. As we have seen for sex-identity coding in the MeA (see section 3.1.1), the predator-activated MeA neurons also form distinct populations (Bergan et al., 2014). Further, MeApv neurons already encode the nature of

the predator (e.g., cat versus snake) (Carvalho et al., 2015). Predator signals detected by different structures (i.e., VNO, MOE, GG, and Taars) also activate the MeApv (Pérez-Gómez et al., 2015), suggesting that it could be a hub to trigger predator avoidance. The pathway by which predator cues converge into the vomeronasal amygdala is not clear. It might involve the CoApl, which is necessary for MOS-driven odor avoidance and connected to the MeA (Canteras et al., 1995; Root et al., 2014). Downstream to the MeA, the VMH, and particularly the SF1-expressing neurons of the VMHdm are crucial to mediate predator avoidance (Silva et al., 2013; Wang et al., 2015). Like in the MeA, VMHdm neurons are activated by AOS and MOS signaling (Pérez-Gómez et al., 2015), and different predators activate different neural ensembles (Carvalho et al., 2020). Activation of the VMHdm led to adaptive behavioral responses (e.g., freeze or flight) according to the context through the activation of distinct downstream pathways (Wang et al., 2015). Current knowledge argues for the participation of the anterior hypothalamic nucleus (AHN), dorsal premammilary nucleus, and PAG as routes for the avoidance and fear motor actions (Canteras et al., 2015; Carvalho et al., 2020; Wang et al., 2015) (Figure 24).

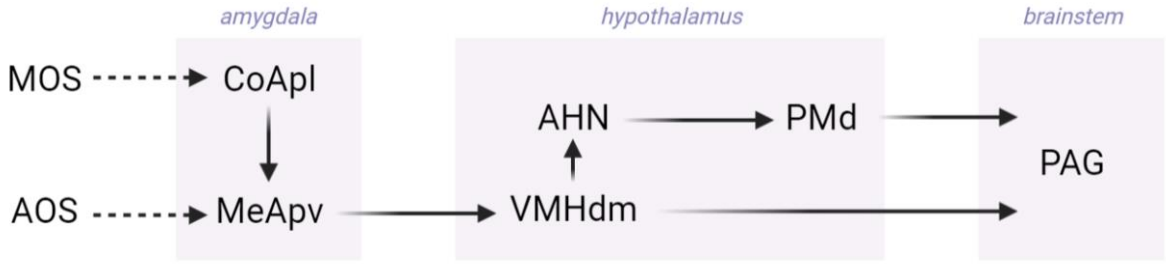

Figure 24: Predator avoidance neural circuit. MOS/AOS, main/accessory olfactory system; CoApl, posterolateral cortical amygdala; MeApv, posteroventral medial amygdala; VMHdm, dorsomedial part of the ventromedial hypothalamus; AHN, anterior hypothalamic nucleus; PMd, dorsal premammillary nucleus; PAG, periaqueductal gray. Adapted from Canteras et al., 2015.

In contrary to predator avoidance, sick conspecific avoidance neural pathway is still largely unexplored. One major pitfall to its comprehension is to discriminate the signal mediating the sick state from the social one. Both are detected by the VNO and activate the AOB (Boillat et al., 2015), but the identity of VSNs mediating sickness-associated cues is unknown. FPRs are good candidates due to their natural affinity for bacterial-derived peptides (Bufe et al., 2012). The avoidance of LPS-treated animals is independent of FPR3. Thus, if detected by FPRs, sickness-associated olfactory cues should be sensed by apical $G\alpha_{i2}$-expressing VSNs. Kwon and colleagues observed that the CoApm, which belongs to the vomeronasal amygdala, was specifically activated after exposure to an LPS-treated female (Kwon et al., 2021). They also showed that CoApm activated cells project to glutamatergic neurons of the MeApv to suppress social engagement. What happens downstream remains unknown, but the MeApv, as it may be a hub to trigger predator avoidance, may act as a decision site between pursuing or not social interactions.

Objectives

In light of the literature review, it appears that the olfactory system has evolved in distinct sensory components working in concert to ensure appropriate behavioral decisions sustained by complex neural circuitry. The place of the VNO in the control of social behaviors is indisputable, but current knowledge is full of gaps and contradictory evidence. The development of molecular and genetic tools allowed progressive insights into VNO sensory function. The fact that rodents' VSNs express two types of evolutionary distinct VRs implies distinct properties and putative functions. Works with the mouse model of $G\alpha_o$ olfactory-restricted deletion partially answered the question for V2Rs-expressing VSNs (Chamero et al., 2011; Oboti et al., 2014; Pérez-Gómez et al., 2015). Three mouse models investigated V1Rs function: the general knockout for $G\alpha_{i2}$ ($G\alpha_{i2}^{-/-}$, Norlin et al., 2003), the olfactory-restricted knockout for $G\gamma_{13}$ ($cG\gamma_{13}^{-/-}$, Liu et al., 2018), and the knockout for V1Ra and V1Rb families (ΔV1rabΔ, Del Punta et al., 2002). The first two induce a mutation leaking outside the VNO, interfering with the evaluation of its function, and the latest only removes 12% of V1Rs, not enough to generalize results with the function of apical VSNs. $G\alpha_{i2}^{-/-}$ mice exhibit a reduced life expectancy due to severe ulcerative colitis and colon adenocarcinoma (Rudolph et al., 1995). Further, they show decreased social behavior linked to cortical development abnormalities (Hamada et al., 2017). The $cG\gamma_{13}^{-/-}$ mouse expresses the Cre recombinase under the OMP promoter, inducing an olfactory-restricted mutation thanks to the Cre-lox system. However, these mice are anosmic due to the role of $G\gamma_{13}$ in OMP-expressing canonical-OSNs (Li et al., 2013). Other deficiencies of these studies are the lack of functional evidence of $G\alpha_{i2}$ implication in VSNs signaling and the limited behavioral paradigms studied.

The main objective of this thesis is to decipher $G\alpha_{i2}$ function in VSNs and $G\alpha_{i2}$-expressing VSNs implication in socio-sexual behaviors. To overcome the limitations of available models, we have generated mice harboring a conditional deletion of $G\alpha_{i2}$ in the olfactory system (the $cG\alpha_{i2}^{-/-}$ mouse). We crossed mice carrying a floxed allele of *Gnai2* (Ustyugova et al., 2012), coding for $G\alpha_{i2}$, with the OMP-Cre mice, in which the coding region for OMP is added with that of Cre recombinase (Li et al., 2004). OMP expression starts in mature olfactory neurons (Katreddi and Forni, 2021), avoiding potential disturbance of VSNs maturation. Further, it has been used to generate many models of olfactory dysfunction (Amjad et al., 2015; Chamero et al., 2011; Dey et al., 2015; Gigante et al., 2017; Green et al., 2018; Koike et al., 2021; Li et al., 2013; Matsuo et al., 2015; Münch et al., 2018; Schmid et al., 2010; Weiss et al., 2011, non-exhaustive list). $G\alpha_{i2}$ is expressed in few cells of the MOE, but it seems limited to basal immature neurons which don't express OMP (Berghard and Buck, 1996). Thus, the $cG\alpha_{i2}^{-/-}$ mouse is an adapted model to study $G\alpha_{i2}$ function. By using this mouse model, this thesis aims to answer three main questions:

i- Is $G\alpha_{i2}$ involved in VSNs signaling?

ii- What behaviors do apical VSNs control, and how?

iii- What can we learn about brain coding and integration of the $G\alpha_{i2}$-dependent olfactory information into social behaviors neural pathways?

To answer these questions, we combined VSNs calcium imaging, behavioral studies in different experimental paradigms, and brain activity mapping using immediate early genes immunostainings. I chose to respect the existing behavioral sexual dimorphism and structured my work accordingly in three chapters. The first unravels $G\alpha_{i2}$ function in VSNs signaling and males' socio-sexual behaviors. The second chapter evaluates the impact of $G\alpha_{i2}$ deletion in VSNs on females' socio-sexual behaviors. Both are presented in their published form as peer-reviewed journal articles. The last chapter investigates the implication of $G\alpha_{i2}$-expressing VSNs in avoidance behaviors. It is presented differently as the underlying results have not yet been submitted to publication and still need complementary investigations to support them.

Results

1 $G\alpha_{i2}$ function in VSNs signaling and males' socio-sexual behaviors

Journal article #1: Central role of G protein $G\alpha_{i2}$ and $G\alpha_{i2}$+ vomeronasal neurons in balancing territorial and infant-directed aggression in male mice

Anne-Charlotte Trouillet[1], Matthieu Keller[1], Jan Weiss[2], Trese leinders-Zufall[2], Lutz Birnbaumer[3,4], Frank Zufall[2], and Pablo Chamero[1]

[1] Laboratoire de Physiologie de la reproduction et des Comportements, UMR OO85-INRAE-CNRS-IFCE-University of Tours, Nouzilly, France

[2] Center for Integrative Physiology and Molecular Medicine, Saarland University, Homburg, Germany

[3] Neurobiology Laboratory, National Institute of Environmental Health Sciences, Durham, NC, United States of America

[4] School of Medical Sciences, Institute of Biomedical Research, Catholic University of Argentina, Buenos Aires, Argentina

Published in Proceedings of the National Academy of Sciences of the United States of America, February 2019.

Abstract

The vomeronasal control of social behaviors depends on two distinct neuronal populations, V1R/$G\alpha_{i2}$- and V2R/$G\alpha_o$-expressing VSNs. $G\alpha_o$ is the primary effector for sensory signaling in V2Rs-expressing VSNs, but the functional role of $G\alpha_{i2}$ in VSNs is not elucidated. The first goal of this study was thus to characterize $G\alpha_{i2}$ function in VSNs signaling. Further, apical VSNs have been associated with the modulation of several social behaviors in males with contradictory results. The second goal of this study was then to elucidate the precise implication of $G\alpha_{i2}$ vomeronasal signaling in the modulation of three social behaviors, namely sexual, aggressive, and parental behaviors.

$G\alpha_{i2}$ is widely expressed in the body, and mice harboring a global $G\alpha_{i2}$ deficiency display severe defects shortening lifespan, thus precluding the analysis of VNO-function and VNO-dependent behaviors in these animals. To overcome this limitation, we created a conditional olfactory-restricted $G\alpha_{i2}$ null mouse ($cG\alpha_{i2}^{-/-}$). We crossed mice carrying a floxed allele of *Gnai2*, the gene coding for $G\alpha_{i2}$, with the OMP-Cre mice, in which the coding region for OMP is added with that of the Cre recombinase. OMP expression starts in mature olfactory neurons, avoiding potential disturbance of VSNs

maturation. In a first step, we combined histological analyzes and mRNA quantifications to validate the mutation and examine the organization of the VNE and MOE. $G\alpha_{i2}$ expression was lost in the VNE and the aAOB-GL, and the mutation reduced the ratio between apical and basal VSNs. However, the structure and function of the MOE were intact.

To establish the cellular function of $G\alpha_{i2}$ in apical VSNs sensory signaling, we performed live-cell Ca^{2+} imaging by using dissociated cells and acute VNO slices in combination with the Ca^{2+} sensors GCaMP6f, fura-2/AM, or fluo-4/AM. As chemostimuli, we used single small organic molecules, sulfated steroids, and urinary peptides detected by V2Rs as control. Subsets of VSNs from controls responded reliably to each of these stimuli. By contrast, such responses were severely diminished or absent in VSNs lacking $G\alpha_{i2}$, except for V2Rs ligands.

We carried out several behavioral experiments on $cG\alpha_{i2}^{-/-}$ males and determined that $G\alpha_{i2}$ vomeronasal signaling is dispensable for the expression of sexual behavior. However, it is required for territorial and pup-directed aggression. On the one hand, $cG\alpha_{i2}^{-/-}$ males were highly aggressive and continue to attack a castrated opponent, suggesting that, although not necessary to trigger the response, $G\alpha_{i2}$ vomeronasal signaling participates in the modulation of the aggressive response. On the other hand, deletion of $G\alpha_{i2}$ suppressed infanticidal behavior and promoted parenting towards neonates in males.

To understand the opposite regulation of male- and pup-directed aggression by $G\alpha_{i2}$ signaling, we mapped brain activation after male and pup exposure using the immediate early gene cFos. Compared to controls, MeApd activation was higher after male exposure and lower after pup exposure, consistent with the behavioral results. Further, close analysis of activated MeApd neurons revealed that male exposure induced the activation of AR-positive neurons, while pup exposure did not.

In conclusion, we showed here an essential role of $G\alpha_{i2}$ in VNO sensory signaling of the apical VSN population that detects small organic molecules, including volatile pheromones and steroid derivatives. Our study identifies $G\alpha_{i2}$+ VSNs as a critical neural component that organizes and balances male-male and infant-directed aggression through distinct neural circuitries.

Check for updates

Central role of G protein Gαi2 and Gαi2$^+$ vomeronasal neurons in balancing territorial and infant-directed aggression of male mice

Anne-Charlotte Trouillet[a], Matthieu Keller[a], Jan Weiss[b], Trese Leinders-Zufall[b], Lutz Birnbaumer[c,d,1], Frank Zufall[b,1], and Pablo Chamero[a,1]

[a]Laboratoire de Physiologie de la Reproduction et des Comportements, UMR Institut National de la Recherche Agronomique (INRA)-CNRS-Institut Français du Cheval et de l'Equitation (IFCE)-University of Tours, 37380 Nouzilly, France; [b]Center for Integrative Physiology and Molecular Medicine, Saarland University, 66421 Homburg, Germany; [c]Neurobiology Laboratory, National Institute of Environmental Health Sciences, National Institutes of Health, Durham, NC 27709; and [d]Institute of Biomedical Research (BIOMED), School of Medical Sciences, Catholic University of Argentina, C1107AAZ Buenos Aires, Argentina

Contributed by Lutz Birnbaumer, January 23, 2019 (sent for review December 18, 2018; reviewed by Peter A. Brennan and Marc Spehr)

Aggression is controlled by the olfactory system in many animal species. In male mice, territorial and infant-directed aggression are tightly regulated by the vomeronasal organ (VNO), but how diverse subsets of sensory neurons convey pheromonal information to limbic centers is not yet known. Here, we employ genetic strategies to show that mouse vomeronasal sensory neurons expressing the G protein subunit Gαi2 regulate male–male and infant-directed aggression through distinct circuit mechanisms. Conditional ablation of Gαi2 enhances male–male aggression and increases neural activity in the medial amygdala (MeA), bed nucleus of the stria terminalis, and lateral septum. By contrast, conditional Gαi2 ablation causes reduced infant-directed aggression and decreased activity in MeA neurons during male–infant interactions. Strikingly, these mice also display enhanced parental behavior and elevated neural activity in the medial preoptic area, whereas sexual behavior remains normal. These results identify Gαi2 as the primary G protein α-subunit mediating the detection of volatile chemosignals in the apical layer of the VNO, and they show that Gαi2$^+$ VSNs and the brain circuits activated by these neurons play a central role in orchestrating and balancing territorial and infant-directed aggression of male mice through bidirectional activation and inhibition of different targets in the limbic system.

olfactory | GCamp6f | V1R receptor | infant-directed aggression | territorial aggression

Aggression is an innate social behavior most commonly displayed in males, typically directed to other males of the same species (1) or to another male's offspring (2). Such behaviors are important for resource competition, establishment of group hierarchies, and access to sexual partners. For example, pup-directed aggression resulting in infanticide ultimately induces endocrine changes in females, which makes them quickly receptive to a male newcomer (3) and thus increases reproductive success. In rodents, the role of the olfactory system is critical for initiating aggression. Pheromonal cues present in secretions from adult males or pups are detected by distinct subsets of sensory neurons in the vomeronasal organ (VNO) (4–7) to initiate neural signals that, in turn, trigger aggressive behavior. However, many of the cellular and molecular mechanisms underlying such aggression-promoting signaling remain unknown.

The mouse VNO contains two major populations of vomeronasal sensory neurons (VSNs): VSNs of the apical layer of the vomeronasal sensory epithelium (VNE) express the G protein Gαi2 and members of the V1R family of vomeronasal G protein-coupled receptors, whereas VSNs of the basal layer express Gαo and members of the V2R receptor family (8–14). Gαo-expressing (i.e., Gαo$^+$) cells have been implicated in male–male aggression by detecting urine-derived high molecular weight (HMW) pheromones, particularly MUP proteins, and ESP1 peptide, both of which are capable to induce aggression (15–19). Conditional ablation of Gαo eliminates VSN transduction of MUPs and ESP1 as well as male–male aggression (16, 20, 21). However, organic low molecular weight (LMW) molecules recognized by Gαi2 VSNs can also induce aggression (22). Furthermore, mice carrying a global deletion of Gαi2 are less aggressive (23), suggesting that both VSN populations may interact to generate aggressive behavior. Thus, whether each VNO subsystem activates independent aggression circuits or whether the two subsystems function in a cooperative and integrative manner to generate territorial aggression is not yet clear.

Infanticidal behavior, in which an adult attacks and kills an alien pup, is observed in virgin adult males and is highly dependent on the VNO. Genetic deletion of the transient receptor potential channel Trpc2, the primary sensory ion channel of VSNs, or surgical VNO ablation strongly reduce aggression toward pups (24, 25). Pup odors in virgin males preferentially activate a region of the accessory olfactory bulb (OB; AOB) innervated by Gαi2 neurons (25), but how molecularly defined VSN subsets influence pup-directed aggression remains unclear. Several regions in the limbic brain are activated during infanticide and male–male aggression, including the medial amygdala (MeA), the bed nucleus of the stria terminalis (BNST),

Significance

Male mice detect pheromones that trigger aggressive behavior toward other males or another male's pups. We found that a subpopulation of chemosensory neurons in the vomeronasal organ organizes and balances both types of aggression by reducing or enhancing each behavioral output. These neurons use a signaling cascade that requires the G protein Gαi2 in the detection of volatile pheromones and steroid derivatives. This subset of sensory neurons conveys pheromonal information to limbic centers in the brain through independent mechanisms, targeting different groups of neurons during male–male or infant-directed aggression. How the mouse olfactory system detects and processes pheromones that trigger different forms of aggression should aid in the identification of neural networks mediating male–male vs. infant-directed social aggression.

Author contributions: M.K., T.L.-Z., L.B., F.Z., and P.C. designed research; A.-C.T., J.W., T.L.-Z., and P.C. performed research; L.B. contributed new reagents/analytic tools; A.-C.T., J.W., T.L.-Z., and P.C. analyzed data; and A.-C.T., F.Z., and P.C. wrote the paper.

Reviewers: P.A.B., University of Bristol; and M.S., RWTH Aachen University.

The authors declare no conflict of interest.

Published under the PNAS license.

Data deposition: The datasets generated and/or analyzed during the present study are available in the Data Inra Dataverse portal (https://data.inra.fr/).

[1]To whom correspondence may be addressed. Email: Birnbau1@gmail.com, frank.zufall@uks.eu, or pablo.chamero-benito@inra.fr.

This article contains supporting information online at www.pnas.org/lookup/suppl/doi:10.1073/pnas.1821492116/-/DCSupplemental.

and the ventromedial hypothalamus (VMH) (25, 26). Current understanding of these neuronal substrates is insufficient to explain whether infanticide and male–male aggression are initiated by the same or different subsets of VSNs. Furthermore, it is not known whether the same or different groups of neurons from these common limbic structures are activated during male–male or infant-directed aggression. One possibility is that neuronal circuits originating from Gαi2^{+} VSNs may independently coordinate infant-directed and male–male aggression.

Because the *Gnai2* gene, which encodes Gαi2, is ubiquitously expressed in the developing brain and cortex (27, 28), analysis of VNO-dependent behaviors in mice carrying a global Gαi2 deletion (28) is impeded. Furthermore, no functional recordings in single VSNs lacking Gαi2 have been performed. To overcome these limitations, we have generated mice harboring a conditional deletion of Gαi2 in the olfactory system. These mice show a striking reduction in the sensory response to LMW organic molecules, demonstrating that Gαi2 is an obligate requirement for normal signaling of apical VSNs. Furthermore, territorial aggression is enhanced in these mutant mice, whereas infant-directed aggression is strongly diminished. Together with c-Fos mapping in aggression-controlling brain centers, our study establishes a critical role of Gαi2, the VSNs that express this G protein, and the circuits derived from Gαi2^{+} VSNs in orchestrating and balancing territorial and infant-directed aggression of male mice.

Results

Conditional Deletion of Gαi2 in VSNs. We used the Cre-*loxP* system to create mice with a tissue-specific and time-dependent deletion of Gαi2. Mice carrying a floxed allele of *Gnai2* (*Gnai2*$^{fx/fx}$) (29) were crossed with OMP-Cre mice (30, 31), in which the coding region for olfactory marker protein (OMP) is replaced by that of Cre recombinase. Conditional Gαi2 mutants (cGαi2$^{-/-}$) were heterozygous for *Cre* (*Gnai2*$^{fx/fx}$*Omp*$^{cre/+}$); mice heterozygous for both alleles (*Gnai2*$^{fx/+}$*Omp*$^{cre/+}$) served as controls (cGαi2$^{+/-}$). All experiments were performed with adult male mice (8–12 wk old).

We used immunohistochemistry (IHC) to examine the VNE in cGαi2$^{+/-}$ and cGαi2$^{-/-}$ males. Gαi2 immunoreactivity was absent in the VNE of cGαi2$^{-/-}$ mice, confirming the loss of Gαi2 protein expression (Fig. 1*A*). Staining was positive for markers of basal (V2R2, family C V2Rs), apical (PDE4A, phosphodiesterase 4A), or both (OMP) VSN populations in control and mutant mice (Fig. 1*A* and *SI Appendix*, Fig. S1*A*), showing that general tissue structure remained intact. By using RT-PCR with whole VNO cDNA from cGαi2$^{+/-}$ or cGαi2$^{-/-}$ males, we identified transcripts for several *V1r* receptors and two *V2r* receptors, *Trpc2* and *Plcb2*, in both genotypes (*SI Appendix*, Fig. S1*B*), indicating that expression of transduction molecules also remained intact. Quantitative RT-PCR analyses showed that relative expression of *Gnai2* in the VNO of cGαi2$^{-/-}$ males was reduced by 1.86 fold ($P <$ 0.001), whereas *Gnao* expression increased by 1.47 fold ($P <$ 0.01; Fig. 1*B*). *Gnai2* expression in the main olfactory epithelium (MOE) of control vs. mutant mice was not significantly different (Fig. 1*B*).

Previous work indicated a role for G protein α-subunits in the survival of VSNs (16, 23, 32). We analyzed PDE4A immunoreactivity, specific for the apical Gαi2-expressing zone (33), and the volume of apical and basal VNE layers in cGαi2$^{+/-}$ and cGαi2$^{-/-}$ mice. The volume of the apical layer was reduced by 1.41 fold whereas that of the basal layer increased 1.35-fold in cGαi2$^{-/-}$ mice ($P <$ 0.001; Fig. 1*C*). Cell density remained unchanged (*SI Appendix*, Fig. S1*C*), indicating that the volume reduction of the apical layer likely resulted from a decrease in the number of VSNs. A reduced volume was also detected in whole AOB of cGαi2$^{-/-}$ mice as shown by IHC for OMP (13% reduction; $P <$ 0.001; *SI Appendix*, Fig. S1*D*). By using IHC for Gαo, we found a reduced glomerular layer in the rostral AOB (31% reduction; $P <$ 0.001), the primary target of Gαi2^{+} VSNs (*SI Appendix*, Fig. S1*D*). The general structure of MOE and glomerular layer of the main OB (MOB) remained unchanged in cGαi2$^{-/-}$ mice (*SI Appendix*, Fig. S1*E*). Thus, conditional Gαi2 deletion caused a selective loss of apical PDE4A-expressing VSNs and rostral AOB glomerular volume. We confirmed that general olfactory performance remained normal in cGαi2$^{-/-}$ males by performing several behavioral tests. There was no significant difference between cGαi2$^{-/-}$ and cGαi2$^{+/-}$ males in a food-finding test (*SI Appendix*, Fig. S1*F*). Likewise, novel odor investigation of female urine and odor discrimination of normal male urine vs. castrated male urine using a habituation–dishabituation paradigm (20, 31) revealed no significant differences between the two genotypes (*SI Appendix*, Fig. S1*G*). Thus, cGαi2$^{-/-}$ mice do not display any obvious defects with respect to main olfactory system function.

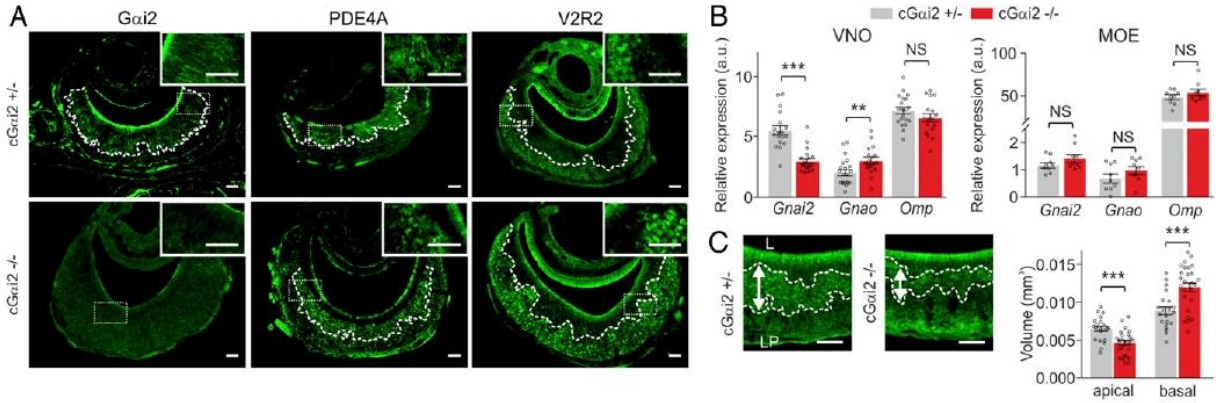

Fig. 1. Expression of marker proteins in the VNO of cGαi2$^{+/-}$ and cGαi2$^{-/-}$ mice. (*A*) Loss of Gαi2 immunoreactivity in cGαi2$^{-/-}$ VNO. Antibodies specific for PDE4A (apical layer) or V2R2 (basal layer) indicate that the laminar VNO organization persists in the absence of Gαi2. (Scale bars, 50 μm.) (*B*) Relative expression (normalized to *Hprt-1*) of *Gnai2*, *Gnao*, and *Omp* genes in VNO (*Left*) and MOE (*Right*). *Gnai2* expression decreased and *Gnao* expression increased, whereas *Omp* expression did not change, in cGαi2$^{-/-}$ VNO [$^{**}P < 0.01$ and $^{***}P < 0.001$; nonsignificant (NS), $P = 0.21$, Mann–Whitney *U* test; cGαi2$^{+/-}$, $n = 20$; cGαi2$^{-/-}$, $n = 18$]. No difference in gene expression in the MOE between the two genotypes was observed (NS, $P = 0.22$–0.53, Mann–Whitney *U* test). (*C*) Analysis of apical and basal VNO layer volume distinguished by PDE4A immunostaining indicates a significant reduction in the apical VNO layer [*t* test, $t(46) = 3.975$; $^{***}P < 0.001$] and an increase in basal VNO layer [*t* test, $t(46) = 3.929$; $^{***}P < 0.001$] of cGαi2$^{-/-}$ ($n = 27$) vs. cGαi2$^{+/-}$ mice ($n = 21$). L, lumen; LP, lamina propria. Data are expressed as means ± SEM. (Scale bars, 50 μm.)

Gαi2 Is Required for Sensory Function of Apical VSNs. VSNs that detect small organic pheromones and steroid derivatives localize to the apical VNO and express V1Rs and Gαi2 (34–37). These neurons do not recognize peptides or proteins (16). To determine whether Gαi2 is required for sensory signaling in apical VSNs, we performed live-cell Ca^{2+} imaging by using dissociated cells (15, 16, 21) and acute VNO slices (33, 34, 38) in combination with the Ca^{2+} sensors GCaMP6f, fura-2/AM, or fluo-4/AM (Fig. 2 and *SI Appendix*, Fig. S2). We crossed *Gnai2*$^{fx/fx}$ *Omp*$^{cre/cre}$ and *Rosa26*-floxstop-GCaMP6f mice (*Methods*) to drive expression of GCaMP6f in *Omp*$^{+}$, *Gnai2*-deficient cells. As chemostimuli, we used nine single compounds (four small organic molecules and five sulfated steroids) or a mix of five sulfated steroids (*SI Appendix*, Fig. S2*A*). Subsets of VSNs from heterozygous controls responded reliably to each of these stimuli (Fig. 2 and *SI Appendix*, Fig. S2 *C–F*). By contrast, such responses were severely diminished or absent in cGαi2$^{-/-}$ VSNs (Fig. 2 and *SI Appendix*, Fig. S2 *C–F*). The response rates of cGαi2$^{-/-}$ VSNs for these ligands were close to those of *Trpc2*$^{-/-}$ VSNs (Fig. 2*B*), indicating a nearly complete loss of sensory function in the apical layer. Importantly, Ca^{2+} responses to a mix of four MHC-binding peptides, known to activate V2R/Gαo^{+} VSNs (19, 33, 38, 39), and high-K^{+} solution remained intact (Fig. 2). Responses to MHC peptides also remained unaffected in *Trpc2*$^{-/-}$ VSNs, consistent with previous results (40). Together, these data establish that Gαi2 is

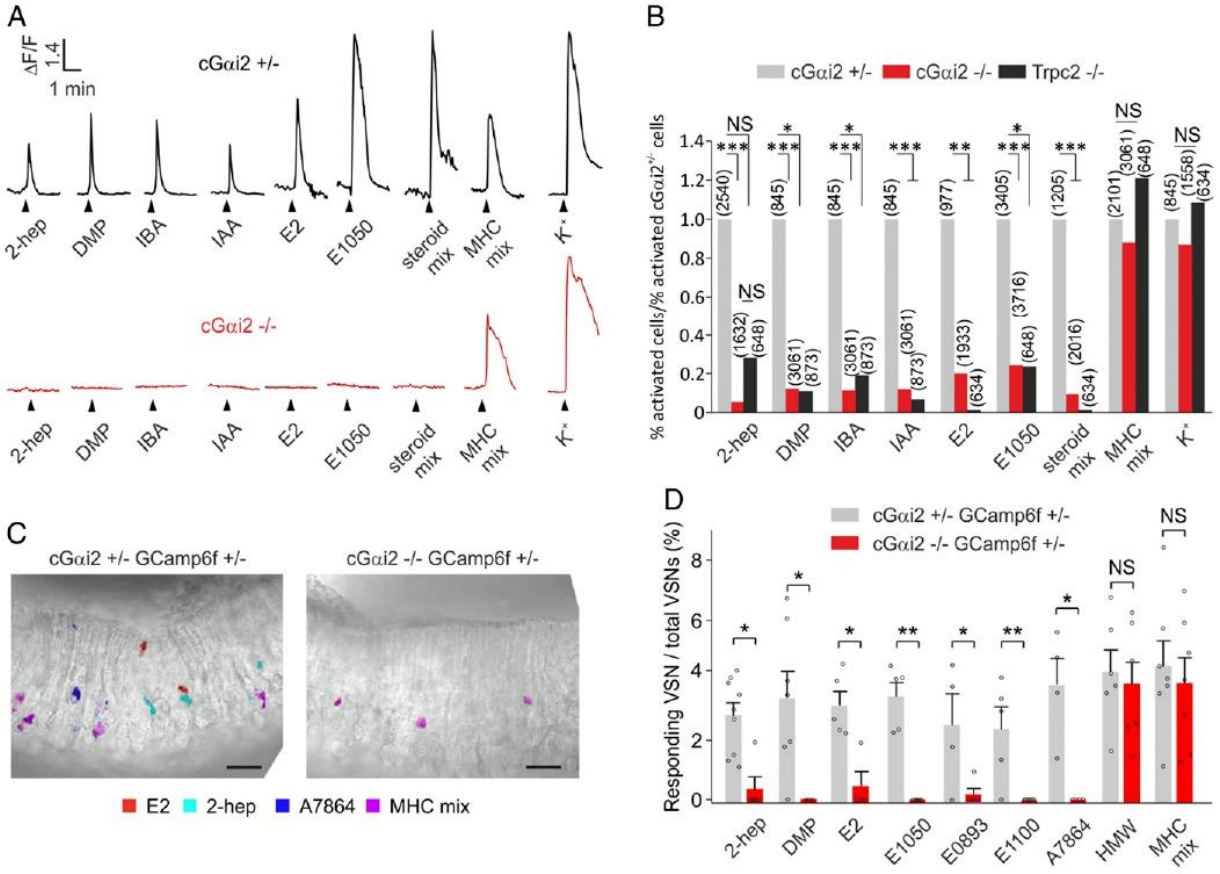

Fig. 2. Essential role of Gαi2 in molecular sensing by apical VSNs. (*A*) Representative Ca^{2+} responses imaged in dissociated VSNs from cGαi2$^{+/-}$ and cGαi2$^{-/-}$ mice. Cells were stimulated with the following stimuli known to activate V1R/Gαi2- or V2R/Gαo-expressing VSNs: 2-heptanone (2-hep, 10^{-8} M); dimethylpyrazine (DMP, 10^{-6} M); isobutylamine (IBA, 10^{-7} M); isoamylamine (IAA, 10^{-7} M); β-estradiol (E2, 1 μM); 1,3,5(10)-estratrien-3,17β-diol disulfate (E1050, 1 μM); sulfated steroid mix E1050, E1100 [1,3,5(10)-estratrien-3,17β-diol 3-sulfate], E0893 [1,3,5(10)-estratrien-3,17α-diol 3-sulfate], and A7864 (5-androsten-3β,17β-diol disulfate), 1 μM each; MHC peptide mix (MHC mix; SYFPEITHI, SYIPSAEKI, AAPDNRETF, SIINFEKL, 10^{-10} M each), and high (50 mM) KCl solution (K^{+}) as viability control. Note that cells from Gαi2$^{-/-}$ mice did not produce Ca^{2+} responses to the V1R ligands but did produce responses to the Gαo-dependent MHC peptide mix and high K^{+}. (*B*) Analysis of ligand-evoked Ca^{2+} responses in dissociated cells from cGαi2$^{+/-}$, cGαi2$^{-/-}$, and Trpc2$^{-/-}$ mice. Data are expressed as the percentage of responding cells to a given stimulus divided by the percentage of responding cells in the cGαi2$^{+/-}$ controls [$*P < 0.05$, $**P < 0.01$, $***P < 0.001$; nonsignificant (NS), $P = 0.07–0.63$, Fisher's exact test]. Number of cells analyzed is indicated above each bar. Each stimulus was tested in 3–16 mice. (*C*) Spatial activation patterns obtained through GCaMP6f imaging in cGαi2$^{+/-}$ and cGαi2$^{-/-}$ VNO slices. Slices were stimulated with the steroids E2 (1 μM; red) and A7864 (1 μM; blue), 2-hep (10^{-8} M; cyan), and MHC mix (SYFPEITHI, SYIPSAEKI, AAPDNRETF, SIINFEKL, 10^{-10} M each; magenta). Stimulus-induced ΔF peak images were digitally superimposed onto the transmitted light image of the same slice (*Methods*; original ΔF peak images are shown in *SI Appendix*, Fig. S2). VSNs in cGαi2$^{-/-}$ slices responded to the MHC peptide mix but not to agonists of apical VSNs. (Scale bar, 25 μm.) (*D*) Percentage of responding VSNs/total VSNs in Gαi2$^{-/-}$ slices is strongly diminished or reduced to zero with stimuli known to activate apical VSNs ($\chi^2 = 40.8$, $P < 0.001$, Kruskal–Wallis ANOVA; $*P < 0.05$, $**P < 0.01$, Mann–Whitney *U* test; $n = 2–3$ slices per mouse from 7 cGαi2$^{+/-}$ and 5 cGαi2$^{-/-}$ GCaMP6f mice). No significant difference in the detection of Gαo-dependent stimuli is observed between the two genotypes [HMW, $t(10) = 0.36$; NS, $P = 0.72$; MHC mix, $t(12) = 0.44$; NS, $P = 0.66$]. Dots indicate the percentage of responding/total VSNs in independent slice recordings. Stimuli were tested one to three times per slice. Each stimulus was tested in at least three mice. Data are expressed as means ± SEM.

required for VSN sensory transduction in the apical VNE layer and plays a central role in detecting small organic molecules and steroid derivatives.

Normal Male Sexual Behavior in Gαi2 Mutants. Trpc2$^{-/-}$ male mice exhibit pronounced alterations in sexual behavior, including elevated mounting and courtship behaviors toward other males (41, 42). To determine whether Gαi2 is also required for male sexual behavior, we first measured serum testosterone levels and the weight of sexual organs (testes, preputial glands, seminal vesicles), but found no significant differences between cGαi2$^{-/-}$ and cGαi2$^{+/-}$ males (*SI Appendix*, Fig. S3 *A* and *B*). We next analyzed sexual behaviors toward females in sexually naïve cGαi2$^{-/-}$ and cGαi2$^{+/-}$ males (*SI Appendix*, Fig. S3 *D–G*). cGαi2$^{-/-}$ and cGαi2$^{+/-}$ males displayed the same level of preference for estrous female urine volatiles and nonvolatiles (*SI Appendix*, Fig. S3*C*). We also scored the number of animals mounting an intruder (female, male, or castrated male) and the mounting episodes (*SI Appendix*, Fig. S3*D*). cGαi2$^{-/-}$ and cGαi2$^{+/-}$ males showed robust mounting and a short latency to mount females, but very rarely displayed sexual behavior toward male or castrated male intruders. Next, we scored the latency to mount female intruders and to ejaculate, and the total mating time (*SI Appendix*, Fig. S3 *E* and *F*). Latency to ejaculate and total mating time of cGαi2$^{-/-}$ males were statistically indistinguishable from those of cGαi2$^{+/-}$ males (P = 0.21–0.89). We further assessed male courtship behavior by measuring ultrasonic vocalizations at high frequencies (30–110 kHz) emitted by resident males. cGαi2$^{-/-}$ and cGαi2$^{+/-}$ males produced high numbers of vocalizations in response to female intruders, whereas few vocalizations were produced during male–male investigation, and there was no significant difference between genotypes (*SI Appendix*, Fig. S3*G*). Together, these findings reveal that cGαi2$^{-/-}$ males display normal sexual behaviors and sexual motivation.

Territorial Aggression Is Enhanced in Gαi2 Mutant Males. Conditional deletion of Gαo in VSNs eliminated male–male aggression (16). This effect could result from cooperation of Gαo and Gαi2 subsystems, or the Gαi2 subsystem could operate relatively independently, being dispensable for aggression and/or controlling a parallel aggression circuit. To distinguish between these hypotheses, we compared territorial aggression of adult cGαi2$^{-/-}$ male mice vs. age-matched cGαi2$^{+/-}$ males in the resident–intruder paradigm (15, 16) (Fig. 3*A*).

Surprisingly, the number of animals attacking an adult male intruder was significantly higher in cGαi2$^{-/-}$ (25 of 27 mice; 93%) vs. cGαi2$^{+/-}$ residents (15 of 23 mice; 65%; $P < 0.05$; Fig. 3*A*), but there was no difference in the intruder investigation time for each genotype (*SI Appendix*, Fig. S4*A*). Total attack duration in three consecutive 10-min trials was high in cGαi2$^{-/-}$ and cGαi2$^{+/-}$ males (130 and 78 s, respectively; $P < 0.05$), showing that Gαi2 is dispensable for the display of aggression. By contrast, castrated male intruders consistently induced less aggression in control cGαi2$^{+/-}$ male residents (37 s; 50% reduction; $P < 0.05$; Fig. 3*A*), whereas attack duration to castrated males was approximately threefold higher in cGαi2$^{-/-}$ residents (129 s; $P < 0.01$) and did not differ from the level of aggression to intact male intruders ($P = 0.8$). Thus, there was no loss of territorial aggression in cGαi2$^{-/-}$ male residents.

Previous work has shown that the HMW (>10 kDa) and LMW (< 10 kDa; includes small peptides) fractions of urine from adult male mice can induce aggression in male residents (15, 16). Therefore, we tested whether cGαi2$^{-/-}$ VSNs are capable of detecting these two fractions. We used Ca^{2+} imaging in cGαi2$^{-/-}$, cGαi2$^{+/-}$, and Trpc2$^{-/-}$ VSNs to record responses to whole urine and the HMW and LMW fractions (Fig. 3*B*). All fractions induced large responses in cGαi2$^{+/-}$ VSNs: 592 of 4,698 cells screened (12%) responded to urine, 250 of 4,698 to LMW fractions (5%), and 402 of 5,577 (7%) to HMW fractions. In cGαi2$^{-/-}$, urine responses were reduced by half (215 of 3,366 activated cells; 6%; $P < 0.001$) and LMW fraction responses by approximately 60% (74 of 3,366; 2%; $P < 0.001$), whereas HMW responses were identical or even slightly elevated (551 of 5,797; 9%; $P = 0.2$; Fig. 3*B*). We identified activated cells by combining Ca^{2+} imaging with post hoc immunostaining (*SI Appendix*, Fig. S2*B*) (15, 16) using antibodies against PDE4A and Gαo (Fig. 3*C*). The vast majority of cells activated by HMW were Gαo^{+} in cGαi2$^{-/-}$ and control VSNs. LMW fraction and castrated male urine activated Gαo^{+} and PDE4A^{+} control VSNs, but nearly all cGαi2$^{-/-}$ activated cells were negative for PDE4A (Fig. 3*C* and *SI Appendix*, Fig. S4*B*). Together, these results indicate that activation of the Gαo^{+} VSN subpopulation is sufficient to induce intermale aggression, irrespective of whether this aggression is promoted by HMW or LMW urine fractions or castrated male urine.

Increased Brain Activation to Male Intruder in Gαi2 Mutant Males. To strengthen these results, we mapped in vivo brain activation in nine distinct regions of the central nervous system implicated in aggression (26) by using immunodetection of the immediate early gene c-Fos. These analyses included subdivisions of the MeA [posterodorsal MeA (MeApd) and posteroventral MeA (MeApv) divisions] and VMH [dorsomedial VMH (VMHdm) and ventrolateral VMH (VMHvl)], the posteromedial part of the medial division of the BNST (BNSTmpm), medial preoptic area (MPOA), and lateral septum (LS). Nonstimulated cGαi2$^{-/-}$ and cGαi2$^{+/-}$ males showed equivalent levels of basal c-Fos activity in all nine brain regions (*SI Appendix*, Fig. S4*C*). Exposure to adult male intruders induced a significant increase in the number of c-Fos^{+} nuclei in three of these regions: MeApd, BNSTmpm, and LS (Fig. 3 *D* and *E*). We did not observe significant differences in some other regions implicated in aggression, such as the VMH (Fig. 3*E*).

Male–male aggression and male pheromones activate a specific subpopulation of MeA neurons that are GABAergic and positive for the androgen receptor (AR) (43, 44). We used double-label IHC for c-Fos and AR, GABA, calbindin (CB), or calretinin (CR) to identify the MeA neurons activated in our experiments. In cGαi2$^{-/-}$ and cGαi2$^{+/-}$ males, c-Fos^{+} nuclei largely colocalized with AR (Fig. 3 *F* and *G*) and GABA, but not with CB and CR (*SI Appendix*, Fig. S4*D*). Moreover, the proportion of c-Fos^{+} neurons positive for AR was even larger in cGαi2$^{-/-}$ males, whereas no change was observed in the absolute number of AR^{+} neurons (Fig. 3*G*). Therefore, conditional Gαi2 deletion resulted in increased neural activation of a population of GABAergic, AR^{+} neurons in the MeA following exposure to a male intruder.

Infant-Directed Aggression Is Diminished in Gαi2 Mutant Males, but Parental Behavior Is Enhanced. Infanticidal behavior in mice, in which an adult attacks and kills a pup, is observed in virgin adult male mice and depends strongly on a functional VNO (24, 25). We investigated infant-directed behavioral consequences of the Gαi2 deletion. We exposed virgin males to 1–2-d-old pups and found that the number of aggressive animals was drastically reduced, whereas attack latency was significantly increased in cGαi2$^{-/-}$ males vs. heterozygous controls ($P < 0.01$; Fig. 4 *A* and *B*). Moreover, two critical measures of parenting behavior—pup grooming and pup retrieval—were significantly increased in cGαi2$^{-/-}$ males ($P < 0.05$ and $P < 0.01$; Fig. 4*B*). Thus, the display of pup-directed aggression is strongly decreased, whereas parental behavior is enhanced, in Gαi2 mutant males.

We used Fos immunodetection to examine whether the lack of apical/Gαi2^{+} sensory inputs alters neural activity in aggression-controlling brain centers during infant-directed aggression (Fig.

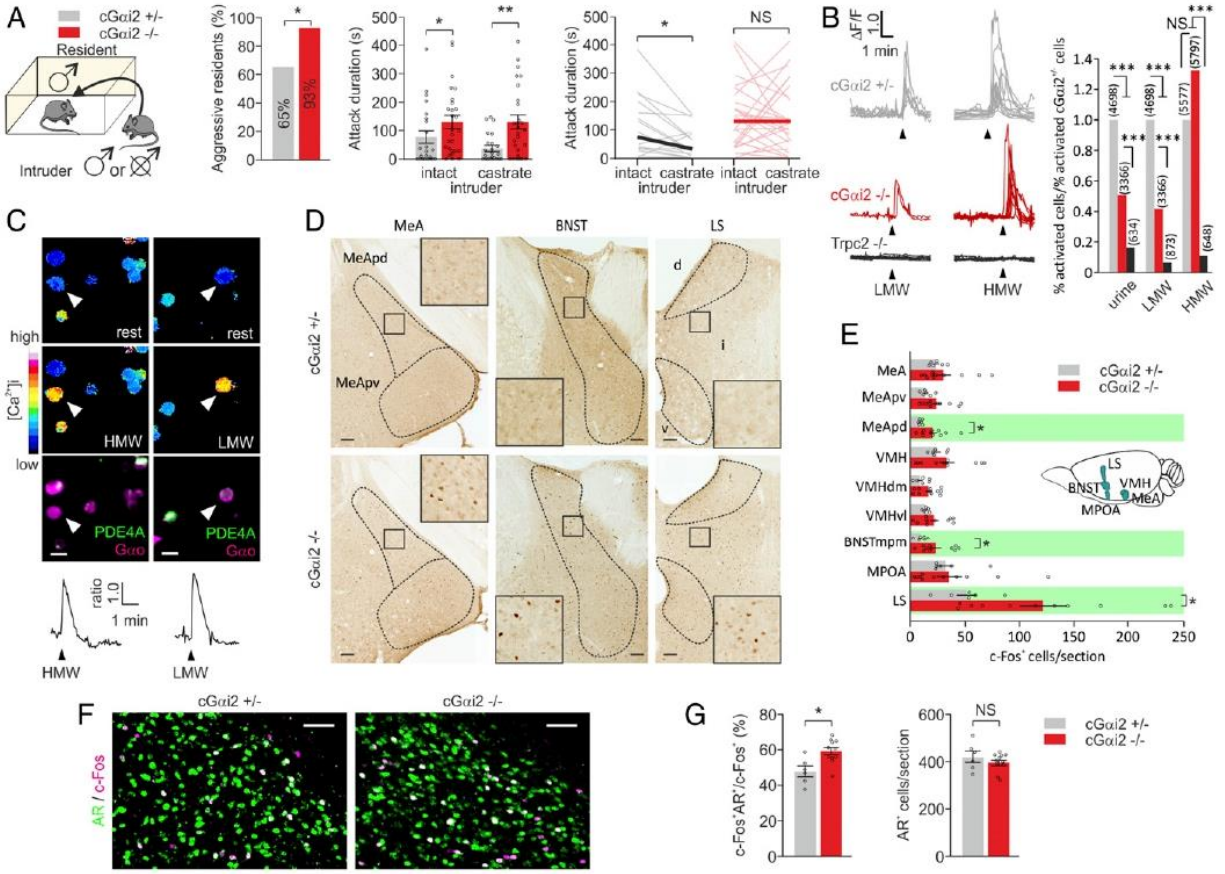

Fig. 3. Loss of Gαi2 enhances territorial aggression and increases activity in aggression-controlling brain centers. (*A*) Territorial aggression is enhanced in sexually experienced cGαi2$^{-/-}$ resident males exposed to intact and castrated intruders in the resident–intruder assay. Fifteen of 23 cGαi2$^{+/-}$ mice (65%) and 25 of 27 (93%) cGαi2$^{-/-}$ resident males were aggressive at least once during three consecutive resident–intruder trials to intact and castrated male intruders (*$P < 0.05$, Fisher's exact test). Cumulative attack duration was higher in cGαi2$^{-/-}$ residents (**$P < 0.01$ and *$P < 0.05$, Mann–Whitney *U* test). Comparison of cGαi2$^{+/-}$ residents' behavior toward gonadally intact vs. castrated intruders indicates the normal reduction in aggression toward a castrate (*$P < 0.05$, Wilcoxon test). This behavior is lost in the cGαi2$^{-/-}$ residents [nonsignificant (NS), $P = 0.8$, Wilcoxon test]. (*B*) Examples of Ca^{2+} transients (*Left*) imaged in dissociated VSNs of cGαi2$^{+/-}$, cGαi2$^{-/-}$, and Trpc2$^{-/-}$ mice stimulated with LMW (1:100) and HMW (1:100) fractions. Analysis of responding cells over total cGαi2$^{+/-}$ responding cells (*Right*) reveals reduced responsivity to urine (1:100) and LMW fraction in cGαi2$^{-/-}$ cells and a loss in Trpc2$^{-/-}$ cells (***$P < 0.001$; NS, $P = 0.2$, Fisher's exact test). Number of cells analyzed is indicated above each bar. Each stimulus was tested in 3–20 mice. (*C*) Fura-2 ratio imaging and post hoc IHC of cGαi2$^{-/-}$ cells indicate that cells activated by LMW and HMW fractions are Gαo^{+} and PDE4A^{-}. Time points of Ca^{2+} images show resting or peak fluorescence levels to stimulation with HMW or LMW fractions. Representative Ca^{2+} transients shown for imaged cells (white arrowheads) are indicated for each condition. (Scale bar, 10 μm.) (*D*) Examples of c-Fos activation in MeA, BNST, and LS of cGαi2$^{+/-}$ and cGαi2$^{-/-}$ male mice exposed to intact male intruder for 10 min. Dashed lines indicate the border of brain areas. Boxes are shown at higher magnification in the *Inset*. (Scale bars, 100 μm.) (*E*) Quantification of c-Fos^{+} cells per section in cGαi2$^{+/-}$ ($n = 6$) and cGαi2$^{-/-}$ residents ($n = 11$) after exposure to an intact intruder reveals an increase in c-Fos expression in MeApd, BNSTmpm, and LS of cGαi2$^{-/-}$ mice (marked in green; *$P < 0.05$; NS, $P = 0.15$–0.99, Mann–Whitney *U* test). (*F*) Gαi2 deletion resulted in increased c-Fos activation of a population of GABAergic, AR^{+} neurons in the MeApd following a 10-min exposure to an intact male intruder. (*G*) Percentage of c-Fos^{+} neurons expressing AR (*Left*) and number of AR^{+} cells per section (*Right*) in the MeApd after a 10-min exposure to an intact male intruder (*$P < 0.05$; NS, $P = 0.46$, Mann–Whitney *U* test). (Scale bars, 50 μm.) d, dorsal LS; i, intermediate LS; v, ventral LS. Data are expressed as means ± SEM.

4 *C* and *D*). We compared the density of c-Fos^{+} nuclei of cGαi2$^{-/-}$ males vs. cGαi2$^{+/-}$ males following pup exposure. In the granular layer of the anterior AOB, c-Fos^{+} cell density was significantly lower in parental cGαi2$^{-/-}$ males vs. aggressive cGαi2$^{+/-}$ male mice ($P < 0.001$; Fig. 4 *C* and *D*), consistent with reduced sensory input from the apical VNO in these mutants. Aggressive cGαi2$^{+/-}$ males also showed more c-Fos^{+} cells in the MeApv and MeApd compared with cGαi2$^{-/-}$ males, suggesting that Gαi2-dependent sensory inputs elicit MeA activation and infant-directed aggression. We also investigated the MPOA of the hypothalamus, a key region in the control of parenting behaviors (45). We observed specific activation during pup interactions in cGαi2$^{-/-}$ males, but this activation was absent in aggressive cGαi2$^{+/-}$ controls (Fig. 4 *C* and *D*). Importantly, our c-Fos mapping revealed significantly higher activation in the medial preoptic nucleus (MPO), the central region of MPOA, of cGαi2$^{-/-}$ males compared with parental controls ($P < 0.05$; Fig. 4 *C* and *D*). Thus, Gαi2-dependent VNO inputs seem to inhibit MPOA activation and subsequent parental behavior.

To identify the activated neurons in the MeA during pup-directed aggression and determine whether they belong to the same AR^{+}, GABAergic neurons activated during male–male aggression, we performed double-label IHC for c-Fos and AR. There was little overlap between c-Fos^{+} and AR^{+} nuclei in aggressive cGαi2$^{+/-}$ males (Fig. 4*E*). c-Fos^{+} nuclei also did not colocalize with CB^{+} or CR^{+} cells in the MeA (*SI Appendix*, Fig. S5).

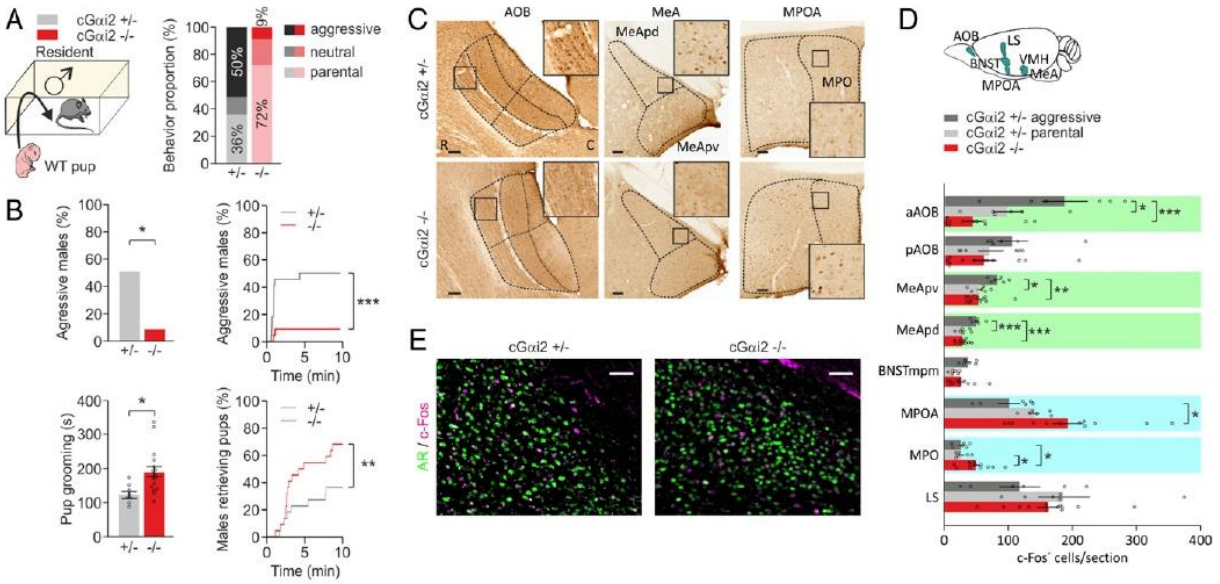

Fig. 4. cGαi2$^{-/-}$ male mice show diminished infant-directed aggression but enhanced parental behavior. (*A*) Comparison of pup-directed behavior of adult cGαi2$^{+/-}$ vs. cGαi2$^{-/-}$ male residents. Pups (WT) were used at postnatal days 1–2. Males attacked (aggressive), ignored (neutral), or retrieved neonates to the nest (parental behavior). cGαi2$^{-/-}$ males were predominantly parental (72%), whereas cGαi2$^{+/-}$ males attacked the pups (50%; $n = 22$ for each genotype). (*B*) Percentages of aggressive males (*$P < 0.05$, Fisher's exact test) and their latency to attack the neonates (***$P < 0.001$, Kolmogorov–Smirnov test), pup grooming times of the cGαi2$^{+/-}$ ($n = 8$) and cGαi2$^{-/-}$ residents ($n = 16$) that showed the behavior [t test: $t(22) = 2.73$, *$P < 0.05$], and percentage of males retrieving pups (**$P < 0.01$, Kolmogorov–Smirnov test). (*C*) Examples of c-Fos activation in AOB, MeA, and MPOA of cGαi2$^{+/-}$ and cGai2$^{-/-}$ males exposed to an alien pup for 10 min. Dashed lines indicate brain areas where c-Fos^{+} cells were counted. Boxes are shown at higher magnification in the *Inset*. C, caudal; R, rostral. (Scale bars, 100 μm.) (*D*) Quantification of c-Fos^{+} cells per section of aggressive cGαi2$^{+/-}$ ($n = 6$), parental cGαi2$^{+/-}$ ($n = 6$), and cGαi2$^{-/-}$ residents ($n = 12$) after exposure to an alien pup reveals increased c-Fos activation in aAOB, MeApd, and MeApv of aggressive cGαi2$^{+/-}$ males [aAOB, $F(2,21) = 10.72$, $P < 0.001$; MeApd, $F(2,21) = 13.98$, $P < 0.001$; MeApv, $F(2,21) = 6.075$, $P < 0.001$, ANOVA; *$P < 0.05$, **$P < 0.01$, ***$P < 0.001$, Tukey test; green]. Enhanced activation is observed in the MPOA (MPO) of cGαi2$^{-/-}$ males [MPOA, $F(2,21) = 5.236$, $P < 0.05$; MPO, $F(2,21) = 4.377$, $P < 0.05$, ANOVA; *$P < 0.05$, Tukey test; blue]. No significant differences are observed in other regions analyzed ($P = 0.06$–0.81, ANOVA). (*E*) Conditional Gαi2 deletion does not cause c-Fos activation of a population of GABAergic, AR^{+} neurons in the MeApd following a 10-min exposure to neonates. (Scale bar, 50 μm.) aAOB, anterior AOB; pAOB, posterior AOB. Data are expressed as means ± SEM.

Therefore, the MeA neurons activated during pup-directed aggression are distinct from those activated during male–male aggression. Together, these results provide strong support for a model in which Gαi2^{+} VSNs control infant-directed aggression by activation of specific aggression nodes that, in turn, inhibit parental-specific circuits.

Discussion

Our results show that the Gαi2^{+} population of VSNs controls important aspects of male–male and infant-directed aggression. We identify Gαi2 as the primary G protein α-subunit mediating the detection of small organic chemosignals by apical VSNs, most likely being responsible for activation of Trpc2 and subsequent Ca^{2+} entry downstream of V1R activation. Gαi2 is an abundant G protein expressed in major cognitive centers such as the cortex and is important for its development, and complete loss or reduction of Gαi2 signaling can result in defective social interaction, increased anxiety, and intellectual disability (27). Therefore, a global Gαi2 mutation may impede investigations of complex VNO-dependent social behaviors. Indeed, our results differ from a report that used global Gαi2-KO mice that exhibited reduced male–male aggression (23). The conditional, olfactory-restricted KO model developed here ablated Gαi2 only in *Omp*-expressing cells, indicating that the observed behavioral deficits depend on the olfactory system. *Omp* is highly expressed in mature sensory neurons of MOE and VNO (46). Although Gαi2 is also expressed in some sensory neurons of the MOE (47), Gαi2 does not seem to participate in known sensory signaling events (48). Our conditional KO mice showed no obvious defects in MOE or MOB morphology and odor-guided behaviors depending on a functional MOE, indicating that the behavioral phenotypes we observe are largely mediated by VNO function.

We found that conditional deletion of Gαi2 suppresses infanticidal behavior, consistent with a direct role of Gαi2 in the detection of pup odor. Furthermore, c-Fos mapping showed less activation in downstream brain areas of the Gαi2 vomeronasal pathway—aAOB and MeA—in Gαi2-deficient virgin male mice exposed to pups. Interestingly, Gαi2 mutant male mice became parental after contact with pups and showed elevated c-Fos in the MPOA, suggesting that this circuit may inhibit proparental MPOA neurons (49). Thus, infanticidal behavior seems to involve the activation of a dedicated circuit, rather than being merely a consequence of the inhibition of parenting behavior.

Our Gαi2 mutant males displayed high levels of male–male aggression, indicating that the Gαi2 subpopulation of VSNs is dispensable for triggering this behavior. Therefore, male–male and infant-directed aggression are initiated by different subsets of VSNs, suggesting that distinct accessory olfactory system circuits control the display of these two forms of aggression. Consistent with this, c-Fos analysis revealed the activation of different populations of MeA neurons in the context of each behavior. Many of these cells were positive for AR in the male–male aggression assay but negative for AR in the pup-directed aggression test. Because deletion of Gαo in the VNO eliminated male–male aggression (16), Gαo^{+} VSNs are probably the key drivers of aggression induced by LMW and HMW urine fractions. The LMW fraction, which includes peptides <10 kDa, is still partially

detected by VSNs from Gαi2-deficient mice, suggesting that LMW-induced aggression is controlled via detection of $G\alpha o^+$ VSNs. However, the $G\alpha o^+$ VSN population is unlikely to govern male–male aggression independently. Gαi2-deficient mice tended to be more aggressive to intact and castrated males, suggesting that $G\alpha i2^+$ VSNs can influence male–male aggression, perhaps by eliciting partial inhibition on Gαo- and/or MOE-dependent targets in limbic brain areas. Consistent with this, we observed higher c-Fos activation in the MeA, BNST, and LS of Gαi2-deficient mice when exposed to males. Similar roles for VNO signaling in inhibiting social behaviors have been observed for sexual behavior toward young conspecifics (50). Thus, $G\alpha o^+$ and $G\alpha i2^+$ VSN populations seem to interact reciprocally to modulate male–male aggression.

Interestingly, we found no difference between Gαi2-deficient males and their heterozygous controls in mounting behavior, indicating that $G\alpha i2^+$ VSNs are not required for mating motivation in males. These results, together with studies in Trpc2 and Gαo mutants (16, 41, 42), are consistent with a relatively minor role of the VNO in the display of male mating behavior. In *Trpc2* mutant mice, however, sex preference is strongly affected, as mutant males attempt to mate with males as frequently as with females (41, 42). By contrast, Gαi2 and Gαo mutant males showed a clear preference for females (ref. 16 and the present study), suggesting that both VNO layers interact to enable sex preference.

Taken together, our results suggest a role of Gαi2 as key element in the coupling of activated V1R receptors to the downstream signal transduction machinery. Downstream signaling has been proposed to occur via Gγ13 because of coexpression with Gαi2 (51). However, because of the absence of functional measurements at the cellular level and the complexity of behavioral phenotype interpretation of Gγ13-null mice—probably affected by a critical function of Gγ13 in MOE signaling and olfaction (52)—this role has not been confirmed thus far. It has been proposed that Gαi2 may also interact with formyl peptide receptors and canonical olfactory receptors, which are mostly expressed in the apical layer of the VNO (53–55). Notably, VSNs expressing *Olfr692* seem to be activated by odors emanating from pups, especially in virgin males, suggesting a potential *Olfr692* role in infant-directed aggression (56). However, *Olfr692* is expressed in basal $G\alpha o^+$ VSNs (56), and no direct functional link has been yet established between *Olfr692* and infanticide. A recent report linked infant-derived chemosensory activity with seven vomeronasal receptors, including three V1Rs and four V2Rs, two of which (Vmn2r65 and Vmn2r88) seem to be partially implicated in infanticide (57). Together with our findings, these results support a non–labeled-line model for infant-directed aggression in which information sensed by apical and basal VSN populations is integrated to generate an aggressive response.

In conclusion, we showed here an essential role of Gαi2 in VNO sensory signaling of the apical VSN population that detects small organic molecules including volatile pheromones and steroid derivatives. Our study identifies $G\alpha i2^+$ VSNs as a critical neural component that organizes and balances male–male and infant-directed aggression. These results provide a framework for dissecting the neuronal networks underlying different forms of social aggression.

Methods

Animal care and experimental procedures were performed in accordance with French, German, and European guidelines on the protection of animals used for scientific purposes and approved by an ethical committee for animal experimentation (Comité d'Etique en Expérimentation Animale Val de Loire and Animal Welfare Committee of Saarland University School of Medicine). Mice were kept under standard 12-h light/dark cycles with food and water ad libitum.

Generation of Conditional Gαi2-Deficient Mice. $Gnai2^{fx/fx}$ mice (mixed 129sv × C57BL/6 background) were crossed to mice carrying a transgene directing the expression of Cre recombinase under the control of the *Omp* promoter [*Omp*-Cre mice; B6; 129P2-$Omp^{tm4(cre)Mom}$/MomJ; Jackson Laboratory, JR 006668; backcrossed into C57BL6/J for eight generations; neomycin cassette absent]. $Gnai2^{fx/fx}$ mice carry *loxP* sites inserted into the introns that flank exons 2 and 4. Breeding established offspring ($cG\alpha i2^{-/-}$) that were homozygous for the floxed *Gnai2* alleles and heterozygous for Cre and *Omp* ($Gnai2^{fx/fx}$ $Omp^{cre/+}$). In these mice, Cre-mediated *Gnai2* deletion was restricted to *Omp*-positive cells. Animals heterozygous for both alleles ($Gnai2^{fx/+}$ $Omp^{cre/+}$) served as controls ($cG\alpha i2^{+/-}$). Homozygous mice containing the Rosa-CAG-LSL-GCaMP6f::ΔNeo conditional allele [B6;129S-*Gt (ROSA)26Sor*$^{tm95.1(CAG-GCaMP6f)Hze}$/J; Jackson Laboratory] were crossed with $Gnai2^{fx/fx}$ to produce mice homozygous for Rosa-CAG-LSL-GCaMP6f::ΔNeo and floxed *Gnai2* alleles. These mice were crossed with homozygous $Gnai2^{fx/fx}$ $Omp^{cre/cre}$ mice to yield mice homozygous for the floxed *Gnai2* allele and heterozygous for Cre, *Omp*, and GCaMP6f ($cG\alpha i2^{-/-}$ $GCaMP6f^{+/-}$). Animals heterozygous for all alleles ($Gnai2^{fx/+}$ $Omp^{cre/+}$ $GCaMP6f^{fx/+}$) served as controls ($cG\alpha i2^{+/-}$ $GCaMP6f^{+/-}$). $Trpc2^{-/-}$ (129S6.129P2-*Trpc2* < *tm1Mom*>/MomJ; Jackson Laboratory, JR 007890; backcrossed into C57BL/6J for six generations) (58) were used for Ca^{2+} imaging in dissociated VSNs. Adults males (8–12 wk) were used.

Immunostaining. Mice were anesthetized by an overdose of pentobarbital (Ceva) and perfused transcardially with 0.9% saline solution followed by 0.1 M phosphate buffer (PB) containing 4% paraformaldehyde (PFA). For c-Fos experiments, mice were perfused 90 min after a 10-min interaction with an intact male or a neonate. Brains, VNOs, and MOEs were removed, post-fixed overnight in 4% PFA, and cryoprotected in 0.1 M PB containing 30% sucrose. Samples were embedded in Tissue-Tek O.C.T. compound, snap-frozen in cold isopentane, and processed on a Leica CM 3050S cryostat. Brains and OBs were cut in 30-μm serial free-floating sections (coronal for brains, sagittal for OB) by using Tris-buffered saline (TBS) solution containing 0.1% sodium azide. Coronal cryosections of olfactory tissues (12-μm thick) were directly mounted on SuperFrost Plus glass slides. Sections were washed (3 × 5 min) with TBS, incubated in blocking solution (TBS solution containing 0.1% Triton X-100 and 5% horse serum) for 2 h at room temperature (RT), incubated overnight at 4 °C in blocking solution supplemented with the primary antibody, and washed in TBS solution and incubated in blocking solution supplemented with secondary antibody for 2 h at RT. Nuclei were counterstained with DAPI (0.5 μg/mL; Sigma) for 5 min. For c-Fos experiments, endogenous peroxidases were blocked for 30 min in TBS solution containing 3% H_2O_2 before the serum blocking step, biotinylated secondary antibody was used, and signals were amplified with Vectastain ABC kit (Vector) and visualized with diaminobenzidine (0.02%, 0.01% H_2O_2 in 0.05 M Tris, pH 7.4). Detailed information about the antibodies used is listed in *SI Appendix*, Table S1. VNO cell density, VNO layer, and AOB volume quantifications were done from images acquired on an Olympus IX71 microscope coupled to a Hamamatsu C10600-10B camera at 10× magnification. Images were analyzed with Fiji/ImageJ [National Institutes of Health (NIH)]. Twenty-five slices of VNO from adult males (five of each genotype) were used. Demarcations of apical vs. basal layers were based on PDE4A immunoreactivity, and $DAPI^+$ cells were counted by using the particle analyzer plugin of Fiji. AOB rostrocaudal demarcation was based on Gαo immunoreactivity from 29 slices from 14 animals per genotype. Tissue volume in cubic micrometers was calculated by multiplying the surface of the immunoreactive area by the thickness of the slice. For c-Fos experiments, slices were scanned by using an automatic slide scanner (AxioScan.Z1; Zeiss). Regions of interest (ROIs) were drawn based on the Paxinos mouse brain atlas by using Zen (blue edition 3.0; Zeiss), and the number of $c\text{-}Fos^+$ cells was automatically counted bilaterally in these regions by using the particle analyzer plugin of Fiji. Numbers of slices counted per animal and region were one for the MPOA and LS; two for AOB, BNST, and VMH; and four for MeA. AR/c-Fos coexpression was quantified in five to eight MeApd images per animal acquired on a Zeiss LSM-700 confocal laser-scanning microscope at 20× magnification. Image regions were analyzed in the entire *z* axis with 3-μm step intervals, and images were reconstituted by using the maximum-intensity projection tool of Zen software. $c\text{-}Fos^+$, AR^+, and $AR/c\text{-}Fos^+$ cells were counted automatically by using the particle analyzer plugin of Fiji.

For combined Ca^{2+} imaging and immunocytochemistry, dissociated VNO cells were fixed by using PBS solution containing 4% PFA (10 min), permeabilized and incubated for 10 min in blocking solution (TST, i.e., 0.1% Triton X-100, 1% FBS, 50 mM NaCl, 100 mM Tris·HCl, pH 7.5), incubated with anti-PDE4A (1:500; 30 min, RT) and anti-Gαo (1:50; 30 min, RT), and washed in TST (5 min), followed by an incubation (30 min, RT) in secondary

NEUROSCIENCE

antibodies (Alexa Fluor 488 goat anti-rabbit, Alexa Fluor 647 goat anti-mouse, 1:500; Invitrogen). Cells were also stained (5 min, RT) with DAPI.

Quantitative RT-PCR. VNOs and MOEs were dissected from cGαi2$^{+/-}$ and cGαi2$^{-/-}$ mice. Pools of VNO or MOE from three animals were established from a total of 21 VNOs and 9 MOEs per genotype. RNA in each pool was isolated with PureLink RNA Mini Kit (Invitrogen). cDNA was synthesized from 1 μg of total RNA by using a Superscript III First-Strand Synthesis System for RT-PCR (Invitrogen). Quantitative PCRs were performed on a CFX96 Touch Real-Time PCR Detection System (Bio-Rad) using SsoAdvanced Universal SYBR green Supermix (Bio-Rad). PCR conditions for all primers were 95 °C for 3 min followed by 39 cycles (95 °C for 10 s, 60 °C for 30 s). PCR specificity was verified by melting curve analysis. Expression of *Hprt-1*, *Omp*, *Gnai2*, and *Gnao* mRNAs were assessed. Each sample was run in triplicate, and data were analyzed with the CFX Manager 3.0 Software (Bio-Rad) normalized to *Hprt-1* expression level to obtain a ΔCt and expressed as $2^{\Delta Ct}$. VNO cDNAs were used to assess *V1re6*, *V1re2*, *V1rf3*, *V1rj2*, *Vmn2r1*, *Vmn2r65*, *Trpc2*, and *Plcb2* expression by endpoint PCR with GoTaq G2 Master Mix. Primer sequences are shown in *SI Appendix*, Table S2. PCR conditions for all primers were 95 °C for 3 min, followed by 39 cycles (95 °C for 45 s, 58 °C for 30 s, and 72 °C for 60 s), and 72 °C for 10 min. Products were run on a 1% agarose gel.

Ca^{2+} Imaging. Ca^{2+} imaging of freshly dissociated VSNs was performed as described previously (15, 16). VNO epithelium was detached from the cartilage and minced in PBS solution at 4 °C. The tissue was incubated (20 min at 37 °C) in PBS solution supplemented with papain (0.22 U/mL) and DNase I (10 U/mL; Fermentas), gently extruded in DMEM (Invitrogen) supplemented with 10% FBS, and centrifuged at 100 × *g* (5 min). Dissociated cells were plated on coverslips previously coated with concanavalin-A type V (0.5 mg/mL, overnight at 4 °C; Sigma). Cells were used immediately for imaging after loading them with fluo-4/AM or fura-2/AM (5 μM; Invitrogen) for 60 min. Coverslips containing VSNs were placed in a laminar-flow chamber (Warner Instruments) and constantly perfused at 22 °C with extracellular solution HBSS (Invitrogen) supplemented with 10 mM Hepes (2-[4-(2-hydroxyethyl) piperazin-1-yl]ethanesulfonic acid). Cells were alternately illuminated at 470 nm for fluo-4 or at 340 and 380 nm for fura-2 imaging, and light emitted above 510 nm was recorded by using a Hamamatsu C10600-10B camera installed on an Olympus IX71 microscope. Images were acquired at 0.25 Hz and analyzed by using ImageJ (NIH), including background subtraction, ROI detection, and signal analyses. ROIs were selected manually and always included the whole cell body. Peak signals were calculated from the temporal profiles of image ratio/fluorescent values. Results are based on recordings from at least three mice for each condition and genotype.

VNO tissue slices were prepared from male cGαi2$^{+/-}$ GCaMP6f$^{+/-}$ and cGαi2$^{-/-}$ GCaMP6f$^{+/-}$ mice by using slicing procedures established previously (33, 34, 39). Briefly, mice were euthanized with CO_2, followed by decapitation. VNOs were quickly removed and submerged in oxygenated extracellular solution 1 (95% O_2/5% CO_2) containing (in mM): 120 NaCl, 25 $NaHCO_3$, 5 KCl, 5 BES, 1 $MgSO_4$, 1 $CaCl_2$, and 10 mM glucose (300 mOsm). The vomer bones were removed, the VNO was embedded in 3% low-gelling temperature agarose, and coronal slices (250 μm) were cut on a vibratome (Microm HM 650 V). VNO tissues slices were imaged by using an upright scanning confocal microscope (LSM 880 Indimo; Zeiss) equipped with a 20 × 1.0 N.A. Plan-Apochromat water-immersion objective and a standard Argon laser for excitation at a wavelength of 488 nm (GCaMP6f excitation). Emitted fluorescence was collected between 500 and 550 nm. All scanning head settings were kept constant during each experiment. Optical sections were ∼7 μm thick. All scanning head settings (i.e., gain, black level, detector aperture, and laser neutral density filter) were kept constant during each experiment. GCaMP6 fluorescence changes are expressed as relative fluorescence changes, i.e., ΔF/F0 (F0 was the average of the fluorescence values 10 s before stimulation). Images were acquired at 1 Hz and analyzed by using a combination of Zen (Zeiss), ImageJ (NIH), and Igor (Wavemetrics) software. To identify and mark responding VSNs, ΔF images (F–F0) were overlaid onto transmitted light images (Fig. 2C) by using Adobe Photoshop's difference tool and slightly adjusting the exposure settings. Original ΔF images of ligand-induced VSN responses are shown in *SI Appendix*, Fig. S2*D*. VNO slices were stimulated successively and in random order by using bath application. The following criteria for stimulus-induced Ca^{2+} responses were applied. (*i*) A response was defined as a stimulus-dependent deviation of GCaMP6f fluorescence that exceeded twice the SD of the mean of the baseline fluorescence noise. (*ii*) Cells showing a response to control buffer were excluded from analysis. (*iii*) A response had to occur within 1 min after stimulus application. In time-series experiments, ligand application was repeated to confirm the repeatability of a given Ca^{2+} response.

Chemostimulation. Chemostimuli for Ca^{2+} imaging were freshly prepared each day and diluted in extracellular solution to give the following final concentrations: urine and HMW and LMW fractions, 1:100 dilution; 2-heptanone, 10^{-8} M (Sigma); 2,5-dimethylpyrazine, 10^{-6} M (Sigma); isobutylamine, 10^{-7} M (Sigma); isoamylamine, 10^{-7} M (Sigma); β-estradiol, 1 μM (E2, Sigma); 1,3,5 (10)-estratrien-3,17β-diol disulfate, 1 μM (E1050; Steraloid or Sigma); 1,3,5 (10)-estratrien-3,17β-diol 3-sulfate, 1 μM (E1100; Steraloid or Sigma); 1,3,5(10)-estratrien-3,17α-diol 3-sulfate, 1 μM (E0893; Steraloid); A7864, 1 μM (5-androsten-3β,17β-diol disulfate; Steraloid); sulfated estrogen mix (E mix) E1050, E1100, E0893, and A7864, each 1 μM; MHC peptide mix SYFPEITHI, SYIPSAEKI, AAPDNRETF, SIINFEKL, 10^{-10} M each (Genscript); and KCl, 50 mM or 60 mM (slice experiments). Sulfated estrogens were initially prepared in DMSO and further diluted in extracellular solution. C57BL/6 males (8–12 wk old; Janvier) served as urine donors. Animals were sexually naïve and were kept group-housed. Equal volumes of freshly collected urine from at least three animals were pooled. To obtain urine fractions, 0.5 mL of fresh urine was size-fractionated by centrifugation (14,000 × *g* for 30 min) by using Microcon (Millipore) or Nanosep (Pall) 10-kDa molecular mass cutoff ultrafiltration columns. The centrifugation supernatant was the LMW fraction, and, to obtain HMW fraction, the retentate was washed with 0.5 mL PBS solution three times and resuspended in 0.5 mL of PBS or oxygenated extracellular solution.

Behavioral Testing. Males were individually housed for 1 wk before testing. Mice were moved to the experimental room 2 h before testing. Assays were conducted 2 h before the start of the dark period.

Resident–intruder male–male aggression assay. Sexually experienced male mice of each genotype (23 cGαi2$^{+/-}$ and 27 cGαi2$^{-/-}$) were tested for territorial aggression. Testing lasted 10 min and began when a sexually inexperienced, gonadally intact, group-housed adult male (i.e., intruder) was placed into the home cage of the test mouse (i.e., resident), whose bedding had not been changed for at least 4 d. Each resident was exposed three times (on consecutive days) to a gonadally intact intruder. After 1 wk, the experiments were repeated with a castrated intruder. Juvenile (postnatal day 18–22) males were castrated under isoflurane general anesthesia and used in adulthood. Residents were not exposed twice to the same intruder. Aggressive behavior was defined as lunging, biting, chasing, tail rattling, wrestling, and kicking. Attack bouts were defined as a succession of aggressive events separated by <3 s. Cumulative attack duration of three consecutive tests, investigation time of the intruder, and number of mounting episodes were scored.

Pup-directed behaviors. Twenty-two sexually naïve males of each genotype were tested for behavior in the presence of an alien 1–2-d-old neonate (C57BL/6 WT) introduced into the home cage of the test mouse for 10 min. To minimize handling and stress to the pups, one single pup was taken from the nest immediately before the test, avoiding prolonged exposure to cold. If harmed, the pup was immediately removed and killed to minimize suffering and to avoid cannibalizing without previous killing. Mice were categorized as aggressive if they presented aggressive behavior (e.g., biting, killing) toward a pup, as parental if they retrieved a pup into their nest, and as neutral if they were indifferent to a pup. Latencies to attack a pup and pup grooming time were scored.

Statistics. Statistical analyses were performed by using GraphPad Prism 7.0 (GraphPad Software), OriginPro 2016G, and OriginPro 2017G (OriginLab). Assumptions of normality and homogeneity of variance were tested before conducting the following statistical approaches. Student's *t* test was used to measure the significance of the differences between two distributions. In case the results failed the test of normality, a Mann–Whitney *U* test was performed. For paired data comparisons, we used the Wilcoxon signed-ranks test, and, for categorical data, we used the Fisher's exact test. Multiple groups were compared by using a one-way or two-way ANOVA with Tukey's multiple comparison test as a post hoc comparison or Kruskal–Wallis ANOVA for nonnormal distributions. The probability of error level (i.e., α) was chosen to be 0.05. Unless otherwise stated, results are presented as means ± SEM and documentation of individual data points.

Further details on testosterone measurements, stimulus delivery, and other behavioral tests are provided in *SI Appendix, Materials and Methods*. The datasets generated and/or analyzed during the present study are available from the Data Inra Dataverse portal (https://data.inra.fr/).

ACKNOWLEDGMENTS. We thank Roberto Tirindelli for V2R2 antibody; Michael Konzmann, Kevin Poissenot, and Chantal Porte for technical assistance; Kerstin Becker, Lisa-Marie Knieriemen, Deborah Crespin, and Aurelie Gasnier for mouse

husbandry; Marie-Claire Blache for help with imaging experiments; and Anne-Lyse Lainé for help with hormone assays. This work was supported by Deutsche Forschungsgemeinschaft Grants Sonderforschungsbereich 894 Project A17 (to F.Z. and T.L.-Z.) and INST 256/427-1 FUGB (to T.L.-Z.), Institut National de la Recherche Agronomique (INRA) "Physiologie Animale et Systèmes d'Elevage" department (P.C.); National Institutes of Health Intramural Research Program Project Z01-ES-101643 (to L.B.); and a grant from the University of Tours and Region Centre Val de Loire (to A.-C.T.).

1. Scott JP (1966) Agonistic behavior of mice and rats: A review. *Am Zool* 6:683–701.
2. Hrdy SB (1979) Infanticide among animals: A review, classification, and examination of the implications for the reproductive strategies of females. *Ethol Sociobiol* 1:13–40.
3. McCarthy MM, Vom Saal FS (1986) Inhibition of infanticide after mating by wild male house mice. *Physiol Behav* 36:203–209.
4. Chamero P, Leinders-Zufall T, Zufall F (2012) From genes to social communication: Molecular sensing by the vomeronasal organ. *Trends Neurosci* 35:597–606.
5. Liberles SD (2014) Mammalian pheromones. *Annu Rev Physiol* 76:151–175.
6. Brennan PA, Keverne EB (2004) Something in the air? New insights into mammalian pheromones. *Curr Biol* 14:R81–R89.
7. Mohrhardt J, Nagel M, Fleck D, Ben-Shaul Y, Spehr M (2018) Signal detection and coding in the accessory olfactory system. *Chem Senses* 43:667–695.
8. Shinohara H, Asano T, Kato K (1992) Differential localization of G-proteins Gi and Go in the accessory olfactory bulb of the rat. *J Neurosci* 12:1275–1279.
9. Jia C, Halpern M (1996) Subclasses of vomeronasal receptor neurons: Differential expression of G proteins (Gi alpha 2 and G(o alpha)) and segregated projections to the accessory olfactory bulb. *Brain Res* 719:117–128.
10. Berghard A, Buck LB (1996) Sensory transduction in vomeronasal neurons: Evidence for G alpha o, G alpha i2, and adenylyl cyclase II as major components of a pheromone signaling cascade. *J Neurosci* 16:909–918.
11. Dulac C, Axel R (1995) A novel family of genes encoding putative pheromone receptors in mammals. *Cell* 83:195–206.
12. Matsunami H, Buck LB (1997) A multigene family encoding a diverse array of putative pheromone receptors in mammals. *Cell* 90:775–784.
13. Ryba NJ, Tirindelli R (1997) A new multigene family of putative pheromone receptors. *Neuron* 19:371–379.
14. Herrada G, Dulac C (1997) A novel family of putative pheromone receptors in mammals with a topographically organized and sexually dimorphic distribution. *Cell* 90:763–773.
15. Chamero P, et al. (2007) Identification of protein pheromones that promote aggressive behaviour. *Nature* 450:899–902.
16. Chamero P, et al. (2011) G protein G(alpha)o is essential for vomeronasal function and aggressive behavior in mice. *Proc Natl Acad Sci USA* 108:12898–12903.
17. Hattori T, et al. (2016) Self-exposure to the male pheromone ESP1 enhances male aggressiveness in mice. *Curr Biol* 26:1229–1234.
18. Kaur AW, et al. (2014) Murine pheromone proteins constitute a context-dependent combinatorial code governing multiple social behaviors. *Cell* 157:676–688.
19. Leinders-Zufall T, et al. (2014) A family of nonclassical class I MHC genes contributes to ultrasensitive chemodetection by mouse vomeronasal sensory neurons. *J Neurosci* 34:5121–5133.
20. Oboti L, et al. (2014) A wide range of pheromone-stimulated sexual and reproductive behaviors in female mice depend on G protein Gαo. *BMC Biol* 12:31.
21. Pérez-Gómez A, et al. (2015) Innate predator odor aversion driven by parallel olfactory subsystems that converge in the ventromedial hypothalamus. *Curr Biol* 25:1340–1346.
22. Novotny M, Harvey S, Jemiolo B, Alberts J (1985) Synthetic pheromones that promote inter-male aggression in mice. *Proc Natl Acad Sci USA* 82:2059–2061.
23. Norlin EM, Gussing F, Berghard A (2003) Vomeronasal phenotype and behavioral alterations in G alpha i2 mutant mice. *Curr Biol* 13:1214–1219.
24. Wu Z, Autry AE, Bergan JF, Watabe-Uchida M, Dulac CG (2014) Galanin neurons in the medial preoptic area govern parental behaviour. *Nature* 509:325–330.
25. Tachikawa KS, Yoshihara Y, Kuroda KO (2013) Behavioral transition from attack to parenting in male mice: A crucial role of the vomeronasal system. *J Neurosci* 33:5120–5126.
26. Trainor BC, Sisk CL, Nelson RJ (2009) Hormones and the development and expression of aggressive behavior. *Hormones, Brain and Behavior*, eds Pfaff DW, Arnold AP, Etgen AM, Fahrbach SE, Rubin RT (Academic, San Diego), 2nd Ed, pp 167–205.
27. Hamada N, et al. (2017) Role of a heterotrimeric G-protein, Gi2, in the corticogenesis: Possible involvement in periventricular nodular heterotopia and intellectual disability. *J Neurochem* 140:82–95.
28. Rudolph U, et al. (1995) Ulcerative colitis and adenocarcinoma of the colon in G alpha i2-deficient mice. *Nat Genet* 10:143–150.
29. Ustyugova IV, Zhi L, Abramowitz J, Birnbaumer L, Wu MX (2012) IEX-1 deficiency protects against colonic cancer. *Mol Cancer Res* 10:760–767.
30. Li J, Ishii T, Feinstein P, Mombaerts P (2004) Odorant receptor gene choice is reset by nuclear transfer from mouse olfactory sensory neurons. *Nature* 428:393–399.
31. Weiss J, et al. (2011) Loss-of-function mutations in sodium channel Nav1.7 cause anosmia. *Nature* 472:186–190.
32. Tanaka M, Treloar H, Kalb RG, Greer CA, Strittmatter SM (1999) G(o) protein-dependent survival of primary accessory olfactory neurons. *Proc Natl Acad Sci USA* 96:14106–14111.
33. Leinders-Zufall T, et al. (2004) MHC class I peptides as chemosensory signals in the vomeronasal organ. *Science* 306:1033–1037.
34. Leinders-Zufall T, et al. (2000) Ultrasensitive pheromone detection by mammalian vomeronasal neurons. *Nature* 405:792–796.
35. Isogai Y, et al. (2011) Molecular organization of vomeronasal chemoreception. *Nature* 478:241–245.
36. Haga-Yamanaka S, et al. (2014) Integrated action of pheromone signals in promoting courtship behavior in male mice. *eLife* 3:e03025.
37. Del Punta K, et al. (2002) Deficient pheromone responses in mice lacking a cluster of vomeronasal receptor genes. *Nature* 419:70–74.
38. Leinders-Zufall T, Ishii T, Mombaerts P, Zufall F, Boehm T (2009) Structural requirements for the activation of vomeronasal sensory neurons by MHC peptides. *Nat Neurosci* 12:1551–1558.
39. Sturm T, et al. (2013) Mouse urinary peptides provide a molecular basis for genotype discrimination by nasal sensory neurons. *Nat Commun* 4:1616.
40. Kelliher KR, Spehr M, Li XH, Zufall F, Leinders-Zufall T (2006) Pheromonal recognition memory induced by TRPC2-independent vomeronasal sensing. *Eur J Neurosci* 23:3385–3390.
41. Leypold BG, et al. (2002) Altered sexual and social behaviors in trp2 mutant mice. *Proc Natl Acad Sci USA* 99:6376–6381.
42. Stowers L, Holy TE, Meister M, Dulac C, Koentges G (2002) Loss of sex discrimination and male-male aggression in mice deficient for TRP2. *Science* 295:1493–1500.
43. Hong W, Kim D-W, Anderson DJ (2014) Antagonistic control of social versus repetitive self-grooming behaviors by separable amygdala neuronal subsets. *Cell* 158:1348–1361.
44. Blake CB, Meredith M (2011) Change in number and activation of androgen receptor-immunoreactive cells in the medial amygdala in response to chemosensory input. *Neuroscience* 190:228–238.
45. Numan M (1974) Medial preoptic area and maternal behavior in the female rat. *J Comp Physiol Psychol* 87:746–759.
46. Margolis FL (1980) A marker protein for the olfactory chemoreceptor neuron. *Proteins of the Nervous System* (Raven Press, New York), pp 59–84.
47. Ibarra-Soria X, Levitin MO, Saraiva LR, Logan DW (2014) The olfactory transcriptomes of mice. *PLoS Genet* 10:e1004593.
48. Scholz P, et al. (2016) Identification of a novel Gnao-mediated alternate olfactory signaling pathway in murine OSNs. *Front Cell Neurosci* 10:63.
49. Kohl J, Autry AE, Dulac C (2017) The neurobiology of parenting: A neural circuit perspective. *BioEssays* 39:1–11.
50. Ferrero DM, et al. (2013) A juvenile mouse pheromone inhibits sexual behaviour through the vomeronasal system. *Nature* 502:368–371.
51. Liu Q, Li S, Lu C, Yu CR, Huang L (2018) G protein γ subunit Gγ13 is essential for olfactory function and aggressive behavior in mice. *Neuroreport* 29:1333–1339.
52. Li F, et al. (2013) Heterotrimeric G protein subunit Gγ13 is critical to olfaction. *J Neurosci* 33:7975–7984.
53. Liberles SD, et al. (2009) Formyl peptide receptors are candidate chemosensory receptors in the vomeronasal organ. *Proc Natl Acad Sci USA* 106:9842–9847.
54. Rivière S, Challet L, Fluegge D, Spehr M, Rodriguez I (2009) Formyl peptide receptor-like proteins are a novel family of vomeronasal chemosensors. *Nature* 459:574–577.
55. Lévai O, Feistel T, Breer H, Strotmann J (2006) Cells in the vomeronasal organ express odorant receptors but project to the accessory olfactory bulb. *J Comp Neurol* 498:476–490.
56. Nakahara TS, et al. (2016) Detection of pup odors by non-canonical adult vomeronasal neurons expressing an odorant receptor gene is influenced by sex and parenting status. *BMC Biol* 14:12.
57. Isogai Y, et al. (2018) Multisensory logic of infant-directed aggression by males. *Cell* 175:1827–1841.e17.
58. Bleymehl K, et al. (2016) A sensor for low environmental oxygen in the mouse main olfactory epithelium. *Neuron* 92:1196–1203.

PNAS
www.pnas.org

Supplementary Information for

Central role of G protein Gαi2 and Gαi2+ vomeronasal neurons in balancing territorial and infant-directed aggression of male mice

Anne-Charlotte Trouillet, Matthieu Keller, Jan Weiss, Trese Leinders-Zufall, Lutz Birnbaumer[1], Frank Zufall[1], Pablo Chamero[1]

Corresponding author: Pablo Chamero

Email: pablo.chamero-benito@inra.fr

This PDF file includes:

Supplementary Materials and Methods
Figs. S1 to S5
Tables S1 to S2
References for SI reference citations

www.pnas.org/cgi/doi/10.1073/pnas.1821492116

Supplementary Information Text

Materials and Methods

Testosterone and Reproductive Organ Measurements: 15 males per genotype were sacrificed to collect trunk blood and to weigh testes, seminal vesicles and preputial glands. Sera were collected by centrifugation (2500 x *g* for 25 min) and levels of testosterone were measured by radioimmunoassay using 3H-testosterone as previously described (1). The assay sensitivity was 0.063 ng/ml; all samples were treated in a single assay.

Behavioral Testing: Experiments were videotaped and subsequently analyzed using Behavioral Observation Research Interactive Software (Boris) (2).

Food localization test. 12 males of each genotype were evaluated for their ability to locate a food source (chocolate cookie) hidden underneath the bedding. One week before testing, mice were familiarized twice with the food used in the experiment. Mice were food-restricted for 8 h before the testing took place. Mice were introduced into a clean cage with a 3-cm-thick layer of bedding and habituated for 5 min. Mice were briefly removed from the cage to bury a piece of cookie and then reintroduced. Time from introduction of a mouse into the cage until retrieval of the food was measured up to a maximum of 900 s. A given male was considered to have uncovered the cookie when he started to eat, holding the food with his forepaws.

Olfactory habituation dishabituation assay. 12 males of each genotype were evaluated for their ability to distinguish different conspecific urine sources (female, male

or castrated male C57BL/6 adult mice). Tests were conducted in the home-cage and an odor stimulus was placed on a cotton-tipped applicator through the hole on the cage lid. Mice were allowed to familiarize themselves with the applicator for 30 min before each test. Mice were first exposed for 1 min to distilled water (50 µl). This procedure was repeated three times with 1-min intervals, followed by presentations of urine samples (50 µl each) from an intact male, a castrated male or an estrous female. Equal urine volumes from 4 animals were pooled.

Olfactory preference test. 12 sexually experienced males of each genotype were tested for their female-directed odor preference in a Y-maze apparatus as described previously (3). Two days before the test assay, mice were accustomed to the maze for 9 min in absence of an odor stimulus. On the experimental test day, each Y-arm received either fresh male or fresh estrous female urine. The estrus status was assessed by analyzing vaginal smear cytology. The urine from a particular source was randomly placed in one of the two arms' ends. Subjects were free to investigate the stimuli for 9 min. Each animal was tested twice: first, with no direct access to the stimuli, which were placed on a filter paper in a plastic weigh boat behind a perforated wall; and second, with direct access to the stimuli (wall removed). Time of investigation of the chemosensory source was recorded. Preference scores were calculated as the difference between time spent sniffing male urine and female urine over total time of chemosensory investigation.

Sexual behavior. 12 sexually naïve males of each genotype were paired overnight in their home cage with a sexually experienced, receptive female. Latencies to mount and ejaculate and the number of mount episodes were recorded, mating duration was calculated as the interval between the first mount and ejaculation. C57BL/6 females (8

weeks old, Janvier, France) served as experimental subjects. Females were ovariectomized and implanted with estradiol silastic capsule (1:1 mix with cholesterol, Sigma) for sexual behavior experiments. Pharmacological estrus was induced by injecting progesterone (1 mg/100 µl in sesame oil, Sigma) 4 h before testing. Females were sexually experienced to show an optimal lordosis behavior in the presence of the test male.

Ultrasonic vocalizations (USVs). Sexually naïve male mice (9 cGαi2$^{+/-}$ and 8 cGαi2$^{-/-}$) were recorded for USV emission in their home-cage in the presence of an intact male or female. Animals were habituated to experimental conditions for 15 min. Animal stimuli were presented on two days, first an adult female, and two days later an adult male. Animal stimuli were introduced into the cage and USVs were recorded using a gold foil electrostatic transducer microphone (Metris B.V., Netherlands). Automatic detection and analysis using SONOTRACK 1.5.0 software (Metris B.V., Netherlands) was employed to count USVs (30 to 100 kHz range bandpass filter). This initial automated analysis was followed by manual inspection of the trials to correct for noise. Number of calls over the first 3 min of an experiment was analyzed.

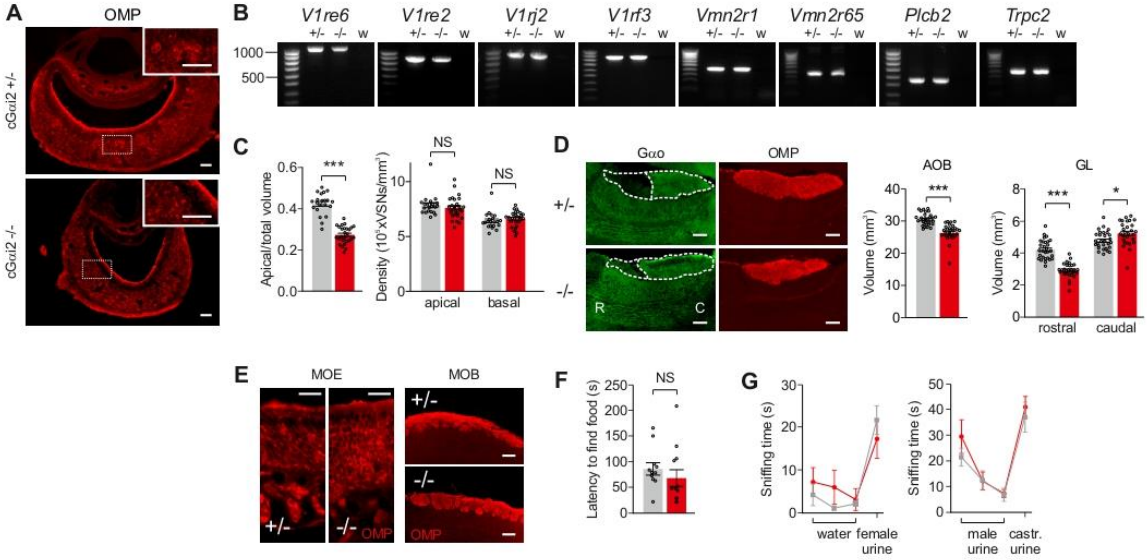
A
OMP
cGαi2 +/-
cGαi2 -/-
B
V1re6
V1re2
V1rj2
V1rf3
Vmn2r1
Vmn2r65
Plcb2
Trpc2
+/- -/- w
1000
500
C
Apical/total volume
***
Density (10³xVSNs/mm²)
NS
NS
apical
basal
D
Gαo
OMP
+/-
-/-
R
C
AOB
GL
Volume (mm³)
***
***
*
rostral
caudal
E
MOE
MOB
+/-
-/-
OMP
F
Latency to find food (s)
NS
G
Sniffing time (s)
water
female urine
male urine
castr. urine

Figure S1

Fig. S1. Olfactory system organization and function in cGαi2$^{-/-}$ mice. (*A*) OMP immunostaining marks the location of all VSNs. Scale bars, 50 µm. (*B*) RT-PCR using whole VNO cDNA of cGαi2$^{+/-}$ and cGαi2$^{-/-}$ mice reveals transcripts of *V1rs* (*V1re6, V1re2, V1rf3, V1rj2*), *V2rs* (*Vmn2r1, Vmn2r65*), and transduction molecules specific to VSN subsets (*Plcb2*) or to all VSNs (*Trpc2*) in cGαi2$^{-/-}$ mice. Water (w) was used as negative control. (*C*) Reduced volume (*left*) of the apical VNO layer in cGαi2$^{-/-}$ mice (n = 27) versus cGαi2$^{+/-}$ mice (n = 21); t-test: t(46) = 11.08, *** $P < 0.001$. Cell density of apical and basal layers (*right*) remained unchanged (Mann-Whitney test: apical, NS, P = 0.37; basal, NS, P = 0.11). The border between the two layers was identified by PDE4A immunoreactivity. (*D*) Gαo and OMP immunolabeling in the AOB of cGαi2$^{+/-}$ (n = 29) and cGαi2$^{-/-}$ mice (n = 28), total AOB volume reduction (Mann-Whitney test; $P < 0.001$), and volume differences of the glomerular layer (GL) (t-test: rostral GL, t(55) = 9.06, *** $P < 0.001$; caudal GL, t(55) = 2.63, *$P < 0.05$). R, rostral; C, caudal. Scale bar, 50 µm. (*E*) No difference of OMP immunostaining in the MOE (*left*) and MOB (*right*) of cGαi2$^{+/-}$ and cGαi2$^{-/-}$ mice. Scale bar, 50 µm. (*F-G*) General olfactory performance in a food localization (*F*) and in habituation-dishabituation assays (*G*) showed no obvious difference between cGαi2$^{+/-}$ and cGαi2$^{-/-}$ mice. Food localization test: Mann-Whitney, NS, P = 0.11 (n = 12 mice per genotype); habituation-dishabituation assay: Two-way ANOVA, F(1, 91) = 1.04 [genotype], P = 0.31 (cGαi2$^{+/-}$, n = 12; cGαi2$^{-/-}$, n = 11). Data are expressed as means ± SEM.

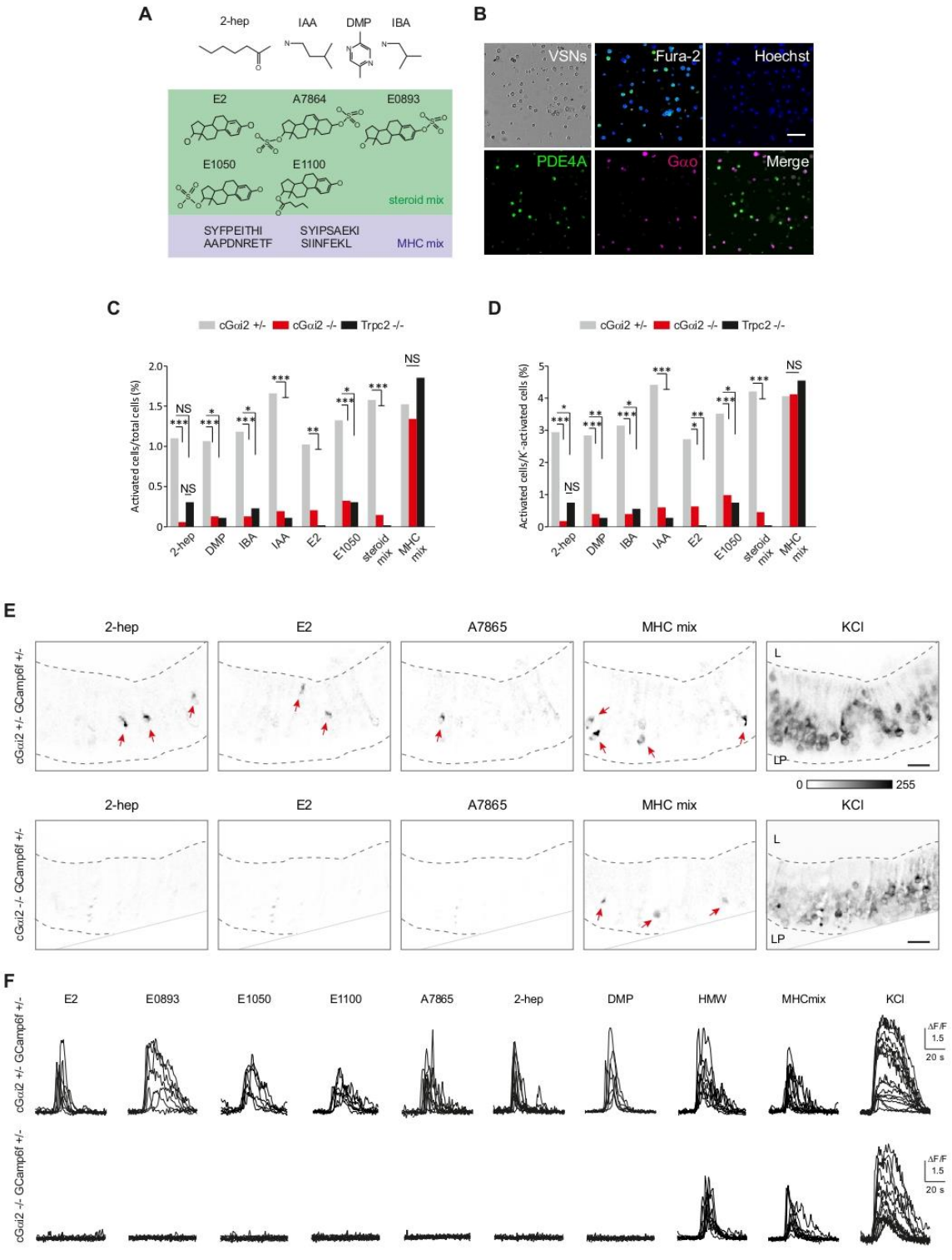
A
2-hep
IAA
DMP
IBA
E2
A7864
E0893
E1050
E1100
steroid mix
SYFPEITHI
AAPDNRETF
SYIPSAEKI
SIINFEKL
MHC mix
B
VSNs
Fura-2
Hoechst
PDE4A
Gαo
Merge
C
cGαi2 +/-
cGαi2 -/-
Trpc2 -/-
Activated cells/total cells (%)
NS
2-hep
DMP
IBA
IAA
E2
E1050
steroid mix
MHC mix
D
cGαi2 +/-
cGαi2 -/-
Trpc2 -/-
Activated cells/K+-activated cells (%)
NS
2-hep
DMP
IBA
IAA
E2
E1050
steroid mix
MHC mix
E
2-hep
E2
A7865
MHC mix
KCl
cGαi2 +/- GCamp6f +/-
cGαi2 -/- GCamp6f +/-
L
LP
0
255
F
E2
E0893
E1050
E1100
A7865
2-hep
DMP
HMW
MHCmix
KCl
cGαi2 +/- GCamp6f +/-
cGαi2 -/- GCamp6f +/-
ΔF/F
1.5
20 s

Figure S2

Fig. S2. (*A*) Chemical structures of compounds used in this study: 2-heptanone (2-hep); isoamylamine (IAA), dimethylpyrazine (DMP); isobutylamine (IBA); steroid mix: β-estradiol (E2), 1,3,5(10)-estratrien-3,17β-diol disulphate (E1050), 1,3,5(10)-estratrien-3,17β-diol 3-sulphate (E1100), 1,3,5(10)-estratrien-3,17α-diol 3-sulphate (E0893), and 5-androsten-3β,17β-diol disulfate (A7864); MHC peptide mix: SYFPEITHI, SYIPSAEKI, AAPDNRETF, SIINFEKL. (*B*) Immunocytochemistry for PDE4A and Gαo after fura-2 Ca^{2+} imaging in dissociated VSNs. Scale bar, 50 µm. (*C*) Ligand-evoked Ca^{2+} responses in dissociated cells from cGαi2$^{+/-}$, cGαi2$^{-/-}$, and Trpc2$^{-/-}$ mice expressed as percentage of responding cells to a given stimulus relative to total cells, or (*D*) relative to cells activated by KCl (50 mM). Cells were stimulated with 2-hep, (10^{-8} M), DMP (10^{-6} M), IBA (10^{-7} M), IAA (10^{-7} M), E2 (1 µM), E1050 (1 µM), sulfated steroid mix (E1050, E1100, E0893 and A7864, each at 1 µM), and MHC peptide mix (SYFPEITHI, SYIPSAEKI, AAPDNRETF, SIINFEKL, 10^{-10} M each). Fisher's exact test: * $P < 0.05$; ** $P < 0.01$; *** $P < 0.001$; No significant differences were observed between cGαi2$^{-/-}$, and Trpc2$^{-/-}$: NS, $P = 0.2 – 1$. (*E*) Spatial activity patterns in VNO slices of cGαi2$^{+/-}$ and cGαi2$^{-/-}$ mice co-expressing the Ca^{2+} reporter GCaMP6f. ΔF images (average intensity of 3 individual images at peak fluorescence) were obtained after simulation with E2 (1 µM), A7865 (1 µM), 2-heptanone (10^{-8} M), MHC mix (SYFPEITHI, SYIPSAEKI, AAPDNRETF, SIINFEKL, 10^{-10} M each), and 60 mM KCl. Red arrows indicate responding cells. L, lumen; LP, lamina propria. Scale bars, 25 µm. (*F*) Comparison of superimposed time courses of somatic VSN GCaMP6f Ca^{2+} responses obtained in cGαi2$^{+/-}$ versus cGαi2$^{-/-}$ slices to E2 (β-estradiol, 1 µM), E0893 (1, 3, 5(10)-estratrien-3, 17α-diol 3-sulphate, 1µM), E1050 (1, 3, 5(10)-estratrien-3, 17β-diol disulphate, 1 µM), E1100 (1, 3, 5(10)-

estratrien-3, 17β-diol 3-sulphate, 1 μM), A7864 (5-androsten-3β, 17β-diol disulfate, 1 μM), 2-hep (2-heptanone, 10^{-8} M), DMP (2,5-dimethylpyrazine, 10^{-6} M), HMW urine fraction (1:100), MHC mix (SYFPEITHI, SYIPSAEKI, AAPDNRETF, SIINFEKL, 10^{-10} M each), or KCl (60 mM).

9

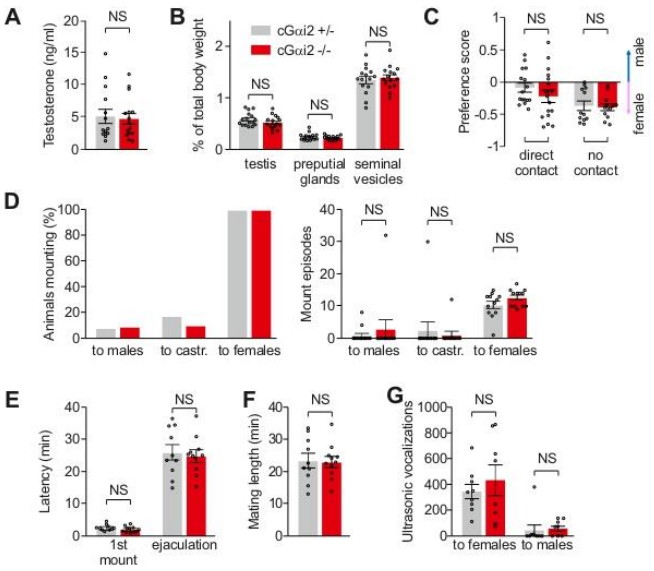
A
Testosterone (ng/ml)
NS
B
% of total body weight
cGαi2 +/-
cGαi2 -/-
NS
NS
NS
testis
preputial glands
seminal vesicles
C
Preference score
NS
NS
male
female
direct contact
no contact
D
Animals mounting (%)
to males
to castr.
to females
Mount episodes
NS
NS
NS
to males
to castr.
to females
E
Latency (min)
NS
NS
1st mount
ejaculation
F
Mating length (min)
NS
G
Ultrasonic vocalizations
NS
NS
to females
to males

Figure S3

Fig. S3. Normal sexual behavior and partner preference in cGαi2$^{-/-}$ males. (*A*) Testosterone levels and (*B*) reproductive organs weight of cGαi2$^{-/-}$ (n = 15) males are not altered compared to cGαi2$^{+/-}$ males (n = 14). Mann-Whitney test; P = 0.92 for testosterone, P = 0.19-0.63 for testis, preputial vesicles, and seminal glands. (*C*) Preference score to examine the social preference of male mice to either female or male urine in a Y-maze shows no difference between cGαi2$^{-/-}$ and cGαi2$^{+/-}$ in their choice for the stimuli to which the mice had either direct (t-test: t(31) = 1.08; NS, P = 0.28; n = 17 and 16, respectively) or no contact (t-test: t(22) = 0.26; NS, P = 0.80; n = 12 for each genotype). (*D*) No difference in mounting behavior of cGαi2$^{-/-}$ and cGαi2$^{+/-}$ male mice to male, castrated males or females was observed. *Left*: percentage of mounting behavior; *Right*: number of mount episodes (ANOVA: genotype, F(1, 64) = 0.43, P = 0.52; sex difference, F(2, 64) = 21.4, P < 0.001; n = 12 per genotype). Both genotypes preferred to mount females (Tukey: *** P < 0.001; NS, P = 0.75-0.81). (*E*) No difference in the latencies to first mount and ejaculation was observed in cGαi2$^{-/-}$ (n = 10) and cGαi2$^{+/-}$ (n = 11) male mice towards female mice (t-test: t(19) = 1.31-0.32; NS, P = 0.21-0.76), (*F*) Mating length was indistinguishable between cGαi2$^{-/-}$ (n = 10) and cGαi2$^{+/-}$ (n = 11) male mice (t-test: t(19) = 1.36; NS, P = 0.89). (*G*) Ultrasonic vocalizations to females measured in cGαi2$^{-/-}$ (n = 8) and cGαi2$^{+/-}$ (n = 9) male mice (Kruskal-Wallis ANOVA: X^2 = 9.48, P < 0.01, all four groups compared, independent samples; Mann-Whitney: NS, P = 0.96, females; P = 0.26, males). Both genotypes preferred to vocalize to females (Mann-Whitney: P < 0.01, for both genotypes). Data are expressed as means ± SEM.

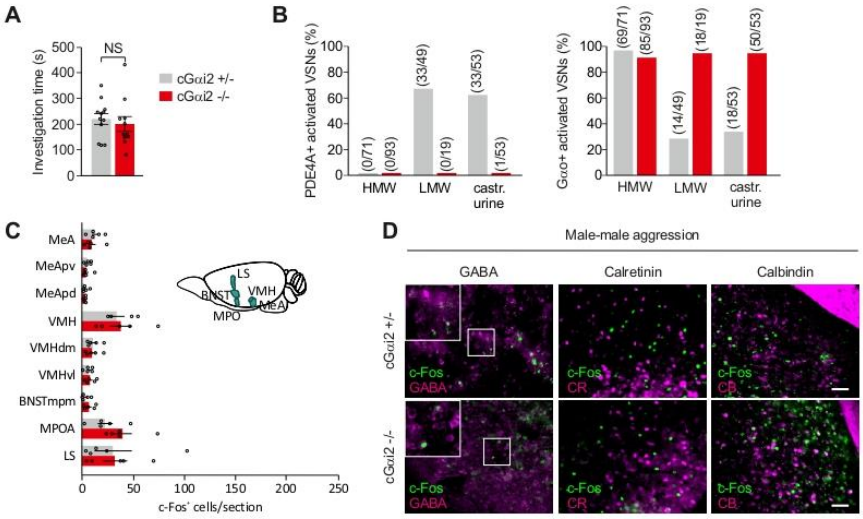
A
Investigation time (s)
NS
cGαi2 +/-
cGαi2 -/-
B
PDE4A+ activated VSNs (%)
(0/71)
(0/93)
(33/49)
(0/19)
(33/53)
(1/53)
HMW
LMW
castr. urine
Gαo+ activated VSNs (%)
(69/71)
(85/93)
(14/49)
(18/19)
(18/53)
(50/53)
C
MeA
MeApv
MeApd
VMH
VMHdm
VMHvl
BNSTmpm
MPOA
LS
c-Fos+ cells/section
D
Male-male aggression
GABA
Calretinin
Calbindin
cGαi2 +/-
cGαi2 -/-
c-Fos
GABA
CR
CB

Figure S4

Fig. S4. (*A*) Intruder investigation time does not differ between cGαi2$^{+/-}$ and cGαi2$^{-/-}$ (*n* = 12, each) in the resident-intruder assay (t-test: t(21) = 0.55; NS, *P* = 0.59). (*B*) Comparison of stimuli detection by PDE4A+ and Gαo+ VSNs. Loss of Gαi2 shifts the detection of stimuli to Gαo+ cells. Ca^{2+} imaging of VNO cells stimulated with HMW (1:100), LMW fractions of urine (1:100) and castrated male urine (1:100), followed by a post-hoc IHC for PDE4A and Gαo was performed on 1207 cells from cGαi2$^{+/-}$ mice (*n* = 4) and 978 cells of cGαi2$^{-/-}$ mice (*n* = 4). LMW and castrated male urine is detected by both PDE4A+ and Gαo+ cells in cGαi2$^{+/-}$, but only by Gαo+ cells in cGαi2$^{-/-}$. Number of PDE4A+ and Gαo+ versus total cells activated by a given stimulus is indicated above each bar. (*C*) Quantification of c-Fos+ cells per section (30 µm thick) of cGαi2$^{+/-}$ and cGαi2$^{-/-}$ residents (*n* = 5, each) without chemostimulation reveals no change in c-Fos expression in the various brain areas (Mann-Whitney: *P* = 0.13-0.96). MeA, medial amygdala (MeApd, posterodorsal; MeApv, posteroventral); VMH, ventromedial hypothalamus (VMHdm, dorsomedial; VMHvl, ventrolateral); BNST, bed nucleus of the stria terminalis (BNSTmpm, posteromedial part of the medial division); MPOA, medial preoptic area; LS, lateral septum (d, dorsal, v, ventral, i, intermediate). Data are expressed as means ± SEM. (*D*) c-Fos co-localization with GABA, calretinin (CR) and calbindin (CB) in the MeApd of cGαi2$^{-/-}$ and cGαi2$^{+/-}$ males after a 10-min exposure to an intact male intruder. NS, not significant. Data are expressed as means ± SEM. Scale bar, 50 µm.

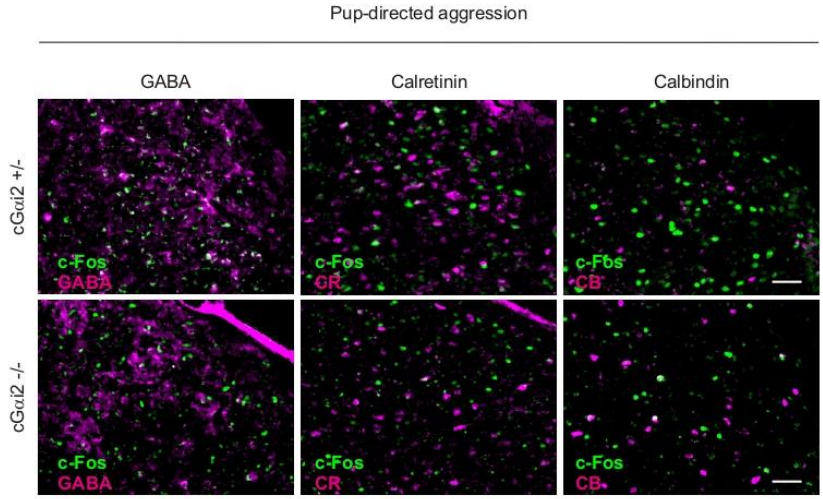
Pup-directed aggression
GABA
Calretinin
Calbindin
cGαi2 +/-
cGαi2 -/-
c-Fos
GABA
c-Fos
CR
c-Fos
CB
c-Fos
GABA
c-Fos
CR
c-Fos
CB

Figure S5

Fig. S5. Co-localization of c-Fos+ nuclei with various markers to identify activated cells in the MeApd of cGαi2$^{-/-}$ and aggressive cGαi2$^{+/-}$ males after exposure to a pup in the pup-directed aggression test. Scale bars, 50 µm. There was no overlap between c-Fos and calretinin (CR) or calbindin (CB).

Table S1. Antibodies, references and concentrations used.

Target	Primary antibody	Concentration
OMP	goat, Wako #544-10001	1:2000
Gαi2	rabbit, Calbiochem #37 1729	1:250
V2R2	rabbit, gift R. Tirindelli, University of Parma, Parma, Italy	1:10 000
PDE4A	rabbit, Fabgennix #PD4-112AP	1:500
Gαo	rabbit, Santa Cruz #sc-387	1:200
	mouse, Santa Cruz #sc-13532	1:200
c-Fos	rabbit, Santa Cruz #sc-52	1:500
		1:200 (IF)
	mouse, Santa Cruz #sc-271243	1:200
AR	rabbit, Santa Cruz #sc-816	1:200
GABA	mouse, Sigma #A0310	1:200
Calbindin	mouse, Sigma #C9848	1:400
Calretinin	goat, Swant #CG1	1:3000
Goat IgG	Donkey anti-goat Alexa-647, Invitrogen #A32849	1:500
Rabbit IgG	Donkey anti-rabbit Alexa-588, Invitrogen #A21206	1:500
	Goat anti-rabbit biotinylated, Jackson #111-065-003	1:1000
Mouse IgG	Donkey anti-mouse Alexa-588, Invitrogen #A21202	1:500
	Donkey anti-mouse Alexa-647, Invitrogen #A3157	1:500

Table S2. Primer sequences.

Gene	Forward primer (5'-3')	Reverse primer (5'-3')	Product size (bp)
Hprt1	GGTCCTTTTCACCAGCAAGCT	TGACACTGGTAAAACAATGCA	94
Omp	GCACAGTTAGCAGGTTCAGCT	GGTTTGCAGTCCTGGCAGC	197
Gnai2	GAGCATGAAGCTGTTTGACAGC	CTCCTTGGTGTCTTTGCGC	220
Gnao	CTCCACGAGGACGAAACCAC	GCCCCGGAGATTGTTGGCA	348
V1re6	ATGATCCTTACACACACATATTCC	TTATGGTATTTTTATATTTCTTGTCCATG	1026
V1re2	ATGGACTTGAGGACCATGATAGTTG	CTAGGTAAAGCAGAATCTGGAAATAGC	897
V1rf3	ATGGAAAACAGTGACATTGTAATTAGTGT	TTAACTGGAGATCACCAGAAAGGGA	870
V1rj2	CATCACTCCCAGTAAYTCTAAGTGGGC	GCTGGGMTCTCTTGTRRTGYCTGTAGA	320
Vmn2r1	TTGTGGGCTGTATTGGGTGC	TGATCCCCCTGATCCAACCA	432
Vmn2r65	GAGTGTAGCACATCCCAAGTG	GGAATGGCCCAAGTATGGCA	401
Trpc2	ATGTTCGGCATGGAAGAGCA	GATGACTCGAAGGCGGTAGG	435
Plcb2	GCCCACGATACACTGCTGAT	ACAGGGACACTAGACGGGAG	563

References

1. Hochereau-de Reviers MT, Perreau C, Pisselet C, Fontaine I, Monet-Kuntz C (1990) Comparisons of endocrinological and testis parameters in 18-month-old Ile de France and Romanov rams. *Domest Anim Endocrinol* 7(1):63–73.

2. Friard O, Gamba M (2016) BORIS: a free, versatile open-source event-logging software for video/audio coding and live observations. *Methods in Ecology and Evolution* 7(11):1325–1330.

3. Jouhanneau M, Cornilleau F, Keller M (2014) Peripubertal exposure to male odors influences female puberty and adult expression of male-directed odor preference in mice. *Horm Behav* 65(2):128–133.

2 Impact of $G\alpha_{i2}$ deletion in VSNs on females' socio-sexual behaviors

Journal article #2: Sensory detection by the vomeronasal organ modulates experience-dependent social behaviors in female

Anne-Charlotte Trouillet[1], Chantal Moussu[1], Kevin Poissenot[1], Matthieu Keller[1], Lutz Birnbaumer[2,3], Trese leinders-Zufall[3], Frank Zufall[3], and Pablo Chamero[1]

[1] Laboratoire de Physiologie de la reproduction et des Comportements, UMR OO85-INRAE-CNRS-IFCE-University of Tours, Nouzilly, France

[2] Neurobiology Laboratory, National Institute of Environmental Health Sciences, Durham, NC, United States of America

[3] School of Medical Sciences, Institute of Biomedical Research, Catholic University of Argentina, Buenos Aires, Argentina

[4] Center for Integrative Physiology and Molecular Medicine, Saarland University, Homburg, Germany

Published in Frontiers in Cellular Neuroscience, February 2021.

Abstract

The onset of female-specific behaviors in mice results from interactions between sensory detection mechanisms and plastic neuronal pathways. Olfactory-driven responses are typically hard-wired, but aspects of female behavior may evolve after social experience. This study aimed to determine the role of $G\alpha_{i2}$ vomeronasal signaling in innate social behaviors in females and, second, determine if sensory detection by this pathway also influences social experience. We choose to focus on male- and pup-directed behaviors since these behaviors are modulated by $G\alpha_{i2}$ vomeronasal signaling in male mice and are modified by social experience in females. We used two different behavioral paradigms, pup retrieval, and sexual receptivity, in which conditional olfactory-restricted $G\alpha_{i2}$ null females mice ($cG\alpha_{i2}^{-/-}$) were naïve or experienced to the stimuli, either a mouse infant or an adult male. After behavioral experiments, brains were mapped for cFos expression to elucidate neural pathways mediating the transformation of the olfactory information into a behavioral decision.

We exposed pup-naïve females to an alien neonate and observed that $G\alpha_{i2}$-dependent VNO inputs participate in pup odor detection, and that the deletion of $G\alpha_{i2}$ reduced pup retrieval, although

pup-parenting behaviors were still displayed after retrieval. Accordingly, we found a reduction of cFos expression in the aAOB but not in parenting-associated hypothalamic areas. Maternity greatly increases parental behaviors and changes male odors' behavioral significance, as lactating females show an aggressive response toward a male instead of sexual attraction. Surprisingly, the retrieving behavior and maternal aggression of $cG\alpha_{i2}^{-/-}$ females were unchanged.

We measured olfactory discrimination abilities of $cG\alpha_{i2}^{-/-}$ females and determined that they could recognize male odors and develop a preference for them. Next, we evaluated their response to sexually experienced males by quantifying their lordosis response to male mounting. In $cG\alpha_{i2}^{-/-}$ females, we did not observe the progressive increase of lordosis responses usually induced by repeating testing. The lordosis quotient of sexually experienced $cG\alpha_{i2}^{-/-}$ females was significantly reduced. This effect was not a consequence of altered reproductive physiology. Rather, we found a reduction of cFos-expressing cells in the kisspeptin-negative RP3V neuronal population, a hypothalamic cell cluster activated by male odors that regulates the lordosis response.

Altogether, our data suggest that the detection of pheromones by the VNO influences olfactory-mediated behavior in females before and after social experience, although with distinctive traits for different behaviors. This may exemplify a mechanism of neuroplasticity in which olfaction in combination with social experience improve social behavior synergistically.

frontiers in Cellular Neuroscience

ORIGINAL RESEARCH
published: 17 February 2021
doi: 10.3389/fncel.2021.638800

Sensory Detection by the Vomeronasal Organ Modulates Experience-Dependent Social Behaviors in Female Mice

*Anne-Charlotte Trouillet[1], Chantal Moussu[1], Kevin Poissenot[1], Matthieu Keller[1], Lutz Birnbaumer[2,3], Trese Leinders-Zufall[4], Frank Zufall[4] and Pablo Chamero[1]**

[1] Laboratoire de Physiologie de la Reproduction et des Comportements, UMR 0085 INRAE-CNRS-IFCE-University of Tours, Nouzilly, France, [2] Neurobiology Laboratory, National Institute of Environmental Health Sciences, National Institutes of Health, Durham, NC, United States, [3] School of Medical Sciences, Institute of Biomedical Research (BIOMED), Catholic University of Argentina, Buenos Aires, Argentina, [4] Center for Integrative Physiology and Molecular Medicine, Saarland University, Homburg, Germany

In mice, social behaviors are largely controlled by the olfactory system. Pheromone detection induces naïve virgin females to retrieve isolated pups to the nest and to be sexually receptive to males, but social experience increases the performance of both types of innate behaviors. Whether animals are intrinsically sensitive to the smell of conspecifics, or the detection of olfactory cues modulates experience for the display of social responses is currently unclear. Here, we employed mice with an olfactory-specific deletion of the G protein Gαi2, which partially eliminates sensory function in the vomeronasal organ (VNO), to show that social behavior in female mice results from interactions between intrinsic mechanisms in the vomeronasal system and experience-dependent plasticity. In pup- and sexually-naïve females, Gαi2 deletion elicited a reduction in pup retrieval behavior, but not in sexual receptivity. By contrast, experienced animals showed normal maternal behavior, but the experience-dependent increase in sexual receptivity was incomplete. Further, lower receptivity was accompanied by reduced neuronal activity in the anterior accessory olfactory bulb and the rostral periventricular area of the third ventricle. Therefore, neural mechanisms utilize intrinsic sensitivity in the mouse vomeronasal system and enable plasticity to display consistent social behavior.

Keywords: olfactory, Gαi2, maternal, lordosis, sex preference, kisspeptin

OPEN ACCESS

Edited by:
Emmanuel Valjent, Centre National de la Recherche Scientifique (CNRS), France

Reviewed by:
Michael Baum, Boston University, United States
Kazushige Touhara, The University of Tokyo, Japan

****Correspondence:***
Pablo Chamero
pablo.chamero-benito@inrae.fr

Specialty section:
This article was submitted to Cellular Neurophysiology, a section of the journal Frontiers in Cellular Neuroscience

Received: *07 December 2020*
Accepted: *28 January 2021*
Published: *17 February 2021*

Citation:
Trouillet A-C, Moussu C, Poissenot K, Keller M, Birnbaumer L, Leinders-Zufall T, Zufall F and Chamero P (2021) Sensory Detection by the Vomeronasal Organ Modulates Experience-Dependent Social Behaviors in Female Mice. Front. Cell. Neurosci. 15:638800. doi: 10.3389/fncel.2021.638800

INTRODUCTION

The onset of female-specific behaviors in mice results from interactions between sensory detection mechanisms and plastic neuronal pathways. Rapid responses in females' behaviour—such as pup care (Lévy et al., 2004), or sexual receptivity to males (Keller et al., 2009)—start with the detection of chemical signals by the olfactory system. Although these olfactory-driven responses are typically hard-wired, aspects of female behavior may evolve after social experience. For example, virgin females recognize pup odors and retrieve isolated pups to the nest to some extent, but maternity greatly increases this type of parental behavior (Stolzenberg and Rissman, 2011; Kohl et al., 2017).

Similarly, the display of sexual receptivity in females, indexed by the incidence of lordosis stance, largely depends on the detection of olfactory signals by the vomeronasal organ (VNO) (Keller et al., 2006; Oboti et al., 2014; Hellier et al., 2018) and is considerably enhanced by experience (Thompson and Edwards, 1971; Bonthuis et al., 2011). Plastic changes in central brain areas have been shown to modulate instinctive olfactory-mediated female behaviors (Stowers and Liberles, 2016), but whether sensory detection by the olfactory system also influences social experience remains unexplored.

Pheromones play a key role in the regulation of innate reproductive responses in female mice and are largely detected by sensory neurons in the VNO (Chamero et al., 2012; Stowers and Kuo, 2015; Ishii and Touhara, 2019). Genetic ablation of Trpc2, the primary signal transduction pathway of VNO neurons, results in several behavioral deficits in mice, such as display of sexual behavior toward both males and females indiscriminately, lack of maternal aggression in females as well as enhanced pup care in males (Leypold et al., 2002; Stowers et al., 2002; Kimchi et al., 2007; Hasen and Gammie, 2009; Wu et al., 2014). We have previously shown that the G protein Gαo is necessary for sensory function of basal vomeronasal sensory neurons (VSNs), maternal aggression, and lordosis behavior in female mice (Chamero et al., 2011; Oboti et al., 2014). By contrast, apical VSNs, which express Gαi2 and V1R receptors, are critical for pup-directed aggression and parental care in males (Trouillet et al., 2019) and have also been associated with maternal aggression (Del Punta et al., 2002; Norlin et al., 2003). This suggests that both apical and basal vomeronasal pathways control female-typical behaviors activating certain behaviors and repressing others. However, the neural VNO mechanisms involved and the role of social experience in controlling the display of female-typical behaviors remain largely unknown.

To uncover the neuronal VNO substrate leading to specific female behaviors, we used female mice with a conditional knockout of Gαi2, in which the apical half of the VNO lacks sensory function (Trouillet et al., 2019). We used two different behavioral paradigms, pup retrieval, and sexual receptivity, in which female mice were naïve to the stimuli, either a mouse infant or an adult male. Mutant females showed reduced pup retrieval behavior, whereas sexual receptivity was not different from control mice in the initial tests. Then, we evaluated the effect of social experience in the display of these behaviors. Remarkably, Gαi2 mutant females displayed normal pup retrieval behavior and maternal aggression after parturition, while sexual experience was not sufficient for Gαi2 mutants to reach control levels of sexual receptivity. These results demonstrate the role of V1R and Gαi2+ neurons in the display of lordosis and detection of pup cues. Unexpectedly, social experience in Gαi2 deficient mice leads to divergent effects on behavior: improvement of pup retrieval without any beneficial effects on the acquisition of high lordosis performance. Altogether, our data suggest that the detection of pheromones by the VNO influences olfactory-mediated behavior in females after social experience, although with distinctive traits for different behaviors.

MATERIALS AND METHODS

Mice

Animal care and experimental procedures were performed following French and European guidelines on the protection of animals used for scientific purposes and approved by an ethical committee for animal experimentation (CEEA Val de Loire project 12785). Mice were kept under standard 12 h light/dark cycles with food and water *ad libitum*. cGαi2$^{-/-}$ and cGαi2$^{+/-}$ mice were generated as described (Trouillet et al., 2019). Briefly, floxed *Gnai2* (*Gnai2*$^{fx/fx}$) mice with mixed 129sv × C57BL/6 background were crossed with mice carrying a transgene directing the expression of Cre recombinase under the control of the OMP promoter (*Omp*-Cre mice; B6; 129P2-*Omp*$^{tm4(cre)Mom}$/ MomJ; The Jackson Laboratory, JR# 006668; backcrossed into C57BL6/J for 8 generations; neomycin cassette is absent). *Gnai2*$^{fx/fx}$ mice carry loxP sites inserted into the introns that flank exons 2 and 4. Breeding established offspring that were homozygous for the floxed *Gnai2* alleles and heterozygous for Cre and *Omp* (*Gnai2*$^{fx/fx}$ *Omp*$^{cre/+}$ or cGαi2$^{-/-}$). In these mice, Cre-mediated *Gnai2* deletion was restricted to *Omp*-positive cells. Animals heterozygous for both alleles (*Gnai2*$^{fx/+}$ *Omp*$^{cre/+}$ or cGαi2$^{+/-}$) served as controls. Adult females (more than 8 weeks) were used except specified otherwise. Adult (8 weeks or older) C57BL/6 males and females (Janvier Labs) and Balb/c males (Janvier Labs) were used as stimulus animals.

Surgery

Stimulus females used for the mounting behavior assay and experimental females used in lordosis, habituation-dishabituation, and olfactory preference tests were ovariectomized under general anesthesia (xylazine 10 mg/kg, ketamine 100 mg/kg), implanted with a SILASTIC capsule filled with estradiol-benzoate (1:1 mix with cholesterol; Sigma-Aldrich). Females were allowed to recover from surgery at least 2 weeks before testing. Females were subcutaneously treated with progesterone (1 mg/100 μl in sesame oil, Sigma-Aldrich) to induce a pharmacological estrus state 4 h before each test. Juvenile (P18-22) C57BL/6 stimulus males were castrated under isoflurane general anesthesia and used in adulthood.

Behavior

Mice were moved to the experimental room 2 h before testing. Assays were conducted 2 h before the start of the dark period. Experiments were videotaped and subsequently analyzed by a blind experimenter.

Parental Behaviors in Virgin Females

Sexually naïve females (N = 12 of each genotype) were tested for behavior in the presence of an alien 1–2 day old C57BL/6 (wild type) neonate introduced into the home-cage of the test mouse for 10 min. Females were individually housed for 1 week before testing. To minimize handling and stress to the pups, one single pup was taken from the nest immediately prior to the test avoiding prolonged exposure to cold. Mice were categorized as parental if they retrieved a pup into their nest, and otherwise

as neutral. We did not observe aggressive behavior. Latency to retrieve a pup, pup grooming, and nesting times were scored.

Maternal Aggression

Sexually naïve females (20 cGαi2$^{+/-}$ and 16 cGαi2$^{-/-}$) were paired with a C57BL/6 male for 1 week. Bedding and nesting materials were changed before parturition and left until the end of the experiments. On postnatal days 2–4, females were tested daily for maternal aggression using the resident—intruder paradigm (Chamero et al., 2011). Before testing, pups were placed in a box next to their mother's cage to avoid potential injuries by the intruder. Testing lasted 10 min and began when a sexually inexperienced intruder (Balb/c adult male, group-housed) was placed in the home cage of the test female mouse (resident). Residents were not exposed twice to the same intruder. Aggressive behavior was defined as lunging, biting, chasing, tail rattling, wrestling, and kicking. Attack bouts were defined as a succession of aggressive events separated by <3 s. Proportion of females attacking the intruder, latency to attack, and cumulative attack duration and episodes of 3 consecutive tests were scored.

Pup Retrieval

After maternal aggression, the same females were tested for retrieval of their own pups. On postnatal day 5, five pups were randomly dispersed at the opposite side of the nest. The latencies to retrieve each pup to the nest were scored.

Olfactory Habituation Dishabituation Assay

Sexually naïve females (10 cGαi2$^{+/-}$ and 9 cGαi2$^{-/-}$) were evaluated for their ability to distinguish urine sources. Females were ovariectomized, supplemented in estradiol, and subcutaneously treated with progesterone 4 h before the experiment. The test was conducted in the female's home-cage and an odor stimulus was placed on a cotton-tipped applicator through the hole of the cage lid. Direct contact with the applicator was allowed. Food and water were removed from the grid and mice were allowed to familiarize themselves with a clean applicator for 30 min before the test. The test started with a first exposition for 1 min to distilled water (10 µl). This procedure was repeated three times with 1 min intervals, followed by a single presentation of intact male urine (10 µl, collected and pooled from 4 C57BL/6 group-housed adult mice). The time spent sniffing in close contact with the applicator was measured for each presentation.

Olfactory Preference Test

Sexually naïve females (10 cGαi2$^{+/-}$ and 9 cGαi2$^{-/-}$) were tested for their male-directed odor preference in a Y-maze apparatus as described previously (Jouhanneau et al., 2014). Females were ovariectomized, supplemented in estradiol, and subcutaneously treated with progesterone 4 h before the experiment. Two days before the test assay, mice were accustomed to the maze for 9 min in absence of an odor stimulus. On test day, urine from two distinct sources were placed in the arms' ends of the Y-maze on a filter paper in a plastic weigh boat behind a perforated wall. The apparatus was cleaned with 20% ethanol between subjects. Each animal was tested twice: first, with either intact male or estrous female urine; and second, with either intact or castrated male urine. Equal urine volumes from 4 C57BL/6 animals per condition were pooled and the estrus status of female donors was assessed by vaginal cytology. The time of chemosensory investigation was recorded. Preference scores were calculated as the difference between times spent on each urine source over total time of chemosensory investigation.

Mounting Behavior

Sexually naïve females (20 cGαi2$^{+/-}$ and 17 cGαi2$^{-/-}$) were individually housed for 1 week before testing. Testing lasted 10 min and began when a sexually inexperienced intruder (either male, female in pharmacological estrus, or castrated male, group-housed) was placed in the home cage of the test mouse (female resident), whose bedding had not been changed for at least 4 days. Each female was tested with every intruder in a randomized order. The proportion of females mounting the intruder was recorded.

Female Sexual Receptivity (Lordosis)

Sexually naïve females (10 cGαi2$^{+/-}$ and 9 cGαi2$^{-/-}$) were tested for their sexual receptivity toward male mounting. Females were ovariectomized, supplemented in estradiol, and subcutaneously treated with progesterone 4 h before the experiment. The test began when the female was introduced in the home cage of a sexually experienced C57BL/6 stud male and lasted for 20 min or until the female received 20 mounts. Stud males were previously trained, and only males showing a mounting latency of less than 5 min were used. Females were not exposed twice to the same stud male. Females were tested three times with a 4 days interval between tests. Lordosis was scored when the female arched her back, lift her tail and adopted a rigid posture standing on all four paws, independently of whether the male was able to achieve intromission. The lordosis quotient (number of lordosis responses/number of mounts) was scored.

Immunostaining

Tissue Preparation

90 min after sexual behavior or interaction with a neonate, mice were anesthetized by an overdose of pentobarbital (Ceva) and perfused transcardially with 0.9% saline solution followed by 0.1 M phosphate buffer (PB) containing 4% paraformaldehyde (PFA). Brains were removed, postfixed overnight in 4% PFA, and cryoprotected in 0.1 M PB containing 30% sucrose. Brain and olfactory bulbs (OB) were embedded separately in Tissue-Tek® O.C.T™ compound, snap-frozen in cold isopentane, and processed on a Leica CM 3050S cryostat. Samples were cut in 30 µm serial free-floating sections (coronal for brains, sagittal for OB) using tris-buffered saline solution (TBS) containing 0.1% sodium azide.

c-Fos Immunolabeling

Sections were washed (3 × 5 min) in TBS, endogenous peroxidases were blocked for 30 min in TBS containing 3% H_2O_2. Sections were incubated in blocking solution (TBS containing 0.1% Triton X-100, TBS-T, and 5% donkey serum) 2 h at room

temperature (RT), and overnight at 4°C in blocking solution supplemented with the c-Fos primary antibody (1:500; rabbit polyclonal #sc-52, Santa Cruz Biotechnology). Sections were then washed in TBS and incubated in TBS-T supplemented with secondary antibody (1:1,000; biotinylated donkey anti-rabbit IgG, Jackson ImmunoResearch) for 2 h at RT. Signals were amplified with VECTASTAIN ABC kit (Vector) and visualized with diaminobenzidine (DAB 0,02%, 0,01% H_2O_2 in 0,05 M Tris, pH 7,4). Slides were mounted with DPX (Sigma-Aldrich).

Kisspeptin/c-Fos Immunolabeling

Sections were washed in TBS, incubated in blocking solution (TBS containing 0.1% Triton X-100, TBS-T, and 5% donkey serum) 2 h at RT, incubated 72 h at 4°C in blocking solution supplemented with c-Fos (1:500; rabbit polyclonal #sc-52, Santa Cruz Biotechnology) and kisspeptin [1:10,000; sheep polyclonal #AC053, generous gift of I. Franceschini (Franceschini et al., 2013)] primary antibodies. Sections were then washed in TBS and incubated in TBS-T supplemented with secondary antibodies (1:500; Cy3 donkey anti-rabbit-IgG and Alexa-488 donkey anti-sheep-IgG, Jackson ImmunoResearch) for 2 h at RT. Nuclei were counterstained with 4′,6-diamidino-2-phenylindole (DAPI; 0.5 μg/ml, Sigma-Aldrich) for 2 min. Slides were mounted with Fluoromount^{TM} (Sigma-Aldrich).

Analysis

For c-Fos experiments, slides were scanned using an automatic slide scanner (Axio Scan.Z1, Zeiss). Regions of interest were drawn based on the Paxinos mouse brain atlas using Zen (blue edition 3.0, Zeiss). The number of c-Fos+ nuclei was automatically counted bilaterally in these regions using the particle analyzer plug-in of Fiji. 2–3 images of the accessory olfactory bulb (AOB), 3 images of the rostral periventricular area of the third ventricle (RP3V), 2 images of the ventrolateral part of the ventromedial hypothalamic nucleus (VMHvl) and 4 images of the medial preoptic area (MPA) per animal were analyzed. Kisspeptin/c-Fos co-expression was quantified in 3–5 RP3V images/animal acquired on a Zeiss LSM-700 confocal laser-scanning microscope at 10× magnification. Images were manually analyzed in the entire *z*-axis with 3 μm step intervals.

Reproductive Physiology

Young prepubertal females (17 cGαi2$^{+/-}$ and 15 cGαi2$^{-/-}$) were monitored daily for evidence of vaginal opening from postnatal day 15, and then for their first estrus by vaginal smears sampling. Briefly, vaginal smears were flushed with 15 μl of NaCl 0.9% solution and the estrus phase was identified by light microscopy after methylene-blue coloration of the smears. Adult females (47 cGαi2$^{+/-}$ and 45 cGαi2$^{-/-}$) were also examined daily for estrus status for 2 weeks using the same protocol. Adult females (61 cGαi2$^{+/-}$ and 49 cGαi2$^{-/-}$) were sacrificed during their diestrus or estrus phase to collect trunk blood and measure the weight of ovaries and uteri. Blood sera were obtained by centrifugation (2,500 × *g* for 25 min) and levels of progesterone were measured by immunoenzymatic assay. Assay sensitivity is 0.25 ng/ml. Sexually naïve females (76 cGαi2$^{+/-}$ and 67 cGαi2$^{-/-}$) were paired for 7 days with a C57BL/6 male. The proportion of pregnant females, the latency to deliver, and the number of pups born were collected.

Statistics

Statistical analyses were performed using GraphPad Prism 9.0 (GraphPad Software, Inc.), and OriginPro 2016G (OriginLab Corporation). Assumptions of normality and homogeneity of variance were tested before conducting the following statistical approaches. Student's *t*-test was used to measure the significance of the differences between two distributions. In case the results failed the test of normality, Mann-Whitney or Kolmogorov-Smirnov test was performed. Multiple groups were compared using a two- or three-way repeated-measures analysis of variance (ANOVA) with Bonferonni's tests as *post hoc* comparison. Kruskal-Wallis test with Dunn's multiple comparisons, or Friedman multiple comparisons in case of paired values, were used for non-normal distributions. Categorical data were analyzed with Fisher's exact test, and correlations were assessed by the Pearson coefficient. The probability of error level (alpha) was chosen to be 0.05. Unless otherwise stated, results are presented as means ± SEM and documentation of individual data points.

RESULTS

Inactivation of the Apical Vomeronasal Cell Layer Reduces Pup Retrieval in Virgin Females

VNO activity is necessary for the display of important pup-directed behaviors in male mice, such as pup-directed aggression (Tachikawa et al., 2013; Wu et al., 2014; Isogai et al., 2018; Trouillet et al., 2019), inhibition of sexual behaviors toward pups (Ferrero et al., 2013), and increased pup-retrieval and parenting behaviors (Wu et al., 2014; Trouillet et al., 2019). In virgin females, the role of the VNO in pup-directed behaviors is less clear. While some studies suggest that genetic ablation of VNO function in Trpc2$^{-/-}$ females increase parenting behavior toward alien juveniles (Nakahara et al., 2016), this view is not supported by others (Wu et al., 2014).

To determine whether the vomeronasal pathway may partially regulate pup parenting in virgin females, we used mice carrying Olfactory Marker Protein (OMP)-dependent deletion of Gαi2 (cGαi2$^{-/-}$), which impairs sensory signaling in apical VNO neurons (Trouillet et al., 2019). We exposed pup-naïve virgin females to 1–2 days old pups (**Figure 1A**) and the majority of females retrieved the pups to the nest, although the proportion of retrieving females was lower in cGαi2$^{-/-}$ when compared to heterozygous controls (58 vs. 92%; **Figure 1A**). Measurement of the latency to retrieve pups showed that cGαi2$^{-/-}$ virgin females retrieved pups with longer latency ($P < 0.05$; **Figure 1B**), even if they displayed more time sniffing the pups before retrieving ($P < 0.05$; **Figure 1B**). Next, we used c-Fos immunolabeling to confirm the role of vomeronasal signaling in pup detection by virgin females

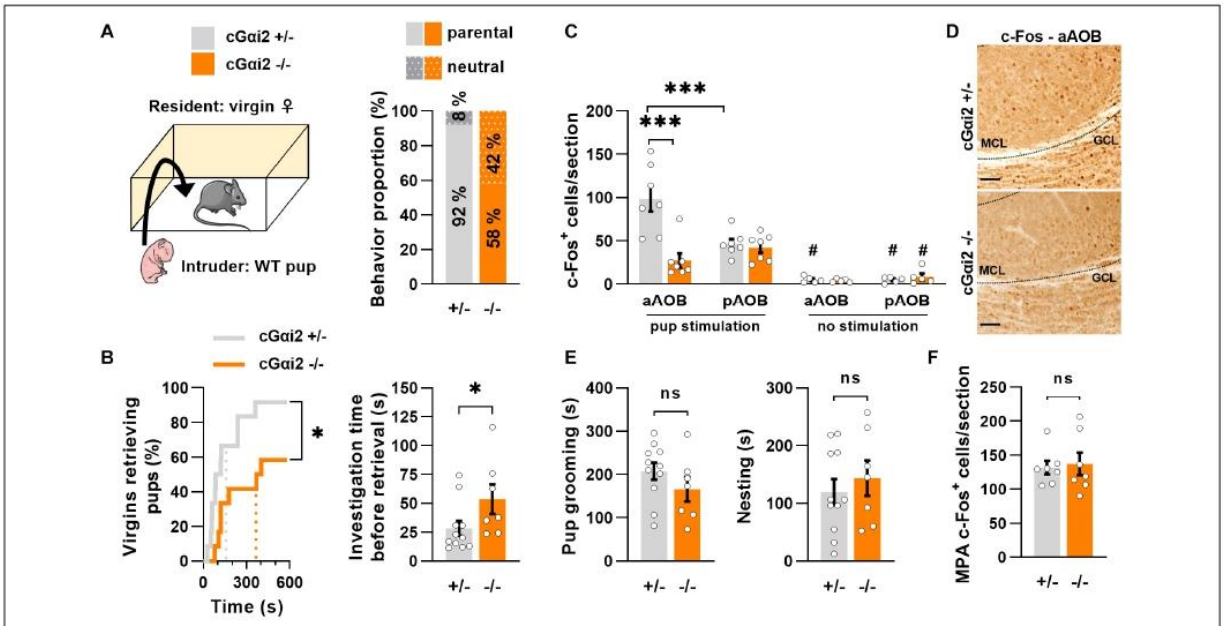

FIGURE 1 | Pup retrieval is altered in virgin cGαi2$^{-/-}$ females. **(A)** Comparison of pup-directed behavior of cGαi2$^{+/-}$ vs. cGαi2$^{-/-}$ virgin female residents ($N = 12$ per genotype). Wild type 1–2 day-old pups served as intruders. Females ignore (neutral) or retrieve neonates to their nest (parental). Females of both genotypes are predominantly parental (11 out of 12; 92% for cGαi2$^{+/-}$ and 7 out of 12; 58% for cGαi2$^{-/-}$). **(B)** *Left*, proportion of females retrieving pups over time (Kolmogorov-Smirnov test: $P < 0.05$). Dotted lines represent the mean latency. *Right*, time spent sniffing the pup before retrieval in cGαi2$^{-/-}$ ($N = 7$) and cGαi2$^{+/-}$ ($N = 11$) parental females (Mann-Whitney: $P < 0.05$). **(C)** Quantification of c-Fos+ cells per section of cGαi2$^{+/-}$ and cGαi2$^{-/-}$ virgin females ($N = 7$ per group) in control condition (no stimulation) and after exposure to an alien pup (pup stimulation) reveals a decreased c-Fos activation in the aAOB of cGαi2$^{-/-}$ compared to cGαi2$^{+/-}$ females, and a higher number of c-Fos+ cells in the anterior compared to the posterior part of the AOB of cGαi2$^{+/-}$ females only [Three-way repeated measures ANOVA: (genotype) $F_{(1,12)} = 6.719$, $P < 0.01$; (region) $F_{(1,12)} = 4.024$, $P = 0.068$; (stimulation) $F_{(1,12)} = 63.21$, $P < 0.001$; (genotype × region × stimulation) $F_{(1,4)} = 14.67$, $P < 0.05$; Bonferroni *post hoc* tests: cGαi2$^{+/-}$ aAOB vs. cGαi2$^{+/-}$ pAOB and cGαi2$^{+/-}$ aAOB vs. cGαi2$^{-/-}$ aAOB $P < 0.001$; $^{\#}P < 0.05$ vs. the stimulated equivalent condition; other comparison $P = 0.3$–0.9]. All three AOB layers were quantified. **(D)** Examples of c-Fos immunodetection in the aAOB of cGαi2$^{+/-}$ and cGαi2$^{-/-}$ virgin females exposed to an alien pup for 10 min. Scale bars, 25 μm. **(E)** The time spent grooming (*left*) and nesting (*right*) the neonates (*t*-test: $P = 0.2$–0.5). **(F)** Quantification of c-Fos^{+} cells per section in the MPA of cGαi2$^{+/-}$ and cGαi2$^{-/-}$ virgin females after exposure to an alien pup is not different (*t*-test: $P = 0.8$). AOB, accessory olfactory bulb (aAOB, anterior AOB; pAOB, posterior AOB); MCL, mitral cell layer; GCL, granular cell layer; MPA, medial preoptic area. $^{*}P < 0.05$; $^{***}P < 0.001$.

and examine whether pup odors were preferentially detected by either the apical or basal vomeronasal subsystems. We compared the density of c-Fos+ nuclei in all three layers of the accessory olfactory bulb (AOB), the first relay station of the pheromonal information transfer in the brain, after pup exposure in cGαi2$^{-/-}$ and cGαi2$^{+/-}$ virgin females (**Figures 1C,D**). After pup exposure, the density of c-Fos+ nuclei was nearly fourfold lower in the anterior part of the AOB of cGαi2$^{-/-}$females ($P < 0.001$; **Figure 1C**), consistent with reduced sensory input from the apical VNO. Furthermore, we observed twofold more c-Fos+ nuclei in the anterior vs. posterior part of the AOB in control females ($P < 0.001$; **Figure 1C**), suggesting a preferential activation of apical Gαi2-expressing VSNs by pup odors. Once pups were retrieved to the nest, measures of parental care—pup grooming and nesting time—were not significantly different in cGαi2$^{-/-}$ females (**Figure 1E**; $P = 0.2$–0.5). Consistent with this, the number of c-Fos+ cells in the medial preoptic area (MPA), a region involved in parenting (Numan, 1974), was also not significantly different in cGαi2$^{-/-}$ females (**Figure 1F**). Together, these results indicate that Gαi2-dependent VNO inputs participate in pup odor detection in virgin females and that deletion of Gαi2 reduces pup retrieval, although pup-parenting behaviors are still displayed after retrieval.

Deletion of Gαi2 Does Not Affect Maternal Behavior in Mothers

Both the main olfactory epithelium and VNO seem to be implicated in maternal behavior. Previous experiments using genetically altered mice showed that an intact main olfactory system is required for pup retrieval in lactating mice mothers (Weiss et al., 2011; Fraser and Shah, 2014), and that the VNO is necessary for the display of maternal aggression (Leypold et al., 2002; Hasen and Gammie, 2009; Chamero et al., 2011). Consequently, impairment of vomeronasal signaling in Trpc2$^{-/-}$ lactating females has no impact on pup retrieval behavior, even though these females are deficient in maternal aggression (Leypold et al., 2002; Hasen and Gammie, 2009).

Yet, the VNO neuronal subpopulation implicated in maternal aggression is not characterized with certainty. While maternal aggression is nearly absent in basal VNO signaling-deficient cGαo$^{-/-}$ females (Chamero et al., 2011), other studies have suggested some mediation from apical Gαi2/V1R-expressing VSNs (Del Punta et al., 2002; Norlin et al., 2003).

Thus, we aimed to investigate the requirement of Gαi2^{+} vomeronasal neurons for parental behaviors in mated females. We first quantified territorial aggression of cGαi2$^{-/-}$ vs. cGαi2$^{+/-}$ lactating females in the resident-intruder paradigm (**Figure 2**). We observed a high number of animals attacking an adult intact male intruder in both cGαi2$^{-/-}$ (14/16 mice; 87%) and cGαi2$^{+/-}$ mothers (14/20 mice; 70%) in three consecutive 10 min tests (P = 0.3; **Figure 2A**). Attack latency, total attack duration, and cumulative attack numbers were high in both cGαi2$^{-/-}$ and cGαi2$^{+/-}$ females (P = 0.4–0.9; **Figure 2B**), indicating that Gαi2 is dispensable for the display of maternal aggression. Consistent with previous findings indicating a minor role of the VNO in the display of pup retrieval behavior in mothers (Wysocki and Lepri, 1991), cGαi2$^{-/-}$ females exhibited normal pup retrieval when compared to heterozygous controls (**Figures 2C,D**). All females retrieved to the nest all of their pups randomly distributed in the home cage (**Figure 2C**), and the mean time to retrieve the 5 pups was less than 80 s in both groups (**Figure 2D**). Taken together, these results show that maternal aggression and pup retrieval by lactating females do not depend on Gαi2+ VSNs.

Incomplete Sexual Receptivity Acquisition in Gαi2-Mutant Females

An intact VNO is required for the display of major female sexual behaviors, such as gender discrimination and sexual receptivity (Leypold et al., 2002; Stowers et al., 2002; Keller et al., 2006; Kimchi et al., 2007; Martel and Baum, 2009; Oboti et al., 2014; Hellier et al., 2018).

To examine whether altered sexual behaviors of VNO-impaired mice might be related to a deficit in Gαi2 signaling, we measured olfactory preference to male odors in cGαi2$^{-/-}$ females. We used adult, sexually naïve females subjected to ovariectomy and primed with estradiol and progesterone to minimize estrus cycle-related variability and increase their motivation for male pheromones. First, we evaluated their ability to recognize urine from an adult male using the habituation-dishabituation paradigm. cGαi2$^{-/-}$ and cGαi2$^{+/-}$ females were exposed to a sequence of three successive odor presentations of water and a final presentation of male urine. All females were able to recognize the urine, as the time spent sniffing the first urine presentation was higher than the previous water presentations (**Figure 3A**). Next, we analyzed the preference for either intact male urine or estrus female urine in a two-choice preference test. cGαi2$^{-/-}$ and cGαi2$^{+/-}$ females displayed the same level of preference for intact male urine (P = 0.8; **Figure 3B**). We then compared the preference for urine from either intact or castrated males (**Figure 3B**). cGαi2$^{-/-}$ and cGαi2$^{+/-}$ females showed a strong preference for intact male urine (P = 0.4;

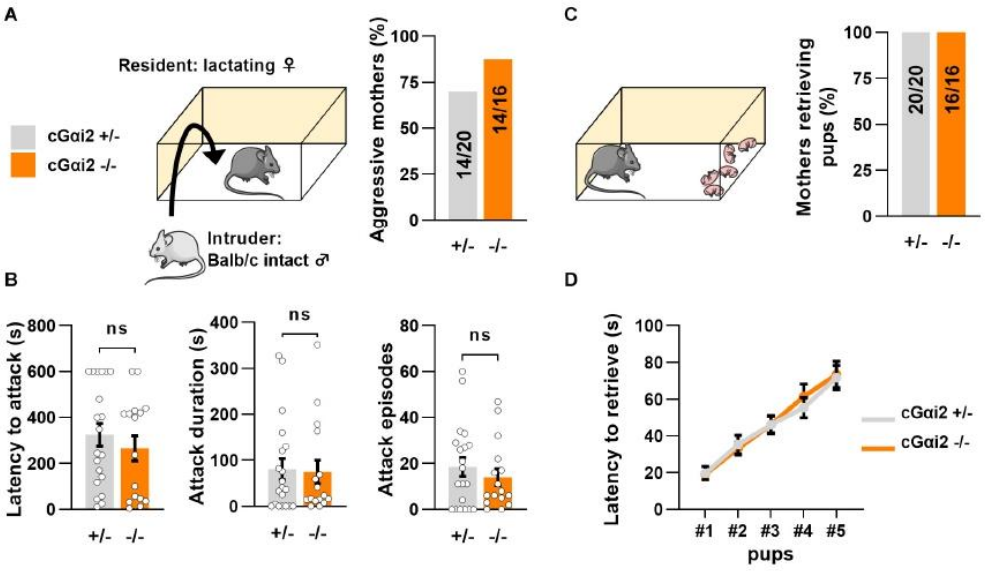

FIGURE 2 | Loss of Gαi2 does not affect maternal behavior in lactating females. **(A)** Maternal aggression in lactating cGαi2$^{+/-}$ (N = 20) vs. cGαi2$^{-/-}$ (N = 16) females during three consecutive exposures to an intact male intruder in the resident-intruder test. 70% of cGαi2$^{+/-}$ and 87% of cGαi2$^{-/-}$ females present at least one aggressive episode (Fisher's exact test: P = 0.3). **(B)** Measure of the aggression parameters latency to attack (*left*), cumulative attack duration (*middle*) and attack episodes (*right*) across genotypes (Mann-Whitney: P = 0.4–0.9). **(C)** 100% of cGαi2$^{+/-}$ (N = 20) and cGαi2$^{-/-}$ (N = 16) mothers retrieve five of their pups previously dispersed in the cage. **(D)** The latency to retrieve pups does not differ between groups (Dunn's multiple comparison tests cGαi2$^{+/-}$ vs. cGαi2$^{-/-}$ for each pup's latency $P > 0.9$).

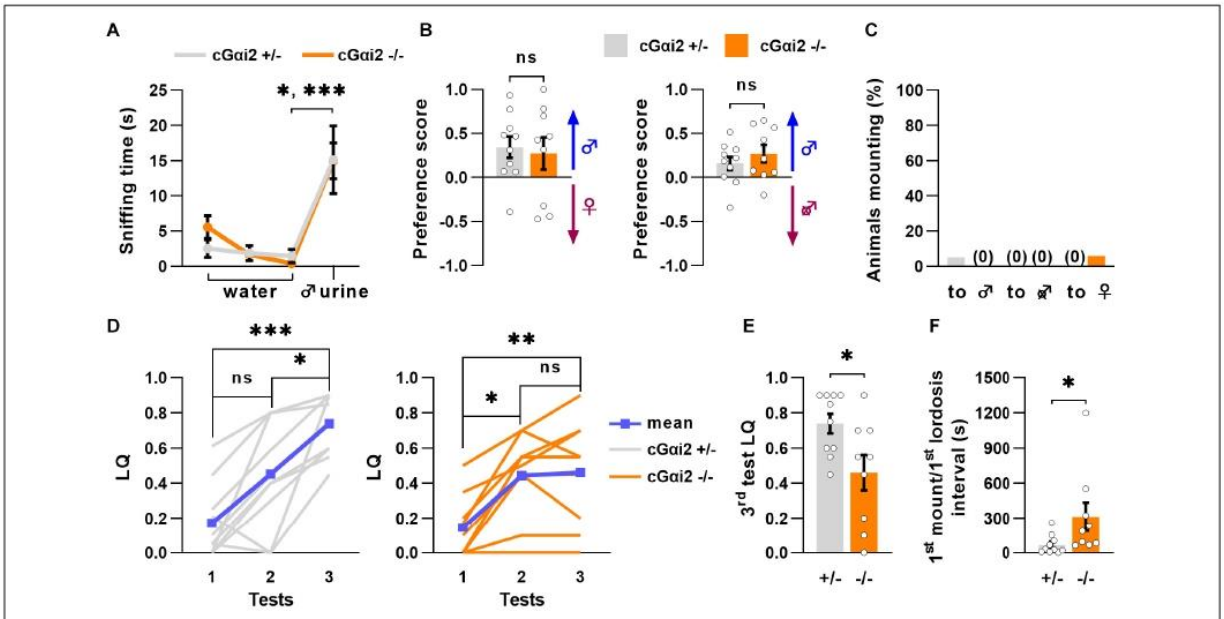

FIGURE 3 | Incomplete sexual receptivity in Gαi2 mutant females. **(A)** cGαi2$^{+/-}$ ($N = 10$) and cGαi2$^{-/-}$ ($N = 9$) are able to detect intact male urine in the habituation—dishabituation paradigm (Kruskal-Wallis: $P < 0.001$, Dunn's multiple comparison tests: water 3 vs. urine 1 cGαi2$^{+/-}$ $P < 0.05$, cGαi2$^{-/-}$ $P < 0.001$). **(B)** Olfactory preference of social cues in cGαi2$^{+/-}$ ($N = 10$) and cGαi2$^{-/-}$ ($N = 9$) female mice in a two-choice test. Females had the choice between male urine vs. estrus female (*left*) or castrated male (*right*) urine. cGαi2$^{+/-}$ and cGαi2$^{-/-}$ animals show a preference for male urine in both tests and no differences between genotypes are found (*t*-test: $P = 0.4$–0.7). **(C)** Ablation of Gαi2 in VSNs does not induce, in females, mounting behavior toward male, castrated male or female. The proportion of animals mounting is similar in cGαi2$^{+/-}$ ($N = 20$) and cGαi2$^{-/-}$ ($N = 17$) females (Fisher's exact test: $P = 0.5$–0.9). **(D–F)** Sexual receptivity of cGαi2$^{+/-}$ ($N = 10$) and cGαi2$^{-/-}$ ($N = 9$) females during exposition to a sexually experienced stud male over three tests. **(D)** The lordosis quotient (LQ) of cGαi2$^{+/-}$ (*left*) follows a normal increase over the tests (Kruskal-Wallis: $P < 0.001$, Friedman multiple comparisons: test 1 vs. 2 $P = 0.5$, test 1 vs. 3 $P < 0.001$, and test 2 vs. 3 $P < 0.05$), but in cGαi2$^{-/-}$ (*right*) the lordosis quotient does not increase in the third test (Kruskal-Wallis: $P < 0.001$, Friedman multiple comparisons: test 1 vs. 2 $P < 0.05$, test 1 vs. 3 $P < 0.01$, and test 2 vs. 3 $P = 0.9$). **(E)** Comparison of the lordosis quotient of cGαi2$^{+/-}$ and cGαi2$^{-/-}$ females during the third test reveals a reduction of sexual receptivity in mutant females (Mann-Whitney: $P < 0.05$). **(F)** Latency to exhibit a lordosis, measured from the first mount received, is significantly longer in cGαi2$^{-/-}$ females (Mann-Whitney: $P < 0.05$). *$P < 0.05$; **$P < 0.01$; ***$P < 0.001$.

Figure 3B), indicating that preference for male odors is intact in cGαi2$^{-/-}$ females.

Next, we assessed cGαi2$^{-/-}$ females for the display of male-typical behaviors by scoring mounting behavior of intact female residents to either male, female, or castrated male intruders, independently introduced into the female resident's home cage during a 10 min test period for 3 consecutive days. Very few animals displayed mounting behavior toward any intruder (female, male, or castrated male) for both cGαi2$^{-/-}$ and cGαi2$^{+/-}$ females. None of the cGαi2$^{-/-}$ females exhibited mounting to male or castrated intruders, although some low levels of mounting were observed in 6% of females, to female intruders (**Figure 3C**). Thus, deletion of Gαi2 in VSNs does not enhance the display of male-specific behaviors in female mice.

We next asked whether normal olfactory preference and lack of mounting to males and females led to normal display of sexual receptivity in cGαi2$^{-/-}$ females. To test this, we measured lordosis behavior, a female sexual stance held in response to male mounting that denotes sexual receptivity. Lordosis requires an intact VNO (Keller et al., 2006; Oboti et al., 2014; Hellier et al., 2018), and is significantly enhanced by experience (Thompson and Edwards, 1971; Bonthuis et al., 2011). Thus, we quantified lordosis response in the presence of a sexually experienced male in three tests separated by 4 days to mimic natural estrus occurrence. We observed low lordosis quotient (LQ; number of lordosis postures divided by the number of mounts received) values during the first test for all animals (LQ = 0.14–0.17; **Figure 3D**). The second test yielded an increase in LQ values of around 0.45, for both cGαi2$^{-/-}$ and cGαi2$^{+/-}$ females (**Figure 3D**). In the third test, however, cGαi2$^{-/-}$ females remained at LQ levels similar to those of the second test (LQ = 0.46; **Figure 3D**), whereas cGαi2$^{+/-}$ control females displayed a further LQ increase (from 0.45 to 0.74; **Figure 3D**). During the third test, each female received 20 mounts from the stud male, but cGαi2$^{-/-}$ females responded displaying less lordosis than cGαi2$^{+/-}$ controls ($P < 0.05$; **Figure 3E**). Furthermore, cGαi2$^{-/-}$ females exhibited a significantly longer latency to show the first lordosis episode (67.4 ± 26.2 s for cGαi2$^{+/-}$ females; 311.8 ± 123.1 s for cGαi2$^{-/-}$; $P < 0.05$; **Figure 3F**). Taken together, these results indicate that Gαi2 vomeronasal neurons play a critical role in the acquisition of complete sexual receptivity in females, but not in olfactory preference and sexual partner choice.

Reduced c-Fos Expression in the AOB and RP3V of Gαi2-Mutant Females

We further investigated neuronal activity after sexual behavior in downstream vomeronasal neural pathways in the brain. First, we quantified c-Fos expression in the AOB (**Figures 4A,B**). In control cGαi2$^{+/-}$ females, the number of c-Fos+ cells in the AOB was elevated (∼100 cells/section) in both the anterior and posterior AOB (**Figure 4A**). By contrast, cGαi2$^{-/-}$ females displayed significantly lower number of c-Fos+ in the anterior AOB (15 cells/section; $P < 0.001$; **Figure 4A**), while c-Fos+ cells in the posterior AOB was not significantly different from cGαi2$^{+/-}$ controls (58 cells/section; $P = 0.06$; **Figure 4A**). This

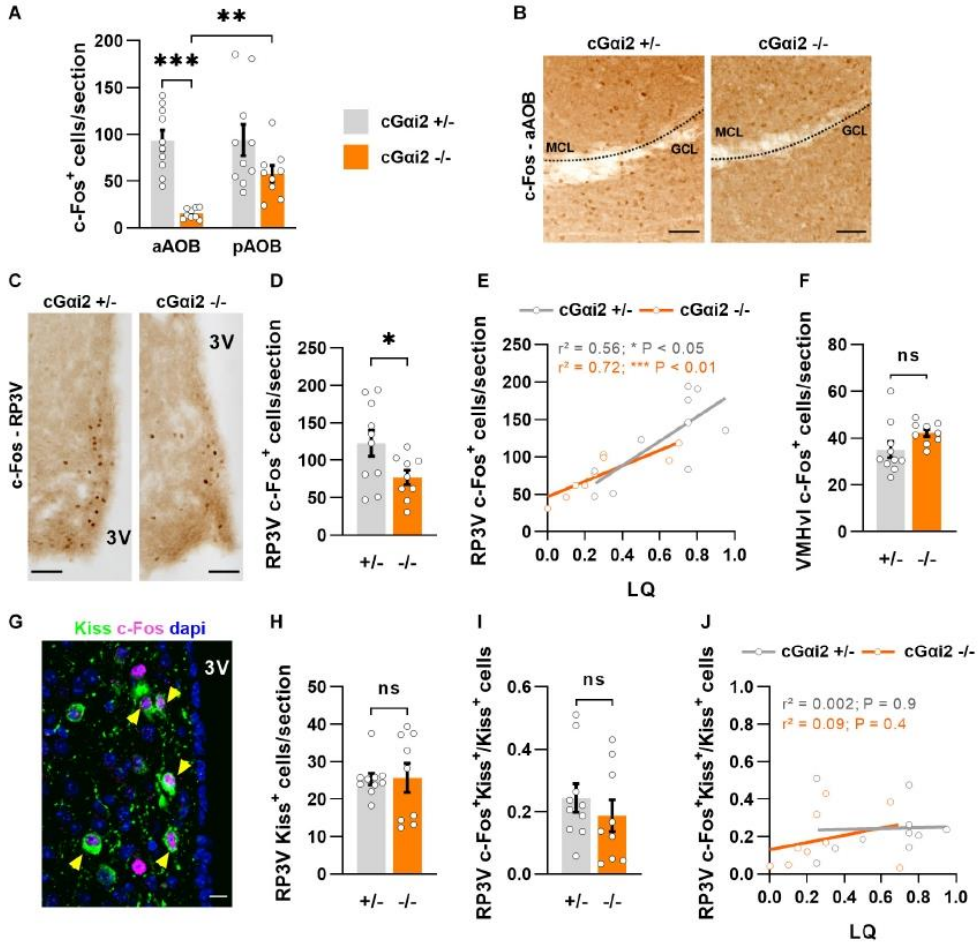

FIGURE 4 | Reduced neural activity in the AOB and RP3V of Gαi2-mutant females. **(A,B)** Analysis of c-Fos immunodetection in the AOB of cGαi2$^{+/-}$ ($N = 10$) and cGαi2$^{-/-}$ ($N = 9$) females after sexual behavior. **(A)** Quantification of c-Fos+ cells per section reveals a decreased c-Fos activation in the aAOB of cGαi2$^{-/-}$ [Two-way repeated measures ANOVA: (genotype) $F_{(1,17)} = 18.28$, $P < 0.001$; (region) $F_{(1,17)} = 5.82$, $P < 0.05$; (genotype × region) $F_{(1,17)} = 5.53$, $P < 0.05$; Bonferroni *post hoc* tests: cGαi2$^{-/-}$ aAOB vs. cGαi2$^{-/-}$ pAOB, $P < 0.01$; cGαi2$^{+/-}$ aAOB vs. cGαi2$^{-/-}$ aAOB $P < 0.001$; other comparisons $P = 0.06$–0.9). All three AOB layers were quantified. **(B)** Examples of c-Fos immunolabeling in the aAOB of cGαi2$^{+/-}$ and cGαi2$^{-/-}$females after sexual behavior. Scale bars, 50 μm. **(C–E)** c-Fos immunodetection in the RP3V of cGαi2$^{+/-}$ ($N = 10$) and cGαi2$^{-/-}$ ($N = 9$) females. **(C)** Examples of c-Fos immunodetection in the RP3V of cGαi2$^{+/-}$ and cGαi2$^{-/-}$females after sexual behavior. Scale bars, 50 μm. **(D)** Quantification of c-Fos+ cells per section in the RP3V of cGαi2$^{-/-}$ (*t*-test: $P < 0.05$). **(E)** Positive correlation between the number of RP3V-c-Fos+ cells and lordosis quotient (LQ) in cGαi2$^{+/-}$ and cGαi2$^{-/-}$ females (Pearson's correlation; cGαi2$^{+/-}$: $r^2 = 0.56$, $P < 0.05$; cGαi2$^{-/-}$: $r^2 = 0.72$, $P < 0.01$). **(F)** c-Fos immunodetection in the VMHvl of cGαi2$^{+/-}$ ($N = 10$) and cGαi2$^{-/-}$ ($N = 9$) females after sexual behavior. Quantification is not different between genotypes (*t*-test: $P = 0.08$). **(G–J)** Analysis of kisspeptin and c-Fos double immunostaining in the RP3V. **(G)** Example of Kiss and c-Fos immunostaining in the RP3V of a cGαi2$^{+/-}$ female. The yellow arrows indicate double labeled c-Fos-Kiss neurons. Scale bar, 10 μm. Quantifications of Kiss+ neurons **(H)** and double-labeled c-Fos+Kiss+ neurons **(I)** are not different between genotypes (Mann-Whitney: $P = 0.9$; *t*-test: $P = 0.4$, respectively). **(J)** Correlative analysis between the number of c-Fos+Kiss+ cells in the RP3V and the LQ (Pearson's correlation; cGαi2$^{+/-}$: $r^2 = 0.002$, $P = 0.9$; cGαi2$^{-/-}$: $r^2 = 0.09$, $P = 0.4$). AOB, accessory olfactory bulb (aAOB, anterior AOB; pAOB, posterior AOB); 3V, third ventricle; RP3V, rostral periventricular area of the third ventricle; VMHvl, ventrolateral part of the ventromedial hypothalamic nucleus; Kiss, kisspeptin. *$P < 0.05$; **$P < 0.01$; ***$P < 0.001$.

result suggests that Gαi2-independent VNO activity is sufficient for the display of basal levels of sexual receptivity.

We further asked whether this reduction of sensory information may have an impact on the neural activity of the rostral periventricular area of the third ventricle (RP3V), a hypothalamic region involved in the control of female sexual behavior and activated by male pheromones (Simerly, 2002; Bakker et al., 2010; Hellier et al., 2018; Inoue et al., 2019; **Figures 4C–E**). We thus counted c-Fos+ nuclei in the RP3V of the same females after sexual behavior. Consistent with a reduced sensory input, the density of c-Fos+ nuclei was lower in cGαi2$^{-/-}$ females vs. cGαi2$^{+/-}$ controls ($P < 0.05$; **Figures 4C,D**). To determine whether the extent of c-Fos+ cells in the RP3V was linked to sexual receptivity, we performed a correlation analysis between c-Fos cell density and LQ (**Figure 4E**). The number of c-Fos+ cells was positively correlated with the LQ in both genotypes (**Figure 4E**), suggesting that the level of sexual receptivity displayed may depend on RP3V neural activity. c-Fos activation in the ventrolateral part of the ventromedial hypothalamic nucleus (VMHvl), a region innervated by RP3V neurons and also involved in the control of female sexual behavior (Pfaff and Sakuma, 1979), revealed no significant differences (**Figure 4F**), suggesting that the observed alterations in cGαi2$^{-/-}$ female receptivity are likely coded upstream of VMHvl neurons.

To further characterize in more detail the activated RP3V neurons in cGαi2$^{-/-}$ females, we asked whether these cells belong to a neuronal subpopulation positive for the neuropeptide kisspeptin (Kiss), which is essential to trigger the lordosis response (Hellier et al., 2018; **Figures 4G–J**). Using double label immunostaining we found neurons that were positive for both c-Fos^{+} and Kiss in all animals (**Figure 4G**). We observed no difference in the density of Kiss^{+} neurons and the number of double-labeled c-Fos^{+}/Kiss^{+} neurons in both cGαi2$^{-/-}$ and cGαi2$^{+/-}$ females (P = 0.4–0.9; **Figures 4H,I**). To establish whether the level of sexual receptivity is linked to the number of activated kisspeptin neurons in the RP3V, we performed a correlation analysis between c-Fos+/Kiss+ cell density and the LQ (**Figure 4J**). We did not observe any obvious correlation between the number of activated kisspeptin neurons and the LQ for any of the two genotypes (r^2 = 0.002 and 0.09; **Figure 4J**), suggesting that an increase in sexual receptivity does not require the recruitment of additional kisspeptin neurons. Collectively, these results indicate that Gαi2 vomeronasal signaling is dispensable for the display of basal levels of lordosis, but participates in the acquisition of complete sexual receptivity, possibly through RP3V kisspeptin-negative neurons.

Gαi2 Deletion Has No Impact on Reproductive Physiology

Reduced receptivity to males could be a consequence of not only defective VNO chemodetection but also of altered reproductive physiology. Indeed, females with a total or partial ablation of VNO function (Trpc2$^{-/-}$ and cGαo$^{-/-}$ females) exhibit profound alterations in puberty onset and estrus cyclicity, even in the absence of external stimuli (Flanagan et al., 2011; Oboti et al., 2014).

Therefore, as a further control and to verify that the described loss of functions by the conditional Gαi2 ablation are indeed caused by a loss of VNO signaling and not by defective reproductive physiology, we investigated the impact of Gαi2 deletion on the timing of estrus and ovulation. First, we characterized puberty onset of juvenile female mice. Control cGαi2$^{+/-}$ and cGαi2$^{-/-}$ females were examined for the onset of vaginal opening and first estrus. Animals from

TABLE 1 | cGαi2$^{-/-}$ females show normal reproductive physiology.

		cGα i2$^{+/-}$	cGα i2$^{-/-}$	Statistic	*P*-value	
Puberty						
	Age at vaginal opening (days)	34.6 ± 0.8 (17)	35.1 ± 0.8 (15)	Unpaired *t*-test	0.6	*ns*
	Age at first estrus (days)	36.2 ± 0.7 (17)	36.8 ± 0.6 (15)	Unpaired *t*-test	0.5	*ns*
Estrus cycle						
	Cycle length (days)	4.9 ± 0.1 (47)	5.5 ± 0.2 (47)	Mann-Whitney	0.1	*ns*
	Proestrus + estrus days	6.6 ± 0.2 (47)	6.4 ± 0.2 (45)	Mann-Whitney	0.5	*ns*
Serum steroids levels						
Progesterone (ng.mL^{-1})	Follicular phase	3.2 ± 0.7 (10)	5.6 ± 1.3 (7)	Mann-Whitney	0.2	*ns*
	Luteal phase	7.9 ± 1.2 (36)	7.9 ± 1.5 (26)	Mann-Whitney	0.9	*ns*
Reproductive organs weight						
Ovaries (%bw)		0.033 ± 0.001 (27)	0.034 ± 0.002 (31)	Mann-Whitney	0.4	*ns*
Uterus (%bw)	Follicular phase	0.29 ± 0.02 (25)	0.32 ± 0.03 (21)	Kruskal-Wallis	0.9	*ns*
	Luteal phase	0.23 ± 0.02 (19) †	0.2 ± 0.01 (28) ‡		0.2	*ns*
Fertility						
	Pregnant females (%)	67/76 (88%)	54/67 (81%)	Fisher's exact test	0.2	*ns*
	Delivery latency (days)	22.4 ± 0.3 (76)	23.3 ± 0.4 (67)	Mann-Whitney	0.2	*ns*
	Litter size	7.8 ± 0.4 (76)	7.1 ± 0.5 (67)	Mann-Whitney	0.3	*ns*

† and ‡, respectively, $P < 0.05$ and $P < 0.001$ vs. the uterus weight during the follicular phase. bw, body weight. Assessment of puberty onset, estrus cyclicity, sex steroids levels, reproductive organs weight, and fertility parameters of control and cGαi2$^{-/-}$ females. Values are means ± SEM of the indicated number (n) of females.

both genotypes displayed vaginal opening around postnatal day 35 (P = 0.6; **Table 1**) and first estrus a day later (P = 0.5; **Table 1**), indicating normal puberty onset in Gαi2 mutants. Next, we analyzed estrus cycles of adult, group-housed female mice during a 2 week interval. Both control cGαi2$^{+/-}$ and cGαi2$^{-/-}$ females displayed consistent estrus cycles with no difference in the mean cycle duration (P = 0.1; **Table 1**) and similar number of proestrus and estrus days (P = 0.5; **Table 1**). Consistent with normal ovarian function, levels of circulating progesterone during the follicular or luteal phases (P = 0.2 and 0.9; **Table 1**), and average ovarian weight were not different between cGαi2$^{-/-}$ and cGαi2$^{+/-}$ females (P = 0.2–0.9; **Table 1**). We measured uterus weight as a proxy for circulating estradiol, and found a weight decrease during the luteal vs. follicular phases (P < 0.001 and 0.05; **Table 1**), but no differences between genotypes (P = 0.2–0.9; **Table 1**). Finally, we compared three fertility parameters—percentage of pregnant females after 7 days, delivery latency and litter size—and found no differences between cGαi2$^{-/-}$ and cGαi2$^{+/-}$ (P = 0.2–0.3; **Table 1**). Together, these findings indicate that reproductive physiology and ovarian function are normal in cGαi2$^{-/-}$ females.

DISCUSSION

The central hypothesis of this study was that detection of environmental stimuli by the VNO modulates experience-dependent plasticity, possibly influencing the display of social behaviors in female mice. To test this hypothesis, we chose an animal model with a conditional mutation for Gαi2 gene, which harbors a partial loss of VNO function (Trouillet et al., 2019), and two experimental paradigms (pup retrieval and sexual receptivity) that are strongly dependent on social experience (repeated contact with pups or the male). We previously showed that Gαi2 is necessary for the detection of small organic pheromones by apical VSNs, and genetic ablation of these neurons severely impairs pup-directed aggression in virgin males (Trouillet et al., 2019). This is consistent with published studies that show that pup cues preferentially activate neurons located in the apical VNO and the anterior AOB in virgin males (Tachikawa et al., 2013; Nakahara et al., 2020). Our results show higher c-Fos activation in the anterior AOB after pup-exposure (**Figures 1C,D**), indicating that pups are also preferentially detected by Gαi2+ VSNs in virgin females.

In contrast to males, we found that deletion of Gαi2 in virgin females does not increase parental care (i.e., grooming) toward pups, but reduces pup retrieval (**Figures 1A,B**). Interestingly, mutant females that retrieve pups still display other types of parenting behaviors such as grooming and nesting, suggesting that different pup care behaviors are controlled independently. Importantly, Gαi2 deletion does not affect pup retrieval and maternal aggression in mothers (**Figure 2**), indicating that other neural substrates different from Gαi2^{+} VSNs control these behaviors, likely by auditory, olfactory and Gαo-dependent signals (Chamero et al., 2011; Weiss et al., 2011; Fraser and Shah, 2014; Marlin et al., 2015).

The mechanism by which social experience drives neural plasticity to modify the behaviors display is unclear. Not only centrally controlled neural changes, but also sensory organ sensitivity to olfactory stimuli have been suggested to have an influence. In particular, previous studies report a decline in VNO activity induced by pup cues in virgin males after cohabitation with a pregnant female (Tachikawa et al., 2013; Nakahara et al., 2020), suggesting the existence of a silencing mechanism at the

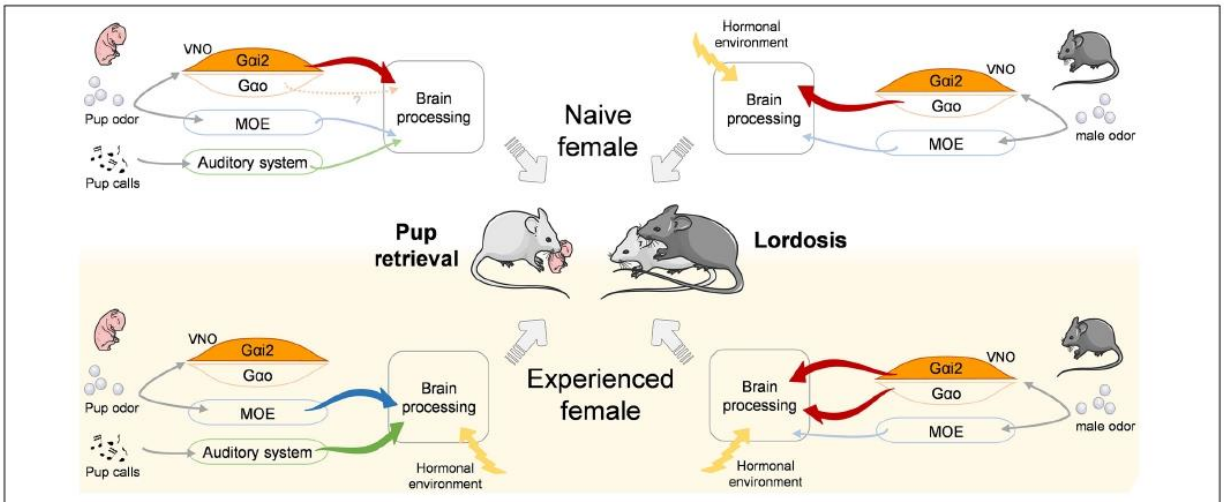

FIGURE 5 | Model for the proposed control of pup retrieval and lordosis behaviors depending on social experience. Olfactory and auditory cues relevant for pup retrieval (***left***) and lordosis (***right***) behaviors are differentially processed by the sensory systems and the brain in naïve (***top***) and experienced (***down***) females. Significantly, Gαi2+ vomeronasal neurons are activated by pup odor in naïve females to trigger retrieval but are dispensable in experienced females. Inversely, they are dispensable in naïve females to trigger the lordosis response but become necessary in experienced females to reach high lordosis levels. VNO, vomeronasal organ; MOE, main olfactory epithelium.

level of VSNs. We can thus speculate that a similar process may occur in females after parturition, either induced by hormonal changes intrinsic to gestation, or by repeated exposure to pups. Indeed, pup retrieval is improved in virgin females after co-housing with a dam and litter, even after ovariectomy (Ehret et al., 1987; Koch and Ehret, 1989; Stolzenberg and Rissman, 2011; Elyada and Mizrahi, 2015), suggesting that pup signals modulate the behavioral response. In this scenario, hormones such as oxytocin may influence experience-dependent plasticity directly at the sensory processing level (Fleming et al., 1979; Marlin et al., 2015; Nakahara et al., 2020).

Studies on Trpc2$^{-/-}$ mice suggest that sex discrimination and opposite-sex preference depend on a functional VNO because of indiscriminate mounting expressed by males and females (Leypold et al., 2002; Stowers et al., 2002; Kimchi et al., 2007). Other studies point to a significant role of testosterone levels (rather than VNO function) to explain the unusual mounting of Trpc2$^{-/-}$ females (Martel and Baum, 2009). The absence of mounting behavior in our Gαi2 mutant females (**Figure 3C**) as well as in conditional Gαo mutants (Oboti et al., 2014), suggest a minor role of the VNO in the control of sexual preference in females. Nonetheless, either the apical or basal VSN layers alone may be sufficient to enable sex preference by using redundant neural pathways (Chamero et al., 2012). Further research is required to elucidate the control of sexual preference.

Although many aspects of sexual receptivity in females may be innate, acquiring elevated levels of lordosis performance depends on the combination of adequate hormonal environment with sensory experience (Thompson and Edwards, 1971). It has been shown that lesions of the VNO and AOB reduce the lordosis quotient of sexually naïve females (Keller et al., 2006; Martel and Baum, 2009) and that acute inhibition of AOB activity reduces the lordosis quotient of sexually experienced females (McCarthy et al., 2017). Our results show that Gαi2-dependent VNO activity is dispensable for the display of basal levels of lordosis (**Figure 3**), which likely depends on Gαo signaling (Oboti et al., 2014). After mating experience, however, we demonstrate that Gαi2+ VSNs play a critical role in the acquisition of complete sexual receptivity in females, transforming weaker responses into more robust and frequent lordosis episodes (**Figure 3**). Thus, synergy between innate and experience-dependent processes may be critical for fast, efficient, and flexible display of complex behaviors.

We have screened for the expression of c-Fos, an early gene linked to neural activity, in the brain and found that the number of c-Fos+ cells was reduced in the anterior AOB and RP3V of cGαi2$^{-/-}$ females after lordosis (**Figure 4**). This reduction in c-Fos+ neurons in both regions is consistent with reduced sensory input from the VNO. However, we observe a positive correlation of the number of c-Fos+ cells in the RP3V with lordosis, also in control animals (**Figure 4E**). Further experiments are needed to establish causality, but these results suggest that neural activity in the RP3V may regulate the level of sexual receptivity integrating sensory information from Gαi2+ neurons. In particular, RP3V-kisspeptin neurons seem to be essential to trigger lordosis (Hellier et al., 2018), although activity of these cells is not lower in cGαi2$^{-/-}$ females (**Figure 4I**). This is in line with the view that the display of basal levels of lordosis is largely Gαi2-independent and suggests that the recruitment of additional RP3V-kisspeptin neurons is not required to increase lordosis performance. In accordance with this, non-kisspeptin neurons in the RP3V, such as tyrosine-hydroxylase (TH) positive neurons, are also sensitive to male odors (Bakker et al., 2010; Taziaux and Bakker, 2015). Remarkably, targeted ablation of TH neurons in the RP3V does not seem to reduce the lordosis quotient in sexually naïve females (Scott et al., 2015). Further research is needed to establish whether TH neurons in the RP3V participate in the acquisition of sexual experience.

Our findings complement recent studies of neural circuits involved in social behavior by revealing that experience-dependent improvement of ethologically important behaviors can be shaped by sensory components (**Figure 5**). This may exemplify a mechanism of neuroplasticity in which olfaction in combination with social experience improve social behavior synergistically.

DATA AVAILABILITY STATEMENT

The raw data supporting the conclusions of this article will be made available by the authors, without undue reservation.

ETHICS STATEMENT

The animal study was reviewed and approved by the CEEA Val de Loire.

AUTHOR CONTRIBUTIONS

PC, MK, LB, FZ, and TL-Z designed the research. A-CT, CM, and KP performed the research. A-CT and CM analyzed the data. PC and A-CT wrote the manuscript with edits of all authors.

FUNDING

This work was supported by the Deutsche Forschungsgemeinschaft (DFG) grants Sonderforschungsbereich-Transregio TRR 152/P10, project 239283807 (FZ and TL-Z) and Sonderforschungsbereich 894 project A17 (FZ and TL-Z), and Region Centre Val de Loire project 201900134883 (PC). LB was supported in part by the Intramural Research Program of the NIH (Project Z01-ES-101643). A-CT was supported by the grant from the University of Tours and Region Centre Val de Loire.

ACKNOWLEDGMENTS

We thank Deborah Crespin, Flora Martin, and Aurelie Gasnier for mice husbandry; Marie-Claire Blache for help with imaging experiments; the staff of the hormonal assay laboratory; and Isabelle Franceschini for the kisspeptin antibody.

REFERENCES

Bakker, J., Pierman, S., and González-Martínez, D. (2010). Effects of aromatase mutation (ArKO) on the sexual differentiation of kisspeptin neuronal numbers and their activation by same versus opposite sex urinary pheromones. *Horm. Behav.* 57, 390–395. doi: 10.1016/j.yhbeh.2009.11.005

Bonthuis, P. J., Patteson, J. K., and Rissman, E. F. (2011). Acquisition of sexual receptivity: roles of chromatin acetylation, estrogen receptor-α, and ovarian hormones. *Endocrinology* 152, 3172–3181. doi: 10.1210/en.2010-1001

Chamero, P., Katsoulidou, V., Hendrix, P., Bufe, B., Roberts, R., Matsunami, H., et al. (2011). G protein G o is essential for vomeronasal function and aggressive behavior in mice. *Proc. Natl. Acad. Sci. U.S.A.* 108, 12898–12903. doi: 10.1073/pnas.1107770108

Chamero, P., Leinders-Zufall, T., and Zufall, F. (2012). From genes to social communication: molecular sensing by the vomeronasal organ. *Trends Neurosci.* 35, 597–606. doi: 10.1016/j.tins.2012.04.011

Del Punta, K., Leinders-Zufall, T., Rodriguez, I., Jukam, D., Wysocki, C. J., Ogawa, S., et al. (2002). Deficient pheromone responses in mice lacking a cluster of vomeronasal receptor genes. *Nature* 419, 70–74. doi: 10.1038/nature00955

Ehret, G., Koch, M., Haack, B., and Markl, H. (1987). Sex and parental experience determine the onset of an instinctive behavior in mice. *Naturwissenschaften* 74, 47–47. doi: 10.1007/BF00367047

Elyada, Y. M., and Mizrahi, A. (2015). Becoming a mother—circuit plasticity underlying maternal behavior. *Curr. Opin. Neurobiol.* 35, 49–56. doi: 10.1016/j.conb.2015.06.007

Ferrero, D. M., Moeller, L. M., Osakada, T., Horio, N., Li, Q., Roy, D. S., et al. (2013). A juvenile mouse pheromone inhibits sexual behaviour through the vomeronasal system. *Nature* 502, 368–371. doi: 10.1038/nature12579

Flanagan, K. A., Webb, W., and Stowers, L. (2011). Analysis of male pheromones that accelerate female reproductive organ development. *PLoS One* 6:e16660. doi: 10.1371/journal.pone.0016660

Fleming, A., Vaccarino, F., Tambosso, L., and Chee, P. (1979). Vomeronasal and olfactory system modulation of maternal behavior in the rat. *Science (80)* 203, 372–374. doi: 10.1126/science.760196

Franceschini, I., Yeo, S. H., Beltramo, M., Desroziers, E., Okamura, H., Herbison, A. E., et al. (2013). Immunohistochemical evidence for the presence of various kisspeptin isoforms in the mammalian brain. *J. Neuroendocrinol.* 25, 839–851. doi: 10.1111/jne.12069

Fraser, E. J., and Shah, N. M. (2014). Complex chemosensory control of female reproductive behaviors. *PLoS One* 9:e90368. doi: 10.1371/journal.pone.0090368

Hasen, N. S., and Gammie, S. C. (2009). Trpc2 gene impacts on maternal aggression, accessory olfactory bulb anatomy and brain activity. *Genes Brain Behav.* 8, 639–649. doi: 10.1111/j.1601-183X.2009.00511.x

Hellier, V., Brock, O., Candlish, M., Desroziers, E., Aoki, M., Mayer, C., et al. (2018). Female sexual behavior in mice is controlled by kisspeptin neurons. *Nat. Commun.* 9:400. doi: 10.1038/s41467-017-02797-2

Inoue, S., Yang, R., Tantry, A., Davis, C., Yang, T., Knoedler, J. R., et al. (2019). Periodic remodeling in a neural circuit governs timing of female sexual behavior. *Cell* 179, 1393–1408.e16. doi: 10.1016/j.cell.2019.10.025

Ishii, K. K., and Touhara, K. (2019). Neural circuits regulating sexual behaviors via the olfactory system in mice. *Neurosci. Res.* 140, 59–76. doi: 10.1016/j.neures.2018.10.009

Isogai, Y., Wu, Z., Love, M. I., Ahn, M. H.-Y., Bambah-Mukku, D., Hua, V., et al. (2018). Multisensory logic of infant-directed aggression by males. *Cell* 175, 1827–1841.e17. doi: 10.1016/j.cell.2018.11.032

Jouhanneau, M., Cornilleau, F., and Keller, M. (2014). Peripubertal exposure to male odors influences female puberty and adult expression of male-directed odor preference in mice. *Horm. Behav.* 65, 128–133. doi: 10.1016/j.yhbeh.2013.12.006

Keller, M., Baum, M. J., Brock, O., Brennan, P. A., and Bakker, J. (2009). The main and the accessory olfactory systems interact in the control of mate recognition and sexual behavior. *Behav. Brain Res.* 200, 268–276. doi: 10.1016/j.bbr.2009.01.020

Keller, M., Pierman, S., Douhard, Q., Baum, M. J., and Bakker, J. (2006). The vomeronasal organ is required for the expression of lordosis behaviour, but not sex discrimination in female mice. *Eur. J. Neurosci.* 23, 521–530. doi: 10.1111/j.1460-9568.2005.04589.x

Kimchi, T., Xu, J., and Dulac, C. (2007). A functional circuit underlying male sexual behaviour in the female mouse brain. *Nature* 448, 1009–1014. doi: 10.1038/nature06089

Koch, M., and Ehret, G. (1989). Estradiol and parental experience, but not prolactin are necessary for ultrasound recognition and pup-retrieving in the mouse. *Physiol. Behav.* 45, 771–776. doi: 10.1016/0031-9384(89)90293-X

Kohl, J., Autry, A. E., and Dulac, C. (2017). The neurobiology of parenting: a neural circuit perspective. *BioEssays* 39, 1–11. doi: 10.1002/bies.201600159

Lévy, F., Keller, M., and Poindron, P. (2004). Olfactory regulation of maternal behavior in mammals. *Horm. Behav.* 46, 284–302. doi: 10.1016/j.yhbeh.2004.02.005

Leypold, B. G., Yu, C. R., Leinders-Zufall, T., Kim, M. M., Zufall, F., and Axel, R. (2002). Altered sexual and social behaviors in trp2 mutant mice. *Proc. Natl. Acad. Sci. U.S.A.* 99, 6376–6381. doi: 10.1073/pnas.082127599

Marlin, B. J., Mitre, M., D'Amour, J. A., Chao, M. V., and Froemke, R. C. (2015). Oxytocin enables maternal behaviour by balancing cortical inhibition. *Nature* 520, 499–504. doi: 10.1038/nature14402

Martel, K. L., and Baum, M. J. (2009). Adult testosterone treatment but not surgical disruption of vomeronasal function augments male-typical sexual behavior in female mice. *J. Neurosci.* 29, 7658–7666. doi: 10.1523/jneurosci.1311-09.2009

McCarthy, E. A., Kunkhyen, T., Korzan, W. J., Naik, A., Maqsudlu, A., Cherry, J. A., et al. (2017). A comparison of the effects of male pheromone priming and optogenetic inhibition of accessory olfactory bulb forebrain inputs on the sexual behavior of estrous female mice. *Horm. Behav.* 89, 104–112. doi: 10.1016/j.yhbeh.2016.12.011

Nakahara, T. S., Camargo, A. P., Magalhães, P. H. M., Souza, M. A. A., Ribeiro, P. G., Martins-Netto, P. H., et al. (2020). Peripheral oxytocin injection modulates vomeronasal sensory activity and reduces pup-directed aggression in male mice. *Sci. Rep.* 10:19943. doi: 10.1038/s41598-020-77061-7

Nakahara, T. S., Cardozo, L. M., Ibarra-Soria, X., Bard, A. D., Carvalho, V. M. A., Trintinalia, G. Z., et al. (2016). Detection of pup odors by non-canonical adult vomeronasal neurons expressing an odorant receptor gene is influenced by sex and parenting status. *BMC Biol.* 14:12. doi: 10.1186/s12915-016-0234-9

Norlin, E. M., Gussing, F., and Berghard, A. (2003). Vomeronasal phenotype and behavioral alterations in Gαi2 mutant mice. *Curr. Biol.* 13, 1214–1219. doi: 10.1016/S0960-9822(03)00452-4

Numan, M. (1974). Medial preoptic area and maternal behavior in the female rat. *J. Comp. Physiol. Psychol.* 87, 746–759. doi: 10.1037/h0036974

Oboti, L., Pérez-Gómez, A., Keller, M., Jacobi, E., Birnbaumer, L., Leinders-Zufall, T., et al. (2014). A wide range of pheromone-stimulated sexual and reproductive behaviors in female mice depend on G protein Gαo. *BMC Biol.* 12:31. doi: 10.1186/1741-7007-12-31

Pfaff, D. W., and Sakuma, Y. (1979). Deficit in the lordosis reflex of female rats caused by lesions in the ventromedial nucleus of the hypothalamus. *J. Physiol.* 288, 203–210. doi: 10.1113/jphysiol.1979.sp012691

Scott, N., Prigge, M., Yizhar, O., and Kimchi, T. (2015). A sexually dimorphic hypothalamic circuit controls maternal care and oxytocin secretion. *Nature* 525, 519–522. doi: 10.1038/nature15378

Simerly, R. B. (2002). Wired for reproduction: organization and development of sexually dimorphic circuits in the mammalian forebrain. *Annu. Rev. Neurosci.* 25, 507–536. doi: 10.1146/annurev.neuro.25.112701.142745

Stolzenberg, D. S., and Rissman, E. F. (2011). Oestrogen-independent, experience-induced maternal behaviour in female mice. *J. Neuroendocrinol.* 23, 345–354. doi: 10.1111/j.1365-2826.2011.02112.x

Stowers, L., Holy, T. E., Meister, M., Dulac, C., and Koentges, G. (2002). Loss of sex discrimination and male-male aggression in mice deficient for TRP2. *Science* 295, 1493–1500. doi: 10.1126/science.1069259

Stowers, L., and Kuo, T.-H. (2015). Mammalian pheromones: emerging properties and mechanisms of detection. *Curr. Opin. Neurobiol.* 34, 103–109. doi: 10.1016/j.conb.2015.02.005

Stowers, L., and Liberles, S. D. (2016). State-dependent responses to sex pheromones in mouse. *Curr. Opin. Neurobiol.* 38, 74–79. doi: 10.1016/j.conb.2016.04.001

Tachikawa, K. S., Yoshihara, Y., and Kuroda, K. O. (2013). Behavioral transition from attack to parenting in male mice: a crucial role of the vomeronasal system. *J. Neurosci.* 33, 5120–5126. doi: 10.1523/JNEUROSCI.2364-12.2013

Taziaux, M., and Bakker, J. (2015). Absence of female-typical pheromone-induced hypothalamic neural responses and kisspeptin neuronal activity in

α-fetoprotein knockout female mice. *Endocrinology* 156, 2595–2607. doi: 10.1210/en.2015-1062

Thompson, M. L., and Edwards, D. A. (1971). Experiential and strain determinants of the estrogen-progesterone induction of sexual receptivity in spayed female mice. *Horm. Behav.* 2, 299–305. doi: 10.1016/0018-506X(71)90004-3

Trouillet, A.-C., Keller, M., Weiss, J., Leinders-Zufall, T., Birnbaumer, L., Zufall, F., et al. (2019). Central role of G protein Gαi2 and Gαi2 + vomeronasal neurons in balancing territorial and infant-directed aggression of male mice. *Proc. Natl. Acad. Sci. U.S.A.* 116, 5135–5143. doi: 10.1073/pnas.1821492116

Weiss, J., Pyrski, M., Jacobi, E., Bufe, B., Willnecker, V., Schick, B., et al. (2011). Loss-of-function mutations in sodium channel Na v 1.7 cause anosmia. *Nature* 472, 186–192. doi: 10.1038/nature09975

Wu, Z., Autry, A. E., Bergan, J. F., Watabe-Uchida, M., and Dulac, C. G. (2014). Galanin neurons in the medial preoptic area govern parental behaviour. *Nature* 509, 325–330. doi: 10.1038/nature13307

Wysocki, C. J., and Lepri, J. J. (1991). Consequences of removing the vomeronasal organ. *J. Steroid Biochem. Mol. Biol.* 39, 661–669. doi: 10.1016/0960-0760(91)90265-7

Conflict of Interest: The authors declare that the research was conducted in the absence of any commercial or financial relationships that could be construed as a potential conflict of interest.

Copyright © 2021 Trouillet, Moussu, Poissenot, Keller, Birnbaumer, Leinders-Zufall, Zufall and Chamero. This is an open-access article distributed under the terms of the Creative Commons Attribution License (CC BY). The use, distribution or reproduction in other forums is permitted, provided the original author(s) and the copyright owner(s) are credited and that the original publication in this journal is cited, in accordance with accepted academic practice. No use, distribution or reproduction is permitted which does not comply with these terms.

3 Control of avoidance behaviors by apical VSNs

3.1 Introduction

Mice are continuously exposed to dangers such as predators or infection during social interactions with congeners. Social species have developed various behavioral mechanisms and responses to minimize their potential exposure to threats while maintaining their vital activities. The olfactory system is crucial in these processes by coding the valence of surrounding odors and thus tipping the balance towards attraction or aversion (Li and Liberles, 2015).

Preys and predators share their environment, and predator cues can be detected by preys to induce avoidance and defensive behaviors. These interspecific chemicals are referred to as kairomones. Kairomones detection is not restricted to a single olfactory subsystem (Pérez-Gómez et al., 2015; Takahashi, 2014). The vomeronasal system was first shown as mediating cat avoidance (Samuelsen and Meredith, 2009). Later, the VNO was also associated with rat, mustelid, snake, and raptor detection and avoidance (Isogai et al., 2011; Papes et al., 2010). Several VRs can be activated by one type of predator and these VRs seem to be clustered, with some predators activating only basal or apical VSNs (Isogai et al., 2011). For example, functional ablation of V2Rs/$G\alpha_o$ basal VSNs abolishes avoidance for cat fur odors (Pérez-Gómez et al., 2015). Conversely, AOS activation by exposure to owl feathers or bedding correlates with the V1R/$G\alpha_{i2}$ signaling pathway (Carvalho et al., 2015; Isogai et al., 2011), but functional evidence is still lacking.

Mice detect sick congeners using smell and actively avoid them to prevent contagion (Kavaliers et al., 2005). The VNO has been proposed to mediate sick conspecific recognition. Bacterial lipopolysaccharides (LPS) injection in mice is a standard protocol to induce a general inflammatory state, thus mimicking pathogen infection, and inducing avoidance by healthy congeners. VNOx and $Trpc2^{-/-}$ mice do not avoid an LPS-treated mice (Boillat et al., 2015; Kwon et al., 2021). The identity of VSNs mediating sickness-associated cues is unknown. FPRs appear as good candidates due to their natural affinity for bacterial-derived peptides (Bufe et al., 2012). However, FPR3-KO mouse still avoid a LPS-treated animal, discarding this receptor in the mediation of this type of avoidance (Bufe et al., 2019). Nonetheless, the analysis of AOB activation after exposure to urine from LPS-treated mice shows increased activation in both anterior and posterior AOB parts (Boillat et al., 2015). Thus, both V2Rs-expressing VSNs or apical VSNs (expressing V1Rs or apical FPRs) are good candidates to mediate this type of avoidance.

The present study is aimed to investigate the role of vomeronasal $G\alpha_{i2}$ signaling on avoidance behaviors. We exposed conditional $G\alpha_{i2}$ null mice ($cG\alpha_{i2}^{-/-}$) to two types of danger-associated cues: predator odors from owls and sickness cues from LPS-treated mice. We combined behavioral experiments with calcium imaging recording and immediate early gene mapping to determine whether $G\alpha_{i2}$-expressing VSNs drive avoidance to both types of cues.

3.2 Methods

Animals. Animal care and experimental procedures were performed following French and European guidelines on the protection of animals used for scientific purposes and approved by an ethical committee for animal experimentation. Mice were kept under standard 12h light/dark cycles with food and water ad libitum. $cG\alpha_{i2}^{-/-}$ and $cG\alpha_{i2}^{+/-}$ mice were generated as described (Trouillet et al., 2019). All animals used were 8 weeks old or older. Males were used for behavioral experiments and immediate early gene mapping. Diestrus females and males were used for calcium imaging experiments. Females' estrus status was assessed by vaginal sampling.

Predator odors collection and preparation. Owl (*Asio otus* and *Tyto alba*) feces were collected directly in bird aviaries. 3 x 3 cm gauzes were put in contact with the feces in a glass jar and incubated at RT for one day (Figure 39C). Gauze and feces were then stored separately at -80°C. Cat (*Felis catus*) fur was collected by brushing. 3 x3 cm gauzes were rubbed onto the cat's neck and face fur (Figure 39A). Gauze and fur were then stored together at -80°C. Snake (*Pantherophis guttatus*) molt was collected in the snake vivarium, cut in 2 x 2 cm pieces, and stored at -80°C (Figure 39B). For calcium imaging experiments, predator odor extracts were prepared by incubating predator samples in 100 mL Hank's balanced salt solution (Invitrogen) supplemented with 10 mM Hepes at RT for 2h on an orbital rotator (Figure 39D). Four solutions were prepared from: 1) a clean gauze; 2) 0.4 g of cat fur and a clean gauze; 3) 3 g of crushed owl feces and a clean gauze; and 4) 0.2 g of crushed snake molt. Solutions were first coarsely filtered to remove solids and then passed through a Nalgene™ Rapid-Flow™ sterile filtering unit (surfactant-free cellulose acetate membrane, pore size 0.2 µm, Thermo Scientific) (Figure 39E). Filtered solutions were stocked at -80°C.

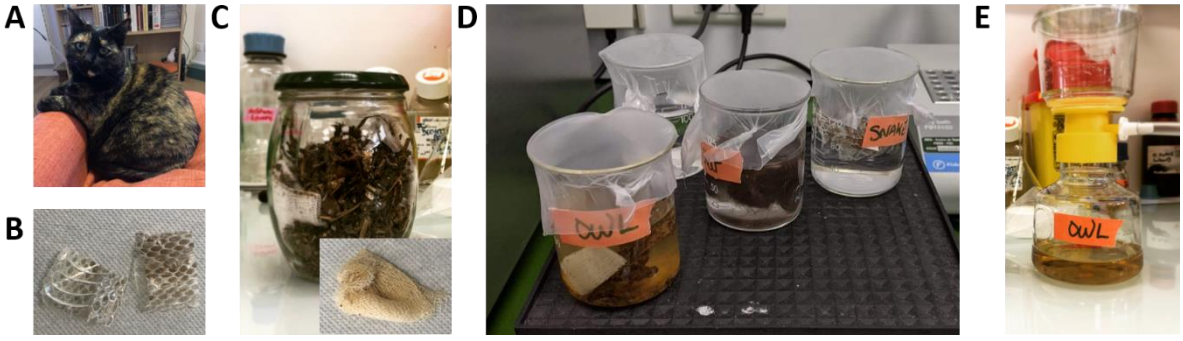

Figure 39: Preparation of predator samples. A) Moquette, the cat used for sampling fur. B) Pieces of snake molt. C) Jar used for incubating gauze with owl feces and resulting gauze after incubation. D) Incubation of predator samples for the preparation of calcium imaging extracts. E) Resulting extract after filtration.

Treatment of mice with LPS and urine collection. C57BL6/J adult group-housed males were injected intraperitoneally with either 200 µL of 1 mg/kg LPS (Lipopolysaccharide L4391, Sigma) or saline solution. 4 h post-injection, urine from mice injected with LPS or saline were collected, pooled

(4 mice per condition), and stored at -80 °C until use. For calcium imaging experiments, fresh urine from healthy male donors was fractioned into high and low molecular weight fractions (HMW and LMW) (Trouillet et al., 2019) and kept at -80 °C. A week later, the same males were injected with 200 µL of 1 mg/kg LPS (Lipopolysaccharide L4391, Sigma), urine was collected 4h later and fractioned before storage.

Behavior. Mice were moved to the experimental room 2 h before testing. Assays were conducted 2 h before the start of the dark period. Experiments were videotaped and subsequently analyzed by a blind experimenter.

Predator odor avoidance. The day before the first test, mice were habituated to the three chambers box for 10 min in absence of stimuli. Mice were then tested 4 times for avoidance to predator odors or neutral stimulus on consecutive days. For each experiment, one chamber contained predator or neutral stimulus and the others were empty. Neutral stimulus was an unscented clean gauze; predator odors were either a piece of snake molt, cat fur and a gauze rubbed on a cat neck, or a gauze incubated with owl feces. Order of stimuli presentation was randomized. The apparatus was cleaned with 20% ethanol between subjects. Stimulus side was randomized to avoid side effects: the entire maze was rotated in order to maintain the predator odor in the same chamber and thus avoiding potential contamination of the empty chambers. Mice were free to investigate the apparatus for 10 min. The time spent in each chamber and the duration of chemosensory investigation were recorded. An avoidance index was calculated as $(T_P — aT_N)/(aT_P + aT_N)$, with T_P as the time an individual mouse investigated a predator odor, aT_P as the average time of all tested mice investigating this stimulus, and aT_N as the average time of all mice investigating the neutral stimulus. Negative values represent avoidance and positive values represent attraction.

Sick conspecific odor avoidance. Two days before the test, mice were daily habituated to the three chambers box for 10 min with unscented stimuli in each side chamber. On test day, 50 µL of urine from LPS-treated and saline-treated males were placed on filter papers sealed to plastic weight boards in each side compartments. Stimulus side was randomized, and the apparatus was cleaned with 20% ethanol between subjects. Mice were left free to investigate the apparatus for 10 min. The time spent in each chamber and the duration of chemosensory investigation were recorded. An avoidance index was calculated as $(T_{LPS} — aT_{veh})/(aT_{LPS} + aT_{veh})$, with T_{LPS} as the time an individual mouse investigated the LPS-treated male urine, aT_{LPS} as the average time of all tested mice investigating this stimulus, and aT_{veh} as the average time of all mice investigating the vehicle-treated male urine. Negative values represent avoidance and positive values represent attraction. We also calculated an individual preference score as $(T_{LPS} — T_{veh})/(T_{LPS} + T_{veh})$, with T_{veh} the time an individual mouse investigated the vehicle-treated male urine. Negative values represent preference for the LPS-urine and positive values represent preference for the veh-urine.

Calcium imaging. Calcium imaging of freshly dissociated VSNs was performed as described previously (Chamero et al., 2007, 2011; Trouillet et al., 2019). Cells were stimulated in a random order during 30 sec with 3 min interval between each stimulation. Chemostimuli were freshly diluted in HBSS/Hepes solution to give the following final concentrations: HMW and LMW fractions from LPS-treated or saline-treated males, 1:100; clean gauze, cat fur, and snake molt extracts, 1:1; owl feces extract, 1:1, 1:2, 1:10, and 1:100; KCl, 50 mM. Cells showing a response to control solution or buffer were excluded from the analysis. Experimental replicates were done by pooling VNO from two mice. Each experimental replicate was tested three times for technical replicates. Mean values obtained from technical replicates and acute number of cells were analyzed.

Immunostaining. *Tissue preparation.* Mice were individually housed for at least 4 days without bedding changing and exposed to either a clean gauze, a gauze incubated with owl feces, a clean filter paper, or a filter paper with LPS-treated male urine. 90 min after exposure, mice were anesthetized by an overdose of pentobarbital (Ceva) and perfused transcardially. Samples were prepared as previously described (Trouillet et al., 2019, 2021). *cFos immunolabeling.* Procedure was done as previously described (Trouillet et al., 2019, 2021). cFos primary antibody (1:1000; mouse monoclonal #sc-271243, Santa Cruz Biotechnology) and biotinylated goat anti-mouse secondary antibody (1:1000; IgG, Jackson ImmunoResearch) were used. *pS6 immunolabeling.* Slides were washed (3 x 5 min) in TBS, incubated in blocking solution (TBS containing 0.3% Triton X-100, TBS-T, and 2% donkey serum) 2h at room temperature (RT), and overnight at 4 °C in blocking solution supplemented with the pS6 primary antibody (1:2500; rabbit polyclonal #44-923G, Invitrogen). Slides were then washed in TBS and incubated in TBS-T supplemented with secondary antibody (1:1000 Cy3-conjugated donkey anti-rabbit IgG, Jackson ImmunoResearch) for 2h at RT. Nuclei were counterstained 5 min at RT with DAPI. Slides were mounted with Fluoromount-G™ (Invitrogen). *Analysis.* Slides were scanned using an automatic slide scanner (Axio Sca.Z1, Zeiss). cFos-positive nuclei were counted using the particle analyzer plug-in of Fiji (Schindelin et al., 2012) on 2-3 images of the AOB per animal and expressed as a density. pS6-positive cells were counted using the Cell Detection process of QuPath (Bankhead et al., 2017) on 6-15 images of the VNE per animals and expressed as a proportion of the total DAPI-positive nuclei number.

Statistics. Statistical analyses were performed by using GraphPad Prism 9.0 (GraphPad Software). Assumptions of normality and homogeneity of variance were tested before conducting the following statistical approaches. Student's t test was used to measure the significance of the difference between two distributions. In case the results failed the test of normality, a Mann–Whitney U test was performed. For categorical data, we used the Fisher's exact test. Multiple groups were compared by using a two-way ANOVA with Fisher LSD multiple comparison tests as a post hoc. The probability of error level (i.e., α) was chosen to be 0.05. Specific statistics and number of samples analyzed are described in the figure captions.

3.3 Results

3.3.1 Apical VSNs mediate sick and predator avoidances

Several pieces of evidence point to a role of $G\alpha_{i2}$-expressing VSNs in mediating innate avoidance behaviors. For example, $Trpc2^{-/-}$ mice do not avoid birds of prey cues (Carvalho et al., 2020), and olfactory detection of this type of predator may be mediated by V1Rs-expressing VSNs (Isogai et al., 2011). To verify this hypothesis, we exposed $cG\alpha_{i2}^{+/-}$ and $cG\alpha_{i2}^{-/-}$ mice to different predator cues (Figure 40A). Each mouse was exposed in independent experiments to a clean gauze (control), cat fur, snake molt, or owl feces in a three-chamber box, and we calculated an aversion index based on the time spent sniffing the stimuli (see methods). Olfactory detection of cat fur has been associated with V2Rs/$G\alpha_o$-expressing VSNs (Pérez-Gómez et al., 2015) and snake molt seems to activate both V1Rs- and V2Rs-expressing VSNs (Isogai et al., 2011). Thus, we used these two stimulations as positive controls. As expected, all predator cues were aversive to naïve $cG\alpha_{i2}^{+/-}$ control mice, as shown by their negative aversion index (owl: -0.3, snake: -0.25, cat: -0.35; Figure 40B). Aversion indexes of $cG\alpha_{i2}^{-/-}$ males for cat and snake stimuli were also negative and statistically similar to those of control animals (-0.33 P = 0.8 and -0.42 P = 0.2, respectively; Figure 40B), indicating that avoidance to these two predators does not require $G\alpha_{i2}$ signaling. However, owl feces failed to induce any aversive effect on $cG\alpha_{i2}^{-/-}$ animals (Figure 40B). Based on the time spent investigating the clean gauze stimulus, exposure of $cG\alpha_{i2}^{-/-}$ mice to owl feces did not elicit avoidance or attraction as shown by the aversion index close to zero (-0.03, $P < 0.05$ versus $cG\alpha_{i2}^{+/-}$, $P < 0.01$ and $P < 0.05$ versus snake and cat stimuli in $cG\alpha_{i2}^{-/-}$; Figure 40B). This indicates that $G\alpha_{i2}$ vomeronasal signaling may be necessary to display innate avoidance to birds of prey.

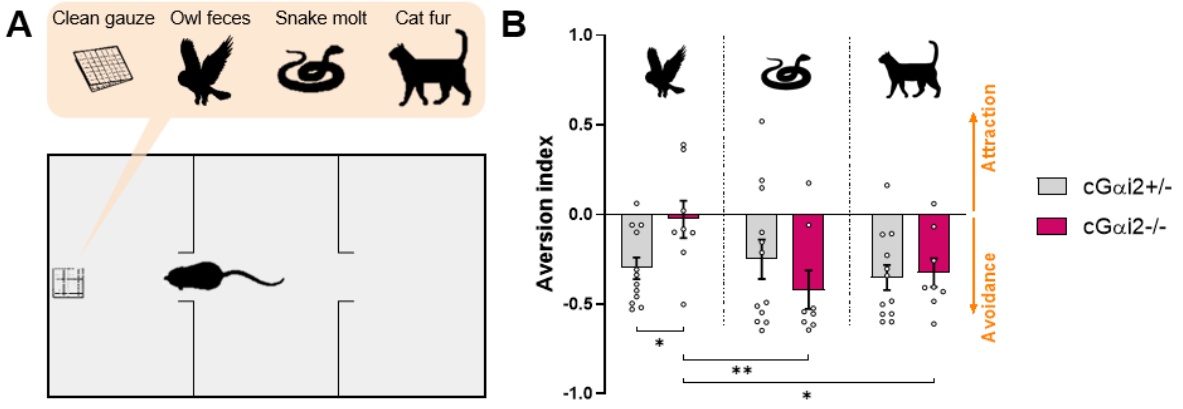

Figure 40: Predator avoidance in $cG\alpha_{i2}^{-/-}$ animals. A) Predator avoidance experimental paradigm. 12 $cG\alpha_{i2}^{+/-}$ and 8 $cG\alpha_{i2}^{-/-}$ males were tested for their innate avoidance toward a clean gauze, owl feces, snake molt, or cat fur in a three-chamber box. B) Average response to a given stimulus, as quantified by the aversion index. Two-way repeated measures ANOVA. Stimulus: $F_{(2, 36)} = 3.924$, $P < 0.05$; genotype : $F_{(1, 18)} = 0.1886$, $P = 0.7$; genotype x stimulus: $F_{(2, 36)} = 4.888$, $P < 0.05$. Posthoc analyzes, LSD Fischer tests: owl feces avoidance, $cG\alpha_{i2}^{+/-}$ vs $cG\alpha_{i2}^{-/-}$ $P < 0.05$; $cG\alpha_{i2}^{-/-}$ owl feces vs snake skin avoidance, $P < 0.01$; $cG\alpha_{i2}^{-/-}$ owl feces vs cat fur avoidance, $P < 0.05$; other comparisons $P = 0.2 – 0.8$. Data are shown as mean ± SEM with individual values.

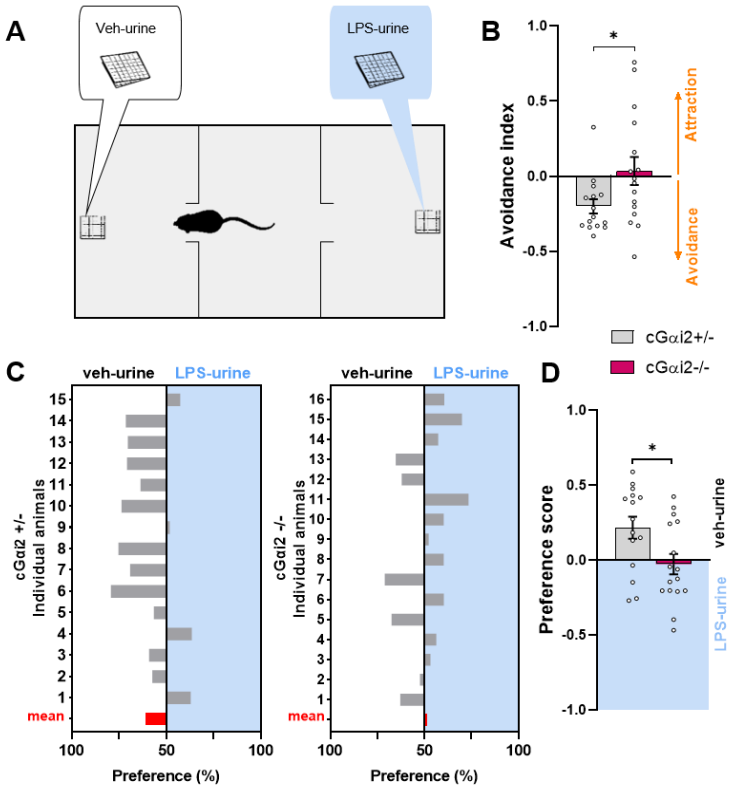

Figure 41: Sick-conspecific avoidance in cGa$_{i2}^{-/-}$ animals. A) Sick-conspecific avoidance experimental paradigm. 15 cGα$_{i2}^{+/-}$ and 16 cGα$_{i2}^{-/-}$ males were tested for their preference between vehicle- (veh-urine) and LPS-treated (LPS-urine) male urine in a three-chamber box. B) Average responses to a given stimulus, as quantified by the aversion index. Mann-Whitney test, P < 0.05. C) Graphs showing investigation time above 50% that individual cGα$_{i2}^{+/-}$ (left) and cGα$_{i2}^{-/-}$ (right) examined either the vehicle or LPS urine. D) Average responses to a given stimulus, as quantified by the preference score. Unpaired t-test, P < 0.05. Data are shown as mean ± SEM with individual values.

Similar to predator cues, Trpc2$^{-/-}$ mice do not discriminate urine from a sick or healthy congener, but VSNs sensing sick-associated cues are not yet identified (Boillat et al., 2015; Bufe et al., 2019). In order to determine if Gα$_{i2}$-expressing VSNs participate in sick-conspecific avoidance, we tested the olfactory preference of cGα$_{i2}^{+/-}$ and cGα$_{i2}^{-/-}$ mice between healthy versus sick same-sex urine (Figure 41A). Male mice were made sick by injection of bacterial lipopolysaccharides (LPS), and their urine (LPS-urine) was used in a two-choice test with urine from healthy males (veh-urine). We calculated an aversion index based on the time spent sniffing the veh-urine (see methods). LPS-urine was aversive to cGα$_{i2}^{+/-}$ control males, as shown by the negative aversion index (-0.2; Figure 41B). However, LPS-urine did not elicit avoidance or attraction to cGα$_{i2}^{-/-}$ mice as shown by an aversion index close to zero (-0.03, P < 0.05 versus cGα$_{i2}^{+/-}$; Figure 41B). Examining data from individual mice showed that most cGα$_{i2}^{+/-}$ animals (11/15) spent more time investigating the veh-urine than the LPS-urine, while only 6 over 16 cGα$_{i2}^{-/-}$ males investigated veh-urine more than LPS-urine (Figure 41C). This indicates that cGα$_{i2}^{+/-}$ males showed a preference for the veh-urine while cGα$_{i2}^{-/-}$ did not. Indeed, the comparison of the individual preference scores (see methods) showed a statistical difference between genotypes (P < 0.05, Figure 41D). Therefore, Gα$_{i2}$ vomeronasal signaling may be necessary for innate sick conspecific avoidance.

3.3.2 Sick and predator associated olfactory cues activate $G\alpha_{i2}$ vomeronasal signaling pathway

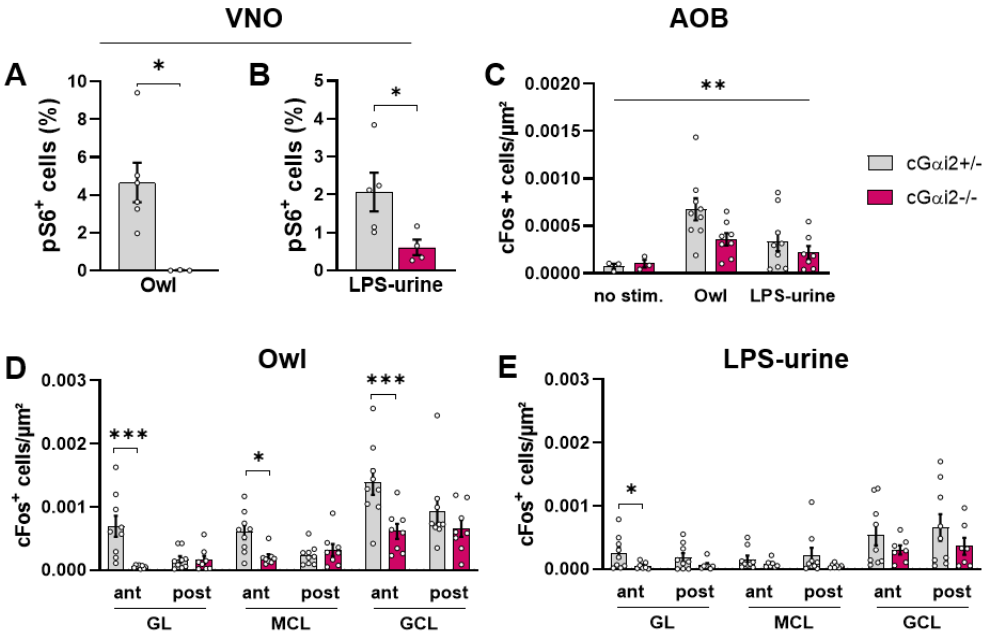

Figure 42: VNO and AOB activation after owl and LPS-urine exposures. A-B) Proportion of pS6-positive cells in the VNO after owl (A) and LPS-urine (B) exposures. A) N = 6 $cG\alpha_{i2}^{+/-}$ and N = 3 $cG\alpha_{i2}^{-/-}$, unpaired t-test P < 0.05. B) N = 5 $cG\alpha_{i2}^{+/-}$ and N = 4 $cG\alpha_{i2}^{-/-}$, unpaired t-test P < 0.05. C) cFos-positive cells density in the AOB of unstimulated and stimulated $cG\alpha_{i2}^{+/-}$ (N = 3 to 9) and $cG\alpha_{i2}^{-/-}$ (N = 3 to 8) mice. Two-way ANOVA, stimulus: $F_{(2, 33)} = 7.432$, P < 0.01 ; genotype : $F_{(1, 33)} = 2.203$, P = 0.1; genotype x stimulus: $F_{(2, 33)} = 1.219$, P = 0.3. D) cFos-positive cells density in each layer of the anterior and posterior AOB of $cG\alpha_{i2}^{+/-}$ (N = 9) and $cG\alpha_{i2}^{-/-}$ (N = 8) mice after exposure to owl feces. Two-way repeated measures ANOVA, area: $F_{(5, 75)} = 30.41$, P < 0.001 ; genotype : $F_{(1, 15)} = 5.914$, P < 0.05; area x genotype: $F_{(5, 75)} = 8.292$, P < 0.001. Posthoc analyzes, LSD Fischer tests: $cG\alpha_{i2}^{+/-}$ vs $cG\alpha_{i2}^{-/-}$ GL-ant P < 0.001; MCL-ant P < 0.05; GCL-ant P < 0.001; other regions P = 0.1 – 0.9. E) cFos-positive cells density in each layer of the anterior and posterior AOB of $cG\alpha_{i2}^{+/-}$ (N = 9) and $cG\alpha_{i2}^{-/-}$ (N = 7) mice after exposure to LPS-urine. Two-way repeated measures ANOVA, area: $F_{(5, 70)} = 9.843$, P < 0.001 ; genotype : $F_{(1, 14)} = 2.3$, P = 0.1; area x genotype: $F_{(5, 70)} = 0.511$, P = 0.8. Posthoc analyzes, LSD Fischer tests: $cG\alpha_{i2}^{+/-}$ vs $cG\alpha_{i2}^{-/-}$ GL-ant P < 0.05; other regions P = 0.1 – 0.6. Data are shown as mean ± SEM with individual values.

Next, we wanted to assess whether $G\alpha_{i2}$-expressing VSNs sense owl and LPS-urine olfactory cues. We exposed singly-housed males to an owl feces impregnated gauze or to urine from an LPS-treated male and analyzed VNO and AOB activation by immunostaining for pS6 or cFos, respectively. Owl exposure induced pS6 expression in 4.6% of VSNs of control $cG\alpha_{i2}^{+/-}$ mice. By contrast, the number of pS6-positive cells was significantly lower in $cG\alpha_{i2}^{-/-}$ animals (0.017%, P < 0.05 versus controls; Figure 42A). Similarly, the proportion of pS6-positive cells in the VNE of $cG\alpha_{i2}^{-/-}$ mice was lower than in controls after LPS-urine exposure (2.07% versus 0.61%, P < 0.05; Figure 42B). At the level of the AOB, each stimulation increased the total cFos expression in both $cG\alpha_{i2}^{+/-}$ and $cG\alpha_{i2}^{-/-}$ mice compared to unstimulated animals (P < 0.01; Figure 42C). Apical and basal VSNs projections to the glomerular layer of the AOB are segregated, with apical V1Rs/$G\alpha_{i2}$ VSNs projecting the anterior AOB and basal V2Rs/$G\alpha_o$ VSNs to the posterior AOB. We thus compared the density of cFos cells in each layer of the AOB (GL, glomerular layer; MCL, mitral cells layer; GCL, granular cells layer) regarding

the anteroposterior segregation (Figure 42D and E). We did not observe differences in the posterior AOB after owl exposure in mutant animals (P = 0.2 – 0.9; Figure 42D). However, the density of cFos positive cells was significantly lower in each layer of the anterior AOB of $cG\alpha_{i2}^{-/-}$ mice (anterior GL and GCL, P < 0.01, anterior MCL, P < 0.05; Figure 42D). LPS-urine exposure did not induce a different activation of the posterior AOB of control and mutant mice (P = 0.1 – 0.2; Figure 42E). In the anterior AOB, a significant difference between $cG\alpha_{i2}^{-/-}$ and $cG\alpha_{i2}^{+/-}$ was found only the GL (P < 0.05, other regions P = 0.1 – 0.6; Figure 42E). Altogether, these results suggest that the the $G\alpha_{i2}$ subsystem may detect owl and LPS-urine olfactory cues.

3.3.3 Deletion of $G\alpha_{i2}$ reduces the detection of owl odors

To strengthen our results and assess the responsiveness of VSNs to predator cues, we performed live-cell Ca^{2+} imaging on dissociated VSNs using Fura2. We prepared extracts from cat fur, snake molt, and owl feces (see methods) and tested the responsiveness of 3334 $cG\alpha_{i2}^{+/-}$ and 2364 $cG\alpha_{i2}^{-/-}$ VSNs. Cat fur and snake molt extracts elicited responses in both control (4% and 3.3%, respectively) and mutant (3.3 and 4.1%, respectively) VSNs (Figure 43A). We analyzed the number and the proportion of responsive cells to these two stimuli and did not found differences between genotypes (Figure 43A and B). By contrast, stimulation with owl extract did activate a much larger fraction of VSNs (>10% versus ~ 3 - 4%) and different amounts of $cG\alpha_{i2}^{-/-}$ and $cG\alpha_{i2}^{+/-}$ VSNs (Figure 43A and B). The overall number of responsive cells was statistically different in $cG\alpha_{i2}^{-/-}$ VSNs ($cG\alpha_{i2}^{-/-}$ 244/2364, 10.3% versus $cG\alpha_{i2}^{+/-}$ 466/3434, 13.6%; χ^2 P < 0.001; Figure 43B). The proportion of activated cells was also decreased in the $cG\alpha_{i2}^{-/-}$ VSNs (P < 0.05, Figure 43A). We then examined the number of cells responsive to exclusively one stimulus (either cat, snake, or owl; Figure 43B and C). Comparing the proportion of monoresponsive cells showed that owl extracts also activated less $cG\alpha_{i2}^{-/-}$ VSNs than control ones (P < 0.01, Figure 43C). We decided to evaluate VSNs responses to several dilutions of the owl feces extract (Figure 43D - G). Surprisingly, in $cG\alpha_{i2}^{+/-}$ controls, [1:2] dilution further increases the number of responses compared to the undiluted ([1:1]) extract (16.7% versus 9.8%), but we observed a reduction of the proportion of responsive cells with the [1:10] and [1:100] dilutions (9.8% versus 5.2% and 3.5%, respectively, Figure 43F). Similar pattern of variation was observed in $cG\alpha_{i2}^{-/-}$ VSNs ([1:1] 6.7%; [1:2] 9.9%, [1:10] 3%; [1:100], 2.5%, Figure 43F). The difference between the number of activated $cG\alpha_{i2}^{-/-}$ and $cG\alpha_{i2}^{+/-}$ VSNs was significant for [1:1] (-33.2%, χ^2 P < 0.01), [1:2] (-40.7%, χ^2 P < 0.001), [1:10] (-43%, χ^2 P < 0.01), but not for [1:100] dilution (-28.7%, χ^2 P = 0.07) (Figure 43E and G). Altogether, these results show that VSNs are responsive to all three predator odors and that $G\alpha_{i2}$-expressing VSNs participate in the detection of owl odors.

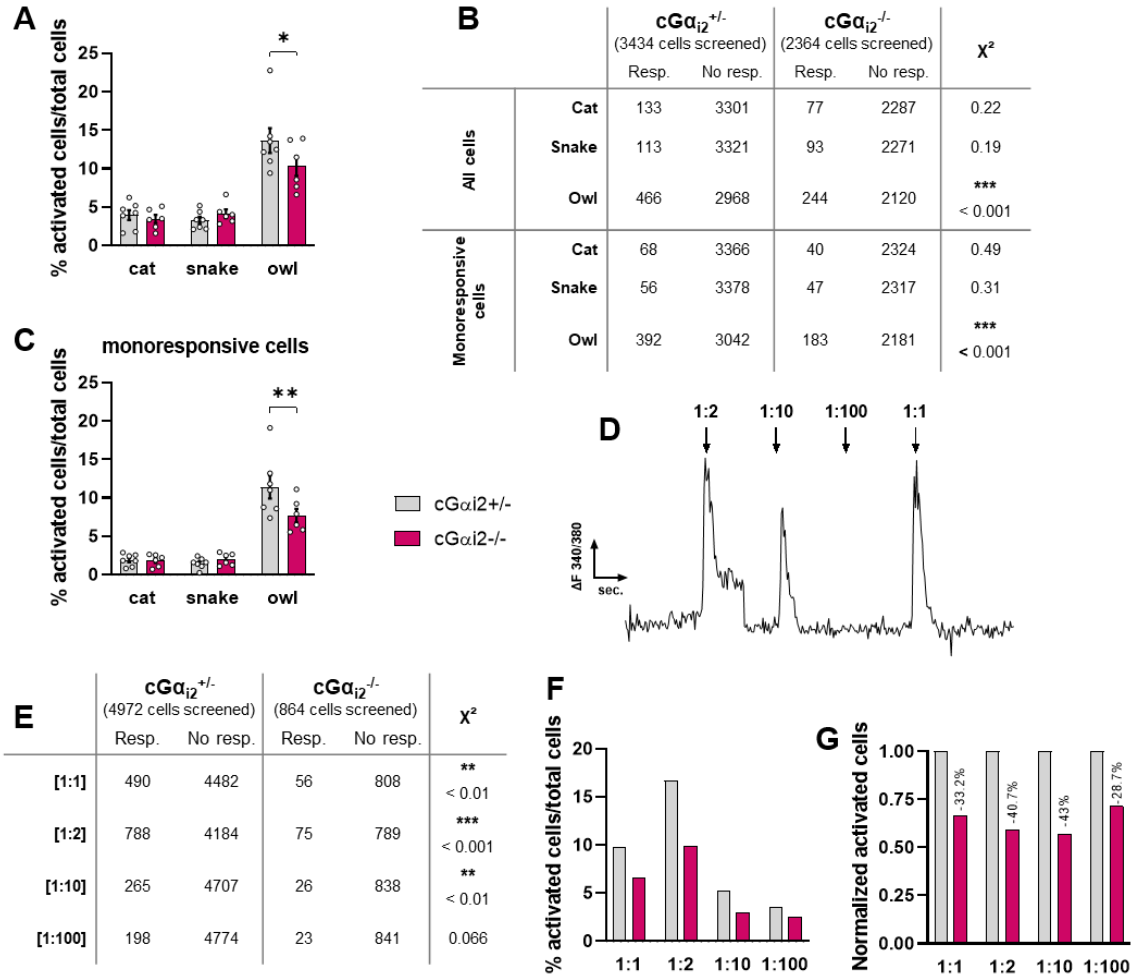

		$cG\alpha_{i2}^{+/-}$ (3434 cells screened)		$cG\alpha_{i2}^{-/-}$ (2364 cells screened)		X^2
		Resp.	No resp.	Resp.	No resp.	
All cells	Cat	133	3301	77	2287	0.22
	Snake	113	3321	93	2271	0.19
	Owl	466	2968	244	2120	*** < 0.001
Monoresponsive cells	Cat	68	3366	40	2324	0.49
	Snake	56	3378	47	2317	0.31
	Owl	392	3042	183	2181	*** < 0.001

	$cG\alpha_{i2}^{+/-}$ (4972 cells screened)		$cG\alpha_{i2}^{-/-}$ (864 cells screened)		X^2
	Resp.	No resp.	Resp.	No resp.	
[1:1]	490	4482	56	808	** < 0.01
[1:2]	788	4184	75	789	*** < 0.001
[1:10]	265	4707	26	838	** < 0.01
[1:100]	198	4774	23	841	0.066

Figure 43: Specific reduction of VSNs activation by owl odors in the absence of Gαi2. A) Analysis of ligand-evoked Ca^{2+} responses in dissociated cells from $cG\alpha_{i2}^{+/-}$ and $cG\alpha_{i2}^{-/-}$ (N = 6 – 7 experiments using cells from 6 mice for each genotype) mice after stimulation by cat fur, snake molt, or owl feces extracts. Two-way ANOVA, stimulus: $F_{(2, 33)} = 47.38$, $P < 0.001$; genotype : $F_{(1, 33)} = 1.521$, $P = 0.2$; stimulus x genotype: $F_{(2, 33)} = 2.332$, $P = 0.1$. Posthoc analyzes, LSD Fischer tests: owl $cG\alpha_{i2}^{+/-}$ vs $cG\alpha_{i2}^{-/-}$ $P < 0.05$; other comparisons $P = 0.5 – 0.7$. B) Table showing the number of (Resp.) and non responsive (No resp.) cells for each stimulation. χ^2 tests, $cG\alpha_{i2}^{+/-}$ versus $cG\alpha_{i2}^{-/-}$ $P < 0.001$ for all cells and for monoresponsive cells only; other comparison $P = 0.2 – 0.5$. C) Analysis of ligand-evoked Ca^{2+} responses in dissociated cells from $cG\alpha_{i2}^{+/-}$ and $cG\alpha_{i2}^{-/-}$ mice (N = 6 – 7 experiments using cells from 6 mice for each genotype) after stimulation by cat fur, snake molt, or owl feces extracts. Only cells responding to one stimulus exclusively are considered. Two-way ANOVA, stimulus: $F_{(2, 33)} = 65.44$, $P < 0.001$; genotype : $F_{(1, 33)} = 2.928$, $P = 0.09$; stimulus x genotype: $F_{(2, 33)} = 4.338$, $P < 0.05$. Posthoc analyzes, LSD Fischer tests: owl extract $cG\alpha_{i2}^{+/-}$ vs $cG\alpha_{i2}^{-/-}$ $P < 0.01$, other comparisons $P = 0.6 – 0.9$. D) Representative Ca^{2+}responses recorded in a $cG\alpha_{i2}^{+/-}$ VSN during stimulation with owl extract at different dilutions ([1:1]; [1:2]; [1:10]; [1:100]). E) Table showing the number of responsive (Resp.) and non responsive (No resp.) cells for each owl extract dilution. χ^2 tests, $cG\alpha_{i2}^{+/-}$ versus $cG\alpha_{i2}^{-/-}$ $P < 0.001$ for [1:2], $P < 0.01$ for [1:1] and [1:10], and $P = 0.066$ for [1:100] dilution. F) Mean proportion of activated cells from $cG\alpha_{i2}^{+/-}$ (N = 4) and $cG\alpha_{i2}^{-/-}$ (N = 2) mice after stimulation with [1:1], [1:2], [1:10], and [1:100] dilutions of the owl extract. G) Normalized percentage of responding cells from $cG\alpha_{i2}^{+/-}$ (N = 4) and $cG\alpha_{i2}^{-/-}$ (N = 2) mice to a given dilution. Data are shown as mean ± SEM with individual values (A and C) or as mean values (F and G).

3.3.4 $G\alpha_{i2}$ deletion does not specifically impact LPS-urine cellular detection

We also analyzed VSNs activation by healthy and sick mouse urine. We previously showed that $cG\alpha_{i2}^{-/-}$ VSNs show fewer responses to the LMW urine fraction from healthy animals, whereas responses to the HMW fraction remained intact (Trouillet et al., 2019). Thus, we hypothesized that LMW urine compounds might mediate avoidance to LPS-urine. We performed live-cell Ca^{2+} imaging

on dissociated VSNs using Fura2 and tested the responsiveness of 5186 cG$\alpha_{i2}^{+/-}$ and 3894 cG$\alpha_{i2}^{-/-}$ VSNs to veh-LMW and LPS-LMW (Figure 44). We observed responses to both stimuli in VSNs from each genotype (Figure 44A and B). As expected, the overall number of responsive cells to veh-urine and LPS-urine was significantly lower in cG$\alpha_{i2}^{-/-}$ VSNs (veh-urine: cG$\alpha_{i2}^{-/-}$ 83/3894, 2.1% versus cG$\alpha_{i2}^{+/-}$ 150/5186, 2.9%; χ^2 P < 0.05; LPS-urine: cG$\alpha_{i2}^{-/-}$ 57/3894, 1.5% versus cG$\alpha_{i2}^{+/-}$ 112/5186, 2.2%; χ^2 P < 0.001; Figure 44B). When comparing the proportion of activated cells among different experiments, we found a global effect of the genotype (two-way ANOVA, P < 0.05; Figure 44A), but no difference between veh- and LPS-urine (P = 0.09; Figure 44A). We also considered cells responsive to exclusively one stimulus (either veh-urine or LPS-urine; Figure 44C). Neither the number nor the proportion of monoresponsive cells differed between genotypes (Figure 44B and C). Consequently, the deletion of Gα_{i2} does not have a major impact on the cellular detection of LPS-urine.

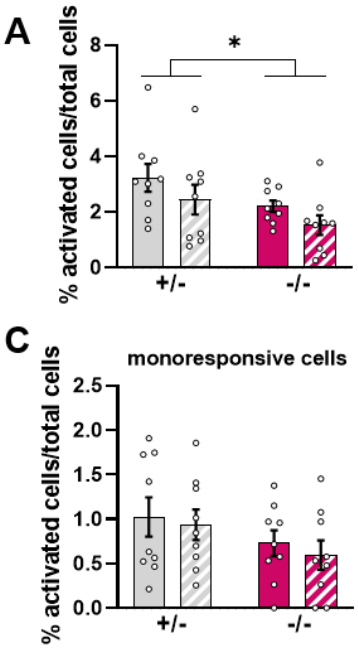

B

		cGα$_{i2}^{+/-}$ (5186 cells screened)		cGα$_{i2}^{-/-}$ (3894 cells screened)		χ^2
		Resp.	No resp.	Resp.	No resp.	
All cells	veh-LMW	150	5036	83	3811	* < 0,05
	LPS-LMW	112	5074	57	3837	*** < 0,001
Monoresponsive cells	veh-LMW	55	5131	28	3866	0,09
	LPS-LMW	43	5143	22	3872	0,17

Figure 44: Gαi2 deletion reduces VSNs responsiveness to sick and healthy LMW urine fractions. A) Analysis of ligand-evoked Ca^{2+} responses in dissociated cells from cGα$_{i2}^{+/-}$ and cGα$_{i2}^{-/-}$ (N = 9 experiments using cells from 6 mice for each genotype) mice after stimulation by veh-urine and LPS-urine. Two-way ANOVA, stimulus: $F_{(1, 32)} = 3.004$, P = 0.09 ; genotype : $F_{(1, 32)} = 5.3$, P < 0.05; stimulus x genotype: $F_{(1, 32)} = 0.016$, P = 0.9. B) Table showing the number of responsive (Resp.) and non responsive (No resp.) cells for each stimulation. χ^2 tests, all cells cGα$_{i2}^{+/-}$ versus cGα$_{i2}^{-/-}$ P < 0.05 for veh-urine and P < 0.001 for LPS-urine; monoresponsive cells P = 0.09 – 0.2. C) Analysis of ligand-evoked Ca^{2+} responses in dissociated cells from cGα$_{i2}^{+/-}$ and cGα$_{i2}^{-/-}$ mice (N = 6 for both genotypes) after stimulation by veh-urine and LPS-urine. Only cells responding to one stimulus exclusively are considered. Two-way ANOVA, stimulus: $F_{(1, 32)} = 0.3759$, P = 0.5 ; genotype : $F_{(1, 32)} = 3.191$, P = 0.08; stimulus x genotype: $F_{(1, 32)} = 0.0168$, P = 0.9.

3.4 Discussion

We used a conditional knockout model for Gα_{i2}, which induces a partial loss of VNO function (Trouillet et al., 2019, 2021), to determine apical VSNs implication in avoidance behaviors. We choose

two types of aversive cues, owl feces and urine from a sick LPS-treated animal, proposed to be detected by apical V1R-$G\alpha_{i2}$ VSNs (Boillat et al., 2015; Isogai et al., 2011). At the behavioral, histological, and cellular levels, we provided evidence that $G\alpha_{i2}$-expressing VSNs detect owl and LPS-urine olfactory cues that induce avoidance behaviors.

We choose three predators based on their differential activation of the accessory olfactory system: cat, snake, and owl. Cat avoidance is shown to be mediated by $G\alpha_o$-expressing VSNs (Pérez-Gómez et al., 2015). Exposure to snake activates both apical and basal VSNs pathways, but the specific requirement of one to induce avoidance is not yet established (Carvalho et al., 2015; Papes et al., 2010). Last, the detection of owl odors is likely to be mediated mainly by apical VSNs (Carvalho et al., 2015; Isogai et al., 2011). This is consistent with our results showing lower neuron activation by owl odors in the VNO and anterior AOB of $cG\alpha_{i2}^{-/-}$ mice (Figure 42). Moreover, $cG\alpha_{i2}^{-/-}$ mice did not display avoidance to owl olfactory cues, which points to a role of apical $G\alpha_{i2}$-expressing VSNs mediating owl avoidance (Figure 40). Further, we showed that snake and cat stimuli avoidances did not require Gαi2 signaling, suggesting that either basal $G\alpha_o$-expressing VSNs and/or sensory neurons in the MOE mediate these effects. We observed that owl exposure also activated the posterior part of the AOB in both genotypes, likely a consequence of basal VSNs signaling, even if the levels of pS6-positive VSNs were low in $cG\alpha_{i2}^{-/-}$ animals (Figure 42A). To assess the detection of owl olfactory cues by $G\alpha_{i2}$-expressing VSNs, we tested responses to owl feces extracts by calcium imaging. As controls, we used extracts from cat fur and snake molt samples. All extracts elicited strong responses in control and mutant VSNs (Figure 43A - C). Consistent with our behavioral results, we did not observe differences in the proportion of responsive cells for cat and snake extracts, but owl extract elicited fewer responses in $cG\alpha_{i2}^{-/-}$ VSNs (Figure 43A - C). Further, this difference was maintained after stimulating with different dilutions of the extract (Figure 43F and G).

To test whether sick conspecific avoidance is mediated by $G\alpha_{i2}$ signaling, we tested avoidance to LPS-urine. LPS injection is a standard protocol used to induce a general inflammatory state characterized by fever. It has also been used to determine VNO implication in sick conspecific avoidance (Boillat et al., 2015; Bufe et al., 2019). $cG\alpha_{i2}^{-/-}$ mice did not avoid LPS-urine and did not show a preference for veh- or LPS-urine (Figure 41). Thus, these results suggest that sickness-associated cues in LPS-urine are not detected in the absence of $G\alpha_{i2}$ signaling. Indeed, we observed fewer pS6-positive cells in the VNO of mutant animals (Figure 42A). However, whether this effect is specific to sickness-associated cues cannot be asserted since $G\alpha_{i2}$ mutation reduces overall VSNs responses to urine (Trouillet et al., 2019). We did not observe significant differences between control and mutant AOB activation, except in the anterior glomerular layer (Figure 42E), where $G\alpha_{i2}$-VSNs project. Again, we cannot determine if this difference specifically results from sickness-associated cues or not. Our calcium imaging experiments did not show a specific effect of LPS-urine on VSNs responses (Figure 44). We observed that $cG\alpha_{i2}^{-/-}$ VSNs showed fewer responses to LMW urine fraction than control VSNs (Figure 44A and B), as we showed previously (Trouillet et al., 2019). However,

responses to the two urine sources were not significantly different for both genotypes. We analyzed the number of cells responding exclusively to one urine source (veh or LPS, Figure 44C), but no differences appeared between veh- and LPS-urine. We evaluated the HMW urine fraction responses but did not find differences between genotypes or urine sources (data not shown). One possibility to explain this lack of differences is that LPS treatment may not induce the secretion of specific components in the urine but instead change the proportion of naturally secreted ones. Accordingly, a comparison of volatiles in urine from mice receiving LPS or other treatments inducing sickness shows that the most divergent molecules were naturally excreted (Millet et al., 2018, 2021). Another possibility is that the abundance or concentration of specific LPS-urine compounds mediating avoidance is below the detection threshold of our experimental setup. Further research is needed to understand the chemical nature of the component driving sick conspecific avoidance.

The brain pathway sustaining predator avoidance starts to be understood (Canteras et al., 2015), but sick conspecific avoidance is still elusive (Arakawa et al., 2011). Determining the brain structures activated during owl feces and LPS-urine exposures would help understand avoidance pathways by delineating each stimulus' neural pathways and identifying convergence sites.

Discussion

Our results have already been discussed in their dedicated sections. I will therefore provide a broader perspective of what combining them tells us. I will also discuss some specific results we obtained in the light of more recent literature and propose perspectives to the remaining and newly broad questions.

1 A model is just a model

We need to keep in mind that genetic constructs are not always perfect. Thus, it is important to consider the potential pitfalls of the cG$\alpha_{i2}^{-/-}$ mouse model. Three main aspects must be examined: *i*- Is the mutation restricted to the tissue of interest? *ii*- What are the effect of the mutation on cells/tissue development? *iii*- Are the observed effect only due to the mutation?

Despite its name, OMP expression is not restricted to the olfactory system and has been reported in many non-olfactory cells and tissues outside the olfactory organs, including the brain (Baker et al., 1989; Kang et al., 2015; Koo et al., 2005). However, OMP expression is restricted to small cell subsets that do not define a specific cell type or a brain nucleus. Similarly, Gα_{i2} is widely expressed (Rudolph et al., 1995). Thus, the probability of coexpression is not null, and we cannot rule out the deletion of Gα_{i2} outside the VNO.

One concern was the MOE. Indeed, the MOE also participates in the regulation of social behaviors, and modifying its function would have distorted our observations. Gα_{i2} mRNA and protein are present in the MOE (Barnes et al., 2020; Barrios et al., 2014; Berghard and Buck, 1996; Ibarra-Soria et al., 2014; Scholz et al., 2016; Wekesa and Anholt, 1999). We provided mRNA quantification of Gα_{i2} transcript in the MOE and, unlike in the VNO, did not found a significant reduction of *Gnai2* gene expression in the MOE. We also showed that cG$\alpha_{i2}^{-/-}$ mice have an intact MOE anatomy, were not anosmic to food odors, and still discriminated social odors in a habituation-dishabituation test. Altogether, this suggests that Gα_{i2} is not critical for OSNs function. OMP and Gα_{i2} coexpression is described in the GG (Brechbühl et al., 2008; Fleischer et al., 2006), but Gα_{i2} expression is controversial (Barrios et al., 2014). We did not investigate the potential coexpression of OMP and Gα_{i2} in the brain. The most robust expression of brain OMP is in the MPOA and PVN. Gα_{i2} is also expressed in the PVN, where it has been recently associated with sodium balance and hypertension (Carmichael et al., 2020). The PVN has many functions and contains distinct neuronal subpopulations controlling them. OMP-PVN neurons have not been characterized, and it is unknown whether they overlap with Gα_{i2}.

We observed a modification of the apical/basal VSNs ratio and an increase of Gα_o mRNA after whole VNO qPCR. However, we did not find differences in the total number of cells composing the VNE (data not shown). Thus, this indicates that the balance between apical and basal VSNs is modified. An increased number of basal VSNs could have behavioral consequences that will be discussed later in the manuscript. Processes by which immature VSNs differentiate into apical or basal lineages are

not clearly established (Katreddi and Forni, 2021). However, OMP expression occurs after $G\alpha_{i2}$/$G\alpha_o$ expression (Enomoto et al., 2011), suggesting that the OMP-Cre-dependent mutation of $G\alpha_{i2}$ cannot modify VSNs lineage choice. $G\alpha_{i2}$ expression could be necessary for the survival of apical VSNs, as $G\alpha_o$ is for basal VSNs (Chamero et al., 2011; Tanaka et al., 1999). Another possibility comes from the coexpression of $G\alpha_o$ and $G\alpha_{i2}$ in maturating VSNs already engaged in apical VSNs lineage (Enomoto et al., 2011). Whether or not OMP expression (and consequently the Cre-dependent deletion of $G\alpha_{i2}$) occurs when both Gα proteins are still present is unknown. The study of VSNs neurogenesis in $cG\alpha_{i2}^{-/-}$ mice could give interesting insights into cell lineage decision and maintenance.

2 The use of two vomeronasal systems in mammals

The coexistence of V1Rs and V2Rs in the mammalian VNO is restricted to some species (Silva and Antunes, 2017). Two main models exist, V1R-only VNO versus V1R/V2R-VNO (with maybe some exceptions, see Schneider et al., 2012). In the mouse, some have suggested that V2Rs may encode general information about the identity, notably sex, whereas V1Rs may encode details about the status of the ligand emitter (Isogai et al., 2011). It has been proposed that the loss of V2R genes in many species might be associated with the emergence of morphological sexual dimorphisms (e.g., body size, fur color, horns) (Suárez et al., 2011). Assessment of sex-identity by non-vomeronasal cues might have induced the relaxation of selective pressure on V2R genes, ultimately leading to their disappearance in many species. Another hypothesis concerning V2Rs maintenance/disappearance is the use or not of proteins and peptides as intraspecific pheromones. V1Rs and V2Rs belong to two different GPCR classes. V2Rs have a long extracellular C-terminus allowing them to bind large molecules, such as peptides and proteins, while V1Rs bind small volatiles with some degree of hydrophobicity. V2Rs genes largely expanded in aquatic and semi-aquatic non-mammalian vertebrates (Tirindelli, 2021). Communication in water implies soluble semiochemicals, and several proteins and peptides pheromones have been described in these species (Wyatt, 2014). Another example comes from the analysis of MUPs expression in mammals. MUPs genes expanded in species expressing V2Rs, while almost no MUPs genes are present in species expressing only V1Rs, such as cattle (Archunan et al., 2014; Chamero et al., 2007).

The biological relevance of the maintenance of one or two vomeronasal pathways remains to be elucidated. Our results on $G\alpha_{i2}$ in mice, combined with those obtained on $G\alpha_o$ (Chamero et al., 2011; Oboti et al., 2014; Pérez-Gómez et al., 2015), could nonetheless help to clarify this issue by providing some insights. First, males and females deficient for $G\alpha_o$ or $G\alpha_{i2}$ discriminate cues from both sexes. Second, ablation of either $G\alpha_o$ or $G\alpha_{i2}$ pathways specifically inhibits the recognition of one type of predator each, cat and owl, respectively. Thus, it seems unlikely that identity cues depend solely on V2Rs, at least not in such a simplistic view. The action of volatile components is usually a result of their blend, whereas peptide and protein pheromones may convey a very specific message due to their

unique amino acid sequence, prompting direct co-evolution of the ligand-receptor pair (Wyatt, 2014). Species that maintained V2Rs may indeed use peptide and protein pheromones as mediators of ethologically defined information. As an example, the trigger of the lordosis response in mice depends on V2Rs (Oboti et al., 2014), while the volatiles' mixture detected by V1Rs enhances the response (our present results). However, in species expressing only V1Rs, such as goats, the absence of V2Rs does not impede sex-dependent olfactory cues to trigger behavioral or physiological responses that are V2R-dependent in other species (Ohara et al., 2014).

3 One pathway, two sexes, many effects

A striking feature of our results is the sexually dimorphic role of $G\alpha_{i2}$ vomeronasal signaling. Most of the behaviors we evaluated are differentially regulated by $G\alpha_{i2}$ signaling in males and females (Figure 45). Further, $G\alpha_{i2}$-VSNs seem to have an active role in stimulating innate behaviors in females, whereas in males, the behavioral readout is rather inhibitory. This is not completely surprising considering that sociosexual behaviors rely on sexually dimorphic brain structures and are tightly modulated by circulated sex steroids (Baum and Bakker, 2013).

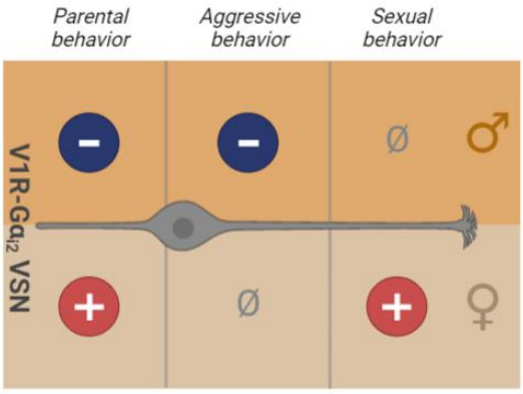

Figure 45: Sexually dimorphic control of sociosexual behaviors by $G\alpha_{i2}$-expressing VSNs. Ø: no effect; ⊖: inhibition; ⊕: activation.

3.1 Experienced-dependent vomeronasal control of sexual behaviors

We have already mentioned and described the atypical mounting behavior of $Trpc2^{-/-}$ animals (see section 2.1.3 from the introduction). $cG\alpha_o^{-/-}$ mice do not show such behavior (Chamero et al., 2011; Oboti et al., 2014), neither do $cG\alpha_{i2}^{-/-}$ animals, as shown here. Two hypotheses are conceivable. First, $G\alpha_o$ and $G\alpha_{i2}$ VSNs may cooperate, each being sufficient to drive the appropriate behavioral response. Second, $Trcp2^{-/-}$ animals exhibit high circulating testosterone levels (Kimchi et al., 2007; Stowers et al., 2002), a phenomenon that may explain the behavior (Martel and Baum, 2009). However, $Trpc2^{-/-}$

females' sexual behavior has been tested under standardized hormonal levels (Fraser and Shah, 2014), which reduced the proportion of mounting females. Thus, it questions Martel and Baum's theory as the sole cause of female mounting behavior (Martel and Baum, 2009). However, it does not exclude a potential organizational effect of high testosterone levels during embryonic and neonatal development. One solution would be to create an inducible time-specific Trpc2$^{-/-}$ mouse model to restrict the mutation to adulthood. Then, we could test males' and females' behaviors in adulthood under a standardized environment to see if indiscriminate mounting is still expressed. If yes, it would mean that, indeed, vomeronasal signaling drives sex preference.

Gα_o and Gα_{i2} cooperate to induce sexual receptivity in females. cG$\alpha_o^{-/-}$ females show reduced lordosis behaviors already when naïve (Oboti et al., 2014). This effect could be due to a lack of activation of AVPV-Kisspeptin neurons, which are necessary for expressing lordosis (Hellier et al., 2018). cG$\alpha_{i2}^{-/-}$ females show intermediate lordosis levels, which are probably caused by the lack of activation of Kisspeptin-negative AVPV-neurons. TH-neurons would be potential candidates. Indeed, dopamine signaling is known to mediate reinforcement of sexual behaviors (Paredes, 2009), and AVPV-TH neurons have been recently linked to male sexual motivation (Zhang et al., 2021). Whether selective ablation of AVPV-TH neurons in sexually experienced females impacts the expression of lordosis behavior may help elucidate this point. Whether activation of this neuronal population depends on Gα_{i2} vomeronasal signaling also remains to be answered (Figure 46).

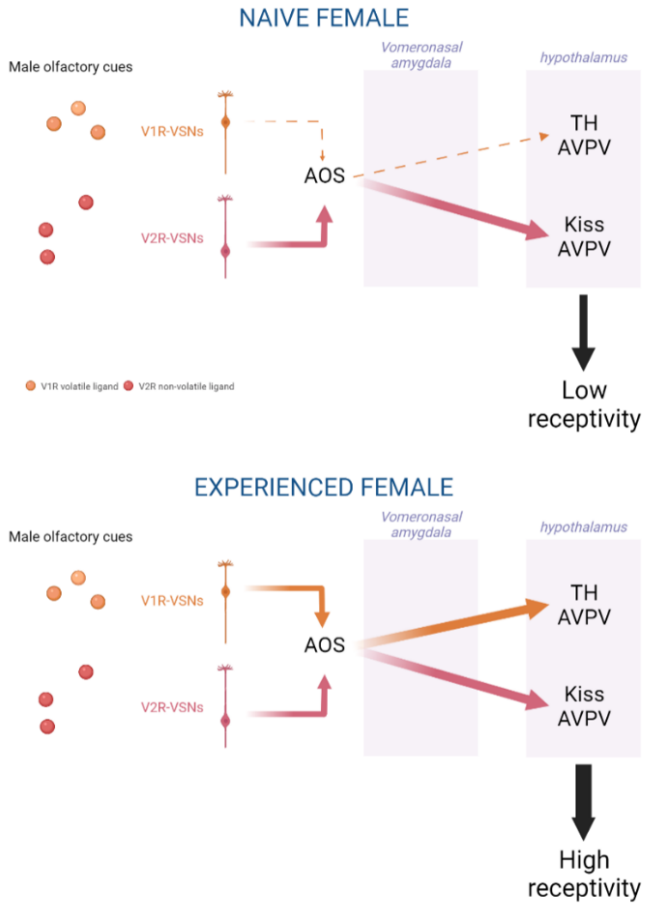

Figure 46: Proposed model of the vomeronasal control of female sexual receptivity. In naïve females, Gα_o signaling induces AVPV-Kisspeptin neurons activation, which triggers lordosis. In experienced females, increased sexual receptivity is due to AVPV-TH neurons activation by Gα_{i2} signaling. This scheme is created in BioRender.com

In males, we did not see differences in the sexual behavior of naïve cG$\alpha_{i2}^{-/-}$ mice. Del Punta and colleagues found that a V1Rs cluster deletion reduces male sexual behavior after three tests (Del Punta et al., 2002). Sexual experience in males produces rearrangements of the MPOA ultrastructure (Jean et al., 2017). This may change the value of Gα_{i2} vomeronasal signaling in driving male sexual behavior, as we observed in females. However, our experiments may not have been long enough to see the effect. Therefore, we cannot exclude the participation of Gα_{i2} vomeronasal signaling in the sexual behavior of experienced males.

Haga and colleagues linked two classes of V1Rs to male mounting behaviors (Haga-Yamanaka et al., 2014). They showed that V1Re9 and V1re12 detect estrus-induced olfactory cues in female urine, and that these compounds stimulate male mounting. Interestingly, Zhang and colleagues showed that stimulating TH-AVPV neurons can stimulate mating toward a diestrus unreceptive female (Zhang et al., 2021). They did not check the origin of TH-AVPV neurons' stimulation, but considering the importance of olfactory cues, we can hypothesize that the olfactory system may provide such stimulus. It is unknown whether compounds highlighted by Haga and coworkers can promote male mounting through TH-AVPV neurons. Nonetheless, AVPV-TH neurons are sexually dimorphic (Simerly et al., 1985). Therefore, this sex difference may allow the integration of opposite-sex olfactory cues into sexual preference and reinforcement of sexual behavior toward an opposite-sex congener. Further research is necessary to clarify this point.

3.2 Contextual regulation of aggressive behaviors

One of the most intriguing behaviors we observed is the intense aggressive behavior of cG$\alpha_{i2}^{-/-}$ male mice towards male intruders, either castrated or not. Using the tube test, a method for measuring territorial dominance through dyadic interactions, it has also been shown that cG$\alpha_{i2}^{-/-}$ males are more likely to win a novel social competition (Pallé et al., 2020). Analyzes of brain activation after a male-male interaction showed increased activation in the vomeronasal amygdala of mutant males. This was peculiarly counterintuitive since, by removing vomeronasal inputs, one might expect a decreased activation of downstream brain pathways. One explanation could come from the modified basal versus apical VSNs ratio we observed. Basal Gα_o-VSNs are necessary to detect compounds from the HMW and LMW urine fractions that trigger aggression (Chamero et al., 2007, 2011). An increased amount of basal Gα_o-expressing VSNs could lead to an overall overactivation of the vomeronasal amygdala and, consequently, increased aggressive behavior. However, this hypothesis is not well suited when considering several aspects of our results and the existing literature. First, we saw increased activation in the BNST, which is known to be activated by the anterior AOB, the Gα_{i2}-expressing VSNs projection site (Mohedano-Moriano et al., 2007). Second, we observed increased activation of AR-expressing MeApd neurons. These cells usually express the enzyme aromatase (Stanić et al., 2014), yet, Aro-MeApd neurons also mainly receive projections from the anterior AOB (Billing et al., 2020). Thus,

our observation cannot be entirely attributed to increased inputs from $G\alpha_o$-expressing VSNs, even though we cannot discard indirect connections. Several hypotheses may explain $cG\alpha_{i2}^{-/-}$ males' phenotype. First, it has been shown that, in the anterior AOB, inhibitory dendrodendritic synapses are needed to shape mitral cells' responses to male-specific olfactory cues (Hendrickson et al., 2008). Further, olfactory stimulation with HMW urine fraction elicits activation of the anterior AOB (Papes et al., 2010), either due to anterior mitral cells connecting posterior glomeruli (Yonekura and Yokoi, 2008) or communication between the two AOB parts. Thus, we can hypothesize that the lack of $G\alpha_{i2}$ signaling modifies the activity of the mitral cells network, ultimately leading to increased activation of downstream brain pathways and aggressive behavior. Second, there are brain pathways dedicated to the inhibition of aggression. For example, the septal rage model in which a lesion of the lateral septum induces excessive aggression in rats (Albert and Chew, 1980) and mice (Wong et al., 2016). Thus, $G\alpha_{i2}$ signaling may convey signals necessary for the activation of these inhibitory pathways. We did analyze the activation in the lateral septum of $cG\alpha_{i2}^{-/-}$ males after male-male aggression. Surprisingly, we found there a higher number of activated cells. However, the lateral septum is a heterogeneous structure with subdivisions projecting to different brain areas through specific cell populations (Risold and Swanson, 1997). A molecular identity analysis of activated cells may reveal specific differences in the cell population downregulating aggressive behaviors.

Male mice do not, or only slightly, attack castrated male intruders (Mugford and Nowell, 1970), yet $cG\alpha_{i2}^{-/-}$ males still do. Urinary levels of MUPs and aggression promoting volatiles, such as the 3,4-dehydro-*exo*-brevicomin, decrease after castration (Hastie et al., 1979; Schwende et al., 1986). It does not support the idea that $cG\alpha_{i2}^{-/-}$ males increased aggression results from the overactivation of $G\alpha_o$/V2R VSNs. However, we do not know if castrated males produce compounds specific to their condition in their urine or other body fluids. Repression of aggression towards castrated animals may not solely result from the lack of aggression promoting pheromones but also from the secretion of inhibitory signals (detected by V1Rs). Inhibitory pheromones have already been described, such as the peptide ESP22, which inhibits male sexual behavior.

We did not observe any modification of maternal aggression in females, and we observed a reduction of infanticide in virgin males. This differential regulation of three ethologically related behaviors opens a new framework to decipher the fine regulation of aggression regarding contextual elements.

3.3 The transition to parenthood

3.3.1 $G\alpha_{i2}$ and the transition to fatherhood

Infanticide by adult males is tightly regulated by the social environment. Mating and cohabitation with pregnant females progressively inhibit this behavior until it completely disappears in favor of parental behaviors around birth (Vom Saal, 1985; Tachikawa et al., 2013). Then, male social isolation

after weaning of the litter restores the expression of infanticide (Vom Saal, 1985). In the wild, this dynamic appears perfectly fitted to the male needs, favoring infanticide to restore ovulation in the lactating female and promoting care only for pups carrying the male's genetic makeup. The neural mechanisms that switch behavior from infanticidal to parental and vice versa are not well characterized. Two main questions emerge: what are the relevant pup-derived chemosignals, and what are the changes at the sensory perception and processing levels during the transition?

Our results show the implication of $G\alpha_{i2}$ vomeronasal signaling in the expression of infanticide by virgin males. Consequently, relevant chemosignals are most likely small components. The chemical signature of young pups varies until weaning (Lacalle-Bergeron et al., 2021), and some specific neonatal small organic compounds could sustain pup-directed behaviors, including infanticide. Specifically, durene, is already known to be detected by VSNs (Sam et al., 2001). Whether $G\alpha_{i2}$-expressing VSNs detect durene and if it is sufficient to induce infanticide is currently unknown. Another study brought out two pairs of peptidic ligand/V2Rs regulating infanticide (Isogai et al., 2018). Genetic invalidation of these receptors reduces infanticide but does not increase parental behaviors. Further, aggression towards other males is also impacted in this model, and ligands identified are likely secreted by mothers rather than by pups. Thus, it is likely that this study identifies new pheromones modulating male aggression in general.

Pup olfactory cues also stimulate parental behaviors. Volatiles identified in pups could be pro-parental or pro-infanticidal, perhaps depending on the sensory organ mediating them. Indeed, certain ligands can activate both VSNs and OSNs (Leinders-Zufall et al., 2000; Sam et al., 2001). One hypothesis is that the VNO is silenced when males need to be parental. Indeed, cohabitation with a pregnant female reduces VNO activation after pup exposure, suggesting that VSNs sensitivity is repressed (Nakahara et al., 2020; Tachikawa et al., 2013). The mechanism modifying VSNs function is not elucidated. The hormonal environment is a potent modulator of VSNs function (Dey et al., 2015; Eckstein et al., 2020), and peripheral oxytocin injection reduces VNO activation after pup exposure (Nakahara et al., 2020). Interestingly, it has been reported that oxytocin levels vary during cohabitation with a pregnant female in males California deer mouse, a monogamous species in which males show infanticide (Gubernick et al., 1995). Levels of oxytocin in males peak after mating and progressively decrease to remain low from before parturition until weaning. It is unknown whether such variation occurs in laboratory mice. It would be interesting to test the effect of oxytocin on VSNs cellular function.

We provide evidence that $G\alpha_{i2}$ vomeronasal signaling represses parental behaviors in virgin males. Strong activation of GABA-MeApd neurons is necessary for the expression of infanticide, while low activation leads to parenting (Chen et al., 2019). $cG\alpha_{i2}^{-/-}$ virgin parental males have fewer cFos-positive cells in the MeApd and more in the MPOA than controls. Thus, we can speculate that the strong activation of GABA-MeApd neurons by the $G\alpha_{i2}$ vomeronasal signaling may activate neural circuits relevant to aggression and inhibit those dedicated to parenting. In the absence of $G\alpha_{i2}$ signaling,

the MPOA is not repressed, and animals show parental behavior. Similarly, in parental animals, VSNs may be silenced, the MPOA not inhibited, and pup olfactory cues promote parenting (Figure 47).

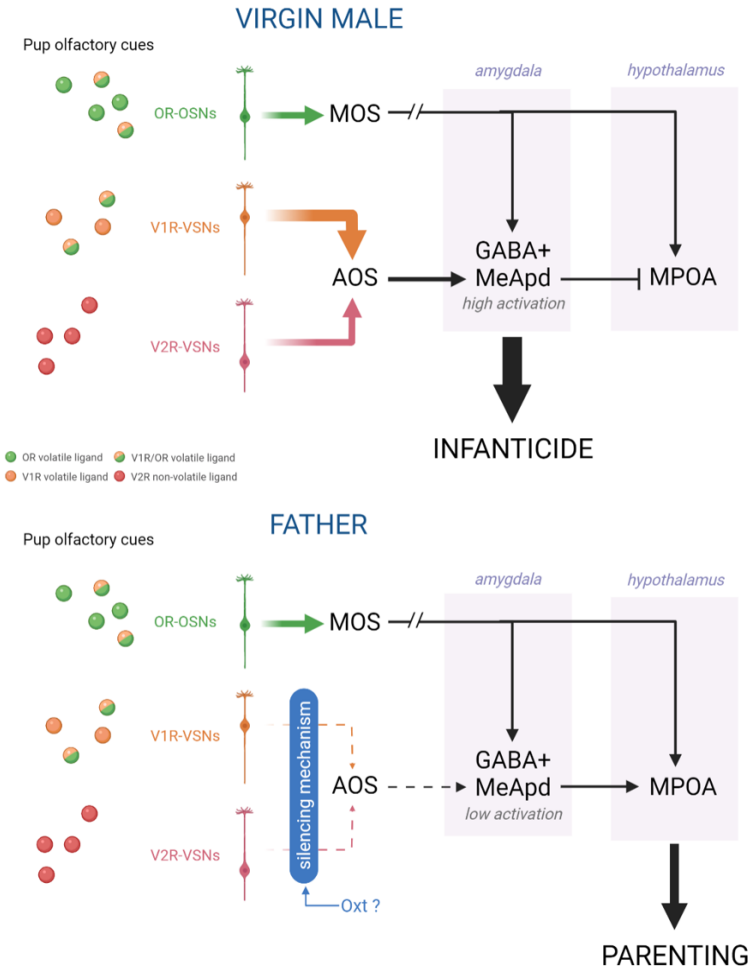

Figure 47: Proposed model for the transition to infanticidal to paternal behaviors in male mouse. In virgin males, detection of pup olfactory cues by the OSNs and VSNs lead to strong activation of GABA-MeApd neurons, triggering infanticide and repressing parenting by inhibition of the MPOA. In fathers, silencing of VSNs signaling decreases GABA-MeApd activation that cannot sufficiently inhibit the MPOA, resulting in the expression of parental behaviors. This scheme is created in BioRender.com.

3.3.2 $G\alpha_{i2}$ and the transition to motherhood

Infanticide is a male-typical behavior and is rarely expressed by virgin females who are spontaneously maternal. Interestingly, activation of GABA-MeApd neurons do not trigger aggression towards a pup in females, whatever the intensity of the stimulation (Chen et al., 2019). This suggests that male and female brains are wired to respond differently to pup sensory cues. Infanticide is testosterone-dependent in males since castration reduces the proportion of aggressive males towards pup (Gandelman and Vom Saal, 1975). However, it seems that the dependence on circulating testosterone could be modulated by neonatal levels of this hormone, suggesting the existence of an organizational mechanism (Gandelman and Vom Saal, 1975). However, no clear consensus has

emerged about if and how sex steroids control infanticidal behavior (Keller et al., 2010; Matsumoto et al., 2003; Ogawa et al., 1998). There is another interesting hypothesis explaining sex differences regarding infanticide. Laboratory mice have been selected by breeding over multiple generations, progressively reducing the proportion of infanticidal females. The analysis of infanticide in wild female mice revealed that this type of behavior is genetically encoded and naturally expressed (Chalfin et al., 2014). One possibility is that laboratory mice's inbreeding has selected non-infanticidal females. To test this hypothesis, we could test if the inhibition of $G\alpha_{i2}$ vomeronasal signaling in wild-derived females reduces infanticide, then compare brain activation in wild males and females, and see if the activated brain pathway in infanticidal animals varies.

We observed that deletion of $G\alpha_{i2}$ does not enhance parental behavior in females, as it does in males, but delays pup-retrieval. This also pleads in a differential wiring of male and female brains regarding the processing of pup olfactory cues. We did not observe any difference potentially explaining how, in the brain, $G\alpha_{i2}$-mediated pup olfactory cues promote retrieval, likely because of the limitations of using cFos as activity reporter. New technics such as *in vivo* calcium imaging would give a better view of pup-retrieval-associated brain areas. Inactivation of ERα-MPOA neurons impairs pup approach and retrieval, and conversely, activating these neurons triggers retrieval (Fang et al., 2018; Wei et al., 2018). Interestingly, the activity of ERα-MPOA neurons seems higher in females than in males at the onset of retrieval (Wei et al., 2018). This increased activation could result from $G\alpha_{i2}$ vomeronasal inputs.

In lactating females, the lack of $G\alpha_{i2}$ vomeronasal signaling does not impair pup-retrieval behavior. This effect may be due to a silencing of vomeronasal signaling in mothers, as in fathers (Nakahara et al., 2020; Tachikawa et al., 2013). However, late pregnant females show strong activation of their VNO after pup exposure (Navarro-Moreno et al., 2020), and $Trpc2^{-/-}$ and $cG\alpha_o^{-/-}$ mothers show intact pup-retrieval behavior. MPOA activity is necessary for maternal behavior, possibly acting as a central hub for sensory inputs (Okabe et al., 2013). Indeed, motherhood enhances the brain activity caused by MOS-driven olfactory and auditory inputs (Marlin et al., 2015; Navarro-Moreno et al., 2020), and the activity of ERα-MPOA neurons during approach and retrieval is higher in lactating females than in virgins (Fang et al., 2018). In the absence of $G\alpha_{i2}$ vomeronasal signaling in mothers, other sensory modalities seem to be sufficient to sustain maternal behaviors.

General conclusion

At the end of this work, we can draw six main conclusions about the role of $G\alpha_{i2}$ vomeronasal signaling in the control of innate sociosexual behaviors:

i- $G\alpha_{i2}$ is a critical component of apical VSNs signaling pathway mediating V1Rs activation;

ii- $G\alpha_{i2}$-expressing VSNs mediate the detection of pup, male, and owl olfactory cues;

iii- $G\alpha_{i2}$ vomeronasal signaling is dispensable for opposite-sex preference;

iv- $G\alpha_{i2}$ vomeronasal signaling is dispensable for male sexual behavior but participates in female sexual receptivity;

v- $G\alpha_{i2}$ vomeronasal signaling is necessary for pup-directed aggression, modulates inter-male aggression, but is dispensable for maternal aggression;

vi- $G\alpha_{i2}$ vomeronasal signaling stimulates parental behavior in females while repressing it in males;

vii- $G\alpha_{i2}$ vomeronasal signaling participates in predator and sick conspecific avoidances.

Most of these observations open new questioning, but that is the beauty of science. Piece by piece, we decipher how our brain is integrating multiple information to produce the best response at each moment. Now that we possess information from apical and basal VSNs pathways, we can design integrating models for the olfactory control of innate behaviors in mice (Figure 48). Such models are relevant if we want to transpose the immense knowledge about rodent social behaviors into humans. We, as human beings, do not sense our environment as rodents. We are not macrosmatic, but the mammalian limbic and hypothalamic systems, where sensory cues converge, is highly conserved. The study of olfactory-mediated behaviors is at the forefront of nowadays psychiatric research. Thus, comprehending sensory perception and social behaviors neurobiology is crucial for understanding and developing new therapeutic regarding many pathologies, such as autistic syndrome, postpartum depression, or innate phobia (e.g., acrophobia).

A complete understanding of innate behaviors neurobiology is also required to comprehend how humans interact with the other wild species surrounding us and, more importantly, how we should treat species that rely on us, the domestic animals. Pets, farm animals, working animals, and laboratory animals are our responsibility. A better understanding of their physiology could avoid them unnecessary suffering to meet our needs.

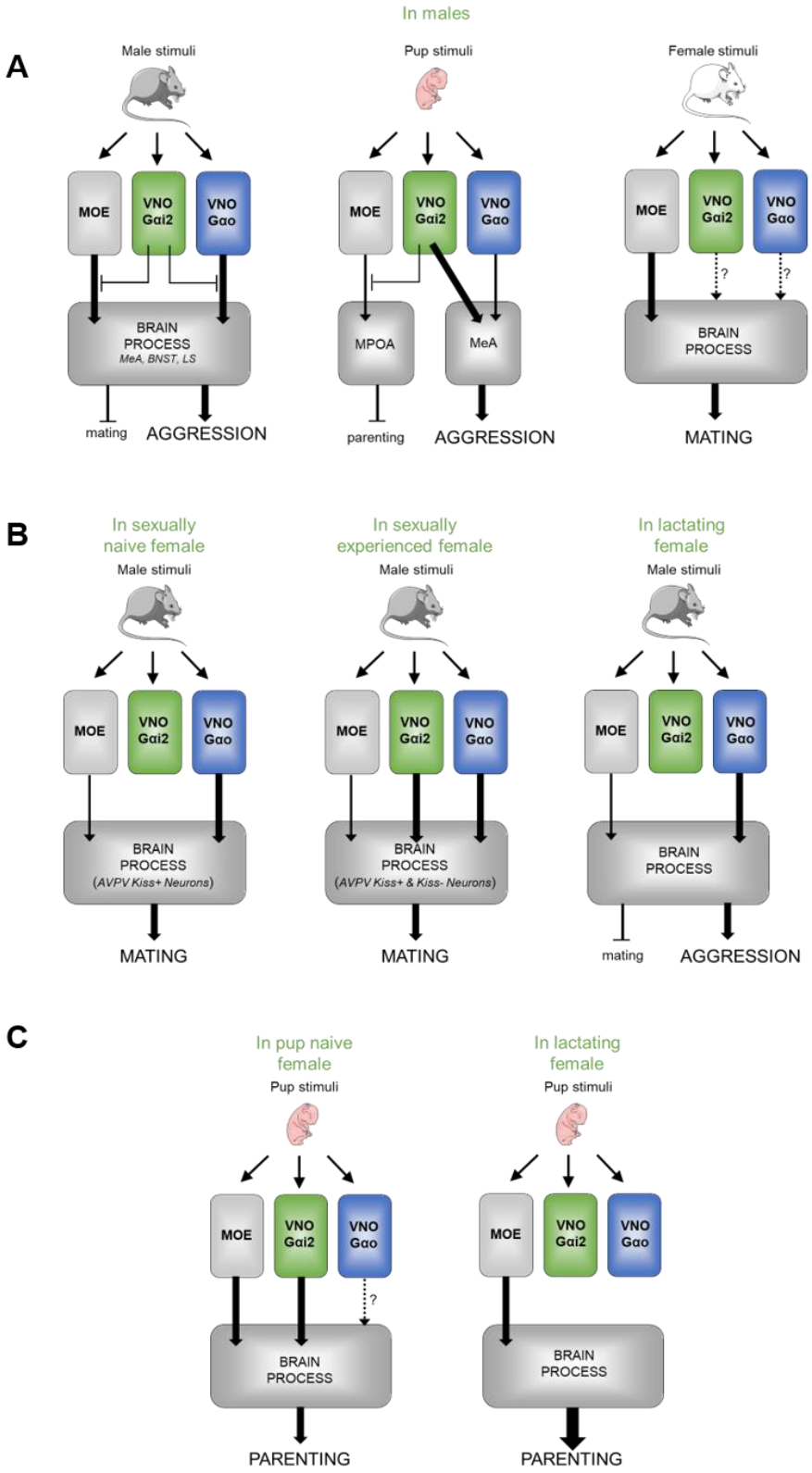

Figure 48: Proposed model of the olfactory control of innate behaviors. A) In males, the MOE and Gαo-VSNs are necessary to trigger aggression towards other males, while Gαi2-VSNs regulate the intensity of the response, probably by modulating signals coming from the other sensory inputs. When confronting an alien neonate, Gαi2 and Gαo signaling activate the MeA to trigger aggression, while Gαi2 signaling represses MOE inputs, thus inhibiting the MPOA and parenting. Last, female-olfactory cues detected by the MOE seem sufficient to drive mating. B) In females, male olfactory cues perception depends on the social experience. In naïve females, MOE and $G\alpha_o$-VSNs allow sexual behaviors, while once experienced, all three components participate. In lactating females, male olfactory cues significance changes and trigger aggression through MOE and $G\alpha_o$ signaling. C) Pup olfactory cues mediation of parental behaviors in females also depend on social experience. In naïve females, MOE and $G\alpha_{i2}$-VSNs cooperate, while the MOE alone is sufficient in lactating females.

Bibliography

Abellán-Álvaro, M., Ayala, G., Barneo-Muñoz, M., Martínez-García, F., Agustín-Pavón, C., and Lanuza, E. (2021). Motherhood-induced gene expression in the mouse medial amygdala: Changes induced by pregnancy and lactation but not by pup stimuli. FASEB J. *35*, 1–21.

Albert, D.J., and Chew, G.L. (1980). The septal forebrain and the inhibitory modulation of attack and defense in the rat. A review. Behav. Neural Biol. *30*, 357–388.

Alsina-Llanes, M., and Olazábal, D.E. (2020). Prefrontal cortex is associated with the rapid onset of parental behavior in inexperienced adult mice (C57BL/6). Behav. Brain Res. *385*, 112556.

Amjad, A., Hernandez-Clavijo, A., Pifferi, S., Maurya, D.K., Boccaccio, A., Franzot, J., Rock, J., and Menini, A. (2015). Conditional knockout of TMEM16A/anoctamin1 abolishes the calciumactivated chloride current in mouse vomeronasal sensory neurons. J. Gen. Physiol. *145*, 285–301.

Amoore, J.E. (1963). Stereochemical Theory of Olfaction. Nature *198*, 271–272.

Apps, P., Mmualefe, L., and McNutt, J.W. (2012). Identification of Volatiles from the Secretions and Excretions of African Wild Dogs (Lycaon pictus). J. Chem. Ecol. *38*, 1450–1461.

Arakawa, H., Cruz, S., and Deak, T. (2011). From models to mechanisms: Odorant communication as a key determinant of social behavior in rodents during illness-associated states. Neurosci. Biobehav. Rev. *35*, 1916–1928.

Archunan, G., Rajanarayanan, S., and Karthikeyan, K. (2014). Cattle Pheromones. In Neurobiology of Chemical Communication, C. Mucignat-Caretta, ed. (CRC Press/Taylor & Francis), pp. 461–487.

Autry, A.E., Wu, Z., Kapoor, V., Kohl, J., Bambah-Mukku, D., Rubinstein, N.D., Marin-Rodriguez, B., Carta, I., Sedwick, V., Tang, M., et al. (2021). Urocortin-3 neurons in the mouse perifornical area promote infant-directed neglect and aggression. Elife *10*.

Bakalyar, H.A., and Reed, R.R. (1990). Identification of a specialized adenylyl cyclase that may mediate odorant detection. Science (80-.). *250*, 1403–1406.

Baker, H., Grillo, M., and Margolis, F.L. (1989). Biochemical and immunocytochemical charaterization of olfactory marker protein in the rodent central nervous system. J. Comp. Neurol. *285*, 246–261.

Baker, H., Cummings, D.M., Munger, S.D., Margolis, J.W., Franzen, L., Reed, R.R., and Margolis, F.L. (1999). Targeted deletion of a cyclic nucleotide-gated channel subunit (OCNC1): Biochemical and morphological consequences in adult mice. J. Neurosci. *19*, 9313–9321.

Bakker, J. (2018). The Sexual Differentiation of the Human Brain: Role of Sex Hormones Versus Sex Chromosomes. In Brain Imaging in Behavioral Neuroscience, pp. 45–67.

Bakker, J., Pierman, S., and González-Martínez, D. (2010). Effects of aromatase mutation (ArKO) on the sexual differentiation of kisspeptin neuronal numbers and their activation by same versus opposite sex urinary pheromones. Horm. Behav. *57*, 390–395.

Ball, G.F., and Balthazart, J. (2008). How useful is the appetitive and consummatory distinction for our understanding of the neuroendocrine control of sexual behavior? Horm. Behav. *53*, 307–311.

Bankhead, P., Loughrey, M.B., Fernández, J.A., Dombrowski, Y., McArt, D.G., Dunne, P.D., McQuaid, S., Gray, R.T., Murray, L.J., Coleman, H.G., et al. (2017). QuPath: Open source software for digital pathology image analysis. Sci. Rep. *7*, 1–7.

Barnes, I.H.A., Ibarra-Soria, X., Fitzgerald, S., Gonzalez, J.M., Davidson, C., Hardy, M.P., Manthravadi, D., Van Gerven, L., Jorissen, M., Zeng, Z., et al. (2020). Expert curation of the human and mouse olfactory receptor gene repertoires identifies conserved coding regions split across two exons. BMC Genomics *21*, 1–15.

Barrios, A.W., Núñez, G., Quinteiro, P.S., and Salazar, I. (2014). Anatomy, histochemistry, and immunohistochemistry of the olfactory subsystems in mice. Front. Neuroanat. *8*, 1–10.

Baum, M.J., and Bakker, J. (2013). Roles of sex and gonadal steroids in mammalian pheromonal communication. Front. Neuroendocrinol. *34*, 268–284.

Baum, M.J., and Kelliher, K.R. (2009). Complementary Roles of the Main and Accessory Olfactory Systems in Mammalian Mate Recognition. Annu. Rev. Physiol. *71*, 141–160.

Bayless, D.W., Yang, T., Mason, M.M., Susanto, A.A.T., Lobdell, A., and Shah, N.M. (2019). Limbic Neurons Shape Sex Recognition and Social Behavior in Sexually Naive Males. Cell *0*, 1–16.

Bean, N.J. (1982). Olfactory and vomeronasal mediation of ultrasonic vocalizations in male mice. Physiol. Behav. *28*, 31–37.

Bean, N.J., and Wysocki, C.J. (1989). Vomeronasal organ removal and female mouse aggression: The role of experience. Physiol. Behav. *45*, 875–882.

Belluscio, L., Gold, G.H., Nemes, A., and Axel, R. (1998). Mice deficient in G(olf) are anosmic. Neuron *20*, 69–81.

Belluscio, L., Koentges, G., Axel, R., and Dulac, C. (1999). A map of pheromone receptor activation in the mammalian brain. Cell *97*, 209–220.

Belluscio, L., Lodovichi, C., Feinstein, P., Mombaerts, P., and Katz, L.C. (2002). Odorant receptors instruct functional circuitry in the mouse olfactory bulb. Nature *419*, 296–300.

Ben-Shaul, Y., Katz, L.C., Mooney, R., and Dulac, C. (2010). In vivo vomeronasal stimulation reveals sensory encoding of conspecific and allospecific cues by the mouse accessory olfactory bulb. Proc. Natl. Acad. Sci. U. S. A. *107*, 5172–5177.

Bentefour, Y., and Bakker, J. (2021). Neuropharmacology Kisspeptin signaling and nNOS neurons in the VMHvl modulate lordosis behavior but not mate preference in female mice. Neuropharmacology *198*, 108762.

Beny-Shefer, Y., Zilkha, N., Lavi-Avnon, Y., Bezalel, N., Rogachev, I., Brandis, A., Dayan, M., and Kimchi, T. (2017). Nucleus Accumbens Dopamine Signaling Regulates Sexual Preference for Females in Male Mice. Cell Rep. *21*, 3079–3088.

Beny, Y., and Kimchi, T. (2016). Conditioned odor aversion induces social anxiety towards females in wild-type and TrpC2 knockout male mice. Genes, Brain Behav. *15*, 722–732.

Bergan, J.F., Ben-Shaul, Y., and Dulac, C. (2014). Sex-specific processing of social cues in the medial amygdala. Elife *3*, e02743.

Berghard, a, and Buck, L.B. (1996). Sensory transduction in vomeronasal neurons: evidence for G alpha o, G alpha i2, and adenylyl cyclase II as major components of a pheromone signaling cascade. J. Neurosci. *16*, 909–918.

Bian, X., Yanagawa, Y., Chen, W.R., and Luo, M. (2008). Cortical-like functional organization of the pheromone-processing circuits in the medial amygdala. J. Neurophysiol. *99*, 77–86.

Billig, G.M., Pál, B., Fidzinski, P., and Jentsch, T.J. (2011). Ca2+-activated Cl- currents are dispensable for olfaction. Nat. Neurosci. *14*, 763–769.

Billing, A., Henrique Correia, M., Kelly, D.A., Li, G.-L., and Bergan, J.F. (2020). Synaptic Connections of Aromatase Circuits in the Medial Amygdala Are Sex Specific. Eneuro *7*, ENEURO.0489-19.2020.

Bleymehl, K., Pérez-Gómez, A., Omura, M., Moreno-Pérez, A., Macías, D., Bai, Z., Johnson, R.S., Leinders-Zufall, T., Zufall, F., and Mombaerts, P. (2016). A Sensor for Low Environmental Oxygen in the Mouse Main Olfactory Epithelium. Neuron *92*, 1196–1203.

Boehm, T., and Zufall, F. (2006). MHC peptides and the sensory evaluation of genotype. Trends Neurosci. *29*, 100–107.

Boillat, M., Challet, L., Rossier, D., Kan, C., Carleton, A., and Rodriguez, I. (2015). The vomeronasal

system mediates sick conspecific avoidance. Curr. Biol. *25*, 251–255.

Boillat, M., Carleton, A., and Rodriguez, I. (2021). From immune to olfactory expression: neofunctionalization of formyl peptide receptors. Cell Tissue Res. *383*, 387–393.

Boisseau, S., Kunert-Keil, C., Lucke, S., and Bouron, A. (2009). Heterogeneous distribution of TRPC proteins in the embryonic cortex. Histochem. Cell Biol. *131*, 355–363.

Bönigk, W., Bradley, J., Müller, F., Sesti, F., Boekhoff, I., Ronnett, G. V., Kaupp, U.B., and Frings, S. (1999). The Native Rat Olfactory Cyclic Nucleotide-Gated Channel Is Composed of Three Distinct Subunits. J. Neurosci. *19*, 5332–5347.

Bonthuis, P.J., Cox, K.H., Searcy, B.T., Kumar, P., Tobet, S., and Rissman, E.F. (2010). Of mice and rats: Key species variations in the sexual differentiation of brain and behavior. Front. Neuroendocrinol. *31*, 341–358.

Bonthuis, P.J., Patteson, J.K., and Rissman, E.F. (2011). Acquisition of Sexual Receptivity: Roles of Chromatin Acetylation, Estrogen Receptor-α, and Ovarian Hormones. Endocrinology *152*, 3172–3181.

Borowsky, B., Adham, N., Jones, K.A., Raddatz, R., Artymyshyn, R., Ogozalek, K.L., Durkin, M.M., Lakhlani, P.P., Bonini, J.A., Pathirana, S., et al. (2001). Trace amines: Identification of a family of mammalian G protein-coupled receptors. Proc. Natl. Acad. Sci. U. S. A. *98*, 8966–8971.

Boschat, C., Pélofi, C., Randin, O., Roppolo, D., Lüscher, C., Broillet, M.C., and Rodriguez, I. (2002). Pheromone detection mediated by a V1r vomeronasal receptor. Nat. Neurosci. *5*, 1261–1262.

Bradley, J., Li, J., Davidson, N., Lester, H.A., and Zinn, K. (1994). Heteromeric olfactory cyclic nucleotide-gated channels: a subunit that confers increased sensitivity to cAMP. Proc. Natl. Acad. Sci. *91*, 8890–8894.

Brann, J.H., and Firestein, S.J. (2014). A lifetime of neurogenesis in the olfactory system. Front. Neurosci. *8*, 1–11.

Brechbühl, J., Klaey, M., and Broillet, M.C. (2008). Grueneberg ganglion cells mediate alarm pheromone detection in mice. Science (80-.). *321*, 1092–1095.

Brechbühl, J., Moine, F., Klaey, M., Nenniger-Tosato, M., Hurni, N., Sporkert, F., Giroud, C., and Broillet, M.C. (2013). Mouse alarm pheromone shares structural similarity with predator scents. Proc. Natl. Acad. Sci. U. S. A. *110*, 4762–4767.

Brennan, P.A., and Zufall, F. (2006). Pheromonal communication in vertebrates. Nature *444*, 308–315.

Brunert, D., and Rothermel, M. (2021). Extrinsic neuromodulation in the rodent olfactory bulb. Cell Tissue Res. *383*, 507–524.

Brunet, L.J., Gold, G.H., and Ngai, J. (1996). General anosmia caused by a targeted disruption of the mouse olfactory cyclic nucleotide-gated cation channel. Neuron *17*, 681–693.

Buck, L., and Axel, R. (1991). A novel multigene family may encode odorant receptors: A molecular basis for odor recognition. Cell *65*, 175–187.

Bufe, B., and Zufall, F. (2016). The sensing of bacteria: Emerging principles for the detection of signal sequences by formyl peptide receptors. Biomol. Concepts *7*, 205–214.

Bufe, B., Schumann, T., and Zufall, F. (2012). Formyl peptide receptors from immune and vomeronasal system exhibit distinct agonist properties. J. Biol. Chem. *287*, 33644–33655.

Bufe, B., Schumann, T., Kappl, R., Bogeski, I., Kummerow, C., Podgórska, M., Smola, S., Hoth, M., and Zufall, F. (2015). Recognition of bacterial signal peptides by mammalian formyl peptide receptors: A new mechanism for sensing pathogens. J. Biol. Chem. *290*, 7369–7387.

Bufe, B., Teuchert, Y., Schmid, A., Pyrski, M., Pérez-Gómez, A., Eisenbeis, J., Timm, T., Ishii, T., Lochnit, G., Bischoff, M., et al. (2019). Bacterial MgrB peptide activates chemoreceptor Fpr3 in mouse accessory olfactory system and drives avoidance behaviour. Nat. Commun. *10*, 4889.

Bumbalo, R., Lieber, M., Lehmann, E., Wolf, I., Breer, H., and Fleischer, J. (2017). Attenuated Chemosensory Responsiveness of the Grueneberg Ganglion in Mouse Pups at Warm Temperatures. Neuroscience *366*, 149–161.

Bunzow, J.R., Sonders, M.S., Arttamangkul, S., Harrison, L.M., Zhang, G., Quigley, D.I., Darland, T., Suchland, K.L., Pasumamula, S., Kennedy, J.L., et al. (2001). Amphetamine, 3,4-methylenedioxymethamphetamine, lysergic acid diethylamide, and metabolites of the catecholamine neurotransmitters are agonists of a rat trace amine receptor. Mol. Pharmacol. *60*, 1181–1188.

Burger, B. V., Visser, R., Moses, A., and Le Roux, M. (2006). Elemental sulfur identified in urine of cheetah, Acinonyx jubatus. J. Chem. Ecol. *32*, 1347–1352.

Canteras, N.S., Simerly, R.B., and Swanson, L.W. (1992). Connections of the posterior nucleus of the amygdala. J. Comp. Neurol. *324*, 143–179.

Canteras, N.S., Simerly, R.B., and Swanson, L.W. (1995). Organization of projections from the medial nucleus of the amygdala: A PHAL study in the rat. J. Comp. Neurol. *360*, 213–245.

Canteras, N.S., Pavesi, E., and Carobrez, A.P. (2015). Olfactory instruction for fear: Neural system analysis. Front. Neurosci. *9*, 1–10.

Carmichael, C.Y., Kuwabara, J.T., Pascale, C.L., Moreira, J.D., Mahne, S.E., Kapusta, D.R., Rosene, D.L., Williams, J.S., Thomas Cunningham, J., and Wainford, R.D. (2020). Hypothalamic paraventricular nucleus Gαi2 (guanine nucleotide-binding protein alpha inhibiting activity polypeptide 2) protein-mediated neural control of the kidney and the salt sensitivity of blood pressure. Hypertension *2*, 1002–1011.

Carvalho, V.M. de A., Nakahara, T.S., Souza, M.A. de A., Cardozo, L.M., Trintinalia, G.Z., Pissinato, L.G., Venancio, J.O., Stowers, L., and Papes, F. (2020). Representation of Olfactory Information in Organized Active Neural Ensembles in the Hypothalamus. Cell Rep. *32*, 108061.

Carvalho, V.M.A., Nakahara, T.S., Cardozo, L.M., Souza, M.A.A., Camargo, A.P.C.B.R., Trintinalia, G.Z., Ferraz, E., and Papes, F. (2015). Lack of spatial segregation in the representation of pheromones and kairomones in the mouse medial amygdala. Front. Neurosci. *9*, 1–19.

Chalfin, L., Dayan, M., Levy, D.R., Austad, S.N., Miller, R.A., Iraqi, F.A., Dulac, C., and Kimchi, T. (2014). Mapping ecologically relevant social behaviours by gene knockout in wild mice. Nat. Commun. *5*, 1–10.

Chamero, P., Marton, T.F., Logan, D.W., Flanagan, K., Cruz, J.R., Saghatelian, A., Cravatt, B.F., and Stowers, L. (2007). Identification of protein pheromones that promote aggressive behaviour. Nature *450*, 899–902.

Chamero, P., Katsoulidou, V., Hendrix, P., Bufe, B., Roberts, R., Matsunami, H., Abramowitz, J., Birnbaumer, L., Zufall, F., and Leinders-Zufall, T. (2011). G protein G o is essential for vomeronasal function and aggressive behavior in mice. Proc. Natl. Acad. Sci. *108*, 12898–12903.

Chamero, P., Leinders-Zufall, T., and Zufall, F. (2012). From genes to social communication: molecular sensing by the vomeronasal organ. Trends Neurosci. *35*, 597–606.

Chamero, P., Weiss, J., Alonso, M.T., Rodríguez-Prados, M., Hisatsune, C., Mikoshiba, K., Leinders-Zufall, T., and Zufall, F. (2017). Type 3 inositol 1,4,5-trisphosphate receptor is dispensable for sensory activation of the mammalian vomeronasal organ. Sci. Rep. *7*, 10260.

Chao, Y., Fleischer, J., and Yang, R. (2018). Guanylyl cyclase-G is an alarm pheromone receptor in mice. EMBO J. *37*, 39–49.

Cheetham, S.A., Thom, M.D., Jury, F., Ollier, W.E.R., Beynon, R.J., and Hurst, J.L. (2007). The Genetic Basis of Individual-Recognition Signals in the Mouse. Curr. Biol. *17*, 1771–1777.

Chen, P., and Hong, W. (2018). Neural Circuit Mechanisms of Social Behavior. Neuron *98*, 16–30.

Chen, P.B., Hu, R.K., Wu, Y.E., Pan, L., Huang, S., Micevych, P.E., and Hong, W. (2019). Sexually

Dimorphic Control of Parenting Behavior by the Medial Amygdala. Cell *176*, 1206-1221.e18.

Choleris, E., Little, S.R., Mong, J.A., Puram, S. V., Langer, R., and Pfaff, D.W. (2007). Microparticle-based delivery of oxytocin receptor antisense DNA in the medial amygdala blocks social recognition in female mice. Proc. Natl. Acad. Sci. U. S. A. *104*, 4670–4675.

Clancy, N., and Nobles, P. (1984). Sexual and Aggression Involvement of the Vomeronasal in Male System ' Mice : J. Neurosci.

Croy, I., Nordin, S., and Hummel, T. (2014). Olfactory disorders and quality of life-an updated review. Chem. Senses *39*, 185–194.

Cuschieri, A., and Bannister, L.H. (1975). The development of the olfactory mucosa in the mouse: electron microscopy. J. Anat. *119*, 471–498.

Cygnar, K.D., and Zhao, H. (2009). Phosphodiesterase 1C is dispensable for rapid response termination of olfactory sensory neurons. Nat. Neurosci. *12*, 454–462.

Desjardins, C., Maruniak, J.A., and Bronson, F.H. (1973). Social rank in house mice: Differentiation revealed by ultraviolet visualization of urinary marking patterns. Science (80-.). *182*, 939–941.

Dewan, A., Pacifico, R., Zhan, R., Rinberg, D., and Bozza, T. (2013). Non-redundant coding of aversive odours in the main olfactory pathway. Nature *497*, 486–489.

Dewan, A., Cichy, A., Zhang, J., Miguel, K., Feinstein, P., Rinberg, D., and Bozza, T. (2018). Single olfactory receptors set odor detection thresholds. Nat. Commun. *9*, 1–12.

Dey, S., and Matsunami, H. (2011). Calreticulin chaperones regulate functional expression of vomeronasal type 2 pheromone receptors. Proc. Natl. Acad. Sci. U. S. A. *108*, 16651–16656.

Dey, S., Chamero, P., Pru, J.K., Chien, M.S., Ibarra-Soria, X., Spencer, K.R., Logan, D.W., Matsunami, H., Peluso, J.J., and Stowers, L. (2015). Cyclic regulation of sensory perception by a female hormone alters behavior. Cell *161*, 1334–1344.

Dhallan, R.S., Yau, K.-W., Schrader, K.A., and Reed, R.R. (1990). Primary structure and functional expression of a cyclic nucleotide-activated channel from olfactory neurons. Nature *347*, 184–187.

Dibattista, M., Al Koborssy, D., Genovese, F., and Reisert, J. (2021). The functional relevance of olfactory marker protein in the vertebrate olfactory system: a never-ending story. Cell Tissue Res. *383*, 409–427.

DiBenedictis, B.T., Ingraham, K.L., Baum, M.J., and Cherry, J.A. (2012). Disruption of urinary odor preference and lordosis behavior in female mice given lesions of the medial amygdala. Physiol. Behav. *105*, 554–559.

Dietschi, Q., Assens, A., Challet, L., Carleton, A., and Rodriguez, I. (2013). Convergence of FPR-rs3-expressing neurons in the mouse accessory olfactory bulb. Mol. Cell. Neurosci. *56*, 140–147.

Dietschi, Q., Tuberosa, J., Rösingh, L., Loichot, G., Ruedi, M., Carleton, A., and Rodriguez, I. (2017). Evolution of immune chemoreceptors into sensors of the outside world. Proc. Natl. Acad. Sci. U. S. A. *114*, 7397–7402.

Døving, K.B., and Trotier, D. (1998). Structure and function of the vomeronasal organ. J. Exp. Biol. *201*, 2913–2925.

Doyle, W.I., Dinser, J.A., Cansler, H.L., Zhang, X., Dinh, D.D., Browder, N.S., Riddington, I.M., and Meeks, J.P. (2016). Faecal bile acids are natural ligands of the mouse accessory olfactory system. Nat. Commun. *7*.

Dulac, C., and Axel, R. (1995). A novel family of genes encoding putative pheromone receptors in mammals. Cell *83*, 195–206.

Eckstein, E., Pyrski, M., Pinto, S., Freichel, M., Vennekens, R., and Zufall, F. (2020). Cyclic regulation of Trpm4 expression in female vomeronasal neurons driven by ovarian sex hormones. Mol. Cell.

Neurosci. *105*, 103495.

Egnor, S.E.R., and Seagraves, K.M. (2016). The contribution of ultrasonic vocalizations to mouse courtship. Curr. Opin. Neurobiol. *38*, 1–5.

Elg, S., Marmigere, F., Mattsson, J.P., and Ernfors, P. (2007). Cellular subtype distribution and developmental regulation of TRPC channel members in the mouse dorsal root ganglion. J. Comp. Neurol. *503*, 35–46.

Ennis, M., and Holy, T.E. (2015). Anatomy and Neurobiology of the Main and Accessory Olfactory Bulbs. In Handbook of Olfaction and Gustation: Third Edition, R. Doty, ed. (John Wiley & Sons, Inc.), pp. 157–182.

Enomoto, T., Ohmoto, M., Iwata, T., Uno, A., Saitou, M., Yamaguchi, T., Kominami, R., Matsumoto, I., and Hirota, J. (2011). Bcl11b/Ctip2 controls the differentiation of vomeronasal sensory neurons in mice. J. Neurosci. *31*, 10159–10173.

Fang, Y.Y., Yamaguchi, T., Song, S.C., Tritsch, N.X., and Lin, D. (2018). A Hypothalamic Midbrain Pathway Essential for Driving Maternal Behaviors. Neuron *98*, 192-207.e10.

Ferguson, J.N., Aldag, J.M., Insel, T.R., and Young, L.J. (2001). Oxytocin in the medial amygdala is essential for social recognition in the mouse. J. Neurosci. *21*, 8278–8285.

Ferrero, D.M., and Liberles, S.D. (2010). The secret codes of mammalian scents. Wiley Interdiscip. Rev. Syst. Biol. Med. *2*, 23–33.

Ferrero, D.M., Lemon, J.K., Fluegge, D., Pashkovski, S.L., Korzan, W.J., Datta, S.R., Spehr, M., Fendt, M., and Liberles, S.D. (2011). Detection and avoidance of a carnivore odor by prey. Proc. Natl. Acad. Sci. U. S. A. *108*, 11235–11240.

Ferrero, D.M., Moeller, L.M., Osakada, T., Horio, N., Li, Q., Roy, D.S., Cichy, A., Spehr, M., Touhara, K., and Liberles, S.D. (2013). A juvenile mouse pheromone inhibits sexual behaviour through the vomeronasal system. Nature *502*, 368–371.

Fleischer, J. (2021). The Grueneberg ganglion: signal transduction and coding in an olfactory and thermosensory organ involved in the detection of alarm pheromones and predator-secreted kairomones. Cell Tissue Res. *383*, 535–548.

Fleischer, J., Hass, N., Schwarzenbacher, K., Besser, S., and Breer, H. (2006). A novel population of neuronal cells expressing the olfactory marker protein (OMP) in the anterior/dorsal region of the nasal cavity. Histochem. Cell Biol. *125*, 337–349.

Fraser, E.J., and Shah, N.M. (2014). Complex chemosensory control of female reproductive behaviors. PLoS One *9*, 5–10.

Fülle, H.J., Vassar, R., Foster, D.C., Yang, R.B., Axel, R., and Garbers, D.L. (1995). A receptor guanylyl cyclase expressed specifically in olfactory sensory neurons. Proc. Natl. Acad. Sci. U. S. A. *92*, 3571–3575.

Fuss, S.H., Omura, M., and Mombaerts, P. (2005). The Grueneberg ganglion of the mouse projects axons to glomeruli in the olfactory bulb. Eur. J. Neurosci. *22*, 2649–2654.

Gandelman, R., and Vom Saal, F.S. (1975). Pup-killing in mice: The effects of gonadectomy and testosterone administration. Physiol. Behav. *15*, 647–651.

Gao, J.L., Chen, H., Filie, J.D., Kozak, C.A., and Murphy, P.M. (1998). Differential expansion of the N-formylpeptide receptor gene cluster in human and mouse. Genomics *51*, 270–276.

Gigante, C.M., Dibattista, M., Dong, F.N., Zheng, X., Yue, S., Young, S.G., Reisert, J., Zheng, Y., and Zhao, H. (2017). Lamin B1 is required for mature neuron-specific gene expression during olfactory sensory neuron differentiation. Nat. Commun. *8*, 1–13.

Gilad, Y., Wiebe, V., Przeworski, M., Lancet, D., and Pääbo, S. (2004). Loss of olfactory receptor

genes coincides with the acquisition of full trichromatic vision in primates. PLoS Biol. *2*, 120–125.

Green, W.W., Uytingco, C.R., Ukhanov, K., Kolb, Z., Moretta, J., McIntyre, J.C., and Martens, J.R. (2018). Peripheral gene therapeutic rescue of an olfactory ciliopathy restores sensory input, axonal pathfinding, and odor-guided behavior. J. Neurosci. *38*, 7462–7475.

Grosmaitre, X., Santarelli, L.C., Tan, J., Luo, M., and Ma, M. (2007). Dual functions of mammalian olfactory sensory neurons as odor detectors and mechanical sensors. Nat. Neurosci. *10*, 348–354.

Grüneberg, H. (1973). A ganglion probably belonging to the N. terminalis system in the nasal mucosa of the mouse. Z. Anat. Entwicklungsgesch. *140*, 39–52.

Grus, W.E., Shi, P., Zhang, Y.P., and Zhang, J. (2005). Dramatic variation of the vomeronasal pheromone receptor gene repertoire among five orders of placental and marsupial mammals. Proc. Natl. Acad. Sci. U. S. A. *102*, 5767–5772.

Gubernick, D.J., Winslow, J.T., Jensen, P., Jeanotte, L., and Bowen, J. (1995). Oxytocin Changes in Males over the Reproductive Cycle in the Monogamous, Biparental California Mouse, Peromyscus californicus. Horm. Behav. *29*, 59–73.

Gutiérrez-Castellanos, N., Pardo-Bellver, C., Martínez-García, F., and Lanuza, E. (2014). The vomeronasal cortex - afferent and efferent projections of the posteromedial cortical nucleus of the amygdala in mice. Eur. J. Neurosci. *39*, 141–158.

Haberly, L.B., and Price, J.L. (1977). The axonal projection patterns of the mitral and tufted cells of the olfactory bulb in the rat. Brain Res. *129*, 152–157.

Haga-Yamanaka, S., Ma, L., He, J., Qiu, Q., Lavis, L.D., Looger, L.L., and Yu, C.R. (2014). Integrated action of pheromone signals in promoting courtship behavior in male mice. Elife *3*, e03025.

Haga, S., Hattori, T., Sato, T., Sato, K., Matsuda, S., Kobayakawa, R., Sakano, H., Yoshihara, Y., Kikusui, T., and Touhara, K. (2010). The male mouse pheromone ESP1 enhances female sexual receptive behaviour through a specific vomeronasal receptor. Nature *466*, 118–122.

Hamada, N., Negishi, Y., Mizuno, M., Miya, F., Hattori, A., Okamoto, N., Kato, M., Tsunoda, T., Yamasaki, M., Kanemura, Y., et al. (2017). Role of a heterotrimeric G-protein, Gi2, in the corticogenesis: possible involvement in periventricular nodular heterotopia and intellectual disability. J. Neurochem. *140*, 82–95.

Hasen, N.S., and Gammie, S.C. (2009). Trpc2 gene impacts on maternal aggression, accessory olfactory bulb anatomy and brain activity. Genes, Brain Behav. *8*, 639–649.

Hashikawa, K., Hashikawa, Y., Tremblay, R., Zhang, J., Feng, J.E., Sabol, A., Piper, W.T., Lee, H., Rudy, B., and Lin, D. (2017). Esr1+ cells in the ventromedial hypothalamus control female aggression. Nat. Neurosci. *20*, 1580–1590.

Hashikawa, K., Hashikawa, Y., Lischinsky, J., and Lin, D. (2018). The Neural Mechanisms of Sexually Dimorphic Aggressive Behaviors. Trends Genet. *34*, 755–776.

Hastie, N.D., Held, W.A., and Toole, J.J. (1979). Multiple genes coding for the androgen-regulated major urinary proteins of the mouse. Cell *17*, 449–457.

Hattori, T., Osakada, T., Masaoka, T., Ooyama, R., Horio, N., Mogi, K., Nagasawa, M., Haga-Yamanaka, S., Touhara, K., and Kikusui, T. (2017). Exocrine Gland-Secreting Peptide 1 Is a Key Chemosensory Signal Responsible for the Bruce Effect in Mice. Curr. Biol. *27*, 3197-3201.e3.

He, J., Ma, L., Kim, S., Nakai, J., and Yu, C.R. (2008). Encoding Gender and Individual Information in the Mouse Vomeronasal Organ. Science (80-.). *320*, 535–538.

Hellier, V., Brock, O., Candlish, M., Desroziers, E., Aoki, M., Mayer, C., Piet, R., Herbison, A., Colledge, W.H., Prévot, V., et al. (2018). Female sexual behavior in mice is controlled by kisspeptin neurons. Nat. Commun. *9*, 1–13.

Hendrickson, R.C., Krauthamer, S., Essenberg, J.M., and Holy, T.E. (2008). Inhibition shapes sex selectivity in the mouse accessory olfactory bulb. J. Neurosci. *28*, 12523–12534.

Herrada, G., and Dulac, C. (1997). A novel family of putative pheromone receptors in mammals with a topographically organized and sexually dimorphic distribution. Cell *90*, 763–773.

Holy, T.E. (2000). Responses of Vomeronasal Neurons to Natural Stimuli. Science (80-.). *289*, 1569–1572.

Hong, W., Kim, D.W., and Anderson, D.J. (2014). Antagonistic control of social versus repetitive self-grooming behaviors by separable amygdala neuronal subsets. Cell *158*, 1348–1361.

Hu, J., Zhong, C., Ding, C., Chi, Q., Walz, A., Mombaerts, P., Matsunami, H., and Luo, M. (2007). Detection of Near-Atmospheric Concentrations of CO2 by an Olfactory Subsystem in the Mouse. Science (80-.). *317*, 953–957.

Hull, E.M., and Dominguez, J.M. (2019). Neuroendocrine regulation of male sexual behavior. Compr. Physiol. *9*, 1383–1410.

Hurst, J.L., and Beynon, R.J. (2004). Scent wars: The chemobiology of competitive signalling in mice. BioEssays *26*, 1288–1298.

Hurst, J.L., Robertson, D.H.L., Tolladay, U., and Beynon, R.J. (1998). Proteins in urine scent marks of male house mice extend the longevity of olfactory signals. Anim. Behav. *55*, 1289–1297.

Hurst, J.L., Payne, C.E., Nevison, C.M., Marie, A.D., Humphries, R.E., Robertson, D.H.L., Cavaggioni, A., and Beynon, R.J. (2001). Individual recognition in mice mediated by major urinary proteins. Nature *414*, 631–634.

Ibarra-Soria, X., Levitin, M.O., Saraiva, L.R., and Logan, D.W. (2014). The Olfactory Transcriptomes of Mice. PLoS Genet. *10*.

Imai, T., Suzuki, M., and Sakano, H. (2006). Odorant Receptor-Derived cAMP Signals Direct Axonal Targeting. Science (80-.). *314*, 657–661.

Inbar, T., Davis, R., and Bergan, J.F. (2021). A sex-specific feedback projection from aromatase-expressing neurons in the medial amygdala to the accessory olfactory bulb. J. Comp. Neurol. cne.25236.

Inoue, S., Yang, R., Tantry, A., Tessier-Lavigne, M., Ding, J.B., Shah Correspondence, N.M., Davis, C.-H., Yang, T., Knoedler, J.R., Wei, Y., et al. (2019). Periodic Remodeling in a Neural Circuit Governs Timing of Female Sexual Behavior Article Periodic Remodeling in a Neural Circuit Governs Timing of Female Sexual Behavior. Cell *179*, 1–16.

Ishii, K.K., and Touhara, K. (2019). Neural circuits regulating sexual behaviors via the olfactory system in mice. Neurosci. Res. *140*, 59–76.

Ishii, T., and Mombaerts, P. (2008). Expression of Nonclassical Class I Major Histocompatibility Genes Defines a Tripartite Organization of the Mouse Vomeronasal System. J. Neurosci. *28*, 2332–2341.

Ishii, K.K., Osakada, T., Mori, H., Miyasaka, N., Yoshihara, Y., Miyamichi, K., and Touhara, K. (2017). A Labeled-Line Neural Circuit for Pheromone-Mediated Sexual Behaviors in Mice. Neuron *95*, 123-137.e8.

Ishii, T., Hirota, J., and Mombaerts, P. (2003). Combinatorial coexpression of neural and immune multigene families in mouse vomeronasal sensory neurons. Curr. Biol. *13*, 394–400.

Isogai, Y., Si, S., Pont-Lezica, L., Tan, T., Kapoor, V., Murthy, V.N., and Dulac, C. (2011). Molecular organization of vomeronasal chemoreception. Nature *478*, 241–245.

Isogai, Y., Wu, Z., Love, M.I., Ahn, M.H.-Y., Bambah-Mukku, D., Hua, V., Farrell, K., and Dulac, C. (2018). Multisensory Logic of Infant-Directed Aggression by Males. Cell *175*, 1827-1841.e17.

Jakupovic, J., Kang, N., and Baum, M.J. (2008). Effect of bilateral accessory olfactory bulb lesions on volatile urinary odor discrimination and investigation as well as mating behavior in male mice. Physiol. Behav. *93*, 467–473.

Jean, A., Bonnet, P., Liere, P., Mhaouty-Kodja, S., and Hardin-Pouzet, H. (2017). Revisiting medial preoptic area plasticity induced in male mice by sexual experience. Sci. Rep. *7*, 1–13.

Jia, C., and Halpern, M. (1996). Subclasses of vomeronasal receptor neurons: differential expression of G proteins (Giα2 and Goα) and segregated projections to the accessory olfactory bulb. Brain Res. *719*, 117–128.

Jia, C., and Halpern, M. (1997). Segregated populations of mitral/tufted cells in the accessory olfactory bulb. Neuroreport *8*, 1887–1890.

Johnson, C.S., Hong, W., and Micevych, P.E. (2021). Posterodorsal medial amygdala regulation of female social behavior: GABA vs Glutamate projections. J. Neurosci. JN-RM-1103-21.

Jones, D.T., and Reed, R.R. (1989). G olf : an Olfactory Neuron Specific-G Protein Involved in Odorant Signal Transduction. Science (80-.). *244*, 790–795.

De Jong, T.R., Beiderbeck, D.I., and Neumann, I.D. (2014). Measuring virgin female aggression in the Female Intruder Test (FIT): Effects of oxytocin, estrous cycle, and anxiety. PLoS One *9*.

Juilfs, D.M., Fülle, H.J., Zhao, A.Z., Houslay, M.D., Garbers, D.L., and Beavo, J.A. (1997). A subset of olfactory neurons that selectively express cGMP-stimulated phosphodiesterase (PDE2) and guanylyl cyclase-D define a unique olfactory signal transduction pathway. Proc. Natl. Acad. Sci. U. S. A. *94*, 3388–3395.

Juntti, S.A., Tollkuhn, J., Wu, M. V., Fraser, E.J., Soderborg, T., Tan, S., Honda, S.I., Harada, N., and Shah, N.M. (2010). The androgen receptor governs the execution, but not programming, of male sexual and territorial behaviors. Neuron *66*, 260–272.

Kang, N.N., Kim, H., Jae, Y.G., Lee, N.H., Ku, C.R., Margolis, F., Lee, E.J., Bahk, Y.Y., Kim, M.S., and Koo, J.H. (2015). Olfactory marker protein expression is an indicator of olfactory receptor-associated events in non-olfactory tissues. PLoS One *10*, 1–21.

Karlson, P., and Lüscher, M. (1959). 'Pheromones': a New Term for a Class of Biologically Active Substances. Nature *183*, 55–56.

Katada, S., Hirokawa, T., Oka, Y., Suwa, M., and Touhara, K. (2005). Structural basis for a broad but selective ligand spectrum of a mouse olfactory receptor: Mapping the odorant-binding site. J. Neurosci. *25*, 1806–1815.

Katreddi, R.R., and Forni, P.E. (2021). Mechanisms underlying pre- and postnatal development of the vomeronasal organ. Cell. Mol. Life Sci.

Kaur, A.W., Ackels, T., Kuo, T.H., Cichy, A., Dey, S., Hays, C., Kateri, M., Logan, D.W., Marton, T.F., Spehr, M., et al. (2014). Murine pheromone proteins constitute a context-dependent combinatorial code governing multiple social behaviors. Cell *157*, 676–688.

Kavaliers, M. (1995). Discrimination by female mice between the odours of parasitized and non-parasitized males. Proc. R. Soc. London. *261*, 31–35.

Kavaliers, M., and Choleris, E. (2001). Antipredator responses and defensive behavior: Ecological and ethological approaches for the neurosciences. Neurosci. Biobehav. Rev. *25*, 577–586.

Kavaliers, M., Choleris, E., and Pfaff, D.W. (2005). Genes, odours and the recognition of parasitized individuals by rodents. Trends Parasitol. *21*, 423–429.

Keller, A. (2007). Getting that first scent of life while we're in the womb. Nature *445*, 593–593.

Keller, M., Pierman, S., Douhard, Q., Baum, M.J., and Bakker, J. (2006). The vomeronasal organ is required for the expression of lordosis behaviour, but not sex discrimination in female mice. Eur. J.

Neurosci. *23*, 521–530.

Keller, M., Pawluski, J.L., Brock, O., Douhard, Q., and Bakker, J. (2010). The α-fetoprotein knock-out mouse model suggests that parental behavior is sexually differentiated under the influence of prenatal estradiol. Horm. Behav. *57*, 434–440.

Kelliher, K.R., Spehr, M., Li, X.H., Zufall, F., and Leinders-Zufall, T. (2006). Pheromonal recognition memory induced by TRPC2-independent vomeronasal sensing. Eur. J. Neurosci. *23*, 3385–3390.

Keshavarzi, S., Sullivan, R.K.P., Ianno, D.J., and Sah, P. (2014). Functional Properties and Projections of Neurons in the Medial Amygdala. J. Neurosci. *34*, 8699–8715.

Kim, S., Ma, L., and Yu, C.R. (2011). Requirement of calcium-activated chloride channels in the activation of mouse vomeronasal neurons. Nat. Commun. *2*, 365–367.

Kim, S., Ma, L., Jensen, K.L., Kim, M.M., Bond, C.T., Adelman, J.P., and Yu, C.R. (2012). Paradoxical contribution of SK3 and GIRK channels to the activation of mouse vomeronasal organ. Nat. Neurosci. *15*, 1236–1244.

Kim, S.S., Ma, L., Unruh, J., McKinney, S., and Yu, C.R. (2015). Intracellular chloride concentration of the mouse vomeronasal neuron. BMC Neurosci. *16*, 4–9.

Kimchi, T., Xu, J., and Dulac, C. (2007). A functional circuit underlying male sexual behaviour in the female mouse brain. Nature *448*, 1009–1014.

Kimoto, H., Sato, K., Nodari, F., Haga, S., Holy, T.E., and Touhara, K. (2007). Sex- and Strain-Specific Expression and Vomeronasal Activity of Mouse ESP Family Peptides. Curr. Biol. *17*, 1879–1884.

Kleine, B., Freudenberg, M.A., and Galanos, C. (1985). Excretion of radioactivity in faeces and urine of rats injected with 3H, 14C-lipopolysaccharide. Br. J. Exp. Pathol. *66*, 303–308.

Kobayakawa, K., Kobayakawa, R., Matsumoto, H., Oka, Y., Imai, T., Ikawa, M., Okabe, M., Ikeda, T., Itohara, S., Kikusui, T., et al. (2007). Innate versus learned odour processing in the mouse olfactory bulb. Nature *450*, 503–508.

Kohl, J., Babayan, B.M., Rubinstein, N.D., Autry, A.E., Marin-Rodriguez, B., Kapoor, V., Miyamishi, K., Zweifel, L.S., Luo, L., Uchida, N., et al. (2018). Functional circuit architecture underlying parental behaviour. Nature *556*, 326–331.

Koike, K., Yoo, S.-J., Bleymehl, K., Omura, M., Zapiec, B., Pyrski, M., Blum, T., Khan, M., Bai, Z., Leinders-Zufall, T., et al. (2021). Danger perception and stress response through an olfactory sensor for the bacterial metabolite hydrogen sulfide. Neuron *109*, 2469-2484.e7.

Koo, J.H., Saraswati, M., and Margolis, F.L. (2005). Immunolocalization of Bex protein in the mouse brain and olfactory system. J. Comp. Neurol. *487*, 1–14.

Koos, D.S., and Fraser, S.E. (2005). The Grueneberg ganglion projects to the olfactory bulb. Neuroreport *16*, 1929–1932.

Kuhn, M. (2016). Molecular physiology of membrane guanylyl cyclase receptors. Physiol. Rev. *96*, 751–804.

Kunkhyen, T., McCarthy, E.A., Korzan, W.J., Doctor, D., Han, X., Baum, M.J., and Cherry, J.A. (2017). Optogenetic activation of accessory olfactory bulb input to the forebrain differentially modulates investigation of opposite versus same-sex urinary chemosignals and stimulates mating in male mice. ENeuro *4*, 1–16.

Kurzweil, V.C., Getman, M., Green, E.D., and Lane, R.P. (2009). Dynamic evolution of V1R putative pheromone receptors between Mus musculus and Mus spretus. BMC Genomics *10*, 1–11.

Kwak, J., Grigsby, C.C., Rizki, M.M., Preti, G., Köksal, M., Josue, J., Yamazaki, K., and Beauchamp, G.K. (2012). Differential binding between volatile ligands and major urinary proteins due to genetic variation in mice. Physiol. Behav. *107*, 112–120.

Kwon, J.T., Ryu, C., Lee, H., Sheffield, A., Fan, J., Cho, D.H., Bigler, S., Sullivan, H.A., Choe, H.K., Wickersham, I.R., et al. (2021). An amygdala circuit that suppresses social engagement. Nature *593*, 114–118.

Labov, J.B., and Wysocki, C.J. (1989). Vomeronasal organ and social factors affect urine marking by male mice. Physiol. Behav. *45*, 443–447.

Labov, J.B., Huck, U.W., Elwood, R.W., and Brooks, R.J. (1985). Current Problems in the Study of Infanticidal Behavior of Rodents. Q. Rev. Biol. *60*, 1–20.

Lacalle-Bergeron, L., Goterris-Cerisuelo, R., Portolés, T., Beltran, J., Sancho, J.V., Navarro-Moreno, C., and Martinez-Garcia, F. (2021). Novel sampling strategy for alive animal volatolome extraction combined with GC-MS based untargeted metabolomics: Identifying mouse pup pheromones. Talanta *235*, 122786.

Larsson, M.C., Domingos, A.I., Jones, W.D., Chiappe, M.E., Amrein, H., and Vosshall, L.B. (2004). Or83b encodes a broadly expressed odorant receptor essential for Drosophila olfaction. Neuron *43*, 703–714.

Lau, Y.E., and Cherry, J.A. (2000). Distribution of PDE4A and G(o) alpha immunoreactivity in the accessory olfactory system of the mouse. Neuroreport *11*, 27–32.

Leinders-Zufall, T., Rand, M.N., Shepherd, G.M., Greer, C.A., and Zufall, F. (1997). Calcium entry through cyclic nucleotide-gated channels in individual cilia of olfactory receptor cells: Spatiotemporal dynamics. J. Neurosci. *17*, 4136–4148.

Leinders-Zufall, T., Lane, A.P., Puche, A.C., Ma, W., Novotny, M. V., Shipley, M.T., and Zufall, F. (2000). Ultrasensitive pheromone detection by mammalian vomeronasal neurons. Nature *405*, 792–796.

Leinders-Zufall, T., Brennan, P., Widmayer, P., Chandramani S., P., Maul-Pavicic, A., Jäger, M., Li, X.H., Breer, H., Zufall, F., and Boehm, T. (2004). MHC class I peptides as chemosensory signals in the vomeronasal organ. Science (80-.). *306*, 1033–1037.

Leinders-Zufall, T., Cockerham, R.E., Michalakis, S., Biel, M., Garbers, D.L., Reed, R.R., Zufall, F., and Munger, S.D. (2007). Contribution of the receptor guanylyl cyclase GC-D to chemosensory function in the olfactory epithelium. Proc. Natl. Acad. Sci. U. S. A. *104*, 14507–14512.

Leinders-Zufall, T., Ishii, T., Mombaerts, P., Zufall, F., and Boehm, T. (2009). Structural requirements for the activation of vomeronasal sensory neurons by MHC peptides. Nat. Neurosci. *12*, 1551–1558.

Leinders-Zufall, T., Ishii, T., Chamero, P., Hendrix, P., Oboti, L., Schmid, A., Kircher, S., Pyrski, M., Akiyoshi, S., Khan, M., et al. (2014). A family of nonclassical class I MHC genes contributes to ultrasensitive chemodetection by mouse vomeronasal sensory neurons. J. Neurosci. *34*, 5121–5133.

Leinders-Zufall, T., Storch, U., Mederos y Schnitzler, M., Ojha, N.K., Koike, K., Gudermann, T., and Zufall, F. (2021). A diacylglycerol photoswitching protocol for studying TRPC channel functions in mammalian cells and tissue slices. STAR Protoc. *2*, 100527.

Lepri, J.J., Wysocki, C.J., and Vandenbergh, J.G. (1985). Mouse vomeronasal organ: Effects on chemosignal production and maternal behavior. Physiol. Behav. *35*, 809–814.

Lévai, O., Feistel, T., Breer, H., and Strotmann, J. (2006). Cells in the vomeronasal organ express odorant receptors but project to the accessory olfactory bulb. J. Comp. Neurol. *498*, 476–490.

Leypold, B.G., Yu, C.R., Leinders-Zufall, T., Kim, M.M., Zufall, F., and Axel, R. (2002). Altered sexual and social behaviors in trp2 mutant mice. Proc. Natl. Acad. Sci. *99*, 6376–6381.

Li, Q., and Liberles, S.D. (2015). Aversion and attraction through olfaction. Curr. Biol. *25*, R120–R129.

Li, F., Ponissery-Saidu, S., Yee, K.K., Wang, H., Chen, M.L., Iguchi, N., Zhang, G., Jiang, P., Reisert, J., and Huang, L. (2013). Heterotrimeric G protein subunit Gγ13 is critical to olfaction. J. Neurosci.

33, 7975–7984.

Li, J., Ishii, T., Feinstein, P., and Mombaerts, P. (2004). Odorant receptor gene choice is reset by nuclear transfer from mouse olfactory sensory neurons. Nature *428*, 393–399.

Li, Y., Mathis, A., Grewe, B.F., Osterhout, J.A., Ahanonu, B., Schnitzer, M.J., Murthy, V.N., and Dulac, C. (2017). Neuronal Representation of Social Information in the Medial Amygdala of Awake Behaving Mice. Cell *171*, 1176-1190.e17.

Liberles, S.D., and Buck, L.B. (2006). A second class of chemosensory receptors in the olfactory epithelium. Nature *442*, 645–650.

Liberles, S.D., Horowitz, L.F., Kuang, D., Contos, J.J., Wilson, K.L., Siltberg-Liberles, J., Liberles, D.A., and Buck, L.B. (2009). Formyl peptide receptors are candidate chemosensory receptors in the vomeronasal organ. Proc. Natl. Acad. Sci. U. S. A. *106*, 9842–9847.

Liman, E.R., and Buck, L.B. (1994). A second subunit of the olfactory cyclic nucleotide-gated channel confers high sensitivity to cAMP. Neuron *13*, 611–621.

Liman, E.R., Corey, D.P., and Dulac, C. (1999). TRP2: A candidate transduction channel for mammalian pheromone sensory signaling. Proc. Natl. Acad. Sci. *96*, 5791–5796.

Lin, D., Boyle, M.P., Dollar, P., Lee, H., Lein, E.S., Perona, P., and Anderson, D.J. (2011). Functional identification of an aggression locus in the mouse hypothalamus. Nature *470*, 221–227.

Lin, W., Arellano, J., Slotnick, B., and Restrepo, D. (2004). Odors Detected Mice Deficient in Cyclic Nucleotide-Gated Channel Subunit A2 Stimulate the Main Olfactory System. J. Neurosci. *24*, 3703–3710.

Van der Linden, C., Jakob, S., Gupta, P., Dulac, C., and Santoro, S.W. (2018). Sex separation induces differences in the olfactory sensory receptor repertoires of male and female mice. Nat. Commun. *9*, 5081.

Liu, Q., Li, S., Lu, C., Yu, C.R., and Huang, L. (2018). G protein γ subunit Gγ13 is essential for olfactory function and aggressive behavior in mice. Neuroreport *29*, 1333–1339.

Liu, Q., Zhang, Y., Wang, P., Guo, X., Wu, Y., Zhang, J.-X.X., and Huang, L. (2019). Two Preputial Gland-Secreted Pheromones Evoke Sexually Dimorphic Neural Pathways in the Mouse Vomeronasal System. Front. Cell. Neurosci. *13*, 1–21.

Lloyd-Thomas, A., and Keverne, E.B. (1982). Role of the brain and accessory olfactory system in the block to pregnancy in mice. Neuroscience *7*, 907–913.

Loconto, J., Papes, F., Chang, E., Stowers, L., Jones, E.P., Takada, T., Kumánovics, A., Lindahl, K.F., and Dulac, C. (2003). Functional expression of murine V2R pheromone receptors involves selective association with the M10 and M1 families of MHC class Ib molecules. Cell *112*, 607–618.

Logan, D.W., Marton, T.F., and Stowers, L. (2008). Species Specificity in Major Urinary Proteins by Parallel Evolution. PLoS One *3*, e3280.

Lowe, G., and Gold, G.H. (1993). Nonlinear amplification by calcium-dependent chloride channels in olfactory receptor cells. Nature *366*, 283–286.

Lucas, P., Ukhanov, K., Leinders-Zufall, T., and Zufall, F. (2003). A diacylglycerol-gated cation channel in vomeronasal neuron dendrites is impaired in TRPC2 mutant mice: Mechanism of pheromone transduction. Neuron *40*, 551–561.

Luo, M. (2003). Encoding Pheromonal Signals in the Accessory Olfactory Bulb of Behaving Mice. Science (80-.). *299*, 1196–1201.

Ma, M., Grosmaitre, X., Iwema, C.L., Baker, H., Greer, C.A., and Shepherd, G.M. (2003). Olfactory signal transduction in the mouse septal organ. J. Neurosci. *23*, 317–324.

Malnic, B., Hirono, J., Sato, T., and Buck, L.B. (1999). Combinatorial receptor codes for odors. Cell

96, 713–723.

Mamasuew, K., Breer, H., and Fleischer, J. (2008). Grueneberg ganglion neurons respond to cool ambient temperatures. Eur. J. Neurosci. *28*, 1775–1785.

Mamasuew, K., Hofmann, N., Kretzschmann, V., Biel, M., Yang, R.B., Breer, H., and Fleischer, J. (2011). Chemo- and thermosensory responsiveness of Grueneberg ganglion neurons relies on cyclic guanosine monophosphate signaling elements. NeuroSignals *19*, 198–209.

Manning, A., and McGill, T.E. (1974). Neonatal androgen and sexual behavior in female house mice. Horm. Behav. *5*, 19–31.

Marlin, B.J., Mitre, M., D'Amour, J.A., Chao, M. V., and Froemke, R.C. (2015). Oxytocin enables maternal behaviour by balancing cortical inhibition. Nature *520*, 499–504.

Martel, K.L., and Baum, M.J. (2009). Adult Testosterone Treatment But Not Surgical Disruption of Vomeronasal Function Augments Male-Typical Sexual Behavior in Female Mice. J. Neurosci. *29*, 7658–7666.

Martín-Sánchez, A., McLean, L., Beynon, R.J., Hurst, J.L., Ayala, G., Lanuza, E., and Martínez-Garcia, F. (2015). From sexual attraction to maternal aggression: when pheromones change their behavioural significance. Horm. Behav. *68*, 65–76.

Martínez-Ricós, J., Agustín-Pavón, C., Lanuza, E., and Martínez-García, F. (2008). Role of the vomeronasal system in intersexual attraction in female mice. Neuroscience *153*, 383–395.

Martini, S., Silvotti, L., Shirazi, A., Ryba, N.J.P., and Tirindelli, R. (2001). Co-expression of putative pheromone receptors in the sensory neurons of the vomeronasal organ. J. Neurosci. *21*, 843–848.

Maruniak, J.A., Wysocki, C.J., and Taylor, J.A. (1986). Mediation of male mouse urine marking and aggression by the vomeronasal organ. Physiol. Behav. *37*, 655–657.

Matsumoto, T., Honda, S.I., and Harada, N. (2003). Alteration in sex-specific behaviors in male mice lacking the aromatase gene. Neuroendocrinology *77*, 416–424.

Matsunami, H., and Buck, L.B. (1997). A Multigene Family Encoding a Diverse Array of Putative Pheromone Receptors in Mammals. Cell *90*, 775–784.

Matsuo, T., Hattori, T., Asaba, A., Inoue, N., Kanomata, N., Kikusui, T., Kobayakawa, R., and Kobayakawa, K. (2015). Genetic dissection of pheromone processing reveals main olfactory system-mediated social behaviors in mice. Proc. Natl. Acad. Sci. *112*, E311–E320.

Mayer, H.S., Crepeau, M., Duque-Wilckens, N., Torres, L.Y., Trainor, B.C., and Stolzenberg, D.S. (2019). Histone deacetylase inhibitor treatment promotes spontaneous caregiving behaviour in non-aggressive virgin male mice. J. Neuroendocrinol. *31*, 1–13.

McCarthy, E.A., Kunkhyen, T., Korzan, W.J., Naik, A., Maqsudlu, A., Cherry, J.A., and Baum, M.J. (2017a). A comparison of the effects of male pheromone priming and optogenetic inhibition of accessory olfactory bulb forebrain inputs on the sexual behavior of estrous female mice. Horm. Behav. *89*, 104–112.

McCarthy, E.A., Maqsudlu, A., Bass, M., Georghiou, S., Cherry, J.A., and Baum, M.J. (2017b). DREADD-induced silencing of the medial amygdala reduces the preference for male pheromones and the expression of lordosis in estrous female mice. Eur. J. Neurosci. *46*, 2035–2046.

McEwen, D.P., Jenkins, P.M., and Martens, J.R. (2008). Olfactory Cilia: Our Direct Neuronal Connection to the External World. In Current Topics in Developmental Biology, (Elesvier Inc.), pp. 333–370.

Mendoza, A.S. (1993). Morphological studies on the rodent main and accessory olfactory systems: The regio olfactoria and vomeronasal organ. Ann. Anat. *175*, 425–446.

Mennella, J.A., and Moltz, H. (1988). Infanticide in the male rat: The role of the vomeronasal organ.

Physiol. Behav. *42*, 303–306.

Meredith, M., and O'Connell, R.J. (1979). Efferent control of stimulus access to the hamster vomeronasal organ. J. Physiol. *286*, 301–316.

Meyer, M.R., Angele, A., Kremmer, E., Kaupp, U.B., and Müller, F. (2000). A cGMP-signaling pathway in a subset of olfactory sensory neurons. Proc. Natl. Acad. Sci. U. S. A. *97*, 10595–10600.

Micevych, P.E., and Meisel, R.L. (2017). Integrating neural circuits controlling female sexual behavior. Front. Syst. Neurosci. *11*, 1–12.

Michalakis, S., Reisert, J., Geiger, H., Wetzel, C., Zong, X., Bradley, J., Spehr, M., Hüttl, S., Gerstner, A., Pfeifer, A., et al. (2006). Loss of CNGB1 protein leads to olfactory dysfunction and subciliary cyclic nucleotide-gated channel trapping. J. Biol. Chem. *281*, 35156–35166.

Millet, P., Opiekun, M., Martin, T., Beauchamp, G.K., and Kimball, B.A. (2018). Cytokine contributions to alterations of the volatile metabolome induced by inflammation. Brain. Behav. Immun. *69*, 312–320.

Millet, P., Martin, T., Opiekun, M., Beauchamp, G.K., and Kimball, B.A. (2021). Differing Alterations of Odor Volatiles Among Pathogenic Stimuli. Chem. Senses *46*, 1–8.

Moffitt, J.R., Bambah-Mukku, D., Eichhorn, S.W., Vaughn, E., Shekhar, K., Perez, J.D., Rubinstein, N.D., Hao, J., Regev, A., Dulac, C., et al. (2018). Molecular, spatial, and functional single-cell profiling of the hypothalamic preoptic region. Science (80-.). *362*, 1–22.

Mohedano-Moriano, A., Pro-Sistiaga, P., Úbeda-Bañón, I., Crespo, C., Insausti, R., and Martinez-Marcos, A. (2007). Segregated pathways to the vomeronasal amygdala: Differential projections from the anterior and posterior divisions of the accessory olfactory bulb. Eur. J. Neurosci. *25*, 2065–2080.

Mohrhardt, J., Nagel, M., Fleck, D., Ben-Shaul, Y., and Spehr, M. (2018). Signal detection and coding in the accessory olfactory system. Chem. Senses *43*, 667–695.

Mombaerts, P. (2004). Genes and ligands for odorant, vomeronasal and taste receptors. Nat. Rev. Neurosci. *5*, 263–278.

Montani, G., Tonelli, S., Sanghez, V., Ferrari, P.F., Palanza, P., Zimmer, A., and Tirindelli, R. (2013). Aggressive behaviour and physiological responses to pheromones are strongly impaired in mice deficient for the olfactory G-protein γ-subunit Gγ8. J. Physiol. *591*, 3949–3962.

Morrison, E.E., and Costanzo, R.M. (1990). Morphology of the human olfactory epithelium. J. Comp. Neurol. *297*, 1–13.

Moulton, D.G., and Beidler, L.M. (1967). Structure and function in the peripheral olfactory system. Physiol. Rev. *47*, 1–52.

Mugford, R.A., and Nowell, N.W. (1970). Pheromones and their Effect on Aggression in Mice. Nature *226*, 967–968.

Münch, J., Billig, G., Hübner, C.A., Leinders-Zufall, T., Zufall, F., and Jentsch, T.J. (2018). Ca2+-activated Cl- currents in the murine vomeronasal organ enhance neuronal spiking but are dispensable for male-male aggression. J. Biol. Chem. *293*, 10392–10403.

Munger, S.D., Lane, A.P., Zhong, H., Leinders-Zufall, T., Yau, K.W., Zufall, F., and Reed, R.R. (2001). Central role of the CNGA4 channel subunit in Ca2+-calmodulin-dependent odor adaptation. Science (80-.). *294*, 2172–2175.

Munger, S.D., Leinders-Zufall, T., and Zufall, F. (2009). Subsystem Organization of the Mammalian Sense of Smell. Annu. Rev. Physiol. *71*, 115–140.

Munger, S.D., Leinders-Zufall, T., McDougall, L.M., Cockerham, R.E., Schmid, A., Wandernoth, P., Wennemuth, G., Biel, M., Zufall, F., and Kelliher, K.R. (2010). An olfactory subsystem that detects carbon disulfide and mediates food-related social learning. Curr. Biol. *20*, 1438–1444.

Nakahara, T.S., Cardozo, L.M., Ibarra-Soria, X., Bard, A.D., Carvalho, V.M.A., Trintinalia, G.Z., Logan, D.W., and Papes, F. (2016). Detection of pup odors by non-canonical adult vomeronasal neurons expressing an odorant receptor gene is influenced by sex and parenting status. BMC Biol. *14*, 12.

Nakahara, T.S., Camargo, A.P., Magalhães, P.H.M., Souza, M.A.A., Ribeiro, P.G., Martins-Netto, P.H., Carvalho, V.M.A., José, J., and Papes, F. (2020). Peripheral oxytocin injection modulates vomeronasal sensory activity and reduces pup-directed aggression in male mice. Sci. Rep. *10*, 1–13.

Nakamura, T., and Gold, G.H. (1987). A cyclic nucleotide-gated conductance in olfactory receptor cilia. Nature *325*, 442–444.

Nakashima, A., Takeuchi, H., Imai, T., Saito, H., Kiyonari, H., Abe, T., Chen, M., Weinstein, L.S., Yu, C.R., Storm, D.R., et al. (2013). Agonist-Independent GPCR Activity Regulates Anterior-Posterior Targeting of Olfactory Sensory Neurons. Cell *154*, 1314–1325.

Navarro-Moreno, C., Sanchez-Catalan, M.J., Barneo-Muñoz, M., Goterris-Cerisuelo, R., Belles, M., Lanuza, E., Agustin-Pavon, C., and Martinez-Garcia, F. (2020). Pregnancy Changes the Response of the Vomeronasal and Olfactory Systems to Pups in Mice. Front. Cell. Neurosci. *14*, 1–19.

Neuhaus, E.M. (2020). Signal Transduction in Olfactory Neurons. In The Senses: A Comprehensive Reference, (Elsevier (Inc.)), pp. 545–564.

Nodari, F., Hsu, F.F., Fu, X., Holekamp, T.F., Kao, L.F., Turk, J., and Holy, T.E. (2008). Sulfated steroids as natural ligands of mouse pheromone-sensing neurons. J. Neurosci. *28*, 6407–6418.

Norlin, E.M.M., Gussing, F., and Berghard, A. (2003). Vomeronasal phenotype and behavioral alterations in Gαi2 mutant mice. Curr. Biol. *13*, 1214–1219.

Novotny, M.V. (2003). Pheromones, binding proteins and receptor responses in rodents. Biochem. Soc. Trans. *31*, 117–122.

Numan, M. (1974). Medial preoptic area and maternal behavior in the female rat. J. Comp. Physiol. Psychol. *87*, 746–759.

Numan, M., and Woodside, B. (2010). Maternity: Neural Mechanisms, Motivational Processes, and Physiological Adaptations. Behav. Neurosci. *124*, 715–741.

Oakley, A.E., Clifton, D.K., and Steiner, R.A. (2009). Kisspeptin signaling in the brain. Endocr. Rev. *30*, 713–743.

Oboti, L., Pérez-Gómez, A., Keller, M., Jacobi, E., Birnbaumer, L., Leinders-Zufall, T., Zufall, F., and Chamero, P. (2014). A wide range of pheromone-stimulated sexual and reproductive behaviors in female mice depend on G protein Gαo. BMC Biol. *12*, 31.

Oboti, L., Ibarra-Soria, X., Pérez-Gómez, A., Schmid, A., Pyrski, M., Paschek, N., Kircher, S., Logan, D.W., Leinders-Zufall, T., Zufall, F., et al. (2015). Pregnancy and estrogen enhance neural progenitor-cell proliferation in the vomeronasal sensory epithelium. BMC Biol. *13*, 1–17.

Ogawa, S., Washburn, T.F., Taylor, J., Lubahn, D.B., Korach, K.S., and Pfaff, D.W. (1998). Modifications of testosterone-dependent behaviors by estrogen receptor- α gene disruption in male mice. Endocrinology *139*, 5058–5069.

Ohara, H., Mogi, K., Ichimaru, T., Ohkura, S., Takeuchi, Y., Mori, Y., and Okamura, H. (2014). Effects of exposure to male goat hair extracts on luteinizing hormone secretion and neuronal activation in seasonally anestrous ewes. J. Vet. Med. Sci. *76*, 1329–1337.

Okabe, S., Nagaswa, M., Koto, M., Koshida, N., Kihara, T., Harada, T., Mogi, K., and Kikusui, T. (2013). Pup odor and ultrasonic vocalizations synergistically stimulate maternal attention in mice. Behav. Neurosci. *127*, 432–438.

Omura, M., and Mombaerts, P. (2014). Trpc2-Expressing Sensory Neurons in the Main Olfactory Epithelium of the Mouse. Cell Rep. *8*, 583–595.

Omura, M., and Mombaerts, P. (2015). Trpc2-expressing sensory neurons in the mouse main olfactory epithelium of type B express the soluble guanylate cyclase Gucy1b2. Mol. Cell. Neurosci. *65*, 114–124.

Osakada, T., Ishii, K.K., Mori, H., Eguchi, R., Ferrero, D.M., Yoshihara, Y., Liberles, S.D., Miyamichi, K., and Touhara, K. (2018). Sexual rejection via a vomeronasal receptor-triggered limbic circuit. Nat. Commun. *9*, 1–15.

Pacifico, R., Dewan, A., Cawley, D., Guo, C., and Bozza, T. (2012). An olfactory subsystem that mediates high-sensitivity detection of volatile amines. Cell Rep. *2*, 76–88.

Padilla, S.L., Qiu, J., Soden, M.E., Sanz, E., Nestor, C.C., Barker, F.D., Quintana, A., Zweifel, L.S., Rønnekleiv, O.K., Kelly, M.J., et al. (2016). Agouti-related peptide neural circuits mediate adaptive behaviors in the starved state. Nat. Neurosci. *19*, 734–741.

Pallé, A., Montero, M., Fernández, S., Tezanos, P., de las Heras, J.A., Luskey, V., Birnbaumer, L., Zufall, F., Chamero, P., and Trejo, J.L. (2020). Gαi2+ vomeronasal neurons govern the initial outcome of an acute social competition. Sci. Rep. *10*, 894.

Pankevich, D.E. (2004). Olfactory Sex Discrimination Persists, Whereas the Preference for Urinary Odorants from Estrous Females Disappears in Male Mice after Vomeronasal Organ Removal. J. Neurosci. *24*, 9451–9457.

Pankevich, D.E., Cherry, J.A., and Baum, M.J. (2006). Effect of vomeronasal organ removal from male mice on their preference for and neural Fos responses to female urinary odors. Behav. Neurosci. *120*, 925–936.

Papes, F., Logan, D.W., and Stowers, L. (2010). The Vomeronasal Organ Mediates Interspecies Defensive Behaviors through Detection of Protein Pheromone Homologs. Cell *141*, 692–703.

Paredes, R.G. (2009). Evaluating the neurobiology of sexual reward. ILAR J. *50*, 15–27.

Parmigiani, S., Brain, P.F., Mainardi, D., and Brunoni, V. (1988). Different patterns of biting attack employed by lactating female mice (Mus domesticus) in encounters with male and female conspecific intruders. J. Comp. Psychol. *102*, 287–293.

Pedersen, P., Stewart, W., Greer, C., and Shepherd, G. (1983). Evidence for olfactory function in utero. Science (80-.). *221*, 478–480.

Pérez-Gómez, A., Bleymehl, K., Stein, B., Pyrski, M., Birnbaumer, L., Munger, S.D., Leinders-Zufall, T., Zufall, F., and Chamero, P. (2015). Innate predator odor aversion driven by parallel olfactory subsystems that converge in the ventromedial hypothalamus. Curr. Biol. *25*, 1340–1346.

Pinching, A.J., and Powell, T.P. (1971). The neuron types of the glomerular layer of the olfactory bulb. J. Cell Sci. *9*, 305–345.

Del Punta, K., Rothman, A., Rodriguez, I., and Mombaerts, P. (2000). Sequence diversity and genomic organization of vomeronasal receptor genes in the mouse. Genome Res. *10*, 1958–1967.

Del Punta, K., Leinders-Zufall, T., Rodriguez, I., Jukam, D., Wysocki, C.J., Ogawa, S., Zufall, F., and Mombaerts, P. (2002). Deficient pheromone responses in mice lacking a cluster of vomeronasal receptor genes. Nature *419*, 70–74.

Raam, T., and Hong, W. (2021). Organization of neural circuits underlying social behavior: A consideration of the medial amygdala. Curr. Opin. Neurobiol. *68*, 124–136.

Renier, N., Adams, E.L., Kirst, C., Wu, Z., Azevedo, R., Kohl, J., Autry, A.E., Kadiri, L., Umadevi Venkataraju, K., Zhou, Y., et al. (2016). Mapping of Brain Activity by Automated Volume Analysis of Immediate Early Genes. Cell *165*, 1789–1802.

Ressler, K.J., Sullivan, S.L., and Buck, L.B. (1994). Information coding in the olfactory system: Evidence for a stereotyped and highly organized epitope map in the olfactory bulb. Cell *79*, 1245–1255.

Reynolds, E. (1971). Urination as a Social Response in Mice. Nature *234*, 481–483.

Ribeiro, A.C., Musatov, S., Shteyler, A., Simanduyev, S., Arrieta-Cruz, I., Ogawa, S., and Pfaff, D.W. (2012). siRNA silencing of estrogen receptor-α expression specifically in medial preoptic area neurons abolishes maternal care in female mice. Proc. Natl. Acad. Sci. U. S. A. *109*, 16324–16329.

Rich, T.J., and Hurst, J.L. (1999). The competing countermarks hypothesis: reliable assessment of competitive ability by potential mates. Anim. Behav. *58*, 1027–1037.

Risold, P.Y., and Swanson, L.W. (1997). Chemoarchitecture of the rat lateral septal nucleus. Brain Res. Rev. *24*, 91–113.

Rivas, F. V., Chervonsky, A. V., and Medzhitov, R. (2014). ART and immunology. Trends Immunol. *35*, 451.

Rivière, S., Challet, L., Fluegge, D., Spehr, M., and Rodriguez, I. (2009). Formyl peptide receptor-like proteins are a novel family of vomeronasal chemosensors. Nature *459*, 574–577.

Roberts, S.A., Simpson, D.M., Armstrong, S.D., Davidson, A.J., Robertson, D.H., McLean, L., Beynon, R.J., and Hurst, J.L. (2010). Darcin: a male pheromone that stimulates female memory and sexual attraction to an individual male's odour. BMC Biol. *8*, 75.

Rodolfo-Masera, T. (1943). Su l'ésistenza di un particolare organo olfattivo nel setoo nasale delà cavia e di altri rodotori. Arch. Ital. Di Anat. e Di Embriol. *48*, 157–212.

Rodriguez, I., Feinstein, P., and Mombaerts, P. (1999). Variable patterns of axonal projections of sensory neurons in the mouse vomeronasal system. Cell *97*, 199–208.

Rodriguez, I., Del Punta, K., Rothman, A., Ishii, T., and Mombaerts, P. (2002). Multiple new and isolated families within the mouse superfamily of V1r vomeronasal receptors. Nat. Neurosci. *5*, 134–140.

Root, C.M., Denny, C.A., Hen, R., and Axel, R. (2014). The participation of cortical amygdala in innate, odour-driven behaviour. Nature *515*, 269–273.

Roppolo, D., Ribaud, V., Jungo, V.P., Lüscher, C., and Rodriguez, I. (2006). Projection of the Grüneberg ganglion to the mouse olfactory bulb. Eur. J. Neurosci. *23*, 2887–2894.

Roppolo, D., Vollery, S., Kan, C. Da, Lüscher, C., Broillet, M.C., and Rodriguez, I. (2007). Gene cluster lock after pheromone receptor gene choice. EMBO J. *26*, 3423–3430.

Rosenson, L.M., and Asheroff, A.K. (1975). Maternal aggression in CD-1 mice: Influence of the hormonal condition of the intruder. Behav. Biol. *15*, 219–224.

Rottman, S.J., and Snowdown, C.T. (1972). Demonstration and analysis of an alarm pheromone in mice. J. Comp. Physiol. Psychol. *81*, 483–490.

Rudolph, U., Srinivasan, Y., Brabet, P., Boulay, G., Birnbaumer, L., Finegold, M.J., Rich, S.S., Harriman, G.R., and Bradley, A. (1995). Ulcerative colitis and adenocarcinoma of the colon in Gαi2-deficient mice. Nat. Genet. *10*, 143–150.

Rünnenburger, K., Breer, H., and Boekhoff, I. (2002). Selective G protein βγ-subunit compositions mediate phospholipase C activation in the vomeronasal organ. Eur. J. Cell Biol. *81*, 539–547.

Ryba, N.J.P., and Tirindelli, R. (1995). A novel GTP-binding protein γ-subunit, Gγ8, is expressed during neurogenesis in the olfactory and vomeronasal neuroepithelia. J. Biol. Chem. *270*, 6757–6767.

Ryba, N.J.P., and Tirindelli, R. (1997). A new multigene family of putative pheromone receptors. Neuron *19*, 371–379.

Vom Saal, F.S. (1985). Time-contingent change in infanticide and parental behavior induced by ejaculation in male mice. Physiol. Behav. *34*, 7–15.

Vom Saal, F.S., and Howard, L.S. (1982). The regulation of infanticide and parental behavior:

Implications for reproductive success in male mice. Science (80-.). *215*, 1270–1272.

Saito, H., Nishizumi, H., Suzuki, S., Matsumoto, H., Ieki, N., Abe, T., Kiyonari, H., Morita, M., Yokota, H., Hirayama, N., et al. (2017). photoactivation of single glomerular species responsive to fox odour TMT. Nat. Commun. *8*, 1–10.

Sam, M., Vora, S., Malnic, B., Ma, W., Novotny, M. V., and Buck, L.B. (2001). Odorants may arouse instinctive behaviours. Nature *412*, 142–142.

Samuelsen, C.L., and Meredith, M. (2009). The vomeronasal organ is required for the male mouse medial amygdala response to chemical-communication signals, as assessed by immediate early gene expression. Neuroscience *164*, 1468–1476.

Sano, K., Tsuda, M.C., Musatov, S., Sakamoto, T., and Ogawa, S. (2013). Differential effects of site-specific knockdown of estrogen receptor α in the medial amygdala, medial pre-optic area, and ventromedial nucleus of the hypothalamus on sexual and aggressive behavior of male mice. Eur. J. Neurosci. *37*, 1308–1319.

Sassoè-Pognetto, M., Cantino, D., Panzanelli, P., Di Cantogno, L.V., Giustetto, M., Margolis, F.L., De Biasi, S., and Fasolo, A. (1993). Presynaptic colocalization of carnosine and glutamate in olfactory neurones. Neuroreport *5*, 7–10.

Sathyanesan, A., Feijoo, A.A., Mehta, S.T., Nimarko, A.F., and Lin, W. (2013). Expression profile of G-protein βγ subunit gene transcripts in the mouse olfactory sensory epithelia. Front. Cell. Neurosci. *7*, 1–19.

Sato, K., Hamasaki, Y., Fukui, K., Ito, K., Miyamichi, K., Minami, M., and Amano, T. (2020). Amygdalohippocampal area neurons that project to the preoptic area mediate infant-directed attack in male mice. J. Neurosci. *40*, 3981–3994.

Schindelin, J., Arganda-Carreras, I., Frise, E., Kaynig, V., Longair, M., Pietzsch, T., Preibisch, S., Rueden, C., Saalfeld, S., Schmid, B., et al. (2012). Fiji: an open-source platform for biological-image analysis. Nat. Methods *9*, 676–682.

Schmid, A., Pyrski, M., Biel, M., Leinders-Zufall, T., and Zufall, F. (2010). Grueneberg ganglion neurons are finely tuned cold sensors. J. Neurosci. *30*, 7563–7568.

Schneider, N.Y., Fletcher, T.P., Shaw, G., and Renfree, M.B. (2012). Goα expression in the vomeronasal organ and olfactory bulb of the tammar wallaby. Chem. Senses *37*, 567–577.

Scholz, P., Mohrhardt, J., Jansen, F., Kalbe, B., Haering, C., Klasen, K., Hatt, H., and Osterloh, S. (2016). Identification of a novel Gnao-mediated alternate olfactory signaling pathway in murine OSNs. Front. Cell. Neurosci. *10*, 1–11.

Schwende, F.J., Wiesler, D., Jorgenson, J.W., Carmack, M., and Novotny, M. (1986). Urinary volatile constituents of the house mouse, Mus musculus, and their endocrine dependency. J. Chem. Ecol. *12*, 277–296.

Seegal, R.F., and Denenberg, V.H. (1974). Maternal experience prevents pup-killing in mice induced by peripheral anosmia. Physiol. Behav. *13*, 339–341.

Serizawa, S., Miyamichi, K., and Sakano, H. (2004). One neuron-one receptor rule in the mouse olfactory system. Trends Genet. *20*, 648–653.

Sharrow, S.D., Vaughn, J.L., Žídek, L., Novotny, M. V., and Stone, M.J. (2009). Pheromone binding by polymorphic mouse major urinary proteins. Protein Sci. *11*, 2247–2256.

Shepherd, G.M., Hines, M.L., Migliore, M., Chen, W.R., and Greer, C.A. (2020). Predicting brain organization with a computational model: 50-year perspective on lateral inhibition and oscillatory gating by dendrodendritic synapses. J. Neurophysiol. *124*, 375–387.

Shi, P., and Zhang, J. (2007). Comparative genomic analysis identifies an evolutionary shift of vomeronasal receptor gene repertoires in the vertebrate transition from water to land. Genome Res. *17*,

166–174.

Silva, L., and Antunes, A. (2017). Vomeronasal Receptors in Vertebrates and the Evolution of Pheromone Detection. Annu. Rev. Anim. Biosci. *5*, 353–370.

Silva, B.A., Mattucci, C., Krzywkowski, P., Murana, E., Illarionova, A., Grinevich, V., Canteras, N.S., Ragozzino, D., and Gross, C.T. (2013). Independent hypothalamic circuits for social and predator fear. Nat. Neurosci. *16*, 1731–1733.

Silvotti, L., Moiani, A., Gatti, R., and Tirindelli, R. (2007). Combinatorial co-expression of pheromone receptors, V2Rs. J. Neurochem. *103*, 1753–1763.

Silvotti, L., Cavalca, E., Gatti, R., Percudani, R., and Tirindelli, R. (2011). A Recent Class of Chemosensory Neurons Developed in Mouse and Rat. PLoS One *6*, e24462.

Simerly, R.B. (2002). Wired for Reproduction: Organization and Development of Sexually Dimorphic Circuits in the Mammalian Forebrain. Annu. Rev. Neurosci. *25*, 507–536.

Simerly, R.B., Swanson, L.W., Handa, R.J., and Gorski, R.A. (1985). Influence of perinatal androgen on the sexually dimorphic distribution of tyrosine hydroxylase-immunoreactive cells and fibers in the anteroventral periventricular nucleus of the rat. Neuroendocrinology *40*, 501–510.

Smrcka, A. V. (2008). G protein βγ subunits: Central mediators of G protein-coupled receptor signaling. Cell. Mol. Life Sci. *65*, 2191–2214.

Song, C., and Leonard, B.E. (2005). The olfactory bulbectomised rat as a model of depression. Neurosci. Biobehav. Rev. *29*, 627–647.

Spehr, J., Hagendorf, S., Weiss, J., Spehr, M., Leinders-Zufall, T., and Zufall, F. (2009). Ca2+-Calmodulin Feedback Mediates Sensory Adaptation and Inhibits Pheromone-Sensitive Ion Channels in the Vomeronasal Organ. J. Neurosci. *29*, 2125–2135.

Spehr, M., Hatt, H., and Wetzel, C.H. (2002). Arachidonic acid plays a role in rat vomeronasal signal transduction. J. Neurosci. *22*, 8429–8437.

Stanić, D., Dubois, S., Chua, H.K., Tonge, B., Rinehart, N., Horne, M.K., and Boon, W.C. (2014). Characterization of Aromatase Expression in the Adult Male and Female Mouse Brain. I. Coexistence with Oestrogen Receptors α and β, and Androgen Receptors. PLoS One *9*, e90451.

Stein, B., Alonso, M.T., Zufall, F., Leinders-Zufall, T., and Chamero, P. (2016). Functional Overexpression of Vomeronasal Receptors Using a Herpes Simplex Virus Type 1 (HSV-1)-Derived Amplicon. PLoS One *11*, e0156092.

Stephan, A.B., Shum, E.Y., Hirsh, S., Cygnar, K.D., Reisert, J., and Zhao, H. (2009). ANO2 is the cilial calcium-activated chloride channel that may mediate olfactory amplification. Proc. Natl. Acad. Sci. U. S. A. *106*, 11776–11781.

Stolzenberg, D.S., and Rissman, E.F. (2011). Oestrogen-Independent, Experience-Induced Maternal Behaviour in Female Mice. J. Neuroendocrinol. *23*, 345–354.

Storan, M.J., and Key, B. (2006). Septal organ of Grüneberg is part of the olfactory system. J. Comp. Neurol. *494*, 834–844.

Stowers, L., Holy, T.E., Meister, M., Dulac, C., and Koentges, G. (2002). Loss of sex discrimination and male-male aggression in mice deficient for TRP2. Science *295*, 1493–1500.

Suárez, R., Fernández-Aburto, P., Manger, P.R., and Mpodozis, J. (2011). Deterioration of the Gαo vomeronasal pathway in sexually dimorphic mammals. PLoS One *6*, 1–6.

Tachikawa, K.S., Yoshihara, Y., and Kuroda, K.O. (2013). Behavioral Transition from Attack to Parenting in Male Mice: A Crucial Role of the Vomeronasal System. J. Neurosci. *33*, 5120–5126.

Takahashi, L.K. (2014). Olfactory systems and neural circuits that modulate predator odor fear. Front. Behav. Neurosci. *8*, 1–13.

Takami, S., and Graziadei, P.P.C. (1991). Light microscopic golgi study of mitral/tufted cells in the accessory olfactory bulb of the adult rat. J. Comp. Neurol. *311*, 65–83.

Takeuchi, H., Inokuchi, K., Aoki, M., Suto, F., Tsuboi, A., Matsuda, I., Suzuki, M., Aiba, A., Serizawa, S., Yoshihara, Y., et al. (2010). Sequential arrival and graded secretion of Sema3F by olfactory neuron axons specify map topography at the bulb. Cell *141*, 1056–1067.

Tan, S., and Stowers, L. (2020). Bespoke behavior: mechanisms that modulate pheromone-triggered behavior. Curr. Opin. Neurobiol. *64*, 143–150.

Tanaka, M., Treloar, H., Kalb, R.G., Greer, C.A., and Strittmatter, S.M. (1999). Go protein-dependent survival of primary accessory olfactory neurons. Proc. Natl. Acad. Sci. U. S. A. *96*, 14106–14111.

Taniguchi, K., Saito, S., and Taniguchi, K. (2011). Phylogenic outline of the olfactory system in vertebrates. J. Vet. Med. Sci. *73*, 139–147.

Thom, M.D., Stockley, P., Jury, F., Ollier, W.E.R., Beynon, R.J., and Hurst, J.L. (2008). The Direct Assessment of Genetic Heterozygosity through Scent in the Mouse. Curr. Biol. *18*, 619–623.

Thompson, M.L., and Edwards, D.A. (1971). Experiential and strain determinants of the estrogen-progesterone induction of sexual receptivity in spayed female mice. Horm. Behav. *2*, 299–305.

Tian, H., and Ma, M. (2004). Molecular organization of the olfactory septal organ. J. Neurosci. *24*, 8383–8390.

Tinbergen, N. (1963). On aims and methods of Ethology. Z. Tierpsychol. *20*, 410–433.

Tirindelli, R. (2021). Coding of pheromones by vomeronasal receptors. Cell Tissue Res. *383*, 367–386.

Tirindelli, R., Dibattista, M., Pifferi, S., and Menini, A. (2009). From Pheromones to Behavior. Physiol. Rev. *89*, 921–956.

Trivers, R.L. (1972). Parental investment and sexual selection. *13*, 136–179.

Trotier, D., and Døving, K.B. (1998). "Anatomical Description of a New Organ in the Nose of Domesticated Animals" by Ludvig Jacobson (1813). Chem. Senses *23*, 743–754.

Trouillet, A.C., Keller, M., Weiss, J., Leinders-Zufall, T., Birnbaumer, L., Zufall, F., and Chamero, P. (2019). Central role of G protein Gαi2 and Gαi2 + vomeronasal neurons in balancing territorial and infant-directed aggression of male mice. Proc. Natl. Acad. Sci. *116*, 5135–5143.

Trouillet, A.C., Moussu, C., Poissenot, K., Keller, M., Birnbaumer, L., Leinders-Zufall, T., Zufall, F., and Chamero, P. (2021). Sensory Detection by the Vomeronasal Organ Modulates Experience-Dependent Social Behaviors in Female Mice. Front. Cell. Neurosci. *15*, 638800.

Tsitoura, C., Malinowski, S.T., Mohrhardt, J., Degen, R., DiBenedictis, B.T., Gao, Y., Watznauer, K., Gerhold, K., Nagel, M., Weber, M., et al. (2020). Synchronous Infra-Slow Oscillations Organize Ensembles of Accessory Olfactory Bulb Projection Neurons into Distinct Microcircuits. J. Neurosci. *40*, 4203–4218.

Tsuneoka, Y., Maruyama, T., Yoshida, S., Nishimori, K., Kato, T., Numan, M., and Kuroda, K.O. (2013). Functional, anatomical, and neurochemical differentiation of medial preoptic area subregions in relation to maternal behavior in the mouse. J. Comp. Neurol. *521*, 1633–1663.

Tsuneoka, Y., Tokita, K., Yoshihara, C., Amano, T., Esposito, G., Huang, A.J., Yu, L.M., Odaka, Y., Shinozuka, K., McHugh, T.J., et al. (2015). Distinct preoptic-BST nuclei dissociate paternal and infanticidal behavior in mice. EMBO J. *34*, 2652–2670.

Tsuneoka, Y., Yoshida, S., Takase, K., Oda, S., Kuroda, M., and Funato, H. (2017). Neurotransmitters and neuropeptides in gonadal steroid receptor-expressing cells in medial preoptic area subregions of the male mouse. Sci. Rep. *7*, 1–16.

Tsunoda, M., Miyamichi, K., Eguchi, R., Sakuma, Y., Yoshihara, Y., Kikusui, T., Kuwahara, M., and

Touhara, K. (2018). Identification of an Intra- and Inter-specific Tear Protein Signal in Rodents. Curr. Biol. *28*, 1213-1223.e6.

Turaga, D., and Holy, T.E. (2012). Organization of Vomeronasal Sensory Coding Revealed by Fast Volumetric Calcium Imaging. J. Neurosci. *32*, 1612–1621.

Uchida, N., Poo, C., and Haddad, R. (2014). Coding and transformations in the olfactory system. Annu. Rev. Neurosci. *37*, 363–385.

Unger, E.K., Burke, K.J., Yang, C.F., Bender, K.J., Fuller, P.M., and Shah, N.M. (2015). Medial amygdalar aromatase neurons regulate aggression in both sexes. Cell Rep. *10*, 453–462.

Ustyugova, I. V., Zhi, L., Abramowitz, J., Birnbaumer, L., and Wu, M.X. (2012). IEX-1 deficiency protects against colonic cancer. Mol. Cancer Res. *10*, 760–767.

Vandenbergh, J.G. (1973). Effects of central and peripheral anosmia on reproduction of female mice. Physiol. Behav. *10*, 257–261.

Vassar, R., Chao, S.K., Sitcheran, R., Nun˜ez, J.M., Vosshall, L.B., and Axel, R. (1994). Topographic organization of sensory projections to the olfactory bulb. Cell *79*, 981–991.

Wachowiak, M., and Shipley, M.T. (2006). Coding and synaptic processing of sensory information in the glomerular layer of the olfactory bulb. Semin. Cell Dev. Biol. *17*, 411–423.

Wagner, S., Gresser, A.L., Torello, A.T., and Dulac, C. (2006). A Multireceptor Genetic Approach Uncovers an Ordered Integration of VNO Sensory Inputs in the Accessory Olfactory Bulb. Neuron *50*, 697–709.

Walz, A., Rodriguez, I., and Mombaerts, P. (2002). Aberrant Sensory Innervation of the Olfactory Bulb in Neuropilin-2 Mutant Mice. J. Neurosci. *22*, 4025–4035.

Walz, A., Feinstein, P., Khan, M., and Mombaerts, P. (2007). Axonal wiring of guanylate cyclase-D-expressing olfactory neurons is dependent on neuropilin 2 and semaphorin 3F. Development *134*, 4063–4072.

Wang, Z., and Storm, D.R. (2011). Maternal behavior is impaired in female mice lacking type 3 adenylyl cyclase. Neuropsychopharmacology *36*, 772–781.

Wang, Z.G., and Ye, R.D. (2002). Characterization of two new members of the formyl peptide receptor gene family from 129S6 mice. Gene *299*, 57–63.

Wang, F., Nemes, A., Mendelsohn, M., and Axel, R. (1998). Odorant receptors govern the formation of a precise topographic map. Cell *93*, 47–60.

Wang, L., Chen, I.Z., and Lin, D. (2015). Collateral Pathways from the Ventromedial Hypothalamus Mediate Defensive Behaviors. Neuron *85*, 1344–1358.

Wei, D., Talwar, V., and Lin, D. (2021). Neural circuits of social behaviors: Innate yet flexible. Neuron *109*, 1600–1620.

Wei, Y.-C., Wang, S.-R., Jiao, Z.-L., Zhang, W., Lin, J.-K., Li, X.-Y., Li, S.-S., Zhang, X., and Xu, X.-H. (2018). Medial preoptic area in mice is capable of mediating sexually dimorphic behaviors regardless of gender. Nat. Commun. *9*, 279.

Weiss, J., Pyrski, M., Jacobi, E., Bufe, B., Willnecker, V., Schick, B., Zizzari, P., Gossage, S.J., Greer, C.A., Leinders-Zufall, T., et al. (2011). Loss-of-function mutations in sodium channel Na v 1.7 cause anosmia. Nature *472*, 186–192.

Wekesa, K.S., and Anholt, R.R.H. (1999). Differential expression of G proteins in the mouse olfactory system. Brain Res. *837*, 117–126.

Wong, L.C., Wang, L., D'Amour, J.A., Yumita, T., Chen, G., Yamaguchi, T., Chang, B.C., Bernstein, H., You, X., Feng, J.E., et al. (2016). Effective Modulation of Male Aggression through Lateral Septum to Medial Hypothalamus Projection. Curr. Biol. *26*, 593–604.

Wong, S.T., Trinh, K., Hacker, B., Chan, G.C.K., Lowe, G., Gaggar, A., Xia, Z., Gold, G.H., and Storm, D.R. (2000). Disruption of the type III adenylyl cyclase gene leads to peripheral and behavioral anosmia in transgenic mice. Neuron *27*, 487–497.

Wong, W.M., Cao, J., Zhang, X., Doyle, W.I., Mercado, L.L., Gautron, L., and Meeks, J.P. (2020). Physiology-forward identification of bile acid–sensitive vomeronasal receptors. Sci. Adv. *6*, eaaz6868.

Wu, M. V., Manoli, D.S., Fraser, E.J., Coats, J.K., Tollkuhn, J., Honda, S.I., Harada, N., and Shah, N.M. (2009). Estrogen Masculinizes Neural Pathways and Sex-Specific Behaviors. Cell *139*, 61–72.

Wu, Z., Autry, A.E., Bergan, J.F., Watabe-Uchida, M., and Dulac, C.G. (2014). Galanin neurons in the medial preoptic area govern parental behaviour. Nature *509*, 325–330.

Wyatt, T.D. (2013). Pheromones and Animal Behavior (Cambridge: Cambridge University Press).

Wyatt, T.D. (2014). Proteins and peptides as pheromone signals and chemical signatures. Anim. Behav. *97*, 273–280.

Wyatt, T.D. (2017). Pheromones. Curr. Biol. *27*, R739–R743.

Wysocki, C.J., and Lepri, J.J. (1991). Consequences of removing the vomeronasal organ. J. Steroid Biochem. Mol. Biol. *39*, 661–669.

Wysocki, C.J., Nyby, J., Whitney, G., Beauchamp, G.K., and Katz, Y. (1982). The vomeronasal organ: Primary role in mouse chemosensory gender recognition. Physiol. Behav. *29*, 315–327.

Yang, C., and Delay, R.J. (2010). Calcium-activated chloride current amplifies the response to urine in mouse vomeronasal sensory neurons. J. Gen. Physiol. *135*, 3–13.

Yang, C.F., Chiang, M.C., Gray, D.C., Prabhakaran, M., Alvarado, M., Juntti, S.A., Unger, E.K., Wells, J.A., and Shah, N.M. (2013). Sexually dimorphic neurons in the ventromedial hypothalamus govern mating in both sexes and aggression in males. Cell *153*, 896–909.

Yang, H., Shi, P., Zhang, Y.P., and Zhang, J. (2005). Composition and evolution of the V2r vomeronasal receptor gene repertoire in mice and rats. Genomics *86*, 306–315.

Yao, S., Bergan, J., Lanjuin, A., and Dulac, C. (2017). Oxytocin signaling in the medial amygdala is required for sex discrimination of social cues. Elife *6*, 1–31.

Yildirim, E., and Birnbaumer, L. (2007). TRPC2: Molecular biology and functional importance. Handb. Exp. Pharmacol. *179*, 53–75.

Yonekura, J., and Yokoi, M. (2008). Conditional genetic labeling of mitral cells of the mouse accessory olfactory bulb to visualize the organization of their apical dendritic tufts. Mol. Cell. Neurosci. *37*, 708–718.

Young, J.M., and Trask, B.J. (2007). V2R gene families degenerated in primates, dog and cow, but expanded in opossum. Trends Genet. *23*, 212–215.

Young, J.M., Massa, H.F., Hsu, L., and Trask, B.J. (2010). Extreme variability among mammalian V1R gene families. Genome Res. *20*, 10–18.

Yu, C.R. (2015). TRICK or TRP? What Trpc2−/− mice tell us about vomeronasal organ mediated innate behaviors. Front. Neurosci. *9*, 1–7.

Zapiec, B., and Mombaerts, P. (2020). The Zonal Organization of Odorant Receptor Gene Choice in the Main Olfactory Epithelium of the Mouse. Cell Rep. *30*, 4220-4234.e5.

Zhang, X., and Firestein, S. (2002). The olfactory receptor gene superfamily of the mouse. Nat. Neurosci. *5*, 124–133.

Zhang, J., Pacifico, R., Cawley, D., Feinstein, P., and Bozza, T. (2013). Ultrasensitive detection of amines by a trace amine-associated receptor. J. Neurosci. *33*, 3228–3239.

Zhang, P., Yang, C., and Delay, R.J. (2008). Urine stimulation activates BK channels in mouse vomeronasal neurons. J. Neurophysiol. *100*, 1824–1834.

Zhang, P., Yang, C., and Delay, R.J. (2010). Odors activate dual pathways, a TRPC2 and a AA-dependent pathway, in mouse vomeronasal neurons. Am. J. Physiol. Physiol. *298*, C1253–C1264.

Zhang, S.X., Lutas, A., Yang, S., Diaz, A., Fluhr, H., Nagel, G., Gao, S., and Andermann, M.L. (2021). Hypothalamic dopamine neurons motivate mating through persistent cAMP signalling. Nature *597*, 245–249.

Appendices

SCIENTIFIC PUBLICATIONS

Peer-reviewed articles

- Photoperiod is involved in the regulation of seasonal breeding in male water voles (*Arvicola terrestris*).
  *Poissenot K., Chorfa A., Moussu C., **Trouillet AC.**, Brachet M., Chesneau D., Chemineau P., Ramadier E., Pinot A., Benoit E., Lattard V., Dardente H., Drevet J., Saez F., Keller M. (2021)* ***Journal of Experimental Biology.*** *224(19), jeb242792.*

- Sensory detection by the vomeronasal organ modulates experience-dependent social behaviors in female mice.
  Trouillet AC.*, Moussu C., Poissenot K., Keller M., Birnbaumer L., Leinders-Zufall T., Zufall F., Chamero P. (2021)* ***Frontiers in Cellular Neurosciences.*** *15, 638800.*

- Effects of neural estrogen receptor beta deletion on social and mood-related behaviors and underlying mechanisms in male mice.
  *Dombret C., Naulé L., **Trouillet AC.**, Parmentier C., Hardin-Pouzet H., Mhaouty-Kodja S. (2020)* ***Scientific Reports.*** *10, 6242.*

- Central role of G protein Gαi2 and Gαi2^{+} vomeronasal neurons in balancing territorial and infant-directed aggression of male mice.
  Trouillet AC.*, Keller M., Weiss J., Leinders-Zufall T., Birnbaumer L., Zufall F., Chamero P. (2019)* ***Proceedings of the National Academy of Sciences USA.*** *116(11), 5135-5143.*

- Phospho-ERK and sex steroids in the mPOA: involvement in male mouse sexual behaviour.
  *Jean A., **Trouillet AC.**, Andrianarivelo NA., Mhaouty-Kodja S., Hardin-Pouzet H. (2017)* ***Journal of Endocrinology.*** *233(3), 257-267.*

- Estradiol-induced neurogenesis in the female olfactory bulb is required for the learning of the male odor.
  *Brus M., **Trouillet AC.**, Hellier V., Bakker J. (2016)* ***Journal of Neurochemistry.*** *138(3), 457-468.*

- Revisiting the neural role of estrogen receptor beta in male sexual behavior by conditional mutagenesis.
  *Naulé L., Marie-Luce C., Parmentier C., Martini M., Albac C., **Trouillet AC.**, Keller M., Hardin-Pouzet H., Mhaouty-Kodja S. (2016)* ***Hormones and Behavior.*** *80, 1-9.*

Oral communications

- 44rd annual meeting of the SNE, 2021, Bordeaux (France): *Sensory detection by Gα_{i2} VSNs modulates experience-dependent social behaviors in female mice.* Selected from abstracts.
- 30th annual meeting of the ECRO, 2021, Cascais (Portugal): *Sensory detection by Gα_{i2} VSNs modulates experience-dependent social behaviors in female mice.* Selected for the Young Investigator Symposium. Supported by a WIOS travel grant.
- 43rd annual meeting of the SNE, 2019, Tours (France): *Role of Gα_{i2} signal transduction mediating reproductive and socio-sexual behaviors in mice.* Selected from abstracts.
- 29th annual meeting of the ECRO, 2019, Trieste (Italie): *Role of Gα_{i2} signal transduction mediating reproductive and socio-sexual behaviors in mice.* Selected for the Young Investigator Symposium. Supported by an ECRO travel grant.

Posters

- 15th Chemical Signals in Vertebrates meeting, 2021, Dijon (France): *Sensory detection by Gα_{i2} VSNs modulates experience-dependent social behaviors in female mice.*
- 46th annual meeting of the SFN, 2016, San Diego (USA): *Neural ERα and ERβ signaling pathways in mice.*
- 41st annual meeting of the SNE, 2016, Corte (France): *Role of neural ERα in male mice sexual behavior.*
- Inaugural symposium of the IBPS, 2015, Paris (France): *Role of neural ERα in sexual behavior of mice.*
- Thematic symposium of the SNE, 2014, Paris (France): *Role of estradiol in the feminization of lordosis behavior.*
- 8th ICHBB, 2014, Liège (Belgium): *Role of estradiol in the feminization of lordosis behavior in female mice.*

"Education is not something you can finish."

Isaac Asimov

SCIENCE POPULARIZATION

School and public animation

- National Science Fair, 2019: whorshop on pheromones and animal reproduction
- National Brain Week, 2017: workshop on neurons observation

Research organizations highlights

- Société des Neurosciences (2019)
- Société de Neuroendocrinologie (2019)
- Département PHASE de l'INRAE (2019)

Press releases

- CNRS Microscoop
  "Une histoire de flair!"
- INRAE and CNRS
  "Comportement paternel et défense du territoire : le fil ne tient qu'à certains neurones olfactifs!"
- France 3 Région Centre-Val de Loire
  "Ces odeurs qui nous gouvernent"

PEER REVIEWED JOURNAL ARTICLES

1 Poissenot K., Chorfa A., Moussu C., **Trouillet AC.**, Brachet M., Chesneau D., Chemineau P., Ramadier E., Pinot A., Benoit E., Lattard V., Dardente H., Drevet J., Saez F., Keller M. **Photoperiod is involved in the regulation of seasonal breeding in male water voles (*Arvicola terrestris*)** Journal of Experimental Biology.224 (19). **2021**.
DOI: 10.1242/jeb.242792

2 **Trouillet AC.**, Moussu C., Poissenot K., Keller M., Birnbaumer L., Leinders-Zufall T., Zufall F., Chamero P. **Sensory detection by the vomeronasal organ modulates experience-dependent social behaviors in female mice.** Frontiers in Celullar Neurosciences. 15, 638800. **2021**.
DOI: 10.3389/fncel.2021.638800

3 Dombret C., Naulé L., **Trouillet AC.**, Parmentier C., Hardin-Pouzet H., Mhaouty-Kodja S. **Effects of neural estrogen receptor beta deletion on social and mood-related behaviors and underlying mechanisms in male mice.** Scientific Reports. 10, 6242. **2020**.
DOI: 2020.10.1038/s41598-020-63427-4

4 **Trouillet AC.**, Keller M., Weiss J., Leinders-Zufall T., Birnbaumer L., Zufall F., Chamero P. **Central role of G protein Gαi2 and Gαi2^{+} vomeronasal neurons in balancing territorial and infant-directed aggression of male mice.** Proceedings of the National Academy of Sciences of the United States of America. 116, 5135-5143. **2019**.
DOI: 10.1073/pnas.1821492116

5 Jean A., **Trouillet AC.**, Andrianarivelo NA., Mhaouty-Kodja S., Hardin-Pouzet H. **Phospho-ERK and sex steroids in the mPOA: involvement in male mouse sexual behaviour.** Journal of Endocrinology. 233, 254-264. **2017**.
DOI: 10.1530/JOE-17-0025

6 Brus M., **Trouillet AC.**, Hellier V., Bakker J. **Estradiol-induced neurogenesis in the female olfactory bulb is required for the learning of the male odor.** Journal of Neurochemistry. 138,457-468. **2016**.
DOI: 10.1111/jnc.13677

7 Naulé L., Marie-Luce C., Parmentier C., Martini M., Albac C., **Trouillet AC.**, Keller M., Hardin-Pouzet H., Mhaouty-Kodja S. **Revisiting the neural role of estrogen receptor beta in male sexual behavior by conditional mutagenesis.** Hormones and Behavior. 80, 1-9. **2016**.
DOI: 10.1016/j.yhbeh.2016.01.014

Une histoire de flair !

Comment les animaux se reconnaissent-ils ? À première vue, toutes les souris se ressemblent. Et pourtant, chacune sait dire qui est l'autre d'un seul coup... de nez !



Savoir qui l'on a en face de soi est indispensable pour exprimer une réponse comportementale adéquate. Nous utilisons nos yeux pour reconnaitre les gens qui nous entourent. Beaucoup de mammifères utilisent, eux, leur nez. Chaque animal produit une combinaison unique d'odeurs qui lui sert de « carte d'identité », indiquant son sexe, son âge, son statut physiologique etc… Lors d'une rencontre, un animal va déterminer ce que représente l'autre à partir de ses odeurs. Une menace ? Un potentiel partenaire sexuel ? Comment cette reconnaissance sociale se passe-t-elle ?

L'ORGANE VOMÉRONASAL, RADAR À PHÉROMONES

Cette « carte d'identité » olfactive est constituée de phéromones sécrétées dans les fluides biologiques. La particularité des phéromones est leur capacité à influencer la physiologie et le comportement de celui qui les perçoit.

Le système olfactif des mammifères comporte plusieurs organes sensoriels contenant des neurones olfactifs. Ce sont les seuls neurones en contact avec le monde chimique extérieur ! Les phéromones sont majoritairement détectées par un organe olfactif particulier, l'organe voméronasal (VNO). Véritable radar à phéromones, le VNO est localisé à la base du septum, dans la cavité nasale de la plupart de mammifères. Les neurones sensoriels du VNO captent les phéromones grâce à des récepteurs spécialisés appartenant à la superfamille des récepteurs couplés aux protéines G (GPCRs). Il existe plusieurs centaines de récepteurs voméronasaux (VRs), chacun spécifiquement dédié à une odeur. Les VRs sont classés en 2 groupes, les V1Rs et les V2Rs, en fonction du type de protéine G qu'ils utilisent, respectivement Gαi2 et Gαo.

LA GOUVERNANCE DES ODEURS

Les études d'ablation chirurgicale et génétique du VNO ont montré l'importance de la détection des phéromones par le VNO dans le contrôle des comportements sociaux. Par exemple, les souris sont de farouches adversaires quand il faut défendre leur territoire. Une souris sans VNO, elle, n'est pas capable de détecter une menace. Elle est douce comme un agneau !

Des phéromones initiatrices de comportements sociaux ont été isolées. Par exemple, les MUPs (Major Urinary Proteins), des protéines sécrétées par les souris mâles dans leurs urines, induisent une réponse agressive. Les phéromones peuvent aussi inhiber certains comportements. C'est le cas de la protéine ESP22 (Exocrine-gland Secreting Peptide 22), sécrétée dans les larmes des souris juvéniles, c'est-à-dire sexuellement immatures. Elle est aussi détectée par le VNO, et va réprimer le comportement sexuel des souris adultes envers les juvéniles.

DES CIRCUITS CÉRÉBRAUX ANCRÉS, MAIS PLASTIQUES

Chez les mammifères, les informations phéromonales sont intégrées à d'autres informations sensorielles internes et externes pour produire un comportement adapté. Les neurones sensoriels du VNO envoient leurs informations dans le bulbe olfactif accessoire via des prolongements nerveux qui traversent la cavité nasale. De là, les informations sont expédiées dans un véritable réseau cérébral interconnecté. Les différents noyaux cérébraux (groupement de neurones associés à une même fonction) de ces réseaux commencent à être connus.

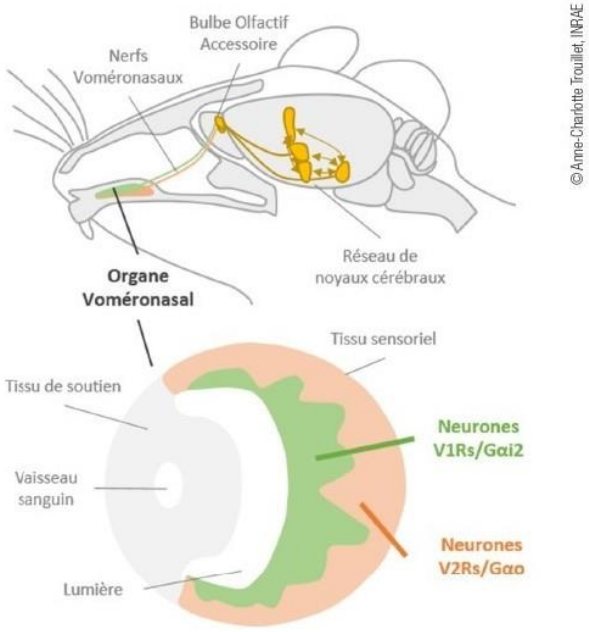

Haut : trajet de l'information olfactive de l'organe voméronasal jusqu'aux noyaux cérébraux. Bas : schéma de l'organisation de l'organe voméronasal

Certains noyaux sont engagés dans plusieurs comportements sociaux. C'est le cas de l'amygdale médiane (un noyau du système limbique) qui est impliquée dans le comportement sexuel, l'agression ou encore le comportement parental. Deux phénomènes l'expliquent. Premièrement, un noyau n'est pas homogène, tous les neurones qui le composent ne sont pas identiques. Il existe des sous-populations de neurones au sein des noyaux, chacune participant à la régulation d'un comportement particulier. Deuxièmement, le cerveau est une structure plastique. Une même stimulation olfactive sera interprétée différemment en fonction du statut de l'animal (âge, expérience, sexe…) et induira différentes réponses comportementales. Par exemple, pour une femelle, un mâle est un potentiel partenaire sexuel. Son cerveau lui dit. Par contre, une femelle qui vient d'avoir des petits va attaquer un mâle qu'elle ne connait pas, car son cerveau lui dit qu'il est une menace pour sa progéniture.

"... déterminer ce que « sentent » les neurones Gαi2."

DE LA PHÉROMONE À LA RÉACTION : DISSECTION

Comment étudier plus finement les circuits nerveux qui contrôlent les comportements sociaux ? La multitude de phéromones et récepteurs associés rend la tâche compliquée. L'idée des chercheurs de l'Unité Physiologie de la Reproduction et des Comportements (UMR 7247 - CNRS/INRAE/IFCE/Université de Tours) a été d'invalider chez la souris le gène codant pour la protéine Gαi2, une sous-unité caractéristique des récepteurs voméronasaux de type V1Rs. Résultat : tous les neurones olfactifs utilisant un des plus de 200 V1Rs, c'est-à-dire la moitié des neurones olfactif du VNO, deviennent non fonctionnels.

Première étape, déterminer ce que « sentent » les neurones Gαi2. L'imagerie calcique permet de voir l'activation d'un neurone instantanément après sa stimulation par une molécule olfactive. Grâce à cette technique, les chercheurs ont déterminé que les neurones Gαi2 détectent les petites molécules organiques comme les dérivés hormonaux présents dans les urines.

Deuxième étape, cibler les comportements que contrôlent les neurones Gαi2. Pour cela, ils ont comparé le comportement de souris avec et sans neurones Gαi2 fonctionnels lors de diverses conditions. Plusieurs comportements étaient impactés : l'agression chez le mâle, le comportement sexuel chez la femelle et le comportement parental chez les deux sexes.

Dernière étape, disséquer les circuits cérébraux modulés par les neurones Gαi2. Les chercheurs ont étudié, dans les noyaux cérébraux connus, quelles populations de neurones étaient activées suite aux différents tests de comportement. Ainsi, ils ont découvert que dans l'amygdale médiane, la réponse agressive chez le mâle est due à l'activation de neurones différents en fonction de la stimulation. Un même type de comportement peut donc découler de l'activation de différents acteurs d'un réseau. Leurs études ont aussi montré que les odeurs de mâles activent plus de neurones de l'hypothalamus chez la femelle sexuellement expérimentée que chez la femelle naïve. Pour une même stimulation, l'expérience de l'animal modifie donc comment le réseau cérébral qui interprète cette stimulation est activé.

Ces études sur l'olfaction sont de puissants outils pour la compréhension des schémas nerveux qui soutiennent les comportements sociaux. Nos comportements humains ne sont pas autant stéréotypés que ceux des rongeurs. Mais nous sommes face à la même problématique qu'eux : intégrer les informations sensorielles qui nous parviennent et adapter nos comportements à la situation. Comprendre ces circuits cérébraux est nécessaire pour le développement de nouvelles approches thérapeutiques des troubles du comportement.

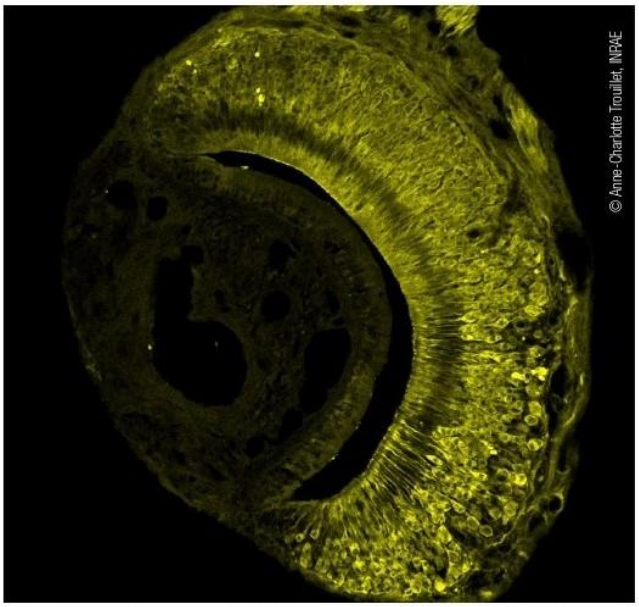

Observation au microscope confocal d'un organe voméronasal de souris et mise en évidence des neurones olfactifs par immunomarquage de l'Olfactory marker Protein (OMP).

Anne-Charlotte TROUILLET < PRC
anne-charlotte.trouillet@inrae.fr
Pablo CHAMERO < PRC
pablo.chamero-benito@inrae.fr
https://www6.val-de-loire.inrae.fr/prc-neuroendo-comp

Anne-Charlotte Trouillet

Rôle des mécanismes de signalisation olfactive impliquant $G\alpha_{i2}$ dans le contrôle des comportements socio-sexuels.

Résumé

Chez la plupart des mammifères, le système olfactif régule les comportements socio-sexuels via la détection d'informations chimiques. Les neurones sensoriels du système olfactif détectent ces signaux par l'intermédiaire de récepteurs couplés aux protéines G, chacun étant exprimé par un seul ensemble de neurones. Les signaux olfactifs pertinents pour la communication sociale sont principalement détectés par l'organe voméronasal, dans lequel au moins deux populations de cellules réceptrices (les VSNs) détectent les phéromones par l'intermédiaire de deux familles de récepteurs couplés aux protéines G, les V1Rs et les V2Rs. Il a été proposé que la liaison d'un ligand à son récepteur, V1R ou V2R, active une protéine G correspondante, respectivement Gαi2 et Gαo. Les neurones exprimant la protéine Gαo détectent des peptides et des protéines modulant plusieurs comportements sociaux. Des études génétiques et comportementales sur la souris indiquent également un rôle potentiel des neurones exprimant Gαi2 comme transducteurs de l'information olfactive et modulateurs de la physiologie et des comportements sexuels. Cependant, la contribution exacte de cette voie de signalisation reste largement méconnue. Par conséquent, l'objectif principal de ce projet est de déterminer comment les comportements socio-sexuels sont contrôlés par le système olfactif, en particulier par les neurones de l'organe voméronasal exprimant V1R-Gαi2.

Pour répondre à cette question, nous avons utilisé le système Cre-lox pour ainsi générer une souris dans laquelle la délétion du gène codant pour Gαi2 est limitée aux neurones sensoriels olfactifs. Tout d'abord, nous avons évalué le rôle fonctionnel de Gαi2 dans le processus de transduction du signal via des techniques d'imagerie calcique sur cellules vivantes. Nous avons ainsi établi que Gαi2 est nécessaire pour la détection des petites molécules organiques et des stéroïdes sulfatés. Ensuite, nous avons étudié le rôle des VSNs exprimant Gαi2/V1Rs dans l'expression des comportements reproducteurs et sociaux. Nous avons testé les comportements sexuels, parentaux et agressifs de souris mâles et femelles déficientes pour Gαi2 et identifié les régions du cerveau transformant l'information olfactive en décision comportementale. Nous avons observé une influence des VSNs exprimant Gαi2 en fonction du sexe avec des effets spécifiques pour chaque comportement. Nous avons constaté que la délétion de Gαi2 dans les VSNs joue un rôle central dans le comportement agressif des mâles en augmentant l'agression territoriale et en réduisant l'agression dirigée vers les nouveau-nés. Cependant, l'agressivité des femelles reste inchangée en l'absence de Gαi2. Le comportement parental est également affecté par la délétion de Gαi2 de façon différente chez chaque sexe, augmenté chez les mâles et inhibé chez les femelles. De plus, l'expérience sociale modifie l'implication de la signalisation voméronasale Gαi2 dans le comportement sexuel des femelles, alors que chez les mâles, la délétion de Gαi2 n'a aucun effet sur le comportement sexuel. Enfin, nous avons identifié un nouveau rôle pour les VSNs exprimant Gαi2 dans les comportements d'aversion médiés par les signaux de prédateurs et de congénères malades.

Toutes les espèces intègrent continuellement des informations environnementales et adaptent leurs réponses en conséquence. Ce projet vise à mettre en lumière les mécanismes neuronaux qui sous-tendent le traitement des signaux chimiques olfactifs, afin de comprendre comment les entrées olfactives périphériques interagissent avec les centres neuronaux qui contrôlent les réponses comportementales. La compréhension de ces mécanismes a une large portée et peut conduire à de nouvelles perspectives dans la compréhension des troubles du comportement et le développement de nouvelles stratégies d'élevage chez les animaux domestiques.

Abstract

In most mammals, the olfactory system drives socio-sexual behaviors through the detection of chemosensory information. Sensory neurons of the olfactory system detect these signals through dedicated G protein-coupled receptors, each expressed by a single ensemble of neurons. Chemosignals relevant for social communication are mainly sensed by the vomeronasal organ in which at least two populations of receptor cells detect pheromones through two families of G-protein-coupled receptors, V1Rs and V2Rs. The binding of ligands to the receptor (V1R or V2R) has been proposed to activate the corresponding G protein, Gαi2 and Gαo, respectively. Gαo-expressing neurons have been shown to detect peptides and proteins modulating several social behaviors. Genetic and behavioral studies on mice also point to a potential role of Gαi2-expressing neurons as transducers of the olfactory information controlling reproductive physiology and behaviors. However, the exact contribution of this signaling pathway remains elusive. Therefore, the main goal of this project is to determine how socio-sexual behaviors are controlled by the olfactory system, particularly by the V1R-Gαi2-expressing neurons of the vomeronasal organ.

To address this point, we used the Cre-lox system to generate a conditional knockout mouse in which the deletion of Gαi2 gene is restricted to olfactory sensory neurons. First, we evaluated the functional role of Gαi2 in the process of VSNs signal transduction using live-cell calcium imaging experiments. We first established that Gαi2 is necessary for the detection of small organic molecules and sulfated steroids in V1Rs-expressing VSNs. Second, we investigated the role of Gαi2/V1Rs-expressing VSNs in displaying reproductive and social behaviors. We tested sexual, parental, and aggressive behaviors of male and female mice deficient for Gαi2 and identified brain regions transforming the olfactory information into a behavioral decision. We observed an influence of Gαi2-expressing VSNs in a sex-dependent manner with distinctive traits for each behavior. We found that the deletion of Gαi2 in VSNs played a central role in male aggressive behavior by increasing territorial aggression and reducing infant-directed aggression. However, female aggression remained unaltered in the absence of Gαi2. Parenting was also differentially affected by Gαi2 deletion in each sex, activated in males and inhibited in females. Further, social experience changed the implication of Gαi2 vomeronasal signaling in female sexual behavior, while in males, Gαi2-deletion had no effect on sexual behavior before or after experience. Last, we identified a new role of Gαi2-expressing VSNs in avoidance behaviors mediated by predators and sick-conspecifics aversive olfactory cues.

All species continuously integrate environmental information and adapt their responses accordingly. This project aims to shed light on neural mechanisms underlying the processing of olfactory chemosignals in order to understand how peripheral olfactory inputs interact with neural centers controlling the behavioral responses. Understanding these mechanisms is of broad relevance and may lead to new insights in the comprehension of behavioral disorders and the development of new breeding strategies in domestic animals.

Version française

INTRODUCTION 1

1 LE SYSTÈME OLFACTIF 3

1.1 LE SYSTÈME OLFACTIF PRINCIPAL 4
1.1.1 L'épithélium olfactif principal 4
1.1.2 Les neurones sensoriels olfactifs canoniques 6
1.1.1 Les neurones sensoriels olfactifs non canoniques 7
1.1.1.1 OSNs exprimant des TAARs 8
1.1.1.2 OSNs exprimant la GC-D 8
1.1.1.1 OSNs exprimant TRPC-2 9
1.1.1 Le bulbe olfactif principal 10
1.2 L'ORGANE SEPTAL DE MASERA 12
1.3 LE GANGLION DE GRÜNEBERG 13
1.4 LE SYSTÈME OLFACTIF ACCESSOIRE 14
1.4.1 L'organe voméronasal 15
1.4.2 Signalisation voméronasale 16
1.4.2.1 V1Rs 17
1.4.2.2 V2Rs 18
1.4.2.3 Cascade sensorielle des VRs 20
1.4.2.4 FPRs 21
1.4.3 Le bulbe olfactif accessoire 22
1.4.1 Ligands voméronasaux 23

2 CONTRÔLE VOMÉRONASAL DES COMPORTEMENTS SOCIO-SEXUELS 26

2.1 COMPORTEMENTS SEXUELS 27
2.1.1 Comportements sexuels mâle 28
2.1.1 Comportements sexuels femelles 31
2.1.2 Le cas curieux de la préférence sexuelle chez les souris Trpc2-/-. 33
2.2 COMPORTEMENTS AGRESSIFS 34
2.2.1 Agressivité territoriale 35
2.2.2 Agressivité maternelle 36
2.2.3 Infanticide 37
2.3 COMPORTEMENTS PARENTAUX 38
2.4 COMPORTEMENTS D'ÉVITEMENT 39
2.4.1 Évitement des prédateurs 40
2.4.2 Évitement des agents pathogènes 41

3 CONTRÔLE NEURONAL DES COMPORTEMENTS SOCIO-SEXUELS 43

3.1 CIRCUITS NEURONAUX DES COMPORTEMENTS SEXUELS 45
3.1.1 Codage du sexe par les informations voméronasales 45
3.1.2 Circuit neuronal du comportement sexuel mâle 47
3.1.1 Circuit neuronal du comportement lordose 48
3.2 CIRCUIT NEURONAL DE L'AGRESSIVITÉ 49
3.3 LES CIRCUITS NEURONAUX DES COMPORTEMENTS PARENTAUX 51
3.4 CIRCUITS NEURONAUX D'ÉVITEMENT DES PRÉDATEURS ET DES CONGÉNÈRES MALADES 53

OBJECTIFS 55

RÉSULTATS 61

1 FONCTION DE GAI2 DANS LA SIGNALISATION DES VSNS ET LES COMPORTEMENTS SOCIO-SEXUELS MÂLES 61

1.1 INTRODUCTION 63
1.2 RESULTS 64
1.2.1 Conditional deletion of $G\alpha_{i2}$ in VSNs 64
1.2.2 $G\alpha_{i2}$ is required for sensory function of apical VSNs 65
1.2.3 Normal male sexual behavior in $G\alpha_{i2}$ mutants 66
1.2.4 Territorial aggression is enhanced in $G\alpha_{i2}$ mutant males 66
1.2.5 Increased brain activation to male intruder in $G\alpha_{i2}$ mutant males 66
1.2.6 Infant-directed aggression is diminished in Gαi2 mutant males, but parental behavior is *enhanced* 66
1.3 DISCUSSION 68
1.4 METHODS 69
1.5 SUPPLEMENTARY INFORMATION 72

2 IMPACT DE LA DÉLÉTION DE GAI2 DANS LES VSNS SUR LES COMPORTEMENTS SOCIO-SEXUELS FEMELLES 91

2.1 INTRODUCTION 93
2.2 METHODS 94
2.3 RESULTS 96
2.3.1 Inactivation of the apical vomeronasal cell layer reduces pup retrieval in virgin females 96
2.3.2 Deletion of $G\alpha_{i2}$ does not affect maternal behavior in mothers 97
2.3.3 Incomplete sexual receptivity acquisition in $G\alpha_{i2}$ mutant females 98
2.3.4 Reduced cFos expression in the AOB and RP3V of $G\alpha_{i2}$ mutant females 100
2.3.5 $G\alpha_{i2}$ deletion has no impact on reproductive physiology 101
2.4 DISCUSSION 102

3 CONTRÔLE DES COMPORTEMENTS D'ÉVITEMENT PAR LES VSN APICAUX 107

3.1 INTRODUCTION 107
3.2 MÉTHODES 108
3.3 RÉSULTATS 111
3.3.1 Apical VSNs mediate sick and predator avoidances 111
3.3.2 Sick and predator associated olfactory cues activate Gαi2 vomeronasal signaling pathway 113
3.3.3 Deletion of $G\alpha_{i2}$ reduces the detection of owl odors 114
3.3.4 $G\alpha_{i2}$ deletion does not specifically impact LPS-urine detection 116
3.4 DISCUSSION 117

DISCUSSION 121

1 UN MODÈLE N'EST QU'UN MODÈLE 123

2 L'UTILISATION DE DEUX SYSTÈMES VOMÉRONASAUX CHEZ LES MAMMIFÈRES 124

3 UNE VOIE DE SIGNALISATION, DEUX SEXES, DE NOMBREUX EFFETS 125

3.1 CONTRÔLE VOMÉRONASAL DÉPENDANT DE L'EXPÉRIENCE SUR LES COMPORTEMENTS SEXUELS 126
3.2 RÉGULATION CONTEXTUELLE DES COMPORTEMENTS AGRESSIFS 128
3.3 LA TRANSITION VERS LA PARENTALITÉ 129
3.3.1 Gαi2 et le passage à la paternité 129
3.3.1 Gαi2 et le passage à la maternité 131

CONCLUSION GÉNÉRALE 132

BIBLIOGRAPHIE 132

Liste d'abbréviations

2-PT: 2-propylthietane
ACIII: adenylyl cyclase III
ANO1/2: anoctamin channel 1/2
AOB: accessory olfactory bulb
AON: anterior olfactory nucleus
AOS: accessory olfactory system
AR: androgen receptor
Aro: aromatase
ATP: adenosine triphosphate
AVPV: anteroventral periventricular nucleus
BNSTp: posterior bed nucleus of the stria terminalis
Ca^{2+}: calcium cation
cAMP: cyclic adenosine-3', 5' monophosphate
$cG\alpha_o^{-/-}$ conditional $G\alpha_o$ KO
$cG\alpha_{i2}^{-/-}$ conditional $G\alpha_{i2}$ KO
cGMP: cyclic guanosine-3', 5' monophosphate
CNG: cyclic nucleotide-gated channel
CNGA2/A3/A4/B1: cyclic nucleotide-gated channel subunit A2/A3/A4/B1
CoA: cortical amygdala posterolateral/posteromedial
DAG: diacylglycerol
ECx: entorhinal cortex
ERα: estrogen receptor alpha
ESP: exocrine secreted protein
FPR: formyl peptide receptor
Fpr-rs1/2/3/4/6/7: formyl peptide receptor related sequence 1/2/3/4/6/7
GABA: gamma aminobutyric acid
GC-D/G: guanylyl-cylcase D/G
GCL: granule cell layer
GDP: guanosine diphosphate
GG: Grüneberg ganglion
GL: glomerular layer
GnRH: gonadotropin-releasing hormone
GPCR: G-protein coupled receptor
GTP: guanosine triphosphate
Gucy1B2: guanylyl cyclase 1B2
$G\alpha_{i2}$: G protein alpha i2 subunit
$G\alpha_o$: G protein alpha o subunit
$G\alpha_{olf}$: G protein alpha olfactory subunit
Gβ/γ: G protein beta/gamma
H2-Mv: major histocompatibility complex molecule
HPA: hypothalamo-pituitary-adrenal
HPG: hypothalamo-pituitary-gonadal
IP_3: inositol-1,4,5-trisphophate
Kiss: kisspeptine
KO: knock-out
LPS: lipopolysaccharides
MC: mitral cell
MCH-Ib: major histocompatibility complex Ib
MCL: mitral cell layer
MeApv/pd: medial amygdala posterodorsal/posteroventral
MOB: main olfactory bulb
MOE: main olfactory epithelium
MOR256-3: mouse olfactory receptor 256-3
MOS: main olfactory system
MPOA: medial preoptic area
MUP: major urinary protein
OB: olfactory bulb
OR: olfactory receptor
OS: olfactory system
OSN: olfactory sensory neuron
OT: olfactory tubercle
Oxt: oxytocin
PAG: periaqueductal grey area
PDE1C/4A: phosphodiesterase 1C/4A
PEA: 2-phenylethylamine
PiCx: piriform cortex
PIP_2: phosphatidylinositol-4,5-bisphosphate
PLCβ2: phospholipase isoform beta 2
PMv: ventral premammillary nucleus
PR: progesterone receptor
SBT: 2-sec-butyl-4,5-dihydrothiazole
SF1: steroidogenic factor 1
SO: septal organ
TAAR: trace amine-associated receptor
TC: tufted cell
TH: tyrosine hydroxylase
TLR-4: Toll-like receptor 4
TMT: 2,5-dihydro-2,4,5-trimethylthiazole
TRP: transient receptor potential
$Trpc2^{-/-}$: TRPC2 KO
TRPC2/6: transient receptor potential channel subfamily C member 2/6
TRPM4/5: transient receptor potential channel subfamily M member 4/5
USVs: ultrasonic vocalizations
V2R2: vomeronasal receptor type 2 family-C
VMHdm/vl: ventromedial hypothalamic nucleus dorsomedial/ventrolateral
VNE: vomeronasal sensory epithelium
VNO vomeronasal organ
VNOx: vomeronasal surgical ablation
VR1/2: vomeronasal receptor type I/II
VSN: vomeronasal sensory neuron

Liste des Figures et Tables

Figure 1: Schematic organization of social interactions. 1

Figure 2: The olfactory system. 3

Figure 3: The main olfactory epithelium. 5

Figure 4: The canonical-OSNs pathway. 7

Figure 5: GC-D-expressing OSNs. 9

Figure 6: Trpc2-expressing OSNs. 10

Figure 7: organization of the main olfactory bulb. 11

Figure 8: The septal organ of Masera. 13

Figure 9: The Grüneberg ganglion. 14

Figure 10: Histology of the vomeronasal organ. 16

Figure 11: Organization of the vomeronasal epithelium and markers associated with VSNs population. 17

Figure 12: Basal VSNs. 20

Figure 13: Vomeronasal signaling pathway. 21

Figure 14: The accessory olfactory bulb. 23

Figure 15: Male sexual behavior sequence. 31

Figure 16: Aggressive behavior sequence. 35

Figure 17: Mechanism of neural sensory processing and integration to socio-behavioral decisions. 43

Figure 18: Neural structures involved in olfactory processing and behavioral responses. 45

Figure 19: Male sexual behavior neural circuit. 48

Figure 20: Female sexual behavior neural circuit. 49

Figure 21: Aggression neural circuit. 50

Figure 22: Disynaptic communication between the MeA and VMH. 51

Figure 23: Parenting neural circuit. 52

Figure 24: Predator avoidance neural circuit. 54

Figure 25: Expression of marker proteins in the VNO of $cG\alpha_{i2}^{+/-}$ and $cG\alpha_{i2}^{-/-}$ mice 64

Figure 26: Essential role of $G\alpha_{i2}$ in molecular sensing by apical VSNs 65

Figure 27: Loss of $G\alpha_{i2}$ enhances territorial aggression and increases activity in aggression-controlling brain centers 67

Figure 28: $cG\alpha_{i2}^{-/-}$ male mice show diminished infant-directed aggression but enhanced parental behavior 68

Figure 29: Relative to figure 25. Olfactory system organization and function in $cG\alpha_{i2}^{-/-}$ mice 76

Figure 30: Relative to figure 26. $G\alpha_{i2}$ role and molecular sensing 78

Figure 31: Normal sexual behavior and partner preference in $cG\alpha_{i2}^{-/-}$ males 81

Figure 32: Relative to figure 27 83

Figure 33: Relative to figure 28 85

Figure 34: Pup retrieval is altered in virgin $cG\alpha_{i2}^{-/-}$ females 97

Figure 35: Loss of $G\alpha_{i2}$ does not affect maternal behavior in lactating females 98

Figure 36: Incomplete sexual receptivity in $G\alpha_{i2}$ mutant females 99

Figure 37: Reduced neural activity in the AOB and RP3V of $G\alpha_{i2}$ mutant females 100

Figure 38: Model for the proposed control of pup retrieval and lordosis behaviors depending on social experience 102

Figure 39: Preparation of predator samples. 109
Figure 40: Predator avoidance in cG$\alpha_{i2}^{-/-}$ animals. 112
Figure 41: Sick-conspecific avoidance in cG$a_{i2}^{-/-}$ animals. 113
Figure 42: VNO and AOB activation after owl and LPS-urine exposures. 114
Figure 43: Specific reduction of VSNs activation by owl odors in the absence of Gα_{i2}. 116
Figure 44: Gα_{i2} deletion reduces VSNs responsiveness to sick and healthy LMW urine fractions. 117
Figure 45: Sexually dimorphic control of sociosexual behaviors by Gα_{i2}-expressing VSNs. 126
Figure 46: Proposed model of the vomeronasal control of female sexual receptivity. 127
Figure 47: Proposed model for the transition to infanticidal to paternal behaviors in male mouse. 131
Figure 48: Proposed model of the olfactory control of innate behaviors. 138

Table 1: Vomeronasal ligands, their receptors. 25
Table 2: Surgical VNO removal and genetic mutation effects on sexual behaviors. 28
Table 3: Antibodies used 87
Table 4: Primer sequences 88
Table 5: cG$\alpha_{i2}^{-/-}$ females show normal reproductive physiology 101

Introduction

Les comportements sociaux constituent l'épine dorsale de toute société. Les individus d'une espèce interagissent pour assurer leur survie et celle de leurs congénères. Agonistiques ou antagonistes, les comportements sociaux sont innés, c'est-à-dire qu'ils sont produits sans apprentissage et consistent en des séquences stéréotypées. Des années d'évolution ont ancré les comportements sociaux en raison de leur contribution à la perpétuation de la vie, et on les retrouve chez la plupart des espèces vivantes. Les interactions sociales résultent de l'intégration de trois composantes : les multiples modalités sensorielles émises par les protagonistes, les informations sur l'état interne et les indices environnementaux/contextuels (figure 1). L'interprétation correcte de cet équilibre délicat permet à un individu d'afficher une réponse comportementale adaptée à chaque situation. Une déficience des systèmes d'interprétation des informations sensorielles conduit à une expression inadéquate des comportements sociaux, compromettant ainsi les chances de survie de l'individu.

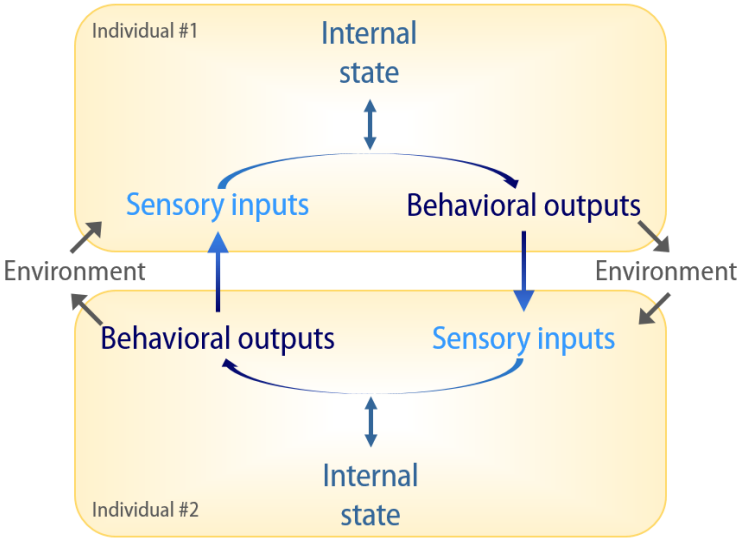

Figure 1 : Organisation schématique des interactions sociales. Les informations sensorielles d'un individu et de l'environnement sont détectées par un autre individu, interprétées en fonction de son état interne, et transformées en réaction comportementale. Ensuite, ce comportement et l'environnement sont perçus comme des informations sensorielles par le deuxième individu. Figure adaptée de Chen et Hong, 2018.

Chez de nombreux animaux, les indices olfactifs prédominent parmi les informations sensorielles émises et reçues. Une odeur est un mélange complexe d'odorants monomoléculaires transportés en panache. Parmi les odorants, les phéromones jouent un rôle particulier dans la régulation des comportements sociaux. P. Karlson et M. Lüscher ont défini le terme phéromone comme "*des substances qui sont sécrétées vers l'extérieur par un individu et reçues par un second individu de la même espèce, chez qui elles déclenchent une réaction spécifique, par exemple, un comportement défini ou un processus physiologique*" (Karlson et Lüscher, 1959). Depuis lors, la frontière entre phéromone et odorant est devenue floue (Wyatt, 2017). Une phéromone peut agir en tant que telle chez une espèce mais être reçue comme un simple odorant chez une autre, et vice-versa. De plus, une phéromone n'est

pas nécessairement odorante ou volatile. À titre anecdotique, à la fin du XIXe siècle, le physiologiste E. Aronsohn a courageusement rempli ses narines de différents odorants dilués, tels que le camphre ou la vanilline, prouvant ainsi que les odeurs pouvaient être liquides (Keller, 2007). Une définition optimale est encore nécessaire, et aucun consensus n'est établi. Plus largement, une phéromone pourrait être définie comme une molécule utilisée pour la communication et qui transporte des informations sur l'individu (par exemple, l'espèce, le sexe et l'âge) même si elle ne provoque pas de manière évidente un changement comportemental ou physiologique. Tout au long de ce manuscrit, les termes phéromone, chimiosignal et odorant seront utilisés indifféremment pour évoquer les odeurs sociales.

L'étude du contrôle olfactif des comportements sociaux innés est un outil puissant pour déchiffrer les circuits cérébraux qui sous-tendent ces comportements. Le système olfactif présente une grande diversité moléculaire, ce qui nous permet de moduler des cibles spécifiques et de déchiffrer les voies cérébrales spécifiques associées à cette cible. En outre, il permet de mieux comprendre comment le cerveau intègre les informations pour assurer des réactions appropriées. Par rapport à d'autres systèmes sensoriels, le traitement de l'information olfactive n'est pas hiérarchisé. Le codage se fait probablement au niveau du système olfactif, puis l'information est intégrée et contextualisée dans les régions cérébrales supérieures. Les circuits olfactifs sont très rationalisés, utilisant quelques connexions synaptiques pour convertir les entrées sensorielles en sorties comportementales. Parmi les systèmes olfactifs, l'organe voméronasal (VNO) joue un rôle central dans la détection des odeurs sociales. Les études sur le contrôle voméronasal des comportements sociaux ont permis des avancées majeures dans la compréhension du contrôle olfactif et du traitement neuronal des comportements sociaux (Chamero et al., 2012; Wyatt, 2013). Cependant, des questions demeurent :

i- Comment les chimiosignaux sont perçus par le VNO et transformés en influx nerveux;
ii- Quels signaux chimiques contrôlent les différents comportements socio-sexuels ?
iii- Comment les signaux chimiques sont intégrés dans les circuits cérébraux soutenant les comportements socio-sexuels.

Ici, je vais d'abord faire le point sur les connaissances actuelles concernant l'organisation du système olfactif chez les rongeurs (mon modèle d'étude), en me concentrant sur les aspects moléculaires des différents organes sensoriels et de leurs ligands. Je décrirai ensuite les comportements induits par l'olfaction et leur contrôle par des odorants spécifiques et les voies moléculaires voméronasales. Dans la dernière partie de cette introduction, je décrirai les voies cérébrales soutenant les comportements socio-sexuels innés et leur régulation par le système voméronasal.

1 Le système olfactif

Qu'est-ce qu'une odeur ? En 1963, J. Amoore exposa sa théorie des récepteurs stéréospécifiques, affirmant que l'odeur perçue d'un produit chimique dépend de sa structure qui est reconnue par un récepteur adapté (Amoore, 1963). L'existence d'une pléthore d'odorants implique donc autant de récepteurs qui leur correspondent. La théorie d'Amoore a été confirmée par la découverte de centaines de récepteurs dans le système olfactif des mammifères. Il a également émis l'hypothèse que des odeurs complexes (comme celle de l'amande, qui a des composantes camphrées, florales et mentholées) peuvent résulter de substances chimiques dont la structure correspond à plusieurs récepteurs. En effet, selon lui, une structure caractéristique confère une odeur. Cela suggère également qu'un récepteur peut détecter des molécules apparentées. Bien qu'il ait clairement conçu l'existence de récepteurs spécifiques dans le système olfactif, sa conception d'une odeur était erronée. La combinaison de plusieurs substances chimiques activant plusieurs récepteurs constitue, en fait, ce que nous appelons une odeur. Nous savons maintenant qu'un composé chimique peut se lier à différents récepteurs, et qu'un récepteur accepte différents ligands, ce qui permet une myriade de combinaisons (Malnic et al., 1999).

La détection et la reconnaissance des substances odorantes nécessitent un odorat très performant. Chez la plupart des mammifères, le système olfactif (OS) comprend des millions de neurones répartis dans des organes sensoriels anatomiquement et fonctionnellement distincts dans la cavité nasale. Comme ils sont en contact étroit avec le monde extérieur et subissent ses agressions, les neurones olfactifs se renouvellent en permanence à partir de cellules progénitrices, ce qui en fait une classe particulière de neurones (Brann et Firestein, 2014). Chaque organe sensoriel diffère des autres par ses mécanismes de transduction du signal, les indices chimiosensoriels qu'il détecte et sa projection axonale vers le cerveau (Munger et al., 2009). Sur la base de ces critères, quatre organes sensoriels sont classiquement décrits chez les rongeurs : l'épithélium olfactif principal (MOE), l'organe voméronasal (VNO), l'organe septal (SO) et le ganglion de Grüneberg (GG) (Figure 2).

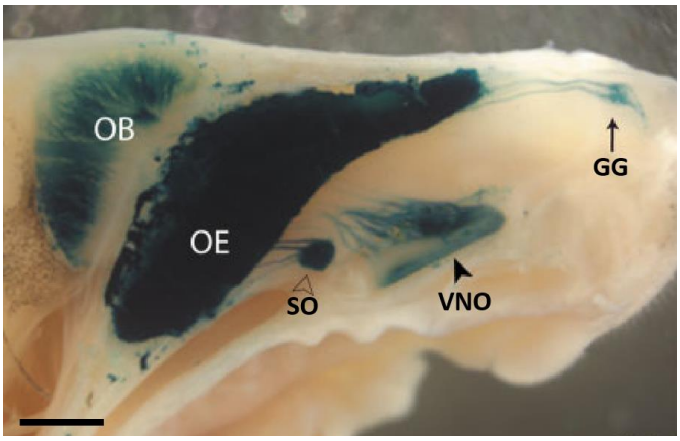

Figure 2 : Le système olfactif. Vue globale de la cavité nasale d'une souris transgénique OMP:tau-LacZ âgée de 7,5 jours. Les neurones olfactifs sont mis en évidence par la coloration LacZ. GG : ganglion de Grüneberg ; OE : épithélium olfactif ; OB : bulbe olfactif ; SO : organe septal ; VNO : organe voméronasal. Barre d'échelle, 500µm. Figure adaptée de Storan et Key, 2006.

Les neurones olfactifs détectent les odorants grâce à des récepteurs spécialisés et obéissent en grande partie à la règle "un neurone - un récepteur" (Serizawa et al., 2004). Ainsi, à chaque respiration, l'environnement est échantillonné et les récepteurs sont activés. Les neurones olfactifs projettent leurs longs axones à travers la cavité nasale pour atteindre leur premier relais cérébral, le bulbe olfactif (OB). Ensuite, l'information est diffusée vers des zones cérébrales interconnectées où elle est intégrée pour produire une réponse adaptée. Le processus de codage des informations olfactives pourrait être considéré comme la lecture en temps réel par l'OB et le cerveau de la carte des neurones olfactifs activés (Wachowiak et Shipley, 2006). Ce processus n'est pas encore clairement établi.

Si la fonction moléculaire de l'épithélium olfactif principal commence à être mieux documentée, les autres organes olfactifs sont moins bien compris. Certains marqueurs et ligands ont été décrits, mais une grande partie de leur fonction reste obscure. Cette première section présentera au lecteur la fonction cellulaire et moléculaire des sous-systèmes olfactifs, une condition préalable pour comprendre comment l'olfaction régule les comportements socio-sexuels.

1.1 Le système olfactif principal

En reniflant, les animaux recueillent les odeurs de leur environnement, les analysent, déterminent celles qui sont pertinentes et agissent en conséquence. Le système olfactif principal (MOS) pourrait être considéré comme un détecteur de fréquences à bande ultra-large. En effet, il détecte la plupart des odorants qui nous entourent et sa déficience entraîne une anosmie globale qui a de graves répercussions sur les comportements sociaux et non sociaux (Song et Leonard, 2005 ; Tirindelli et al., 2009). Chez l'homme, qui dépend principalement du MOS, les troubles olfactifs impactent la qualité de vie et sont fréquemment associés à des états dépressifs (Croy et al., 2014).

Le MOS se compose : *i- de* l'épithélium olfactif principal (MOE), où les odorants sont détectés ; *ii-* du bulbe olfactif principal (MOB), premier relais cérébral de l'information olfactive ; *iii-* des cortex olfactifs, qui reçoivent des informations directes ou indirectes du MOB (Munger et al., 2009). Le MOS est le plus ancien composant du système olfactif des vertébrés (Taniguchi et al., 2011). Façonné par des années d'évolution, il est hétérogène et présente des particularités sensorielles. Ici, je passerai en revue l'organisation du MOS chez les rongeurs.

1.1.1 L'épithélium olfactif principal

L'épithélium olfactif principal (MOE), organe sensoriel du MOS, est situé dans le toit de la partie postérieure de la cavité nasale et recouvre les cornets nasaux. Il naît de la placode olfactive vers le 9e jour embryonnaire chez la souris et présente les caractéristiques d'un tissu organisé au 13e jour embryonnaire (Cuschieri et Bannister, 1975). Le MOE adulte est un épithélium pseudostratifié composé, de bas en haut, de trois couches cellulaires : les cellules souches basales (cellules basales

horizontales et globulaires), les neurones sensoriels olfactifs (matures et immatures) et les cellules de soutien (cellules sustentaculaires) (Moulton et Beidler, 1967). Il comprend également des glandes qui sécrètent du mucus pour protéger les cellules et capturer les substances odorantes en suspension dans l'air (figure 3) (Moulton et Beidler, 1967).

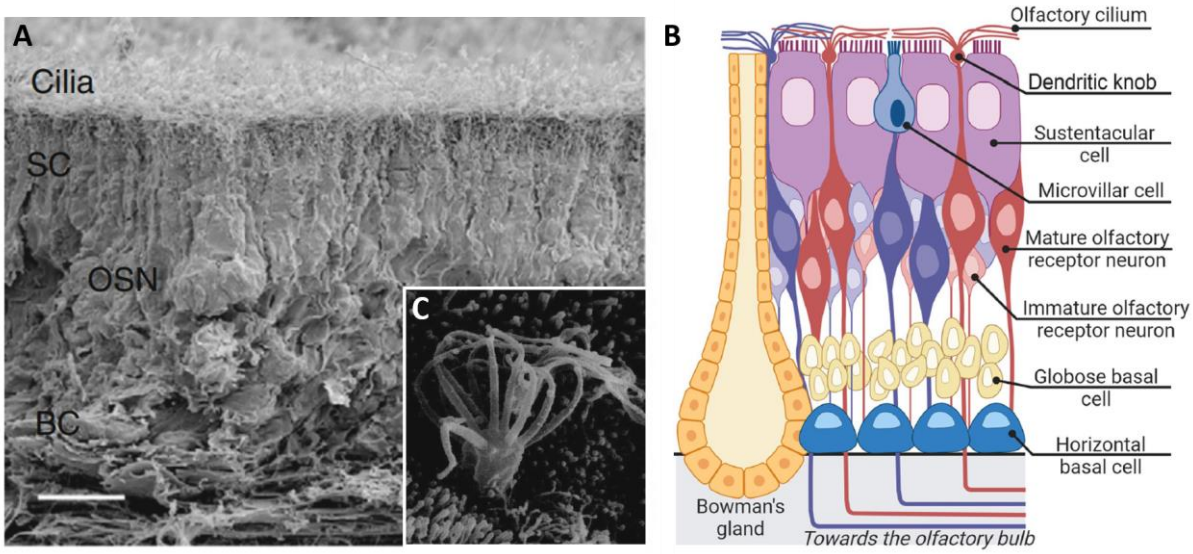

Figure 3 : L'épithélium olfactif principal. A) Micrographie électronique à balayage de la vue latérale d'un épithélium olfactif de souris décrivant les différentes couches cellulaires. Zoom 1030x ; barre d'échelle, 10 µm. BC : cellule basale ; OSN : neurone sensoriel olfactif ; SC : cellule sustentaculaire. D'après McEwen et al. 2008. B) Représentation schématique des couches cellulaires du MOE. D'après Dibattista et al. 2021. C) Micrographie électronique à balayage d'un bouton dendritique de l'OSN humain émergeant à la surface de la MOE. Zoom 18 525x. D'après Morrison et Costanzo, 1990.

Les neurones sensoriels olfactifs (OSN) sont bipolaires, avec une dendrite et un axone uniques. L'axone des OSN est non myélinisé ; il se fascicule avec d'autres pour former le nerf olfactif et atteindre le bulbe olfactif à travers la plaque criblée de l'os ethmoïde. La dendrite s'étend jusqu'à la surface de l'épithélium et forme un bouton terminal à partir duquel plusieurs cils s'étendent dans le mucus pour agrandir la surface réceptive (Figure 3) (Mendoza, 1993). La surface des cils est recouverte de récepteurs olfactifs (OR) qui fixent les substances odorantes. Elle contient également toutes les protéines nécessaires au déclenchement de la dépolarisation du neurone (Munger et al., 2009). Les OSNs forment des sous-populations distinctes à partir de leur machinerie interne et de leur localisation. Tout d'abord, en fonction de leur bagage moléculaire, les OSNs sont classés comme canoniques ou non canoniques (Munger et al., 2009). Une description détaillée de ces voies de signalisation est faite ci-après. Deuxièmement, une étude récente a montré que les OSNs exprimant un type d'OR ne sont pas dispersés au hasard dans la MOE (Zapiec et Mombaerts, 2020). Ils ont élégamment cartographié l'aire d'expression de plusieurs ORS et défini des zones de chevauchement, suggérant l'existence d'une distribution zonale des types d'OSNs, chacun d'entre eux étant restreint dans son choix de OR.

1.1.2 Les neurones sensoriels olfactifs canoniques

La grande majorité des OSNs du MOE partagent des caractéristiques communes et sont catégorisés comme OSNs classiques ou canoniques. Parmi les similitudes, les OSNs canoniques détectent l'odorant par des récepteurs spécialisés : les ORs. L. Buck et R. Axel ont découvert la nouvelle famille multigénique codant pour les ORs en 1991 (Buck et Axel, 1991) ; un travail récompensé par un prix Nobel en 2004 qui a fourni de nouvelles pistes sur la logique du traitement olfactif. Depuis, nous savons que les mammifères expriment jusqu'à 1500 gènes codant pour les ORs (Mombaerts, 2004). À ce jour, le répertoire des ORs de la souris comprend 1141 gènes codant pour des protéines et 342 pseudogènes (Barnes et al., 2020). Une vague de pseudogénisation s'est produite dans le répertoire des ORs des primates pour atteindre 50% des pseudogènes d'OR chez l'homme (Gilad et al., 2004). Ceci est cohérent avec une transition d'une perception sensorielle primaire basée sur l'olfaction vers une perception basée sur la vision.

Les ORs appartiennent à la superfamille des récepteurs couplés aux protéines G (GPCR), caractérisés par 7 segments transmembranaires (Buck et Axel, 1991). Leur nombre et leurs caractéristiques communes font des ORs une classe à part de GPCR. Les ORs présentent plusieurs petits motifs d'acides aminés conservés dans leurs segments transmembranaires, une caractéristique qui a servi à les mettre en évidence dans le génome (Zhang et Firestein, 2002). La liaison du ligand se fait dans la poche de liaison dédiée formée par les parties hydrophobes des segments transmembranaires (Katada et al., 2005). Une grande variabilité est trouvée dans ces régions (Buck et Axel, 1991), permettant un large spectre de repliement 3D, nécessaire pour s'adapter à la variété des ligands possibles. Il est intéressant de noter qu'une seule modification d'un acide aminé peut changer la spécificité d'un OR donné (Katada et al., 2005).

La voie de signalisation des OSNs canoniques est composée d'un élément variable, l'OR, qui active une machinerie moléculaire unique (Figure 4). En tant que GPCR, le principal effecteur de l'activation des ORs est la triade de sous-unités de la protéine Gα/β/γ. Les ORs utilisent une sous-unité Gα particulière appelée Gαolf (Belluscio et al., 1998 ; Jones et Reed, 1988). La liaison des ORs à leur ligand déclenche l'hydrolyse de la guanosine triphosphate (GTP) en guanosine diphosphate (GDP) par les protéines G, libérant ainsi Gαolf de la triade. Le Gαolf active alors l'adénylyl cyclase III (ACIII) sensible au calcium (Ca^{2+}), qui convertit l'adénosine triphosphate (ATP) en adénosine-3', 5' monophosphate (AMPc) cyclique (Bakalyar et Reed, 1990 ; Wong et al., 2000). L'augmentation de la concentration d'AMPc active un canal cationique par les nucléotides cycliques (CNG), permettant l'augmentation du Ca^{2+} intracellulaire et la dépolarisation du neurone (Brunet et al., 1996 ; Dhallan et al., 1990 ; Leinders-Zufall et al., 1997 ; Nakamura et Gold, 1987). Le CNG olfactif est tétramérique et résulte de l'association de 2 CNGA2 avec une sous-unité CNGA4 et une CNGB1 (Bönigk et al., 1999 ; Bradley et al., 1994 ; Dhallan et al., 1990 ; Liman et Buck, 1994). Le CNGA2 est nécessaire à la formation du canal et sa perte provoque une anosmie (Brunet et al., 1996). Les deux autres sous-unités

modulent la sensibilité du canal (Bradley et al., 1994 ; Liman et Buck, 1994 ; Lin et al., 2004 ; Michalakis et al., 2006 ; Munger et al., 2001).

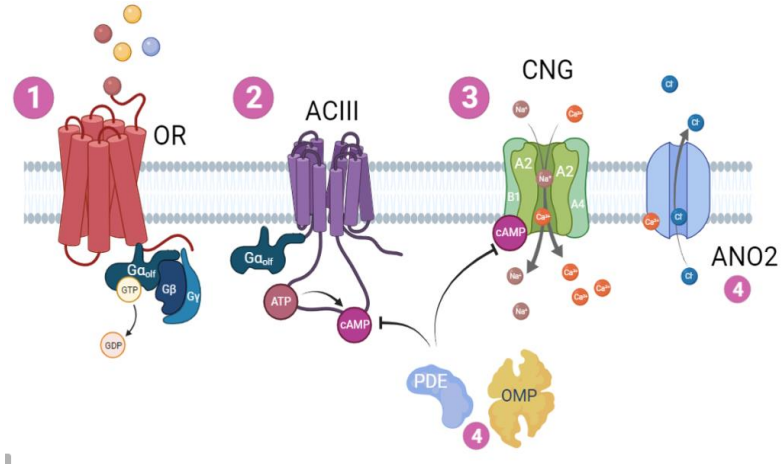

Figure 4 : La voie canonique-OSNs. ① Étape 1 : la liaison de l'odorant au récepteur olfactif (OR) active l'hydrolyse du GTP en GDP par le complexe protéique G. ② Étape 2 : le Gαolf active l'adénylyl cyclase III (ACIII), qui transforme à son tour l'ATP en AMPc. ③ Étape 3 : l'AMPc active le canal CNG, permettant l'entrée de Na+ et de Ca2+. ④ Étape 4 : plusieurs protéines intracellulaires modulent le signal. Le canal anoctamine 2 (ANO2) amplifie la dépolarisation par un courant Cl- ; les phosphodiestérases (PDE) régulent les niveaux d'AMPc ; l'action de la protéine marqueur olfactive (OMP) n'est pas clairement établie (voir pour revue Dibattista et al., 2021). Ce schéma est créé via BioRender.com.

Après cette cascade de signalisation primaire, d'autres effecteurs modulent le signal et régulent la concentration en Ca2+ pour rétablir le potentiel d'excitation du neurone. De nombreux acteurs ont été identifiés (voir pour revue Neuhaus, 2020). Dans le cadre de ce travail nous pouvons retenir, le canal activé par le Ca2+, l'anoctamine-2 (ANO2) qui amplifie le signal (Billig et al., 2011 ; Lowe et Gold, 1993 ; Stephan et al, 2009) ; les phosphodiestérases PDE1C et PDE4A qui hydrolysent l'AMPc (Cygnar et Zhao, 2009) ; la protéine marqueur olfactive (OMP), qui module la cinétique et la terminaison du signal (voir pour revue Dibattista et al., 2021) (Figure 4). L'OMP, comme son nom l'indique, est un marqueur constitutif des neurones olfactifs présent dans tous les organes sensoriels. Sa fonction précise reste largement inconnue, mais grâce à son expression quasi exclusive dans les neurones olfactifs, elle a été largement utilisée pour générer un ciblage génique restreint à l'olfaction chez les rongeurs (Li et al., 2004).

1.1.1 Les neurones sensoriels olfactifs non canoniques

Il a longtemps été admis que la voie de signalisation de l'AMPc était obligatoire pour la détection olfactive. D'autres voies ont été théorisées (Baker et al., 1999), et une étude sur un modèle de souris portant une délétion génétique de la sous-unité CNGA2 a révélé qu'une voie indépendante de l'AMPc transmettait la détection de certains odorants (Lin et al., 2004). Depuis lors, nous savons que

des OSNs utilisant différents types de récepteurs ou de protéines de transduction existent dans la MOE. Ils sont donc appelés OSNs non-canoniques. Ici, je vais présenter trois types d'OSNs non-canoniques dont la fonction est connue et pertinente pour ce travail.

1.1.1.1 OSNs exprimant des TAARs

Les récepteurs associés aux amines-traces (TAAR) constituent une famille distincte de GPCR exprimés dans divers tissus (Borowsky et al., 2001 ; Bunzow et al., 2001). Ils sont devenus intéressants pour le monde olfactif lorsqu'il a été démontré que 14 des 15 gènes TAAR de souris étaient exprimés dans le MOE (Liberles et Buck, 2006). Les OSNs exprimant les TAARs et les OSNs canoniques partagent de nombreuses similitudes. Les TAARs ne sont exprimés qu'un par un dans les OSNs matures (Pacifico et al., 2012) ; les OSNs exprimant un TAAR spécifique sont localisés dans une zone spatiale limitée et se projettent vers des glomérules dédiés dans le MOB (Pacifico et al., 2012) ; les OSNs exprimant des TAAR utilisent le même composant clé pour la transduction du signal (Liberles et Buck, 2006 ; Zhang et al., 2013).

Alors que les OSN canoniques détectent un large éventail de signaux chimiques, les OSNs exprimant les TAAR sont adaptés pour détection des amines biogènes (Liberles et Buck, 2006). Les amines biogènes résultent de la dégradation des acides aminés et sont donc enrichies dans certains fluides corporels comme l'urine. Les TAARs ne sont pas le seul capteur d'amines, mais ils règlent le seuil de sensibilité des OSNs aux amines (Dewan et al., 2018). Nous pouvons spéculer que leur capacité de détection fine pourrait être pertinente sur le plan évolutif, d'où le développement d'un système de détection parallèle.

1.1.1.2 OSNs exprimant la GC-D

Un sous-ensemble d'OSNs dispersés n'utilise pas l'AMPc pour soutenir la transduction du signal. Les récepteurs de la guanylyl-cyclase (GC) sont des récepteurs à un segment transmembranaire qui catalysent le GTP en GMPc lors de leur activation (Kuhn, 2016). Plusieurs GC sont exprimés dans divers tissus, mais l'expression de GC-D semble principalement limitée à la MOE (Figure 5) (Fülle et al., 1995). Les OSNs exprimant GC-D n’ont pas les composants clés de la cascade canonique de transduction de l'odeur des OSNs et utilisent à la place le canal CNGA3 et la phosphodiestérase PDE2 (Juilfs et al., 1997 ; Meyer et al., 2000). Une autre spécificité est leur schéma de projection dans le MOB. Les OSNs exprimant GC-D se projettent vers plusieurs glomérules en forme d'anneau interconnectés postérieurement, appelés glomérules en collier (Figure 5) (Juilfs et al., 1997).

Le GC-D est resté un récepteur orphelin pendant une décennie après sa découverte. Les peptides hormonaux guanyline et uroguanyline ont été les premiers ligands découverts (Leinders-Zufall et al., 2007). Ces peptides sont produits par le système digestif et sont naturellement présents

dans les fèces et les urines. Plus tard, Munger et ses collègues ont montré que les neurones GC-D répondent également au gaz CS2 dans le contexte de la préférence alimentaire et olfactive (Munger et al., 2010). Les souris peuvent transmettre la présence d'une source de nourriture sûre par leur haleine. La combinaison du CS2 avec l'odeur de nourriture dans l'haleine est détectée et apprise par un congénère, et, lorsqu'il est confronté à l'odeur de cette nourriture, il peut se souvenir de sa sécurité. Enfin, le GC-D peut répondre aux variations de CO2 autour des niveaux atmosphériques, ce qui pourrait constituer un avantage comportemental pour éviter les environnements dangereux (Hu et al., 2007).

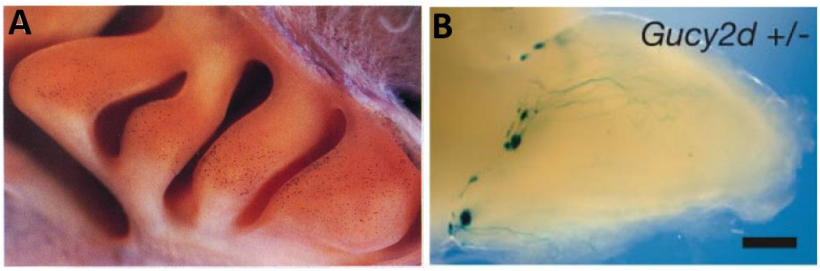

Figure 5 : OSNs exprimant le GC-D. A) Hybridation in situ de l'ARNm GC-D dans une MOE entière. D'après Fülle et al. 1995. B) Vue complète du bulbe olfactif d'une souris transgénique GC-D:LacZ. Les axones positifs GC-D, mis en évidence par la coloration LacZ, sont rassemblés dans les glomérules du collier. Barre d'échelle, 500µm. D'après Leinders-Zufall et al. 2007.

1.1.1.1 OSNs exprimant TRPC-2

Les canaux TRP (Transient Receptor Potential) sont impliqués dans une pléthore de fonctions cellulaires (Yildirim et Birnbaumer, 2007). TRPC2 est le principal canal cationique exprimé dans l'organe voméronasal (Liman et al., 1999) (voir section 1.4.2.3 pour une description détaillée) et on a longtemps pensé qu'il était restreint à cet organe sensoriel olfactif. En 2014, M. Omura et P. Mombaerts ont mis en évidence des cellules de la MOE exprimant TRPC2 et ont fourni une description détaillée de cette nouvelle population cellulaire (Omura et Mombaerts, 2014, 2015).

Sur la base d'autres marqueurs cellulaires, ils ont déterminé deux types de cellules (Figure 6) : Les cellules de type A expriment CNGA2 et ACIII mais sont négatives pour Gucy1B2 (une autre guanylyl cyclase) ; inversement, les cellules de type B expriment CNGA2 et Gucy1b2 mais sont négatives pour ACIII. La fonction des cellules de type A reste inconnue, mais elles expriment certains ORs et ACIII, ce qui suggère une fonction similaire à celle des OSNs canoniques (Omura et Mombaerts, 2014). Les cellules de type B sont des capteurs des gazes O2 et H2S (Bleymehl et al., 2016 ; Koike et al., 2021). Il est intéressant de noter que dans les cellules de type B, chaque canal cationique (CNGA2 et TRPC2) est dédié à un gaz, et que la détection a lieu dans des compartiments subcellulaires distincts (Figure 6) (Koike et al., 2021).

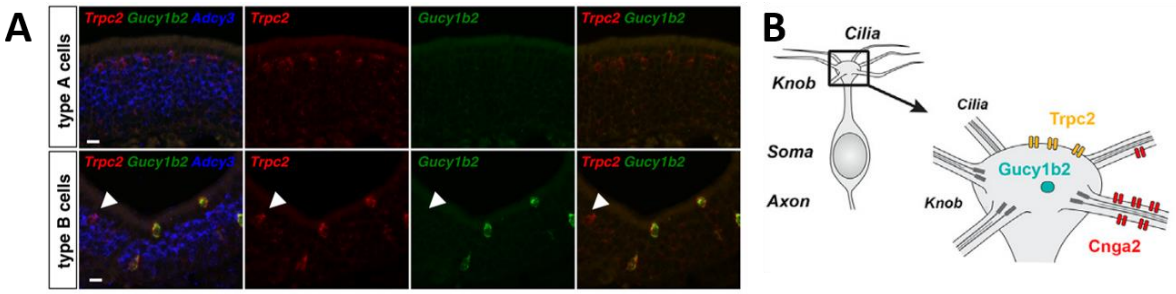

Les cellules de type A sont positives pour Adcy3 (adenylyl cyclase III) mais pas pour Gucy1b2 (guanylyl cyclase 1b2), inversement pour les cellules de type 2. La pointe de flèche représente une cellule de type A dans la région des cellules de type B. Barre d'échelle, 10 µm. D'après Omura et Mombaerts, 2015. B) Représentation schématique de l'expression compartimentée de Trpc2, Cnga2 et Gucy1b2 dans le bouton et les cils des OSNs. D'après Koike et al. 2021.

1.1.1 Le bulbe olfactif principal

Les axones des OSNs atteignent le bulbe olfactif (OB) pour former leur premier relais dans le système nerveux central. Le bulbe olfactif principal (MOB) est une subdivision de l'OB qui reçoit spécifiquement les entrées du MOE. Le MOB est une structure laminée en forme de haricot dont les couches forment des cercles concentriques (figure 7). Les glomérules sont dépourvus de corps cellulaires mais contiennent l'une des plus fortes densités de synapses. À l'intérieur des glomérules, les axones des OSNs entrent en contact avec les dendrites des cellules mitrales et en panache (MCs et TCs) (Figure 7) (Pinching et Powell, 1971) par une synapse glutamatergique (Sassoè-Pognetto et al., 1993). Les MCs et TCs activées projettent ensuite vers les cortex olfactifs (Figure 7) (Haberly et Price, 1977). Des mécanismes de régulation intrinsèques impliquant d'autres types de cellules existent au sein du MOB (voir pour revue Ennis et Holy, 2015). Notamment, un type de synapse peu commun existe au sein du MOB, la synapse dendrodendritique (Figure 7). Elle implique les cellules granuleuses, un type particulier d'interneurone sans axone dont les dendrites entrent en contact avec les dendrites des MCs et des TCs. Cette interaction est réciproque et on pense qu'elle module plusieurs aspects du signal olfactif, tels que la synchronisation ou la spécificité (voir pour revue Shepherd et al., 2020).

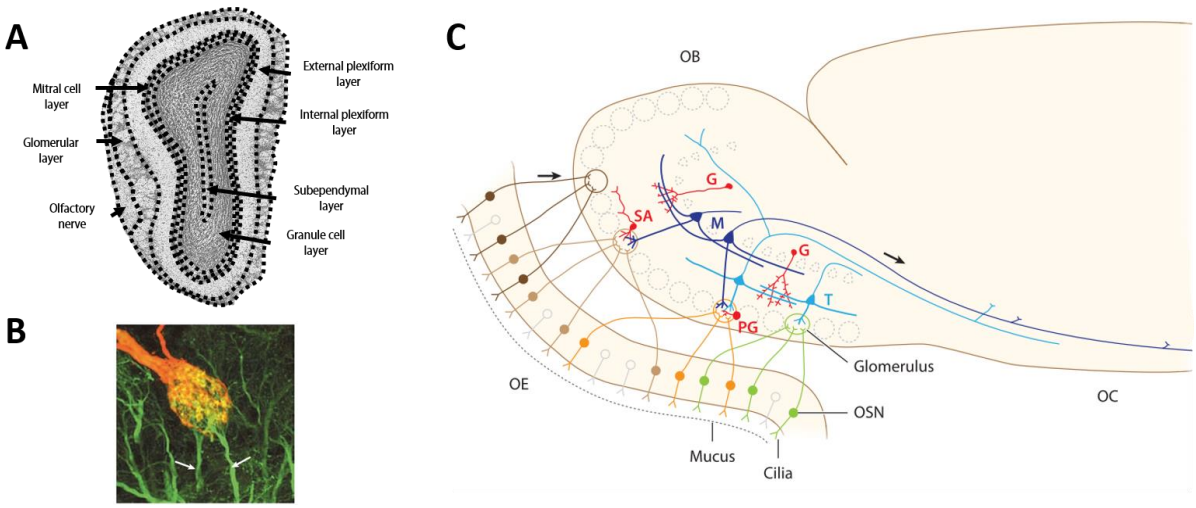

Figure 7 : organisation du bulbe olfactif principal. A) Une coupe coronale colorée au Nissl d'un bulbe olfactif de souris montre son organisation laminaire. Chaque couche est étiquetée. L'image provient du Paxinos Mouse Brain Atlas. B) Micrographie fluorescente montrant les axones des OSNs (rouge) formant un glomérule. Les dendrites des cellules mitrales (vert) contactent les axones des OSNs à l'intérieur du glomérule. D'après Belluscio et al. 2002. C) Organisation cellulaire schématique du MOB. Les OSNs exprimant un OR similaire projettent dans le même glomérule. À l'intérieur du glomérule, les cellules mitrales (M) et les cellules en panache (T), les cellules périglomérulaires (PG) et les cellules à axone court (SA) contactent les axones des OSNs. Les cellules granuleuses (G) forment des synapses dendrodendritiques avec les cellules M et T. Les cellules M et T projettent dans les cortex olfactifs (OC). D'après Uchida et al. 2014.

Les OSNs ne se projettent pas aléatoirement dans les glomérules. Comme les cartes des OSNs dans la MOE, il existe des cartes des glomérules dans le MOB. Un OSN se projette vers un ou deux glomérules, et un glomérule ne reçoit des entrées que des OSNs exprimant le même OR (Ressler et al., 1994 ; Vassar et al., 1994). Il est intéressant de noter que certains glomérules accordés pour un OR donné sont en miroir, l'un étant situé sur le côté médial du M'OB et l'autre latéralement opposé (Ressler et al., 1994 ; Vassar et al., 1994). Ces deux glomérules isofonctionnels sont interconnectés (Belluscio et al., 2002), mais l'impact de cette connexion sur le décodage des odeurs reste inconnu. Plusieurs mécanismes assurent un ciblage correct des OSNs vers les glomérules. La présence de l'OR est obligatoire. En effet, la mutation ou la délétion d'un OR entraîne un déplacement de l'axone (Wang et al., 1998). L'identité de l'OR, et donc sa place au sein du MOE, contraint la zone de projection dorso-ventrale (Takeuchi et al., 2010). La signalisation AMPc est également un élément clé du ciblage axonal. La modulation des niveaux d'AMPc dans les OSNs déplace les sites de projection axonale le long de l'axe antéro-postérieur du MOB en modifiant l'expression des molécules de guidage axonal (Imai et al., 2006 ; Nakashima et al., 2013).

L'information olfactive va directement du bulbe aux cortex olfactifs, sans relais thalamique, soulignant la place particulière de l'information olfactive parmi les autres entrées sensorielles. Le MOB innerve directement le cortex piriforme, le tubercule olfactif, le noyau olfactif antérieur, l'amygdale corticale et le cortex entorhinal (Tirindelli et al., 2009). La plupart de ces régions corticales projettent aussi en retour vers le bulbe olfactif principal (Brunert et Rothermel, 2021) et d'autres zones du

cerveau, notamment le thalamus, l'hypothalamus, l'hippocampe et le système limbique (Tirindelli et al., 2009).

1.2 L'organe septal de Masera

L'organe septal (SO) est un petit épithélium situé près de la base du septum nasal (figures 2 et 8) (Rodolfo-Masera, 1943). La grande majorité des neurones du SO expriment des ORs, des protéines de la voie canonique-OSNs, sont OMP-positifs et se projettent vers le MOB (Ma et al., 2003 ; Tian et Ma, 2004). Il est intéressant de noter que 50 % des neurones expriment le même OR, le MOR256-3 (figure 8), un OR à large spectre, et que l'on ne trouve qu'environ 80 ORs différents dans le SO (Tian et Ma, 2004). Quelques cellules expriment néanmoins le récepteur GC-D et projettent vers les glomérules du collier (Figure 8) (Ma et al., 2003 ; Walz et al., 2007).

L'organisation de l'épithélium du SO se superpose à celle du MOE, ce qui suggère une fonction redondante dans le système olfactif. Une étude a rapporté que les neurones du SO sont des capteurs mécaniques, en plus d'être des capteurs d'odeurs (Grosmaitre et al., 2007). Ils ont proposé deux hypothèses intéressantes à cette nouvelle fonction. Premièrement, pendant un reniflement intense, l'augmentation de la pression du flux d'air active les mécanorécepteurs en plus des ORs. Cela pourrait augmenter la probabilité qu'un neurone se déclenche en réponse à une faible stimulation olfactive. En se basant sur le peu d'ORs exprimés dans le SO, nous pouvons spéculer que ceux-ci pourraient détecter des signaux éthologiquement pertinents, augmentant ainsi la sensibilité du système olfactif à ces odorants. Deuxièmement, le couplage de la mécanosensibilité avec la sensibilité olfactive peut synchroniser la respiration et la détection des odeurs pour faciliter le codage des odeurs au niveau du MOB.

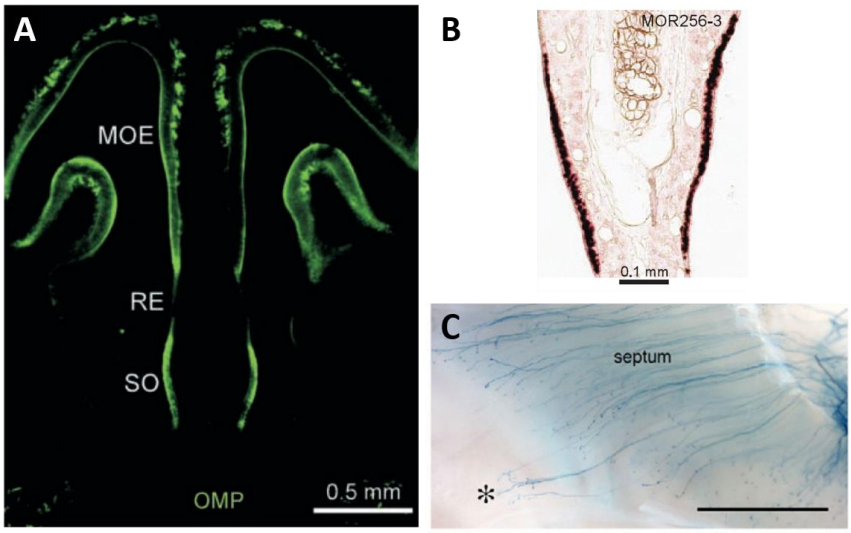

Figure 8 : L'organe septal de Masera. A) Visualisation de la protéine marqueur olfactive (OMP) sur une coupe sagittale d'un museau de souris. L'organe septal (SO) est séparé de l'épithélium olfactif principal (MOE) par l'épithélium respiratoire (RE). D'après Ma et al. 2003. B) L'hybridation in situ pour MOR256-3 montre une forte expression à travers le SO. D'après Tian et Ma, 2004. C) Vue globale de la zone septale d'une souris transgénique GC-D:tau-LacZ. Les axones positifs GC-D sont mis en évidence par la coloration LacZ, et l'astérisque indique les axones émergeant de l'organe septal. Barre d'échelle, 40 µm. D'après Walz et al. 2007.

1.3 Le ganglion de Grüneberg

En 1973, H. Grüneberg a décrit un groupe de cellules résidant dans la région la plus rostrale de la cavité nasale de la souris (figures 2 et 9) (Grüneberg, 1973). Plusieurs années plus tard, plusieurs laboratoires l'ont classé parmi les organes sensoriels olfactifs et l'ont nommé ganglion de Grüneberg (GG) (Fleischer et al., 2006 ; Fuss et al., 2005 ; Koos et Fraser, 2005 ; Roppolo et al., 2006 ; Storan et Key, 2006). Le GG n'est pas un épithélium. Il comprend plutôt des cellules non neuronales et des cellules neuronales OMP-positives, recouvertes d'une enveloppe kératinisée (Figure 9) (Brechbühl et al., 2008).

Les neurones GG utilisent une voie de signalisation dépendante du GMPc au lieu de la voie classique dépendante de l'AMPc des OSN canoniques. Ils utilisent la guanylyl-cyclase GC-G et la sous-unité de canal CNGA3 pour détecter plusieurs types de signaux chimiques (figure 9) (Mamasuew et al., 2011). Comme les OSNs exprimant la GC-D, les neurones GG se projettent vers plusieurs glomérules postérieurs interconnectés (figure 9) (Fuss et al., 2005 ; Koos et Fraser, 2005). D'autres récepteurs ont été décrits, certains coexprimés avec le GC-G, ce qui est un scénario inhabituel dans le système olfactif (Figure 9) (voir pour revue Fleischer, 2021).

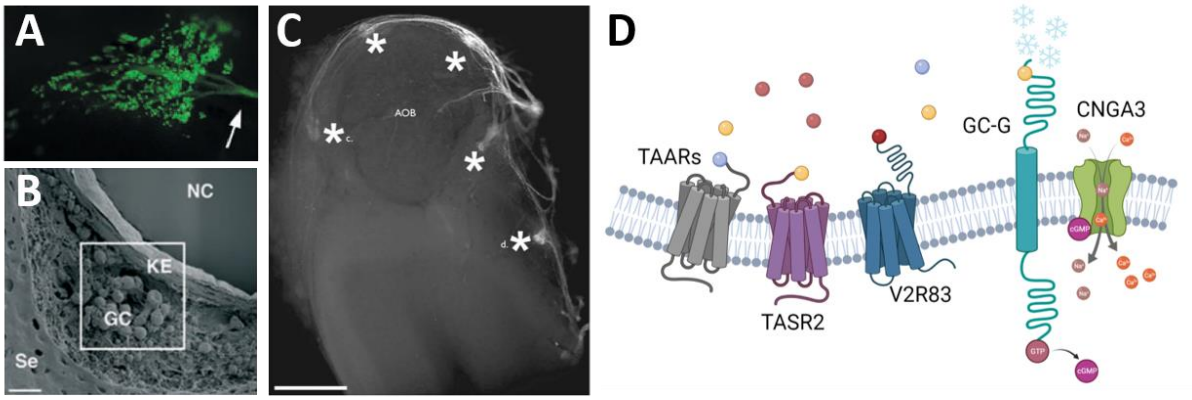

Figure 9 : Le ganglion de Grüneberg. A) La vue du ganglion de Grüneberg d'une souris OMP-GFP met en évidence les neurones du GG. La flèche indique les axones des neurones du GG qui fasciculent pour former un seul nerf. D'après Fuss et al. 2005. B) Micrographie électronique à balayage d'une section coronale de GG. Barre d'échelle, 20 µm. GC : cellules GG ; KE : épithélium kératinisé ; NC : cavité nasale ; Se : septum. D'après Brechbühl et al. 2008. C) Traçage antérograde des neurones du GG vers l'OB postérieur d'une souris âgée de 7 jours. Les astérisques indiquent les glomérules innervés par le GG. Barre d'échelle 500 µm. D'après Koos et Fraser, 2005. D) Voies de signalisation dans les neurones du GG. Les neurones du GG expriment le récepteur GC-G qui active le CNGA3 en hydrolysant le GTP en GMPc. D'autres récepteurs, comme les TAAR, TASR2 ou V2R83, sont exprimés dans les neurones du GG. Le froid (symbolisé par les flocons de neige) peut également activer les neurones du GG, très probablement par le biais du GC-G. Ce schéma est créé sur BioRender.com.

Le GG est un organe sensoriel double. D'un côté, il détecte les phéromones d'alarme et les kairomones des prédateurs (Brechbühl et al., 2008, 2013 ; Chao et al., 2018 ; Mamasuew et al., 2011 ; Pérez-Gómez et al., 2015), qui sont également détectées par la MOE et la VNO. Ensuite, il a été proposé que le GG ne participe pas à la discrimination de ces odorants mais envoient plutôt le signal d'alarme *per se* pour induire des réponses comportementales et physiologiques adéquates (par exemple, la sécrétion de cortisol) (Fleischer, 2021). D'autre part, le froid active les neurones GG, en particulier chez les nouveau-nés qui sont très sensibles aux températures froides (Mamasuew et al., 2008 ; Schmid et al., 2010). Il est intéressant de noter que ces deux fonctions sont entremêlées. La chaleur réduit la réactivité des neurones du GG aux odorants (Bumbalo et al., 2017). Ce phénomène pourrait être pertinent sur le plan éthologique. Les rongeurs sont des animaux nocturnes. Ils explorent leur environnement pendant la période la plus froide pour trouver de la nourriture et se reposent au chaud pour dormir pendant la journée. Avoir une plus grande sensibilité au danger uniquement en cas de besoin pourrait être avantageux pour cette espèce (Fleischer, 2021).

1.4 Le système olfactif accessoire

Outre le MOS, de nombreux mammifères possèdent un système secondaire, le système olfactif accessoire (AOS), dédié à la communication socio-sexuelle (Munger et al., 2009). L'AOS a longtemps été associé à la détection de phéromones non volatiles, tandis que le MOS était associé aux substances odorantes volatiles dans l'environnement. Cette stricte ségrégation fonctionnelle n'est plus valable. Nous savons maintenant que les deux systèmes peuvent détecter des substances chimiques volatiles et

non volatiles et que la nature phéromonale des odorants ne se limite pas à la définition initiale des phéromones faite par Karlson et Lüscher (Brennan et Zufall, 2006). Malgré ce chevauchement de sensibilité, le rôle principal de l'AOS dans la communication chimique est bien établi. En effet, l'altération de l'AOS impacte gravement l'expression de comportements socio-sexuels innés (Mohrhardt et al., 2018).

L'AOS comprend : *i*- l'organe voméronasal (VNO), où sont détectés les odorants ; *ii*- le bulbe olfactif accessoire (AOB), premier relais cérébral de l'information olfactive ; *iii*- l'amygdale voméronasale, qui reçoit des informations directes ou indirectes de l'AOB (Munger et al., 2009). L'organisation de l'AOS en tant que système indépendant s'est produite avec le développement du poumon respiratoire chez les amphibiens mais n'a pas persisté chez tous les taxons (Taniguchi et al., 2011). Parmi les mammifères, il existe une hétérogénéité dans l'expression des marqueurs moléculaires de l'AOS, et certains ne possèdent pas d'AOS fonctionnel, comme les primates supérieurs (y compris les humains), les cétacés et presque toutes les chauves-souris (Tirindelli, 2021). Je passerai ici en revue l'organisation de l'AOS chez les rongeurs.

1.4.1 L'organe voméronasal

En 1813, L. Jacobson a décrit en détail un nouvel organe dans le nez des animaux domestiques qui *"peut être utile au sens de l'odorat"* (voir la traduction de l'article fondateur de Jacobson dans Trotier et Døving, 1998). Il a ensuite été rebaptisé *organe voméronasal* en raison de sa localisation à la base du vomer. Le VNO est une structure tubulaire entourée d'une coiffe cartilagineuse qui communique avec les cavités nasales et orales par les canaux voméronasal et nasopalatin. Sur une coupe coronale du VNO, on peut délimiter des structures histologiques distinctes (figure 10) : des glandes situées dorsalement le long du septum nasal ; l'épithélium sensoriel voméronasal (VNE) en forme de croissant, médialement ; un gros vaisseau sanguin entouré de tissu caverneux, latéralement. Le VNO est borgne, et sa lumière est pleine de mucus sécrété par les glandes dorsales. Le transfert de l'odeur vers la lumière du VNO se produit par un processus de pompage actif déclenché par l'innervation sympathique (Meredith et O'Connell, 1979). Le pompage peut être induit pendant une investigation olfactive et activé par l'excitation, le stress ou la peur (Tirindelli, 2021).

Le VNE dérive de la placode olfactive vers le 11e jour embryonnaire chez la souris et présente les caractéristiques d'un tissu organisé au 13e jour embryonnaire (Cuschieri et Bannister, 1975). Il est intéressant de noter que des preuves suggèrent que le VNO est fonctionnel *in utero* bien que son développement complet ne soit atteint qu'après la naissance (Pedersen et al., 1983). Le VNE est composé de neurones sensoriels voméronasaux (VSN) OMP-positifs, de cellules de soutien et de cellules souches (Figure 10). Contrairement à la MOE, les cellules souches ne sont pas seulement basales mais forment deux niches neurogéniques aux extrémités du croissant du VNE (Figure 11) (Brann et Firestein, 2014).

Les VSNs sont bipolaires, avec une dendrite et un axone uniques (Figure 10). Les axones des VSNs sont non myélinisés, ils fasciculent pour former le nerf voméronasal et atteindre le bulbe olfactif accessoire. La dendrite s'étend jusqu'à la lumière du VNO et forme un bouton terminal à partir duquel plusieurs microvillosités s'étendent dans le mucus pour agrandir la surface réceptive (Mendoza, 1993). Comme les cils des OSNs, les microvillosités contiennent toute la machinerie moléculaire nécessaire au processus de transduction des odeurs (Munger et al., 2009).

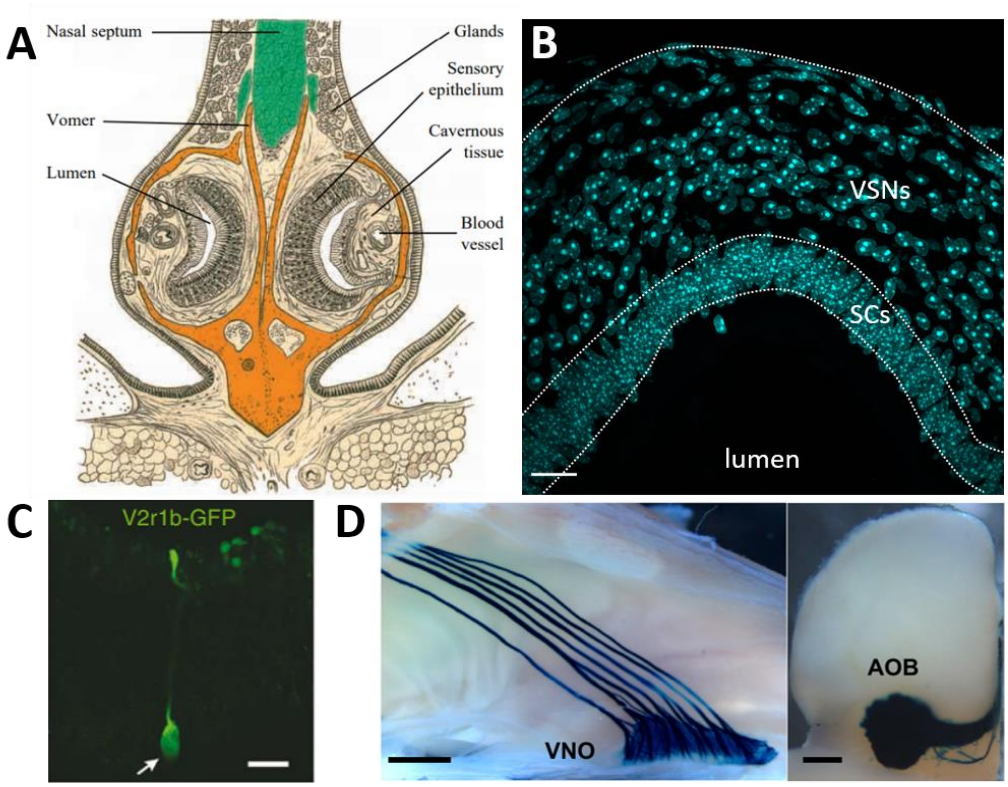

Figure 10 : Histologie de l'organe voméronasal. A) Schéma d'une coupe coronale entière du VNO montrant ses différentes structures histologiques. D'après Døving et Trotier, 1998 B) Coloration Dapi du VNE. Les cellules de soutien (SCs) sont situées apicalement à la limite de la lumière. Barre d'échelle, 20 µm. C) Visualisation d'un VSN. La flèche pointe vers le corps cellulaire situé dans le VNE. La dendrite s'étend jusqu'à la limite de la lumière et forme un bouton saillant. Barre d'échelle, 10 µm. D'après Leinders-Zufall et al. 2009. D) Vue en plan du VNO (à gauche) et de l'AOB (à droite) d'une souris Trpc2-IRES-taulacZ, mettant en évidence la projection des axones des VSNs vers l'AOB. Barre d'échelle, 200 µm (gauche) et 50 µm (droite). D'après Omura et Mombaerts, 2014.

1.4.2 Signalisation voméronasale

La signalisation vomeronasale résulte de l'activation de trois types de GPCR : Les récepteurs voméronasaux de type I et de type II, à savoir les V1R et les V2R, et les récepteurs des peptides formylés, les FPR (Munger et al., 2009). De plus, certains VSNs expriment un OR (Lévai et al., 2006 ; Nakahara et al., 2016). Les VSN exprimant des V1Rs et des V2Rs forment des populations qui ne se chevauchent pas au sein du VNE, chacune étant associée à des marqueurs moléculaires spécifiques (Munger et al., 2009) (Figure 11). Les V1Rs sont limités aux VSNs apicaux positifs pour la sous-unité

de la protéine Gαi2, la phosphodiestérase PDE4A et la sémaphorine neuropiline 2 ; à l'inverse, les V2Rs sont limités aux VSNs basaux positifs pour Gαo et β2-microglobuline (Ishii et al., 2003 ; Jia et Halpern, 1996 ; Lau et Cherry, 2000 ; Matsunami et Buck, 1997 ; Walz et al., 2002).

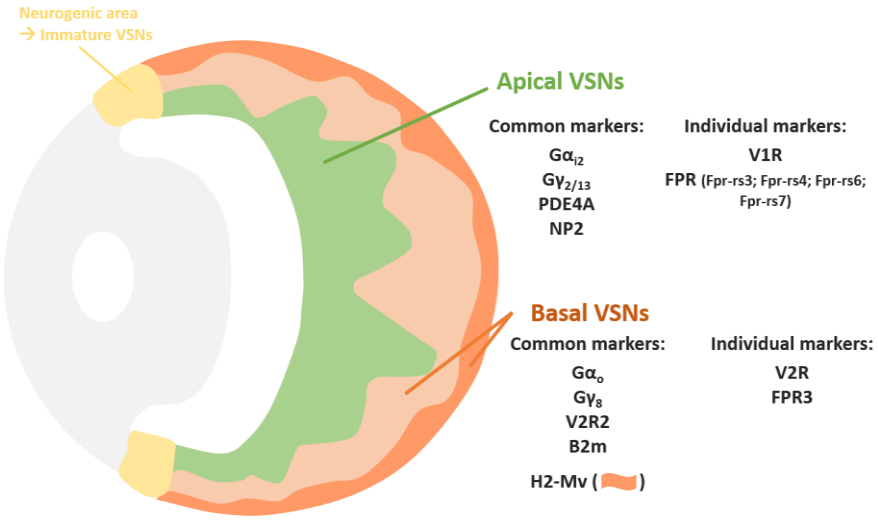

Figure 11 : Organisation de l'épithélium voméronasal et marqueurs associés à la population des VSNs. Les populations apicales et basales de VSNs ont chacune des marqueurs spécifiques (marqueurs communs), et les neurones individuels de chaque population expriment un récepteur (marqueurs individuels). Notez que les VSNs basaux sont également divisées en deux populations distinctes, la plus basale exprimant H2-Mv (orange foncé).

1.4.2.1 V1Rs

La famille des V1Rs a été la première découverte en 1995 via le criblage d'une bibliothèque de gènes provenant de VSNs individuels (Dulac et Axel, 1995). Sept membres ont été initialement isolés et des analyses ultérieures chez la souris ont conduit à un répertoire complet de 250 gènes, dont 150 gènes codants, regroupés en 12 familles de 1 à 30 représentants (Boschat et al., 2002 ; Del Punta et al., 2000 ; Roppolo et al., 2007 ; Young et al., 2010). Les répertoires de V1Rs sont hautement spécifiques aux espèces (Grus et al., 2005 ; Silva et Antunes, 2017 ; Young et al., 2010), même entre espèces étroitement apparentées (Kurzweil et al., 2009), ce qui suggère des changements adaptatifs rapides et éthologiquement pertinents dans les V1Rs fonctionnels. Il est intéressant de noter que de nombreux mammifères comme la chèvre, le mouton et la plupart des animaux domestiques expriment des V1Rs mais pas des V2Rs (Silva et Antunes, 2017). En outre, les humains possèdent plusieurs pseudogènes *V1R* et cinq gènes *de type V1R* codant potentiellement pour des récepteurs fonctionnels (Rodriguez et al., 2002). Cela suggère des origines distinctes pour les deux familles de VRs, les V1Rs se développant chez les mammifères jusqu'à la disparition d'un VNO fonctionnel dans certaines branches.

Les V1Rs sont co-exprimés avec la protéine Gαi2, mais aucun lien fonctionnel entre cette protéine G et l'initiation de la signalisation intracellulaire n'a été proposé. Une preuve indirecte provient

du modèle de souris knockout global Gαi2 (Gαi2-/-) dans lequel l'exposition de la litière souillée ne parvient pas à activer les sites de projection apicaux dans l'AOB (Norlin et al., 2003a). Structurellement, les V1Rs possèdent une courte région extracellulaire, ce qui suggère que la liaison du ligand se produit au niveau des domaines transmembranaires (Del Punta et al., 2000). Cela signifie également que les odorants détectés doivent être à un certain degré hydrophobes pour atteindre la poche de liaison. D'autres études ont confirmé cette hypothèse. La première à attribuer un rôle fonctionnel aux V1Rs résulte de l'inactivation génétique des clusters A et B des V1Rs (Del Punta et al., 2002). Elle a révélé que les V1Rs détectent de petits composés organiques volatils, et plusieurs études ont ensuite ajouté les stéroïdes sulfatés à la liste (Boschat et al., 2002 ; Haga-Yamanaka et al., 2014 ; Nodari et al., 2008 ; Turaga et Holy, 2012). Récemment, les acides biliaires ont également été associés aux V1Rs (Wong et al., 2020). En 2011, Isogai et ses collègues ont cartographié l'activation des VSNs chez la souris après une stimulation par des signaux hétéro ou homospécifiques (Isogai et al., 2011). Ils ont révélé que la plupart des familles de V1Rs détectent des signaux chimiques communs à plusieurs espèces, ce qui suggère qu'ils pourraient ne pas coder d'informations sur l'identité de l'émetteur mais plutôt sur son statut physiologique.

1.4.2.2 V2Rs

Trois groupes ont découvert simultanément les V2Rs en 1997 (Herrada et Dulac, 1997 ; Matsunami et Buck, 1997 ; Ryba et Tirindelli, 1997). Actuellement, le répertoire des V2Rs de la souris comprend 280 gènes, dont 120 gènes codants, regroupés en 4 familles (A à D) de 1 à plus de 100 membres (Shi et Zhang, 2007 ; Yang et al., 2005 ; Young et Trask, 2007). Les V2Rs sont très répandus chez les amphibiens et les reptiles mais sont largement absents chez la plupart des mammifères, à l'exception des rongeurs, des lagomorphes, de certains marsupiaux, de l'ornithorynque et des primates inférieurs (Shi et Zhang, 2007 ; Young et Trask, 2007). Cette divergence entre les répertoires V1Rs et V2Rs chez les mammifères suggère que les rongeurs (et autres taxons exprimant des V2Rs) peuvent être confrontés à un environnement phéromonal plus complexe, d'où le maintien d'une deuxième famille de VRs.

Les VSNs exprimant des V2Rs constituent l'exception notable à la règle " un neurone-un récepteur " qui prévaut parmi les neurones olfactifs (Rodriguez et al., 1999 ; Serizawa et al., 2004). Les V2Rs de la famille C comprennent sept récepteurs hautement homologues (également appelés V2R2) dont au moins un membre est exprimé simultanément avec les V2Rs des familles A, B, ou D dans chaque VSN basal (Figure 12) (Belluscio et al., 1999 ; Martini et al., 2001 ; Silvotti et al., 2007, 2011). Certains postulent que V2R2 pourrait servir de partenaire de dimérisation chaperon pour les sous-unités V2R (Mohrhardt et al., 2018), comme cela est postulé pour le récepteur constitutif Orco chez les insectes (Larsson et al., 2004).

Les V2Rs sont co-exprimés avec la protéine Gαo, qui est nécessaire pour déclencher la signalisation des VSNs après la détection du ligand (Chamero et al., 2011). Les V2Rs n'appartiennent pas à la même famille de GPCR que les ORs et les V1Rs. Ces derniers sont de type rhodopsine (classe A), alors que les V2Rs sont de classe C, comme les récepteurs du glutamate, ce qui signifie qu'ils possèdent un long domaine N-terminal extracellulaire hydrophobe (également appelé module Venus Flytrap) (Matsunami et Buck, 1997 ; Mombaerts, 2004). Cette conformation structurelle prédit que les V2Rs doivent détecter de grandes molécules telles que les peptides et les protéines. En 2003, la découverte d'une deuxième classe de récepteurs exprimés dans les VSN basaux a conforté cette théorie (Ishii et al., 2003 ; Loconto et al., 2003). Les gènes *H2-Mv* codent pour le MCH de classe Ib non classique (une classe de glycoprotéines qui lient les protéines extracellulaires pour les présenter au système immunitaire). Des études ont révélé que les VSNs les plus basaux coexpriment l'un de ces gènes *H2-Mv* avec les V2Rs (figure 12) (Ishii et Mombaerts, 2008 ; Ishii et al., 2003 ; Loconto et al., 2003 ; Silvotti et al., 2007). Par la suite, Leinders-Zufall et ses collègues ont montré que les ligands peptidiques du MHC-Ib servent également de ligands des V2Rs (Leinders-Zufall et al., 2004, 2009). De plus, ils ont démontré que la délétion de *H2-Mv* diminue la sensibilité des V2Rs à leurs ligands naturels, ce qui suggère une interaction entre eux.

Les peptides du MHC ont été la première classe de ligands de V2Rs identifiée. Ensuite, d'autres familles de ligands ont été découvertes, comme les protéines urinaires majeures (MUPs), les peptides sécrétés exocrines (ESPs), et les peptides salivaires (Chamero et al., 2007, 2011 ; Dey et Matsunami, 2011 ; Haga et al., 2010a ; Isogai et al., 2018 ; Osakada et al., 2018a ; Stein et al., 2016). Ces protéines sécrétées portent des informations robustes sur les caractéristiques de leur émetteur (Ferrero et Liberles, 2010 ; Hurst et Beynon, 2004). Si l'on considère que les VSNs basaux peuvent exprimer simultanément trois types de récepteurs, V2R2, V2RA/B/D et H2-Mv, cela pourrait leur permettre de coder un message très raffiné. Dans leur analyse globale de l'activation des VSNs, Isogai et ses collègues ont constaté que les V2Rs individuels sont principalement sensibles aux signaux d'un contexte éthologique unique (c'est-à-dire ceux d'un congénère ou d'une autre espèce particulière) (Isogai et al., 2011). Par conséquent, les V2Rs seraient de bons candidats pour encoder des informations sur l'identité de l'émetteur.

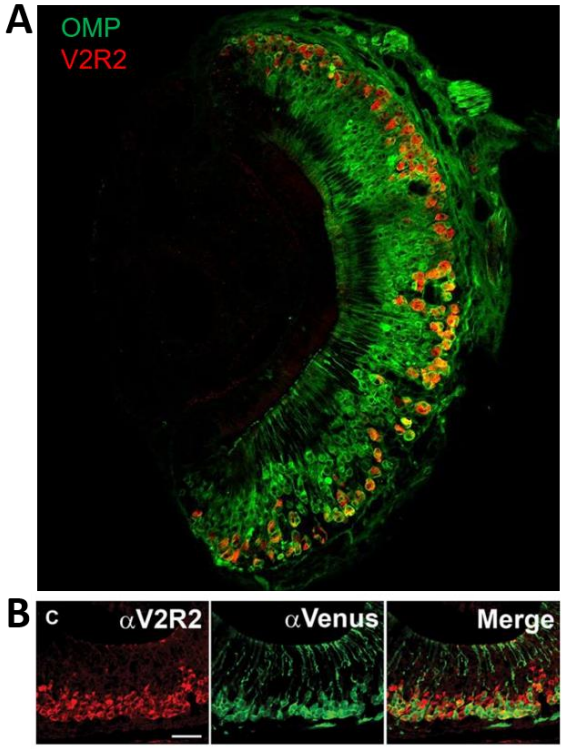

Figure 12 : VSNs basales. A) Immunomarquage d'une section coronale du VNE. Les VSNs expriment l'OMP (vert) et les VSNs basaux sont mis en évidence par la coloration de la famille V2R2. B) Les VSNs basaaux (exprimant V2R2, en rouge) sont séparées en deux populations, les plus basaaux exprimant H2-Mv (révélé par le transgène Venus chez une souris M10.2-Venus). Barre d'échelle 50 µm. D'après Ishii et Mombaerts, 2008.

1.4.2.3 Cascade sensorielle des VRs

Comme mentionné précédemment, les V1Rs et V2Rs utilisent respectivement Gαi2 et Gαo comme sous-unité primaire α de la protéine G (Chamero et al., 2011 ; Jia et Halpern, 1996 ; Norlin et al., 2003c). Le reste de la voie de signalisation intracellulaire est alors commun aux deux population de VSNs (Figure 13). Lors de l'activation par un ligand, la sous-unité Gα hydrolyse le GTP en GDP et libère le complexe Gβ/γ. L'activation cellulaire ultérieure ne dépend pas d'une enzyme activée par le GDP, comme dans les OSNs, mais implique plutôt le complexe Gβ/γ. Sa nature varie dans les VSNs basaaux et apicaux (Sathyanesan et al., 2013), mais il semble que l'activité fonctionnelle repose sur l'association de Gβ2/γ8 dans les VSNs basaux (Montani et al., 2013 ; Rünnenburger et al., 2002 ; Ryba et Tirindelli, 1995) et de Gβ2/γ2 ou γ13 dans les VSNs apicaux (Liu et al., 2018 ; Rünnenburger et al., 2002). Les différents complexes Gβ/γ activent la phospholipase C (PLC) (Holy, 2000 ; Smrcka, 2008 ; Spehr et al., 2002), qui hydrolyse à son tour le phosphatidylinositol-4,5-bisphosphate (PIP2) en les seconds messagers diacylglycérol (DAG) et inositol-1,4,5-trisphosphate (IP3). Le rôle fonctionnel de l'isoforme PLC β2 (PLCβ2) a été attesté dans les VSNs, mais elle ne compte pas pour la majorité des isoformes PLC exprimées dans le VNO, un rôle fonctionnel des autres manquant n'est pas montré (Dey et al., 2015). En aval du remaniement lipideque dépendant des PLC, IP3 n'est pas nécessaire à la signalisation du VNO (Chamero et al., 2017). La délétion génétique du récepteur IP3 de type 3 modifie le courant initial mais n'empêche pas la dépolarisation du VSN, suggérant qu'il participe uniquement à la modulation du signal. Le DAG active le TRPC2, un canal cationique membre de la famille des récepteurs à potentiel transitoire (TRP), pour déclencher la dépolarisation des VSNs (Leinders-Zufall

et al., 2018 ; Liman et al., 1999 ; Lucas et al., 2003). Secondairement à l'activation de TRPC2, l'influx de Ca2+ induit active les canaux chlorure anoctamine 1 (ANO1) pour dépolariser davantage la cellule (Amjad et al., 2015 ; Münch et al., 2018 ; Yang et Delay, 2010).

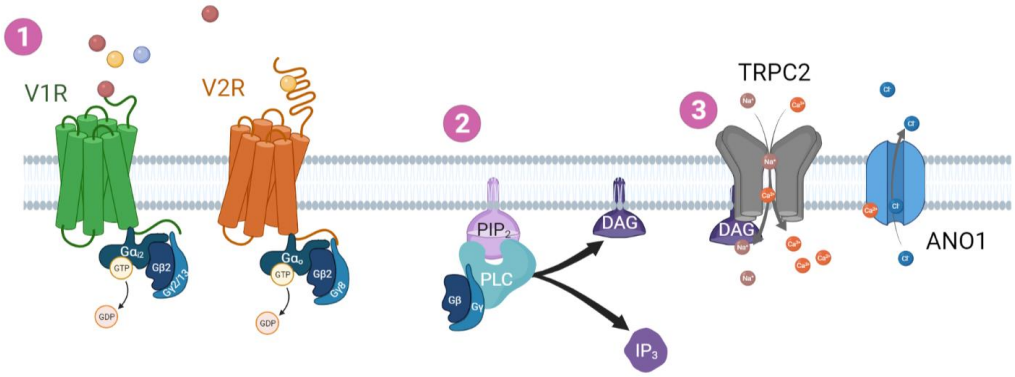

Figure 13 : Voie de signalisation voméronasale. ① Étape 1 : la liaison de l'odorant au récepteur voméronasal (V1R, V2R) active l'hydrolyse du GTP en GDP par le complexe de la protéine G. ② Étape 2 : le complexe Gβ/γ active la phospholipase C (PLC), qui hydrolyse à son tour le phosphatidylinositol-4,5-bisphosphate (PIP2) en seconds messagers diacylglycérol (DAG) et inositol-1,4,5-trisphosphate (IP3). ③ Étape 3 : Le DAG active le canal TRPC2, permettant l'entrée de Na+ et de Ca2+. Le Ca2+ intracellulaire active alors le canal anoctamine 1 (ANO1) pour amplifier la dépolarisation par un courant Cl-. Ce schéma est créé dans BioRender.com.

Plusieurs études montrent qu'un certain degré de signalisation peut être atteint sans TRPC2 dans les VSNs. Le premier indice est venu d'une étude montrant *in vitro* que les peptides de liaison au MHC activent les VSNs de souris knock-out TRPC2 (TRPC2-KO ; Trpc2-/-) (Kelliher et al., 2006). D'autres études ont renforcé cette hypothèse et mis en évidence l'existence d'autres canaux cationiques (Kim et al., 2012 ; Zhang et al., 2008, 2010). Certaines ont même montré que le courant chlorure pouvait à lui seul déclencher la dépolarisation des VSNs, probablement du fait que la concentration en chlore au sein du bouton dendritique est assez élevée (Kim et al., 2011, 2015 ; Spehr et al., 2009). Une question demeure quant au rôle de ces voies indépendantes de TRPC2. Il reste à savoir si elles soutiennent la transmission d'odorants spécifiques, si elles complètent le signal électrique déclenché par TRPC2, ou si elles prennent simplement en charge la fonction de TRPC2 en son absence.

1.4.2.4 FPRs

Outre les VRs, certains VSNs expriment une troisième famille de GPCR de type rhodopsine, les récepteurs des peptides formiques (FPR) (Liberles et al., 2009 ; Rivière et al., 2009). Les FPR sont exprimés dans de nombreux tissus et types de cellules du système immunitaire, où ils participent aux mécanismes de défense contre les agents pathogènes (Boillat et al., 2021). La plupart des mammifères possèdent deux FPR immunitaires, mais le répertoire des FPR des rongeurs s'est considérablement étendu, et les souris possèdent sept gènes codant des FPR. Deux d'entre eux sont des orthologues des FPR immunitaires (Fpr1 et Fpr-rs2), tandis que les cinq autres résultent de la duplication de Fpr-rs2

(Dietschi et al., 2017 ; Gao et al., 1998 ; Wang et Ye, 2002). Le rôle de ces cinq FPR supplémentaires (Fpr-rs1/3/4/6/7) est resté insaisissable jusqu'à ce que deux laboratoires découvrent qu'ils étaient presque exclusivement exprimés dans le VNO (Liberles et al., 2009 ; Rivière et al., 2009). L'existence de FPR voméronasaux implique que les rongeurs peuvent sentir les pathogènes. Une autre utilisation de ces récepteurs serait l'évaluation du microbiote des congénères (Boillat et al., 2021).

Les VSN exprimant des FPRs constituent 4% du total des VSNs (Boillat et al., 2021) et observent la même règle "un neurone-un récepteur" que la plupart des neurones olfactifs (Bufe et al., 2019 ; Dietschi et al., 2013 ; Liberles et al., 2009 ; Rivière et al., 2009). Les FPRs voméronasaux sont spatialement ségrégués : FPR3 (Fpr-rs1) est restreint aux VSNs exprimant Gαo et les autres aux VSNs exprimant Gαi2, ce qui suggère qu'ils dérivent de deux événements génétiques indépendants (Dietschi et al., 2017 ; Liberles et al., 2009 ; Rivière et al., 2009). Ils sont sensibles aux ligands classiques du FPRs (Rivière et al., 2009), mais une confirmation *in vivo* n'a été apportée que pour le FPR3 (Bufe et al., 2019). Cette dernière étude a également démontré l'exigence de Gαo et TRPC2 pour la signalisation *in vivo du* FPR3. Cela suggère que les FPR voméronasaux utilisent probablement la même voie intracellulaire que les VR même si une confirmation pour les FPR localisés apicalement est encore nécessaire.

1.4.3 Le bulbe olfactif accessoire

Les axones du VSNs atteignent le bulbe olfactif (OB) pour former leur premier relais dans le système nerveux central. Le bulbe olfactif accessoire (AOB) est une subdivision dorsale de l'OB qui reçoit spécifiquement les entrées du VNO. Comme le MOB, l'AOB est organisé en différentes couches cellulaires, bien que non concentriques. De la partie dorsale à la partie ventrale, la couche glomérulaire (GL) reçoit les axones des VSN à l'intérieur des glomérules ; la couche des cellules mitrales (MCL) contient des interneurones qui transmettent les informations des VSN au cerveau, et la couche des cellules granuleuses (GCL) contient des neurones sans axone qui établissent des synapses dendrodendritiques avec les cellules mitrales (MC) (Figure 14) (Mohrhardt et al., 2018).

Le GL-AOB conserve la dichotomie structurelle observée dans le VNO et les VSN exprimant V1Rs et V2Rs ciblent des régions distinctes du GL-AOB le long de son axe rostro-caudal. Les VSN apicaux font synapse dans les glomérules antérieurs, et les VSN basaux dans les glomérules postérieurs (Figure 14) (Belluscio et al., 1999 ; Ishii et Mombaerts, 2008 ; Jia et Halpern, 1997 ; Rodriguez et al., 1999). Une étude suggère une carte tripartite de la partie postérieure, encore subdivisée pour organiser les entrées des VSN basaux positifs ou négatifs à *H2-Mv* (figure 14) (Ishii et Mombaerts, 2008).

La ségrégation topographique de l'AOB n'est pas aussi stricte que pour la MOB. Premièrement, les axones peuvent se diviser pour innerver plusieurs glomérules (jusqu'à 30) (Belluscio et al., 1999 ; Rodriguez et al., 1999). Il a également été signalé que certains glomérules, principalement les plus grands, reçoivent des entrées de VSN exprimant des VR différents, chacun étant limité à des

microdomaines à l'intérieur du glomérule (Belluscio et al., 1999). Cependant, les glomérules recevant des axones de VSN exprimant des VR de la même famille (par exemple, V1Rj ou V2R1) sont regroupés en domaines (Wagner et al., 2006) (Figure 14). Dans la MOB, les MCs reçoivent des entrées dans un seul glomérule. Au contraire, les AOB-MCs ont des dendrites ramifiées qui contactent plusieurs glomérules (Takami et Graziadei, 1991 ; Yonekura et Yokoi, 2008). Ils respectent la ségrégation rostrocaudale de l'AOB-GL, c'est-à-dire que les MCs antérieures contactent les glomérules antérieurs et vice-versa, mais une certaine connectivité croisée a néanmoins été rapportée (Yonekura et Yokoi, 2008). Cette organisation plaide pour un calcul et une intégration directs des informations olfactives dans l'AOB. Ceci est cohérent avec le fait que les AOB-MCs ne projettent pas dans des cortex dédiés mais activent plutôt directement les structures cérébrales limbiques et hypothalamiques. Ces régions sont de grandes plaques tournantes pour les informations sensorielles, d'où le codage des informations en amont.

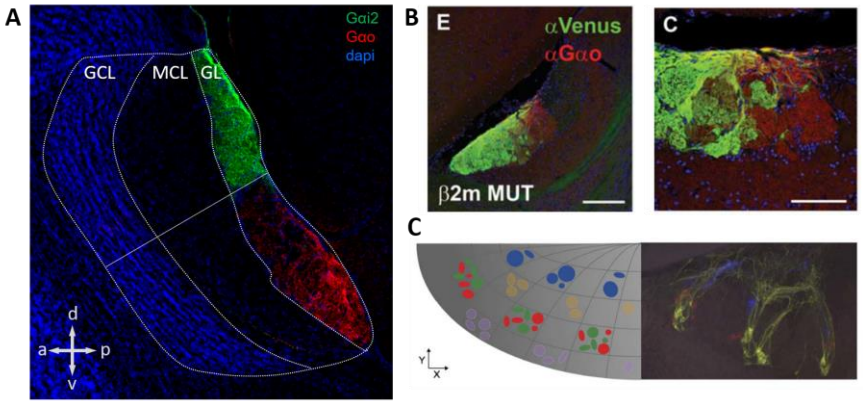

Figure 14 : Le bulbe olfactif accessoire. A) Coupe sagittale de l'AOB. La coloration Dapi (bleu) permet de délimiter les différentes couches cellulaires (GL, MCL, GCL). Le GL-AOB reflète l'organisation topographique du VNO avec des VSNs Gαi2 (vert) se projetant vers le GL antérieur et des VSNs Gαo (rouge) vers le GL postérieur. B) Le GL postérieur est également subdivisé, la partie la plus postérieure recevant les entrées des VSN exprimant H2-Mv (représentés ici par le transgène Venus chez une souris M10.2-Venus). Barres d'échelle, 200 µm (gauche) et 100 µm (droite). D'après Ishii et Mombaerts, 2008. C) Les VSN exprimant des récepteurs de la même famille se projettent vers des glomérules regroupés en domaines. A droite : organisation schématique proposée. A gauche : tracé expérimental. Ici, les VSNs exprimant la famille A de V1R, représentés par des fibres rouges et jaunes (provenant respectivement de VSNs positifs pour V1Ra1 et V1Ra3) se projettent vers des glomérules ventraux proches, alors que les VSNs exprimant la famille B de V1R, représentés ici par des fibres bleues (provenant de VSNs positifs pour V1Rb1) se projettent vers des glomérules dorsaux. D'après Wagner et al. 2006.

1.4.1 Ligands voméronasaux

Parmi les centaines de récepteurs exprimés dans le VNO, seule une poignée a été associée à leur(s) ligand(s). Le criblage à grande échelle par hybridation in situ ou séquençage de l'ARNm (Isogai et al., 2011a ; Wong et al., 2020), les modèles de souris KO pour les VR (Haga et al., 2010a ; Osakada et al, 2018a), et des modèles génétiques de souris permettant la présence d'un rapporteur fluorescent

dans les VSN exprimant un VR spécifique (Boschat et al., 2002 ; Haga-Yamanaka et al., 2014 ; Leinders-Zufall et al., 2009, 2014 ; Del Punta et al., 2002) ont permis d'identifier quelques paires. Ces travaux sont très techniques, longs et coûteux, donc inadaptés pour couvrir le grand répertoire de VR. La principale contrainte à la découverte des ligands des VR est le manque de modèles *in vitro* appropriés. Les systèmes d'expression hétérologue sont complexes à adapter à l'expression des VR en raison des exigences particulières pour l'arrimage à la membrane de ces récepteurs (Dey et Matsunami, 2011). Néanmoins, de tels systèmes existent et ont permis l'identification de ligands voméronasaux supplémentaires (Bufe et al., 2012, 2015, 2019 ; Dey et Matsunami, 2011 ; Stein et al., 2016). Le tableau 1 contient les paires connues de VR et de ligands. En outre, il énumère les ligands voméronasaux dont les récepteurs sont inconnus et indique s'ils activent un type spécifique de VSN (par exemple, les VSN exprimant Gαo).

Certains des ligands voméronasaux agissent comme une phéromone pure, conformément à la définition initiale de Karlson et Lüscher (Karlson et Lüscher, 1959). Un exemple clair est ESP22, un peptide sécrété dans les larmes de souris juvéniles qui inhibe le comportement sexuel des adultes (Ferrero et al., 2013 ; Osakada et al., 2018a). D'autres ont été liés à des comportements ou à des processus physiologiques spécifiques, mais pas strictement à un en particulier. Comme mentionné dans l'introduction générale, nous devons repenser la définition de la phéromone : une phéromone pourrait être définie comme une molécule utilisée pour la communication qui transporte des informations sur l'individu. Chaque individu émet une combinaison d'odorants, lue par les autres pour adapter leur comportement.

Maintenant que le lecteur est familiarisé avec le système olfactif des rongeurs, je décrirai les comportements socio-sexuels des souris et la manière dont le système voméronasal les contrôle.

Deorphanized receptors

	receptor name	gene	ligand(s)	biological source	reference
V1Rs	V1Rb2	*Vmn1r49*	2-heptanone	urine	1
	V1Re2	*Vmn1r226*	sulfated corticosteroids	urine	2, 3
	V1Re6	*Vmn1r227*	sulfated corticosteroids	urine	2
	V1Rf3	*Vmn1r237*	sulfated estrogen		
	V1Rj2	*Vmn1r89*	sulfated androgens sulfated estrogens	urine	2, 3
	V1Rj3	*Vmn1r85*	sulfated estrogens	urine	3
	V1Rc28	*Vmn1r21*	deoxycholic acid	bile	4, 5
	V1Rc29	*Vmn1r16*	cholic acid		
	V1Rl1	*Vmn1r70*	lithocholic acid	bile	4
V2Rs	V2Rp5	*Vmn2r116*	ESP1	male tears	6
	V2Rp1	*Vmn2r112*	ESP5 ESP6	male tears	7
	V2Rp2	*Vmn2r111*	ESP5		
	V2Rp4	*Vmn2r115*	ESP22	juvenile tears	8
	n/a	*Vmn2r65*	submandibular gland protein C	female saliva	9
	n/a	*Vmn2r88*	haemoglobin	blood	9
	n/a	*Vmn2r28*	CRP1	rat tears	10
	n/a	*Vmn2r52*			
	V2R1b	*Vmn2r26*	MHC-proteins	urine	11
	V2Rf2	*Vmn2r81*	MHC-proteins formyl peptide	urine	12
FPRs	FRP3	*Frpr-rs1*	MgrB peptide W-peptide	bacteria	13, 14

Partially deorphanized receptors and unmatched ligands

VSNs marker	gene	ligand(s)	biological source	reference
V1Rc1 V1Rc30	*Vmn1r10* *Vmn1r9*		neonate	9
V1Re9 V1Re12	*Vmn1r69* *Vmn1r185*		female urine	3
V1Ra & V1Rb	*n/a*	n-pentylacetate isobutylamine 6-hydroxy-6-methyl-3-heptanone	urine	15
$G\alpha_o$	*Gnao*	MUPs MHC-proteins mitochondrial formyl-peptides LMW fraction	urine	16
		Feld4	cat fur	17
n/a	*n/a*	α/β-farnesene 2-*sec*-butyl-4,5-dihydrothiazole 2,5-dimethylpyrazine 2,3-dehydro-*exo*-brevicomin	urine	18
n/a	*n/a*	hexadecanol hexadecyl acetate	urine	19
n/a	*n/a*	sulfated androgens sulfated estrogens sulfated progestagens sulfated corticosteroids	urine	20, 21

Table 1: Vomeronasal ligands, their receptors. n/a: not applicable. [1] Boschat et al., 2002; [2] Isogai et al., 2011; [3] Haga-Yamanaka et al., 2014; [4] Doyle et al., 2016; [5] Wong et al., 2020; [6] Haga et al., 2010; [7] Dey and Matsunami, 2011; [8] Osakada et al., 2018; [9] Isogai et al., 2018; [10] Tsunoda et al., 2018; [11] Leinders-Zufall et al., 2009; [12] Leinders-Zufall et al., 2014; [13] Bufe et al., 2012; [14] Bufe et al., 2019; [15] Del Punta et al., 2002; [16] Chamero et al., 2011; [17] Pérez-Gómez et al., 2015; [18] Leinders-Zufall et al., 2000; [19] (Liu et al., 2019); [20] Nodari et al., 2008; [21] Turaga and Holy, 2012

2 Contrôle voméronasal des comportements socio-sexuels

Les individus d'une espèce interagissent pour assurer leur survie et celle de leurs congénères. De quoi dépend la survie ? L'alimentation, l'accouplement, les soins de la progéniture, la défense et l'évitement du danger sont cruciaux, et tous dépendent de la détection et de l'interprétation des signaux olfactifs. Tinbergen a théorisé quatre façons d'étudier les comportements : la causalité (comment fonctionne-t-il), l'ontogenèse (comment est-il mis en œuvre), la fonction (quelle est sa valeur de survie) et l'évolution (comment évolue-t-il) (Tinbergen, 1963). Ici, nous nous intéresserons principalement à la causalité des comportements sociaux, notamment leur contrôle et leur modulation voméronasale.

Agonistiques ou antagonistes, les comportements sociaux sont innés, c'est-à-dire qu'ils sont produits sans apprentissage et consistent en des séquences stéréotypées. Cependant, l'inné n'est en aucun cas statique. L'état reproductif, l'expérience sociale, l'état interne et les facteurs environnementaux influencent la décision d'action et sa réalisation. Les modèles de comportement social sont bien caractérisés et leur plasticité est de plus en plus étudiée (Tan et Stowers, 2020 ; Wei et al., 2021). En outre, les comportements sociaux sont fortement sexuellement dimorphiques. L'émergence de la reproduction sexuée a conduit au développement de réponses comportementales spécifiques au sexe, adaptées au rôle complémentaire de chaque sexe dans la perpétuation de l'espèce. Cette section décrira quatre catégories de comportement : les comportements sexuels, agressifs, parentaux et d'évitement.

Plusieurs modèles ont démêlé l'implication de la VNO dans le contrôle des comportements sociaux (Chamero et al., 2012). Avant l'explosion des outils génétiques, l'ablation chirurgicale du VNO (le modèle VNOx) a jeté les bases de ce domaine de recherche (Wysocki et Lepri, 1991). Ensuite, la dissection génétique des comportements dépendants du VNO a commencé avec la souris TRPC2-KO (Trpc2-/-), qui induit une anosmie voméronasale (Leypold et al., 2002 ; Stowers et al., 2002). La dissection plus fine des voies voméronasales a suivi, avec des modèles d'ablation génétique de messagers intracellulaires ou de VRs (Chamero et al., 2011 ; Haga et al., 2010a ; Isogai et al., 2018 ; Kim et al, 2012 ; Leinders-Zufall et al., 2014 ; Liu et al., 2018 ; Loconto et al., 2003 ; Montani et al., 2013 ; Münch et al., 2018 ; Norlin et al., 2003b ; Osakada et al., 2018a ; Del Punta et al., 2002). Un pas énorme dans la compréhension précise de la fonction voméronasale est venu de la délétion conditionnelle de Gαo (souris cGαo-/-), l'effecteur primaire des VSNs positifs aux V2Rs (Chamero et al., 2011 ; Oboti et al., 2014 ; Pérez-Gómez et al., 2015). Cependant, des informations similaires concernant les VSNs V1R/Gαi2 font encore défaut.

Le VNO est un acteur crucial des comportements sociaux, mais l'implication des autres organes sensoriels olfactifs ne doit pas être sous-estimée. L'ablation de la fonction du MOS induit une anosmie globale, ce qui rend difficile la détermination de son implication précise. Des avancées récentes ont permis un dysfonctionnement partiel du MOS, révélant ainsi sa coopération avec le VNO pour assurer

des réponses comportementales complètes (Kobayakawa et al., 2007 ; Matsuo et al., 2015). Lorsque cela sera pertinent, je mentionnerai la participation de voies non-voméronasales.

2.1 Comportements sexuels

Certains diraient que l'accouplement est la plus belle réussite de la vie d'un animal. Si ce n'est pour perpétuer l'espèce, pourquoi vivrait-on ? Au-delà des questions philosophiques qu'elle peut soulever, la reproduction occupe en effet une place particulière dans la vie de la plupart des animaux, empiétant souvent sur d'autres activités. Dans des cas extrêmes, la reproduction devient la seule et unique activité, à l'instar du papillon paon de nuit géant, qui n'a pas de trompe pour se nourrir et qui consacre toute sa semaine de vie à l'accouplement.

Le comportement sexuel des rongeurs est composé d'une phase appétitive, qui englobe la détection, l'approche et l'investigation de la cible, suivie d'une phase consommatoire, l'acte sexuel proprement dit (Figure 15) (Ball et Balthazart, 2008). La nécessité de l'olfaction pour détecter et approcher un partenaire potentiel est parfaitement logique mais ne se limite pas à cela. Les rongeurs détectent et suivent la signature olfactive d'un congénère. Une fois trouvés, des contacts nasaux étroits leur permettent de déterminer s'il s'agit d'un choix approprié pour s'accoupler. Enfin, certains signaux olfactifs peuvent stimuler les rapports sexuels. La discrimination entre un effet direct des signaux olfactifs sur la phase de consommation et un effet indirect provenant d'une modification de la phase d'appétit n'est pas toujours facile (Baum et Kelliher, 2009). Il existe des paradigmes de tests comportementaux spécifiques pour chaque phase, mais leurs résultats doivent toujours être interprétés avec précaution en fonction de la séquence comportementale globale (tableau 2).

		Olfactory sex discrimination			olfactory sex preference		USVs (to ♀)	urine marking (to ♀)	male sexual behavior						opposite sex mounting	female sexual behavior (lordosis)
		♂ vs ♀	♂ vs cast ♂	♀ vs ovx ♀	nonvolatiles	volatiles			latency to mount		mounting		ejaculation			
VNOx	♂	✓ 1, 2		✓ 1	✗ 1, 2		↘ 7, 8, 9	↘ 13	✓ 1	↘ 14	✓ 1	↘ 9, 14	✓ 1	↘ 14	✗ 1	
	♀	✓ 20	✓ 21		✗ 20, 22	✓ 20, 22									✗ 20	↘ 22
AOBx	♂	✓ 3		✓ 3			✗ 7		✓ 3		✓ 3		✓ 3			
	♀														✗ 20	
Trpc2$^{-/-}$	♂	✓ 4, 5				✗ 4, 5	✓ 10, 11		✓ 15		✓ 10, 15				✓ 10, 11, 15	↘ 24
	♀														✓ 11, 23	
cGao$^{-/-}$	♂		✓ 6						✓ 16		✓ 16				✗ 6	
	♀					✓ 16									✗ 16	✗ 16
ΔV1rabΔ$^{-/-}$	♂						✓ 12				↘ 12		↘ 12		✗ 12	
Gai2$^{-/-}$	♂										✓ 18				✗ 18	
SK3$^{-/-}$	♂								↘ 17		↘ 17				✗ 17	
GIRK1$^{-/-}$	♂								↘ 17		↘ 17				✗ 17	
β2m$^{-/-}$	♂														✗ 19	
H2Mv$^{-/-}$	♂															↘ 25

Table 2: Surgical VNO removal and genetic mutation effects on sexual behaviors. ✓ : no effect; ✗ : absence; ↘ : decrease. Numbers refer to research articles demonstrating the effect. [1] Pankevich, 2004; [2] Pankevich et al., 2006; [3] Jakupovic et al., 2008; [4] Beny and Kimchi, 2016; [5] Beny-Shefer et al., 2017; [6] Chamero et al., 2011; [7] Bean, 1982; [8] Wysocki et al., 1982; [9] Wysocki and Lepri, 1991; [10] Stowers et al., 2002; [11] Kimchi et al., 2007; [12] Del Punta et al., 2002; [13] Maruniak et al., 1986; [14] Clancy and Nobles, 1984; [15] Leypold et al., 2002; [16] Oboti et al., 2014; [17] Kim et al., 2012; [18] Norlin et al., 2003; [19] Loconto et al., 2003; [20] Martel and Baum, 2009; [21] Lloyd-Thomas and Keverne, 1982; [22] Keller et al., 2006; [23] Chalfin et al., 2014; [24] Fraser and Shah, 2014; [25] Leinders-Zufall et al., 2014.

2.1.1 Comportements sexuels mâle

Les souris mâles ont un potentiel copulatoire élevé. Ils s'accouplent avec toutes les femelles réceptives qu'ils rencontrent afin de disséminer leur bagage génétique autant que possible. En explorant leur territoire, ils doivent détecter la présence d'une femelle et l'attirer en montrant leur aptitude à la reproduction (Figure 15). La détection d'un partenaire potentiel se fait principalement par l'analyse des urines et des fèces déposées par les congénères. Par conséquent, les souris doivent discriminer le sexe de l'émetteur. De manière intrigante, ni l'ablation chirurgicale du VNO (modèle VNOx) ni l'ablation de l'AOB n'affectent la discrimination du sexe à partir de l'urine chez les souris mâles (Jakupovic et al., 2008 ; Pankevich, 2004 ; Pankevich et al., 2006b). Ainsi, le MOS est suffisant pour favoriser la discrimination sexuelle. Les rongeurs préfèrent les odeurs provenant du sexe opposé. L'implication de l'AOS par rapport au MOS dans ce phénomène n'est cependant pas claire. Lorsqu'ils n'ont pas accès à la source de l'odeur dans un test à deux choix (par exemple, un papier filtre imbibé urine), ce qui signifie que seuls les composants volatils sont disponibles, les animaux préfèrent les indices du sexe opposé, ce qui suggère que le MOS peut soutenir seul la préférence sexuelle (Baum et Kelliher, 2009). Lorsque l'accès à la source d'odeur est accordé, les mâles VNOx ne montrent pas de préférence et reniflent les odeurs des mâles et des femelles de manière égale (Pankevich, 2004 ; Pankevich et al.,

2006b). De même, une étude a montré que la préférence olfactive des mâles Trpc2-/- est affectée (Bayless et al., 2019). Soutenant le rôle du VNO dans la discrimination et la préférence sexuelle, une carte des VSNs activés par les urines mâles ou femelles a révélé l'existence de VSNs accordés pour chaque indice sexuel (Ben-Shaul et al., 2010 ; He et al., 2008). Ainsi, il apparaît que le MOS et l'AOS peuvent avoir des rôles complémentaires dans l'induction d'une préférence sexuelle olfactive : le MOS est à l'origine de l'attraction et de la discrimination initiales ; ensuite, l'AOS maintient l'intérêt pour les signaux du sexe opposé (Baum et Kelliher, 2009).

Une fois qu'un mâle a détecté une femelle, il doit l'attirer en utilisant des comportements de parade nuptiale (Figure 15). Tout d'abord, les mâles répandent de petites spots d'urine pour montrer leur présence (Reynolds, 1971). Si la femelle détectée passe par là, elle suivra l'odeur et trouvera le mâle. Une autre aptitude du marquage urinaire est de présenter un statut génétique et social à la femelle. En effet, l'urine contient des molécules portant des informations individuelles sur son expéditeur (Ferrero et Liberles, 2010 ; Hurst et Beynon, 2004). Les premières études ont montré que les mâles VNOx marquaient moins que les mâles sham-opérés en réponse à la stimulation urinaire de la femelle (Labov et Wysocki, 1989 ; Maruniak et al., 1986). Ainsi, les stimuli dépendants du VNO peuvent être à l'origine de la motivation à s'engager dans des comportements de séduction. Outre le marquage, les mâles émettent également des vocalisations ultrasoniques (USV) pour attirer une femelle. Celles-ci peuvent être déclenchées par l'urine de la femelle et ne sont pas émises en direction des mâles. Comme les marques olfactives urinaires, les USV sont caractéristiques d'un individu et servent au choix du partenaire par les femelles (Egnor et Seagraves, 2016). Les premiers travaux ont également montré que l'ablation des VNO réduit les émissions d'USVs (Bean, 1982 ; Wysocki et Lepri, 1991). Cependant, les mâles Trpc2-/- conservent de fortes vocalisations (Kimchi et al., 2007 ; Stowers et al., 2002), remettant en question la validité des résultats précédents. L'ablation partielle de la fonction MOS a révélé que le MOS et l'AOS participent touts deux à l'induction des USVs (Matsuo et al., 2015). Il est possible qu'en l'absence de signalisation TRPC2 au cours du développement, le MOS fournisse une entrée suffisante pour générer des USVs chez les souris Trpc2-/-.

Le comportement sexuel consommatoire du mâle commence lorsque le mâle monte une femelle. S'ensuit une série de montées avec intromissions et poussées pelviennes vigoureuses, ponctuées de séances de toilettage anogénital pour maintenir l'érection, pour finalement aboutir à l'éjaculation (Figure 15). Les premières études ont rapporté un effet de l'ablation chirurgicale du VNO sur la motivation à commencer un rapport sexuel (augmentation de la latence à monter) et sur la performance sexuelle (réduction du nombre de montées et augmentation de la latence à éjaculer) (Clancy et Nobles, 1984 ; Wysocki et Lepri, 1991). Cependant, des études plus récentes n'ont montré aucun effet de l'altération de l'AOS (Jakupovic et al., 2008 ; Pankevich, 2004). Cette divergence pourrait s'expliquer par les protocoles expérimentaux utilisés dans chaque expérience. Les études plus anciennes ont examiné le comportement sur une période limitée, trop courte pour voir toutes les phases du rapport sexuel, alors que les plus récentes ont analysé le comportement des mâles jusqu'à

l'éjaculation. Les modifications génétiques de la fonction VNO ont également donné des résultats contradictoires. D'une part, les mâles Trpc2-/-, cGαo-/- et Gαi2-/- présentent un comportement similaire à celui de leurs congénères témoins (Kimchi et al., 2007 ; Leypold et al., 2002 ; Norlin et al., 2003c ; Oboti et al., 2014 ; Stowers et al., 2002). D'autre part, la délétion d'un groupe de gènes *V1R* réduit la proportion de mâles qui montent (Del Punta et al., 2002). Cette divergence majeure sur la fonction des V1Rs peut résulter du modèle Gαi2-/- de Norlin et ses collègues, qui induit une délétion de Gαi2 sur l'ensemble du corps, et par conséquent, un dysfonctionnement des cellules non sensorielles comme les neurones cérébraux (Hamada et al., 2017 ; Rudolph et al., 1995). Aucune de ces études n'a analysé le comportement sur l'ensemble de sa séquence, de la première monte à l'éjaculation, ce qui ne permet pas de tirer des conclusions claires. Del Punta et ses collègues ont rapporté que les mâles mutants engagés dans des rapports sexuels affichaient un niveau égal d'activité sexuelle en termes de latences et de nombre de montes. Cette affirmation suggère que le VNO pourrait être le moteur de la motivation à initier un comportement sexuel, comme cela est suggéré pour les comportements de séduction. Dans l'ensemble, les connaissances actuelles ne permettent pas de conclure à un rôle majeur du VNO dans le comportement sexuel consommatoire des males. Néanmoins, une meilleure investigation de la signalisation V1Rs/Gαi2 est nécessaire puisque les modèles disponibles donnent des résultats contradictoires (Norlin et al., 2003b ; Del Punta et al., 2002).

Bien que ne contrôlant pas le comportement sexuel dans les conditions basales, la signalisation VNO peut l'influencer. ESP22, un peptide lacrymal juvénile détecté par V2Rp4, inhibe complètement les comportements sexuels des adultes (Ferrero et al., 2013 ; Osakada et al., 2018b). D'autre part, l'exposition aux œstrogènes sulfatés, détectés par V1Rj2 et V1Rj3, augmente le comportement de monte des mâles sexuellement naïfs (Haga-Yamanaka et al., 2014). Le comportement sexuel dépend de voies cérébrales organisées avant la naissance et situées sur les sites cérébraux de convergence des entrées sensorielles (Simerly, 2002). Ainsi, on pourrait supposer que la suppression d'une de ces entrées sensorielles, ici les voméronasales, est insuffisante pour abolir un tel comportement ancré. Étant donné la place du VNO dans la transduction des phéromones, il doit participer à la régulation du comportement sexuel. Les résultats suggèrent que ce pourrait être en motivant les mâles à attirer activement les femelles, puis en maintenant la motivation à s'engager dans des rapports sexuels. Les conditions expérimentales en laboratoire peuvent masquer le rôle naturel du VNO, et on pourrait penser que les animaux sauvages dépourvus d'un VNO fonctionnel ne se reproduiraient pas efficacement.

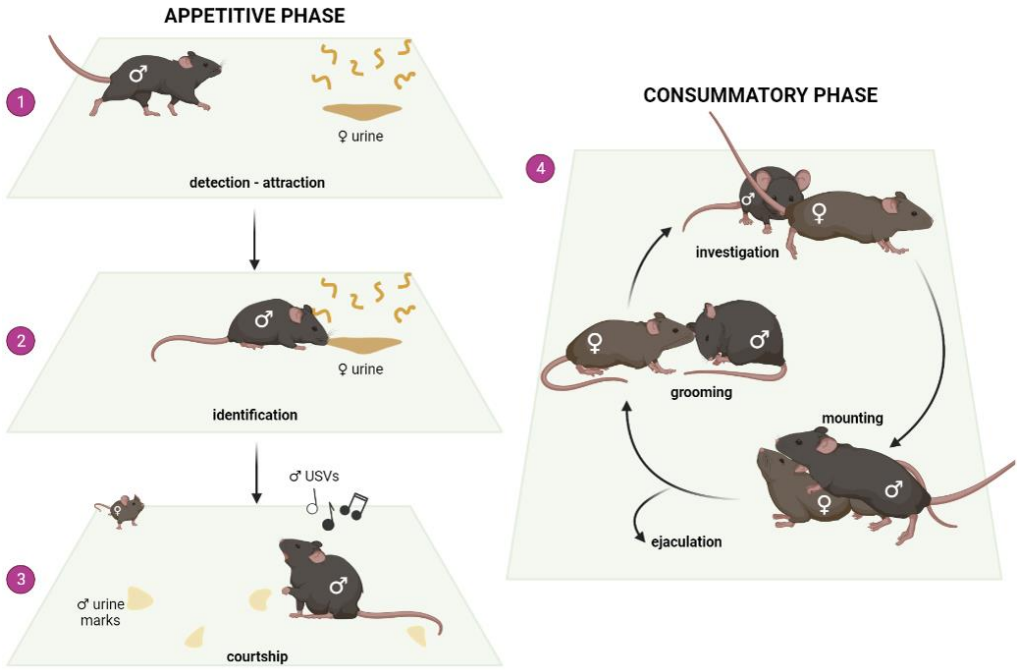

Figure 15 : Séquence du comportement sexuel masculin. Le comportement sexuel du mâle est composé d'une phase appétitive (à gauche) et d'une phase consommatoire (à droite). ① Le mâle détecte la présence d'une femelle et est attiré par son odeur. ② Une investigation olfactive rapprochée permet d'identifier les caractéristiques de l'émetteur de l'odeur. ③ Le mâle entame une série de comportements de parade nuptiale pour attirer la femelle, comme le marquage olfactif et les USV. ④ La phase consommatoire commence par l'investigation olfactive rapprochée de la femelle ; puis suit une série de montages avec intromissions et poussées pelviennes vigoureuses facilitées par la posture de lordose de la femelle, ponctuées de séances de toilettage anogénital pour maintenir l'érection, pour finalement arriver à l'éjaculation. Ce schéma est créé dans BioRender.com.

2.1.1 Comportements sexuels femelles

Les comportements sexuels appétitifs des souris femelles sont différents de ceux des mâles. Alors que les mâles peuvent multiplier les partenaires, les femelles doivent choisir le meilleur. Premièrement, l'accouplement des femelles a lieu pendant leur période ovulatoire, limitée à une douzaine d'heures tous les quatre ou cinq jours. Ensuite, les femelles portent et élèvent des petits jusqu'au sevrage, ce qui limite encore une fois les possibilités d'accouplement. Par conséquent, les femelles doivent sélectionner leurs partenaires afin d'assurer un bagage génétique robuste à leur progéniture (Trivers, 1972).

L'ablation chirurgicale ou génétique (limitée aux VSN basaux) du VNO n'a pas d'incidence sur la capacité des femelles à distinguer et à montrer une préférence pour les signaux olfactifs volatils provenant de mâles intacts sur le plan gonadique (Keller et al., 2006 ; Lloyd-Thomas et Keverne, 1982 ; Oboti et al., 2014). Cependant, la préférence pour les odeurs urinaires non volatiles d'un mâle gonadiquement intact par rapport à un mâle castré ou à une femelle est perdue chez les femelles VNOx (Keller et al., 2006 ; Martínez-Ricós et al., 2008). Ainsi, comme chez les mâles, le MOS et l'AOS peuvent avoir des rôles complémentaires dans l'induction d'une préférence sexuelle olfactive (Baum et

Kelliher, 2009). En effet, une série d'attractifs chimiques ont été identifiés dans l'urine des mâles, certains détectés à la fois par le MOS et le AOS (Ishii et Touhara, 2018 ; Novotny, 2003). Une fois détectée, l'évaluation de l'urine du mâle permet à la femelle d'évaluer la fitness de l'émetteur. Dans une vision simpliste, les femelles recherchent un partenaire génétiquement riche et distant. Trois familles de peptides détectés par le VNO pourraient servir de tels indices : les peptides du MCH, les MUP et les ESP. L'expression de chacun de ces peptides est spécifique à la génétique des animaux (Boehm et Zufall, 2006 ; Kimoto et al., 2007 ; Logan et al., 2008), et tous sont détectés par les VSN basaux (Chamero et al., 2011 ; Hattori et al., 2017 ; Leinders-Zufall et al., 2004).

Les MUP sont particulièrement intéressants. Tout d'abord, leur combinaison dans l'urine est porteuse d'informations individuelles (Cheetham et al., 2007 ; Hurst et al., 2001 ; Kaur et al., 2014). Les femelles évaluent l'hétérozygotie génétique d'un partenaire potentiel, un marqueur de diversité génétique apportant un bénéfice, par la détection de ses MUPs (Thom et al., 2008). Ensuite, certaines MUPs isolées comme la Darcine (MUP20) peuvent induire une attraction de la femelle (Roberts et al., 2010). Les MUPs sont également des protéines porteuses, séquestrant ainsi des volatiles attractifs dans l'urine pour prolonger leur longévité (Hurst et al., 1998 ; Kwak et al., 2012 ; Sharrow et al., 2009). La signalisation par les MUP est, par conséquent, un outil puissant agissant comme un attracteur et un informateur. En dehors de la période ovulatoire de la femelle, un tel message n'est pas pertinent. Une étude élégante a montré un mécanisme permettant de réduire au silence les VSNs détectant les MUPs en dehors de la période ovulatoire et donc d'inhiber l'attractivité des MUPs (Dey et al., 2015). Des niveaux élevés de progestérone en dehors de la période ovulatoire inhibent PLCβ2 par phosphorylation, empêchant ainsi l'activation des VSNs par les MUPs. Cette étude a apporté un nouvel éclairage sur le potentiel de plasticité de la signalisation des VSN. Récemment, Eckstein et ses collègues ont mis en évidence l'existence d'un autre canal TRP dans le VNO, TRPM4 (Eckstein et al., 2020). De manière intéressante, l'expression de TRPM4 suit le cycle œstral de la femelle et est plus élevée pendant la période ovulatoire. Aucune régulation du comportement ou de la fonction des VNO n'a été associée à ce canal. Cependant, il serait un excellent candidat pour renforcer les signaux pertinents ou réduire au silence les signaux non pertinents pendant la période critique de la réceptivité sexuelle.

En plus d'être attirées par les odeurs des mâles, les femelles expriment un comportement spécifique en réponse aux montes des mâles pendant leur période ovulatoire, le comportement de lordose. L'appellation lordose provient de la posture adoptée par les femelles : elles cambrent le dos, écartent les pattes et lèvent la queue pour faciliter l'intromission du mâle (Figure 15). La réaction de lordose est déclenchée par la montée du mâle mais ne peut être induite en dehors de la période ovulatoire (Bonthuis et al., 2010). L'environnement hormonal est essentiel pour favoriser le comportement de lordose, mais les signaux olfactifs sont tout aussi importants. L'ablation chirurgicale ou génétique du VNO diminue l'expression des réponses de lordose, même sous des niveaux hormonaux contrôlés (Fraser et Shah, 2014 ; Hellier et al., 2018 ; Keller et al., 2006). De même, l'invalidation génétique restreinte à l'olfaction de Gαo diminue la réceptivité sexuelle des femelles

(Oboti et al., 2014). De plus, le peptide lacrymal ESP1 détecté par V2Rp5 est capable de promouvoir la réponse de lordose chez les femelles sexuellement naïves (Haga et al., 2010). Dans des conditions de laboratoire, les souris femelles démontrent de façon prévisible une augmentation graduelle de la réceptivité (Bonthuis et al., 2011 ; Thompson et Edwards, 1971). De manière intéressante, l'inhibition optogénétique aiguë des cellules mitrales de l'AOB diminue les réponses de lordose des femelles sexuellement expérimentées jusqu'aux niveaux basaux habituellement observés chez les femelles sexuellement naïves (McCarthy et al., 2017a), ce qui renforce l'importance de la signalisation voméronasale dans la réceptivité sexuelle.

2.1.2 Le cas curieux de la préférence sexuelle chez les souris Trpc2-/-.

Le modèle de souris knock-out pour TRPC2 (Trpc2-/-) a été largement utilisé pour étudier la fonction voméronasale, la régulation des comportements socio-sexuels, permettant de grandes découvertes (Boillat et al., 2015 ; Ferrero et al., 2013 ; Haga et al., 2010a ; Hasen et Gammie, 2009 ; Kimchi et al., 2007 ; Leypold et al., 2002 ; Papes et al., 2010 ; Stowers et al., 2002 ; Wu et al., 2014). les articles séminaux ont rapporté un comportement de monte indiscriminé chez les mâles Trpc2-/- (Leypold et al., 2002 ; Stowers et al., 2002), et une étude ultérieure a montré un comportement similaire chez les femelles Trpc2-/- (Kimchi et al., 2007). De plus, les souris Trpc2-/- des deux sexes produisent des USVs envers les congénères mâles et femelles (Kimchi et al., 2007 ; Stowers et al., 2002). Cette découverte a conduit les auteurs à émettre l'hypothèse que le VNO est essentiel pour la discrimination sexuelle et assure des comportements spécifiques au sex. Tout à fait passionnant mais discutable.

La première et principale objection provient des études sur les animaux VNOx. La seule étude dans laquelle un comportement de monte homosexuel a été rapporté chez les souris VNOx est la même que celle qui le montre chez les souris Trpc2-/- (Kimchi et al., 2007). De plus, les lignées de souris transgéniques présentant un déficit partiel de la signalisation du VNO ne montrent pas de comportement de monte indiscriminé (tableau 2) (Chamero et al., 2011 ; Kim et al., 2012 ; Norlin et al., 2003c ; Oboti et al., 2014 ; Del Punta et al., 2002). Deuxièmement, outre les VSN, l'expression de TRPC2 est rapportée dans les OSN (voir section 1.1.3.3) et le système nerveux en développement (Boisseau et al., 2009 ; Elg et al., 2007). Le modèle Trpc2-/- consiste en une délétion génétique germinale ; par conséquent, la fonction des MOE est affectée et le développement du cerveau peut être altéré. Troisièmement, comme mentionné dans la description de la signalisation voméronasale, des mécanismes indépendants de TRPC2 existent dans les VSN (voir section 1.4.2.3). Par conséquent, la détection voméronasale peut ne pas être entièrement abolie chez les souris Trpc2-/-. Enfin, Kimchi et ses collègues ont déclaré que puisque les femelles Trpc2-/- présentent un comportement de montage, les circuits neuronaux fonctionnels qui sous-tendent ce comportement existent dans le cerveau féminin et sont naturellement réprimés par les entrées voméronasales (Kimchi et al., 2007). Cette hypothèse contredit le rôle admis de l'environnement hormonal prénatal organisant les circuits cérébraux du

comportement sexuel masculin (Simerly, 2002). De plus, des études montrent que le traitement néonatal ou adulte avec des stéroïdes sexuels peut augmenter le comportement de monte chez les souris femelles (Manning et McGill, 1974 ; Wu et al., 2009). Ceci est particulièrement intéressant puisque les souris Trpc2-/- présentent des niveaux élevés de testostérone (Kimchi et al., 2007 ; Stowers et al., 2002) et qu'une étude a réussi à reproduire le phénotype des femelles Trpc2-/- en combinant ovariectomie, supplémentation en testostérone et ablation chirurgicale de la VNO (Martel et Baum, 2009). Pour toutes ces raisons, le comportement de monte indiscriminé des souris Trpc2-/- ne doit pas être considéré comme le strict reflet de l'absence de fonction du VNO.

Plusieurs laboratoires ont observé le même comportement (Fraser et Shah, 2014 ; Haga et al., 2010a ; Kim et al., 2012 ; Leypold et al., 2002 ; Stowers et al., 2002). En outre, Chalflin et ses collègues ont rétrocroisé leurs souris de laboratoire Trpc2-/- avec une souche de souris sauvages (Chalfin et al., 2014). Les témoins sauvages et de laboratoire présentent des comportements innés basaux différents, mais la mutation de TRPC2 induit le même effet sur le comportement de monte dans les deux souches. Reste encore la question de son explication. Leypold et ses collègues ont déjà émis la possibilité d'un comportement de déplacement (Leypold et al., 2002). La réaction de déplacement correspond à l'affichage d'un comportement particulier hors de son contexte en raison de pulsions conflictuelles. Ici, en raison de l'origine génétique du comportement de Trpc2-/-, Yu a proposé de parler plutôt de comportement néomorphique (Yu, 2015). Une façon de répondre à cette question serait de créer des modèles alternatifs de dysfonctionnement voméronasal complet ou partiel. Une délétion Cre inductible de TRPC2 à l'âge adulte permettrait d'éviter les effets potentiels sur le développement. Alternativement, une délétion de Gαi2 restreinte à l'olfaction permettrait d'obtenir des informations complémentaires correspondant à celles du modèle cGαo-/-. Enfin, la délétion combinée des gènes Gαi2 et Gαo dans les neurones olfactifs pourrait représenter un meilleur modèle de dysfonctionnement du VNO.

2.2 Comportements agressifs

L'agression peut être, en fait, un mécanisme de défense. La défense du territoire pour garder l'accès à la nourriture, aux partenaires d'accouplement et protéger la progéniture est cruciale pour la survie des individus. Le comportement agressif commence par une phase appétitive au cours de laquelle le résident investigue et intimide l'intrus, suivie d'une phase consommatoire comprenant une séquence d'attaques (Figure 16). L'agression est coûteuse ; elle exige un investissement énergétique élevé et fait courir à l'agresseur le risque d'être blessé. D'un autre côté, la décision d'attaquer doit être prise rapidement face à une menace potentielle. Ainsi, une détection olfactive précise et l'identification des congénères potentiellement dangereux sont cruciales.

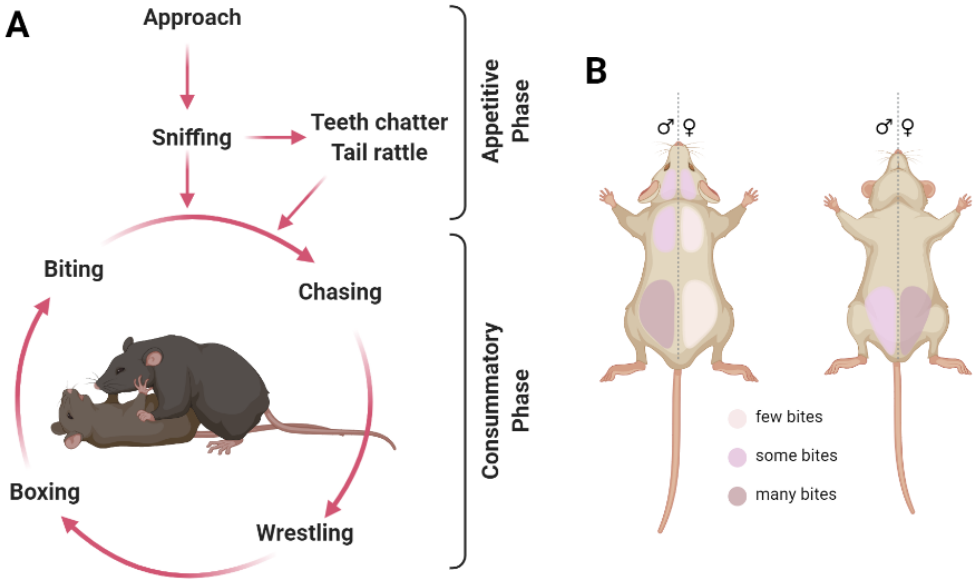

Figure 16 : Séquence du comportement agressif. A) L'agression est composée d'une phase appétitive (haut) et d'une phase de consommation (bas). Pendant la phase appétitive, le résident s'approche de l'intrus, l'examine pour déterminer sa nature et l'intimide. Suit alors une série d'attaques composées d'événements séquentiels de poursuite, de lutte, de coups et de morsure. B) Différence entre les sites d'attaque des mâles et des femelles. Les mâles fournissent de nombreuses morsures sur le dos de l'intrus, alors que les femelles attaquent surtout l'abdomen et la région anogénitale. Adapté de Hashikawa et al., 2018. Ce schéma est créé dans BioRender.com.

2.2.1 Agressivité territoriale

Dans les conditions naturelles, les souris mâles règnent sur un territoire et une ou plusieurs femelles. Dans les conditions de laboratoire, les mâles isolés considèrent leur cage comme leur territoire, et toute intrusion déclenche des réponses territoriales. La plus étudiée est l'agression offensive. Dans le paradigme comportemental résident/intrus, la souris résidente (un mâle isolé) défend son territoire en attaquant les intrus. Ni les mâles VNOx ni les mâles Trpc2-/- ne présentent d'agression envers les intrus, ce qui indique un rôle majeur du VNO dans le contrôle de l'agression territoriale (Clancy et Nobles, 1984 ; Leypold et al., 2002 ; Maruniak et al., 1986 ; Stowers et al., 2002 ; Wysocki et Lepri, 1991). Une étude ultérieure a montré que les VSN basaux Gαo-positifs sont essentiels pour exprimer un comportement agressif (Chamero et al., 2011).

Les composés chimiques favorisant l'agression sont sécrétés dans l'urine, et leur production est androgéno-dépendante (Mugford et Nowell, 1970). En effet, un intrus mâle castré n'est pas attaqué, mais imbiber son dos avec l'urine d'un mâle gonadiquement intact rétablit la réponse agressive du résident. Dans l'urine, plusieurs composés de faible ou haut poids moléculaire (LMW, HMW) peuvent susciter des attaques d'intensité similaire (Chamero et al., 2007, 2011 ; Kaur et al., 2014). Les MUP sont responsables de l'activité d'agression de la fraction HMW. Imbiber le dos d'un mâle castré avec des MUP synthétiques déclenche une réponse agressive, ce qui suggère que les MUP agissent par elles-mêmes comme des phéromones (Chamero et al., 2007). De manière intéressante, les mâles cGαo-/- ne parviennent pas à attaquer un intrus mâle castré imbibé avec la fraction d'urine contenant MUP

(Chamero et al., 2011). La détection de plusieurs petites molécules volatiles a été liée aux VSN apicaux, et les mâles Gαi2-/- présentent des comportements agressifs réduits (Leinders-Zufall et al., 2000 ; Norlin et al., 2003c). Dans l'ensemble, les données suggèrent que les VSN apicaux et basaux peuvent travailler de concert pour promouvoir l'agressivité. Gαo semble être un facteur plus critique pour initier le comportement mais la fonction de Gαi2 reste élusive.

En plus d'attaquer, les mâles territoriaux contremarquent les taches d'urine d'un intrus. Les signaux olfactifs sont suffisants pour provoquer la contremarque d'urine (Desjardins et al., 1973 ; Rich et Hurst, 1999), et les mâles VNOx et Trpc2-/- ne parviennent pas à contremarquer lorsqu'ils sont exposés à l'urine d'un mâle (Kaur et al., 2014 ; Maruniak et al., 1986 ; Wysocki et Lepri, 1991). Il est intéressant de noter que les mâles Trpc2-/- isolés contremarquent en présence d'un intrus (Leypold et al., 2002), ce qui indique que des signaux non olfactifs sont également utilisés pour induire la contremarque. Les mâles hébergés en groupe utilisent également la contremarque pour affirmer leur statut au sein du groupe. Les mâles dominants contremarquent alors que les subordonnés ne le font pas (Desjardins et al., 1973). Il est intéressant de noter que, lorsqu'ils sont hébergés en groupe, les mâles Trpc2-/- continuent de contremarquer, ce qui suggère qu'ils ne parviennent pas à établir des relations de dominance territoriale puisqu'ils ne présentent pas d'interactions agressives (Leypold et al., 2002). Cependant, il n'existe pas d'évaluation stricte de la dynamique hiérarchique au sein des groupes de mâles Trpc2-/-. Les mâles cGαi2-/- sont capables de former des groupes stables (Pallé et al., 2020), ce qui suggère que si une désorganisation de la hiérarchie du groupe existe chez les mâles Trpc2-/-, elle devrait résulter de la perte de la fonction des VSN basaux. Malheureusement, la hiérarchie des groupes chez les mâles cGαo-/- n'a pas été évaluée.

2.2.2 Agressivité maternelle

Les souris femelles de laboratoire présentent rarement des comportements agressifs, sauf lorsqu'elles allaitent. Au cours de la première semaine suivant la mise bas, les femelles défendent ardemment leur progéniture. Comparée à l'agression territoriale des mâles, l'agression maternelle des femelles est beaucoup plus dangereuse pour l'intrus puisque les femelles allaitantes attaquent directement les régions vulnérables de l'intrus, comme l'abdomen ou la région anogénitale (Figure 16) (Parmigiani et al., 1988 ; Unger et al., 2015a). La manifestation de l'agression maternelle est sous un contrôle complexe de facteurs hormonaux et sensoriels internes, mais les signaux olfactifs émis par l'intrus sont cruciaux pour déclencher la réponse comportementale (Martín-Sánchez et al., 2015).

Là encore, les entrées olfactives voméronasales jouent un rôle essentiel dans la perception des signaux induisant une agression. Les femelles allaitantes VNOx et Trpc2-/- n'attaquent pas un intrus (Bean et Wysocki, 1989 ; Hasen et Gammie, 2009 ; Kimchi et al., 2007 ; Leypold et al., 2002). L'implication différentielle des VSN basaux et apicaux dans ce processus n'est pas claire. Chamero et ses collègues ont montré que les VSN basaux sont essentiels puisque pratiquement aucune des femelles

cGαo-/- n'attaque un intrus (Chamero et al., 2011). Inversement, l'ablation germinale de Gαi2 ou la délétion d'un groupe de gènes V1R diminue l'agression maternelle (Norlin et al., 2003c ; Del Punta et al., 2002). Ainsi, les deux systèmes peuvent coopérer pour promouvoir l'agression maternelle, et, comme pour l'agression territoriale, les VSNs exprimant Gαo semblent plus critiques pour initier le comportement.

On sait moins de choses sur les substances chimiques induisant l'agression chez les femelles en lactation. Des études suggèrent que les mères sont plus susceptibles d'attaquer un intrus mâle intact qu'un mâle castré ou une femelle (Parmigiani et al., 1988 ; Rosenson et Asheroff, 1975). Les femelles allaitantes attaquent un intrus mâle castré imbibé de fractions d'urine LMW ou HMW, ce qui suggère une fois de plus que ces deux fractions contiennent des substances chimiques qui favorisent l'agression (Chamero et al., 2011). De manière intéressante, l'absence de réponse agressive chez les femelles cGαo-/- est observée quel que soit l'intrus, soutenant un rôle plus important de Gαo pour induire une réponse agressive (Chamero et al., 2011). À ce jour, une seule phéromone a été testée pour son potentiel à favoriser l'agression chez les femelles allaitantes, la Darcine (Martín-Sánchez et al., 2015), qui suscite des niveaux d'agression équivalents à l'urine de mâle intact.

2.2.3 Infanticide

Le comportement d'infanticide est un comportement bien connu mais peu étudié, principalement exprimé par les souris mâles vierges. Sa valeur évolutive n'est pas claire, mais certains suggèrent que les mâles ont intérêt à tuer des jeunes non apparentés pour supprimer l'investissement parental dans une progéniture qu'ils n'ont pas engendrée et restaurer la capacité des mères à être fécondées (Labov et al., 1985 ; Vom Saal et Howard, 1982). Le rôle du VNO dans l'infanticide a été démontré pour la première fois chez le rat (Mennella et Moltz, 1988). Plus tard, il a également été démontré que les souris mâles VNOx et Trpc2-/- ne tuent pas les petits étrangers (Nakahara et al., 2016 ; Tachikawa et al., 2013 ; Wu et al., 2014). L'exposition aux petits active les parties antérieure et postérieure de l'AOB, ce qui suggère que les couches basales et apicales des VSNs participent à la détection des signaux des petits, bien que l'activation soit plus importante dans l'AOB antérieur (Tachikawa et al., 2013). L'implication de chaque couche VSNs est inconnue puisque le comportement infanticide n'a pas été testé dans les modèles de souris cGαo-/- et Gαi2-/-.

Deux études ont investigué plus profondément la détection aiguë des signaux olfactifs des petits. Tout d'abord, Nakahara et ses collègues ont montré que le récepteur olfactif ectopique Olfr692, l'un des rares ORs exprimés dans le VNO, détecte spécifiquement les signaux des petits (Nakahara et al., 2016). Ils ont montré que l'extraction de l'odeur des petits par incubation dans un tampon induit toujours l'activation des VSNs Olfr692-positifs. De manière intéressante, ils ont constaté que l'exposition des petits active Olfr692 chez les mâles mais pas chez les femelles, ce qui indique un rôle de ce récepteur dans l'infanticide. Malheureusement, ils n'ont pas fourni de preuve fonctionnelle de

cette implication. Deuxièmement, Isogai et ses collègues ont mis en évidence les VRs activés par les petits par un criblage basé sur l'hybridation *in situ* (Isogai et al., 2018). Ils ont identifié 5 VRs potentiellement activées par les signaux des petits : V1Rc1, V1Rc30, V2R88, V2R65, et V2R122/123. Cependant, aucun de ces récepteurs n'était exclusivement activé par les odeurs de petits. Ils ont concentré leur attention sur V2R65 et V2R88, auxquels ils ont trouvé un ligand, la protéine C de la glande submandibulaire et l'hémoglobine, respectivement. L'ablation génétique d'un de ces 2 VRs a un léger impact sur l'infanticide. Par contre, une mutation combinée réduit significativement l'infanticide. Pendant la rédaction de ce travail, une étude ingénieuse a vu le jour dans laquelle le volatolome de petits a été extrait et analysé (Lacalle-Bergeron et al., 2021). Leurs données mettent en évidence 11 composants dont la concentration diminue après une semaine d'âge, et qui sont donc potentiellement des phéromones spécifiques aux petits. L'un d'entre eux, le durène, est déjà connu pour être détecté par le VNO et pourrait être impliqué dans le déclenchement d'infanticides (Sam et al., 2001).

2.3 Comportements parentaux

Le comportement parental augmente la probabilité de survie de la progéniture. Chez les rongeurs, plusieurs comportements parentaux sont décrits, notamment l'allaitement, la récupération, le toilettage, la construction du nid et la défense des petits. Chez les souris, les mères et les pères participent tous deux à ces soins, à l'exception de la lactation assurée uniquement par les femelles. De multiples modalités sensorielles déclenchent la réponse parentale, et l'olfaction est l'une des plus importantes chez les souris.

Chez les femelles, nous avons vu dans la section précédente que la défense des petits (agression maternelle) repose sur l'organe voméronasal ; cependant, d'autres comportements parentaux dépendent plutôt principalement de la signalisation du MOS. Les premières études n'ont montré aucun effet de l'ablation chirurgicale du VNO sur la survie de la progéniture et le temps d'interaction des mères avec leurs petits (Bean et Wysocki, 1989 ; Lepri et al., 1985). En revanche, la lésion chimique du MOE a un impact sur la survie des petits et réduit les soins prodigués par les mères (Seegal et Denenberg, 1974 ; Vandenbergh, 1973), et l'ablation génétique de la voie de signalisation des OSNs réduit les comportements parentaux (Belluscio et al., 1998 ; Fraser et Shah, 2014 ; Wang et Storm, 2011). Pourtant, l'implication du VNO dans les comportements parentaux ne doit pas être négligée. L'exposition à des petits active les VSN chez les femelles vierges et les mères (Isogai et al., 2018 ; Navarro-Moreno et al., 2020). L'évaluation longitudinale du comportement maternel sur 14 jours a révélé une diminution progressive de l'investissement des femelles Trpc2-/- envers leurs petits (Kimchi et al., 2007). Ce déficit a pu être manqué chez les femelles VNOx puisque les tests n'ont été effectués que pendant la période post-partum précoce. On pourrait émettre l'hypothèse que l'environnement hormonal particulier qui accompagne la parturition masque l'implication potentielle du VNO dans la parentalité. Les femelles vierges sont naturellement maternelles et s'occupent d'un petit étranger, mais

des expositions répétées au petits augmentent la qualité des soins (par exemple, une latence plus courte pour récupérer) (Stolzenberg et Rissman, 2011). En outre, ce phénomène est indépendant du statut hormonal de la femelle (Stolzenberg et Rissman, 2011). Ainsi, la détection des signaux des petits par le VNO pourrait être impliquée dans la stimulation du comportement parental en dehors de la période péripartum, un phénomène nécessaire au maintien de la parentalité.

Les souris mâles vierges sont infanticides, mais ce comportement disparaît progressivement lorsqu'elles cohabitent avec des femelles gestantes (Vom Saal, 1985 ; Tachikawa et al., 2013). L'activation du VNO par les odoeurs des petits diminue également au fil du temps passé avec une femelle et cesse chez les pères (Nakahara et al., 2020a ; Tachikawa et al., 2013). Une possibilité est que le VNO subisse un remodelage après l'accouplement, réduisant au silence sa réponse aux signaux olfactifs des petits afin d'inhiber le comportement d'infanticide et de promouvoir le rôle parental. Soutenant cette hypothèse, les mâles vierges Trpc2-/- sont parentaux lorsqu'ils sont exposés à un nouveau-né étranger (Wu et al., 2014). Malheureusement, aucune étude n'a examiné le contrôle voméronasal des comportements parentaux de la souris chez les pères. Les pères redeviennent infanticides après le sevrage de leurs petits (Vom Saal, 1985). Ainsi, l'expression du comportement parental chez les souris mâles semble étroitement contrôlée, peut-être par l'exposition à une femelle enceinte. Le processus exact par lequel la sensibilité de la VNO aux signaux des petits est modifiée, ainsi que l'étendue de cette modification, sont encore inconnus. L'accouplement induit la sécrétion d'ocytocine (Waldherr et Neumann, 2007), et le traitement à l'ocytocine inhibe l'activation du VNO par les signaux des petits (Nakahara et al., 2020). Ainsi, il a été proposé que l'ocytocine puisse être le messager d'une progéniture à venir. En agissant sur la sensibilité des VNO, puisque les VSN expriment le récepteur de l'ocytocine (Nakahara et al., 2020), elle peut permettre l'expression du comportement parental. Cependant, il est possible que les comportements parentaux et infanticides soient plus que les deux faces d'une même pièce. Chacun peut avoir besoin de son mécanisme d'activation-inhibition. Ainsi, une étude a montré que l'inhibition de la désacétylation des histones (libérant la chromatine et favorisant l'expression génétique) augmentait l'expression des comportements paternels chez les mâles non agressifs sans modifier l'expression de l'infanticide chez les mâles agressifs (Mayer et al., 2019). Cependant, on ne sait rien des signaux voméronasaux potentiels stimulant les comportements paternels.

2.4 Comportements d'évitement

L'un des principaux coûts des comportements sociaux est le risque accru d'exposition aux dangers. Les rongeurs sont souvent des proies, et le fait de parcourir leur territoire pour trouver de la nourriture ou s'accoupler expose les souris au risque de rencontrer des prédateurs. Un autre défi quotidien est l'exposition aux parasites et aux infections lors des interactions sociales avec les congénères. Les espèces sociales ont développé divers mécanismes comportementaux et réponses pour minimiser leur exposition potentielle aux menaces tout en maintenant leurs activités sociales. Le

système olfactif est également crucial dans ces processus en codant la valence des odeurs environnantes et en faisant ainsi pencher la balance vers l'attraction ou l'aversion (Li et Liberles, 2015).

2.4.1 Évitement des prédateurs

Les proies et les prédateurs partagent leur environnement, et tous deux y libèrent des substances sémiochimiques pour communiquer. Au cours de l'évolution, les signaux des prédateurs ont été incorporés dans la mémoire des proies et induisent naturellement des comportements d'évitement et de défense. Ces substances chimiques interspécifiques sont appelées kairomones. Plusieurs taxons prédatent fortement les souris, comme les mammifères carnivores (par exemple, les mustélidés, les félidés ou les canidés), les rapaces (par exemple, les faucons et les hiboux), les reptiles ou les araignées. Plusieurs comportements sont associés à l'évitement des prédateurs, tels que l'évaluation du risque, l'immobilisation, ou la fuite active, et tous peuvent être induits par l'exposition à la seule odeur du prédateur (Kavaliers et Choleris, 2001). La détection des kairomones n'est pas limitée à un seul sous-système olfactif, mais certains semblent dédiés à transmettre des informations limitées à une classe de prédateurs (Pérez-Gómez et al., 2015 ; Takahashi, 2014).

En raison de son implication dans la détection des phéromones, on a rapidement pensé que le système voméronasal était le médiateur de la détection des kairomones. En effet, les souris VNOx n'évitent pas les odeurs de chat (Samuelsen et Meredith, 2009). Plus tard, le VNO a également été associé à l'évitement des rats et des serpents (Papes et al., 2010). Isogai et ses collègues ont ajouté les oiseaux de proie, les mustélidés et autres carnivores à la liste des prédateurs détectés par le VNO (Isogai et al., 2011). De manière intéressante, cette étude montre que les VRs activés par un type de prédateur sont regroupés, certains prédateurs n'activant même que les VSN basaux ou apicaux. En accord avec ces résultats, l'ablation de la fonction des VSN basaux abolit l'évitement pour les odeurs de fourrure de chat (Pérez-Gómez et al., 2015).

Des kairomones spécifiques à certaines espèces ont été identifiées. Les chercheurs se sont tournés vers les MUP, leurs orthologues chez les prédateurs, en se basant sur l'activité phéromonale de cette classe de molécules. Il a ainsi été prouvé qu'une MUP de rat, MUP-Rn13, et une lipocaline de type MUP de chat, Feld4, agissaient comme des kairomones et entraînaient l'évitement via le VNO (Papes et al., 2010 ; Pérez-Gómez et al., 2015). Les urines des mammifères carnivores sont enrichies en amines biogènes en raison de la consommation de viande. L'une d'elles, la 2-phényléthylamine (PEA), active précisément TAAR4 et induit l'évitement (Dewan et al., 2013 ; Ferrero et al., 2011). Les TAARs sont principalement exprimés dans la MOE, certains sont retrouvés dans la GG, mais aucun n'est décrit dans le VNO. Néanmoins, l'urine des mammifères carnivores active le VNO, ce qui suggère que plusieurs composés urinaires pourraient être porteurs d'indices d'évitement (Ben-Shaul et al., 2010 ; Isogai et al., 2011a). Deux composés volatils, le 2-propylthiétane (2-PT) et le 2,5-dihydro-2,4,5-triméthylthiazole (TMT), respectivement présents dans la glande anale de la hermine et les excréments

du renard, activent des neurones dédiés dans le GG et induisent l'évitement (Brechbühl et al., 2013 ; Pérez-Gómez et al., 2015). Le 2-PT n'a pas d'autre détecteur connu, mais le TMT est également détecté par le MOE mais pas par le VNO (Kobayakawa et al., 2007 ; Papes et al., 2010 ; Saito et al., 2017).

Après avoir détecté une menace potentielle, les rongeurs peuvent avertir leur congénère en sécrétant des phéromones d'alarme (Rottman et Snowdown, 1972). Il est intéressant de noter que certaines phéromones d'alarme, comme le 2-sec-butyl-4,5-dihydrothiazole (SBT), présentent des similitudes structurelles avec les kairomones des prédateurs et sont détectées par le GG et le MOE (Brechbühl et al., 2008, 2013 ; Matsuo et al., 2015). Ainsi, des voies génériques de signalisation du danger peuvent exister, bien que les voies de détection olfactive spécifique ne soient pas totalement identifiées.

2.4.2 Évitement des agents pathogènes

Les animaux sauvages sont fréquemment exposés à divers agents pathogènes, notamment des bactéries, des virus et des vers parasites. Pour contrer cette menace permanente, les animaux ont développé plusieurs mécanismes de défense et d'évitement, de résistance et de tolérance aux agents pathogènes (Rivas et al., 2014). Les souris sont macrosmatiques, elles détectent les maladies de leurs congénères par l'odeur et les évitent activement pour éviter la contagion (Kavaliers et al., 2005). La reconnaissance des congénères parasités intervient également dans la sélection des partenaires, les femelles préférant copuler avec des mâles sains (Kavaliers, 1995).

Le VNO a été proposé comme médiateur de la reconnaissance d'un congénère malade. En effet, les souris VNOx et Trpc2-/- n'évitent pas une souris traitée au LPS (Boillat et al., 2015). L'injection de lipopolysaccharides bactériens (LPS) est un protocole standard pour induire un état inflammatoire général, mimant ainsi une infection pathogène. Les mâles VNOx perdent également leur préférence naturelle pour s'accoupler avec une femelle saine lorsqu'ils ont le choix avec une femelle traitée au LPS (Kwon et al., 2021). L'urine d'animaux traités au LPS est suffisante pour induire l'évitement (Boillat et al., 2015 ; Kwon et al., 2021), mais la modification de l'urine par le traitement au LPS est inconnue. Certains LPS sont directement excrétés dans les urines (Kleine et al., 1985). Les LPS se lient au récepteur Toll-like 4 (TLR-4), dont l'ARNm a été détecté après séquençage des VSN (Ibarra-Soria et al., 2014). Ainsi, une détection directe au niveau des VSNs pourrait avoir lieu. Deux études ont mis en évidence deux composés distincts de l'urine traitée au LPS, le SBT et le diméthyl sulfone (Millet et al., 2018, 2021). De manière surprenante, le SBT est présent dans l'urine de souris et a été proposé comme une phéromone d'alarme (Brechbühl et al., 2013), et le diméthyl sulfone est présent dans les urines de différents prédateurs (Apps et al., 2012 ; Burger et al., 2006). Cela suggère que la maladie pourrait être détectée par des phéromones d'alarme ou des analogues aux signaux des prédateurs, ce qui implique que l'évitement des maladies et des prédateurs peut résulter de processus similaires.

Les VNO expriment des FPRs, récepteurs naturels pour les peptides bactériens (Bufe et Zufall, 2016). Les FPRs voméronasaux, à l'exception du FPR3, ne répondent pas aux ligands FPRs immunitaires classiques, ce qui suggère une néofonctionnalisation de ces récepteurs (Bufe et al., 2012). Bufe et ses collègues ont montré que le FPR3, le seul FPR exprimé dans les VSN basaux (voir section 1.4.2.4), présente une grande sélectivité pour les protéines associées à la virulence bactérienne MgrB (Bufe et al., 2019). De plus, l'ajout du peptide MgrB dans l'urine des femelles induit une aversion et la délétion génétique de FPR3 ou Gαo la supprime, ce qui suggère que FPR3 est impliqué dans l'évitement des pathogènes. De manière intéressante, la délétion du FPR3 n'abolit pas l'évitement des souris traitées par le LPS. L'étude de l'implication des FPR apicaux dans la détection de l'urine LPS ou dans l'évitement des congénères malades serait particulièrement intéressante.

Maintenant que le lecteur est familiarisé avec les comportements socio-sexuels des souris et la manière dont le système voméronasal les contrôle, je vais décrire la voie neuronale générale qui les soutient.

3 Contrôle neuronal des comportements socio-sexuels

L'expression d'une réaction comportementale adaptée survient après l'intégration neuronale des informations sensorielles avec les états sociaux et internes, déclenchant la décision de l'action motrice (Figure 17). Ce travail se concentre sur les indices sensoriels olfactifs, mais d'autres modalités sensorielles (auditives, visuelles et somatosensorielles) sont également compilées. Toutes ces informations sont mises en balance avec l'état de l'animal. L'expérience sociale est particulièrement importante pour le comportement social, car elle accélère le processus de décision (par exemple, un mâle ayant une expérience sexuelle commence plus rapidement à avoir des rapports sexuels). En outre, l'état neuroendocrinien de l'animal favorise ou inhibe l'expression de certaines réponses comportementales (par exemple, une femelle ne s'accouple que pendant sa période d'ovulation).

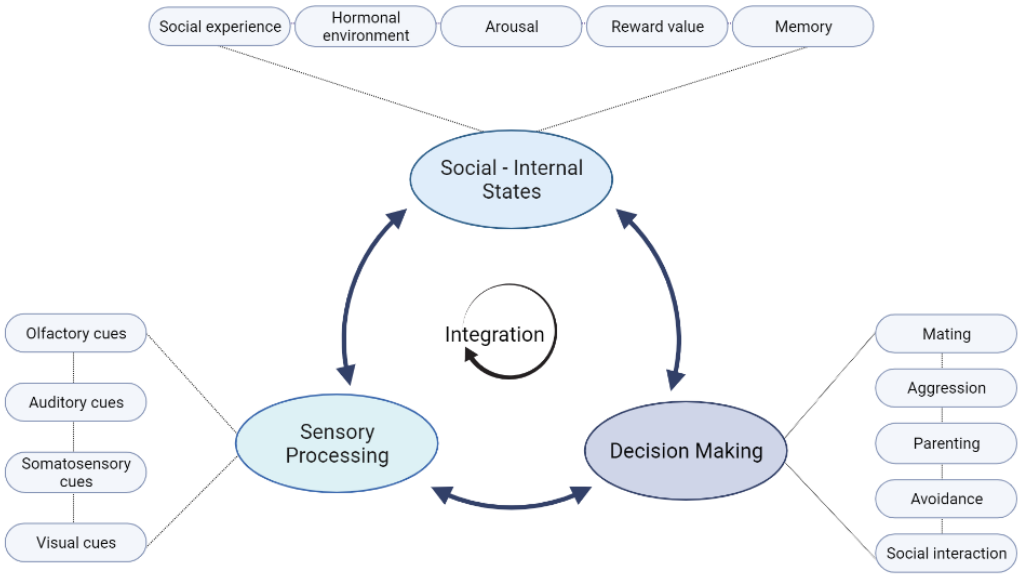

Figure 17 : Mécanisme de traitement sensoriel neuronal et d'intégration aux décisions socio-comportementales. Adapté de Chen et Hong, 2018. *Ce schéma est créé dans BioRender.com.*

Le MOB se projette vers les cortex olfactifs, tandis que l'AOB envoie des informations vers l'amygdale voméronasale, qui est composée de la partie postérieure du noyau du lit de la strie terminalis (BNSTp), de l'amygdale médiane (MeA) et de l'amygdale corticale postéromédiale (CoApm) (Figure 18). La ségrégation apparente entre les cortex olfactifs et l'amygdale voméronasale suggère un traitement différentiel de l'information, mais, comme le MOS et l'AOS coopèrent pour détecter l'odorant et déclencher des réponses comportementales, les informations qu'ils transportent respectivement sont intégrées ensemble. Dans l'AOS, les projections apicales et basales des VSN sont initialement séparées. Les VSN apicaux se projettent vers l' aAOB et atteignent ensuite la BNSTp, la CoApm et la MeA, tandis que les VSN basaux envoient leurs axones vers le pAOB qui n'est connectée qu'avec la CoApm et la MeA (Gutiérrez-Castellanos et al., 2014 ; Mohedano-Moriano et al., 2007). Ces régions sont néanmoins connectées entre elles. On ne sait pas si la ségrégation des entrées

V1Rs/Gαi2 et V2Rs/Gαo est maintenue une fois arrivée dans l'amygdale voméronasale. Cependant, les informations transportées par la voie de signalisation V1Rs/Gαi2 peuvent subir un traitement spécifique dans la BNSTp, avant d'être intégrées aux entrées V2Rs/Gαo dans la MeA. Le site de convergence des informations MOS et AOS n'est pas clair non plus, mais la MeA semble centrale puisque l'amygdale corticale postérolatérale (CoApl, qui fait partie des cortex olfactifs) se projette vers la MeA (Canteras et al., 1992).

Les comportements socio-sexuels sont sexuellement dimorphiques ; par conséquent, il existe des dimorphismes sexuels parmi les régions cérébrales qui les contrôlent. Des décennies d'études de lésions et de stimulations chez les rongeurs ont révélé un ensemble limité et chevauchant de régions hypothalamiques et limbiques du cerveau contrôlant les comportements sociaux (figure 18). Parmi celles-ci, la MeA, la BNST, l'aire préoptique médiane (MPOA) et le noyau hypothalamique ventromédian (VMH) présentent un intérêt particulier. Dans ces noyaux, des populations cellulaires distinctes contrôlent différents aspects des comportements socio-sexuels (Wei et al., 2021). Un défi majeur à relever est d'attribuer une fonction précise à chacun de ces noyaux et populations de neurones dans la boucle interprétation - intégration - décision (Figure 17). Le traitement des entrées voméronasales se produit très probablement au niveau de l'amygdale médiane (Raam et Hong, 2021) et l'intégration des états sociaux et internes peut se produire tout au long du circuit, depuis les VSN (Dey et al., 2015 ; Oboti et al., 2015) jusqu'au cerveau (Wei et al., 2021). En ce qui concerne l'aire de décision, de nombreuses études montrent que la stimulation d'un des noyaux ou d'une des populations de neurones d'une voie cérébrale dédiée au comportement, même ceux très en amont, peut suffire à déclencher le schéma moteur correspondant (Raam et Hong, 2021). Ici, je me concentrerai sur les noyaux membres de l'amygdale voméronasale et mentionnerai les zones en aval lorsque cela sera nécessaire.

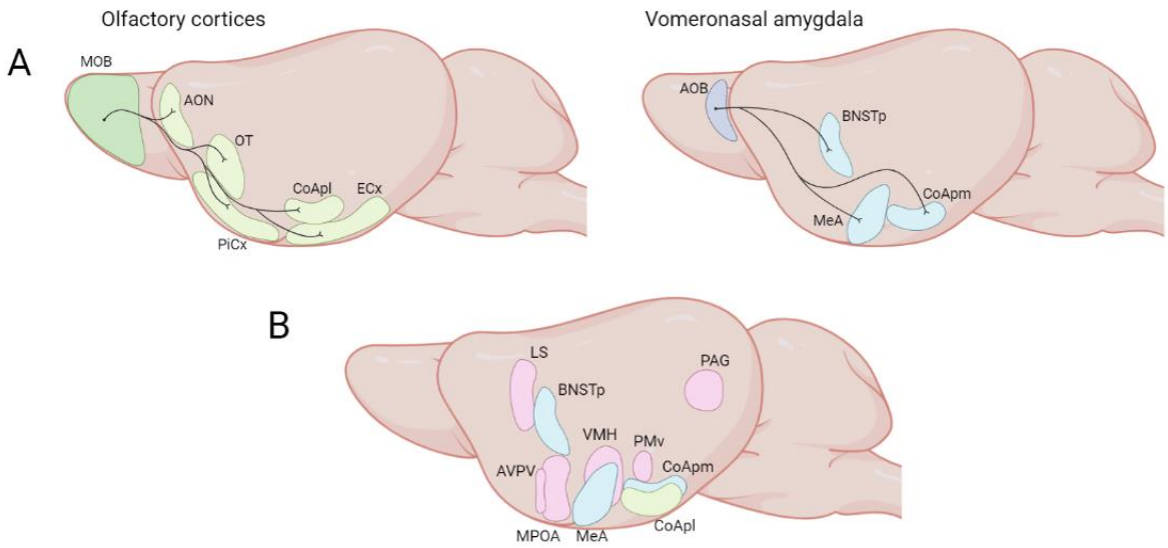

Figure 18 : Structures neuronales impliquées dans le traitement olfactif et les réponses comportementales. A) Le MOB se projette vers les cortex olfactifs (gauche), composés du noyau olfactif antérieur (AON), du tubercule olfactif (OT), du cortex piriforme (PiCx), de l'amygdale corticale postérolatérale (CoApl) et du cortex entorhinal (ECx). L'AOB se projette vers l'amygdale voméronasale (à droite), composée de la partie postérieure du noyau du lit de la strie terminale (BNSTp), de l'amygdale médiane (MeA) et de l'amygdale corticale postéromédiale (CoApm). B) Principaux noyaux cérébraux impliqués dans les réponses comportementales. Les noyaux bleus appartiennent à l'amygdale voméronasale et les verts aux cortex olfactifs. LS : septum latéral, AVPV : noyau périventriculaire antéroventral, MPOA : aire préoptique médiale, VMH : noyau hypothalamique ventromédial, PMv : noyau prémammillaire ventral, PAG : aire grise périaqueducale. Ce schéma a été créé avec BioRender.com.

3.1 Circuits neuronaux des comportements sexuels

3.1.1 Codage du sexe par les informations voméronasales

Avant de s'engager dans une interaction sociale, il faut d'abord déterminer l'identité de la personne rencontrée, notamment son sexe, car il conditionne le type de réponse comportementale à déclencher (par exemple, accouplement versus agression). Pour comprendre comment les informations sensorielles sont intégrées, il faut rappeler que les cerveaux masculins et féminins sont organisés par les stéroïdes sexuels au cours du développement et de la maturation, permettant ainsi l'expression à l'âge adulte de comportements sexuellement dimorphiques (Bakker, 2018). En bref, le cerveau masculin subit une masculinisation lors du pic périnatal de testostérone, tandis que le cerveau féminin est féminisé pendant la période péripubertaire par les œstrogènes ovariens. Les dimorphismes sexuels de la taille des noyaux cérébraux, de l'expression des neuropeptides et de la connectivité sont donc établis de façon permanente. Il convient de mentionner que les répertoires de VRs masculins et féminins sont relativement similaires, à quelques exceptions près (Van der Linden et al., 2018). Par exemple, le VNO féminin est enrichi en V2Rp5, le récepteur du peptide ESP1 stimulant la lordose, et le VNO masculin contient davantage de V1Rj2, le récepteur des œstrogènes sulfatés urinaires induits par l'ovulation.

Le schéma de réponse du message arrivant au niveau de l'AOB semble essentiellement similaire chez les mâles et les femelles (Ben-Shaul et al., 2010 ; Luo, 2003). Si et comment le codage se produit au niveau de l'AOB n'est pas clair, mais l'AOB-MCL forme des microcircuits synchrones, ce qui suggère fortement un rôle dans le traitement de l'information (Tsitoura et al., 2020). En outre, il pourrait exister un dimorphisme sexuel dans la fonction de l'AOB puisqu'une étude récente a signalé une projection descendante spécifique aux mâles de la MeA vers l'AOB (Inbar et al., 2021). On ignore si cette connexion module ou non le signal, mais on peut spéculer qu'elle façonne l'information, activant ensuite le circuit dédié à la réponse comportementale appropriée.

En aval de l'AOB, la MeA reçoit en grande partie des entrées glutamatergiques de l'AOB-MCL (Mohedano-Moriano et al., 2007). La MeA est une structure hétérogène avec une organisation tripartite : la MeA antérieure (MeAa), la MeA postérodorsale (MeApd), et la MeA postéroventrale (MeApv). La MeApd et la MeApv se distinguent en outre par des marqueurs moléculaires : la MeApv contient principalement des neurones glutamatergiques, tandis que la plupart des neurones de la MeApd sont GABAergiques et expriment l'aromatase (Aro, l'enzyme qui transforme la testostérone en estradiol), les récepteurs des androgènes et de la progestérone (AR et PR) (Bian et al, 2008 ; Juntti et al., 2010 ; Keshavarzi et al., 2014 ; Wu et al., 2009 ; Yang et al., 2013a). La MeA est également enrichie en neurones exprimant l'ocytocine (Oxt), dont il a été démontré très tôt qu'ils sont nécessaires à la reconnaissance sociale (Choleris et al., 2007 ; Ferguson et al., 2001). Au sein de la MeA, la stimulation sociale induit l'activation des neurones d'une manière spécifique au sexe (Bergan et al., 2014). La carte d'activation des mâles est biaisée vers les signaux féminins, tandis que la carte des femelles est biaisée vers les signaux masculins. De plus, l'établissement de ces cartes est organisé par les stéroïdes sexuels néonataux et nécessite l'activation des neurones MeApd exprimant Aro et Oxt chez les mâles uniquement (Bergan et al., 2014 ; Yao et al., 2017). Ainsi, la MeA est probablement un centre d'intégration des indices associés au sexe avec leur valeur comportementale. De manière intéressante, le séquençage de l'ARN unicellulaire de la MeApd n'a pas révélé de dimorphisme sexuel dans les populations cellulaires exprimant Aro ou Oxt (Chen et al., 2019). Ainsi, l'activation différentielle de ces neurones chez les mâles et les femelles découle plutôt de propriétés physiologiques intracellulaires différentielles ou de différences de câblage.

L'expérience sociale et sexuelle façonne la carte d'activation de la MeA (Li et al., 2017). Les mâles et les femelles sexuellement naïfs présentent des schémas d'activation similaires, et des différences apparaissent après une expérience sexuelle. Le BNSTp montre également une activation spécifique au sexe après une stimulation masculine ou féminine, notamment une activité plus élevée dans les neurones exprimant Aro lors de l'exposition à des femelles chez les mâles (Bayless et al., 2019). Cependant, contrairement à la MeA, l'activation du BNSTp est déjà sexuellement dimorphique chez les animaux sexuellement naïfs. Bayless et ses collègues ont proposé que les neurones BNSTp puissent coder le sexe d'un congénère, tandis que le MeA définit la façon de réagir à ce sexe, un processus façonné par l'expérience. Les mâles Trpc2-/- présentent une activation similaire des neurones

Aro-BNSTp après une exposition à un mâle ou une femelle, ce qui suggère que les entrées voméronasales transportent des informations supplémentaires définissant le sexe (Bayless et al., 2019). En leur absence, une activation égale des neurones Aro-BNSTp pourrait entraîner un comportement de monte indiscriminé. La source de ces entrées voméronasales est inconnue, mais le BNSTp ne reçoit que des informations directes de l'aAOB (Mohedano-Moriano et al., 2007), ce qui indique que la signalisation V1Rs/Gαi2 est le médiateur des signaux associés au sexe. L'activation du BNSTp pourrait également résulter d'entrées voméronasales indirectes provenant des VSN apicaux et basaux transitant par la MeA.

3.1.2 Circuit neuronal du comportement sexuel mâle

Nous avons vu que MeA et BNSTp, en particulier les neurones Aro-positifs, sont nécessaires pour renforcer les signaux de femelles dans le cerveau des mâles. Il est intéressant de noter que l'ablation des cellules BNSTp-Aro, mais pas des cellules MeApd-Aro, inhibe le comportement sexuel mâle (Bayless et al., 2019 ; Unger et al., 2015b). Le BNST est fortement interconnectée avec l'aire préoptique médiane (MPOA), une structure clé dans le comportement sexuel mâle (Hull et Dominguez, 2019). L'action des stéroïdes sexuels dans cette structure est primordiale pour permettre la monte (Sano et al., 2013 ; Wei et al., 2018), en plus d'autres neuropeptides (Hull et Dominguez, 2019). Le rôle de la signalisation de la dopamine est particulièrement intéressant. Les signaux sexuels sont hautement récompensant, et les structures associées au système de la récompense sont connectées à la MPOA (Paredes, 2009). Une étude récente a révélé que la libération de dopamine dans la MPOA stimule l'intérêt des mâles pour l'accouplement pendant plusieurs minutes (Zhang et al., 2021). La source de dopamine est constituée par les neurones à tyrosine-hydroxylase (TH) du noyau périventriculaire antéroventral (AVPV), une sous-structure de l'aire préoptique. Les auteurs n'ont pas fourni de lien avec le système olfactif, mais les neurones AVPV-TH des mâles sont activés par les signaux de femelles, et non par les signaux de mâles (Taziaux et Bakker, 2015), suggérant que ce mécanisme appartient au processus de transformation des signaux olfactifs en une décision comportementale. La stimulation optogénétique des neurones AOB-MCL suite à un contact nasal avec une femelle augmente l'occurrence de l'intromission (Kunkhyen et al., 2017), soutenant l'idée que les signaux voméronasaux stimulent le circuit neuronal du comportement sexuel. D'autres structures complètent le circuit, comme le VMH et la zone grise périaqueducale (PAG). La figure 19 montre un circuit potentiel soutenant le comportement sexuel mâle proposé par Wei et ses collègues (Wei et al., 2021).

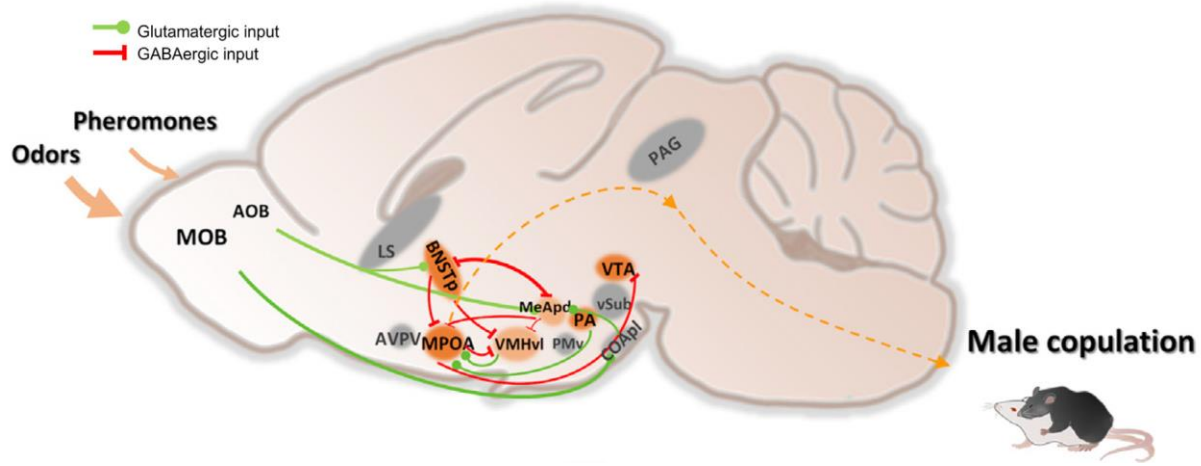

Figure 19 : Circuit neuronal du comportement sexuel masculin. Les lignes pleines indiquent les voies connues qui sont impliquées dans la médiation du comportement. Les lignes pointillées indiquent les voies potentielles à explorer davantage. Les régions orange favorisent le comportement, l'orange clair indique les régions qui jouent un rôle mineur dans le comportement, les régions grises ne sont pas essentielles pour les comportements ou n'ont pas encore été étudiées. La taille de la flèche indique l'importance de l'entrée sensorielle. La largeur de la ligne indique la force de la connexion. Toutes les connexions connues ne sont pas représentées. MOB/AOB, bulbe olfactif principal/accessoire ; AVPV, noyau périventriculaire antéroventral ; BNSTp, partie postérieure du noyau du lit de la stria terminalis ; CoApl, amygdale corticale postérolatérale ; LS, septum latéral ; MeA, amygdale médiane ; MPOA, aire préoptique médiane ; PA, amygdale postérieure ; PAG, gris périaqueducal ; PMv, noyau prémammillaire ventral ; VMHvl, partie ventrolatérale de l'hypothalamus ventromédial ; vSUB, subiculum ventral ; VTA : aire tegmentale ventrale. D'après Wei et al. 2021.

3.1.1 Circuit neuronal du comportement lordose

Le réflexe de lordose est déclenché par des indices somatosensoriels fournis par le mâle pendant la monte, mais des indices olfactifs sont nécessaires pour le permettre (Keller et al., 2006). Ishii et ses collègues ont dessiné un circuit cérébral linéaire étiqueté soutenant l'amélioration de la lordose par la stimulation avec le peptide ESP1 (Ishii et al., 2017). La détection de l'ESP1 par les VSN exprimant V2Rp5 active les neurones glutamatergiques du MeApv, puis les neurones SF1-VMHdm (SF1, facteur stéroïdogénique 1) et ERα-PAG (ERα, récepteur alpha des œstrogènes). L'ESP1 n'est sécrété que par certaines souches de souris (Kimoto et al., 2007), et les femelles présentent une lordose lors de la monte par des mâles déficients en ESP1. Ainsi, le circuit cérébral activé par ESP1 n'est pas nécessairement le circuit qui soutient l'initiation du réflexe de lordose. La réduction de la réponse de lordose chez les femelles cGαo-/- et après une inhibition aiguë de l'AOB soutient l'implication des entrées voméronasales dans le circuit cérébral de la lordose (McCarthy et al., 2017a ; Oboti et al., 2014). La lésion ou l'inhibition pharmacologique de la MeA réduit le comportement de lordose, même si ces études ne discriminent pas la participation de chaque subdivision de la MeA (DiBenedictis et al., 2012 ; McCarthy et al., 2017b). Récemment, Johnson et ses collègues ont désigné les neurones GABAergiques, mais pas glutamatergiques, de la MeA comme médiateurs du réflexe de lordose (Johnson et al., 2021). Le VMH peut être subdivisé en une partie postéroventrale et une partie dorsomédiale (VMHvl et VMHdm). Des preuves claires montrent que le VMHvl est également

nécessaire au comportement de lordose (Bentefour et Bakker, 2021 ; Hashikawa et al., 2017 ; Micevych et Meisel, 2017 ; Yang et al., 2013b). La figure 20 montre un circuit potentiel soutenant le comportement sexuel féminin proposé par Wei et ses collègues (Wei et al., 2021).

L'AVPV, plus précisément les neurones Kisspeptin-AVPV, sont les gardiens de la réponse de lordose (Hellier et al., 2018). La Kisspeptine (Kiss) est un neuropeptide régulant l'axe hypothalamo-hypophyso-gonadique (HPG) en médiant la rétroaction des stéroïdes sexuels sur les neurones hypothalamiques GnRH (gonadotropin-releasing hormone) (Oakley et al., 2009). Les neurones Kiss-AVPV sont activés par les odeurs masculines (Bakker et al., 2010), et leur inhibition abolit la préférence olfactive et le comportement de lordose (Hellier et al., 2018). En outre, une étude a révélé que l'environnement hormonal déclenche la fonction de l'AVPV (Inoue et al., 2019). Les œstrogènes augmentent les projections du VMHvl vers l'AVPV. Les auteurs n'ont pas analysé si les neurones de l'AVPV innervés par le VMHvl expriment Kiss. Néanmoins, les neurones Kiss apparaissent comme un candidat parfait pour transformer les signaux olfactifs en une décision comportementale.

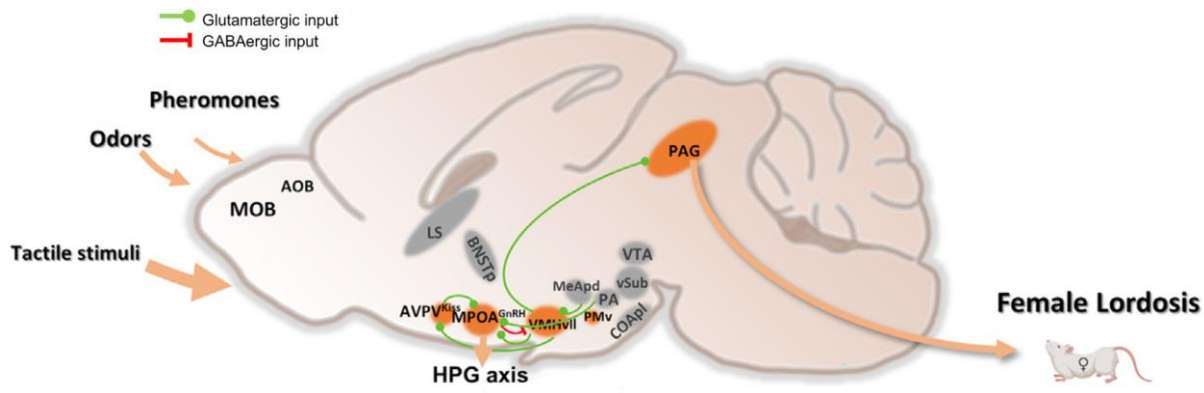

Figure 20 : Circuit neuronal du comportement sexuel féminin. Les régions orange favorisent le comportement, les régions grises ne sont pas essentielles pour les comportements ou n'ont pas encore été étudiées. La taille des flèches indique l'importance de l'entrée sensorielle. La largeur de la ligne indique la force de la connexion. Toutes les connexions connues ne sont pas représentées. MOB/AOB, bulbe olfactif principal/accessoire ; AVPV, noyau périventriculaire antéroventral ; BNSTp, partie postérieure du noyau du lit de la stria terminalis ; CoApl, amygdale corticale postérolatérale ; LS, septum latéral ; MeA, amygdale médiane ; MPOA, aire préoptique médiane ; PA, amygdale postérieure ; PAG, gris périaqueducal ; PMv, noyau prémammillaire ventral ; VMHvl, partie ventrolatérale de l'hypothalamus ventromédial ; vSUB, subiculum ventral ; VTA : aire tegmentale ventrale. D'après Wei et al. 2021.

3.2 Circuit neuronal de l'agressivité

Le comportement agressif des mâles et des femelles est qualitativement dimorphique et s'exprime dans des circonstances différentes (voir section 2.2). Cependant, il est contrôlé par la signalisation voméronasale dans les deux sexes et presque toutes les régions associées à l'agression masculine sont également impliquées dans l'agression féminine, ce qui indique un circuit d'agression commun dans une certaine mesure (Hashikawa et al., 2018). La figure 21 montre un circuit potentiel soutenant le comportement agressif proposé par Wei et ses collègues (Wei et al., 2021).

Les neurones GABA-MeApd induisent une réponse agressive envers un intrus adulte, indépendamment du sexe ou du statut gonadique (Hong et al., 2014). Il est surprenant de constater qu'elle ne peut être obtenue que par une activation robuste, alors qu'une faible activation des neurones GABA-MeApd entraîne un comportement de monte. De même, une faible activité des neurones GABA-MeApd entraîne un comportement parental chez un mâle exposé à un nouveau-né, alors qu'une forte activité déclenche un infanticide dans des conditions similaires (Chen et al., 2019). Ainsi, la mesure de l'activité de MeApd est déjà un proxy de la réponse comportementale. On ignore si la signalisation voméronasale pourrait augmenter l'activation des neurones GABA-MeApd pour conduire à des comportements agressifs.

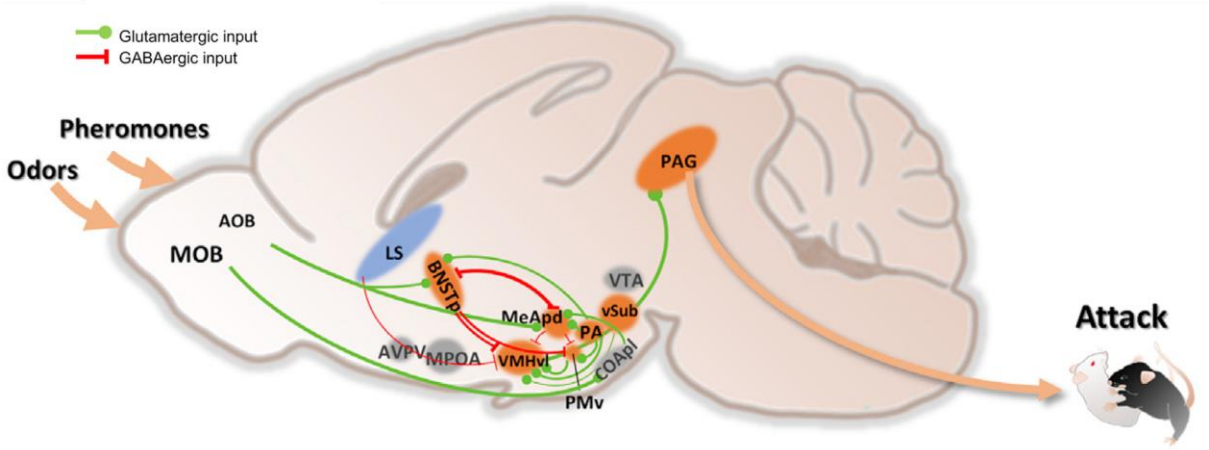

Figure 21 : Circuit neuronal de l'agression. Les régions bleues suppriment le comportement, tandis que les régions orange le favorisent. Les régions grises ne sont pas essentielles au comportement ou n'ont pas encore été étudiées. La taille des flèches indique l'importance de l'entrée sensorielle. La largeur de la ligne indique la force de la connexion. Toutes les connexions connues ne sont pas représentées. MOB/AOB, bulbe olfactif principal/accessoire ; AVPV, noyau périventriculaire antéroventral ; BNSTp, partie postérieure du noyau du lit de la stria terminalis ; CoApl, amygdale corticale postérolatérale ; LS, septum latéral ; MeA, amygdale médiane ; MPOA, aire préoptique médiane ; PA, amygdale postérieure ; PAG, gris périaqueducal ; PMv, noyau prémammillaire ventral ; VMHvl, partie ventrolatérale de l'hypothalamus ventromédial ; vSUB, subiculum ventral ; VTA : aire tegmentale ventrale. D'après Wei et al. 2021.

Les MeA projettent vers le VMH, qui est un nœud crucial pour l'expression de l'agressivité (Canteras et al., 1995 ; Lin et al., 2011). Comment les neurones inhibiteurs GABA-MeApd pourraient-ils favoriser l'activation du VMH ? Padilla et ses collègues ont révélé une voie disynaptique entre la MeA, le BNSTp et le VMH contrôlant l'agressivité (Padilla et al., 2016). Les neurones BNSTp sont principalement GABAergiques, projettent vers le VMH, et l'inhibition des neurones Aro-BNSTp (également GABAergiques) a un impact sur l'agressivité (Bayless et al., 2019). Par conséquent, un circuit d'inhibition-désinhibition pourrait transmettre des informations du MeApd au VMH via le BNSTp (figure 22).

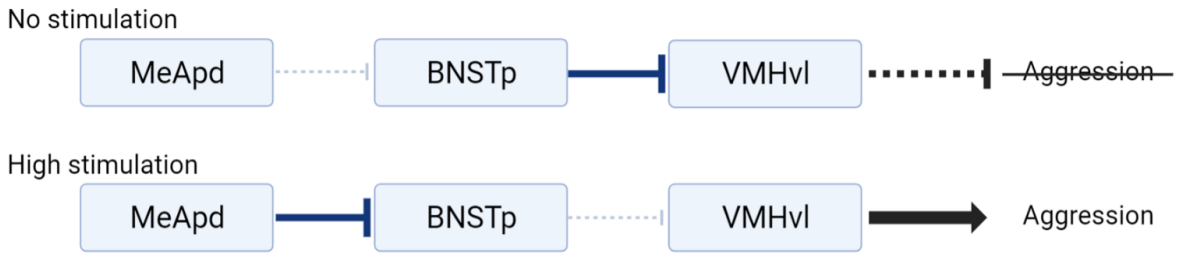

Figure 22 : Communication disynaptique entre le MeA et le VMH. En l'absence de stimulation, les neurones GABA-MeApd sont silencieux et le BNSTp inhibe le VMHvl, freinant l'expression de l'agressivité. Lors d'une forte stimulation, les neurones GABA-MeApd inhibent le BNSTp, libérant l'inhibition du BNSTp sur le VMH et permettant l'expression de l'agression.

Les stéroïdes sexuels sont des facteurs permissifs de l'agression. Les mâles castrés ne présentent pas d'agression territoriale, et l'AR, l'ER et Aro sont présents dans de nombreux noyaux cérébraux du circuit de l'agression (Hashikawa et al., 2018). Les neurones à aromatase sont en effet fortement impliqués dans les comportements agressifs (Bayless et al., 2019 ; Unger et al., 2015a). Chez les rats femelles, la fluctuation rapide des niveaux d'hormones pendant le cycle estrien n'induit pas de réactions agressives (De Jong et al., 2014). Cependant, le passage à la maternité s'accompagne d'un changement majeur et durable de l'environnement hormonal. Il induit une modification profonde de l'agressivité féminine : le mâle devient une menace au lieu d'un partenaire sexuel. Ce changement de signification comportementale n'est pas encore expliqué. Le cerveau féminin subit un remodelage autour de la parturition, modifiant l'activation cellulaire (Moffitt et al., 2018) et l'expression des gènes (Abellán-Álvaro et al., 2021). La grossesse remodèle également le VNO en renforçant la neurogenèse et en modifiant le répertoire des VRs (Oboti et al., 2015). Ces deux mécanismes agissent probablement de concert pour induire un changement aussi drastique des comportements.

3.3 Les circuits neuronaux des comportements parentaux

L'implication de la signalisation voméronasale dans les comportements parentaux n'est pas clairement établie (voir section 2.3). Cependant, des études sur le rat suggèrent que la MeA régule négativement la parentalité (Numan et Woodside, 2010) et que l'exposition à des petits induit une activation cellulaire dans la MeA (Alsina-Llanes et Olazábal, 2020), ce qui suggère que les entrées voméronasales peuvent être intégrées au circuit neuronal de la parentalité. Les premières études menées sur des rats ont également révélé le rôle central de la MPOA dans les comportements parentaux (Numan, 1974). La MPOA est une structure vaste et hétérogène fortement activée lors des comportements parentaux chez la souris (Tsuneoka et al., 2013). La combinaison de marqueurs anatomiques et moléculaires permet de délimiter plusieurs subdivisions (Moffitt et al., 2018 ; Tsuneoka et al., 2013). Cependant, il n'existe pas de marqueurs clairs permettant une discrimination stricte. La dissection génétique des cellules de la MPOA modulant des comportements parentaux a mis en

évidence des neurones exprimant ERα et galanine (Fang et al., 2018 ; Kohl et al., 2018 ; Wei et al., 2018 ; Wu et al., 2014). Les neurones ERα-MPOA sont nécessaires à l'expression des comportements parentaux et sexuels (Ribeiro et al., 2012 ; Sano et al., 2013). Cependant, la stimulation séquentielle avec un petit et un congénère adulte active des populations neuronales exprimant ERα distinctes (Wei et al., 2018). Une sous-population de neurones ERα exprime le neuropeptide galanine (Tsuneoka et al., 2017), mais l'ablation des neurones exprimant la galanine abolit également le comportement sexuel (Wu et al., 2014). La figure 23 montre un circuit potentiel soutenant les comportements parentaux proposé par Wei et ses collègues (Wei et al., 2021).

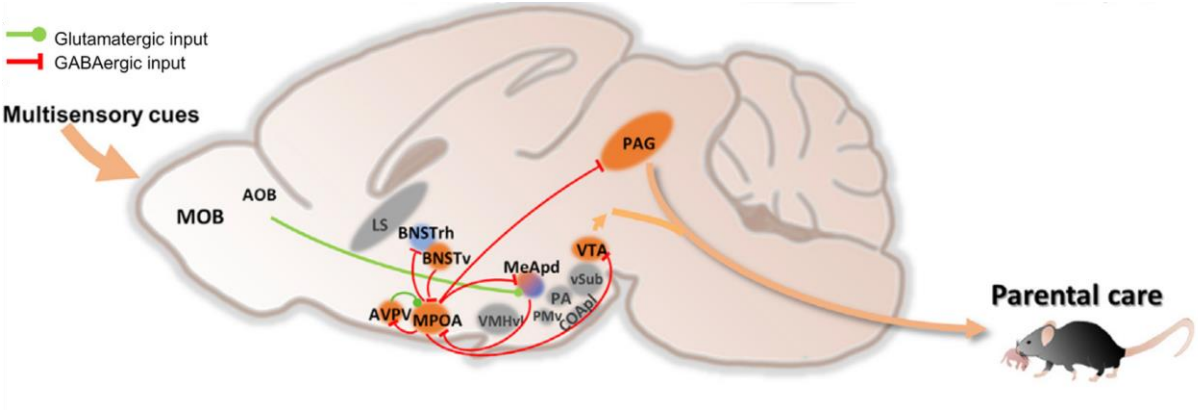

Figure 23 : Circuit neuronal du comportement parental. Les régions bleues suppriment le comportement, tandis que les régions orange le favorisent. Les régions grises ne sont pas essentielles au comportement ou n'ont pas encore été étudiées. La taille des flèches indique l'importance de l'entrée sensorielle. La largeur de la ligne indique la force de la connexion. Toutes les connexions connues ne sont pas représentées. MOB/AOB, bulbe olfactif principal/accessoire ; AVPV, noyau périventriculaire antéroventral ; BNSTp, partie postérieure du noyau du lit de la stria terminalis ; CoApl, amygdale corticale postérolatérale ; LS, septum latéral ; MeA, amygdale médiane ; MPOA, aire préoptique médiane ; PA, amygdale postérieure ; PAG, gris périaqueducal ; PMv, noyau prémammillaire ventral ; VMHvl, partie ventrolatérale de l'hypothalamus ventromédial ; vSUB, subiculum ventral ; VTA : aire tegmentale ventrale. D'après Wei et al. 2021.

La parentalité semble étroitement liée à l'infanticide. Le circuit cérébral de l'infanticide n'est pas élucidé, mais la MeApd, le BNSTp, la MPOA, l'hypothalamus antérieure et l'aire amygdalohippocampique semblent être impliquées (Autry et al., 2021 ; Chen et al., 2019 ; Sato et al., 2020 ; Tachikawa et al., 2013 ; Tsuneoka et al., 2013, 2015 ; Wu et al., 2014). Chez les animaux vierges, l'inhibition des noyaux cérébraux infanticides stimule la parentalité, et inversement, l'activation des noyaux cérébraux parentaux inhibe l'infanticide (Sato et al., 2020 ; Tsuneoka et al., 2013, 2015 ; Wu et al., 2014). Une comparaison des régions activées dans le cerveau entre une femelle allaitante et un mâle infanticide montre un nombre plus élevé de régions suractivées chez les mâles (Renier et al., 2016). Cependant, il n'est pas clair si cette différence résulte d'un manque d'inhibition dans le cerveau mâle ou d'une activation sensorielle spécifique au mâle. Le VNO détecte les odeurs de petits chez les mâles vierges qui peuvent agir comme des indices pro-infanticide (Isogai et al., 2018 ; Nakahara et al., 2020a ; Tachikawa et al., 2013). Chen et ses collègues ont montré qu'une forte

activation des neurones GABA-MeApd déclenche l'infanticide chez les mâles, même chez les pères (Chen et al., 2019). De manière intéressante, la réduction de l'intensité de la stimulation des neurones GABA-MeApd rendait les mâles vierges parentaux. On ne sait pas dans quelle mesure la signalisation voméronasale peut conduire à cette forte activation de la MeApd. L'équilibre entre l'activation des circuits pro-parentaux et pro-infanticide est loin d'être compris. Une discrimination rigoureuse des facteurs liés au sexe et à l'expérience fait défaut.

3.4 Circuits neuronaux d'évitement des prédateurs et des congénères malades

Les circuits neuronaux d'évitement des prédateurs sont étroitement liés à ceux qui soutiennent les comportements sociaux. Les deux types de signaux sont traités par le système olfactif et convergent vers les mêmes structures cérébrales. Comme nous l'avons vu pour le codage du sexe dans la MeA (voir section 3.1.1), les neurones de la MeA activés par les prédateurs forment également des populations distinctes (Bergan et al., 2014). De plus, les neurones de la MeApv codent déjà la nature du prédateur (par exemple, chat contre serpent) (Carvalho et al., 2015). Les signaux de prédateurs détectés par différentes structures (c'est-à-dire VNO, MOE, GG et Taars) activent également la MeApv (Pérez-Gómez et al., 2015), ce qui suggère que cette région pourrait être une plaque tournante pour déclencher l'évitement des prédateurs. La voie par laquelle les signaux des prédateurs convergent vers l'amygdale voméronasale n'est pas claire. Elle pourrait impliquer la CoApl, qui est nécessaire pour l'évitement des odeurs induit par le MOS et qui est connecté à la MeA (Canteras et al., 1995 ; Root et al., 2014). En aval de la MeA, le VMH, et en particulier les neurones exprimant SF1 du VMHdm, sont essentiels pour la médiation de l'évitement des prédateurs (Silva et al., 2013 ; Wang et al., 2015). Comme dans la MeA, les neurones du VMHdm sont activés par les signaux venant de l'AOS et du MOS (Pérez-Gómez et al., 2015), et différents prédateurs activent différents ensembles neuronaux (Carvalho et al., 2020). L'activation du VMHdm a conduit à des réponses comportementales adaptatives (par exemple, l'immobilisation ou la fuite) en fonction du contexte par l'activation de voies distinctes en aval (Wang et al., 2015). Les connaissances actuelles plaident pour la participation du noyau hypothalamique antérieur (AHN), du noyau prémammilaire dorsal et de la PAG comme voies pour les actions motrices de peur et d'évitement (Canteras et al., 2015 ; Carvalho et al., 2020 ; Wang et al., 2015) (Figure 24).

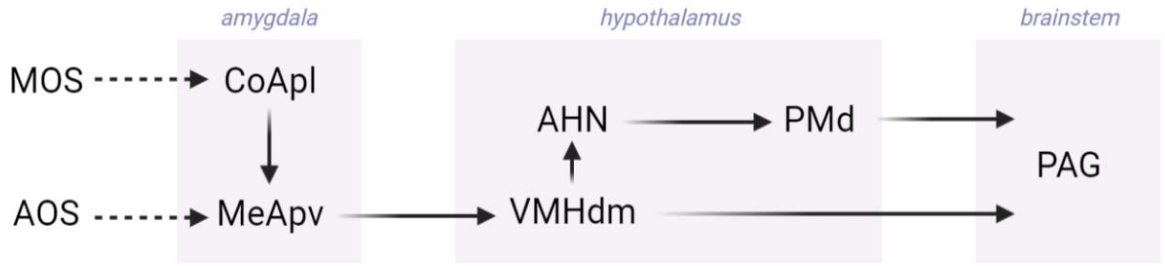

Figure 24 : Circuit neuronal d'évitement des prédateurs. MOS/AOS, système olfactif principal/accessoire ; CoApl, amygdale corticale postérolatérale ; MeApv, amygdale médiale postéroventrale ; VMHdm, partie dorsomédiale de l'hypothalamus ventromédial ; AHN, noyau hypothalamique antérieur ; PMd, noyau prémammillaire dorsal ; PAG, gris périaqueducal. Adapté de Canteras et al. 2015.

Contrairement à l'évitement des prédateurs, la voie neuronale de l'évitement des congénères malades est encore largement inexplorée. L'un des principaux écueils à sa compréhension est de discriminer le signal médiateur de l'état malade de celui de l'état social. Les deux sont détectés par le VNO et activent l'AOB (Boillat et al., 2015), mais l'identité des VSNs qui médient les signaux associés à la maladie est inconnue. Les FPR sont de bons candidats en raison de leur affinité naturelle pour les peptides d'origine bactérienne (Bufe et al., 2012). L'évitement des animaux traités par le LPS est indépendant du FPR3. Ainsi, s'ils sont détectés par les FPR, les signaux olfactifs associés à la maladie devraient être détectés par les VSN apicaux exprimant Gαi2. Kwon et ses collègues ont observé que la CoApm, qui appartient à l'amygdale voméronasale, était spécifiquement activée après l'exposition à une femelle traitée au LPS (Kwon et al., 2021). Ils ont également montré que les cellules activées par le CoApm projettent vers les neurones glutamatergiques de la MeApv pour supprimer l'engagement social. Ce qui se passe en aval reste inconnu, mais la MeApv, comme elle semble être une plaque tournante pour déclencher l'évitement des prédateurs, peut agir comme un site de décision entre la poursuite ou non des interactions sociales.

Objectifs

À la lumière de la littérature, il apparaît que le système olfactif a évolué en composants sensoriels distincts travaillant de concert pour assurer des décisions comportementales appropriées soutenues par des circuits neuronaux complexes. La place du VNO dans le contrôle des comportements sociaux est indiscutable, mais les connaissances actuelles sont pleines de lacunes et de preuves contradictoires. Le développement d'outils moléculaires et génétiques a permis une compréhension progressive de la fonction sensorielle du VNO. Le fait que les VSNs de rongeurs expriment deux types de VR distincts sur le plan évolutif implique des propriétés et des fonctions putatives distinctes. Les travaux réalisés avec le modèle murin de délétion restreinte de Gαo au système olfactif ont partiellement répondu à la question pour les VSNs exprimant les V2Rs (Chamero et al., 2011 ; Oboti et al., 2014 ; Pérez-Gómez et al., 2015). Trois modèles de souris ont étudié la fonction des V1Rs : le knockout général pour Gαi2 (Gαi2-/-, Norlin et al., 2003b), le knockout restreint au système olfactif pour Gγ13 (cGγ13-/-, Liu et al., 2018), et le knockout pour les familles V1Ra et V1Rb (ΔV1rabΔ, Del Punta et al., 2002). Les deux premiers induisent une mutation fuyant à l'extérieur du VNO, interférant avec l'évaluation de sa fonction, et le dernier ne supprime que 12% des V1Rs, ce qui n'est pas suffisant pour généraliser les résultats avec la fonction des VSNs apicaux. Les souris Gαi2-/- présentent une espérance de vie réduite en raison de colites ulcéreuses sévères et d'adénocarcinomes du côlon (Rudolph et al., 1995). De plus, elles présentent un comportement social diminué lié à des anomalies du développement cortical (Hamada et al., 2017). La souris cGγ13-/- exprime la Cre recombinase sous le promoteur OMP, induisant une mutation restreinte au système olfactif grâce au système Cre-lox. Cependant, ces souris sont anosmiques en raison du rôle de Gγ13 dans les OSNs canoniques exprimant l'OMP (Li et al., 2013). Une autre lacune de ces études est le manque de preuves fonctionnelles de l'implication de Gαi2 dans la signalisation des VSNs et le peu de paradigmes comportementaux étudiés.

L'**objectif principal de cette thèse est de décrypter la fonction de Gαi2 dans les VSNs et l'implication des VSNs exprimant Gαi2 dans les comportements socio-sexuels.** Pour surmonter les limites des modèles disponibles, nous avons généré une souris portant une délétion conditionnelle de Gαi2 dans le système olfactif (la souris cGαi2-/-). Nous avons croisé des souris portant un allèle floxé de *Gnai2* (Ustyugova et al., 2012), codant pour Gαi2, avec les souris OMP-Cre, dans lesquelles la région codante de la Cre recombinase est ajoutée à celle de l'OMP (Li et al., 2004). L'expression de l'OMP commence dans les neurones olfactifs matures (Katreddi et Forni, 2021), évitant ainsi une perturbation potentielle de la maturation des VSNs. De plus, ce modèle a été utilisée pour générer de nombreux modèles de dysfonctionnement olfactif (Amjad et al., 2015 ; Chamero et al., 2011 ; Dey et al., 2015 ; Gigante et al., 2017 ; Green et al., 2018 ; Koike et al., 2021 ; Li et al., 2013 ; Matsuo et al., 2015 ; Münch et al., 2018 ; Schmid et al., 2010 ; Weiss et al., 2011, liste non exhaustive). Gαi2 est exprimé dans quelques cellules de la MOE, mais il semble limité aux neurones immatures basaux qui n'expriment pas l'OMP (Berghard et Buck, 1996). Ainsi, la souris cGαi2-/- est un modèle adapté pour étudier la fonction de Gαi2. En utilisant ce modèle de souris, cette thèse vise à répondre à trois questions principales :

i- Gαi2 est-il impliqué dans la signalisation des VSNs ?

ii- Quels comportements les VSNs apicaux contrôlent-ils, et comment ?

iii- Que pouvons-nous apprendre sur le codage cérébral et l'intégration des informations olfactives dépendantes de Gαi2 dans les voies neuronales régulant les comportements sociaux ?

Pour répondre à ces questions, nous avons combiné l'imagerie calcique de VSNs, des études comportementales dans différents paradigmes expérimentaux et la cartographie de l'activité cérébrale à l'aide d'immunomarquages de gènes précoces immédiats. J'ai choisi de respecter le dimorphisme sexuel comportemental existant et j'ai structuré mon travail en conséquence en trois chapitres. Le premier dévoile la fonction de Gαi2 dans la signalisation des VSNs et les comportements socio-sexuels des mâles. Le deuxième chapitre évalue l'impact de la délétion de Gαi2 dans les VSNs sur les comportements socio-sexuels des femelles. Les deux chapitres sont présentés sous leur forme publiée en tant qu'articles de journaux évalués par des pairs. Le dernier chapitre étudie l'implication des VSNs exprimant Gαi2 dans les comportements d'évitement. Il est présenté différemment car les résultats sous-jacents n'ont pas encore été soumis à publication et nécessitent encore des investigations complémentaires pour les étayer.

Résultats

1 Fonction de Gαi2 dans la signalisation des VSNs et les comportements socio-sexuels mâles

Journal article #1: Central role of G protein $G\alpha_{i2}$ and $G\alpha_{i2}$+ vomeronasal neurons in balancing territorial and infant-directed aggression in male mice

Anne-Charlotte Trouillet[1], Matthieu Keller[1], Jan Weiss[2], Trese leinders-Zufall[2], Lutz Birnbaumer[3,4], Frank Zufall[2], and Pablo Chamero[1]

[1] Laboratoire de Physiologie de la reproduction et des Comportements, UMR OO85-INRAE-CNRS-IFCE-University of Tours, Nouzilly, France

[2] Center for Integrative Physiology and Molecular Medicine, Saarland University, Homburg, Germany

[3] Neurobiology Laboratory, National Institute of Environmental Health Sciences, Durham, NC, United States of America

[4] School of Medical Sciences, Institute of Biomedical Research, Catholic University of Argentina, Buenos Aires, Argentina

Published in Proceedings of the National Academy of Sciences of the United States of America, February 2019.

Résumé

Le contrôle voméronasal des comportements sociaux dépend de deux populations neuronales distinctes, les VSNs exprimant V1R/Gαi2 et V2R/Gαo. Gαo est le principal effecteur de la signalisation sensorielle dans les VSNs exprimant V2Rs, mais le rôle fonctionnel de Gαi2 dans les VSNs n'est pas élucidé. Le premier objectif de cette étude était donc de caractériser la fonction de Gαi2 dans la signalisation des VSNs. De plus, les VSNs apicaux ont été associés à la modulation de plusieurs comportements sociaux chez les mâles avec des résultats contradictoires. Le second objectif de cette étude était alors d'élucider l'implication précise de la signalisation voméronasale Gαi2 dans la modulation de trois comportements sociaux, à savoir les comportements sexuels, agressifs et parentaux.

Gαi2 est largement exprimé dans l'organisme, et les souris avec une déficience globale de Gαi2 présentent des défauts sévères raccourcissant leur durée de vie, empêchant ainsi l'analyse de la fonction du VNO et des comportements dépendant du VNO chez ces animaux. Pour surmonter cette limitation, nous avons créé une souris Gαi2 nulle conditionnellement restreinte à l'olfaction (cGαi2-/-). Nous

avons croisé des souris portant un allèle floxé de *Gnai2*, le gène codant pour Gαi2, avec les souris OMP-Cre, dans lesquelles la région codante de la Cre recombinase est ajoutée à celle de l'OMP. L'expression de l'OMP commence dans les neurones olfactifs matures, évitant une perturbation potentielle de la maturation des VSNs. Dans un premier temps, nous avons combiné des analyses histologiques et des quantifications d'ARNm pour valider la mutation et examiner l'organisation du VNE et de la MOE. L'expression de Gαi2 était absente dans le VNE et l'aAOB-GL, et la mutation reduisait le ratio entre les VSNs apicaux et basaux. Cependant, la structure et la fonction de la MOE étaient intactes.

Pour établir la fonction cellulaire de Gαi2 dans la signalisation sensorielle des VSNs apicaux, nous avons réalisé une imagerie calcique sur cellules vivantes en utilisant des cellules dissociées et des tranches de VNO en combinaison avec les senseur calciques GCaMP6f, fura-2/AM ou fluo-4/AM. Comme chimiostimuli, nous avons utilisé de petites molécules organiques, des stéroïdes sulfatés et des peptides urinaires détectés par les V2Rs comme contrôle. Des sous-ensembles de VSNs témoins répondaient de manière fiable à chacun de ces stimuli. En revanche, ces réponses étaient sévèrement diminuées ou absentes dans les VSNs dépourvus de Gαi2, sauf pour les ligands des V2Rs.

Nous avons réalisé plusieurs expériences comportementales sur des mâles cGαi2-/- et déterminé que la signalisation voméronasale Gαi2 est dispensable pour l'expression du comportement sexuel. Cependant, elle est nécessaire pour l'agression territoriale et l'agression dirigée vers les petits. D'une part, les mâles cGαi2-/- sont très agressifs et continuent d'attaquer un adversaire castré, ce qui suggère que, bien que non nécessaire au déclenchement de la réponse, la signalisation voméronasale Gαi2 participe à la modulation de la réponse agressive. D'autre part, la délétion de Gαi2 supprime le comportement infanticide et favorise la parentalité envers les nouveau-nés chez les mâles.

Pour comprendre la régulation opposée de l'agression dirigée vers des mâles et des petits par la signalisation Gαi2, nous avons cartographié l'activation du cerveau après l'exposition à des mâles et à des petits en utilisant le gène précoce immédiat cFos. Par rapport aux témoins, l'activation de la MeApd était plus élevée après l'exposition au mâle et plus faible après l'exposition au petit, ce qui correspond aux résultats comportementaux. En outre, une analyse approfondie des neurones de la MeApd activés a révélé que l'exposition au mâle induisait l'activation des neurones AR-positifs, alors que l'exposition au petit ne le faisait pas.

En conclusion, nous avons montré ici un rôle essentiel de Gαi2 dans la signalisation sensorielle du VNO et de la population apicale des VSNs qui détecte les petites molécules organiques, notamment les phéromones volatiles et les dérivés stéroïdiens. Notre étude identifie les VSNs Gαi2+ comme un composant neuronal critique qui organise et équilibre l'agression dirigée vers les mâles et les nouveau-nés à travers des circuits neuronaux distincts

Check for updates

Central role of G protein Gαi2 and Gαi2$^+$ vomeronasal neurons in balancing territorial and infant-directed aggression of male mice

Anne-Charlotte Trouillet[a], Matthieu Keller[a], Jan Weiss[b], Trese Leinders-Zufall[b], Lutz Birnbaumer[c,d,1], Frank Zufall[b,1], and Pablo Chamero[a,1]

[a]Laboratoire de Physiologie de la Reproduction et des Comportements, UMR Institut National de la Recherche Agronomique (INRA)-CNRS-Institut Français du Cheval et de l'Equitation (IFCE)-University of Tours, 37380 Nouzilly, France; [b]Center for Integrative Physiology and Molecular Medicine, Saarland University, 66421 Homburg, Germany; [c]Neurobiology Laboratory, National Institute of Environmental Health Sciences, National Institutes of Health, Durham, NC 27709; and [d]Institute of Biomedical Research (BIOMED), School of Medical Sciences, Catholic University of Argentina, C1107AAZ Buenos Aires, Argentina

Contributed by Lutz Birnbaumer, January 23, 2019 (sent for review December 18, 2018; reviewed by Peter A. Brennan and Marc Spehr)

Aggression is controlled by the olfactory system in many animal species. In male mice, territorial and infant-directed aggression are tightly regulated by the vomeronasal organ (VNO), but how diverse subsets of sensory neurons convey pheromonal information to limbic centers is not yet known. Here, we employ genetic strategies to show that mouse vomeronasal sensory neurons expressing the G protein subunit Gαi2 regulate male–male and infant-directed aggression through distinct circuit mechanisms. Conditional ablation of Gαi2 enhances male–male aggression and increases neural activity in the medial amygdala (MeA), bed nucleus of the stria terminalis, and lateral septum. By contrast, conditional Gαi2 ablation causes reduced infant-directed aggression and decreased activity in MeA neurons during male–infant interactions. Strikingly, these mice also display enhanced parental behavior and elevated neural activity in the medial preoptic area, whereas sexual behavior remains normal. These results identify Gαi2 as the primary G protein α-subunit mediating the detection of volatile chemosignals in the apical layer of the VNO, and they show that Gαi2$^+$ VSNs and the brain circuits activated by these neurons play a central role in orchestrating and balancing territorial and infant-directed aggression of male mice through bidirectional activation and inhibition of different targets in the limbic system.

olfactory | GCamp6f | V1R receptor | infant-directed aggression | territorial aggression

Aggression is an innate social behavior most commonly displayed in males, typically directed to other males of the same species (1) or to another male's offspring (2). Such behaviors are important for resource competition, establishment of group hierarchies, and access to sexual partners. For example, pup-directed aggression resulting in infanticide ultimately induces endocrine changes in females, which makes them quickly receptive to a male newcomer (3) and thus increases reproductive success. In rodents, the role of the olfactory system is critical for initiating aggression. Pheromonal cues present in secretions from adult males or pups are detected by distinct subsets of sensory neurons in the vomeronasal organ (VNO) (4–7) to initiate neural signals that, in turn, trigger aggressive behavior. However, many of the cellular and molecular mechanisms underlying such aggression-promoting signaling remain unknown.

The mouse VNO contains two major populations of vomeronasal sensory neurons (VSNs): VSNs of the apical layer of the vomeronasal sensory epithelium (VNE) express the G protein Gαi2 and members of the V1R family of vomeronasal G protein-coupled receptors, whereas VSNs of the basal layer express Gαo and members of the V2R receptor family (8–14). Gαo-expressing (i.e., Gαo$^+$) cells have been implicated in male–male aggression by detecting urine-derived high molecular weight (HMW) pheromones, particularly MUP proteins, and ESP1 peptide, both of which are capable to induce aggression (15–19). Conditional ablation of Gαo eliminates VSN transduction of MUPs and ESP1 as well as male–male aggression (16, 20, 21). However, organic low molecular weight (LMW) molecules recognized by Gαi2 VSNs can also induce aggression (22). Furthermore, mice carrying a global deletion of Gαi2 are less aggressive (23), suggesting that both VSN populations may interact to generate aggressive behavior. Thus, whether each VNO subsystem activates independent aggression circuits or whether the two subsystems function in a cooperative and integrative manner to generate territorial aggression is not yet clear.

Infanticidal behavior, in which an adult attacks and kills an alien pup, is observed in virgin adult males and is highly dependent on the VNO. Genetic deletion of the transient receptor potential channel Trpc2, the primary sensory ion channel of VSNs, or surgical VNO ablation strongly reduce aggression toward pups (24, 25). Pup odors in virgin males preferentially activate a region of the accessory olfactory bulb (OB; AOB) innervated by Gαi2 neurons (25), but how molecularly defined VSN subsets influence pup-directed aggression remains unclear. Several regions in the limbic brain are activated during infanticide and male–male aggression, including the medial amygdala (MeA), the bed nucleus of the stria terminalis (BNST),

Significance

Male mice detect pheromones that trigger aggressive behavior toward other males or another male's pups. We found that a subpopulation of chemosensory neurons in the vomeronasal organ organizes and balances both types of aggression by reducing or enhancing each behavioral output. These neurons use a signaling cascade that requires the G protein Gαi2 in the detection of volatile pheromones and steroid derivatives. This subset of sensory neurons conveys pheromonal information to limbic centers in the brain through independent mechanisms, targeting different groups of neurons during male–male or infant-directed aggression. How the mouse olfactory system detects and processes pheromones that trigger different forms of aggression should aid in the identification of neural networks mediating male–male vs. infant-directed social aggression.

Author contributions: M.K., T.L.-Z., L.B., F.Z., and P.C. designed research; A.-C.T., J.W., T.L.-Z., and P.C. performed research; L.B. contributed new reagents/analytic tools; A.-C.T., J.W., T.L.-Z., and P.C. analyzed data; and A.-C.T., F.Z., and P.C. wrote the paper.

Reviewers: P.A.B., University of Bristol; and M.S., RWTH Aachen University.

The authors declare no conflict of interest.

Published under the PNAS license.

Data deposition: The datasets generated and/or analyzed during the present study are available in the Data Inra Dataverse portal (https://data.inra.fr/).

[1]To whom correspondence may be addressed. Email: Birnbau1@gmail.com, frank.zufall@uks.eu, or pablo.chamero-benito@inra.fr.

This article contains supporting information online at www.pnas.org/lookup/suppl/doi:10.1073/pnas.1821492116/-/DCSupplemental.

and the ventromedial hypothalamus (VMH) (25, 26). Current understanding of these neuronal substrates is insufficient to explain whether infanticide and male–male aggression are initiated by the same or different subsets of VSNs. Furthermore, it is not known whether the same or different groups of neurons from these common limbic structures are activated during male–male or infant-directed aggression. One possibility is that neuronal circuits originating from Gαi2^{+} VSNs may independently coordinate infant-directed and male–male aggression.

Because the *Gnai2* gene, which encodes Gαi2, is ubiquitously expressed in the developing brain and cortex (27, 28), analysis of VNO-dependent behaviors in mice carrying a global Gαi2 deletion (28) is impeded. Furthermore, no functional recordings in single VSNs lacking Gαi2 have been performed. To overcome these limitations, we have generated mice harboring a conditional deletion of Gαi2 in the olfactory system. These mice show a striking reduction in the sensory response to LMW organic molecules, demonstrating that Gαi2 is an obligate requirement for normal signaling of apical VSNs. Furthermore, territorial aggression is enhanced in these mutant mice, whereas infant-directed aggression is strongly diminished. Together with c-Fos mapping in aggression-controlling brain centers, our study establishes a critical role of Gαi2, the VSNs that express this G protein, and the circuits derived from Gαi2^{+} VSNs in orchestrating and balancing territorial and infant-directed aggression of male mice.

Results

Conditional Deletion of Gαi2 in VSNs. We used the Cre-*loxP* system to create mice with a tissue-specific and time-dependent deletion of Gαi2. Mice carrying a floxed allele of *Gnai2* (*Gnai2*$^{fx/fx}$) (29) were crossed with OMP-Cre mice (30, 31), in which the coding region for olfactory marker protein (OMP) is replaced by that of Cre recombinase. Conditional Gαi2 mutants (cGαi2$^{-/-}$) were heterozygous for *Cre* (*Gnai2*$^{fx/fx}$*Omp*$^{cre/+}$); mice heterozygous for both alleles (*Gnai2*$^{fx/+}$*Omp*$^{cre/+}$) served as controls (cGαi2$^{+/-}$). All experiments were performed with adult male mice (8–12 wk old).

We used immunohistochemistry (IHC) to examine the VNE in cGαi2$^{+/-}$ and cGαi2$^{-/-}$ males. Gαi2 immunoreactivity was absent in the VNE of cGαi2$^{-/-}$ mice, confirming the loss of Gαi2 protein expression (Fig. 1*A*). Staining was positive for markers of basal (V2R2, family C V2Rs), apical (PDE4A, phosphodiesterase 4A), or both (OMP) VSN populations in control and mutant mice (Fig. 1*A* and *SI Appendix*, Fig. S1*A*), showing that general tissue structure remained intact. By using RT-PCR with whole VNO cDNA from cGαi2$^{+/-}$ or cGαi2$^{-/-}$ males, we identified transcripts for several *V1r* receptors and two *V2r* receptors, *Trpc2* and *Plcb2*, in both genotypes (*SI Appendix*, Fig. S1*B*), indicating that expression of transduction molecules also remained intact. Quantitative RT-PCR analyses showed that relative expression of *Gnai2* in the VNO of cGαi2$^{-/-}$ males was reduced by 1.86 fold ($P <$ 0.001), whereas *Gnao* expression increased by 1.47 fold ($P <$ 0.01; Fig. 1*B*). *Gnai2* expression in the main olfactory epithelium (MOE) of control vs. mutant mice was not significantly different (Fig. 1*B*).

Previous work indicated a role for G protein α-subunits in the survival of VSNs (16, 23, 32). We analyzed PDE4A immunoreactivity, specific for the apical Gαi2-expressing zone (33), and the volume of apical and basal VNE layers in cGαi2$^{+/-}$ and cGαi2$^{-/-}$ mice. The volume of the apical layer was reduced by 1.41 fold whereas that of the basal layer increased 1.35-fold in cGαi2$^{-/-}$ mice ($P <$ 0.001; Fig. 1*C*). Cell density remained unchanged (*SI Appendix*, Fig. S1*C*), indicating that the volume reduction of the apical layer likely resulted from a decrease in the number of VSNs. A reduced volume was also detected in whole AOB of cGαi2$^{-/-}$ mice as shown by IHC for OMP (13% reduction; $P <$ 0.001; *SI Appendix*, Fig. S1*D*). By using IHC for Gαo, we found a reduced glomerular layer in the rostral AOB (31% reduction; $P <$ 0.001), the primary target of Gαi2^{+} VSNs (*SI Appendix*, Fig. S1*D*). The general structure of MOE and glomerular layer of the main OB (MOB) remained unchanged in cGαi2$^{-/-}$ mice (*SI Appendix*, Fig. S1*E*). Thus, conditional Gαi2 deletion caused a selective loss of apical PDE4A-expressing VSNs and rostral AOB glomerular volume. We confirmed that general olfactory performance remained normal in cGαi2$^{-/-}$ males by performing several behavioral tests. There was no significant difference between cGαi2$^{-/-}$ and cGαi2$^{+/-}$ males in a food-finding test (*SI Appendix*, Fig. S1*F*). Likewise, novel odor investigation of female urine and odor discrimination of normal male urine vs. castrated male urine using a habituation–dishabituation paradigm (20, 31) revealed no significant differences between the two genotypes (*SI Appendix*, Fig. S1*G*). Thus, cGαi2$^{-/-}$ mice do not display any obvious defects with respect to main olfactory system function.

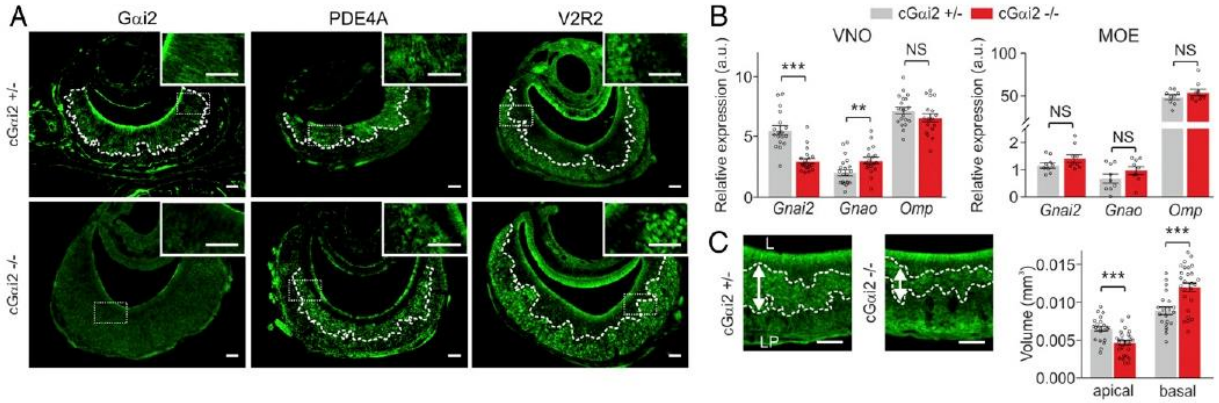

Fig. 1. Expression of marker proteins in the VNO of cGαi2$^{+/-}$ and cGαi2$^{-/-}$ mice. (*A*) Loss of Gαi2 immunoreactivity in cGαi2$^{-/-}$ VNO. Antibodies specific for PDE4A (apical layer) or V2R2 (basal layer) indicate that the laminar VNO organization persists in the absence of Gαi2. (Scale bars, 50 μm.) (*B*) Relative expression (normalized to *Hprt-1*) of *Gnai2*, *Gnao*, and *Omp* genes in VNO (*Left*) and MOE (*Right*). *Gnai2* expression decreased and *Gnao* expression increased, whereas *Omp* expression did not change, in cGαi2$^{-/-}$ VNO [$^{**}P < 0.01$ and $^{***}P < 0.001$; nonsignificant (NS), $P = 0.21$, Mann–Whitney *U* test; cGαi2$^{+/-}$, $n = 20$; cGαi2$^{-/-}$, $n = 18$]. No difference in gene expression in the MOE between the two genotypes was observed (NS, $P = 0.22$–0.53, Mann–Whitney *U* test). (*C*) Analysis of apical and basal VNO layer volume distinguished by PDE4A immunostaining indicates a significant reduction in the apical VNO layer [*t* test, $t(46) = 3.975$; $^{***}P < 0.001$] and an increase in basal VNO layer [*t* test, $t(46) = 3.929$; $^{***}P < 0.001$] of cGαi2$^{-/-}$ ($n = 27$) vs. cGαi2$^{+/-}$ mice ($n = 21$). L, lumen; LP, lamina propria. Data are expressed as means ± SEM. (Scale bars, 50 μm.)

Gαi2 Is Required for Sensory Function of Apical VSNs. VSNs that detect small organic pheromones and steroid derivatives localize to the apical VNO and express V1Rs and Gαi2 (34–37). These neurons do not recognize peptides or proteins (16). To determine whether Gαi2 is required for sensory signaling in apical VSNs, we performed live-cell Ca^{2+} imaging by using dissociated cells (15, 16, 21) and acute VNO slices (33, 34, 38) in combination with the Ca^{2+} sensors GCaMP6f, fura-2/AM, or fluo-4/AM (Fig. 2 and *SI Appendix*, Fig. S2). We crossed *Gnai2*$^{fx/fx}$ *Omp*$^{cre/cre}$ and *Rosa26*-floxstop-GCaMP6f mice (*Methods*) to drive expression of GCaMP6f in *Omp*$^{+}$, *Gnai2*-deficient cells. As chemostimuli, we used nine single compounds (four small organic molecules and five sulfated steroids) or a mix of five sulfated steroids (*SI Appendix*, Fig. S2*A*). Subsets of VSNs from heterozygous controls responded reliably to each of these stimuli (Fig. 2 and *SI Appendix*, Fig. S2 *C–F*). By contrast, such responses were severely diminished or absent in cGαi2$^{-/-}$ VSNs (Fig. 2 and *SI Appendix*, Fig. S2 *C–F*). The response rates of cGαi2$^{-/-}$ VSNs for these ligands were close to those of *Trpc2*$^{-/-}$ VSNs (Fig. 2*B*), indicating a nearly complete loss of sensory function in the apical layer. Importantly, Ca^{2+} responses to a mix of four MHC-binding peptides, known to activate V2R/Gαo^{+} VSNs (19, 33, 38, 39), and high-K^{+} solution remained intact (Fig. 2). Responses to MHC peptides also remained unaffected in *Trpc2*$^{-/-}$ VSNs, consistent with previous results (40). Together, these data establish that Gαi2 is

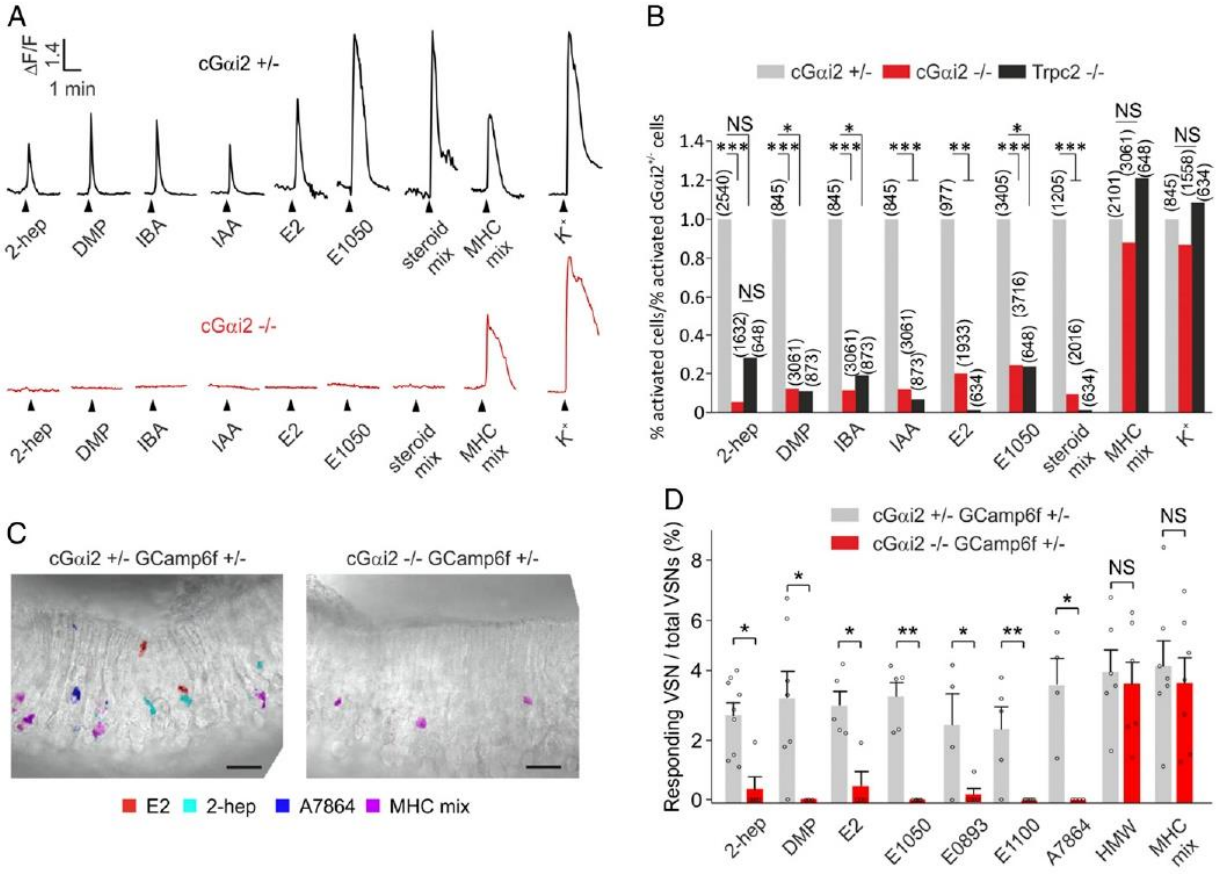

Fig. 2. Essential role of Gαi2 in molecular sensing by apical VSNs. (*A*) Representative Ca^{2+} responses imaged in dissociated VSNs from cGαi2$^{+/-}$ and cGαi2$^{-/-}$ mice. Cells were stimulated with the following stimuli known to activate V1R/Gαi2- or V2R/Gαo-expressing VSNs: 2-heptanone (2-hep, 10^{-8} M); dimethylpyrazine (DMP, 10^{-6} M); isobutylamine (IBA, 10^{-7} M); isoamylamine (IAA, 10^{-7} M); β-estradiol (E2, 1 μM); 1,3,5(10)-estratrien-3,17β-diol disulfate (E1050, 1 μM); sulfated steroid mix E1050, E1100 [1,3,5(10)-estratrien-3,17β-diol 3-sulfate], E0893 [1,3,5(10)-estratrien-3,17α-diol 3-sulfate], and A7864 (5-androsten-3β,17β-diol disulfate), 1 μM each; MHC peptide mix (MHC mix; SYFPEITHI, SYIPSAEKI, AAPDNRETF, SIINFEKL, 10^{-10} M each), and high (50 mM) KCl solution (K^{+}) as viability control. Note that cells from Gαi2$^{-/-}$ mice did not produce Ca^{2+} responses to the V1R ligands but did produce responses to the Gαo-dependent MHC peptide mix and high K^{+}. (*B*) Analysis of ligand-evoked Ca^{2+} responses in dissociated cells from cGαi2$^{+/-}$, cGαi2$^{-/-}$, and Trpc2$^{-/-}$ mice. Data are expressed as the percentage of responding cells to a given stimulus divided by the percentage of responding cells in the cGαi2$^{+/-}$ controls [$*P < 0.05$, $**P < 0.01$, $***P < 0.001$; nonsignificant (NS), $P = 0.07–0.63$, Fisher's exact test]. Number of cells analyzed is indicated above each bar. Each stimulus was tested in 3–16 mice. (*C*) Spatial activation patterns obtained through GCaMP6f imaging in cGαi2$^{+/-}$ and cGαi2$^{-/-}$ VNO slices. Slices were stimulated with the steroids E2 (1 μM; red) and A7864 (1 μM; blue), 2-hep (10^{-8} M; cyan), and MHC mix (SYFPEITHI, SYIPSAEKI, AAPDNRETF, SIINFEKL, 10^{-10} M each; magenta). Stimulus-induced ΔF peak images were digitally superimposed onto the transmitted light image of the same slice (*Methods*; original ΔF peak images are shown in *SI Appendix*, Fig. S2). VSNs in cGαi2$^{-/-}$ slices responded to the MHC peptide mix but not to agonists of apical VSNs. (Scale bar, 25 μm.) (*D*) Percentage of responding VSNs/total VSNs in Gαi2$^{-/-}$ slices is strongly diminished or reduced to zero with stimuli known to activate apical VSNs ($\chi^2 = 40.8$, $P < 0.001$, Kruskal–Wallis ANOVA; $*P < 0.05$, $**P < 0.01$, Mann–Whitney *U* test; $n = 2–3$ slices per mouse from 7 cGαi2$^{+/-}$ and 5 cGαi2$^{-/-}$ GCaMP6f mice). No significant difference in the detection of Gαo-dependent stimuli is observed between the two genotypes [HMW, $t(10) = 0.36$; NS, $P = 0.72$; MHC mix, $t(12) = 0.44$; NS, $P = 0.66$]. Dots indicate the percentage of responding/total VSNs in independent slice recordings. Stimuli were tested one to three times per slice. Each stimulus was tested in at least three mice. Data are expressed as means ± SEM.

required for VSN sensory transduction in the apical VNE layer and plays a central role in detecting small organic molecules and steroid derivatives.

Normal Male Sexual Behavior in Gαi2 Mutants. Trpc2$^{-/-}$ male mice exhibit pronounced alterations in sexual behavior, including elevated mounting and courtship behaviors toward other males (41, 42). To determine whether Gαi2 is also required for male sexual behavior, we first measured serum testosterone levels and the weight of sexual organs (testes, preputial glands, seminal vesicles), but found no significant differences between cGαi2$^{-/-}$ and cGαi2$^{+/-}$ males (*SI Appendix*, Fig. S3 *A* and *B*). We next analyzed sexual behaviors toward females in sexually naïve cGαi2$^{-/-}$ and cGαi2$^{+/-}$ males (*SI Appendix*, Fig. S3 *D–G*). cGαi2$^{-/-}$ and cGαi2$^{+/-}$ males displayed the same level of preference for estrous female urine volatiles and nonvolatiles (*SI Appendix*, Fig. S3*C*). We also scored the number of animals mounting an intruder (female, male, or castrated male) and the mounting episodes (*SI Appendix*, Fig. S3*D*). cGαi2$^{-/-}$ and cGαi2$^{+/-}$ males showed robust mounting and a short latency to mount females, but very rarely displayed sexual behavior toward male or castrated male intruders. Next, we scored the latency to mount female intruders and to ejaculate, and the total mating time (*SI Appendix*, Fig. S3 *E* and *F*). Latency to ejaculate and total mating time of cGαi2$^{-/-}$ males were statistically indistinguishable from those of cGαi2$^{+/-}$ males (P = 0.21–0.89). We further assessed male courtship behavior by measuring ultrasonic vocalizations at high frequencies (30–110 kHz) emitted by resident males. cGαi2$^{-/-}$ and cGαi2$^{+/-}$ males produced high numbers of vocalizations in response to female intruders, whereas few vocalizations were produced during male–male investigation, and there was no significant difference between genotypes (*SI Appendix*, Fig. S3*G*). Together, these findings reveal that cGαi2$^{-/-}$ males display normal sexual behaviors and sexual motivation.

Territorial Aggression Is Enhanced in Gαi2 Mutant Males. Conditional deletion of Gαo in VSNs eliminated male–male aggression (16). This effect could result from cooperation of Gαo and Gαi2 subsystems, or the Gαi2 subsystem could operate relatively independently, being dispensable for aggression and/or controlling a parallel aggression circuit. To distinguish between these hypotheses, we compared territorial aggression of adult cGαi2$^{-/-}$ male mice vs. age-matched cGαi2$^{+/-}$ males in the resident–intruder paradigm (15, 16) (Fig. 3*A*).

Surprisingly, the number of animals attacking an adult male intruder was significantly higher in cGαi2$^{-/-}$ (25 of 27 mice; 93%) vs. cGαi2$^{+/-}$ residents (15 of 23 mice; 65%; $P < 0.05$; Fig. 3*A*), but there was no difference in the intruder investigation time for each genotype (*SI Appendix*, Fig. S4*A*). Total attack duration in three consecutive 10-min trials was high in cGαi2$^{-/-}$ and cGαi2$^{+/-}$ males (130 and 78 s, respectively; $P < 0.05$), showing that Gαi2 is dispensable for the display of aggression. By contrast, castrated male intruders consistently induced less aggression in control cGαi2$^{+/-}$ male residents (37 s; 50% reduction; $P < 0.05$; Fig. 3*A*), whereas attack duration to castrated males was approximately threefold higher in cGαi2$^{-/-}$ residents (129 s; $P < 0.01$) and did not differ from the level of aggression to intact male intruders ($P = 0.8$). Thus, there was no loss of territorial aggression in cGαi2$^{-/-}$ male residents.

Previous work has shown that the HMW (>10 kDa) and LMW (< 10 kDa; includes small peptides) fractions of urine from adult male mice can induce aggression in male residents (15, 16). Therefore, we tested whether cGαi2$^{-/-}$ VSNs are capable of detecting these two fractions. We used Ca^{2+} imaging in cGαi2$^{-/-}$, cGαi2$^{+/-}$, and Trpc2$^{-/-}$ VSNs to record responses to whole urine and the HMW and LMW fractions (Fig. 3*B*). All fractions induced large responses in cGαi2$^{+/-}$ VSNs: 592 of 4,698 cells screened (12%) responded to urine, 250 of 4,698 to LMW fractions (5%), and 402 of 5,577 (7%) to HMW fractions. In cGαi2$^{-/-}$, urine responses were reduced by half (215 of 3,366 activated cells; 6%; $P < 0.001$) and LMW fraction responses by approximately 60% (74 of 3,366; 2%; $P < 0.001$), whereas HMW responses were identical or even slightly elevated (551 of 5,797; 9%; $P = 0.2$; Fig. 3*B*). We identified activated cells by combining Ca^{2+} imaging with post hoc immunostaining (*SI Appendix*, Fig. S2*B*) (15, 16) using antibodies against PDE4A and Gαo (Fig. 3*C*). The vast majority of cells activated by HMW were Gαo^{+} in cGαi2$^{-/-}$ and control VSNs. LMW fraction and castrated male urine activated Gαo^{+} and PDE4A^{+} control VSNs, but nearly all cGαi2$^{-/-}$ activated cells were negative for PDE4A (Fig. 3*C* and *SI Appendix*, Fig. S4*B*). Together, these results indicate that activation of the Gαo^{+} VSN subpopulation is sufficient to induce intermale aggression, irrespective of whether this aggression is promoted by HMW or LMW urine fractions or castrated male urine.

Increased Brain Activation to Male Intruder in Gαi2 Mutant Males. To strengthen these results, we mapped in vivo brain activation in nine distinct regions of the central nervous system implicated in aggression (26) by using immunodetection of the immediate early gene c-Fos. These analyses included subdivisions of the MeA [posterodorsal MeA (MeApd) and posteroventral MeA (MeApv) divisions] and VMH [dorsomedial VMH (VMHdm) and ventrolateral VMH (VMHvl)], the posteromedial part of the medial division of the BNST (BNSTmpm), medial preoptic area (MPOA), and lateral septum (LS). Nonstimulated cGαi2$^{-/-}$ and cGαi2$^{+/-}$ males showed equivalent levels of basal c-Fos activity in all nine brain regions (*SI Appendix*, Fig. S4*C*). Exposure to adult male intruders induced a significant increase in the number of c-Fos^{+} nuclei in three of these regions: MeApd, BNSTmpm, and LS (Fig. 3 *D* and *E*). We did not observe significant differences in some other regions implicated in aggression, such as the VMH (Fig. 3*E*).

Male–male aggression and male pheromones activate a specific subpopulation of MeA neurons that are GABAergic and positive for the androgen receptor (AR) (43, 44). We used double-label IHC for c-Fos and AR, GABA, calbindin (CB), or calretinin (CR) to identify the MeA neurons activated in our experiments. In cGαi2$^{-/-}$ and cGαi2$^{+/-}$ males, c-Fos^{+} nuclei largely colocalized with AR (Fig. 3 *F* and *G*) and GABA, but not with CB and CR (*SI Appendix*, Fig. S4*D*). Moreover, the proportion of c-Fos^{+} neurons positive for AR was even larger in cGαi2$^{-/-}$ males, whereas no change was observed in the absolute number of AR^{+} neurons (Fig. 3*G*). Therefore, conditional Gαi2 deletion resulted in increased neural activation of a population of GABAergic, AR^{+} neurons in the MeA following exposure to a male intruder.

Infant-Directed Aggression Is Diminished in Gαi2 Mutant Males, but Parental Behavior Is Enhanced. Infanticidal behavior in mice, in which an adult attacks and kills a pup, is observed in virgin adult male mice and depends strongly on a functional VNO (24, 25). We investigated infant-directed behavioral consequences of the Gαi2 deletion. We exposed virgin males to 1–2-d-old pups and found that the number of aggressive animals was drastically reduced, whereas attack latency was significantly increased in cGαi2$^{-/-}$ males vs. heterozygous controls ($P < 0.01$; Fig. 4 *A* and *B*). Moreover, two critical measures of parenting behavior—pup grooming and pup retrieval—were significantly increased in cGαi2$^{-/-}$ males ($P < 0.05$ and $P < 0.01$; Fig. 4*B*). Thus, the display of pup-directed aggression is strongly decreased, whereas parental behavior is enhanced, in Gαi2 mutant males.

We used Fos immunodetection to examine whether the lack of apical/Gαi2^{+} sensory inputs alters neural activity in aggression-controlling brain centers during infant-directed aggression (Fig.

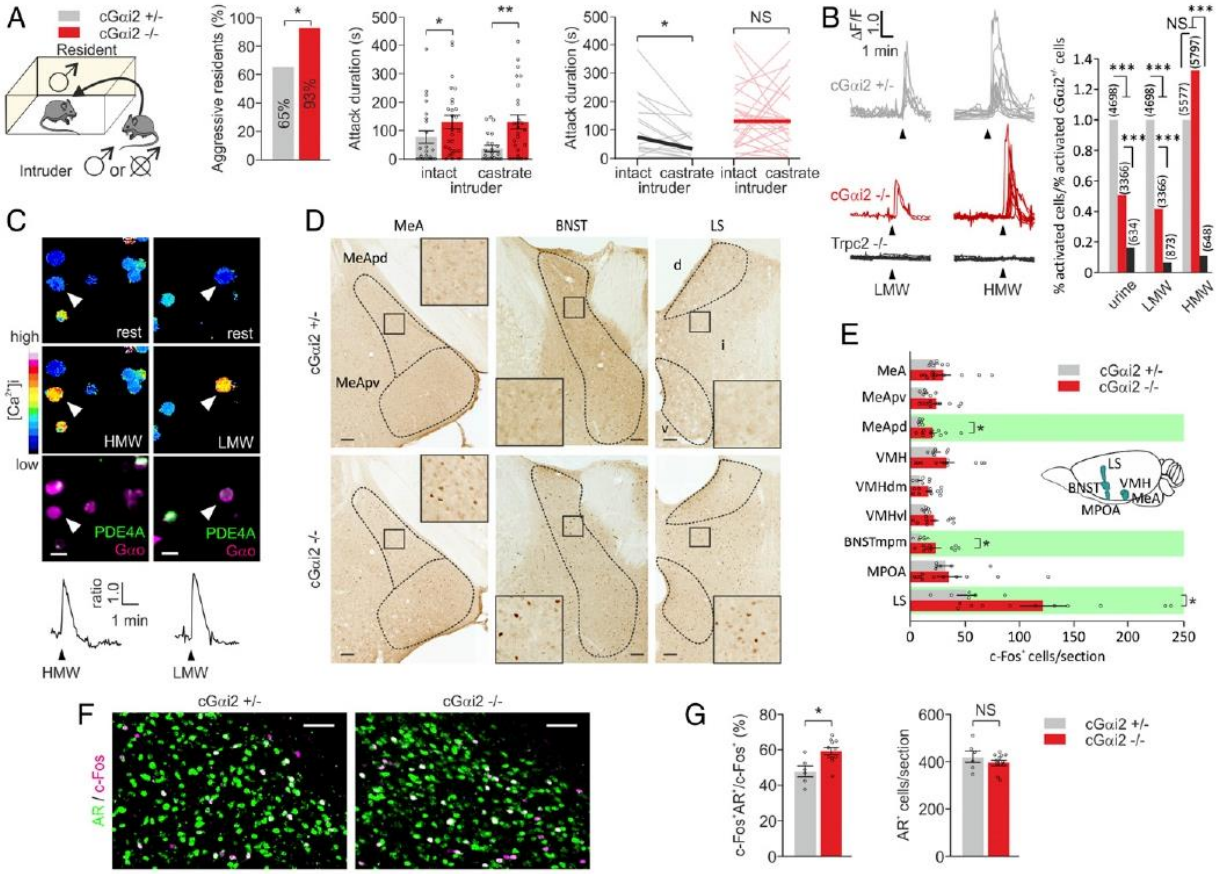

Fig. 3. Loss of Gαi2 enhances territorial aggression and increases activity in aggression-controlling brain centers. (*A*) Territorial aggression is enhanced in sexually experienced cGαi2$^{-/-}$ resident males exposed to intact and castrated intruders in the resident–intruder assay. Fifteen of 23 cGαi2$^{+/-}$ mice (65%) and 25 of 27 (93%) cGαi2$^{-/-}$ resident males were aggressive at least once during three consecutive resident–intruder trials to intact and castrated male intruders (*$P < 0.05$, Fisher's exact test). Cumulative attack duration was higher in cGαi2$^{-/-}$ residents (**$P < 0.01$ and *$P < 0.05$, Mann–Whitney *U* test). Comparison of cGαi2$^{+/-}$ residents' behavior toward gonadally intact vs. castrated intruders indicates the normal reduction in aggression toward a castrate (*$P < 0.05$, Wilcoxon test). This behavior is lost in the cGαi2$^{-/-}$ residents [nonsignificant (NS), $P = 0.8$, Wilcoxon test]. (*B*) Examples of Ca^{2+} transients (*Left*) imaged in dissociated VSNs of cGαi2$^{+/-}$, cGαi2$^{-/-}$, and Trpc2$^{-/-}$ mice stimulated with LMW (1:100) and HMW (1:100) fractions. Analysis of responding cells over total cGαi2$^{+/-}$ responding cells (*Right*) reveals reduced responsivity to urine (1:100) and LMW fraction in cGαi2$^{-/-}$ cells and a loss in Trpc2$^{-/-}$ cells (***$P < 0.001$; NS, $P = 0.2$, Fisher's exact test). Number of cells analyzed is indicated above each bar. Each stimulus was tested in 3–20 mice. (*C*) Fura-2 ratio imaging and post hoc IHC of cGαi2$^{-/-}$ cells indicate that cells activated by LMW and HMW fractions are Gαo^{+} and PDE4A^{-}. Time points of Ca^{2+} images show resting or peak fluorescence levels to stimulation with HMW or LMW fractions. Representative Ca^{2+} transients shown for imaged cells (white arrowheads) are indicated for each condition. (Scale bar, 10 μm.) (*D*) Examples of c-Fos activation in MeA, BNST, and LS of cGαi2$^{+/-}$ and cGαi2$^{-/-}$ male mice exposed to intact male intruder for 10 min. Dashed lines indicate the border of brain areas. Boxes are shown at higher magnification in the *Inset*. (Scale bars, 100 μm.) (*E*) Quantification of c-Fos^{+} cells per section in cGαi2$^{+/-}$ ($n = 6$) and cGαi2$^{-/-}$ residents ($n = 11$) after exposure to an intact intruder reveals an increase in c-Fos expression in MeApd, BNSTmpm, and LS of cGαi2$^{-/-}$ mice (marked in green; *$P < 0.05$; NS, $P = 0.15$–0.99, Mann–Whitney *U* test). (*F*) Gαi2 deletion resulted in increased c-Fos activation of a population of GABAergic, AR^{+} neurons in the MeApd following a 10-min exposure to an intact male intruder. (*G*) Percentage of c-Fos^{+} neurons expressing AR (*Left*) and number of AR^{+} cells per section (*Right*) in the MeApd after a 10-min exposure to an intact male intruder (*$P < 0.05$; NS, $P = 0.46$, Mann–Whitney *U* test). (Scale bars, 50 μm.) d, dorsal LS; i, intermediate LS; v, ventral LS. Data are expressed as means ± SEM.

4 *C* and *D*). We compared the density of c-Fos^{+} nuclei of cGαi2$^{-/-}$ males vs. cGαi2$^{+/-}$ males following pup exposure. In the granular layer of the anterior AOB, c-Fos^{+} cell density was significantly lower in parental cGαi2$^{-/-}$ males vs. aggressive cGαi2$^{+/-}$ male mice ($P < 0.001$; Fig. 4 *C* and *D*), consistent with reduced sensory input from the apical VNO in these mutants. Aggressive cGαi2$^{+/-}$ males also showed more c-Fos^{+} cells in the MeApv and MeApd compared with cGαi2$^{-/-}$ males, suggesting that Gαi2-dependent sensory inputs elicit MeA activation and infant-directed aggression. We also investigated the MPOA of the hypothalamus, a key region in the control of parenting behaviors (45). We observed specific activation during pup interactions in cGαi2$^{-/-}$ males, but this activation was absent in aggressive cGαi2$^{+/-}$ controls (Fig. 4 *C* and *D*). Importantly, our c-Fos mapping revealed significantly higher activation in the medial preoptic nucleus (MPO), the central region of MPOA, of cGαi2$^{-/-}$ males compared with parental controls ($P < 0.05$; Fig. 4 *C* and *D*). Thus, Gαi2-dependent VNO inputs seem to inhibit MPOA activation and subsequent parental behavior.

To identify the activated neurons in the MeA during pup-directed aggression and determine whether they belong to the same AR^{+}, GABAergic neurons activated during male–male aggression, we performed double-label IHC for c-Fos and AR. There was little overlap between c-Fos^{+} and AR^{+} nuclei in aggressive cGαi2$^{+/-}$ males (Fig. 4*E*). c-Fos^{+} nuclei also did not colocalize with CB^{+} or CR^{+} cells in the MeA (*SI Appendix*, Fig. S5).

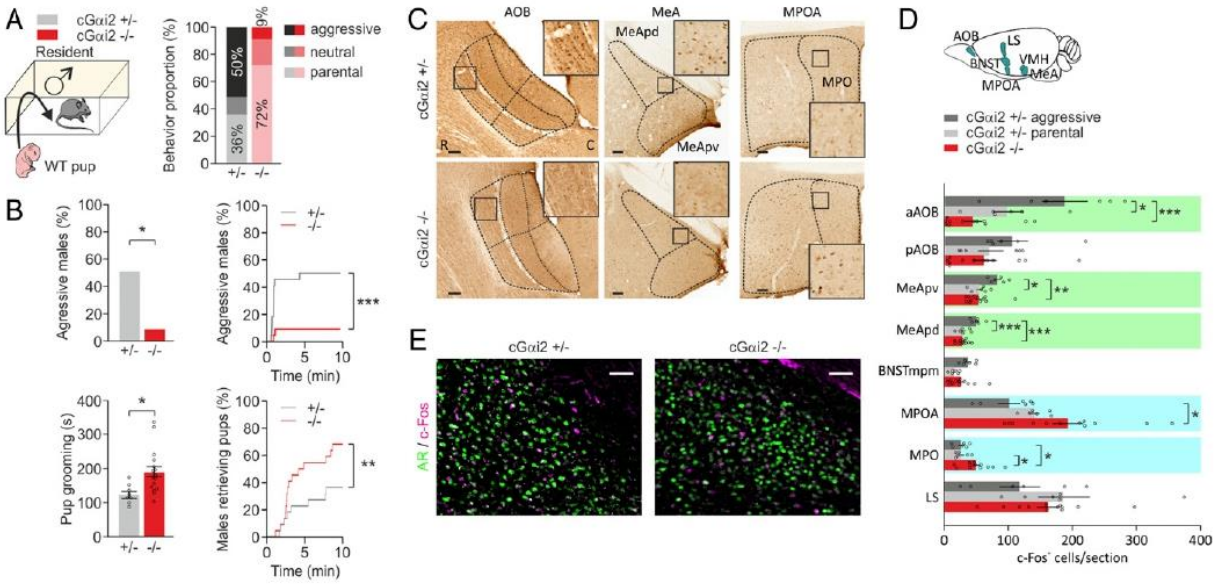

Fig. 4. cGαi2$^{-/-}$ male mice show diminished infant-directed aggression but enhanced parental behavior. (*A*) Comparison of pup-directed behavior of adult cGαi2$^{+/-}$ vs. cGαi2$^{-/-}$ male residents. Pups (WT) were used at postnatal days 1–2. Males attacked (aggressive), ignored (neutral), or retrieved neonates to the nest (parental behavior). cGαi2$^{-/-}$ males were predominantly parental (72%), whereas cGαi2$^{+/-}$ males attacked the pups (50%; $n = 22$ for each genotype). (*B*) Percentages of aggressive males (*$P < 0.05$, Fisher's exact test) and their latency to attack the neonates (***$P < 0.001$, Kolmogorov–Smirnov test), pup grooming times of the cGαi2$^{+/-}$ ($n = 8$) and cGαi2$^{-/-}$ residents ($n = 16$) that showed the behavior [t test: $t(22) = 2.73$, *$P < 0.05$], and percentage of males retrieving pups (**$P < 0.01$, Kolmogorov–Smirnov test). (*C*) Examples of c-Fos activation in AOB, MeA, and MPOA of cGαi2$^{+/-}$ and cGai2$^{-/-}$ males exposed to an alien pup for 10 min. Dashed lines indicate brain areas where c-Fos^{+} cells were counted. Boxes are shown at higher magnification in the *Inset*. C, caudal; R, rostral. (Scale bars, 100 μm.) (*D*) Quantification of c-Fos^{+} cells per section of aggressive cGαi2$^{+/-}$ ($n = 6$), parental cGαi2$^{+/-}$ ($n = 6$), and cGαi2$^{-/-}$ residents ($n = 12$) after exposure to an alien pup reveals increased c-Fos activation in aAOB, MeApd, and MeApv of aggressive cGαi2$^{+/-}$ males [aAOB, $F(2,21) = 10.72$, $P < 0.001$; MeApd, $F(2,21) = 13.98$, $P < 0.001$; MeApv, $F(2,21) = 6.075$, $P < 0.001$, ANOVA; *$P < 0.05$, **$P < 0.01$, ***$P < 0.001$, Tukey test; green]. Enhanced activation is observed in the MPOA (MPO) of cGαi2$^{-/-}$ males [MPOA, $F(2,21) = 5.236$, $P < 0.05$; MPO, $F(2,21) = 4.377$, $P < 0.05$, ANOVA; *$P < 0.05$, Tukey test; blue]. No significant differences are observed in other regions analyzed ($P = 0.06$–0.81, ANOVA). (*E*) Conditional Gαi2 deletion does not cause c-Fos activation of a population of GABAergic, AR^{+} neurons in the MeApd following a 10-min exposure to neonates. (Scale bar, 50 μm.) aAOB, anterior AOB; pAOB, posterior AOB. Data are expressed as means ± SEM.

Therefore, the MeA neurons activated during pup-directed aggression are distinct from those activated during male–male aggression. Together, these results provide strong support for a model in which Gαi2^{+} VSNs control infant-directed aggression by activation of specific aggression nodes that, in turn, inhibit parental-specific circuits.

Discussion

Our results show that the Gαi2^{+} population of VSNs controls important aspects of male–male and infant-directed aggression. We identify Gαi2 as the primary G protein α-subunit mediating the detection of small organic chemosignals by apical VSNs, most likely being responsible for activation of Trpc2 and subsequent Ca^{2+} entry downstream of V1R activation. Gαi2 is an abundant G protein expressed in major cognitive centers such as the cortex and is important for its development, and complete loss or reduction of Gαi2 signaling can result in defective social interaction, increased anxiety, and intellectual disability (27). Therefore, a global Gαi2 mutation may impede investigations of complex VNO-dependent social behaviors. Indeed, our results differ from a report that used global Gαi2-KO mice that exhibited reduced male–male aggression (23). The conditional, olfactory-restricted KO model developed here ablated Gαi2 only in *Omp*-expressing cells, indicating that the observed behavioral deficits depend on the olfactory system. *Omp* is highly expressed in mature sensory neurons of MOE and VNO (46). Although Gαi2 is also expressed in some sensory neurons of the MOE (47), Gαi2 does not seem to participate in known sensory signaling events (48). Our conditional KO mice showed no obvious defects in MOE or MOB morphology and odor-guided behaviors depending on a functional MOE, indicating that the behavioral phenotypes we observe are largely mediated by VNO function.

We found that conditional deletion of Gαi2 suppresses infanticidal behavior, consistent with a direct role of Gαi2 in the detection of pup odor. Furthermore, c-Fos mapping showed less activation in downstream brain areas of the Gαi2 vomeronasal pathway—aAOB and MeA—in Gαi2-deficient virgin male mice exposed to pups. Interestingly, Gαi2 mutant male mice became parental after contact with pups and showed elevated c-Fos in the MPOA, suggesting that this circuit may inhibit proparental MPOA neurons (49). Thus, infanticidal behavior seems to involve the activation of a dedicated circuit, rather than being merely a consequence of the inhibition of parenting behavior.

Our Gαi2 mutant males displayed high levels of male–male aggression, indicating that the Gαi2 subpopulation of VSNs is dispensable for triggering this behavior. Therefore, male–male and infant-directed aggression are initiated by different subsets of VSNs, suggesting that distinct accessory olfactory system circuits control the display of these two forms of aggression. Consistent with this, c-Fos analysis revealed the activation of different populations of MeA neurons in the context of each behavior. Many of these cells were positive for AR in the male–male aggression assay but negative for AR in the pup-directed aggression test. Because deletion of Gαo in the VNO eliminated male–male aggression (16), Gαo^{+} VSNs are probably the key drivers of aggression induced by LMW and HMW urine fractions. The LMW fraction, which includes peptides <10 kDa, is still partially

detected by VSNs from Gαi2-deficient mice, suggesting that LMW-induced aggression is controlled via detection of $G\alpha o^+$ VSNs. However, the $G\alpha o^+$ VSN population is unlikely to govern male–male aggression independently. Gαi2-deficient mice tended to be more aggressive to intact and castrated males, suggesting that $G\alpha i2^+$ VSNs can influence male–male aggression, perhaps by eliciting partial inhibition on Gαo- and/or MOE-dependent targets in limbic brain areas. Consistent with this, we observed higher c-Fos activation in the MeA, BNST, and LS of Gαi2-deficient mice when exposed to males. Similar roles for VNO signaling in inhibiting social behaviors have been observed for sexual behavior toward young conspecifics (50). Thus, $G\alpha o^+$ and $G\alpha i2^+$ VSN populations seem to interact reciprocally to modulate male–male aggression.

Interestingly, we found no difference between Gαi2-deficient males and their heterozygous controls in mounting behavior, indicating that $G\alpha i2^+$ VSNs are not required for mating motivation in males. These results, together with studies in Trpc2 and Gαo mutants (16, 41, 42), are consistent with a relatively minor role of the VNO in the display of male mating behavior. In *Trpc2* mutant mice, however, sex preference is strongly affected, as mutant males attempt to mate with males as frequently as with females (41, 42). By contrast, Gαi2 and Gαo mutant males showed a clear preference for females (ref. 16 and the present study), suggesting that both VNO layers interact to enable sex preference.

Taken together, our results suggest a role of Gαi2 as key element in the coupling of activated V1R receptors to the downstream signal transduction machinery. Downstream signaling has been proposed to occur via Gγ13 because of coexpression with Gαi2 (51). However, because of the absence of functional measurements at the cellular level and the complexity of behavioral phenotype interpretation of Gγ13-null mice—probably affected by a critical function of Gγ13 in MOE signaling and olfaction (52)—this role has not been confirmed thus far. It has been proposed that Gαi2 may also interact with formyl peptide receptors and canonical olfactory receptors, which are mostly expressed in the apical layer of the VNO (53–55). Notably, VSNs expressing *Olfr692* seem to be activated by odors emanating from pups, especially in virgin males, suggesting a potential *Olfr692* role in infant-directed aggression (56). However, *Olfr692* is expressed in basal $G\alpha o^+$ VSNs (56), and no direct functional link has been yet established between *Olfr692* and infanticide. A recent report linked infant-derived chemosensory activity with seven vomeronasal receptors, including three V1Rs and four V2Rs, two of which (Vmn2r65 and Vmn2r88) seem to be partially implicated in infanticide (57). Together with our findings, these results support a non–labeled-line model for infant-directed aggression in which information sensed by apical and basal VSN populations is integrated to generate an aggressive response.

In conclusion, we showed here an essential role of Gαi2 in VNO sensory signaling of the apical VSN population that detects small organic molecules including volatile pheromones and steroid derivatives. Our study identifies $G\alpha i2^+$ VSNs as a critical neural component that organizes and balances male–male and infant-directed aggression. These results provide a framework for dissecting the neuronal networks underlying different forms of social aggression.

Methods

Animal care and experimental procedures were performed in accordance with French, German, and European guidelines on the protection of animals used for scientific purposes and approved by an ethical committee for animal experimentation (Comité d'Etique en Expérimentation Animale Val de Loire and Animal Welfare Committee of Saarland University School of Medicine). Mice were kept under standard 12-h light/dark cycles with food and water ad libitum.

Generation of Conditional Gαi2-Deficient Mice. $Gnai2^{fx/fx}$ mice (mixed 129sv × C57BL/6 background) were crossed to mice carrying a transgene directing the expression of Cre recombinase under the control of the *Omp* promoter [*Omp*-Cre mice; B6; 129P2-$Omp^{tm4(cre)Mom}$/MomJ; Jackson Laboratory, JR 006668; backcrossed into C57BL6/J for eight generations; neomycin cassette absent]. $Gnai2^{fx/fx}$ mice carry *loxP* sites inserted into the introns that flank exons 2 and 4. Breeding established offspring ($cG\alpha i2^{-/-}$) that were homozygous for the floxed *Gnai2* alleles and heterozygous for Cre and *Omp* ($Gnai2^{fx/fx}$ $Omp^{cre/+}$). In these mice, Cre-mediated *Gnai2* deletion was restricted to *Omp*-positive cells. Animals heterozygous for both alleles ($Gnai2^{fx/+}$ $Omp^{cre/+}$) served as controls ($cG\alpha i2^{+/-}$). Homozygous mice containing the Rosa-CAG-LSL-GCaMP6f::ΔNeo conditional allele [B6;129S-*Gt (ROSA)26Sor*$^{tm95.1(CAG-GCaMP6f)Hze}$/J; Jackson Laboratory] were crossed with $Gnai2^{fx/fx}$ to produce mice homozygous for Rosa-CAG-LSL-GCaMP6f::ΔNeo and floxed *Gnai2* alleles. These mice were crossed with homozygous $Gnai2^{fx/fx}$ $Omp^{cre/cre}$ mice to yield mice homozygous for the floxed *Gnai2* allele and heterozygous for Cre, *Omp*, and GCaMP6f ($cG\alpha i2^{-/-}$ $GCaMP6f^{+/-}$). Animals heterozygous for all alleles ($Gnai2^{fx/+}$ $Omp^{cre/+}$ $GCaMP6f^{fx/+}$) served as controls ($cG\alpha i2^{+/-}$ $GCaMP6f^{+/-}$). $Trpc2^{-/-}$ (129S6.129P2-*Trpc2* < *tm1Mom*>/MomJ; Jackson Laboratory, JR 007890; backcrossed into C57BL/6J for six generations) (58) were used for Ca^{2+} imaging in dissociated VSNs. Adults males (8–12 wk) were used.

Immunostaining. Mice were anesthetized by an overdose of pentobarbital (Ceva) and perfused transcardially with 0.9% saline solution followed by 0.1 M phosphate buffer (PB) containing 4% paraformaldehyde (PFA). For c-Fos experiments, mice were perfused 90 min after a 10-min interaction with an intact male or a neonate. Brains, VNOs, and MOEs were removed, post-fixed overnight in 4% PFA, and cryoprotected in 0.1 M PB containing 30% sucrose. Samples were embedded in Tissue-Tek O.C.T. compound, snap-frozen in cold isopentane, and processed on a Leica CM 3050S cryostat. Brains and OBs were cut in 30-μm serial free-floating sections (coronal for brains, sagittal for OB) by using Tris-buffered saline (TBS) solution containing 0.1% sodium azide. Coronal cryosections of olfactory tissues (12-μm thick) were directly mounted on SuperFrost Plus glass slides. Sections were washed (3 × 5 min) with TBS, incubated in blocking solution (TBS solution containing 0.1% Triton X-100 and 5% horse serum) for 2 h at room temperature (RT), incubated overnight at 4 °C in blocking solution supplemented with the primary antibody, and washed in TBS solution and incubated in blocking solution supplemented with secondary antibody for 2 h at RT. Nuclei were counterstained with DAPI (0.5 μg/mL; Sigma) for 5 min. For c-Fos experiments, endogenous peroxidases were blocked for 30 min in TBS solution containing 3% H_2O_2 before the serum blocking step, biotinylated secondary antibody was used, and signals were amplified with Vectastain ABC kit (Vector) and visualized with diaminobenzidine (0.02%, 0.01% H_2O_2 in 0.05 M Tris, pH 7.4). Detailed information about the antibodies used is listed in *SI Appendix*, Table S1. VNO cell density, VNO layer, and AOB volume quantifications were done from images acquired on an Olympus IX71 microscope coupled to a Hamamatsu C10600-10B camera at 10× magnification. Images were analyzed with Fiji/ImageJ [National Institutes of Health (NIH)]. Twenty-five slices of VNO from adult males (five of each genotype) were used. Demarcations of apical vs. basal layers were based on PDE4A immunoreactivity, and $DAPI^+$ cells were counted by using the particle analyzer plugin of Fiji. AOB rostrocaudal demarcation was based on Gαo immunoreactivity from 29 slices from 14 animals per genotype. Tissue volume in cubic micrometers was calculated by multiplying the surface of the immunoreactive area by the thickness of the slice. For c-Fos experiments, slices were scanned by using an automatic slide scanner (AxioScan.Z1; Zeiss). Regions of interest (ROIs) were drawn based on the Paxinos mouse brain atlas by using Zen (blue edition 3.0; Zeiss), and the number of $c\text{-}Fos^+$ cells was automatically counted bilaterally in these regions by using the particle analyzer plugin of Fiji. Numbers of slices counted per animal and region were one for the MPOA and LS; two for AOB, BNST, and VMH; and four for MeA. AR/c-Fos coexpression was quantified in five to eight MeApd images per animal acquired on a Zeiss LSM-700 confocal laser-scanning microscope at 20× magnification. Image regions were analyzed in the entire *z* axis with 3-μm step intervals, and images were reconstituted by using the maximum-intensity projection tool of Zen software. $c\text{-}Fos^+$, AR^+, and $AR/c\text{-}Fos^+$ cells were counted automatically by using the particle analyzer plugin of Fiji.

For combined Ca^{2+} imaging and immunocytochemistry, dissociated VNO cells were fixed by using PBS solution containing 4% PFA (10 min), permeabilized and incubated for 10 min in blocking solution (TST, i.e., 0.1% Triton X-100, 1% FBS, 50 mM NaCl, 100 mM Tris·HCl, pH 7.5), incubated with anti-PDE4A (1:500; 30 min, RT) and anti-Gαo (1:50; 30 min, RT), and washed in TST (5 min), followed by an incubation (30 min, RT) in secondary

antibodies (Alexa Fluor 488 goat anti-rabbit, Alexa Fluor 647 goat anti-mouse, 1:500; Invitrogen). Cells were also stained (5 min, RT) with DAPI.

Quantitative RT-PCR. VNOs and MOEs were dissected from cGαi2$^{+/-}$ and cGαi2$^{-/-}$ mice. Pools of VNO or MOE from three animals were established from a total of 21 VNOs and 9 MOEs per genotype. RNA in each pool was isolated with PureLink RNA Mini Kit (Invitrogen). cDNA was synthesized from 1 μg of total RNA by using a Superscript III First-Strand Synthesis System for RT-PCR (Invitrogen). Quantitative PCRs were performed on a CFX96 Touch Real-Time PCR Detection System (Bio-Rad) using SsoAdvanced Universal SYBR green Supermix (Bio-Rad). PCR conditions for all primers were 95 °C for 3 min followed by 39 cycles (95 °C for 10 s, 60 °C for 30 s). PCR specificity was verified by melting curve analysis. Expression of *Hprt-1*, *Omp*, *Gnai2*, and *Gnao* mRNAs were assessed. Each sample was run in triplicate, and data were analyzed with the CFX Manager 3.0 Software (Bio-Rad) normalized to *Hprt-1* expression level to obtain a ΔCt and expressed as $2^{\Delta Ct}$. VNO cDNAs were used to assess *V1re6*, *V1re2*, *V1rf3*, *V1rj2*, *Vmn2r1*, *Vmn2r65*, *Trpc2*, and *Plcb2* expression by endpoint PCR with GoTaq G2 Master Mix. Primer sequences are shown in *SI Appendix*, Table S2. PCR conditions for all primers were 95 °C for 3 min, followed by 39 cycles (95 °C for 45 s, 58 °C for 30 s, and 72 °C for 60 s), and 72 °C for 10 min. Products were run on a 1% agarose gel.

Ca^{2+} Imaging. Ca^{2+} imaging of freshly dissociated VSNs was performed as described previously (15, 16). VNO epithelium was detached from the cartilage and minced in PBS solution at 4 °C. The tissue was incubated (20 min at 37 °C) in PBS solution supplemented with papain (0.22 U/mL) and DNase I (10 U/mL; Fermentas), gently extruded in DMEM (Invitrogen) supplemented with 10% FBS, and centrifuged at 100 × *g* (5 min). Dissociated cells were plated on coverslips previously coated with concanavalin-A type V (0.5 mg/mL, overnight at 4 °C; Sigma). Cells were used immediately for imaging after loading them with fluo-4/AM or fura-2/AM (5 μM; Invitrogen) for 60 min. Coverslips containing VSNs were placed in a laminar-flow chamber (Warner Instruments) and constantly perfused at 22 °C with extracellular solution HBSS (Invitrogen) supplemented with 10 mM Hepes (2-[4-(2-hydroxyethyl) piperazin-1-yl]ethanesulfonic acid). Cells were alternately illuminated at 470 nm for fluo-4 or at 340 and 380 nm for fura-2 imaging, and light emitted above 510 nm was recorded by using a Hamamatsu C10600-10B camera installed on an Olympus IX71 microscope. Images were acquired at 0.25 Hz and analyzed by using ImageJ (NIH), including background subtraction, ROI detection, and signal analyses. ROIs were selected manually and always included the whole cell body. Peak signals were calculated from the temporal profiles of image ratio/fluorescent values. Results are based on recordings from at least three mice for each condition and genotype.

VNO tissue slices were prepared from male cGαi2$^{+/-}$ GCaMP6f$^{+/-}$ and cGαi2$^{-/-}$ GCaMP6f$^{+/-}$ mice by using slicing procedures established previously (33, 34, 39). Briefly, mice were euthanized with CO_2, followed by decapitation. VNOs were quickly removed and submerged in oxygenated extracellular solution 1 (95% O_2/5% CO_2) containing (in mM): 120 NaCl, 25 $NaHCO_3$, 5 KCl, 5 BES, 1 $MgSO_4$, 1 $CaCl_2$, and 10 mM glucose (300 mOsm). The vomer bones were removed, the VNO was embedded in 3% low-gelling temperature agarose, and coronal slices (250 μm) were cut on a vibratome (Microm HM 650 V). VNO tissues slices were imaged by using an upright scanning confocal microscope (LSM 880 Indimo; Zeiss) equipped with a 20 × 1.0 N.A. Plan-Apochromat water-immersion objective and a standard Argon laser for excitation at a wavelength of 488 nm (GCaMP6f excitation). Emitted fluorescence was collected between 500 and 550 nm. All scanning head settings were kept constant during each experiment. Optical sections were ∼7 μm thick. All scanning head settings (i.e., gain, black level, detector aperture, and laser neutral density filter) were kept constant during each experiment. GCaMP6 fluorescence changes are expressed as relative fluorescence changes, i.e., ΔF/F0 (F0 was the average of the fluorescence values 10 s before stimulation). Images were acquired at 1 Hz and analyzed by using a combination of Zen (Zeiss), ImageJ (NIH), and Igor (Wavemetrics) software. To identify and mark responding VSNs, ΔF images (F–F0) were overlaid onto transmitted light images (Fig. 2C) by using Adobe Photoshop's difference tool and slightly adjusting the exposure settings. Original ΔF images of ligand-induced VSN responses are shown in *SI Appendix*, Fig. S2*D*. VNO slices were stimulated successively and in random order by using bath application. The following criteria for stimulus-induced Ca^{2+} responses were applied. (*i*) A response was defined as a stimulus-dependent deviation of GCaMP6f fluorescence that exceeded twice the SD of the mean of the baseline fluorescence noise. (*ii*) Cells showing a response to control buffer were excluded from analysis. (*iii*) A response had to occur within 1 min after stimulus application. In time-series experiments, ligand application was repeated to confirm the repeatability of a given Ca^{2+} response.

Chemostimulation. Chemostimuli for Ca^{2+} imaging were freshly prepared each day and diluted in extracellular solution to give the following final concentrations: urine and HMW and LMW fractions, 1:100 dilution; 2-heptanone, 10^{-8} M (Sigma); 2,5-dimethylpyrazine, 10^{-6} M (Sigma); isobutylamine, 10^{-7} M (Sigma); isoamylamine, 10^{-7} M (Sigma); β-estradiol, 1 μM (E2, Sigma); 1,3,5 (10)-estratrien-3,17β-diol disulfate, 1 μM (E1050; Steraloid or Sigma); 1,3,5 (10)-estratrien-3,17β-diol 3-sulfate, 1 μM (E1100; Steraloid or Sigma); 1,3,5(10)-estratrien-3,17α-diol 3-sulfate, 1 μM (E0893; Steraloid); A7864, 1 μM (5-androsten-3β,17β-diol disulfate; Steraloid); sulfated estrogen mix (E mix) E1050, E1100, E0893, and A7864, each 1 μM; MHC peptide mix SYFPEITHI, SYIPSAEKI, AAPDNRETF, SIINFEKL, 10^{-10} M each (Genscript); and KCl, 50 mM or 60 mM (slice experiments). Sulfated estrogens were initially prepared in DMSO and further diluted in extracellular solution. C57BL/6 males (8–12 wk old; Janvier) served as urine donors. Animals were sexually naïve and were kept group-housed. Equal volumes of freshly collected urine from at least three animals were pooled. To obtain urine fractions, 0.5 mL of fresh urine was size-fractionated by centrifugation (14,000 × *g* for 30 min) by using Microcon (Millipore) or Nanosep (Pall) 10-kDa molecular mass cutoff ultrafiltration columns. The centrifugation supernatant was the LMW fraction, and, to obtain HMW fraction, the retentate was washed with 0.5 mL PBS solution three times and resuspended in 0.5 mL of PBS or oxygenated extracellular solution.

Behavioral Testing. Males were individually housed for 1 wk before testing. Mice were moved to the experimental room 2 h before testing. Assays were conducted 2 h before the start of the dark period.

Resident–intruder male–male aggression assay. Sexually experienced male mice of each genotype (23 cGαi2$^{+/-}$ and 27 cGαi2$^{-/-}$) were tested for territorial aggression. Testing lasted 10 min and began when a sexually inexperienced, gonadally intact, group-housed adult male (i.e., intruder) was placed into the home cage of the test mouse (i.e., resident), whose bedding had not been changed for at least 4 d. Each resident was exposed three times (on consecutive days) to a gonadally intact intruder. After 1 wk, the experiments were repeated with a castrated intruder. Juvenile (postnatal day 18–22) males were castrated under isoflurane general anesthesia and used in adulthood. Residents were not exposed twice to the same intruder. Aggressive behavior was defined as lunging, biting, chasing, tail rattling, wrestling, and kicking. Attack bouts were defined as a succession of aggressive events separated by <3 s. Cumulative attack duration of three consecutive tests, investigation time of the intruder, and number of mounting episodes were scored.

Pup-directed behaviors. Twenty-two sexually naïve males of each genotype were tested for behavior in the presence of an alien 1–2-d-old neonate (C57BL/6 WT) introduced into the home cage of the test mouse for 10 min. To minimize handling and stress to the pups, one single pup was taken from the nest immediately before the test, avoiding prolonged exposure to cold. If harmed, the pup was immediately removed and killed to minimize suffering and to avoid cannibalizing without previous killing. Mice were categorized as aggressive if they presented aggressive behavior (e.g., biting, killing) toward a pup, as parental if they retrieved a pup into their nest, and as neutral if they were indifferent to a pup. Latencies to attack a pup and pup grooming time were scored.

Statistics. Statistical analyses were performed by using GraphPad Prism 7.0 (GraphPad Software), OriginPro 2016G, and OriginPro 2017G (OriginLab). Assumptions of normality and homogeneity of variance were tested before conducting the following statistical approaches. Student's *t* test was used to measure the significance of the differences between two distributions. In case the results failed the test of normality, a Mann–Whitney *U* test was performed. For paired data comparisons, we used the Wilcoxon signed-ranks test, and, for categorical data, we used the Fisher's exact test. Multiple groups were compared by using a one-way or two-way ANOVA with Tukey's multiple comparison test as a post hoc comparison or Kruskal–Wallis ANOVA for nonnormal distributions. The probability of error level (i.e., α) was chosen to be 0.05. Unless otherwise stated, results are presented as means ± SEM and documentation of individual data points.

Further details on testosterone measurements, stimulus delivery, and other behavioral tests are provided in *SI Appendix*, *Materials and Methods*. The datasets generated and/or analyzed during the present study are available from the Data Inra Dataverse portal (https://data.inra.fr/).

ACKNOWLEDGMENTS. We thank Roberto Tirindelli for V2R2 antibody; Michael Konzmann, Kevin Poissenot, and Chantal Porte for technical assistance; Kerstin Becker, Lisa-Marie Knieriemen, Deborah Crespin, and Aurelie Gasnier for mouse

husbandry; Marie-Claire Blache for help with imaging experiments; and Anne-Lyse Lainé for help with hormone assays. This work was supported by Deutsche Forschungsgemeinschaft Grants Sonderforschungsbereich 894 Project A17 (to F.Z. and T.L.-Z.) and INST 256/427-1 FUGB (to T.L.-Z.), Institut National de la Recherche Agronomique (INRA) "Physiologie Animale et Systèmes d'Elevage" department (P.C.); National Institutes of Health Intramural Research Program Project Z01-ES-101643 (to L.B.); and a grant from the University of Tours and Region Centre Val de Loire (to A.-C.T.).

1. Scott JP (1966) Agonistic behavior of mice and rats: A review. *Am Zool* 6:683–701.
2. Hrdy SB (1979) Infanticide among animals: A review, classification, and examination of the implications for the reproductive strategies of females. *Ethol Sociobiol* 1:13–40.
3. McCarthy MM, Vom Saal FS (1986) Inhibition of infanticide after mating by wild male house mice. *Physiol Behav* 36:203–209.
4. Chamero P, Leinders-Zufall T, Zufall F (2012) From genes to social communication: Molecular sensing by the vomeronasal organ. *Trends Neurosci* 35:597–606.
5. Liberles SD (2014) Mammalian pheromones. *Annu Rev Physiol* 76:151–175.
6. Brennan PA, Keverne EB (2004) Something in the air? New insights into mammalian pheromones. *Curr Biol* 14:R81–R89.
7. Mohrhardt J, Nagel M, Fleck D, Ben-Shaul Y, Spehr M (2018) Signal detection and coding in the accessory olfactory system. *Chem Senses* 43:667–695.
8. Shinohara H, Asano T, Kato K (1992) Differential localization of G-proteins Gi and Go in the accessory olfactory bulb of the rat. *J Neurosci* 12:1275–1279.
9. Jia C, Halpern M (1996) Subclasses of vomeronasal receptor neurons: Differential expression of G proteins (Gi alpha 2 and G(o alpha)) and segregated projections to the accessory olfactory bulb. *Brain Res* 719:117–128.
10. Berghard A, Buck LB (1996) Sensory transduction in vomeronasal neurons: Evidence for G alpha o, G alpha i2, and adenylyl cyclase II as major components of a pheromone signaling cascade. *J Neurosci* 16:909–918.
11. Dulac C, Axel R (1995) A novel family of genes encoding putative pheromone receptors in mammals. *Cell* 83:195–206.
12. Matsunami H, Buck LB (1997) A multigene family encoding a diverse array of putative pheromone receptors in mammals. *Cell* 90:775–784.
13. Ryba NJ, Tirindelli R (1997) A new multigene family of putative pheromone receptors. *Neuron* 19:371–379.
14. Herrada G, Dulac C (1997) A novel family of putative pheromone receptors in mammals with a topographically organized and sexually dimorphic distribution. *Cell* 90:763–773.
15. Chamero P, et al. (2007) Identification of protein pheromones that promote aggressive behaviour. *Nature* 450:899–902.
16. Chamero P, et al. (2011) G protein G(alpha)o is essential for vomeronasal function and aggressive behavior in mice. *Proc Natl Acad Sci USA* 108:12898–12903.
17. Hattori T, et al. (2016) Self-exposure to the male pheromone ESP1 enhances male aggressiveness in mice. *Curr Biol* 26:1229–1234.
18. Kaur AW, et al. (2014) Murine pheromone proteins constitute a context-dependent combinatorial code governing multiple social behaviors. *Cell* 157:676–688.
19. Leinders-Zufall T, et al. (2014) A family of nonclassical class I MHC genes contributes to ultrasensitive chemodetection by mouse vomeronasal sensory neurons. *J Neurosci* 34:5121–5133.
20. Oboti L, et al. (2014) A wide range of pheromone-stimulated sexual and reproductive behaviors in female mice depend on G protein Gαo. *BMC Biol* 12:31.
21. Pérez-Gómez A, et al. (2015) Innate predator odor aversion driven by parallel olfactory subsystems that converge in the ventromedial hypothalamus. *Curr Biol* 25:1340–1346.
22. Novotny M, Harvey S, Jemiolo B, Alberts J (1985) Synthetic pheromones that promote inter-male aggression in mice. *Proc Natl Acad Sci USA* 82:2059–2061.
23. Norlin EM, Gussing F, Berghard A (2003) Vomeronasal phenotype and behavioral alterations in G alpha i2 mutant mice. *Curr Biol* 13:1214–1219.
24. Wu Z, Autry AE, Bergan JF, Watabe-Uchida M, Dulac CG (2014) Galanin neurons in the medial preoptic area govern parental behaviour. *Nature* 509:325–330.
25. Tachikawa KS, Yoshihara Y, Kuroda KO (2013) Behavioral transition from attack to parenting in male mice: A crucial role of the vomeronasal system. *J Neurosci* 33:5120–5126.
26. Trainor BC, Sisk CL, Nelson RJ (2009) Hormones and the development and expression of aggressive behavior. *Hormones, Brain and Behavior*, eds Pfaff DW, Arnold AP, Etgen AM, Fahrbach SE, Rubin RT (Academic, San Diego), 2nd Ed, pp 167–205.
27. Hamada N, et al. (2017) Role of a heterotrimeric G-protein, Gi2, in the corticogenesis: Possible involvement in periventricular nodular heterotopia and intellectual disability. *J Neurochem* 140:82–95.
28. Rudolph U, et al. (1995) Ulcerative colitis and adenocarcinoma of the colon in G alpha i2-deficient mice. *Nat Genet* 10:143–150.
29. Ustyugova IV, Zhi L, Abramowitz J, Birnbaumer L, Wu MX (2012) IEX-1 deficiency protects against colonic cancer. *Mol Cancer Res* 10:760–767.
30. Li J, Ishii T, Feinstein P, Mombaerts P (2004) Odorant receptor gene choice is reset by nuclear transfer from mouse olfactory sensory neurons. *Nature* 428:393–399.
31. Weiss J, et al. (2011) Loss-of-function mutations in sodium channel Nav1.7 cause anosmia. *Nature* 472:186–190.
32. Tanaka M, Treloar H, Kalb RG, Greer CA, Strittmatter SM (1999) G(o) protein-dependent survival of primary accessory olfactory neurons. *Proc Natl Acad Sci USA* 96:14106–14111.
33. Leinders-Zufall T, et al. (2004) MHC class I peptides as chemosensory signals in the vomeronasal organ. *Science* 306:1033–1037.
34. Leinders-Zufall T, et al. (2000) Ultrasensitive pheromone detection by mammalian vomeronasal neurons. *Nature* 405:792–796.
35. Isogai Y, et al. (2011) Molecular organization of vomeronasal chemoreception. *Nature* 478:241–245.
36. Haga-Yamanaka S, et al. (2014) Integrated action of pheromone signals in promoting courtship behavior in male mice. *eLife* 3:e03025.
37. Del Punta K, et al. (2002) Deficient pheromone responses in mice lacking a cluster of vomeronasal receptor genes. *Nature* 419:70–74.
38. Leinders-Zufall T, Ishii T, Mombaerts P, Zufall F, Boehm T (2009) Structural requirements for the activation of vomeronasal sensory neurons by MHC peptides. *Nat Neurosci* 12:1551–1558.
39. Sturm T, et al. (2013) Mouse urinary peptides provide a molecular basis for genotype discrimination by nasal sensory neurons. *Nat Commun* 4:1616.
40. Kelliher KR, Spehr M, Li XH, Zufall F, Leinders-Zufall T (2006) Pheromonal recognition memory induced by TRPC2-independent vomeronasal sensing. *Eur J Neurosci* 23:3385–3390.
41. Leypold BG, et al. (2002) Altered sexual and social behaviors in trp2 mutant mice. *Proc Natl Acad Sci USA* 99:6376–6381.
42. Stowers L, Holy TE, Meister M, Dulac C, Koentges G (2002) Loss of sex discrimination and male-male aggression in mice deficient for TRP2. *Science* 295:1493–1500.
43. Hong W, Kim D-W, Anderson DJ (2014) Antagonistic control of social versus repetitive self-grooming behaviors by separable amygdala neuronal subsets. *Cell* 158:1348–1361.
44. Blake CB, Meredith M (2011) Change in number and activation of androgen receptor-immunoreactive cells in the medial amygdala in response to chemosensory input. *Neuroscience* 190:228–238.
45. Numan M (1974) Medial preoptic area and maternal behavior in the female rat. *J Comp Physiol Psychol* 87:746–759.
46. Margolis FL (1980) A marker protein for the olfactory chemoreceptor neuron. *Proteins of the Nervous System* (Raven Press, New York), pp 59–84.
47. Ibarra-Soria X, Levitin MO, Saraiva LR, Logan DW (2014) The olfactory transcriptomes of mice. *PLoS Genet* 10:e1004593.
48. Scholz P, et al. (2016) Identification of a novel Gnao-mediated alternate olfactory signaling pathway in murine OSNs. *Front Cell Neurosci* 10:63.
49. Kohl J, Autry AE, Dulac C (2017) The neurobiology of parenting: A neural circuit perspective. *BioEssays* 39:1–11.
50. Ferrero DM, et al. (2013) A juvenile mouse pheromone inhibits sexual behaviour through the vomeronasal system. *Nature* 502:368–371.
51. Liu Q, Li S, Lu C, Yu CR, Huang L (2018) G protein γ subunit Gγ13 is essential for olfactory function and aggressive behavior in mice. *Neuroreport* 29:1333–1339.
52. Li F, et al. (2013) Heterotrimeric G protein subunit Gγ13 is critical to olfaction. *J Neurosci* 33:7975–7984.
53. Liberles SD, et al. (2009) Formyl peptide receptors are candidate chemosensory receptors in the vomeronasal organ. *Proc Natl Acad Sci USA* 106:9842–9847.
54. Rivière S, Challet L, Fluegge D, Spehr M, Rodriguez I (2009) Formyl peptide receptor-like proteins are a novel family of vomeronasal chemosensors. *Nature* 459:574–577.
55. Lévai O, Feistel T, Breer H, Strotmann J (2006) Cells in the vomeronasal organ express odorant receptors but project to the accessory olfactory bulb. *J Comp Neurol* 498:476–490.
56. Nakahara TS, et al. (2016) Detection of pup odors by non-canonical adult vomeronasal neurons expressing an odorant receptor gene is influenced by sex and parenting status. *BMC Biol* 14:12.
57. Isogai Y, et al. (2018) Multisensory logic of infant-directed aggression by males. *Cell* 175:1827–1841.e17.
58. Bleymehl K, et al. (2016) A sensor for low environmental oxygen in the mouse main olfactory epithelium. *Neuron* 92:1196–1203.

PNAS
www.pnas.org

Supplementary Information for

Central role of G protein Gαi2 and Gαi2+ vomeronasal neurons in balancing territorial and infant-directed aggression of male mice

Anne-Charlotte Trouillet, Matthieu Keller, Jan Weiss, Trese Leinders-Zufall, Lutz Birnbaumer[1], Frank Zufall[1], Pablo Chamero[1]

Corresponding author: Pablo Chamero

Email: pablo.chamero-benito@inra.fr

This PDF file includes:

Supplementary Materials and Methods
Figs. S1 to S5
Tables S1 to S2
References for SI reference citations

www.pnas.org/cgi/doi/10.1073/pnas.1821492116

Supplementary Information Text

Materials and Methods

Testosterone and Reproductive Organ Measurements: 15 males per genotype were sacrificed to collect trunk blood and to weigh testes, seminal vesicles and preputial glands. Sera were collected by centrifugation (2500 x *g* for 25 min) and levels of testosterone were measured by radioimmunoassay using 3H-testosterone as previously described (1). The assay sensitivity was 0.063 ng/ml; all samples were treated in a single assay.

Behavioral Testing: Experiments were videotaped and subsequently analyzed using Behavioral Observation Research Interactive Software (Boris) (2).

Food localization test. 12 males of each genotype were evaluated for their ability to locate a food source (chocolate cookie) hidden underneath the bedding. One week before testing, mice were familiarized twice with the food used in the experiment. Mice were food-restricted for 8 h before the testing took place. Mice were introduced into a clean cage with a 3-cm-thick layer of bedding and habituated for 5 min. Mice were briefly removed from the cage to bury a piece of cookie and then reintroduced. Time from introduction of a mouse into the cage until retrieval of the food was measured up to a maximum of 900 s. A given male was considered to have uncovered the cookie when he started to eat, holding the food with his forepaws.

Olfactory habituation dishabituation assay. 12 males of each genotype were evaluated for their ability to distinguish different conspecific urine sources (female, male

or castrated male C57BL/6 adult mice). Tests were conducted in the home-cage and an odor stimulus was placed on a cotton-tipped applicator through the hole on the cage lid. Mice were allowed to familiarize themselves with the applicator for 30 min before each test. Mice were first exposed for 1 min to distilled water (50 µl). This procedure was repeated three times with 1-min intervals, followed by presentations of urine samples (50 µl each) from an intact male, a castrated male or an estrous female. Equal urine volumes from 4 animals were pooled.

Olfactory preference test. 12 sexually experienced males of each genotype were tested for their female-directed odor preference in a Y-maze apparatus as described previously (3). Two days before the test assay, mice were accustomed to the maze for 9 min in absence of an odor stimulus. On the experimental test day, each Y-arm received either fresh male or fresh estrous female urine. The estrus status was assessed by analyzing vaginal smear cytology. The urine from a particular source was randomly placed in one of the two arms' ends. Subjects were free to investigate the stimuli for 9 min. Each animal was tested twice: first, with no direct access to the stimuli, which were placed on a filter paper in a plastic weigh boat behind a perforated wall; and second, with direct access to the stimuli (wall removed). Time of investigation of the chemosensory source was recorded. Preference scores were calculated as the difference between time spent sniffing male urine and female urine over total time of chemosensory investigation.

Sexual behavior. 12 sexually naïve males of each genotype were paired overnight in their home cage with a sexually experienced, receptive female. Latencies to mount and ejaculate and the number of mount episodes were recorded, mating duration was calculated as the interval between the first mount and ejaculation. C57BL/6 females (8

weeks old, Janvier, France) served as experimental subjects. Females were ovariectomized and implanted with estradiol silastic capsule (1:1 mix with cholesterol, Sigma) for sexual behavior experiments. Pharmacological estrus was induced by injecting progesterone (1 mg/100 µl in sesame oil, Sigma) 4 h before testing. Females were sexually experienced to show an optimal lordosis behavior in the presence of the test male.

Ultrasonic vocalizations (USVs). Sexually naïve male mice (9 cGαi2$^{+/-}$ and 8 cGαi2$^{-/-}$) were recorded for USV emission in their home-cage in the presence of an intact male or female. Animals were habituated to experimental conditions for 15 min. Animal stimuli were presented on two days, first an adult female, and two days later an adult male. Animal stimuli were introduced into the cage and USVs were recorded using a gold foil electrostatic transducer microphone (Metris B.V., Netherlands). Automatic detection and analysis using SONOTRACK 1.5.0 software (Metris B.V., Netherlands) was employed to count USVs (30 to 100 kHz range bandpass filter). This initial automated analysis was followed by manual inspection of the trials to correct for noise. Number of calls over the first 3 min of an experiment was analyzed.

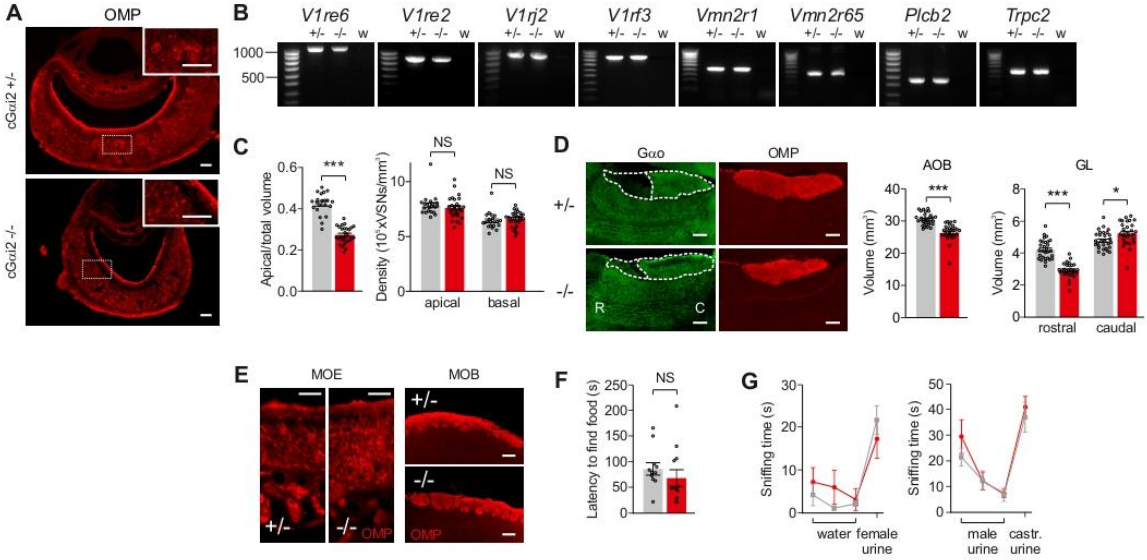
A
OMP
cGαi2 +/-
cGαi2 -/-
B
V1re6
V1re2
V1rj2
V1rf3
Vmn2r1
Vmn2r65
Plcb2
Trpc2
+/- -/- w
1000
500
C
Apical/total volume
Density (10³xVSNs/mm²)
***
NS
NS
apical
basal
D
Gαo
OMP
+/-
-/-
R
C
AOB
GL
Volume (mm³)
***
***
*
rostral
caudal
E
MOE
MOB
+/-
-/-
OMP
F
Latency to find food (s)
NS
G
Sniffing time (s)
water
female urine
male urine
castr. urine

Figure S1

Fig. S1. Olfactory system organization and function in cGαi2$^{-/-}$ mice. (*A*) OMP immunostaining marks the location of all VSNs. Scale bars, 50 µm. (*B*) RT-PCR using whole VNO cDNA of cGαi2$^{+/-}$ and cGαi2$^{-/-}$ mice reveals transcripts of *V1rs* (*V1re6, V1re2, V1rf3, V1rj2*), *V2rs* (*Vmn2r1, Vmn2r65*), and transduction molecules specific to VSN subsets (*Plcb2*) or to all VSNs (*Trpc2*) in cGαi2$^{-/-}$ mice. Water (w) was used as negative control. (*C*) Reduced volume (*left*) of the apical VNO layer in cGαi2$^{-/-}$ mice (n = 27) versus cGαi2$^{+/-}$ mice (n = 21); t-test: t(46) = 11.08, *** $P < 0.001$. Cell density of apical and basal layers (*right*) remained unchanged (Mann-Whitney test: apical, NS, P = 0.37; basal, NS, P = 0.11). The border between the two layers was identified by PDE4A immunoreactivity. (*D*) Gαo and OMP immunolabeling in the AOB of cGαi2$^{+/-}$ (n = 29) and cGαi2$^{-/-}$ mice (n = 28), total AOB volume reduction (Mann-Whitney test; $P < 0.001$), and volume differences of the glomerular layer (GL) (t-test: rostral GL, t(55) = 9.06, *** $P < 0.001$; caudal GL, t(55) = 2.63, *$P < 0.05$). R, rostral; C, caudal. Scale bar, 50 µm. (*E*) No difference of OMP immunostaining in the MOE (*left*) and MOB (*right*) of cGαi2$^{+/-}$ and cGαi2$^{-/-}$ mice. Scale bar, 50 µm. (*F-G*) General olfactory performance in a food localization (*F*) and in habituation-dishabituation assays (*G*) showed no obvious difference between cGαi2$^{+/-}$ and cGαi2$^{-/-}$ mice. Food localization test: Mann-Whitney, NS, P = 0.11 (n = 12 mice per genotype); habituation-dishabituation assay: Two-way ANOVA, F(1, 91) = 1.04 [genotype], P = 0.31 (cGαi2$^{+/-}$, n = 12; cGαi2$^{-/-}$, n = 11). Data are expressed as means ± SEM.

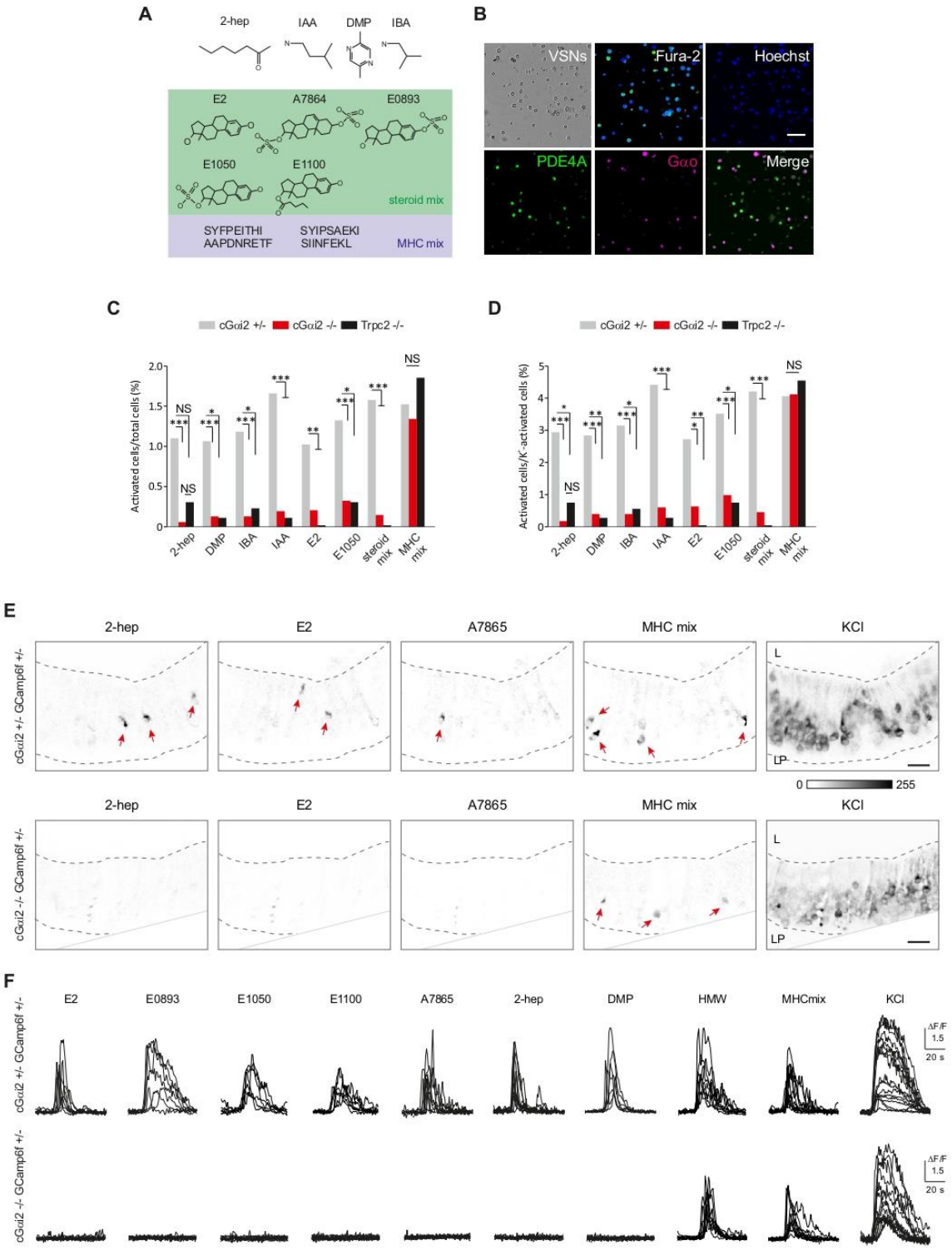
A
2-hep
IAA
DMP
IBA
E2
A7864
E0893
E1050
E1100
steroid mix
SYFPEITHI
AAPDNRETF
SYIPSAEKI
SIINFEKL
MHC mix
B
VSNs
Fura-2
Hoechst
PDE4A
Gαo
Merge
C
cGαi2 +/-
cGαi2 -/-
Trpc2 -/-
Activated cells/total cells (%)
NS
2-hep
DMP
IBA
IAA
E2
E1050
steroid mix
MHC mix
D
cGαi2 +/-
cGαi2 -/-
Trpc2 -/-
Activated cells/K+-activated cells (%)
NS
2-hep
DMP
IBA
IAA
E2
E1050
steroid mix
MHC mix
E
2-hep
E2
A7865
MHC mix
KCl
cGαi2 +/- GCamp6f +/-
cGαi2 -/- GCamp6f +/-
L
LP
0
255
F
E2
E0893
E1050
E1100
A7865
2-hep
DMP
HMW
MHCmix
KCl
cGαi2 +/- GCamp6f +/-
cGαi2 -/- GCamp6f +/-
ΔF/F
1.5
20 s

Figure S2

Fig. S2. (*A*) Chemical structures of compounds used in this study: 2-heptanone (2-hep); isoamylamine (IAA), dimethylpyrazine (DMP); isobutylamine (IBA); steroid mix: β-estradiol (E2), 1,3,5(10)-estratrien-3,17β-diol disulphate (E1050), 1,3,5(10)-estratrien-3,17β-diol 3-sulphate (E1100), 1,3,5(10)-estratrien-3,17α-diol 3-sulphate (E0893), and 5-androsten-3β,17β-diol disulfate (A7864); MHC peptide mix: SYFPEITHI, SYIPSAEKI, AAPDNRETF, SIINFEKL. (*B*) Immunocytochemistry for PDE4A and Gαo after fura-2 Ca^{2+} imaging in dissociated VSNs. Scale bar, 50 µm. (*C*) Ligand-evoked Ca^{2+} responses in dissociated cells from cGαi2$^{+/-}$, cGαi2$^{-/-}$, and Trpc2$^{-/-}$ mice expressed as percentage of responding cells to a given stimulus relative to total cells, or (*D*) relative to cells activated by KCl (50 mM). Cells were stimulated with 2-hep, (10^{-8} M), DMP (10^{-6} M), IBA (10^{-7} M), IAA (10^{-7} M), E2 (1 µM), E1050 (1 µM), sulfated steroid mix (E1050, E1100, E0893 and A7864, each at 1 µM), and MHC peptide mix (SYFPEITHI, SYIPSAEKI, AAPDNRETF, SIINFEKL, 10^{-10} M each). Fisher's exact test: * $P < 0.05$; ** $P < 0.01$; *** $P < 0.001$; No significant differences were observed between cGαi2$^{-/-}$, and Trpc2$^{-/-}$: NS, $P = 0.2 – 1$. (*E*) Spatial activity patterns in VNO slices of cGαi2$^{+/-}$ and cGαi2$^{-/-}$ mice co-expressing the Ca^{2+} reporter GCaMP6f. ΔF images (average intensity of 3 individual images at peak fluorescence) were obtained after simulation with E2 (1 µM), A7865 (1 µM), 2-heptanone (10^{-8} M), MHC mix (SYFPEITHI, SYIPSAEKI, AAPDNRETF, SIINFEKL, 10^{-10} M each), and 60 mM KCl. Red arrows indicate responding cells. L, lumen; LP, lamina propria. Scale bars, 25 µm. (*F*) Comparison of superimposed time courses of somatic VSN GCaMP6f Ca^{2+} responses obtained in cGαi2$^{+/-}$ versus cGαi2$^{-/-}$ slices to E2 (β-estradiol, 1 µM), E0893 (1, 3, 5(10)-estratrien-3, 17α-diol 3-sulphate, 1µM), E1050 (1, 3, 5(10)-estratrien-3, 17β-diol disulphate, 1 µM), E1100 (1, 3, 5(10)-

estratrien-3, 17β-diol 3-sulphate, 1 μM), A7864 (5-androsten-3β, 17β-diol disulfate, 1 μM), 2-hep (2-heptanone, 10^{-8} M), DMP (2,5-dimethylpyrazine, 10^{-6} M), HMW urine fraction (1:100), MHC mix (SYFPEITHI, SYIPSAEKI, AAPDNRETF, SIINFEKL, 10^{-10} M each), or KCl (60 mM).

9

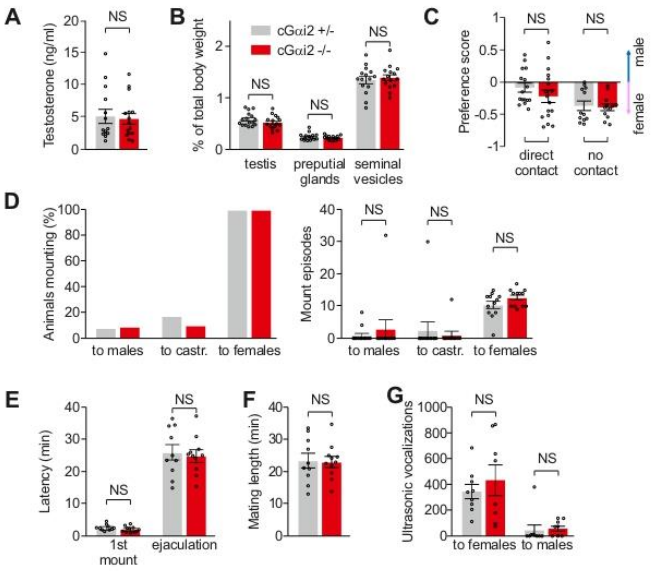
A
Testosterone (ng/ml)
NS
B
% of total body weight
cGαi2 +/-
cGαi2 -/-
NS
NS
NS
testis
preputial glands
seminal vesicles
C
Preference score
NS
NS
male
female
direct contact
no contact
D
Animals mounting (%)
to males
to castr.
to females
Mount episodes
NS
NS
NS
to males
to castr.
to females
E
Latency (min)
NS
NS
1st mount
ejaculation
F
Mating length (min)
NS
G
Ultrasonic vocalizations
NS
NS
to females
to males

Figure S3

Fig. S3. Normal sexual behavior and partner preference in cGαi2$^{-/-}$ males. (*A*) Testosterone levels and (*B*) reproductive organs weight of cGαi2$^{-/-}$ (n = 15) males are not altered compared to cGαi2$^{+/-}$ males (n = 14). Mann-Whitney test; P = 0.92 for testosterone, P = 0.19-0.63 for testis, preputial vesicles, and seminal glands. (*C*) Preference score to examine the social preference of male mice to either female or male urine in a Y-maze shows no difference between cGαi2$^{-/-}$ and cGαi2$^{+/-}$ in their choice for the stimuli to which the mice had either direct (t-test: t(31) = 1.08; NS, P = 0.28; n = 17 and 16, respectively) or no contact (t-test: t(22) = 0.26; NS, P = 0.80; n = 12 for each genotype). (*D*) No difference in mounting behavior of cGαi2$^{-/-}$ and cGαi2$^{+/-}$ male mice to male, castrated males or females was observed. *Left*: percentage of mounting behavior; *Right*: number of mount episodes (ANOVA: genotype, F(1, 64) = 0.43, P = 0.52; sex difference, F(2, 64) = 21.4, P < 0.001; n = 12 per genotype). Both genotypes preferred to mount females (Tukey: *** P < 0.001; NS, P = 0.75-0.81). (*E*) No difference in the latencies to first mount and ejaculation was observed in cGαi2$^{-/-}$ (n = 10) and cGαi2$^{+/-}$ (n = 11) male mice towards female mice (t-test: t(19) = 1.31-0.32; NS, P = 0.21-0.76), (*F*) Mating length was indistinguishable between cGαi2$^{-/-}$ (n = 10) and cGαi2$^{+/-}$ (n = 11) male mice (t-test: t(19) = 1.36; NS, P = 0.89). (*G*) Ultrasonic vocalizations to females measured in cGαi2$^{-/-}$ (n = 8) and cGαi2$^{+/-}$ (n = 9) male mice (Kruskal-Wallis ANOVA: X^2 = 9.48, P < 0.01, all four groups compared, independent samples; Mann-Whitney: NS, P = 0.96, females; P = 0.26, males). Both genotypes preferred to vocalize to females (Mann-Whitney: P < 0.01, for both genotypes). Data are expressed as means ± SEM.

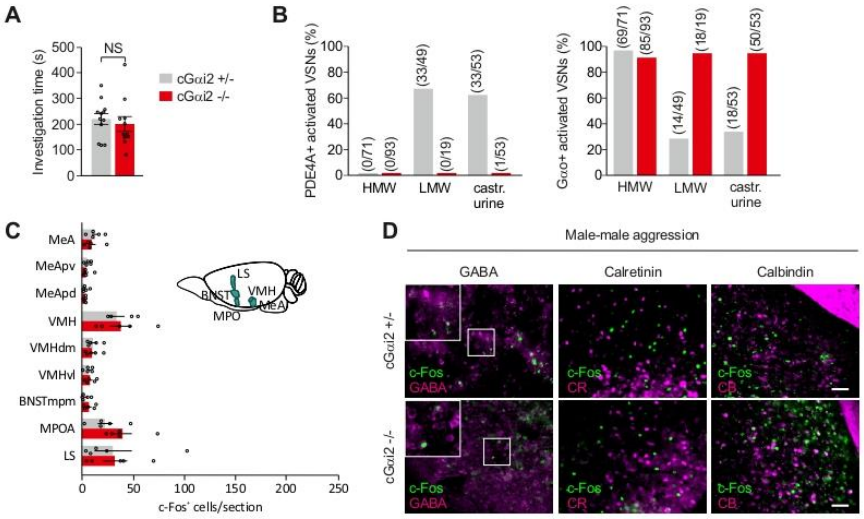
A
Investigation time (s)
NS
cGαi2 +/-
cGαi2 -/-
B
PDE4A+ activated VSNs (%)
(0/71)
(0/93)
(33/49)
(0/19)
(33/53)
(1/53)
HMW
LMW
castr. urine
Gαo+ activated VSNs (%)
(69/71)
(85/93)
(14/49)
(18/19)
(18/53)
(50/53)
C
MeA
MeApv
MeApd
VMH
VMHdm
VMHvl
BNSTmpm
MPOA
LS
c-Fos+ cells/section
D
Male-male aggression
GABA
Calretinin
Calbindin
cGαi2 +/-
cGαi2 -/-
c-Fos
GABA
CR
CB

Figure S4

Fig. S4. (*A*) Intruder investigation time does not differ between cGαi2$^{+/-}$ and cGαi2$^{-/-}$ (*n* = 12, each) in the resident-intruder assay (t-test: t(21) = 0.55; NS, *P* = 0.59). (*B*) Comparison of stimuli detection by PDE4A+ and Gαo+ VSNs. Loss of Gαi2 shifts the detection of stimuli to Gαo+ cells. Ca^{2+} imaging of VNO cells stimulated with HMW (1:100), LMW fractions of urine (1:100) and castrated male urine (1:100), followed by a post-hoc IHC for PDE4A and Gαo was performed on 1207 cells from cGαi2$^{+/-}$ mice (*n* = 4) and 978 cells of cGαi2$^{-/-}$ mice (*n* = 4). LMW and castrated male urine is detected by both PDE4A+ and Gαo+ cells in cGαi2$^{+/-}$, but only by Gαo+ cells in cGαi2$^{-/-}$. Number of PDE4A+ and Gαo+ versus total cells activated by a given stimulus is indicated above each bar. (*C*) Quantification of c-Fos+ cells per section (30 µm thick) of cGαi2$^{+/-}$ and cGαi2$^{-/-}$ residents (*n* = 5, each) without chemostimulation reveals no change in c-Fos expression in the various brain areas (Mann-Whitney: *P* = 0.13-0.96). MeA, medial amygdala (MeApd, posterodorsal; MeApv, posteroventral); VMH, ventromedial hypothalamus (VMHdm, dorsomedial; VMHvl, ventrolateral); BNST, bed nucleus of the stria terminalis (BNSTmpm, posteromedial part of the medial division); MPOA, medial preoptic area; LS, lateral septum (d, dorsal, v, ventral, i, intermediate). Data are expressed as means ± SEM. (*D*) c-Fos co-localization with GABA, calretinin (CR) and calbindin (CB) in the MeApd of cGαi2$^{-/-}$ and cGαi2$^{+/-}$ males after a 10-min exposure to an intact male intruder. NS, not significant. Data are expressed as means ± SEM. Scale bar, 50 µm.

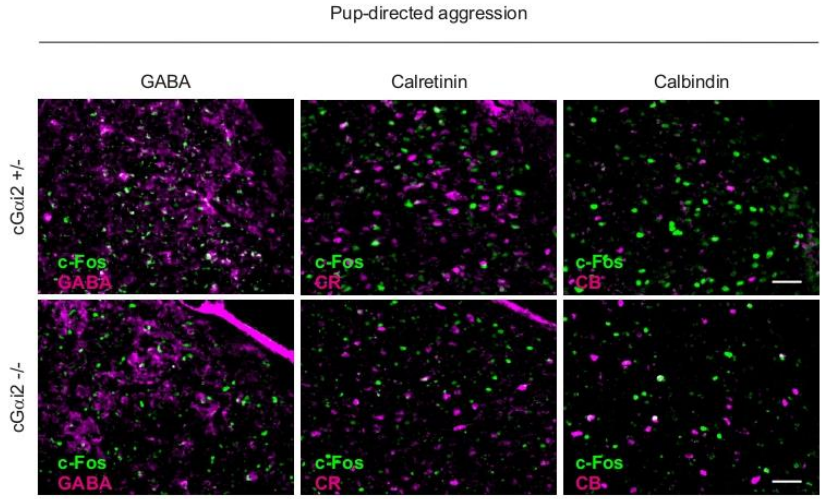
Pup-directed aggression
GABA
Calretinin
Calbindin
cGαi2 +/-
cGαi2 -/-
c-Fos
GABA
c-Fos
CR
c-Fos
CB
c-Fos
GABA
c-Fos
CR
c-Fos
CB

Figure S5

Fig. S5. Co-localization of c-Fos+ nuclei with various markers to identify activated cells in the MeApd of cGαi2$^{-/-}$ and aggressive cGαi2$^{+/-}$ males after exposure to a pup in the pup-directed aggression test. Scale bars, 50 µm. There was no overlap between c-Fos and calretinin (CR) or calbindin (CB).

Table S1. Antibodies, references and concentrations used.

Target	Primary antibody	Concentration
OMP	goat, Wako #544-10001	1:2000
Gαi2	rabbit, Calbiochem #37 1729	1:250
V2R2	rabbit, gift R. Tirindelli, University of Parma, Parma, Italy	1:10 000
PDE4A	rabbit, Fabgennix #PD4-112AP	1:500
Gαo	rabbit, Santa Cruz #sc-387	1:200
	mouse, Santa Cruz #sc-13532	1:200
c-Fos	rabbit, Santa Cruz #sc-52	1:500
		1:200 (IF)
	mouse, Santa Cruz #sc-271243	1:200
AR	rabbit, Santa Cruz #sc-816	1:200
GABA	mouse, Sigma #A0310	1:200
Calbindin	mouse, Sigma #C9848	1:400
Calretinin	goat, Swant #CG1	1:3000
Goat IgG	Donkey anti-goat Alexa-647, Invitrogen #A32849	1:500
Rabbit IgG	Donkey anti-rabbit Alexa-588, Invitrogen #A21206	1:500
	Goat anti-rabbit biotinylated, Jackson #111-065-003	1:1000
Mouse IgG	Donkey anti-mouse Alexa-588, Invitrogen #A21202	1:500
	Donkey anti-mouse Alexa-647, Invitrogen #A3157	1:500

Table S2. Primer sequences.

Gene	Forward primer (5'-3')	Reverse primer (5'-3')	Product size (bp)
Hprt1	GGTCCTTTTCACCAGCAAGCT	TGACACTGGTAAAACAATGCA	94
Omp	GCACAGTTAGCAGGTTCAGCT	GGTTTGCAGTCCTGGCAGC	197
Gnai2	GAGCATGAAGCTGTTTGACAGC	CTCCTTGGTGTCTTTGCGC	220
Gnao	CTCCACGAGGACGAAACCAC	GCCCCGGAGATTGTTGGCA	348
V1re6	ATGATCCTTACACACACATATTCC	TTATGGTATTTTTATATTTCTTGTCCATG	1026
V1re2	ATGGACTTGAGGACCATGATAGTTG	CTAGGTAAAGCAGAATCTGGAAATAGC	897
V1rf3	ATGGAAAACAGTGACATTGTAATTAGTGT	TTAACTGGAGATCACCAGAAAGGGA	870
V1rj2	CATCACTCCCAGTAAYTCTAAGTGGGC	GCTGGGMTCTCTTGTRRTGYCTGTAGA	320
Vmn2r1	TTGTGGGCTGTATTGGGTGC	TGATCCCCCTGATCCAACCA	432
Vmn2r65	GAGTGTAGCACATCCCAAGTG	GGAATGGCCCAAGTATGGCA	401
Trpc2	ATGTTCGGCATGGAAGAGCA	GATGACTCGAAGGCGGTAGG	435
Plcb2	GCCCACGATACACTGCTGAT	ACAGGGACACTAGACGGGAG	563

References

1. Hochereau-de Reviers MT, Perreau C, Pisselet C, Fontaine I, Monet-Kuntz C (1990) Comparisons of endocrinological and testis parameters in 18-month-old Ile de France and Romanov rams. *Domest Anim Endocrinol* 7(1):63–73.

2. Friard O, Gamba M (2016) BORIS: a free, versatile open-source event-logging software for video/audio coding and live observations. *Methods in Ecology and Evolution* 7(11):1325–1330.

3. Jouhanneau M, Cornilleau F, Keller M (2014) Peripubertal exposure to male odors influences female puberty and adult expression of male-directed odor preference in mice. *Horm Behav* 65(2):128–133.

2 Impact de la délétion de Gαi2 dans les VSNs sur les comportements socio-sexuels femelles

Journal article #2: Sensory detection by the vomeronasal organ modulates experience-dependent social behaviors in female

Anne-Charlotte Trouillet[1], Chantal Moussu[1], Kevin Poissenot[1], Matthieu Keller[1], Lutz Birnbaumer[2,3], Trese leinders-Zufall[3], Frank Zufall[3], and Pablo Chamero[1]

[1] Laboratoire de Physiologie de la reproduction et des Comportements, UMR OO85-INRAE-CNRS-IFCE-University of Tours, Nouzilly, France

[2] Neurobiology Laboratory, National Institute of Environmental Health Sciences, Durham, NC, United States of America

[3] School of Medical Sciences, Institute of Biomedical Research, Catholic University of Argentina, Buenos Aires, Argentina

[4] Center for Integrative Physiology and Molecular Medicine, Saarland University, Homburg, Germany

Published in Frontiers in Cellular Neuroscience, February 2021.

Résumé

L'apparition de comportements spécifiques aux femelles chez les souris résulte d'interactions entre les mécanismes de détection sensorielle et des voies neuronales plastiques. Les réponses olfactives sont généralement câblées, mais certains aspects du comportement femelle peuvent évoluer après une expérience sociale. Cette étude visait à déterminer le rôle de la signalisation voméronasale Gαi2 dans les comportements sociaux innés chez les femelles et, ensuite, à déterminer si la détection sensorielle par cette voie influence également l'expérience sociale. Nous avons choisi de nous concentrer sur les comportements dirigés vers les mâles et les petits puisque ces comportements sont modulés par la signalisation voméronasale Gαi2 chez les souris mâles et sont modifiés par l'expérience sociale chez les femelles. Nous avons utilisé deux paradigmes comportementaux différents, la récupération des petits et la réceptivité sexuelle, dans lesquels des souris femelles Gαi2 nulle conditionnellement restreinte à l'olfaction (cGαi2-/-) étaient naïves ou expérimentées face aux stimuli, soit un nouveau-né, soit un mâle adulte. Après les expériences comportementales, les cerveaux ont été

cartographiés pour l'expression de cFos afin d'élucider les voies neurales médiant la transformation de l'information olfactive en une décision comportementale.

Nous avons exposé des femelles naïves à un nouveau-né étranger et avons observé que les entrées dépendantes de Gαi2 participent à la détection de l'odeur des petits, et que la délétion de Gαi2 réduit la récupération des petits, bien que les comportements de soin des petits soient toujours présents après la récupération. En conséquence, nous avons trouvé une réduction de l'expression de cFos dans l'aAOB mais pas dans les zones hypothalamiques associées à la parentalité. La maternité augmente considérablement les comportements parentaux et modifie la signification comportementale des odeurs de mâles, car les femelles allaitantes montrent une réponse agressive envers un mâle au lieu d'une attraction sexuelle. De manière surprenante, le comportement de récupération des petits et l'agressivité maternelle des femelles cGαi2-/- sont inchangés.

Nous avons mesuré les capacités de discrimination olfactive des femelles cGαi2-/- et déterminé qu'elles pouvaient reconnaître les odeurs de mâles et développer une préférence pour eux. Ensuite, nous avons évalué leur réponse aux mâles sexuellement expérimentés en quantifiant leur réponse à la monte de mâles, la lordose. Chez les femelles cGαi2-/-, nous n'avons pas observé l'augmentation progressive des réponses de lordose habituellement induite par la répétition des tests. Le quotient de lordose des femelles cGαi2-/- sexuellement expérimentées était significativement réduit. Cet effet n'était pas la conséquence d'une physiologie altérée des organes reproducteurs. Nous avons plutôt constaté une réduction des cellules exprimant le cFos dans la population neuronale du RP3V négative à la kisspeptine, un groupe hypothalamique de cellules activé par les odeurs de mâle et qui régule la lordose.

Dans l'ensemble, nos données suggèrent que la détection des phéromones par le VNO influence les comportements contrôlés par l’olfaction chez les femelles avant et après une expérience sociale, bien qu'avec des traits distincts pour les différents comportements. Cela pourrait illustrer un mécanisme de neuroplasticité dans lequel l'olfaction, combinée à l'expérience sociale, améliore le comportement social de manière synergique.

frontiers in Cellular Neuroscience

ORIGINAL RESEARCH
published: 17 February 2021
doi: 10.3389/fncel.2021.638800

Sensory Detection by the Vomeronasal Organ Modulates Experience-Dependent Social Behaviors in Female Mice

*Anne-Charlotte Trouillet[1], Chantal Moussu[1], Kevin Poissenot[1], Matthieu Keller[1], Lutz Birnbaumer[2,3], Trese Leinders-Zufall[4], Frank Zufall[4] and Pablo Chamero[1]**

[1] Laboratoire de Physiologie de la Reproduction et des Comportements, UMR 0085 INRAE-CNRS-IFCE-University of Tours, Nouzilly, France, [2] Neurobiology Laboratory, National Institute of Environmental Health Sciences, National Institutes of Health, Durham, NC, United States, [3] School of Medical Sciences, Institute of Biomedical Research (BIOMED), Catholic University of Argentina, Buenos Aires, Argentina, [4] Center for Integrative Physiology and Molecular Medicine, Saarland University, Homburg, Germany

In mice, social behaviors are largely controlled by the olfactory system. Pheromone detection induces naïve virgin females to retrieve isolated pups to the nest and to be sexually receptive to males, but social experience increases the performance of both types of innate behaviors. Whether animals are intrinsically sensitive to the smell of conspecifics, or the detection of olfactory cues modulates experience for the display of social responses is currently unclear. Here, we employed mice with an olfactory-specific deletion of the G protein Gαi2, which partially eliminates sensory function in the vomeronasal organ (VNO), to show that social behavior in female mice results from interactions between intrinsic mechanisms in the vomeronasal system and experience-dependent plasticity. In pup- and sexually-naïve females, Gαi2 deletion elicited a reduction in pup retrieval behavior, but not in sexual receptivity. By contrast, experienced animals showed normal maternal behavior, but the experience-dependent increase in sexual receptivity was incomplete. Further, lower receptivity was accompanied by reduced neuronal activity in the anterior accessory olfactory bulb and the rostral periventricular area of the third ventricle. Therefore, neural mechanisms utilize intrinsic sensitivity in the mouse vomeronasal system and enable plasticity to display consistent social behavior.

Keywords: olfactory, Gαi2, maternal, lordosis, sex preference, kisspeptin

OPEN ACCESS

Edited by:
Emmanuel Valjent, Centre National de la Recherche Scientifique (CNRS), France

Reviewed by:
Michael Baum, Boston University, United States
Kazushige Touhara, The University of Tokyo, Japan

****Correspondence:***
Pablo Chamero
pablo.chamero-benito@inrae.fr

Specialty section:
This article was submitted to Cellular Neurophysiology, a section of the journal Frontiers in Cellular Neuroscience

Received: *07 December 2020*
Accepted: *28 January 2021*
Published: *17 February 2021*

Citation:
Trouillet A-C, Moussu C, Poissenot K, Keller M, Birnbaumer L, Leinders-Zufall T, Zufall F and Chamero P (2021) Sensory Detection by the Vomeronasal Organ Modulates Experience-Dependent Social Behaviors in Female Mice. Front. Cell. Neurosci. 15:638800. doi: 10.3389/fncel.2021.638800

INTRODUCTION

The onset of female-specific behaviors in mice results from interactions between sensory detection mechanisms and plastic neuronal pathways. Rapid responses in females' behaviour—such as pup care (Lévy et al., 2004), or sexual receptivity to males (Keller et al., 2009)—start with the detection of chemical signals by the olfactory system. Although these olfactory-driven responses are typically hard-wired, aspects of female behavior may evolve after social experience. For example, virgin females recognize pup odors and retrieve isolated pups to the nest to some extent, but maternity greatly increases this type of parental behavior (Stolzenberg and Rissman, 2011; Kohl et al., 2017).

Similarly, the display of sexual receptivity in females, indexed by the incidence of lordosis stance, largely depends on the detection of olfactory signals by the vomeronasal organ (VNO) (Keller et al., 2006; Oboti et al., 2014; Hellier et al., 2018) and is considerably enhanced by experience (Thompson and Edwards, 1971; Bonthuis et al., 2011). Plastic changes in central brain areas have been shown to modulate instinctive olfactory-mediated female behaviors (Stowers and Liberles, 2016), but whether sensory detection by the olfactory system also influences social experience remains unexplored.

Pheromones play a key role in the regulation of innate reproductive responses in female mice and are largely detected by sensory neurons in the VNO (Chamero et al., 2012; Stowers and Kuo, 2015; Ishii and Touhara, 2019). Genetic ablation of Trpc2, the primary signal transduction pathway of VNO neurons, results in several behavioral deficits in mice, such as display of sexual behavior toward both males and females indiscriminately, lack of maternal aggression in females as well as enhanced pup care in males (Leypold et al., 2002; Stowers et al., 2002; Kimchi et al., 2007; Hasen and Gammie, 2009; Wu et al., 2014). We have previously shown that the G protein Gαo is necessary for sensory function of basal vomeronasal sensory neurons (VSNs), maternal aggression, and lordosis behavior in female mice (Chamero et al., 2011; Oboti et al., 2014). By contrast, apical VSNs, which express Gαi2 and V1R receptors, are critical for pup-directed aggression and parental care in males (Trouillet et al., 2019) and have also been associated with maternal aggression (Del Punta et al., 2002; Norlin et al., 2003). This suggests that both apical and basal vomeronasal pathways control female-typical behaviors activating certain behaviors and repressing others. However, the neural VNO mechanisms involved and the role of social experience in controlling the display of female-typical behaviors remain largely unknown.

To uncover the neuronal VNO substrate leading to specific female behaviors, we used female mice with a conditional knockout of Gαi2, in which the apical half of the VNO lacks sensory function (Trouillet et al., 2019). We used two different behavioral paradigms, pup retrieval, and sexual receptivity, in which female mice were naïve to the stimuli, either a mouse infant or an adult male. Mutant females showed reduced pup retrieval behavior, whereas sexual receptivity was not different from control mice in the initial tests. Then, we evaluated the effect of social experience in the display of these behaviors. Remarkably, Gαi2 mutant females displayed normal pup retrieval behavior and maternal aggression after parturition, while sexual experience was not sufficient for Gαi2 mutants to reach control levels of sexual receptivity. These results demonstrate the role of V1R and Gαi2+ neurons in the display of lordosis and detection of pup cues. Unexpectedly, social experience in Gαi2 deficient mice leads to divergent effects on behavior: improvement of pup retrieval without any beneficial effects on the acquisition of high lordosis performance. Altogether, our data suggest that the detection of pheromones by the VNO influences olfactory-mediated behavior in females after social experience, although with distinctive traits for different behaviors.

MATERIALS AND METHODS

Mice

Animal care and experimental procedures were performed following French and European guidelines on the protection of animals used for scientific purposes and approved by an ethical committee for animal experimentation (CEEA Val de Loire project 12785). Mice were kept under standard 12 h light/dark cycles with food and water *ad libitum*. cGαi2$^{-/-}$ and cGαi2$^{+/-}$ mice were generated as described (Trouillet et al., 2019). Briefly, floxed *Gnai2* (*Gnai2*$^{fx/fx}$) mice with mixed 129sv × C57BL/6 background were crossed with mice carrying a transgene directing the expression of Cre recombinase under the control of the OMP promoter (*Omp*-Cre mice; B6; 129P2-*Omp*$^{tm4(cre)Mom}$/ MomJ; The Jackson Laboratory, JR# 006668; backcrossed into C57BL6/J for 8 generations; neomycin cassette is absent). *Gnai2*$^{fx/fx}$ mice carry loxP sites inserted into the introns that flank exons 2 and 4. Breeding established offspring that were homozygous for the floxed *Gnai2* alleles and heterozygous for Cre and *Omp* (*Gnai2*$^{fx/fx}$ *Omp*$^{cre/+}$ or cGαi2$^{-/-}$). In these mice, Cre-mediated *Gnai2* deletion was restricted to *Omp*-positive cells. Animals heterozygous for both alleles (*Gnai2*$^{fx/+}$ *Omp*$^{cre/+}$ or cGαi2$^{+/-}$) served as controls. Adult females (more than 8 weeks) were used except specified otherwise. Adult (8 weeks or older) C57BL/6 males and females (Janvier Labs) and Balb/c males (Janvier Labs) were used as stimulus animals.

Surgery

Stimulus females used for the mounting behavior assay and experimental females used in lordosis, habituation-dishabituation, and olfactory preference tests were ovariectomized under general anesthesia (xylazine 10 mg/kg, ketamine 100 mg/kg), implanted with a SILASTIC capsule filled with estradiol-benzoate (1:1 mix with cholesterol; Sigma-Aldrich). Females were allowed to recover from surgery at least 2 weeks before testing. Females were subcutaneously treated with progesterone (1 mg/100 μl in sesame oil, Sigma-Aldrich) to induce a pharmacological estrus state 4 h before each test. Juvenile (P18-22) C57BL/6 stimulus males were castrated under isoflurane general anesthesia and used in adulthood.

Behavior

Mice were moved to the experimental room 2 h before testing. Assays were conducted 2 h before the start of the dark period. Experiments were videotaped and subsequently analyzed by a blind experimenter.

Parental Behaviors in Virgin Females

Sexually naïve females (N = 12 of each genotype) were tested for behavior in the presence of an alien 1–2 day old C57BL/6 (wild type) neonate introduced into the home-cage of the test mouse for 10 min. Females were individually housed for 1 week before testing. To minimize handling and stress to the pups, one single pup was taken from the nest immediately prior to the test avoiding prolonged exposure to cold. Mice were categorized as parental if they retrieved a pup into their nest, and otherwise

as neutral. We did not observe aggressive behavior. Latency to retrieve a pup, pup grooming, and nesting times were scored.

Maternal Aggression

Sexually naïve females (20 cGαi2$^{+/-}$ and 16 cGαi2$^{-/-}$) were paired with a C57BL/6 male for 1 week. Bedding and nesting materials were changed before parturition and left until the end of the experiments. On postnatal days 2–4, females were tested daily for maternal aggression using the resident—intruder paradigm (Chamero et al., 2011). Before testing, pups were placed in a box next to their mother's cage to avoid potential injuries by the intruder. Testing lasted 10 min and began when a sexually inexperienced intruder (Balb/c adult male, group-housed) was placed in the home cage of the test female mouse (resident). Residents were not exposed twice to the same intruder. Aggressive behavior was defined as lunging, biting, chasing, tail rattling, wrestling, and kicking. Attack bouts were defined as a succession of aggressive events separated by <3 s. Proportion of females attacking the intruder, latency to attack, and cumulative attack duration and episodes of 3 consecutive tests were scored.

Pup Retrieval

After maternal aggression, the same females were tested for retrieval of their own pups. On postnatal day 5, five pups were randomly dispersed at the opposite side of the nest. The latencies to retrieve each pup to the nest were scored.

Olfactory Habituation Dishabituation Assay

Sexually naïve females (10 cGαi2$^{+/-}$ and 9 cGαi2$^{-/-}$) were evaluated for their ability to distinguish urine sources. Females were ovariectomized, supplemented in estradiol, and subcutaneously treated with progesterone 4 h before the experiment. The test was conducted in the female's home-cage and an odor stimulus was placed on a cotton-tipped applicator through the hole of the cage lid. Direct contact with the applicator was allowed. Food and water were removed from the grid and mice were allowed to familiarize themselves with a clean applicator for 30 min before the test. The test started with a first exposition for 1 min to distilled water (10 µl). This procedure was repeated three times with 1 min intervals, followed by a single presentation of intact male urine (10 µl, collected and pooled from 4 C57BL/6 group-housed adult mice). The time spent sniffing in close contact with the applicator was measured for each presentation.

Olfactory Preference Test

Sexually naïve females (10 cGαi2$^{+/-}$ and 9 cGαi2$^{-/-}$) were tested for their male-directed odor preference in a Y-maze apparatus as described previously (Jouhanneau et al., 2014). Females were ovariectomized, supplemented in estradiol, and subcutaneously treated with progesterone 4 h before the experiment. Two days before the test assay, mice were accustomed to the maze for 9 min in absence of an odor stimulus. On test day, urine from two distinct sources were placed in the arms' ends of the Y-maze on a filter paper in a plastic weigh boat behind a perforated wall. The apparatus was cleaned with 20% ethanol between subjects. Each animal was tested twice: first, with either intact male or estrous female urine; and second, with either intact or castrated male urine. Equal urine volumes from 4 C57BL/6 animals per condition were pooled and the estrus status of female donors was assessed by vaginal cytology. The time of chemosensory investigation was recorded. Preference scores were calculated as the difference between times spent on each urine source over total time of chemosensory investigation.

Mounting Behavior

Sexually naïve females (20 cGαi2$^{+/-}$ and 17 cGαi2$^{-/-}$) were individually housed for 1 week before testing. Testing lasted 10 min and began when a sexually inexperienced intruder (either male, female in pharmacological estrus, or castrated male, group-housed) was placed in the home cage of the test mouse (female resident), whose bedding had not been changed for at least 4 days. Each female was tested with every intruder in a randomized order. The proportion of females mounting the intruder was recorded.

Female Sexual Receptivity (Lordosis)

Sexually naïve females (10 cGαi2$^{+/-}$ and 9 cGαi2$^{-/-}$) were tested for their sexual receptivity toward male mounting. Females were ovariectomized, supplemented in estradiol, and subcutaneously treated with progesterone 4 h before the experiment. The test began when the female was introduced in the home cage of a sexually experienced C57BL/6 stud male and lasted for 20 min or until the female received 20 mounts. Stud males were previously trained, and only males showing a mounting latency of less than 5 min were used. Females were not exposed twice to the same stud male. Females were tested three times with a 4 days interval between tests. Lordosis was scored when the female arched her back, lift her tail and adopted a rigid posture standing on all four paws, independently of whether the male was able to achieve intromission. The lordosis quotient (number of lordosis responses/number of mounts) was scored.

Immunostaining

Tissue Preparation

90 min after sexual behavior or interaction with a neonate, mice were anesthetized by an overdose of pentobarbital (Ceva) and perfused transcardially with 0.9% saline solution followed by 0.1 M phosphate buffer (PB) containing 4% paraformaldehyde (PFA). Brains were removed, postfixed overnight in 4% PFA, and cryoprotected in 0.1 M PB containing 30% sucrose. Brain and olfactory bulbs (OB) were embedded separately in Tissue-Tek® O.C.T™ compound, snap-frozen in cold isopentane, and processed on a Leica CM 3050S cryostat. Samples were cut in 30 µm serial free-floating sections (coronal for brains, sagittal for OB) using tris-buffered saline solution (TBS) containing 0.1% sodium azide.

c-Fos Immunolabeling

Sections were washed (3 × 5 min) in TBS, endogenous peroxidases were blocked for 30 min in TBS containing 3% H_2O_2. Sections were incubated in blocking solution (TBS containing 0.1% Triton X-100, TBS-T, and 5% donkey serum) 2 h at room

temperature (RT), and overnight at 4°C in blocking solution supplemented with the c-Fos primary antibody (1:500; rabbit polyclonal #sc-52, Santa Cruz Biotechnology). Sections were then washed in TBS and incubated in TBS-T supplemented with secondary antibody (1:1,000; biotinylated donkey anti-rabbit IgG, Jackson ImmunoResearch) for 2 h at RT. Signals were amplified with VECTASTAIN ABC kit (Vector) and visualized with diaminobenzidine (DAB 0,02%, 0,01% H_2O_2 in 0,05 M Tris, pH 7,4). Slides were mounted with DPX (Sigma-Aldrich).

Kisspeptin/c-Fos Immunolabeling

Sections were washed in TBS, incubated in blocking solution (TBS containing 0.1% Triton X-100, TBS-T, and 5% donkey serum) 2 h at RT, incubated 72 h at 4°C in blocking solution supplemented with c-Fos (1:500; rabbit polyclonal #sc-52, Santa Cruz Biotechnology) and kisspeptin [1:10,000; sheep polyclonal #AC053, generous gift of I. Franceschini (Franceschini et al., 2013)] primary antibodies. Sections were then washed in TBS and incubated in TBS-T supplemented with secondary antibodies (1:500; Cy3 donkey anti-rabbit-IgG and Alexa-488 donkey anti-sheep-IgG, Jackson ImmunoResearch) for 2 h at RT. Nuclei were counterstained with 4′,6-diamidino-2-phenylindole (DAPI; 0.5 μg/ml, Sigma-Aldrich) for 2 min. Slides were mounted with Fluoromount^{TM} (Sigma-Aldrich).

Analysis

For c-Fos experiments, slides were scanned using an automatic slide scanner (Axio Scan.Z1, Zeiss). Regions of interest were drawn based on the Paxinos mouse brain atlas using Zen (blue edition 3.0, Zeiss). The number of c-Fos+ nuclei was automatically counted bilaterally in these regions using the particle analyzer plug-in of Fiji. 2–3 images of the accessory olfactory bulb (AOB), 3 images of the rostral periventricular area of the third ventricle (RP3V), 2 images of the ventrolateral part of the ventromedial hypothalamic nucleus (VMHvl) and 4 images of the medial preoptic area (MPA) per animal were analyzed. Kisspeptin/c-Fos co-expression was quantified in 3–5 RP3V images/animal acquired on a Zeiss LSM-700 confocal laser-scanning microscope at 10× magnification. Images were manually analyzed in the entire *z*-axis with 3 μm step intervals.

Reproductive Physiology

Young prepubertal females (17 cGαi2$^{+/-}$ and 15 cGαi2$^{-/-}$) were monitored daily for evidence of vaginal opening from postnatal day 15, and then for their first estrus by vaginal smears sampling. Briefly, vaginal smears were flushed with 15 μl of NaCl 0.9% solution and the estrus phase was identified by light microscopy after methylene-blue coloration of the smears. Adult females (47 cGαi2$^{+/-}$ and 45 cGαi2$^{-/-}$) were also examined daily for estrus status for 2 weeks using the same protocol. Adult females (61 cGαi2$^{+/-}$ and 49 cGαi2$^{-/-}$) were sacrificed during their diestrus or estrus phase to collect trunk blood and measure the weight of ovaries and uteri. Blood sera were obtained by centrifugation (2,500 × *g* for 25 min) and levels of progesterone were measured by immunoenzymatic assay. Assay sensitivity is 0.25 ng/ml. Sexually naïve females (76 cGαi2$^{+/-}$ and 67 cGαi2$^{-/-}$) were paired for 7 days with a C57BL/6 male. The proportion of pregnant females, the latency to deliver, and the number of pups born were collected.

Statistics

Statistical analyses were performed using GraphPad Prism 9.0 (GraphPad Software, Inc.), and OriginPro 2016G (OriginLab Corporation). Assumptions of normality and homogeneity of variance were tested before conducting the following statistical approaches. Student's *t*-test was used to measure the significance of the differences between two distributions. In case the results failed the test of normality, Mann-Whitney or Kolmogorov-Smirnov test was performed. Multiple groups were compared using a two- or three-way repeated-measures analysis of variance (ANOVA) with Bonferonni's tests as *post hoc* comparison. Kruskal-Wallis test with Dunn's multiple comparisons, or Friedman multiple comparisons in case of paired values, were used for non-normal distributions. Categorical data were analyzed with Fisher's exact test, and correlations were assessed by the Pearson coefficient. The probability of error level (alpha) was chosen to be 0.05. Unless otherwise stated, results are presented as means ± SEM and documentation of individual data points.

RESULTS

Inactivation of the Apical Vomeronasal Cell Layer Reduces Pup Retrieval in Virgin Females

VNO activity is necessary for the display of important pup-directed behaviors in male mice, such as pup-directed aggression (Tachikawa et al., 2013; Wu et al., 2014; Isogai et al., 2018; Trouillet et al., 2019), inhibition of sexual behaviors toward pups (Ferrero et al., 2013), and increased pup-retrieval and parenting behaviors (Wu et al., 2014; Trouillet et al., 2019). In virgin females, the role of the VNO in pup-directed behaviors is less clear. While some studies suggest that genetic ablation of VNO function in Trpc2$^{-/-}$ females increase parenting behavior toward alien juveniles (Nakahara et al., 2016), this view is not supported by others (Wu et al., 2014).

To determine whether the vomeronasal pathway may partially regulate pup parenting in virgin females, we used mice carrying Olfactory Marker Protein (OMP)-dependent deletion of Gαi2 (cGαi2$^{-/-}$), which impairs sensory signaling in apical VNO neurons (Trouillet et al., 2019). We exposed pup-naïve virgin females to 1–2 days old pups (**Figure 1A**) and the majority of females retrieved the pups to the nest, although the proportion of retrieving females was lower in cGαi2$^{-/-}$ when compared to heterozygous controls (58 vs. 92%; **Figure 1A**). Measurement of the latency to retrieve pups showed that cGαi2$^{-/-}$ virgin females retrieved pups with longer latency ($P < 0.05$; **Figure 1B**), even if they displayed more time sniffing the pups before retrieving ($P < 0.05$; **Figure 1B**). Next, we used c-Fos immunolabeling to confirm the role of vomeronasal signaling in pup detection by virgin females

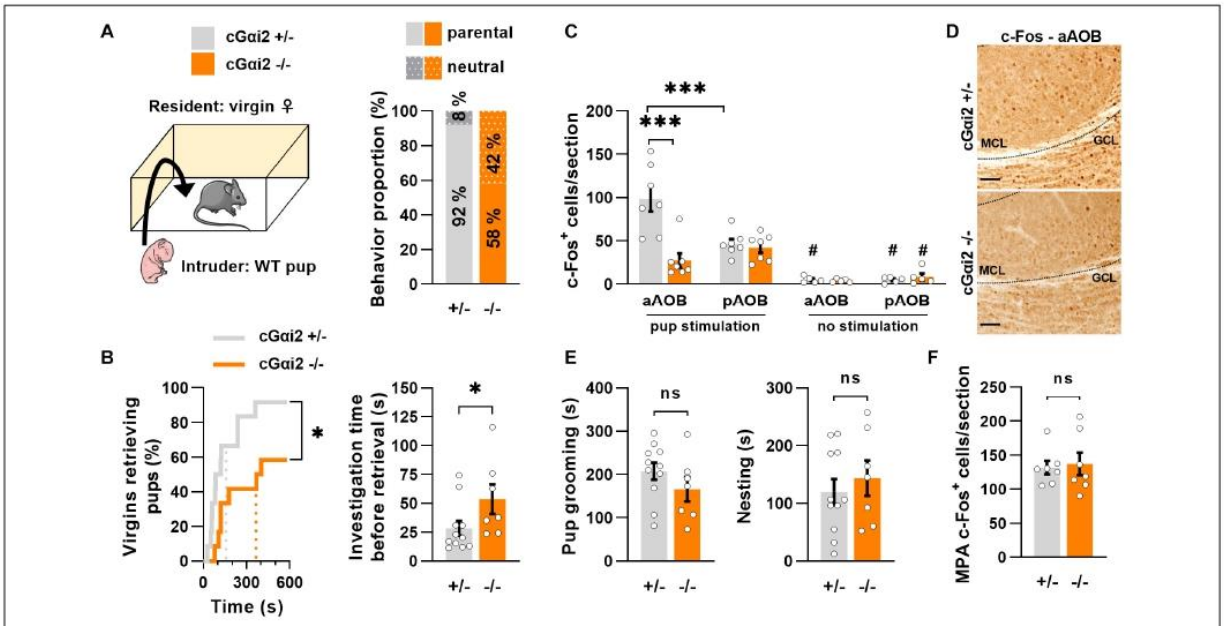

FIGURE 1 | Pup retrieval is altered in virgin cGαi2$^{-/-}$ females. **(A)** Comparison of pup-directed behavior of cGαi2$^{+/-}$ vs. cGαi2$^{-/-}$ virgin female residents ($N = 12$ per genotype). Wild type 1–2 day-old pups served as intruders. Females ignore (neutral) or retrieve neonates to their nest (parental). Females of both genotypes are predominantly parental (11 out of 12; 92% for cGαi2$^{+/-}$ and 7 out of 12; 58% for cGαi2$^{-/-}$). **(B)** *Left*, proportion of females retrieving pups over time (Kolmogorov-Smirnov test: $P < 0.05$). Dotted lines represent the mean latency. *Right*, time spent sniffing the pup before retrieval in cGαi2$^{-/-}$ ($N = 7$) and cGαi2$^{+/-}$ ($N = 11$) parental females (Mann-Whitney: $P < 0.05$). **(C)** Quantification of c-Fos+ cells per section of cGαi2$^{+/-}$ and cGαi2$^{-/-}$ virgin females ($N = 7$ per group) in control condition (no stimulation) and after exposure to an alien pup (pup stimulation) reveals a decreased c-Fos activation in the aAOB of cGαi2$^{-/-}$ compared to cGαi2$^{+/-}$ females, and a higher number of c-Fos+ cells in the anterior compared to the posterior part of the AOB of cGαi2$^{+/-}$ females only [Three-way repeated measures ANOVA: (genotype) $F_{(1,12)} = 6.719$, $P < 0.01$; (region) $F_{(1,12)} = 4.024$, $P = 0.068$; (stimulation) $F_{(1,12)} = 63.21$, $P < 0.001$; (genotype × region × stimulation) $F_{(1,4)} = 14.67$, $P < 0.05$; Bonferroni *post hoc* tests: cGαi2$^{+/-}$ aAOB vs. cGαi2$^{+/-}$ pAOB and cGαi2$^{+/-}$ aAOB vs. cGαi2$^{-/-}$ aAOB $P < 0.001$; $^{\#}P < 0.05$ vs. the stimulated equivalent condition; other comparison $P = 0.3$–0.9]. All three AOB layers were quantified. **(D)** Examples of c-Fos immunodetection in the aAOB of cGαi2$^{+/-}$ and cGαi2$^{-/-}$ virgin females exposed to an alien pup for 10 min. Scale bars, 25 μm. **(E)** The time spent grooming (*left*) and nesting (*right*) the neonates (*t*-test: $P = 0.2$–0.5). **(F)** Quantification of c-Fos^{+} cells per section in the MPA of cGαi2$^{+/-}$ and cGαi2$^{-/-}$ virgin females after exposure to an alien pup is not different (*t*-test: $P = 0.8$). AOB, accessory olfactory bulb (aAOB, anterior AOB; pAOB, posterior AOB); MCL, mitral cell layer; GCL, granular cell layer; MPA, medial preoptic area. $^{*}P < 0.05$; $^{***}P < 0.001$.

and examine whether pup odors were preferentially detected by either the apical or basal vomeronasal subsystems. We compared the density of c-Fos+ nuclei in all three layers of the accessory olfactory bulb (AOB), the first relay station of the pheromonal information transfer in the brain, after pup exposure in cGαi2$^{-/-}$ and cGαi2$^{+/-}$ virgin females (**Figures 1C,D**). After pup exposure, the density of c-Fos+ nuclei was nearly fourfold lower in the anterior part of the AOB of cGαi2$^{-/-}$females ($P < 0.001$; **Figure 1C**), consistent with reduced sensory input from the apical VNO. Furthermore, we observed twofold more c-Fos+ nuclei in the anterior vs. posterior part of the AOB in control females ($P < 0.001$; **Figure 1C**), suggesting a preferential activation of apical Gαi2-expressing VSNs by pup odors. Once pups were retrieved to the nest, measures of parental care—pup grooming and nesting time—were not significantly different in cGαi2$^{-/-}$ females (**Figure 1E**; $P = 0.2$–0.5). Consistent with this, the number of c-Fos+ cells in the medial preoptic area (MPA), a region involved in parenting (Numan, 1974), was also not significantly different in cGαi2$^{-/-}$ females (**Figure 1F**). Together, these results indicate that Gαi2-dependent VNO inputs participate in pup odor detection in virgin females and that deletion of Gαi2 reduces pup retrieval, although pup-parenting behaviors are still displayed after retrieval.

Deletion of Gαi2 Does Not Affect Maternal Behavior in Mothers

Both the main olfactory epithelium and VNO seem to be implicated in maternal behavior. Previous experiments using genetically altered mice showed that an intact main olfactory system is required for pup retrieval in lactating mice mothers (Weiss et al., 2011; Fraser and Shah, 2014), and that the VNO is necessary for the display of maternal aggression (Leypold et al., 2002; Hasen and Gammie, 2009; Chamero et al., 2011). Consequently, impairment of vomeronasal signaling in Trpc2$^{-/-}$ lactating females has no impact on pup retrieval behavior, even though these females are deficient in maternal aggression (Leypold et al., 2002; Hasen and Gammie, 2009).

Yet, the VNO neuronal subpopulation implicated in maternal aggression is not characterized with certainty. While maternal aggression is nearly absent in basal VNO signaling-deficient cGαo$^{-/-}$ females (Chamero et al., 2011), other studies have suggested some mediation from apical Gαi2/V1R-expressing VSNs (Del Punta et al., 2002; Norlin et al., 2003).

Thus, we aimed to investigate the requirement of Gαi2^{+} vomeronasal neurons for parental behaviors in mated females. We first quantified territorial aggression of cGαi2$^{-/-}$ vs. cGαi2$^{+/-}$ lactating females in the resident-intruder paradigm (**Figure 2**). We observed a high number of animals attacking an adult intact male intruder in both cGαi2$^{-/-}$ (14/16 mice; 87%) and cGαi2$^{+/-}$ mothers (14/20 mice; 70%) in three consecutive 10 min tests (P = 0.3; **Figure 2A**). Attack latency, total attack duration, and cumulative attack numbers were high in both cGαi2$^{-/-}$ and cGαi2$^{+/-}$ females (P = 0.4–0.9; **Figure 2B**), indicating that Gαi2 is dispensable for the display of maternal aggression. Consistent with previous findings indicating a minor role of the VNO in the display of pup retrieval behavior in mothers (Wysocki and Lepri, 1991), cGαi2$^{-/-}$ females exhibited normal pup retrieval when compared to heterozygous controls (**Figures 2C,D**). All females retrieved to the nest all of their pups randomly distributed in the home cage (**Figure 2C**), and the mean time to retrieve the 5 pups was less than 80 s in both groups (**Figure 2D**). Taken together, these results show that maternal aggression and pup retrieval by lactating females do not depend on Gαi2+ VSNs.

Incomplete Sexual Receptivity Acquisition in Gαi2-Mutant Females

An intact VNO is required for the display of major female sexual behaviors, such as gender discrimination and sexual receptivity (Leypold et al., 2002; Stowers et al., 2002; Keller et al., 2006; Kimchi et al., 2007; Martel and Baum, 2009; Oboti et al., 2014; Hellier et al., 2018).

To examine whether altered sexual behaviors of VNO-impaired mice might be related to a deficit in Gαi2 signaling, we measured olfactory preference to male odors in cGαi2$^{-/-}$ females. We used adult, sexually naïve females subjected to ovariectomy and primed with estradiol and progesterone to minimize estrus cycle-related variability and increase their motivation for male pheromones. First, we evaluated their ability to recognize urine from an adult male using the habituation-dishabituation paradigm. cGαi2$^{-/-}$ and cGαi2$^{+/-}$ females were exposed to a sequence of three successive odor presentations of water and a final presentation of male urine. All females were able to recognize the urine, as the time spent sniffing the first urine presentation was higher than the previous water presentations (**Figure 3A**). Next, we analyzed the preference for either intact male urine or estrus female urine in a two-choice preference test. cGαi2$^{-/-}$ and cGαi2$^{+/-}$ females displayed the same level of preference for intact male urine (P = 0.8; **Figure 3B**). We then compared the preference for urine from either intact or castrated males (**Figure 3B**). cGαi2$^{-/-}$ and cGαi2$^{+/-}$ females showed a strong preference for intact male urine (P = 0.4;

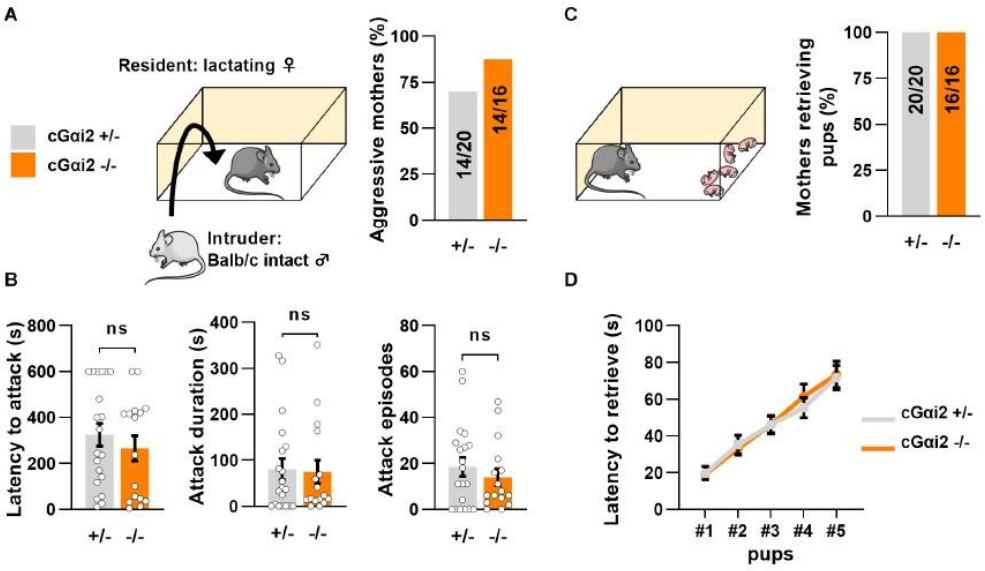

FIGURE 2 | Loss of Gαi2 does not affect maternal behavior in lactating females. **(A)** Maternal aggression in lactating cGαi2$^{+/-}$ (N = 20) vs. cGαi2$^{-/-}$ (N = 16) females during three consecutive exposures to an intact male intruder in the resident-intruder test. 70% of cGαi2$^{+/-}$ and 87% of cGαi2$^{-/-}$ females present at least one aggressive episode (Fisher's exact test: P = 0.3). **(B)** Measure of the aggression parameters latency to attack (*left*), cumulative attack duration (*middle*) and attack episodes (*right*) across genotypes (Mann-Whitney: P = 0.4–0.9). **(C)** 100% of cGαi2$^{+/-}$ (N = 20) and cGαi2$^{-/-}$ (N = 16) mothers retrieve five of their pups previously dispersed in the cage. **(D)** The latency to retrieve pups does not differ between groups (Dunn's multiple comparison tests cGαi2$^{+/-}$ vs. cGαi2$^{-/-}$ for each pup's latency $P > 0.9$).

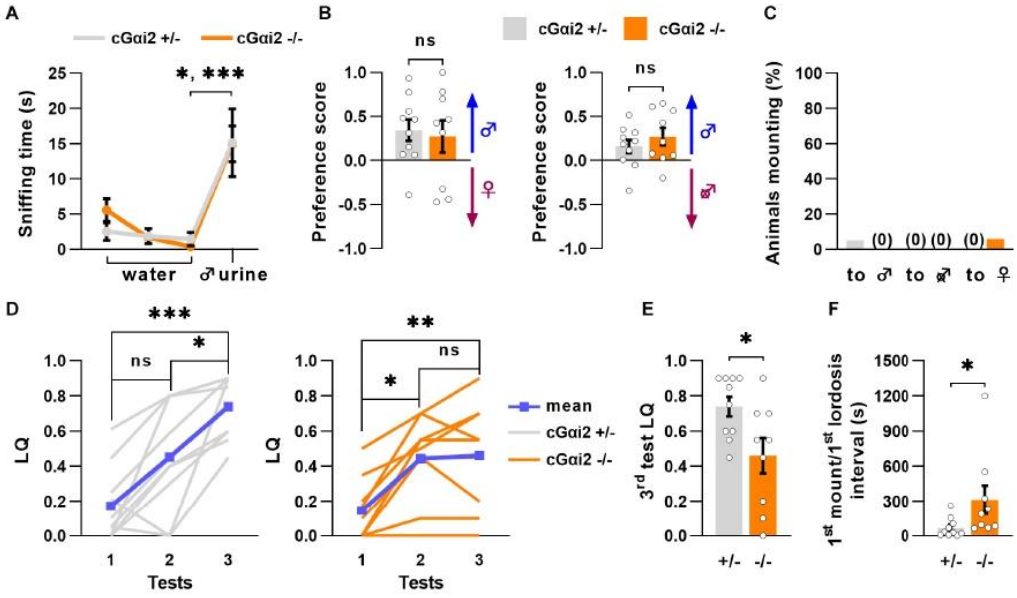

FIGURE 3 | Incomplete sexual receptivity in Gαi2 mutant females. **(A)** cGαi2$^{+/-}$ ($N = 10$) and cGαi2$^{-/-}$ ($N = 9$) are able to detect intact male urine in the habituation—dishabituation paradigm (Kruskal-Wallis: $P < 0.001$, Dunn's multiple comparison tests: water 3 vs. urine 1 cGαi2$^{+/-}$ $P < 0.05$, cGαi2$^{-/-}$ $P < 0.001$). **(B)** Olfactory preference of social cues in cGαi2$^{+/-}$ ($N = 10$) and cGαi2$^{-/-}$ ($N = 9$) female mice in a two-choice test. Females had the choice between male urine vs. estrus female (*left*) or castrated male (*right*) urine. cGαi2$^{+/-}$ and cGαi2$^{-/-}$ animals show a preference for male urine in both tests and no differences between genotypes are found (*t*-test: $P = 0.4$–0.7). **(C)** Ablation of Gαi2 in VSNs does not induce, in females, mounting behavior toward male, castrated male or female. The proportion of animals mounting is similar in cGαi2$^{+/-}$ ($N = 20$) and cGαi2$^{-/-}$ ($N = 17$) females (Fisher's exact test: $P = 0.5$–0.9). **(D–F)** Sexual receptivity of cGαi2$^{+/-}$ ($N = 10$) and cGαi2$^{-/-}$ ($N = 9$) females during exposition to a sexually experienced stud male over three tests. **(D)** The lordosis quotient (LQ) of cGαi2$^{+/-}$ (*left*) follows a normal increase over the tests (Kruskal-Wallis: $P < 0.001$, Friedman multiple comparisons: test 1 vs. 2 $P = 0.5$, test 1 vs. 3 $P < 0.001$, and test 2 vs. 3 $P < 0.05$), but in cGαi2$^{-/-}$ (*right*) the lordosis quotient does not increase in the third test (Kruskal-Wallis: $P < 0.001$, Friedman multiple comparisons: test 1 vs. 2 $P < 0.05$, test 1 vs. 3 $P < 0.01$, and test 2 vs. 3 $P = 0.9$). **(E)** Comparison of the lordosis quotient of cGαi2$^{+/-}$ and cGαi2$^{-/-}$ females during the third test reveals a reduction of sexual receptivity in mutant females (Mann-Whitney: $P < 0.05$). **(F)** Latency to exhibit a lordosis, measured from the first mount received, is significantly longer in cGαi2$^{-/-}$ females (Mann-Whitney: $P < 0.05$). *$P < 0.05$; **$P < 0.01$; ***$P < 0.001$.

Figure 3B), indicating that preference for male odors is intact in cGαi2$^{-/-}$ females.

Next, we assessed cGαi2$^{-/-}$ females for the display of male-typical behaviors by scoring mounting behavior of intact female residents to either male, female, or castrated male intruders, independently introduced into the female resident's home cage during a 10 min test period for 3 consecutive days. Very few animals displayed mounting behavior toward any intruder (female, male, or castrated male) for both cGαi2$^{-/-}$ and cGαi2$^{+/-}$ females. None of the cGαi2$^{-/-}$ females exhibited mounting to male or castrated intruders, although some low levels of mounting were observed in 6% of females, to female intruders (**Figure 3C**). Thus, deletion of Gαi2 in VSNs does not enhance the display of male-specific behaviors in female mice.

We next asked whether normal olfactory preference and lack of mounting to males and females led to normal display of sexual receptivity in cGαi2$^{-/-}$ females. To test this, we measured lordosis behavior, a female sexual stance held in response to male mounting that denotes sexual receptivity. Lordosis requires an intact VNO (Keller et al., 2006; Oboti et al., 2014; Hellier et al., 2018), and is significantly enhanced by experience (Thompson and Edwards, 1971; Bonthuis et al., 2011). Thus, we quantified lordosis response in the presence of a sexually experienced male in three tests separated by 4 days to mimic natural estrus occurrence. We observed low lordosis quotient (LQ; number of lordosis postures divided by the number of mounts received) values during the first test for all animals (LQ = 0.14–0.17; **Figure 3D**). The second test yielded an increase in LQ values of around 0.45, for both cGαi2$^{-/-}$ and cGαi2$^{+/-}$ females (**Figure 3D**). In the third test, however, cGαi2$^{-/-}$ females remained at LQ levels similar to those of the second test (LQ = 0.46; **Figure 3D**), whereas cGαi2$^{+/-}$ control females displayed a further LQ increase (from 0.45 to 0.74; **Figure 3D**). During the third test, each female received 20 mounts from the stud male, but cGαi2$^{-/-}$ females responded displaying less lordosis than cGαi2$^{+/-}$ controls ($P < 0.05$; **Figure 3E**). Furthermore, cGαi2$^{-/-}$ females exhibited a significantly longer latency to show the first lordosis episode (67.4 ± 26.2 s for cGαi2$^{+/-}$ females; 311.8 ± 123.1 s for cGαi2$^{-/-}$; $P < 0.05$; **Figure 3F**). Taken together, these results indicate that Gαi2 vomeronasal neurons play a critical role in the acquisition of complete sexual receptivity in females, but not in olfactory preference and sexual partner choice.

Reduced c-Fos Expression in the AOB and RP3V of Gαi2-Mutant Females

We further investigated neuronal activity after sexual behavior in downstream vomeronasal neural pathways in the brain. First, we quantified c-Fos expression in the AOB (**Figures 4A,B**). In control cGαi2$^{+/-}$ females, the number of c-Fos+ cells in the AOB was elevated (∼100 cells/section) in both the anterior and posterior AOB (**Figure 4A**). By contrast, cGαi2$^{-/-}$ females displayed significantly lower number of c-Fos+ in the anterior AOB (15 cells/section; $P < 0.001$; **Figure 4A**), while c-Fos+ cells in the posterior AOB was not significantly different from cGαi2$^{+/-}$ controls (58 cells/section; $P = 0.06$; **Figure 4A**). This

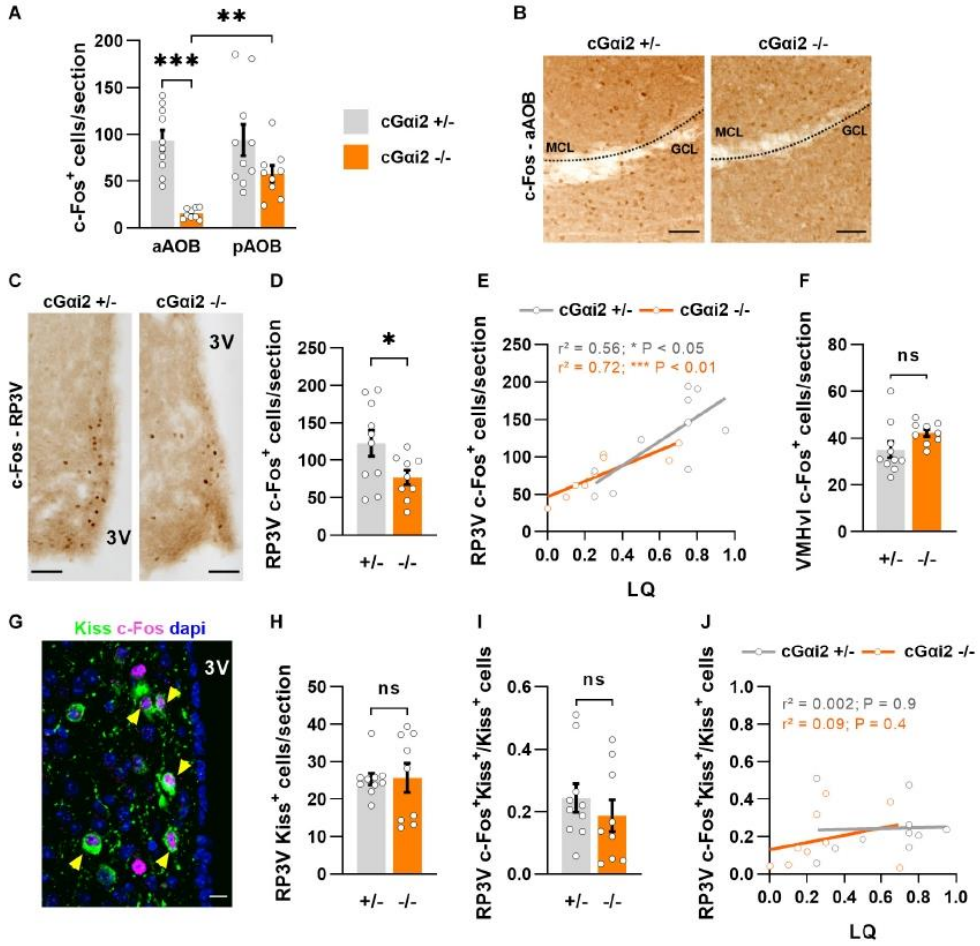

FIGURE 4 | Reduced neural activity in the AOB and RP3V of Gαi2-mutant females. **(A,B)** Analysis of c-Fos immunodetection in the AOB of cGαi2$^{+/-}$ ($N = 10$) and cGαi2$^{-/-}$ ($N = 9$) females after sexual behavior. **(A)** Quantification of c-Fos+ cells per section reveals a decreased c-Fos activation in the aAOB of cGαi2$^{-/-}$ [Two-way repeated measures ANOVA: (genotype) $F_{(1,17)} = 18.28$, $P < 0.001$; (region) $F_{(1,17)} = 5.82$, $P < 0.05$; (genotype × region) $F_{(1,17)} = 5.53$, $P < 0.05$; Bonferroni *post hoc* tests: cGαi2$^{-/-}$ aAOB vs. cGαi2$^{-/-}$ pAOB, $P < 0.01$; cGαi2$^{+/-}$ aAOB vs. cGαi2$^{-/-}$ aAOB $P < 0.001$; other comparisons $P = 0.06$–0.9). All three AOB layers were quantified. **(B)** Examples of c-Fos immunolabeling in the aAOB of cGαi2$^{+/-}$ and cGαi2$^{-/-}$females after sexual behavior. Scale bars, 50 μm. **(C–E)** c-Fos immunodetection in the RP3V of cGαi2$^{+/-}$ ($N = 10$) and cGαi2$^{-/-}$ ($N = 9$) females. **(C)** Examples of c-Fos immunodetection in the RP3V of cGαi2$^{+/-}$ and cGαi2$^{-/-}$females after sexual behavior. Scale bars, 50 μm. **(D)** Quantification of c-Fos+ cells per section in the RP3V of cGαi2$^{-/-}$ (*t*-test: $P < 0.05$). **(E)** Positive correlation between the number of RP3V-c-Fos+ cells and lordosis quotient (LQ) in cGαi2$^{+/-}$ and cGαi2$^{-/-}$ females (Pearson's correlation; cGαi2$^{+/-}$: $r^2 = 0.56$, $P < 0.05$; cGαi2$^{-/-}$: $r^2 = 0.72$, $P < 0.01$). **(F)** c-Fos immunodetection in the VMHvl of cGαi2$^{+/-}$ ($N = 10$) and cGαi2$^{-/-}$ ($N = 9$) females after sexual behavior. Quantification is not different between genotypes (*t*-test: $P = 0.08$). **(G–J)** Analysis of kisspeptin and c-Fos double immunostaining in the RP3V. **(G)** Example of Kiss and c-Fos immunostaining in the RP3V of a cGαi2$^{+/-}$ female. The yellow arrows indicate double labeled c-Fos-Kiss neurons. Scale bar, 10 μm. Quantifications of Kiss+ neurons **(H)** and double-labeled c-Fos+Kiss+ neurons **(I)** are not different between genotypes (Mann-Whitney: $P = 0.9$; *t*-test: $P = 0.4$, respectively). **(J)** Correlative analysis between the number of c-Fos+Kiss+ cells in the RP3V and the LQ (Pearson's correlation; cGαi2$^{+/-}$: $r^2 = 0.002$, $P = 0.9$; cGαi2$^{-/-}$: $r^2 = 0.09$, $P = 0.4$). AOB, accessory olfactory bulb (aAOB, anterior AOB; pAOB, posterior AOB); 3V, third ventricle; RP3V, rostral periventricular area of the third ventricle; VMHvl, ventrolateral part of the ventromedial hypothalamic nucleus; Kiss, kisspeptin. *$P < 0.05$; **$P < 0.01$; ***$P < 0.001$.

result suggests that Gαi2-independent VNO activity is sufficient for the display of basal levels of sexual receptivity.

We further asked whether this reduction of sensory information may have an impact on the neural activity of the rostral periventricular area of the third ventricle (RP3V), a hypothalamic region involved in the control of female sexual behavior and activated by male pheromones (Simerly, 2002; Bakker et al., 2010; Hellier et al., 2018; Inoue et al., 2019; **Figures 4C–E**). We thus counted c-Fos+ nuclei in the RP3V of the same females after sexual behavior. Consistent with a reduced sensory input, the density of c-Fos+ nuclei was lower in cGαi2$^{-/-}$ females vs. cGαi2$^{+/-}$ controls ($P < 0.05$; **Figures 4C,D**). To determine whether the extent of c-Fos+ cells in the RP3V was linked to sexual receptivity, we performed a correlation analysis between c-Fos cell density and LQ (**Figure 4E**). The number of c-Fos+ cells was positively correlated with the LQ in both genotypes (**Figure 4E**), suggesting that the level of sexual receptivity displayed may depend on RP3V neural activity. c-Fos activation in the ventrolateral part of the ventromedial hypothalamic nucleus (VMHvl), a region innervated by RP3V neurons and also involved in the control of female sexual behavior (Pfaff and Sakuma, 1979), revealed no significant differences (**Figure 4F**), suggesting that the observed alterations in cGαi2$^{-/-}$ female receptivity are likely coded upstream of VMHvl neurons.

To further characterize in more detail the activated RP3V neurons in cGαi2$^{-/-}$ females, we asked whether these cells belong to a neuronal subpopulation positive for the neuropeptide kisspeptin (Kiss), which is essential to trigger the lordosis response (Hellier et al., 2018; **Figures 4G–J**). Using double label immunostaining we found neurons that were positive for both c-Fos^{+} and Kiss in all animals (**Figure 4G**). We observed no difference in the density of Kiss^{+} neurons and the number of double-labeled c-Fos^{+}/Kiss^{+} neurons in both cGαi2$^{-/-}$ and cGαi2$^{+/-}$ females (P = 0.4–0.9; **Figures 4H,I**). To establish whether the level of sexual receptivity is linked to the number of activated kisspeptin neurons in the RP3V, we performed a correlation analysis between c-Fos+/Kiss+ cell density and the LQ (**Figure 4J**). We did not observe any obvious correlation between the number of activated kisspeptin neurons and the LQ for any of the two genotypes (r^2 = 0.002 and 0.09; **Figure 4J**), suggesting that an increase in sexual receptivity does not require the recruitment of additional kisspeptin neurons. Collectively, these results indicate that Gαi2 vomeronasal signaling is dispensable for the display of basal levels of lordosis, but participates in the acquisition of complete sexual receptivity, possibly through RP3V kisspeptin-negative neurons.

Gαi2 Deletion Has No Impact on Reproductive Physiology

Reduced receptivity to males could be a consequence of not only defective VNO chemodetection but also of altered reproductive physiology. Indeed, females with a total or partial ablation of VNO function (Trpc2$^{-/-}$ and cGαo$^{-/-}$ females) exhibit profound alterations in puberty onset and estrus cyclicity, even in the absence of external stimuli (Flanagan et al., 2011; Oboti et al., 2014).

Therefore, as a further control and to verify that the described loss of functions by the conditional Gαi2 ablation are indeed caused by a loss of VNO signaling and not by defective reproductive physiology, we investigated the impact of Gαi2 deletion on the timing of estrus and ovulation. First, we characterized puberty onset of juvenile female mice. Control cGαi2$^{+/-}$ and cGαi2$^{-/-}$ females were examined for the onset of vaginal opening and first estrus. Animals from

TABLE 1 | cGαi2$^{-/-}$ females show normal reproductive physiology.

		cGα i2$^{+/-}$	cGα i2$^{-/-}$	Statistic	*P*-value	
Puberty						
	Age at vaginal opening (days)	34.6 ± 0.8 (17)	35.1 ± 0.8 (15)	Unpaired *t*-test	0.6	*ns*
	Age at first estrus (days)	36.2 ± 0.7 (17)	36.8 ± 0.6 (15)	Unpaired *t*-test	0.5	*ns*
Estrus cycle						
	Cycle length (days)	4.9 ± 0.1 (47)	5.5 ± 0.2 (47)	Mann-Whitney	0.1	*ns*
	Proestrus + estrus days	6.6 ± 0.2 (47)	6.4 ± 0.2 (45)	Mann-Whitney	0.5	*ns*
Serum steroids levels						
Progesterone (ng.mL^{-1})	Follicular phase	3.2 ± 0.7 (10)	5.6 ± 1.3 (7)	Mann-Whitney	0.2	*ns*
	Luteal phase	7.9 ± 1.2 (36)	7.9 ± 1.5 (26)	Mann-Whitney	0.9	*ns*
Reproductive organs weight						
Ovaries (%bw)		0.033 ± 0.001 (27)	0.034 ± 0.002 (31)	Mann-Whitney	0.4	*ns*
Uterus (%bw)	Follicular phase	0.29 ± 0.02 (25)	0.32 ± 0.03 (21)	Kruskal-Wallis	0.9	*ns*
	Luteal phase	0.23 ± 0.02 (19) †	0.2 ± 0.01 (28) ‡		0.2	*ns*
Fertility						
	Pregnant females (%)	67/76 (88%)	54/67 (81%)	Fisher's exact test	0.2	*ns*
	Delivery latency (days)	22.4 ± 0.3 (76)	23.3 ± 0.4 (67)	Mann-Whitney	0.2	*ns*
	Litter size	7.8 ± 0.4 (76)	7.1 ± 0.5 (67)	Mann-Whitney	0.3	*ns*

† and ‡, respectively, $P < 0.05$ and $P < 0.001$ vs. the uterus weight during the follicular phase. bw, body weight. Assessment of puberty onset, estrus cyclicity, sex steroids levels, reproductive organs weight, and fertility parameters of control and cGαi2$^{-/-}$ females. Values are means ± SEM of the indicated number (n) of females.

both genotypes displayed vaginal opening around postnatal day 35 (P = 0.6; **Table 1**) and first estrus a day later (P = 0.5; **Table 1**), indicating normal puberty onset in Gαi2 mutants. Next, we analyzed estrus cycles of adult, group-housed female mice during a 2 week interval. Both control cGαi2$^{+/-}$ and cGαi2$^{-/-}$ females displayed consistent estrus cycles with no difference in the mean cycle duration (P = 0.1; **Table 1**) and similar number of proestrus and estrus days (P = 0.5; **Table 1**). Consistent with normal ovarian function, levels of circulating progesterone during the follicular or luteal phases (P = 0.2 and 0.9; **Table 1**), and average ovarian weight were not different between cGαi2$^{-/-}$ and cGαi2$^{+/-}$ females (P = 0.2–0.9; **Table 1**). We measured uterus weight as a proxy for circulating estradiol, and found a weight decrease during the luteal vs. follicular phases (P < 0.001 and 0.05; **Table 1**), but no differences between genotypes (P = 0.2–0.9; **Table 1**). Finally, we compared three fertility parameters—percentage of pregnant females after 7 days, delivery latency and litter size—and found no differences between cGαi2$^{-/-}$ and cGαi2$^{+/-}$ (P = 0.2–0.3; **Table 1**). Together, these findings indicate that reproductive physiology and ovarian function are normal in cGαi2$^{-/-}$ females.

DISCUSSION

The central hypothesis of this study was that detection of environmental stimuli by the VNO modulates experience-dependent plasticity, possibly influencing the display of social behaviors in female mice. To test this hypothesis, we chose an animal model with a conditional mutation for Gαi2 gene, which harbors a partial loss of VNO function (Trouillet et al., 2019), and two experimental paradigms (pup retrieval and sexual receptivity) that are strongly dependent on social experience (repeated contact with pups or the male). We previously showed that Gαi2 is necessary for the detection of small organic pheromones by apical VSNs, and genetic ablation of these neurons severely impairs pup-directed aggression in virgin males (Trouillet et al., 2019). This is consistent with published studies that show that pup cues preferentially activate neurons located in the apical VNO and the anterior AOB in virgin males (Tachikawa et al., 2013; Nakahara et al., 2020). Our results show higher c-Fos activation in the anterior AOB after pup-exposure (**Figures 1C,D**), indicating that pups are also preferentially detected by Gαi2+ VSNs in virgin females.

In contrast to males, we found that deletion of Gαi2 in virgin females does not increase parental care (i.e., grooming) toward pups, but reduces pup retrieval (**Figures 1A,B**). Interestingly, mutant females that retrieve pups still display other types of parenting behaviors such as grooming and nesting, suggesting that different pup care behaviors are controlled independently. Importantly, Gαi2 deletion does not affect pup retrieval and maternal aggression in mothers (**Figure 2**), indicating that other neural substrates different from Gαi2^{+} VSNs control these behaviors, likely by auditory, olfactory and Gαo-dependent signals (Chamero et al., 2011; Weiss et al., 2011; Fraser and Shah, 2014; Marlin et al., 2015).

The mechanism by which social experience drives neural plasticity to modify the behaviors display is unclear. Not only centrally controlled neural changes, but also sensory organ sensitivity to olfactory stimuli have been suggested to have an influence. In particular, previous studies report a decline in VNO activity induced by pup cues in virgin males after cohabitation with a pregnant female (Tachikawa et al., 2013; Nakahara et al., 2020), suggesting the existence of a silencing mechanism at the

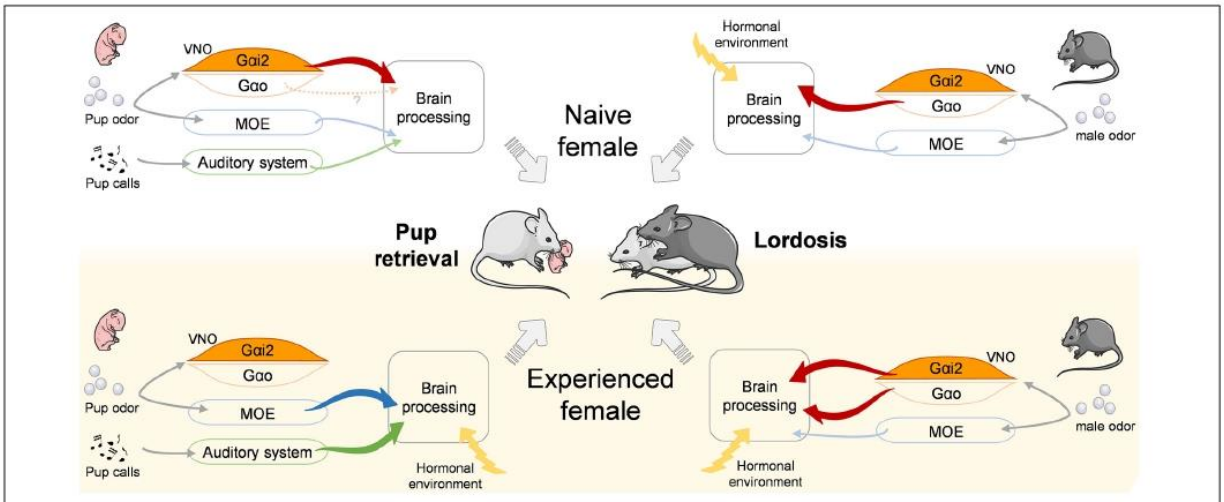

FIGURE 5 | Model for the proposed control of pup retrieval and lordosis behaviors depending on social experience. Olfactory and auditory cues relevant for pup retrieval (***left***) and lordosis (***right***) behaviors are differentially processed by the sensory systems and the brain in naïve (***top***) and experienced (***down***) females. Significantly, Gαi2+ vomeronasal neurons are activated by pup odor in naïve females to trigger retrieval but are dispensable in experienced females. Inversely, they are dispensable in naïve females to trigger the lordosis response but become necessary in experienced females to reach high lordosis levels. VNO, vomeronasal organ; MOE, main olfactory epithelium.

level of VSNs. We can thus speculate that a similar process may occur in females after parturition, either induced by hormonal changes intrinsic to gestation, or by repeated exposure to pups. Indeed, pup retrieval is improved in virgin females after co-housing with a dam and litter, even after ovariectomy (Ehret et al., 1987; Koch and Ehret, 1989; Stolzenberg and Rissman, 2011; Elyada and Mizrahi, 2015), suggesting that pup signals modulate the behavioral response. In this scenario, hormones such as oxytocin may influence experience-dependent plasticity directly at the sensory processing level (Fleming et al., 1979; Marlin et al., 2015; Nakahara et al., 2020).

Studies on Trpc2$^{-/-}$ mice suggest that sex discrimination and opposite-sex preference depend on a functional VNO because of indiscriminate mounting expressed by males and females (Leypold et al., 2002; Stowers et al., 2002; Kimchi et al., 2007). Other studies point to a significant role of testosterone levels (rather than VNO function) to explain the unusual mounting of Trpc2$^{-/-}$ females (Martel and Baum, 2009). The absence of mounting behavior in our Gαi2 mutant females (**Figure 3C**) as well as in conditional Gαo mutants (Oboti et al., 2014), suggest a minor role of the VNO in the control of sexual preference in females. Nonetheless, either the apical or basal VSN layers alone may be sufficient to enable sex preference by using redundant neural pathways (Chamero et al., 2012). Further research is required to elucidate the control of sexual preference.

Although many aspects of sexual receptivity in females may be innate, acquiring elevated levels of lordosis performance depends on the combination of adequate hormonal environment with sensory experience (Thompson and Edwards, 1971). It has been shown that lesions of the VNO and AOB reduce the lordosis quotient of sexually naïve females (Keller et al., 2006; Martel and Baum, 2009) and that acute inhibition of AOB activity reduces the lordosis quotient of sexually experienced females (McCarthy et al., 2017). Our results show that Gαi2-dependent VNO activity is dispensable for the display of basal levels of lordosis (**Figure 3**), which likely depends on Gαo signaling (Oboti et al., 2014). After mating experience, however, we demonstrate that Gαi2+ VSNs play a critical role in the acquisition of complete sexual receptivity in females, transforming weaker responses into more robust and frequent lordosis episodes (**Figure 3**). Thus, synergy between innate and experience-dependent processes may be critical for fast, efficient, and flexible display of complex behaviors.

We have screened for the expression of c-Fos, an early gene linked to neural activity, in the brain and found that the number of c-Fos+ cells was reduced in the anterior AOB and RP3V of cGαi2$^{-/-}$ females after lordosis (**Figure 4**). This reduction in c-Fos+ neurons in both regions is consistent with reduced sensory input from the VNO. However, we observe a positive correlation of the number of c-Fos+ cells in the RP3V with lordosis, also in control animals (**Figure 4E**). Further experiments are needed to establish causality, but these results suggest that neural activity in the RP3V may regulate the level of sexual receptivity integrating sensory information from Gαi2+ neurons. In particular, RP3V-kisspeptin neurons seem to be essential to trigger lordosis (Hellier et al., 2018), although activity of these cells is not lower in cGαi2$^{-/-}$ females (**Figure 4I**). This is in line with the view that the display of basal levels of lordosis is largely Gαi2-independent and suggests that the recruitment of additional RP3V-kisspeptin neurons is not required to increase lordosis performance. In accordance with this, non-kisspeptin neurons in the RP3V, such as tyrosine-hydroxylase (TH) positive neurons, are also sensitive to male odors (Bakker et al., 2010; Taziaux and Bakker, 2015). Remarkably, targeted ablation of TH neurons in the RP3V does not seem to reduce the lordosis quotient in sexually naïve females (Scott et al., 2015). Further research is needed to establish whether TH neurons in the RP3V participate in the acquisition of sexual experience.

Our findings complement recent studies of neural circuits involved in social behavior by revealing that experience-dependent improvement of ethologically important behaviors can be shaped by sensory components (**Figure 5**). This may exemplify a mechanism of neuroplasticity in which olfaction in combination with social experience improve social behavior synergistically.

DATA AVAILABILITY STATEMENT

The raw data supporting the conclusions of this article will be made available by the authors, without undue reservation.

ETHICS STATEMENT

The animal study was reviewed and approved by the CEEA Val de Loire.

AUTHOR CONTRIBUTIONS

PC, MK, LB, FZ, and TL-Z designed the research. A-CT, CM, and KP performed the research. A-CT and CM analyzed the data. PC and A-CT wrote the manuscript with edits of all authors.

FUNDING

This work was supported by the Deutsche Forschungsgemeinschaft (DFG) grants Sonderforschungsbereich-Transregio TRR 152/P10, project 239283807 (FZ and TL-Z) and Sonderforschungsbereich 894 project A17 (FZ and TL-Z), and Region Centre Val de Loire project 201900134883 (PC). LB was supported in part by the Intramural Research Program of the NIH (Project Z01-ES-101643). A-CT was supported by the grant from the University of Tours and Region Centre Val de Loire.

ACKNOWLEDGMENTS

We thank Deborah Crespin, Flora Martin, and Aurelie Gasnier for mice husbandry; Marie-Claire Blache for help with imaging experiments; the staff of the hormonal assay laboratory; and Isabelle Franceschini for the kisspeptin antibody.

REFERENCES

Bakker, J., Pierman, S., and González-Martínez, D. (2010). Effects of aromatase mutation (ArKO) on the sexual differentiation of kisspeptin neuronal numbers and their activation by same versus opposite sex urinary pheromones. *Horm. Behav.* 57, 390–395. doi: 10.1016/j.yhbeh.2009.11.005

Bonthuis, P. J., Patteson, J. K., and Rissman, E. F. (2011). Acquisition of sexual receptivity: roles of chromatin acetylation, estrogen receptor-α, and ovarian hormones. *Endocrinology* 152, 3172–3181. doi: 10.1210/en.2010-1001

Chamero, P., Katsoulidou, V., Hendrix, P., Bufe, B., Roberts, R., Matsunami, H., et al. (2011). G protein G o is essential for vomeronasal function and aggressive behavior in mice. *Proc. Natl. Acad. Sci. U.S.A.* 108, 12898–12903. doi: 10.1073/pnas.1107770108

Chamero, P., Leinders-Zufall, T., and Zufall, F. (2012). From genes to social communication: molecular sensing by the vomeronasal organ. *Trends Neurosci.* 35, 597–606. doi: 10.1016/j.tins.2012.04.011

Del Punta, K., Leinders-Zufall, T., Rodriguez, I., Jukam, D., Wysocki, C. J., Ogawa, S., et al. (2002). Deficient pheromone responses in mice lacking a cluster of vomeronasal receptor genes. *Nature* 419, 70–74. doi: 10.1038/nature00955

Ehret, G., Koch, M., Haack, B., and Markl, H. (1987). Sex and parental experience determine the onset of an instinctive behavior in mice. *Naturwissenschaften* 74, 47–47. doi: 10.1007/BF00367047

Elyada, Y. M., and Mizrahi, A. (2015). Becoming a mother—circuit plasticity underlying maternal behavior. *Curr. Opin. Neurobiol.* 35, 49–56. doi: 10.1016/j.conb.2015.06.007

Ferrero, D. M., Moeller, L. M., Osakada, T., Horio, N., Li, Q., Roy, D. S., et al. (2013). A juvenile mouse pheromone inhibits sexual behaviour through the vomeronasal system. *Nature* 502, 368–371. doi: 10.1038/nature12579

Flanagan, K. A., Webb, W., and Stowers, L. (2011). Analysis of male pheromones that accelerate female reproductive organ development. *PLoS One* 6:e16660. doi: 10.1371/journal.pone.0016660

Fleming, A., Vaccarino, F., Tambosso, L., and Chee, P. (1979). Vomeronasal and olfactory system modulation of maternal behavior in the rat. *Science (80)* 203, 372–374. doi: 10.1126/science.760196

Franceschini, I., Yeo, S. H., Beltramo, M., Desroziers, E., Okamura, H., Herbison, A. E., et al. (2013). Immunohistochemical evidence for the presence of various kisspeptin isoforms in the mammalian brain. *J. Neuroendocrinol.* 25, 839–851. doi: 10.1111/jne.12069

Fraser, E. J., and Shah, N. M. (2014). Complex chemosensory control of female reproductive behaviors. *PLoS One* 9:e90368. doi: 10.1371/journal.pone.0090368

Hasen, N. S., and Gammie, S. C. (2009). Trpc2 gene impacts on maternal aggression, accessory olfactory bulb anatomy and brain activity. *Genes Brain Behav.* 8, 639–649. doi: 10.1111/j.1601-183X.2009.00511.x

Hellier, V., Brock, O., Candlish, M., Desroziers, E., Aoki, M., Mayer, C., et al. (2018). Female sexual behavior in mice is controlled by kisspeptin neurons. *Nat. Commun.* 9:400. doi: 10.1038/s41467-017-02797-2

Inoue, S., Yang, R., Tantry, A., Davis, C., Yang, T., Knoedler, J. R., et al. (2019). Periodic remodeling in a neural circuit governs timing of female sexual behavior. *Cell* 179, 1393–1408.e16. doi: 10.1016/j.cell.2019.10.025

Ishii, K. K., and Touhara, K. (2019). Neural circuits regulating sexual behaviors via the olfactory system in mice. *Neurosci. Res.* 140, 59–76. doi: 10.1016/j.neures.2018.10.009

Isogai, Y., Wu, Z., Love, M. I., Ahn, M. H.-Y., Bambah-Mukku, D., Hua, V., et al. (2018). Multisensory logic of infant-directed aggression by males. *Cell* 175, 1827–1841.e17. doi: 10.1016/j.cell.2018.11.032

Jouhanneau, M., Cornilleau, F., and Keller, M. (2014). Peripubertal exposure to male odors influences female puberty and adult expression of male-directed odor preference in mice. *Horm. Behav.* 65, 128–133. doi: 10.1016/j.yhbeh.2013.12.006

Keller, M., Baum, M. J., Brock, O., Brennan, P. A., and Bakker, J. (2009). The main and the accessory olfactory systems interact in the control of mate recognition and sexual behavior. *Behav. Brain Res.* 200, 268–276. doi: 10.1016/j.bbr.2009.01.020

Keller, M., Pierman, S., Douhard, Q., Baum, M. J., and Bakker, J. (2006). The vomeronasal organ is required for the expression of lordosis behaviour, but not sex discrimination in female mice. *Eur. J. Neurosci.* 23, 521–530. doi: 10.1111/j.1460-9568.2005.04589.x

Kimchi, T., Xu, J., and Dulac, C. (2007). A functional circuit underlying male sexual behaviour in the female mouse brain. *Nature* 448, 1009–1014. doi: 10.1038/nature06089

Koch, M., and Ehret, G. (1989). Estradiol and parental experience, but not prolactin are necessary for ultrasound recognition and pup-retrieving in the mouse. *Physiol. Behav.* 45, 771–776. doi: 10.1016/0031-9384(89)90293-X

Kohl, J., Autry, A. E., and Dulac, C. (2017). The neurobiology of parenting: a neural circuit perspective. *BioEssays* 39, 1–11. doi: 10.1002/bies.201600159

Lévy, F., Keller, M., and Poindron, P. (2004). Olfactory regulation of maternal behavior in mammals. *Horm. Behav.* 46, 284–302. doi: 10.1016/j.yhbeh.2004.02.005

Leypold, B. G., Yu, C. R., Leinders-Zufall, T., Kim, M. M., Zufall, F., and Axel, R. (2002). Altered sexual and social behaviors in trp2 mutant mice. *Proc. Natl. Acad. Sci. U.S.A.* 99, 6376–6381. doi: 10.1073/pnas.082127599

Marlin, B. J., Mitre, M., D'Amour, J. A., Chao, M. V., and Froemke, R. C. (2015). Oxytocin enables maternal behaviour by balancing cortical inhibition. *Nature* 520, 499–504. doi: 10.1038/nature14402

Martel, K. L., and Baum, M. J. (2009). Adult testosterone treatment but not surgical disruption of vomeronasal function augments male-typical sexual behavior in female mice. *J. Neurosci.* 29, 7658–7666. doi: 10.1523/jneurosci.1311-09.2009

McCarthy, E. A., Kunkhyen, T., Korzan, W. J., Naik, A., Maqsudlu, A., Cherry, J. A., et al. (2017). A comparison of the effects of male pheromone priming and optogenetic inhibition of accessory olfactory bulb forebrain inputs on the sexual behavior of estrous female mice. *Horm. Behav.* 89, 104–112. doi: 10.1016/j.yhbeh.2016.12.011

Nakahara, T. S., Camargo, A. P., Magalhães, P. H. M., Souza, M. A. A., Ribeiro, P. G., Martins-Netto, P. H., et al. (2020). Peripheral oxytocin injection modulates vomeronasal sensory activity and reduces pup-directed aggression in male mice. *Sci. Rep.* 10:19943. doi: 10.1038/s41598-020-77061-7

Nakahara, T. S., Cardozo, L. M., Ibarra-Soria, X., Bard, A. D., Carvalho, V. M. A., Trintinalia, G. Z., et al. (2016). Detection of pup odors by non-canonical adult vomeronasal neurons expressing an odorant receptor gene is influenced by sex and parenting status. *BMC Biol.* 14:12. doi: 10.1186/s12915-016-0234-9

Norlin, E. M., Gussing, F., and Berghard, A. (2003). Vomeronasal phenotype and behavioral alterations in Gαi2 mutant mice. *Curr. Biol.* 13, 1214–1219. doi: 10.1016/S0960-9822(03)00452-4

Numan, M. (1974). Medial preoptic area and maternal behavior in the female rat. *J. Comp. Physiol. Psychol.* 87, 746–759. doi: 10.1037/h0036974

Oboti, L., Pérez-Gómez, A., Keller, M., Jacobi, E., Birnbaumer, L., Leinders-Zufall, T., et al. (2014). A wide range of pheromone-stimulated sexual and reproductive behaviors in female mice depend on G protein Gαo. *BMC Biol.* 12:31. doi: 10.1186/1741-7007-12-31

Pfaff, D. W., and Sakuma, Y. (1979). Deficit in the lordosis reflex of female rats caused by lesions in the ventromedial nucleus of the hypothalamus. *J. Physiol.* 288, 203–210. doi: 10.1113/jphysiol.1979.sp012691

Scott, N., Prigge, M., Yizhar, O., and Kimchi, T. (2015). A sexually dimorphic hypothalamic circuit controls maternal care and oxytocin secretion. *Nature* 525, 519–522. doi: 10.1038/nature15378

Simerly, R. B. (2002). Wired for reproduction: organization and development of sexually dimorphic circuits in the mammalian forebrain. *Annu. Rev. Neurosci.* 25, 507–536. doi: 10.1146/annurev.neuro.25.112701.142745

Stolzenberg, D. S., and Rissman, E. F. (2011). Oestrogen-independent, experience-induced maternal behaviour in female mice. *J. Neuroendocrinol.* 23, 345–354. doi: 10.1111/j.1365-2826.2011.02112.x

Stowers, L., Holy, T. E., Meister, M., Dulac, C., and Koentges, G. (2002). Loss of sex discrimination and male-male aggression in mice deficient for TRP2. *Science* 295, 1493–1500. doi: 10.1126/science.1069259

Stowers, L., and Kuo, T.-H. (2015). Mammalian pheromones: emerging properties and mechanisms of detection. *Curr. Opin. Neurobiol.* 34, 103–109. doi: 10.1016/j.conb.2015.02.005

Stowers, L., and Liberles, S. D. (2016). State-dependent responses to sex pheromones in mouse. *Curr. Opin. Neurobiol.* 38, 74–79. doi: 10.1016/j.conb.2016.04.001

Tachikawa, K. S., Yoshihara, Y., and Kuroda, K. O. (2013). Behavioral transition from attack to parenting in male mice: a crucial role of the vomeronasal system. *J. Neurosci.* 33, 5120–5126. doi: 10.1523/JNEUROSCI.2364-12.2013

Taziaux, M., and Bakker, J. (2015). Absence of female-typical pheromone-induced hypothalamic neural responses and kisspeptin neuronal activity in

α-fetoprotein knockout female mice. *Endocrinology* 156, 2595–2607. doi: 10.1210/en.2015-1062

Thompson, M. L., and Edwards, D. A. (1971). Experiential and strain determinants of the estrogen-progesterone induction of sexual receptivity in spayed female mice. *Horm. Behav.* 2, 299–305. doi: 10.1016/0018-506X(71)90004-3

Trouillet, A.-C., Keller, M., Weiss, J., Leinders-Zufall, T., Birnbaumer, L., Zufall, F., et al. (2019). Central role of G protein Gαi2 and Gαi2 + vomeronasal neurons in balancing territorial and infant-directed aggression of male mice. *Proc. Natl. Acad. Sci. U.S.A.* 116, 5135–5143. doi: 10.1073/pnas.1821492116

Weiss, J., Pyrski, M., Jacobi, E., Bufe, B., Willnecker, V., Schick, B., et al. (2011). Loss-of-function mutations in sodium channel Na v 1.7 cause anosmia. *Nature* 472, 186–192. doi: 10.1038/nature09975

Wu, Z., Autry, A. E., Bergan, J. F., Watabe-Uchida, M., and Dulac, C. G. (2014). Galanin neurons in the medial preoptic area govern parental behaviour. *Nature* 509, 325–330. doi: 10.1038/nature13307

Wysocki, C. J., and Lepri, J. J. (1991). Consequences of removing the vomeronasal organ. *J. Steroid Biochem. Mol. Biol.* 39, 661–669. doi: 10.1016/0960-0760(91)90265-7

Conflict of Interest: The authors declare that the research was conducted in the absence of any commercial or financial relationships that could be construed as a potential conflict of interest.

Copyright © 2021 Trouillet, Moussu, Poissenot, Keller, Birnbaumer, Leinders-Zufall, Zufall and Chamero. This is an open-access article distributed under the terms of the Creative Commons Attribution License (CC BY). The use, distribution or reproduction in other forums is permitted, provided the original author(s) and the copyright owner(s) are credited and that the original publication in this journal is cited, in accordance with accepted academic practice. No use, distribution or reproduction is permitted which does not comply with these terms.

3 Contrôle des comportements d'évitement par les VSN apicaux

3.1 Introduction

Les souris sont continuellement exposées à des dangers tels que les prédateurs ou les infections lors des interactions sociales avec leurs congénères. Les espèces sociales ont développé divers mécanismes comportementaux pour minimiser leur exposition potentielle aux menaces tout en maintenant leurs activités vitales. Le système olfactif est crucial dans ces processus en codant la valence des odeurs environnantes et en faisant ainsi pencher la balance vers l'attraction ou l'aversion (Li et Liberles, 2015).

Les proies et les prédateurs partagent leur environnement, et les signaux des prédateurs peuvent être détectés par les proies pour induire des comportements d'évitement et de défense. Ces substances chimiques interspécifiques sont appelées kairomones. La détection des kairomones ne se limite pas à un seul sous-système olfactif (Pérez-Gómez et al., 2015 ; Takahashi, 2014). Le système voméronasal a d'abord été montré comme médiateur de l'évitement des chats (Samuelsen et Meredith, 2009). Plus tard, le VNO a également été associé à la détection et à l'évitement des rats, des mustélidés, des serpents et des rapaces (Isogai et al., 2011a ; Papes et al., 2010). Plusieurs VRs peuvent être activés par un type de prédateur et ces VRs semblent être regroupés, certains prédateurs n'activant que les VSN basaux ou apicaux (Isogai et al., 2011). Par exemple, l'ablation fonctionnelle des VSNs basaux V2Rs/Gαo abolit l'évitement pour les odeurs de fourrure de chat (Pérez-Gómez et al., 2015). À l'inverse, l'activation des VSNs par l'exposition aux plumes ou à la litière de chouettes est corrélée à la voie de signalisation V1R/Gαi2 (Carvalho et al., 2015 ; Isogai et al., 2011b), mais les preuves fonctionnelles font encore défaut.

Les souris détectent les congénères malades à l'aide de l'odorat et les évitent activement pour prévenir la contagion (Kavaliers et al., 2005). Le VNO a été proposé comme médiateur de la reconnaissance des congénères malades. L'injection de lipopolysaccharides bactériens (LPS) chez la souris est un protocole standard pour induire un état inflammatoire général, imitant ainsi l'infection par un pathogène, et induisant l'évitement par des congénères sains. Les souris VNOx et Trpc2-/- n'évitent pas une souris traitée au LPS (Boillat et al., 2015 ; Kwon et al., 2021). L'identité des VSNs médiant les signaux associés à la maladie est inconnue. Les FPR semblent être de bons candidats en raison de leur affinité naturelle pour les peptides d'origine bactérienne (Bufe et al., 2012). Cependant, les souris FPR3-KO évitent toujours un animal traité au LPS, écartant ce récepteur dans la médiation de ce type d'évitement (Bufe et al., 2019). Néanmoins, l'analyse de l'activation de l'AOB après exposition à l'urine de souris traitées au LPS montre une activation accrue dans les parties antérieures et postérieures de l'AOB (Boillat et al., 2015). Ainsi, les VSNs exprimant les V2Rs ou les VSNs apicaux (exprimant les V1Rs ou les FPRs apicaux) sont de bons candidats pour médier ce type d'évitement.

La présente étude vise à étudier le rôle de la signalisation voméronasale Gαi2 sur les comportements d'évitement. Nous avons exposé des souris conditionnellement dépourvues de Gαi2

(cGαi2-/-) à deux types d'indices associés au danger : des odeurs de prédateur provenant de hiboux et des indices de maladie provenant de souris traitées au LPS. Nous avons combiné des expériences comportementales avec des enregistrement par imagerie calcique et la cartographie des gènes précoces immédiats pour déterminer si les VSNs exprimant Gαi2 conduisent l'évitement des deux types d'indices olfactifs.

3.2 Méthodes

Animals. Animal care and experimental procedures were performed following French and European guidelines on the protection of animals used for scientific purposes and approved by an ethical committee for animal experimentation. Mice were kept under standard 12h light/dark cycles with food and water ad libitum. $cG\alpha_{i2}^{-/-}$ and $cG\alpha_{i2}^{+/-}$ mice were generated as described (Trouillet et al., 2019). All animals used were 8 weeks old or older. Males were used for behavioral experiments and immediate early gene mapping. Diestrus females and males were used for calcium imaging experiments. Females' estrus status was assessed by vaginal sampling.

Predator odors collection and preparation. Owl (*Asio otus* and *Tyto alba*) feces were collected directly in bird aviaries. 3 x 3 cm gauzes were put in contact with the feces in a glass jar and incubated at RT for one day (Figure 39C). Gauze and feces were then stored separately at -80°C. Cat (*Felis catus*) fur was collected by brushing. 3 x3 cm gauzes were rubbed onto the cat's neck and face fur (Figure 39A). Gauze and fur were then stored together at -80°C. Snake (*Pantherophis guttatus*) molt was collected in the snake vivarium, cut in 2 x 2 cm pieces, and stored at -80°C (Figure 39B). For calcium imaging experiments, predator odor extracts were prepared by incubating predator samples in 100 mL Hank's balanced salt solution (Invitrogen) supplemented with 10 mM Hepes at RT for 2h on an orbital rotator (Figure 39D). Four solutions were prepared from: 1) a clean gauze; 2) 0.4 g of cat fur and a clean gauze; 3) 3 g of crushed owl feces and a clean gauze; and 4) 0.2 g of crushed snake molt. Solutions were first coarsely filtered to remove solids and then passed through a Nalgene™ Rapid-Flow™ sterile filtering unit (surfactant-free cellulose acetate membrane, pore size 0.2 µm, Thermo Scientific) (Figure 39E). Filtered solutions were stocked at -80°C.

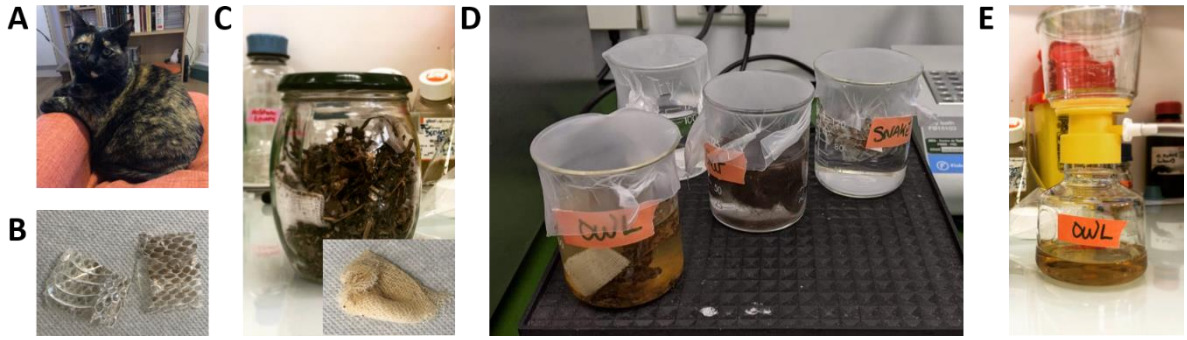

Figure 39: Preparation of predator samples. A) Moquette, the cat used for sampling fur. B) Pieces of snake molt. C) Jar used for incubating gauze with owl feces and resulting gauze after incubation. D) Incubation of predator samples for the preparation of calcium imaging extracts. E) Resulting extract after filtration.

Treatment of mice with LPS and urine collection. C57BL6/J adult group-housed males were injected intraperitoneally with either 200 µL of 1 mg/kg LPS (Lipopolysaccharide L4391, Sigma) or saline solution. 4 h post-injection, urine from mice injected with LPS or saline were collected, pooled (4 mice per condition), and stored at -80 °C until use. For calcium imaging experiments, fresh urine from healthy male donors was fractioned into high and low molecular weight fractions (HMW and LMW) (Trouillet et al., 2019) and kept at -80 °C. A week later, the same males were injected with 200 µL of 1 mg/kg LPS (Lipopolysaccharide L4391, Sigma), urine was collected 4h later and fractioned before storage.

Behavior. Mice were moved to the experimental room 2 h before testing. Assays were conducted 2 h before the start of the dark period. Experiments were videotaped and subsequently analyzed by a blind experimenter.

Predator odor avoidance. The day before the first test, mice were habituated to the three chambers box for 10 min in absence of stimuli. Mice were then tested 4 times for avoidance to predator odors or neutral stimulus on consecutive days. For each experiment, one chamber contained predator or neutral stimulus and the others were empty. Neutral stimulus was an unscented clean gauze; predator odors were either a piece of snake molt, cat fur and a gauze rubbed on a cat neck, or a gauze incubated with owl feces. Order of stimuli presentation was randomized. The apparatus was cleaned with 20% ethanol between subjects. Stimulus side was randomized to avoid side effects: the entire maze was rotated in order to maintain the predator odor in the same chamber and thus avoiding potential contamination of the empty chambers. Mice were free to investigate the apparatus for 10 min. The time spent in each chamber and the duration of chemosensory investigation were recorded. An avoidance index was calculated as $(T_P — aT_N)/(aT_P + aT_N)$, with T_P as the time an individual mouse investigated a predator odor, aT_P as the average time of all tested mice investigating this stimulus, and aT_N as the average time of all mice investigating the neutral stimulus. Negative values represent avoidance and positive values represent attraction.

Sick conspecific odor avoidance. Two days before the test, mice were daily habituated to the three chambers box for 10 min with unscented stimuli in each side chamber. On test day, 50 µL of urine from LPS-treated and saline-treated males were placed on filter papers sealed to plastic weight boards in each side compartments. Stimulus side was randomized, and the apparatus was cleaned with 20% ethanol between subjects. Mice were left free to investigate the apparatus for 10 min. The time spent in each chamber and the duration of chemosensory investigation were recorded. An avoidance index was calculated as $(T_{LPS} — aT_{veh})/(aT_{LPS} + aT_{veh})$, with T_{LPS} as the time an individual mouse investigated the LPS-treated male urine, aT_{LPS} as the average time of all tested mice investigating this stimulus, and aT_{veh} as the average time of all mice investigating the vehicle-treated male urine. Negative values represent avoidance and positive values represent attraction. We also calculated an individual preference score as $(T_{LPS} — T_{veh})/(T_{LPS} + T_{veh})$, with T_{veh} the time an individual mouse investigated the vehicle-treated male urine. Negative values represent preference for the LPS-urine and positive values represent preference for the veh-urine.

Calcium imaging. Calcium imaging of freshly dissociated VSNs was performed as described previously (Chamero et al., 2007, 2011; Trouillet et al., 2019). Cells were stimulated in a random order during 30 sec with 3 min interval between each stimulation. Chemostimuli were freshly diluted in HBSS/Hepes solution to give the following final concentrations: HMW and LMW fractions from LPS-treated or saline-treated males, 1:100; clean gauze, cat fur, and snake molt extracts, 1:1; owl feces extract, 1:1, 1:2, 1:10, and 1:100; KCl, 50 mM. Cells showing a response to control solution or buffer were excluded from the analysis. Experimental replicates were done by pooling VNO from two mice. Each experimental replicate was tested three times for technical replicates. Mean values obtained from technical replicates and acute number of cells were analyzed.

Immunostaining. *Tissue preparation.* Mice were individually housed for at least 4 days without bedding changing and exposed to either a clean gauze, a gauze incubated with owl feces, a clean filter paper, or a filter paper with LPS-treated male urine. 90 min after exposure, mice were anesthetized by an overdose of pentobarbital (Ceva) and perfused transcardially. Samples were prepared as previously described (Trouillet et al., 2019, 2021). *cFos immunolabeling.* Procedure was done as previously described (Trouillet et al., 2019, 2021). cFos primary antibody (1:1000; mouse monoclonal #sc-271243, Santa Cruz Biotechnology) and biotinylated goat anti-mouse secondary antibody (1:1000; IgG, Jackson ImmunoResearch) were used. *pS6 immunolabeling.* Slides were washed (3 x 5 min) in TBS, incubated in blocking solution (TBS containing 0.3% Triton X-100, TBS-T, and 2% donkey serum) 2h at room temperature (RT), and overnight at 4 °C in blocking solution supplemented with the pS6 primary antibody (1:2500; rabbit polyclonal #44-923G, Invitrogen). Slides were then washed in TBS and incubated in TBS-T supplemented with secondary antibody (1:1000 Cy3-conjugated donkey anti-rabbit IgG, Jackson ImmunoResearch) for 2h at RT. Nuclei were counterstained 5 min at RT with DAPI. Slides were mounted with Fluoromount-G™ (Invitrogen). *Analysis.* Slides were scanned using an automatic slide scanner (Axio Sca.Z1, Zeiss). cFos-positive

nuclei were counted using the particle analyzer plug-in of Fiji (Schindelin et al., 2012) on 2-3 images of the AOB per animal and expressed as a density. pS6-positive cells were counted using the Cell Detection process of QuPath (Bankhead et al., 2017) on 6-15 images of the VNE per animals and expressed as a proportion of the total DAPI-positive nuclei number.

Statistics. Statistical analyses were performed by using GraphPad Prism 9.0 (GraphPad Software). Assumptions of normality and homogeneity of variance were tested before conducting the following statistical approaches. Student's t test was used to measure the significance of the difference between two distributions. In case the results failed the test of normality, a Mann–Whitney U test was performed. For categorical data, we used the Fisher's exact test. Multiple groups were compared by using a two-way ANOVA with Fisher LSD multiple comparison tests as a post hoc. The probability of error level (i.e., α) was chosen to be 0.05. Specific statistics and number of samples analyzed are described in the figure captions.

3.3 Résultats

3.3.1 Apical VSNs mediate sick and predator avoidances

Several pieces of evidence point to a role of $G\alpha_{i2}$-expressing VSNs in mediating innate avoidance behaviors. For example, $Trpc2^{-/-}$ mice do not avoid birds of prey cues (Carvalho et al., 2020), and olfactory detection of this type of predator may be mediated by V1Rs-expressing VSNs (Isogai et al., 2011). To verify this hypothesis, we exposed $cG\alpha_{i2}^{+/-}$ and $cG\alpha_{i2}^{-/-}$ mice to different predator cues (Figure 40A). Each mouse was exposed in independent experiments to a clean gauze (control), cat fur, snake molt, or owl feces in a three-chamber box, and we calculated an aversion index based on the time spent sniffing the stimuli (see methods). Olfactory detection of cat fur has been associated with V2Rs/$G\alpha_o$-expressing VSNs (Pérez-Gómez et al., 2015) and snake molt seems to activate both V1Rs- and V2Rs-expressing VSNs (Isogai et al., 2011). Thus, we used these two stimulations as positive controls. As expected, all predator cues were aversive to naïve $cG\alpha_{i2}^{+/-}$ control mice, as shown by their negative aversion index (owl: -0.3, snake: -0.25, cat: -0.35; Figure 40B). Aversion indexes of $cG\alpha_{i2}^{-/-}$ males for cat and snake stimuli were also negative and statistically similar to those of control animals (-0.33 P = 0.8 and -0.42 P = 0.2, respectively; Figure 40B), indicating that avoidance to these two predators does not require $G\alpha_{i2}$ signaling. However, owl feces failed to induce any aversive effect on $cG\alpha_{i2}^{-/-}$ animals (Figure 40B). Based on the time spent investigating the clean gauze stimulus, exposure of $cG\alpha_{i2}^{-/-}$ mice to owl feces did not elicit avoidance or attraction as shown by the aversion index close to zero (-0.03, $P < 0.05$ versus $cG\alpha_{i2}^{+/-}$, $P < 0.01$ and $P < 0.05$ versus snake and cat stimuli in $cG\alpha_{i2}^{-/-}$; Figure 40B). This indicates that $G\alpha_{i2}$ vomeronasal signaling may be necessary to display innate avoidance to birds of prey.

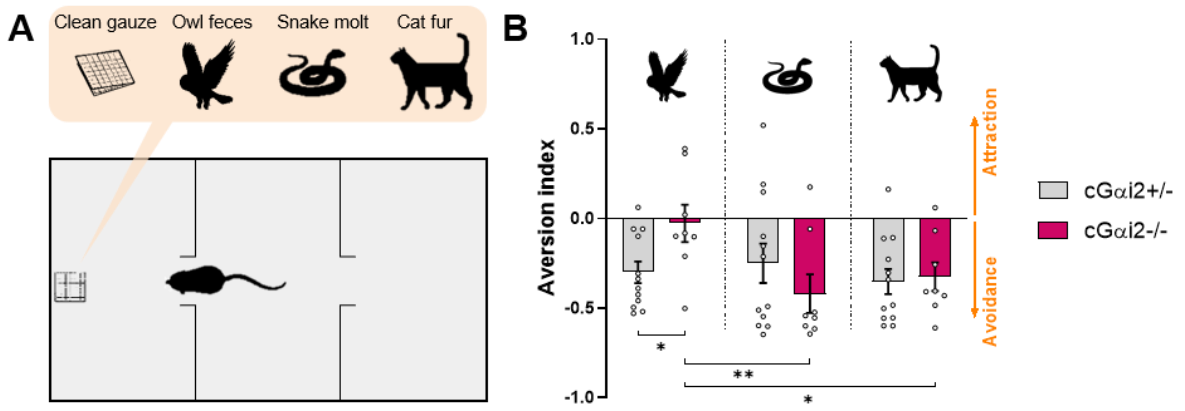

Figure 40: Predator avoidance in cGα$_{i2}^{-/-}$ animals. A) Predator avoidance experimental paradigm. 12 cGα$_{i2}^{+/-}$ and 8 cGα$_{i2}^{-/-}$ males were tested for their innate avoidance toward a clean gauze, owl feces, snake molt, or cat fur in a three-chamber box. B) Average response to a given stimulus, as quantified by the aversion index. Two-way repeated measures ANOVA. Stimulus: $F_{(2, 36)} = 3.924$, $P < 0.05$; genotype : $F_{(1, 18)} = 0.1886$, $P = 0.7$; genotype x stimulus: $F_{(2, 36)} = 4.888$, $P < 0.05$. Posthoc analyzes, LSD Fischer tests: owl feces avoidance, cGα$_{i2}^{+/-}$ vs cGα$_{i2}^{-/-}$ $P < 0.05$; cGα$_{i2}^{-/-}$ owl feces vs snake skin avoidance, $P < 0.01$; cGα$_{i2}^{-/-}$ owl feces vs cat fur avoidance, $P < 0.05$; other comparisons $P = 0.2 – 0.8$. Data are shown as mean ± SEM with individual values.

Similar to predator cues, Trpc2$^{-/-}$ mice do not discriminate urine from a sick or healthy congener, but VSNs sensing sick-associated cues are not yet identified (Boillat et al., 2015; Bufe et al., 2019). In order to determine if Gα$_{i2}$-expressing VSNs participate in sick-conspecific avoidance, we tested the olfactory preference of cGα$_{i2}^{+/-}$ and cGα$_{i2}^{-/-}$ mice between healthy versus sick same-sex urine (Figure 41A). Male mice were made sick by injection of bacterial lipopolysaccharides (LPS), and their urine (LPS-urine) was used in a two-choice test with urine from healthy males (veh-urine). We calculated an aversion index based on the time spent sniffing the veh-urine (see methods). LPS-urine was aversive to cGα$_{i2}^{+/-}$ control males, as shown by the negative aversion index (-0.2; Figure 41B). However, LPS-urine did not elicit avoidance or attraction to cGα$_{i2}^{-/-}$ mice as shown by an aversion index close to zero (-0.03, $P < 0.05$ versus cGα$_{i2}^{+/-}$; Figure 41B). Examining data from individual mice showed that most cGα$_{i2}^{+/-}$ animals (11/15) spent more time investigating the veh-urine than the LPS-urine, while only 6 over 16 cGα$_{i2}^{-/-}$ males investigated veh-urine more than LPS-urine (Figure 41C). This indicates that cGα$_{i2}^{+/-}$ males showed a preference for the veh-urine while cGα$_{i2}^{-/-}$ did not. Indeed, the comparison of the individual preference scores (see methods) showed a statistical difference between genotypes ($P < 0.05$, Figure 41D). Therefore, Gα$_{i2}$ vomeronasal signaling may be necessary for innate sick conspecific avoidance.

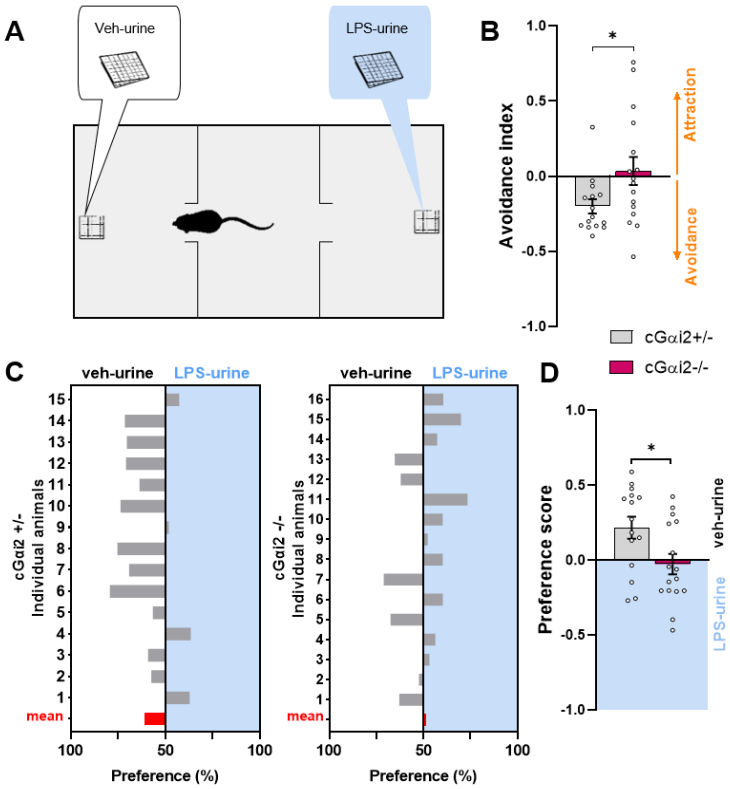

Figure 41: Sick-conspecific avoidance in cGa$i2^{-/-}$ animals. A) Sick-conspecific avoidance experimental paradigm. 15 cGa$i2^{+/-}$ and 16 cGa$i2^{-/-}$ males were tested for their preference between vehicle- (veh-urine) and LPS-treated (LPS-urine) male urine in a three-chamber box. B) Average responses to a given stimulus, as quantified by the aversion index. Mann-Whitney test, P < 0.05. C) Graphs showing investigation time above 50% that individual cGa$i2^{+/-}$ (left) and cGa$i2^{-/-}$ (right) examined either the vehicle or LPS urine. D) Average responses to a given stimulus, as quantified by the preference score. Unpaired t-test, P < 0.05. Data are shown as mean ± SEM with individual values.

3.3.2 Sick and predator associated olfactory cues activate Gαi2 vomeronasal signaling pathway

Next, we wanted to assess whether Gαi2-expressing VSNs sense owl and LPS-urine olfactory cues. We exposed singly-housed males to an owl feces impregnated gauze or to urine from an LPS-treated male and analyzed VNO and AOB activation by immunostaining for pS6 or cFos, respectively. Owl exposure induced pS6 expression in 4.6% of VSNs of control cG$\alpha_{i2}^{+/-}$ mice. By contrast, the number of pS6-positive cells was significantly lower in cG$\alpha_{i2}^{-/-}$ animals (0.017%, $P < 0.05$ versus controls; Figure 42A). Similarly, the proportion of pS6-positive cells in the VNE of cG$\alpha_{i2}^{-/-}$ mice was lower than in controls after LPS-urine exposure (2.07% versus 0.61%, $P < 0.05$; Figure 42B). At the level of the AOB, each stimulation increased the total cFos expression in both cG$\alpha_{i2}^{+/-}$ and cG$\alpha_{i2}^{-/-}$ mice compared to unstimulated animals ($P < 0.01$; Figure 42C). Apical and basal VSNs projections to the glomerular layer of the AOB are segregated, with apical V1Rs/Gα_{i2} VSNs projecting the anterior AOB and basal V2Rs/Gα_o VSNs to the posterior AOB. We thus compared the density of cFos cells in each layer of the AOB (GL, glomerular layer; MCL, mitral cells layer; GCL, granular cells layer) regarding the anteroposterior segregation (Figure 42D and E). We did not observe differences in the posterior AOB after owl exposure in mutant animals ($P = 0.2 – 0.9$; Figure 42D). However, the density of cFos

positive cells was significantly lower in each layer of the anterior AOB of cGα$_{i2}^{-/-}$ mice (anterior GL and GCL, P < 0.01, anterior MCL, P < 0.05; Figure 42D). LPS-urine exposure did not induce a different activation of the posterior AOB of control and mutant mice (P = 0.1 – 0.2; Figure 42E). In the anterior AOB, a significant difference between cGα$_{i2}^{-/-}$ and cGα$_{i2}^{+/-}$ was found only the GL (P < 0.05, other regions P = 0.1 – 0.6; Figure 42E). Altogether, these results suggest that the the Gα$_{i2}$ subsystem may detect owl and LPS-urine olfactory cues.

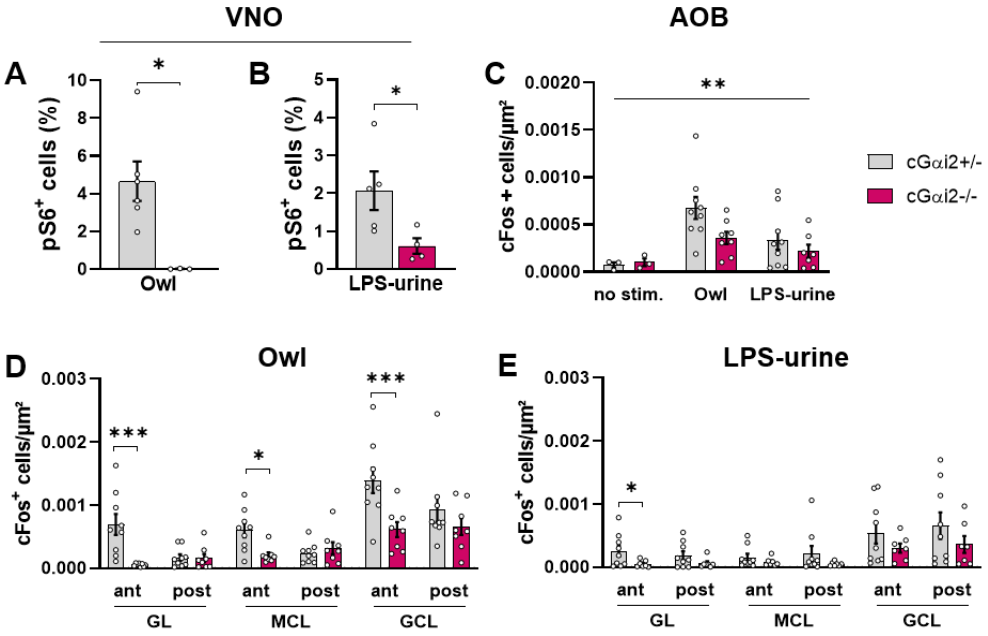

Figure 42: VNO and AOB activation after owl and LPS-urine exposures. A-B) Proportion of pS6-positive cells in the VNO after owl (A) and LPS-urine (B) exposures. A) N = 6 cGα$_{i2}^{+/-}$ and N = 3 cGα$_{i2}^{-/-}$, unpaired t-test P < 0.05. B) N = 5 cGα$_{i2}^{+/-}$ and N = 4 cGα$_{i2}^{-/-}$, unpaired t-test P < 0.05. C) cFos-positive cells density in the AOB of unstimulated and stimulated cGα$_{i2}^{+/-}$ (N = 3 to 9) and cGα$_{i2}^{-/-}$ (N = 3 to 8) mice. Two-way ANOVA, stimulus: $F_{(2, 33)}$ = 7.432, P < 0.01 ; genotype : $F_{(1, 33)}$ = 2.203, P = 0.1; genotype x stimulus: $F_{(2, 33)}$ = 1.219, P = 0.3. D) cFos-positive cells density in each layer of the anterior and posterior AOB of cGα$_{i2}^{+/-}$ (N = 9) and cGα$_{i2}^{-/-}$ (N = 8) mice after exposure to owl feces. Two-way repeated measures ANOVA, area: $F_{(5, 75)}$ = 30.41, P < 0.001 ; genotype : $F_{(1, 15)}$ = 5.914, P < 0.05; area x genotype: $F_{(5, 75)}$ = 8.292, P < 0.001. Posthoc analyzes, LSD Fischer tests: cGα$_{i2}^{+/-}$ vs cGα$_{i2}^{-/-}$ GL-ant P < 0.001; MCL-ant P < 0.05; GCL-ant P < 0.001; other regions P = 0.1 – 0.9. E) cFos-positive cells density in each layer of the anterior and posterior AOB of cGα$_{i2}^{+/-}$ (N = 9) and cGα$_{i2}^{-/-}$ (N = 7) mice after exposure to LPS-urine. Two-way repeated measures ANOVA, area: $F_{(5, 70)}$ = 9.843, P < 0.001 ; genotype : $F_{(1, 14)}$ = 2.3, P = 0.1; area x genotype: $F_{(5, 70)}$ = 0.511, P = 0.8. Posthoc analyzes, LSD Fischer tests: cGα$_{i2}^{+/-}$ vs cGα$_{i2}^{-/-}$ GL-ant P < 0.05; other regions P = 0.1 – 0.6. Data are shown as mean ± SEM with individual values.

3.3.3 Deletion of Gα$_{i2}$ reduces the detection of owl odors

To strengthen our results and assess the responsiveness of VSNs to predator cues, we performed live-cell Ca^{2+} imaging on dissociated VSNs using Fura2. We prepared extracts from cat fur, snake molt, and owl feces (see methods) and tested the responsiveness of 3334 cGα$_{i2}^{+/-}$ and 2364 cGα$_{i2}^{-/-}$ VSNs. Cat fur and snake molt extracts elicited responses in both control (4% and 3.3%, respectively) and mutant (3.3 and 4.1%, respectively) VSNs (Figure 43A). We analyzed the number and the proportion of responsive cells to these two stimuli and did not found differences between genotypes

(Figure 43A and B). By contrast, stimulation with owl extract did activate a much larger fraction of VSNs (>10% versus ~ 3 - 4%) and different amounts of cG$\alpha_{i2}^{-/-}$ and cG$\alpha_{i2}^{+/-}$ VSNs (Figure 43A and B). The overall number of responsive cells was statistically different in cG$\alpha_{i2}^{-/-}$ VSNs (cG$\alpha_{i2}^{-/-}$ 244/2364, 10.3% versus cG$\alpha_{i2}^{+/-}$ 466/3434, 13.6%; χ^2 $P < 0.001$; Figure 43B). The proportion of activated cells was also decreased in the cG$\alpha_{i2}^{-/-}$ VSNs ($P < 0.05$, Figure 43A). We then examined the number of cells responsive to exclusively one stimulus (either cat, snake, or owl; Figure 43B and C). Comparing the proportion of monoresponsive cells showed that owl extracts also activated less cG$\alpha_{i2}^{-/-}$ VSNs than control ones ($P < 0.01$, Figure 43C). We decided to evaluate VSNs responses to several dilutions of the owl feces extract (Figure 43D - G). Surprisingly, in cG$\alpha_{i2}^{+/-}$ controls, [1:2] dilution further increases the number of responses compared to the undiluted ([1:1]) extract (16.7% versus 9.8%), but we observed a reduction of the proportion of responsive cells with the [1:10] and [1:100] dilutions (9.8% versus 5.2% and 3.5%, respectively, Figure 43F). Similar pattern of variation was observed in cG$\alpha_{i2}^{-/-}$ VSNs ([1:1] 6.7%; [1:2] 9.9%, [1:10] 3%; [1:100], 2.5%, Figure 43F). The difference between the number of activated cG$\alpha_{i2}^{-/-}$ and cG$\alpha_{i2}^{+/-}$ VSNs was significant for [1:1] (-33.2%, χ^2 $P < 0.01$), [1:2] (-40.7%, χ^2 $P < 0.001$), [1:10] (-43%, χ^2 $P < 0.01$), but not for [1:100] dilution (-28.7%, χ^2 $P = 0.07$) (Figure 43E and G). Altogether, these results show that VSNs are responsive to all three predator odors and that Gα_{i2}-expressing VSNs participate in the detection of owl odors.

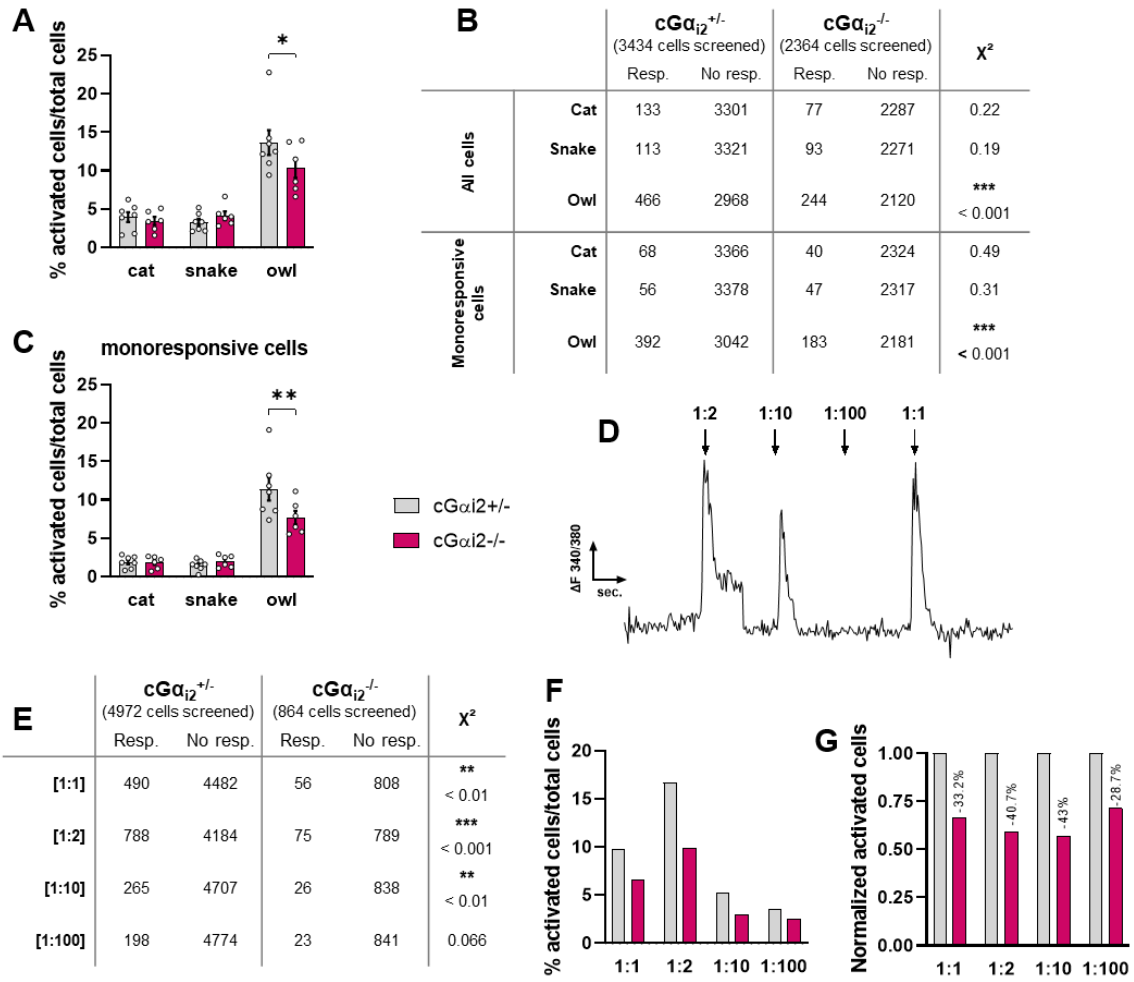

B		$cG\alpha_{i2}^{+/-}$ (3434 cells screened)		$cG\alpha_{i2}^{-/-}$ (2364 cells screened)		χ^2
		Resp.	No resp.	Resp.	No resp.	
All cells	Cat	133	3301	77	2287	0.22
	Snake	113	3321	93	2271	0.19
	Owl	466	2968	244	2120	*** < 0.001
Monoresponsive cells	Cat	68	3366	40	2324	0.49
	Snake	56	3378	47	2317	0.31
	Owl	392	3042	183	2181	*** < 0.001

E	$cG\alpha_{i2}^{+/-}$ (4972 cells screened)		$cG\alpha_{i2}^{-/-}$ (864 cells screened)		χ^2
	Resp.	No resp.	Resp.	No resp.	
[1:1]	490	4482	56	808	** < 0.01
[1:2]	788	4184	75	789	*** < 0.001
[1:10]	265	4707	26	838	** < 0.01
[1:100]	198	4774	23	841	0.066

Figure 43: Specific reduction of VSNs activation by owl odors in the absence of Gαi2. A) Analysis of ligand-evoked Ca^{2+} responses in dissociated cells from $cG\alpha_{i2}^{+/-}$ and $cG\alpha_{i2}^{-/-}$ (N = 6 – 7 experiments using cells from 6 mice for each genotype) mice after stimulation by cat fur, snake molt, or owl feces extracts. Two-way ANOVA, stimulus: $F_{(2, 33)} = 47.38$, $P < 0.001$; genotype : $F_{(1, 33)} = 1.521$, $P = 0.2$; stimulus x genotype: $F_{(2, 33)} = 2.332$, $P = 0.1$. Posthoc analyzes, LSD Fischer tests: owl $cG\alpha_{i2}^{+/-}$ vs $cG\alpha_{i2}^{-/-}$ $P < 0.05$; other comparisons $P = 0.5 – 0.7$. B) Table showing the number of (Resp.) and non responsive (No resp.) cells for each stimulation. χ^2 tests, $cG\alpha_{i2}^{+/-}$ versus $cG\alpha_{i2}^{-/-}$ $P < 0.001$ for all cells and for monoresponsive cells only; other comparison $P = 0.2 – 0.5$. C) Analysis of ligand-evoked Ca^{2+} responses in dissociated cells from $cG\alpha_{i2}^{+/-}$ and $cG\alpha_{i2}^{-/-}$ mice (N = 6 for both genotypes) after stimulation by cat fur, snake molt, or owl feces extracts. Only cells responding to one stimulus exclusively are considered. Two-way ANOVA, stimulus: $F_{(2, 33)} = 65.44$, $P < 0.001$; genotype : $F_{(1, 33)} = 2.928$, $P = 0.09$; stimulus x genotype: $F_{(2, 33)} = 4.338$, $P < 0.05$. Posthoc analyzes, LSD Fischer tests: owl extract $cG\alpha_{i2}^{+/-}$ vs $cG\alpha_{i2}^{-/-}$ $P < 0.01$, other comparisons $P = 0.6 – 0.9$. D) Representative Ca^{2+}responses recorded in a $cG\alpha_{i2}^{+/-}$ VSN during stimulation with owl extract at different dilutions ([1:1]; [1:2]; [1:10]; [1:100]). E) Table showing the number of responsive (Resp.) and non responsive (No resp.) cells for each owl extract dilution. χ^2 tests, $cG\alpha_{i2}^{+/-}$ versus $cG\alpha_{i2}^{-/-}$ $P < 0.001$ for [1:2], $P < 0.01$ for [1:1] and [1:10], and $P = 0.066$ for [1:100] dilution. F) Mean proportion of activated cells from $cG\alpha_{i2}^{+/-}$ (N = 4) and $cG\alpha_{i2}^{-/-}$ (N = 2) mice after stimulation with [1:1], [1:2], [1:10], and [1:100] dilutions of the owl extract. G) Normalized percentage of responding cells from $cG\alpha_{i2}^{+/-}$ (N = 4) and $cG\alpha_{i2}^{-/-}$ (N = 2) mice to a given dilution. Data are shown as mean ± SEM with individual values (A and C) or as mean values (F and G).

3.3.4 $G\alpha_{i2}$ deletion does not specifically impact LPS-urine detection

We also analyzed VSNs activation by healthy and sick mouse urine. We previously showed that $cG\alpha_{i2}^{-/-}$ VSNs show fewer responses to the LMW urine fraction from healthy animals, whereas responses to the HMW fraction remained intact (Trouillet et al., 2019). Thus, we hypothesized that LMW urine compounds might mediate avoidance to LPS-urine. We performed live-cell Ca^{2+} imaging

on dissociated VSNs using Fura2 and tested the responsiveness of 5186 cG$\alpha_{i2}^{+/-}$ and 3894 cG$\alpha_{i2}^{-/-}$ VSNs to veh-LMW and LPS-LMW (Figure 44). We observed responses to both stimuli in VSNs from each genotype (Figure 44A and B). As expected, the overall number of responsive cells to veh-urine and LPS-urine was significantly lower in cG$\alpha_{i2}^{-/-}$ VSNs (veh-urine: cG$\alpha_{i2}^{-/-}$ 83/3894, 2.1% versus cG$\alpha_{i2}^{+/-}$ 150/5186, 2.9%; χ^2 $P < 0.05$; LPS-urine: cG$\alpha_{i2}^{-/-}$ 57/3894, 1.5% versus cG$\alpha_{i2}^{+/-}$ 112/5186, 2.2%; χ^2 $P < 0.001$; Figure 44B). When comparing the proportion of activated cells among different experiments, we found a global effect of the genotype (two-way ANOVA, $P < 0.05$; Figure 44A), but no difference between veh- and LPS-urine ($P = 0.09$; Figure 44A). We also considered cells responsive to exclusively one stimulus (either veh-urine or LPS-urine; Figure 44C). Neither the number nor the proportion of monresponsive cells differed between genotypes (Figure 44B and C). Consequently, the deletion of Gα_{i2} does not have a major impact on the detection of LPS-urine.

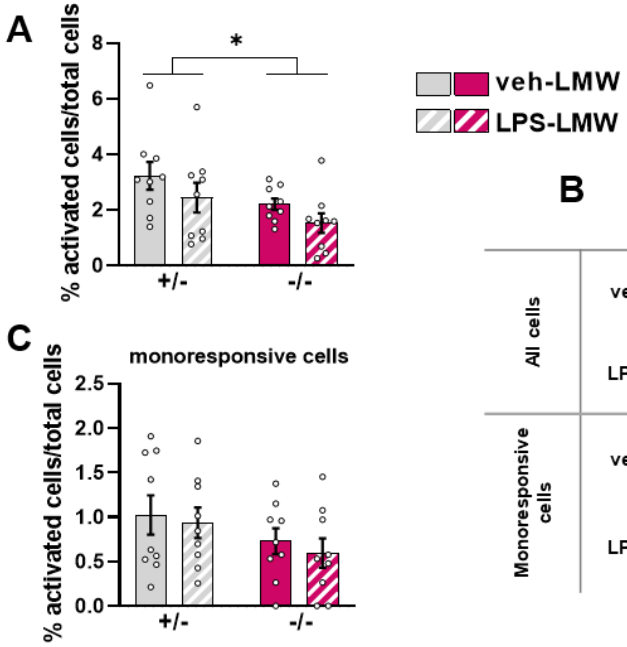

B

		cGα$_{i2}^{+/-}$ (5186 cells screened)		cGα$_{i2}^{-/-}$ (3894 cells screened)		χ^2
		Resp.	No resp.	Resp.	No resp.	
All cells	veh-LMW	150	5036	83	3811	* < 0,05
	LPS-LMW	112	5074	57	3837	*** < 0,001
Monoresponsive cells	veh-LMW	55	5131	28	3866	0,09
	LPS-LMW	43	5143	22	3872	0,17

Figure 44: Gαi2 deletion reduces VSNs responsiveness to sick and healthy LMW urine fractions. A) Analysis of ligand-evoked Ca^{2+} responses in dissociated cells from cG$\alpha_{i2}^{+/-}$ and cG$\alpha_{i2}^{-/-}$ (N = 9 experiments using cells from 6 mice for each genotype) mice after stimulation by veh-urine and LPS-urine. Two-way ANOVA, stimulus: $F_{(1, 32)} = 3.004$, $P = 0.09$; genotype : $F_{(1, 32)} = 5.3$, $P < 0.05$; stimulus x genotype: $F_{(1, 32)} = 0.016$, $P = 0.9$. B) Table showing the number of responsive (Resp.) and non responsive (No resp.) cells for each stimulation. χ^2 tests, all cells cG$\alpha_{i2}^{+/-}$ versus cG$\alpha_{i2}^{-/-}$ $P < 0.05$ for veh-urine and $P < 0.001$ for LPS-urine; monoresponsive cells $P = 0.09 – 0.2$. C) Analysis of ligand-evoked Ca^{2+} responses in dissociated cells from cG$\alpha_{i2}^{+/-}$ and cG$\alpha_{i2}^{-/-}$ mice (N = 6 for both genotypes) after stimulation by veh-urine and LPS-urine. Only cells responding to one stimulus exclusively are considered. Two-way ANOVA, stimulus: $F_{(1, 32)} = 0.3759$, $P = 0.5$; genotype : $F_{(1, 32)} = 3.191$, $P = 0.08$; stimulus x genotype: $F_{(1, 32)} = 0.0168$, $P = 0.9$.

3.4 Discussion

We used a conditional knockout model for Gα_{i2}, which induces a partial VNO function loss (Trouillet et al., 2019, 2021), to determine apical VSNs implication in avoidance behaviors. We choose

two types of aversive cues, owl feces and urine from a sick LPS-treated animal, proposed to be detected by apical V1R-Gα_{i2} VSNs (Boillat et al., 2015; Isogai et al., 2011). At the behavioral, histological, and cellular levels, we provided evidence that Gα_{i2}-expressing VSNs detect owl and LPS-urine olfactory cues that induce avoidance behaviors.

We choose three predators based on their differential activation of the accessory olfactory system: cat, snake, and owl. Cat avoidance is shown to be mediated by Gα_o-expressing VSNs (Pérez-Gómez et al., 2015). Exposure to snake activates both apical and basal VSNs pathways, but the specific requirement of one to induce avoidance is not yet established (Carvalho et al., 2015; Papes et al., 2010). Last, the detection of owl odors is likely to be mediated mainly by apical VSNs (Carvalho et al., 2015; Isogai et al., 2011). This is consistent with our results showing lower neuron activation by owl odors in the VNO and anterior AOB of cG$\alpha_{i2}^{-/-}$ mice (Figure 42). Moreover, cG$\alpha_{i2}^{-/-}$ mice did not display avoidance to owl olfactory cues, which points to a role of apical Gα_{i2}-expressing VSNs mediating owl avoidance (Figure 40). Further, we showed that snake and cat stimuli avoidance did not require Gαi2 signaling, suggesting that either basal Gα_o-expressing VSNs and/or sensory neurons in the MOE mediate these effects. We observed that owl exposure also activated the posterior part of the AOB in both genotypes, likely a consequence of basal VSNs signaling, even if the levels of pS6-positive VSNs were low in cG$\alpha_{i2}^{-/-}$ animals (Figure 42A). To assess the detection of owl olfactory cues by Gα_{i2}-expressing VSNs, we tested responses to owl feces extracts by calcium imaging. As controls, we used extracts from cat fur and snake molt samples. All extracts elicited strong responses in control and mutant VSNs (Figure 43A - C). Consistent with our behavioral results, we did not observe differences in the proportion of responsive cells for cat and snake extracts, but owl extract elicited fewer responses in cG$\alpha_{i2}^{-/-}$ VSNs (Figure 43A - C). Further, this difference was maintained after stimulating with different dilutions of the extract (Figure 43F and G).

To test whether sick conspecific avoidance is mediating by Gα_{i2} signaling, we tested avoidance to LPS-urine. LPS injection is a standard protocol used to induce a general inflammatory state characterized by fever. It has also been used to determine VNO implication in sick conspecific avoidance (Boillat et al., 2015; Bufe et al., 2019). cG$\alpha_{i2}^{-/-}$ mice did not avoid LPS-urine and did not show a preference for veh- or LPS-urine (Figure 41). Thus, these results suggest that sickness-associated cues in LPS-urine are not detected in the absence of Gα_{i2} signaling. Indeed, we observed fewer pS6-positive cells in the VNO of mutant animals (Figure 42A). However, whether this effect is specific to sickness-associated cues cannot be asserted since Gα_{i2} mutation reduces overall VSNs responses to urine (Trouillet et al., 2019). We did not observe significant differences between control and mutant AOB activation, except in the anterior glomerular layer (Figure 42E), where Gα_{i2}-VSNs project. Again, we cannot determine if this difference specifically results from sickness-associated cues or not. Our calcium imaging experiments did not show a specific effect of LPS-urine on VSNs responses (Figure 44). We observed that cG$\alpha_{i2}^{-/-}$ VSNs showed fewer responses to LMW urine fraction than control VSNs (Figure 44A and B), as we showed previously (Trouillet et al., 2019). However,

responses to the two urine sources were not significantly different for both genotypes. We analyzed the number of cells responding exclusively to one urine source (veh or LPS, Figure 44C), but no differences appeared between veh- and LPS-urine. We evaluated the HMW urine fraction responses but did not find differences between genotypes or urine sources (data not shown). One possibility to explain this lack of differences is that LPS treatment may not induce the secretion of specific components in the urine but instead change the proportion of naturally secreted ones. Accordingly, a comparison of volatiles in urine from mice receiving LPS or other treatments inducing sickness shows that the most divergent molecules were naturally excreted (Millet et al., 2018, 2021). Another possibility is that the abundance or concentration of specific LPS-urine compounds mediating avoidance is below the detection threshold of our experimental setup. Further research is needed to understand the chemical nature of the component driving sick conspecific avoidance.

The brain pathway sustaining predator avoidance starts to be understood (Canteras et al., 2015), but sick conspecific avoidance is still elusive (Arakawa et al., 2011). Determining the brain structures activated during owl feces and LPS-urine exposures would help understand avoidance pathways by delineating each stimulus' neural pathways and identifying convergence sites.

Discussion

Nos résultats ont déjà été discutés dans les sections qui leur sont consacrées. Je vais donc fournir une perspective plus large de ce que leur combinaison nous apprend. Je discuterai également de certains résultats spécifiques que nous avons obtenus à la lumière d'une littérature plus récente et proposerai des perspectives pour les questions restantes et les nouvellement apportées.

1 Un modèle n'est qu'un modèle

Il faut garder à l'esprit que les constructions génétiques ne sont pas toujours parfaites. Ainsi, il est important de considérer les pièges potentiels du modèle de souris cGαi2-/-. Trois aspects principaux doivent être examinés : *i*- La mutation est-elle limitée au tissu d'intérêt ? *ii*- Quels sont les effets de la mutation sur le développement des cellules/tissus ? *iii*- Les effets observés sont-ils uniquement dus à la mutation ?

Malgré son nom, l'expression de l'OMP n'est pas limitée au système olfactif et a été rapportée dans de nombreuses cellules et tissus non olfactifs, y compris le cerveau (Baker et al., 1989 ; Kang et al., 2015 ; Koo et al., 2005). Cependant, l'expression de l'OMP est limitée à de petits sous-ensembles cellulaires qui ne définissent pas un type cellulaire spécifique ou un noyau cérébral. De même, Gαi2 est largement exprimé (Rudolph et al., 1995). Ainsi, la probabilité de coexpression n'est pas nulle, et nous ne pouvons pas exclure la délétion de Gαi2 en dehors du VNO.

L'une des préoccupations était la MOE. En effet, la MOE participe également à la régulation des comportements sociaux, et modifier sa fonction aurait faussé nos observations. L'ARNm et la protéine Gαi2 sont présents dans la MOE (Barnes et al., 2020 ; Barrios et al., 2014 ; Berghard et Buck, 1996 ; Ibarra-Soria et al., 2014 ; Scholz et al., 2016 ; Wekesa et Anholt, 1999). Nous avons fourni une quantification de l'ARNm du transcrit Gαi2 dans la MOE et, contrairement au VNO, nous n'avons pas trouvé de réduction significative de l'expression du gène *Gnai2* dans la MOE. Nous avons également montré que les souris cGαi2-/- ont une anatomie de la MOE intacte, ne sont pas anosmiques aux odeurs alimentaires et discriminent encore les odeurs sociales dans un test d'habituation-déshabituation. Dans l'ensemble, cela suggère que Gαi2 n'est pas critique pour la fonction des OSN. La coexpression de l'OMP et de Gαi2 est décrite dans le GG (Brechbühl et al., 2008 ; Fleischer et al., 2006), mais l'expression de Gαi2 y est controversée (Barrios et al., 2014). Nous n'avons pas étudié la coexpression potentielle de l'OMP et de Gαi2 dans le cerveau. L'expression la plus robuste de l'OMP cérébrale se trouve dans le MPOA et le PVN. Gαi2 est également exprimé dans le PVN, où il a été récemment associé à l'équilibre du sodium et à l'hypertension (Carmichael et al., 2020). Le PVN a de nombreuses fonctions et contient des sous-populations neuronales distinctes qui les contrôlent. Les neurones de l'OMP-PVN n'ont pas été caractérisés, et on ne sait pas s'ils chevauchent avec Gαi2.

Nous avons observé une modification du ratio des VSNs apical/basal et une augmentation de l'ARNm de Gαo après une qPCR du VNO entier. Cependant, nous n'avons pas trouvé de différences

dans le nombre total de cellules composant le VNE (données non présentées). Cela indique donc que l'équilibre entre les VSN apicales et basales est modifié. Un nombre accru de VSN basaux pourrait avoir des conséquences comportementales qui seront discutées plus loin dans le manuscrit. Les processus par lesquels les VSN immatures se différencient en lignées apicales ou basales ne sont pas clairement établis (Katreddi et Forni, 2021). Cependant, l'expression de l'OMP intervient après l'expression de Gαi2/Gαo (Enomoto et al., 2011), ce qui suggère que la mutation de Gαi2 dépendante de l'OMP-Cre ne peut pas modifier le choix du lignage des VSNs. L'expression de Gαi2 pourrait être nécessaire à la survie des VSNs apicaux, comme Gαo l'est pour les VSNs basaux (Chamero et al., 2011 ; Tanaka et al., 1999). Une autre possibilité provient de la coexpression de Gαo et Gαi2 dans les VSN en maturation déjà engagés dans le lignage des VSN apicaux (Enomoto et al., 2011). On ignore si l'expression de l'OMP (et par conséquent la délétion de Gαi2 dépendante de Cre) se produit lorsque les deux protéines Gα sont encore présentes. L'étude de la neurogenèse des VSNs chez les souris cGαi2-/- pourrait donner des indications intéressantes sur la décision et le maintien du lignage cellulaire.

2 L'utilisation de deux systèmes voméronasaux chez les mammifères

La coexistence de V1Rs et V2Rs dans le VNO des mammifères est limitée à certaines espèces (Silva et Antunes, 2017). Il existe deux modèles principaux, le VNO à V1R seul et le VNO à V1R/V2R (avec peut-être quelques exceptions, voir Schneider et al., 2012). Chez la souris, certains ont suggéré que les V2R peuvent encoder des informations générales sur l'identité, notamment le sexe, tandis que les V1R peuvent encoder des détails sur le statut de l'émetteur du ligand (Isogai et al., 2011). Il a été proposé que la perte des gènes V2R chez de nombreuses espèces puisse être associée à l'émergence de dimorphismes sexuels morphologiques (par exemple, la taille du corps, la couleur de la fourrure, les cornes) (Suárez et al., 2011). L'évaluation du sexe par des indices non-voméronasaux pourrait avoir induit un relâchement de la pression sélective sur les gènes V2R, conduisant finalement à leur disparition chez de nombreuses espèces. Une autre hypothèse concernant le maintien/disparition des V2R est l'utilisation ou non de protéines et de peptides comme phéromones intraspécifiques. Les V1R et les V2R appartiennent à deux classes différentes de GPCR. Les V2R ont une longue extrémité C-terminale extracellulaire qui leur permet de se lier à de grosses molécules, comme les peptides et les protéines, tandis que les V1R se lient à de petites molécules volatiles présentant un certain degré d'hydrophobie. Les gènes V2Rs se sont largement développés chez les vertébrés non mammaliens aquatiques et semi-aquatiques (Tirindelli, 2021). La communication dans l'eau implique des substances sémiochimiques solubles, et plusieurs phéromones de type protéines et peptides ont été décrits chez ces espèces (Wyatt, 2014). Un autre exemple provient de l'analyse de l'expression des MUPs chez les mammifères. Les gènes MUPs se sont développés chez les espèces exprimant des V2Rs, alors que

presque aucun gène MUPs n'est présent chez les espèces exprimant uniquement des V1Rs, comme la majorité des animaux d'élevage (Archunan et al., 2014 ; Chamero et al., 2007).

La pertinence biologique du maintien d'une ou deux voies voméronasales reste à élucider. Nos résultats sur Gαi2 chez la souris, combinés à ceux obtenus sur Gαo (Chamero et al., 2011 ; Oboti et al., 2014 ; Pérez-Gómez et al., 2015), pourraient néanmoins contribuer à clarifier cette question en apportant quelques éléments de réponse. Premièrement, les mâles et les femelles déficients pour Gαo ou Gαi2 discriminent les signaux provenant des deux sexes. Deuxièmement, l'ablation des voies Gαo ou Gαi2 inhibe spécifiquement la reconnaissance d'un type de prédateur chacun, le chat et le hibou, respectivement. Ainsi, il semble peu probable que les indices d'identité dépendent uniquement des V2R, du moins pas dans une vision aussi simpliste. L'action des composants volatils résulte généralement de leur mélange, tandis que les phéromones peptidiques et protéiques peuvent transmettre un message très spécifique en raison de leur séquence unique d'acides aminés, ce qui entraîne une coévolution directe de la paire ligand-récepteur (Wyatt, 2014). Les espèces qui ont maintenu les V2R peuvent en effet utiliser les phéromones peptidiques et protéiques comme médiateurs d'informations éthologiquement définies. Par exemple, le déclenchement de la réponse de lordose chez les souris dépend des V2R (Oboti et al., 2014), tandis que le mélange de volatiles détecté par les V1R renforce la réponse (nos présents résultats). Cependant, chez les espèces n'exprimant que des V1Rs, comme les chèvres, l'absence de V2Rs n'empêche pas les signaux olfactifs dépendants du sexe de déclencher des réponses comportementales ou physiologiques qui sont V2R-dépendantes chez d'autres espèces (Ohara et al., 2014).

3 Une voie de signalisation, deux sexes, de nombreux effets

Une caractéristique frappante de ces résultats est le dimorphisme sexuel du rôle de signalisation voméronasale de Gαi2. La plupart des comportements que nous avons évalués sont régulés de manière différentielle par la signalisation Gαi2 chez les mâles et les femelles (Figure 45). De plus, les VSNs Gαi2 semblent avoir un rôle actif dans la stimulation des comportements innés chez les femelles, alors que chez les mâles, la résultante comportementale est plutôt inhibitrice. Cela n'est pas complètement surprenant si l'on considère que les comportements sociosexuels reposent sur des structures cérébrales sexuellement dimorphiques et sont étroitement modulés par les stéroïdes sexuels circulants (Baum et Bakker, 2013).

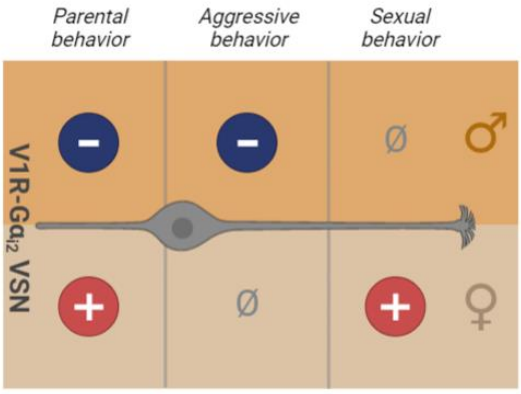

Figure 45 : Contrôle sexuellement dimorphe des comportements sociosexuels par les VSNs exprimant Gαi2. Ø : aucun effet ; ⊖ : inhibition ; ⊕ : activation.

3.1 Contrôle voméronasal dépendant de l'expérience sur les comportements sexuels

Nous avons déjà mentionné et décrit le comportement de monte atypique des animaux Trpc2-/- (voir section 2.1.3 de l'introduction). Les souris cGαo-/- ne présentent pas un tel comportement (Chamero et al., 2011 ; Oboti et al., 2014), ni les animaux cGαi2-/-, comme montré ici. Deux hypothèses sont envisageables. Premièrement, les VSN Gαo et Gαi2 peuvent coopérer, chacun étant suffisant pour conduire la réponse comportementale appropriée. Deuxièmement, les animaux Trcp2-/- présentent des niveaux élevés de testostérone circulants (Kimchi et al., 2007 ; Stowers et al., 2002), un phénomène qui pourrait expliquer le comportement (Martel et Baum, 2009). Cependant, le comportement sexuel des femelles Trpc2-/- a été testé sous des niveaux hormonaux standardisés (Fraser et Shah, 2014), ce qui a réduit la proportion de femelles montantes. Ainsi, cela remet en question la théorie de Martel et Baum comme seule cause du comportement de monte des femelles (Martel et Baum, 2009). Cependant, elle n'exclut pas un potentiel effet organisateur de la testostérone au cours du développement embryonnaire et néonatal. Une solution serait de créer un modèle de souris Trpc2-/- inductible dans le temps afin de restreindre la mutation à l'âge adulte. Ensuite, nous pourrions tester les comportements des mâles et des femelles à l'âge adulte dans un environnement hormonal standardisé pour voir si le comportement de monte sans discrimination est toujours exprimé. Si c'est le cas, cela signifierait que, effectivement, la signalisation voméronasale détermine la préférence sexuelle.

Gαo et Gαi2 coopèrent pour induire la réceptivité sexuelle chez les femelles. Les femelles cGαo-/- présentent des comportements de lordose réduits déjà lorsqu'elles sont naïves (Oboti et al., 2014). Cet effet pourrait être dû à un manque d'activation des neurones AVPV-Kisspeptin, qui sont nécessaires à l'expression de la lordose (Hellier et al., 2018). Les femelles cGαi2-/- présentent des niveaux de lordose intermédiaires, qui sont probablement causés par le manque d'activation des neurones AVPV-négatifs pour la Kisspeptine. Les neurones TH seraient des candidats potentiels. En effet, la signalisation dopaminergique est connue pour son rôle de médiateur dans le renforcement des

comportements sexuels (Paredes, 2009), et les neurones AVPV-TH ont récemment été associés à la motivation sexuelle chez le mâle (Zhang et al., 2021). Déterminer si l'ablation sélective des neurones AVPV-TH chez les femelles sexuellement expérimentées a un impact sur l'expression du comportement de lordose pourrait aider à élucider ce point. Il reste également à déterminer si l'activation de cette population neuronale dépend de la signalisation voméronasale Gαi2 (Figure 46).

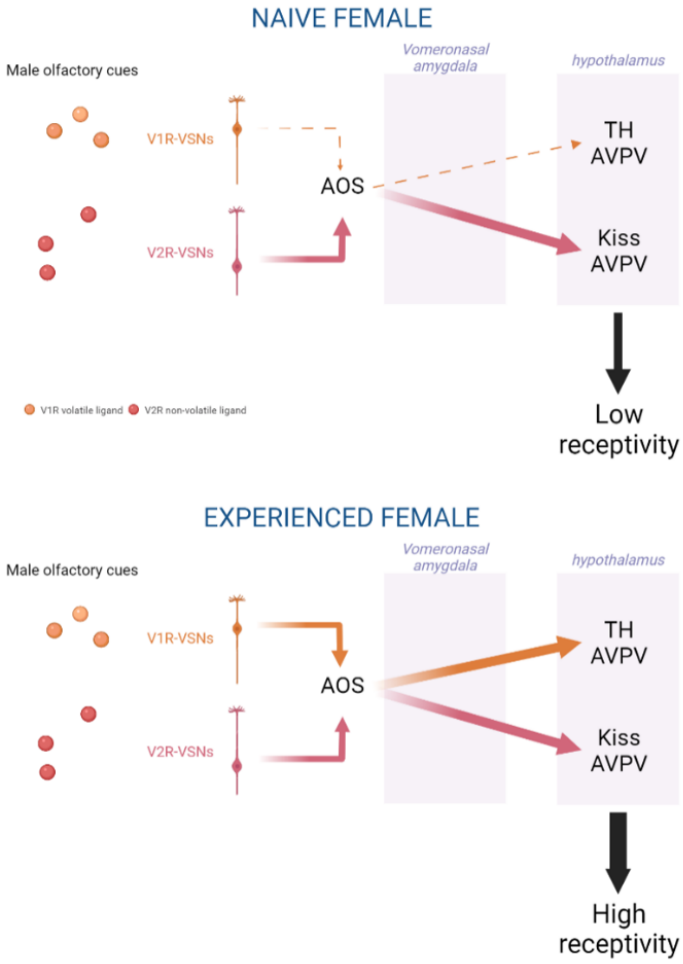

Figure 46 : Modèle proposé du contrôle voméronasal de la réceptivité sexuelle féminine. Chez les femelles naïves, la signalisation Gαo induit l'activation des neurones AVPV-Kisspeptin, ce qui déclenche la lordose. Chez les femelles expérimentées, l'augmentation de la réceptivité sexuelle est due à l'activation des neurones AVPV-TH par la signalisation Gαi2. Ce schéma est créé dans BioRender.com

Chez les mâles, nous n'avons pas observé de différences de comportement sexuel des mâles naïfs. Del Punta et ses collègues ont constaté qu'une délétion du cluster V1Rs réduit le comportement sexuel des mâles après trois tests (Del Punta et al., 2002). L'expérience sexuelle chez les mâles produit des réarrangements de l'ultrastructure du MPOA (Jean et al., 2017). Cela peut modifier la valeur de la signalisation voméronasale Gαi2 dans la régulation du comportement sexuel mâle, comme nous l'avons observé chez les femelles. Cependant, nos expériences peuvent ne pas avoir été assez longues pour observer cet effet. Par conséquent, nous ne pouvons pas exclure la participation de la signalisation voméronasale Gαi2 dans le comportement sexuel des mâles expérimentés.

Haga et ses collègues ont établi un lien entre deux classes de V1Rs et les comportements de monte des mâles (Haga-Yamanaka et al., 2014). Ils ont montré que V1Re9 et V1re12 détectent les signaux olfactifs induits par l'œstrus dans l'urine des femelles, et que ces composés stimulent la monte des

mâles. De façon intéressante, Zhang et ses collègues ont montré que la stimulation des neurones TH-AVPV peut stimuler l'accouplement vers une femelle non réceptive en diestrus (Zhang etal., 2021). Ils n'ont pas vérifié l'origine de la stimulation des neurones TH-AVPV, mais compte tenu de l'importance des signaux olfactifs, nous pouvons émettre l'hypothèse que le système olfactif peut fournir un tel stimulus. On ne sait pas si les composés mis en évidence par Haga et ses collègues peuvent favoriser la monte des mâles par l'intermédiaire des neurones TH-AVPV. Néanmoins, les neurones AVPV-TH sont sexuellement dimorphiques (Simerly et al., 1985). Par conséquent, cette différence sexuelle peut permettre l'intégration de signaux olfactifs de sexe opposé dans la préférence sexuelle et le renforcement du comportement sexuel envers un congénère de sexe opposé. Des recherches supplémentaires sont nécessaires pour clarifier ce point.

3.2 Régulation contextuelle des comportements agressifs

L'un des comportements les plus intrigants que nous avons observé est le comportement agressif intense des souris mâles cGαi2-/- envers les intrus mâles, qu'ils soient castrés ou non. En utilisant le test du tube, une méthode de mesure de la dominance territoriale par le biais d'interactions dyadiques, il a également été montré que les mâles cGαi2-/- sont plus susceptibles de gagner une compétition sociale (Pallé et al., 2020). Les analyses de l'activation cérébrale après une interaction mâle-mâle ont montré une activation accrue dans l'amygdale voméronasale des mâles mutants. Ce résultat était particulièrement contre-intuitif puisque, en supprimant les entrées voméronasales, on pourrait s'attendre à une diminution de l'activation des voies cérébrales en aval. Une explication pourrait venir du rapport modifié entre les VSN basaux et apicaaux que nous avons observé. Les Gαo-VSN basaux sont nécessaires pour détecter les composés des fractions urinaires HMW et LMW qui déclenchent l'agression (Chamero et al., 2007, 2011). Une quantité accrue de VSNs basaux exprimant Gαo pourrait conduire à une suractivation globale de l'amygdale voméronasale et, par conséquent, à une augmentation du comportement agressif. Cependant, cette hypothèse n'est pas bien adaptée si l'on considère plusieurs aspects de nos résultats et de la littérature existante. Premièrement, nous avons observé une activation accrue du BNST, dont on sait qu'il est activée par l'AOB antérieur, le site de projection des VSN exprimant Gαi2 (Mohedano-Moriano et al., 2007). Deuxièmement, nous avons observé une activation accrue des neurones de la MeApd exprimant l'AR. Ces cellules expriment généralement l'enzyme aromatase (Stanić et al., 2014), or, les neurones Aro-MeApd reçoivent aussi principalement des projections de l'AOB antérieur (Billing et al., 2020). Ainsi, notre observation ne peut pas être entièrement attribuée à une augmentation des entrées provenant des VSN exprimant Gαo, même si nous ne pouvons pas écarter les connexions indirectes. Plusieurs hypothèses peuvent expliquer le phénotype des mâles cGαi2-/-. Premièrement, il a été démontré que, dans l'AOB antérieur, des synapses dendrodendritiques inhibitrices sont nécessaires pour façonner les réponses des cellules mitrales aux signaux olfactifs spécifiques aux mâles (Hendrickson et al., 2008). De plus, la stimulation olfactive avec la fraction d'urine HMW provoque l'activation de l'AOB antérieur (Papes et al., 2010),

soit en raison de la connexion des cellules mitrales antérieures avec les glomérules postérieurs (Yonekura et Yokoi, 2008), soit en raison de la communication entre les deux parties de l'AOB. Ainsi, nous pouvons émettre l'hypothèse que l'absence de signalisation Gαi2 modifie l'activité du réseau de cellules mitrales, conduisant finalement à une activation accrue des voies cérébrales en aval et à un comportement agressif. Deuxièmement, il existe des voies cérébrales dédiées à l'inhibition de l'agressivité. Par exemple, le modèle de rage septale dans lequel une lésion du septum latéral induit une agressivité excessive chez les rats (Albert et Chew, 1980) et les souris (Wong et al., 2016). Ainsi, la signalisation Gαi2 pourrait véhiculer des signaux nécessaires à l'activation de ces voies inhibitrices. Nous avons effectivement analysé l'activation dans le septum latéral des mâles cGαi2-/- après une agression entre mâles. De manière surprenante, nous y avons trouvé un nombre plus élevé de cellules activées. Cependant, le septum latéral est une structure hétérogène avec des subdivisions projetant vers différentes zones du cerveau par le biais de populations cellulaires spécifiques (Risold et Swanson, 1997). Une analyse de l'identité moléculaire des cellules activées pourrait révéler des différences spécifiques dans la population de cellules régulant les comportements agressifs.

Les souris mâles n'attaquent pas, ou peu, les intrus mâles castrés (Mugford et Nowell, 1970), pourtant les mâles cGαi2-/- le font toujours. Les niveaux urinaires de MUP et de volatiles favorisant l'agression, tels que la 3,4-déhydro-exo-brevicomine, diminuent après la castration (Hastie et al., 1979 ; Schwende et al., 1986). Cela ne soutient pas l'idée que l'agressivité accrue des mâles cGαi2-/- résulte de la suractivation des VSN Gαo/V2R. Cependant, nous ne savons pas si les mâles castrés produisent des composés spécifiques à leur condition dans leur urine ou d'autres fluides corporels. La répression de l'agression envers les animaux castrés pourrait ne pas résulter uniquement de l'absence de phéromones favorisant l'agression, mais également de la sécrétion de signaux inhibiteurs (détectés par les V1R). Des phéromones inhibitrices ont déjà été décrites, comme le peptide ESP22, qui inhibe le comportement sexuel des mâles.

Nous n'avons pas observé de modification de l'agression maternelle chez les femelles, et nous avons observé une réduction de l'infanticide chez les mâles vierges. Cette régulation différentielle de trois comportements éthologiquement proches ouvre un nouveau cadre pour décrypter la régulation fine de l'agression en fonction d'éléments contextuels.

3.3 La transition vers la parentalité

3.3.1 Gαi2 et le passage à la paternité

L'infanticide par les mâles adultes est étroitement régulé par son environnement social. L'accouplement et la cohabitation avec des femelles gestantes inhibent progressivement ce comportement jusqu'à le faire disparaître complètement au profit de comportements parentaux autour de la naissance (Vom Saal, 1985 ; Tachikawa et al., 2013). Puis, l'isolement social du mâle après le sevrage de la portée restaure l'expression de l'infanticide (Vom Saal, 1985). Dans la nature, cette

dynamique semble parfaitement adaptée aux besoins du mâle, favorisant l'infanticide pour restaurer l'ovulation chez la femelle allaitante et promouvant les soins uniquement aux petits porteurs du patrimoine génétique du mâle. Les mécanismes neuronaux qui font passer le comportement de l'infanticide à parental et vice versa ne sont pas bien caractérisés. Deux questions principales se posent : quels sont les signaux chimiques pertinents dérivés des petits, et quels sont les changements au niveau de la perception et du traitement sensoriels pendant la transition ?

Nos résultats montrent l'implication de la signalisation voméronasale Gαi2 dans l'expression de l'infanticide par les mâles vierges. Par conséquent, les chimiosignaux pertinents sont très probablement de petits composés. La signature chimique des petits varie jusqu'au sevrage (Lacalle-Bergeron et al., 2021), et certains petits composés organiques néonataux spécifiques pourraient soutenir des comportements dirigés vers les petits, y compris l'infanticide. On sait déjà que le durène, en particulier, est détecté par les VSN (Sam et al., 2001). On ignore actuellement si les VSN exprimant Gαi2 détectent le durène et si cela est suffisant pour induire l'infanticide. Une autre étude a mis en évidence deux paires de ligand peptidique/V2Rs régulant l'infanticide (Isogai et al., 2018). L'invalidation génétique de ces récepteurs réduit l'infanticide mais n'augmente pas les comportements parentaux. De plus, l'agressivité envers les autres mâles est également impactée dans ce modèle, et les ligands identifiés sont probablement sécrétés par les mères plutôt que par les petits. Ainsi, il est probable que cette étude identifie de nouvelles phéromones modulant l'agressivité masculine en général.

Les signaux olfactifs des petits stimulent également les comportements parentaux. Les substances volatiles identifiées chez les petits pourraient être pro-parentales ou pro-infanticides, peut-être en fonction de l'organe sensoriel qui les détecte. En effet, certains ligands peuvent activer à la fois les VSN et les OSN (Leinders-Zufall et al., 2000 ; Sam et al., 2001). Une hypothèse est que le VNO est réduit au silence lorsque les mâles ont besoin d'être parentaux. En effet, la cohabitation avec une femelle enceinte réduit l'activation du VNO après l'exposition des petits, ce qui suggère que la sensibilité des VSNs est réprimée (Nakahara et al., 2020 ; Tachikawa et al., 2013). Le mécanisme modifiant la fonction des VSNs n'est pas élucidé. L'environnement hormonal est un puissant modulateur de la fonction des VSN (Dey et al., 2015 ; Eckstein et al., 2020), et l'injection périphérique d'ocytocine réduit l'activation des VNO après l'exposition à des petits (Nakahara et al., 2020). De façon intéressante, il a été rapporté que les niveaux d'ocytocine varient pendant la cohabitation avec une femelle enceinte chez la souris de Californie mâle, une espèce monogame chez laquelle les mâles font preuve d'infanticide (Gubernick et al., 1995). Les niveaux d'ocytocine chez les mâles atteignent un pic après l'accouplement et diminuent progressivement avant la parturition pour rester faibles jusqu'au sevrage. On ne sait pas si une telle variation se produit chez les souris de laboratoire.

Nous apportons la preuve que la signalisation voméronasale Gαi2 réprime les comportements parentaux chez les mâles vierges. Une forte activation des neurones GABA-MeApd est nécessaire pour l'expression de l'infanticide, tandis qu'une faible activation conduit au comportement parental (Chen et

al., 2019). Les mâles vierges parentaux cGαi2-/- ont moins de cellules cFos-positives dans la MeApd et plus dans la MPOA que les témoins. Ainsi, nous pouvons spéculer que la forte activation des neurones GABA-MeApd par la signalisation voméronasale Gαi2 peut activer les circuits neuronaux pertinents pour l'agression et inhiber ceux dédiés aux comportements parentaux. En l'absence de signalisation Gαi2, la MPOA n'est pas réprimée, et les animaux présentent un comportement parental. De même, chez les animaux parentaux, les VSN peuvent être réduits au silence, la MPOA n'est pas inhibée et les signaux olfactifs des petits favorisent le comportement parental (Figure 47).

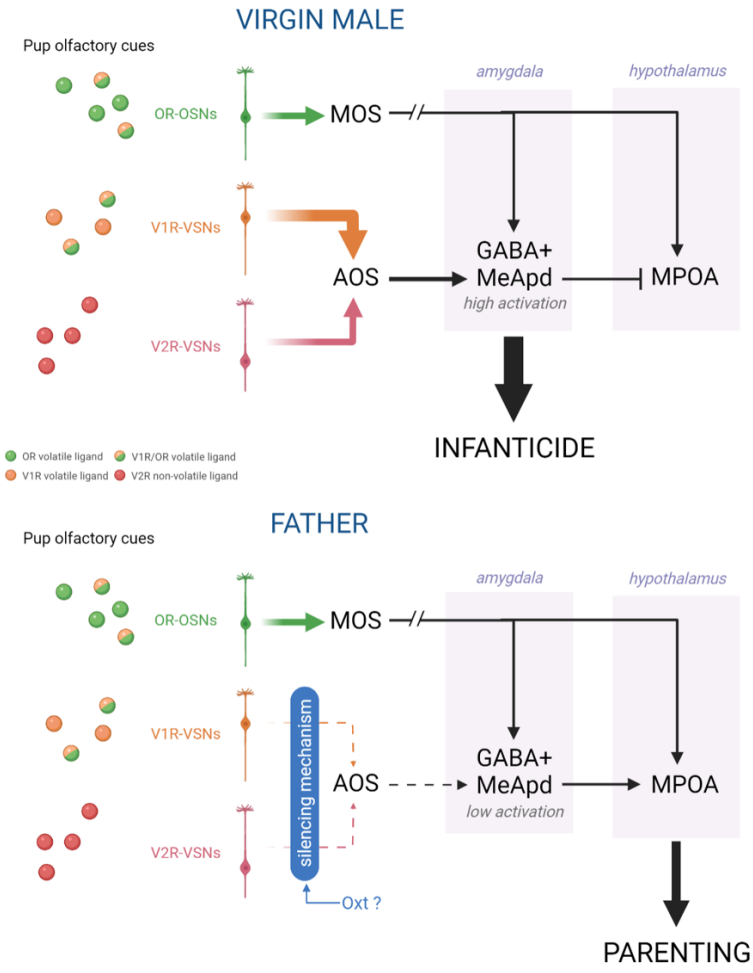

Figure 47 : Modèle proposé pour la transition entre les comportements infanticide et paternel chez la souris mâle. Chez les mâles vierges, la détection des signaux olfactifs des petits par les OSNs et les VSNs conduit à une forte activation des neurones GABA-MeApd, déclenchant l'infanticide et réprimant la parentalité par inhibition du MPOA. Chez le père, l'extinction de la signalisation des VSNs diminue l'activation du GABA-MeApd qui ne peut pas inhiber suffisamment le MPOA, ce qui entraîne l'expression des comportements parentaux. Ce schéma est créé dans BioRender.com.

3.3.1 Gαi2 et le passage à la maternité

L'infanticide est un comportement typiquement masculin et est rarement exprimé par les femelles vierges qui sont spontanément maternelles. De manière intéressante, l'activation des neurones GABA-MeApd ne déclenche pas d'agression envers un petit chez les femelles, quelle que soit

l'intensité de la stimulation (Chen et al., 2019). Cela suggère que les cerveaux des mâles et des femelles sont câblés pour répondre différemment aux signaux sensoriels des petits. L'infanticide est dépendant de la testostérone chez les mâles puisque la castration réduit la proportion de mâles agressifs envers les petits (Gandelman et Vom Saal, 1975). Cependant, il semble que la dépendance à la testostérone circulante puisse être modulée par les niveaux néonataux de cette hormone, ce qui suggère l'existence d'un mécanisme d'organisation (Gandelman et Vom Saal, 1975). Cependant, aucun consensus clair n'a émergé pour savoir si et comment les stéroïdes sexuels contrôlent le comportement infanticide (Keller et al., 2010 ; Matsumoto et al., 2003 ; Ogawa et al., 1998). Il existe une autre hypothèse intéressante pour expliquer les différences entre les sexes en matière d'infanticide. Les souris de laboratoire ont été sélectionnées par reproduction sur plusieurs générations, réduisant progressivement la proportion de femelles infanticides. L'analyse de l'infanticide chez les souris femelles sauvages a révélé que ce type de comportement est génétiquement codé et naturellement exprimé (Chalfin et al., 2014). Une possibilité est que la consanguinité des souris de laboratoire ait sélectionné des femelles non infanticides. Pour vérifier cette hypothèse, nous pourrions tester si l'inhibition de la signalisation voméronasale Gαi2 chez les femelles sauvages réduit l'infanticide, puis comparer l'activation cérébrale chez les mâles et les femelles sauvages, et voir si la voie cérébrale activée chez les animaux infanticides varie.

Nous avons observé que la délétion de Gαi2 n'améliore pas le comportement parental chez les femelles, comme elle le fait chez les mâles, mais retarde la récupération des petits. Ceci plaide également pour un câblage différentiel des cerveaux mâles et femelles concernant le traitement des signaux olfactifs des petits. Nous n'avons pas observé de différence qui pourrait expliquer comment, dans le cerveau, les signaux olfactifs des petits médiés par Gαi2 favorisent la récupération, probablement en raison des limites de l'utilisation de cFos comme rapporteur d'activité. De nouvelles techniques, telles que l'imagerie calcique *in vivo,* permettraient de mieux visualiser les zones du cerveau associées à la récupération des petits. L'inactivation des neurones ERα-MPOA entrave l'approche et la récupération des petits, et inversement, l'activation de ces neurones déclenche la récupération (Fang et al., 2018 ; Wei et al., 2018). De manière intéressante, l'activité des neurones ERα-MPOA semble plus élevée chez les femelles que chez les mâles au début de la récupération (Wei et al., 2018). Cette activation accrue pourrait résulter des entrées voméronasales Gαi2.

Chez les femelles allaitantes, l'absence de signalisation voméronasale Gαi2 n'altère pas le comportement de récupération des petits. Cet effet pourrait être dû à une extinction de la signalisation voméronasale chez les mères, comme chez les pères (Nakahara et al., 2020 ; Tachikawa et al., 2013). Cependant, les femelles en fin de grossesse montrent une forte activation de leur VNO après exposition des petits (Navarro-Moreno et al., 2020), et les mères Trpc2-/- et cGαo-/- montrent un comportement intact de récupération des petits. L'activité du MPOA est nécessaire pour le comportement maternel, agissant probablement comme un hub central pour les entrées sensorielles (Okabe et al., 2013). En effet, la maternité renforce l'activité cérébrale causée par les entrées olfactives pilotées par le MOS et

auditives (Marlin et al., 2015 ; Navarro-Moreno et al., 2020), et l'activité des neurones ERα-MPOA pendant l'approche et la récupération est plus élevée chez les femelles allaitantes que chez les vierges (Fang et al., 2018). En l'absence de signalisation voméronasale Gαi2 chez les mères, d'autres modalités sensorielles semblent être suffisantes pour soutenir les comportements maternels.

Conclusion Générale

Au terme de ce travail, nous pouvons tirer six conclusions principales sur le rôle de la signalisation voméronasale Gαi2 dans le contrôle des comportements sociosexuels innés :

i- Gαi2 est un composant critique de la voie de signalisation des VSNs apicaux médiant l'activation des V1Rs ;

ii- Les VSN exprimant Gαi2 sont les médiateurs de la détection des signaux olfactifs des nouveau-nés, des mâles et des oiseaux de proies ;

iii- La signalisation voméronasale Gαi2 n'est pas nécessaire pour la préférence au sexe opposé ;

iv- La signalisation voméronasale Gαi2 est dispensable pour le comportement sexuel mâle mais participe à la réceptivité sexuelle chez la femelle ;

v- La signalisation voméronasale Gαi2 est nécessaire pour l'agression dirigée vers les petits, module l'agression entre mâles, mais est dispensable pour l'agression maternelle ;

vi- La signalisation voméronasale Gαi2 stimule le comportement parental chez les femelles tout en le réprimant chez les mâles ;

vii- La signalisation voméronasale Gαi2 participe à l'évitement des prédateurs et des congénères malades.

La plupart de ces observations ouvrent de nouveaux questionnements, mais c'est là toute la beauté de la science. Pièce par pièce, nous déchiffrons comment notre cerveau intègre de multiples informations pour produire la meilleure réponse à chaque instant. Maintenant que nous possédons des informations provenant des voies des VSNs apicaux et basaux, nous pouvons concevoir des modèles d'intégration du contrôle olfactif des comportements innés chez la souris (Figure 48). De tels modèles sont pertinents si nous voulons transposer à l'homme les immenses connaissances sur les comportements sociaux des rongeurs. En tant qu'êtres humains, nous ne percevons pas notre environnement comme les rongeurs. Nous ne sommes pas macrosmatiques, mais les systèmes limbiques et hypothalamiques des mammifères, où convergent les signaux sensoriels, est hautement conservé. L'étude des comportements à médiation olfactive est à la pointe de la recherche psychiatrique actuelle. Ainsi, la compréhension de la neurobiologie de la perception sensorielle et des comportements sociaux est cruciale pour comprendre et développer de nouvelles thérapies concernant de nombreuses pathologies, telles que le syndrome autistique, la dépression post-partum ou les phobies innées (par exemple, l'acrophobie).

Une compréhension complète de la neurobiologie des comportements innés est également nécessaire pour comprendre comment les humains interagissent avec les autres espèces sauvages qui nous entourent et, plus important encore, comment nous devons traiter les espèces qui dépendent de nous, les animaux domestiques. Les animaux de compagnie, les animaux de ferme, les animaux de travail et les animaux de laboratoire sont sous notre responsabilité. Une meilleure compréhension de leur physiologie pourrait leur éviter des souffrances inutiles pour répondre à nos besoins.

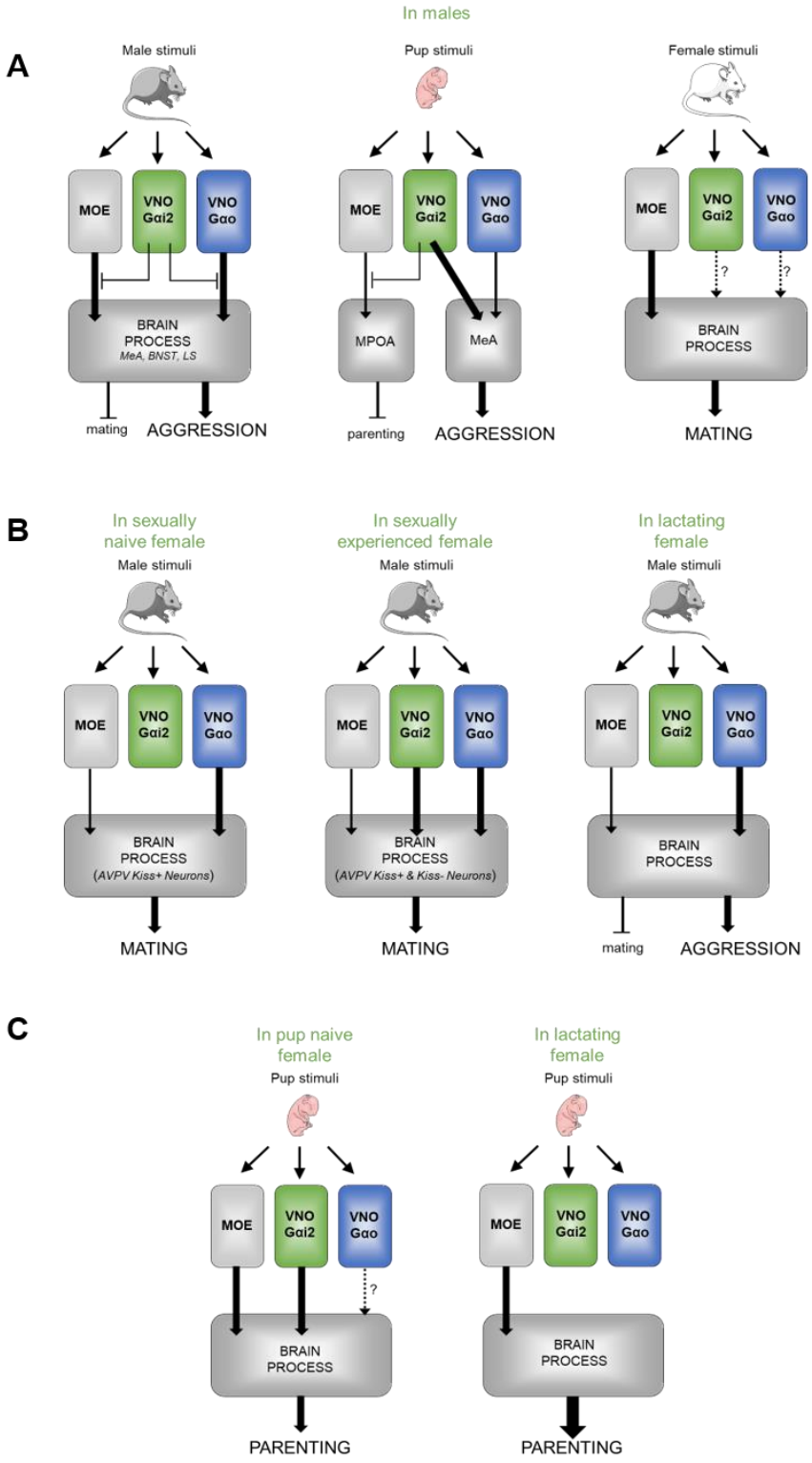

Figure 48 : Modèle proposé du contrôle olfactif des comportements innés. A) Chez les mâles, la MeA et les Gαo-VSN sont nécessaires pour déclencher l'agression envers les autres mâles, tandis que les Gαi2-VSN régulent l'intensité de la réponse, probablement en modulant les signaux provenant des autres entrées sensorielles. Lors de la confrontation avec un nouveau-né étranger, la signalisation Gαi2 et Gαo active la MeA pour déclencher l'agression, tandis que la signalisation Gαi2 réprime les entrées de la MeA, inhibant ainsi la MPOA et le parentage. Enfin, les signaux olfactifs femelles détectés par le MOE semblent suffisants pour conduire l'accouplement. B) Chez les femelles, la perception des signaux olfactifs masculins dépend de l'expérience sociale. Chez les femelles naïves, la MOE et les Gαo-VSNs permettent les comportements sexuels, alors qu'une fois expérimentés, les trois composants participent. Chez les femelles en lactation, la signification des signaux olfactifs des mâles change et déclenche l'agression par le biais des signaux MOE et Gαo. C) La médiation des signaux olfactifs des chiots sur les comportements parentaux des femelles dépend également de l'expérience sociale. Chez les femelles naïves, la MOE et les Gαi2-VSNs coopèrent, alors que la MOE seule est suffisante chez les femelles en lactation..

Bibliographie

Abellán-Álvaro, M., Ayala, G., Barneo-Muñoz, M., Martínez-García, F., Agustín-Pavón, C., and Lanuza, E. (2021). Motherhood-induced gene expression in the mouse medial amygdala: Changes induced by pregnancy and lactation but not by pup stimuli. FASEB J. *35*, 1–21.

Albert, D.J., and Chew, G.L. (1980). The septal forebrain and the inhibitory modulation of attack and defense in the rat. A review. Behav. Neural Biol. *30*, 357–388.

Alsina-Llanes, M., and Olazábal, D.E. (2020). Prefrontal cortex is associated with the rapid onset of parental behavior in inexperienced adult mice (C57BL/6). Behav. Brain Res. *385*, 112556.

Amjad, A., Hernandez-Clavijo, A., Pifferi, S., Maurya, D.K., Boccaccio, A., Franzot, J., Rock, J., and Menini, A. (2015). Conditional knockout of TMEM16A/anoctamin1 abolishes the calciumactivated chloride current in mouse vomeronasal sensory neurons. J. Gen. Physiol. *145*, 285–301.

Amoore, J.E. (1963). Stereochemical Theory of Olfaction. Nature *198*, 271–272.

Apps, P., Mmualefe, L., and McNutt, J.W. (2012). Identification of Volatiles from the Secretions and Excretions of African Wild Dogs (Lycaon pictus). J. Chem. Ecol. *38*, 1450–1461.

Arakawa, H., Cruz, S., and Deak, T. (2011). From models to mechanisms: Odorant communication as a key determinant of social behavior in rodents during illness-associated states. Neurosci. Biobehav. Rev. *35*, 1916–1928.

Archunan, G., Rajanarayanan, S., and Karthikeyan, K. (2014). Cattle Pheromones. In Neurobiology of Chemical Communication, C. Mucignat-Caretta, ed. (CRC Press/Taylor & Francis), pp. 461–487.

Autry, A.E., Wu, Z., Kapoor, V., Kohl, J., Bambah-Mukku, D., Rubinstein, N.D., Marin-Rodriguez, B., Carta, I., Sedwick, V., Tang, M., et al. (2021). Urocortin-3 neurons in the mouse perifornical area promote infant-directed neglect and aggression. Elife *10*.

Bakalyar, H.A., and Reed, R.R. (1990). Identification of a specialized adenylyl cyclase that may mediate odorant detection. Science (80-.). *250*, 1403–1406.

Baker, H., Grillo, M., and Margolis, F.L. (1989). Biochemical and immunocytochemical charaterization of olfactory marker protein in the rodent central nervous system. J. Comp. Neurol. *285*, 246–261.

Baker, H., Cummings, D.M., Munger, S.D., Margolis, J.W., Franzen, L., Reed, R.R., and Margolis, F.L. (1999). Targeted deletion of a cyclic nucleotide-gated channel subunit (OCNC1): Biochemical and morphological consequences in adult mice. J. Neurosci. *19*, 9313–9321.

Bakker, J. (2018). The Sexual Differentiation of the Human Brain: Role of Sex Hormones Versus Sex Chromosomes. In Brain Imaging in Behavioral Neuroscience, pp. 45–67.

Bakker, J., Pierman, S., and González-Martínez, D. (2010). Effects of aromatase mutation (ArKO) on the sexual differentiation of kisspeptin neuronal numbers and their activation by same versus opposite sex urinary pheromones. Horm. Behav. *57*, 390–395.

Ball, G.F., and Balthazart, J. (2008). How useful is the appetitive and consummatory distinction for our understanding of the neuroendocrine control of sexual behavior? Horm. Behav. *53*, 307–311.

Bankhead, P., Loughrey, M.B., Fernández, J.A., Dombrowski, Y., McArt, D.G., Dunne, P.D., McQuaid, S., Gray, R.T., Murray, L.J., Coleman, H.G., et al. (2017). QuPath: Open source software for digital pathology image analysis. Sci. Rep. *7*, 1–7.

Barnes, I.H.A., Ibarra-Soria, X., Fitzgerald, S., Gonzalez, J.M., Davidson, C., Hardy, M.P., Manthravadi, D., Van Gerven, L., Jorissen, M., Zeng, Z., et al. (2020). Expert curation of the human and mouse olfactory receptor gene repertoires identifies conserved coding regions split across two exons. BMC Genomics *21*, 1–15.

Barrios, A.W., Núñez, G., Quinteiro, P.S., and Salazar, I. (2014). Anatomy, histochemistry, and immunohistochemistry of the olfactory subsystems in mice. Front. Neuroanat. *8*, 1–10.

Baum, M.J., and Bakker, J. (2013). Roles of sex and gonadal steroids in mammalian pheromonal communication. Front. Neuroendocrinol. *34*, 268–284.

Baum, M.J., and Kelliher, K.R. (2009). Complementary Roles of the Main and Accessory Olfactory Systems in Mammalian Mate Recognition. Annu. Rev. Physiol. *71*, 141–160.

Bayless, D.W., Yang, T., Mason, M.M., Susanto, A.A.T., Lobdell, A., and Shah, N.M. (2019). Limbic Neurons Shape Sex Recognition and Social Behavior in Sexually Naive Males. Cell *0*, 1–16.

Bean, N.J. (1982). Olfactory and vomeronasal mediation of ultrasonic vocalizations in male mice. Physiol. Behav. *28*, 31–37.

Bean, N.J., and Wysocki, C.J. (1989). Vomeronasal organ removal and female mouse aggression: The role of experience. Physiol. Behav. *45*, 875–882.

Belluscio, L., Gold, G.H., Nemes, A., and Axel, R. (1998). Mice deficient in G(olf) are anosmic. Neuron *20*, 69–81.

Belluscio, L., Koentges, G., Axel, R., and Dulac, C. (1999). A map of pheromone receptor activation in the mammalian brain. Cell *97*, 209–220.

Belluscio, L., Lodovichi, C., Feinstein, P., Mombaerts, P., and Katz, L.C. (2002). Odorant receptors instruct functional circuitry in the mouse olfactory bulb. Nature *419*, 296–300.

Ben-Shaul, Y., Katz, L.C., Mooney, R., and Dulac, C. (2010). In vivo vomeronasal stimulation reveals sensory encoding of conspecific and allospecific cues by the mouse accessory olfactory bulb. Proc. Natl. Acad. Sci. U. S. A. *107*, 5172–5177.

Bentefour, Y., and Bakker, J. (2021). Neuropharmacology Kisspeptin signaling and nNOS neurons in the VMHvl modulate lordosis behavior but not mate preference in female mice. Neuropharmacology *198*, 108762.

Beny-Shefer, Y., Zilkha, N., Lavi-Avnon, Y., Bezalel, N., Rogachev, I., Brandis, A., Dayan, M., and Kimchi, T. (2017). Nucleus Accumbens Dopamine Signaling Regulates Sexual Preference for Females in Male Mice. Cell Rep. *21*, 3079–3088.

Beny, Y., and Kimchi, T. (2016). Conditioned odor aversion induces social anxiety towards females in wild-type and TrpC2 knockout male mice. Genes, Brain Behav. *15*, 722–732.

Bergan, J.F., Ben-Shaul, Y., and Dulac, C. (2014). Sex-specific processing of social cues in the medial amygdala. Elife *3*, e02743.

Berghard, a, and Buck, L.B. (1996). Sensory transduction in vomeronasal neurons: evidence for G alpha o, G alpha i2, and adenylyl cyclase II as major components of a pheromone signaling cascade. J. Neurosci. *16*, 909–918.

Bian, X., Yanagawa, Y., Chen, W.R., and Luo, M. (2008). Cortical-like functional organization of the pheromone-processing circuits in the medial amygdala. J. Neurophysiol. *99*, 77–86.

Billig, G.M., Pál, B., Fidzinski, P., and Jentsch, T.J. (2011). Ca2+-activated Cl- currents are dispensable for olfaction. Nat. Neurosci. *14*, 763–769.

Billing, A., Henrique Correia, M., Kelly, D.A., Li, G.-L., and Bergan, J.F. (2020). Synaptic Connections of Aromatase Circuits in the Medial Amygdala Are Sex Specific. Eneuro *7*, ENEURO.0489-19.2020.

Bleymehl, K., Pérez-Gómez, A., Omura, M., Moreno-Pérez, A., Macías, D., Bai, Z., Johnson, R.S., Leinders-Zufall, T., Zufall, F., and Mombaerts, P. (2016). A Sensor for Low Environmental Oxygen in the Mouse Main Olfactory Epithelium. Neuron *92*, 1196–1203.

Boehm, T., and Zufall, F. (2006). MHC peptides and the sensory evaluation of genotype. Trends Neurosci. *29*, 100–107.

Boillat, M., Challet, L., Rossier, D., Kan, C., Carleton, A., and Rodriguez, I. (2015). The vomeronasal

system mediates sick conspecific avoidance. Curr. Biol. *25*, 251–255.

Boillat, M., Carleton, A., and Rodriguez, I. (2021). From immune to olfactory expression: neofunctionalization of formyl peptide receptors. Cell Tissue Res. *383*, 387–393.

Boisseau, S., Kunert-Keil, C., Lucke, S., and Bouron, A. (2009). Heterogeneous distribution of TRPC proteins in the embryonic cortex. Histochem. Cell Biol. *131*, 355–363.

Bönigk, W., Bradley, J., Müller, F., Sesti, F., Boekhoff, I., Ronnett, G. V., Kaupp, U.B., and Frings, S. (1999). The Native Rat Olfactory Cyclic Nucleotide-Gated Channel Is Composed of Three Distinct Subunits. J. Neurosci. *19*, 5332–5347.

Bonthuis, P.J., Cox, K.H., Searcy, B.T., Kumar, P., Tobet, S., and Rissman, E.F. (2010). Of mice and rats: Key species variations in the sexual differentiation of brain and behavior. Front. Neuroendocrinol. *31*, 341–358.

Bonthuis, P.J., Patteson, J.K., and Rissman, E.F. (2011). Acquisition of Sexual Receptivity: Roles of Chromatin Acetylation, Estrogen Receptor-α, and Ovarian Hormones. Endocrinology *152*, 3172–3181.

Borowsky, B., Adham, N., Jones, K.A., Raddatz, R., Artymyshyn, R., Ogozalek, K.L., Durkin, M.M., Lakhlani, P.P., Bonini, J.A., Pathirana, S., et al. (2001). Trace amines: Identification of a family of mammalian G protein-coupled receptors. Proc. Natl. Acad. Sci. U. S. A. *98*, 8966–8971.

Boschat, C., Pélofi, C., Randin, O., Roppolo, D., Lüscher, C., Broillet, M.C., and Rodriguez, I. (2002). Pheromone detection mediated by a V1r vomeronasal receptor. Nat. Neurosci. *5*, 1261–1262.

Bradley, J., Li, J., Davidson, N., Lester, H.A., and Zinn, K. (1994). Heteromeric olfactory cyclic nucleotide-gated channels: a subunit that confers increased sensitivity to cAMP. Proc. Natl. Acad. Sci. *91*, 8890–8894.

Brann, J.H., and Firestein, S.J. (2014). A lifetime of neurogenesis in the olfactory system. Front. Neurosci. *8*, 1–11.

Brechbühl, J., Klaey, M., and Broillet, M.C. (2008). Grueneberg ganglion cells mediate alarm pheromone detection in mice. Science (80-.). *321*, 1092–1095.

Brechbühl, J., Moine, F., Klaey, M., Nenniger-Tosato, M., Hurni, N., Sporkert, F., Giroud, C., and Broillet, M.C. (2013). Mouse alarm pheromone shares structural similarity with predator scents. Proc. Natl. Acad. Sci. U. S. A. *110*, 4762–4767.

Brennan, P.A., and Zufall, F. (2006). Pheromonal communication in vertebrates. Nature *444*, 308–315.

Brunert, D., and Rothermel, M. (2021). Extrinsic neuromodulation in the rodent olfactory bulb. Cell Tissue Res. *383*, 507–524.

Brunet, L.J., Gold, G.H., and Ngai, J. (1996). General anosmia caused by a targeted disruption of the mouse olfactory cyclic nucleotide-gated cation channel. Neuron *17*, 681–693.

Buck, L., and Axel, R. (1991). A novel multigene family may encode odorant receptors: A molecular basis for odor recognition. Cell *65*, 175–187.

Bufe, B., and Zufall, F. (2016). The sensing of bacteria: Emerging principles for the detection of signal sequences by formyl peptide receptors. Biomol. Concepts *7*, 205–214.

Bufe, B., Schumann, T., and Zufall, F. (2012). Formyl peptide receptors from immune and vomeronasal system exhibit distinct agonist properties. J. Biol. Chem. *287*, 33644–33655.

Bufe, B., Schumann, T., Kappl, R., Bogeski, I., Kummerow, C., Podgórska, M., Smola, S., Hoth, M., and Zufall, F. (2015). Recognition of bacterial signal peptides by mammalian formyl peptide receptors: A new mechanism for sensing pathogens. J. Biol. Chem. *290*, 7369–7387.

Bufe, B., Teuchert, Y., Schmid, A., Pyrski, M., Pérez-Gómez, A., Eisenbeis, J., Timm, T., Ishii, T., Lochnit, G., Bischoff, M., et al. (2019). Bacterial MgrB peptide activates chemoreceptor Fpr3 in mouse accessory olfactory system and drives avoidance behaviour. Nat. Commun. *10*, 4889.

Bumbalo, R., Lieber, M., Lehmann, E., Wolf, I., Breer, H., and Fleischer, J. (2017). Attenuated Chemosensory Responsiveness of the Grueneberg Ganglion in Mouse Pups at Warm Temperatures. Neuroscience *366*, 149–161.

Bunzow, J.R., Sonders, M.S., Arttamangkul, S., Harrison, L.M., Zhang, G., Quigley, D.I., Darland, T., Suchland, K.L., Pasumamula, S., Kennedy, J.L., et al. (2001). Amphetamine, 3,4-methylenedioxymethamphetamine, lysergic acid diethylamide, and metabolites of the catecholamine neurotransmitters are agonists of a rat trace amine receptor. Mol. Pharmacol. *60*, 1181–1188.

Burger, B. V., Visser, R., Moses, A., and Le Roux, M. (2006). Elemental sulfur identified in urine of cheetah, Acinonyx jubatus. J. Chem. Ecol. *32*, 1347–1352.

Canteras, N.S., Simerly, R.B., and Swanson, L.W. (1992). Connections of the posterior nucleus of the amygdala. J. Comp. Neurol. *324*, 143–179.

Canteras, N.S., Simerly, R.B., and Swanson, L.W. (1995). Organization of projections from the medial nucleus of the amygdala: A PHAL study in the rat. J. Comp. Neurol. *360*, 213–245.

Canteras, N.S., Pavesi, E., and Carobrez, A.P. (2015). Olfactory instruction for fear: Neural system analysis. Front. Neurosci. *9*, 1–10.

Carmichael, C.Y., Kuwabara, J.T., Pascale, C.L., Moreira, J.D., Mahne, S.E., Kapusta, D.R., Rosene, D.L., Williams, J.S., Thomas Cunningham, J., and Wainford, R.D. (2020). Hypothalamic paraventricular nucleus Gαi2 (guanine nucleotide-binding protein alpha inhibiting activity polypeptide 2) protein-mediated neural control of the kidney and the salt sensitivity of blood pressure. Hypertension *2*, 1002–1011.

Carvalho, V.M. de A., Nakahara, T.S., Souza, M.A. de A., Cardozo, L.M., Trintinalia, G.Z., Pissinato, L.G., Venancio, J.O., Stowers, L., and Papes, F. (2020). Representation of Olfactory Information in Organized Active Neural Ensembles in the Hypothalamus. Cell Rep. *32*, 108061.

Carvalho, V.M.A., Nakahara, T.S., Cardozo, L.M., Souza, M.A.A., Camargo, A.P.C.B.R., Trintinalia, G.Z., Ferraz, E., and Papes, F. (2015). Lack of spatial segregation in the representation of pheromones and kairomones in the mouse medial amygdala. Front. Neurosci. *9*, 1–19.

Chalfin, L., Dayan, M., Levy, D.R., Austad, S.N., Miller, R.A., Iraqi, F.A., Dulac, C., and Kimchi, T. (2014). Mapping ecologically relevant social behaviours by gene knockout in wild mice. Nat. Commun. *5*, 1–10.

Chamero, P., Marton, T.F., Logan, D.W., Flanagan, K., Cruz, J.R., Saghatelian, A., Cravatt, B.F., and Stowers, L. (2007). Identification of protein pheromones that promote aggressive behaviour. Nature *450*, 899–902.

Chamero, P., Katsoulidou, V., Hendrix, P., Bufe, B., Roberts, R., Matsunami, H., Abramowitz, J., Birnbaumer, L., Zufall, F., and Leinders-Zufall, T. (2011). G protein G o is essential for vomeronasal function and aggressive behavior in mice. Proc. Natl. Acad. Sci. *108*, 12898–12903.

Chamero, P., Leinders-Zufall, T., and Zufall, F. (2012). From genes to social communication: molecular sensing by the vomeronasal organ. Trends Neurosci. *35*, 597–606.

Chamero, P., Weiss, J., Alonso, M.T., Rodríguez-Prados, M., Hisatsune, C., Mikoshiba, K., Leinders-Zufall, T., and Zufall, F. (2017). Type 3 inositol 1,4,5-trisphosphate receptor is dispensable for sensory activation of the mammalian vomeronasal organ. Sci. Rep. *7*, 10260.

Chao, Y., Fleischer, J., and Yang, R. (2018). Guanylyl cyclase-G is an alarm pheromone receptor in mice. EMBO J. *37*, 39–49.

Cheetham, S.A., Thom, M.D., Jury, F., Ollier, W.E.R., Beynon, R.J., and Hurst, J.L. (2007). The Genetic Basis of Individual-Recognition Signals in the Mouse. Curr. Biol. *17*, 1771–1777.

Chen, P., and Hong, W. (2018). Neural Circuit Mechanisms of Social Behavior. Neuron *98*, 16–30.

Chen, P.B., Hu, R.K., Wu, Y.E., Pan, L., Huang, S., Micevych, P.E., and Hong, W. (2019). Sexually

Dimorphic Control of Parenting Behavior by the Medial Amygdala. Cell *176*, 1206-1221.e18.

Choleris, E., Little, S.R., Mong, J.A., Puram, S. V., Langer, R., and Pfaff, D.W. (2007). Microparticle-based delivery of oxytocin receptor antisense DNA in the medial amygdala blocks social recognition in female mice. Proc. Natl. Acad. Sci. U. S. A. *104*, 4670–4675.

Clancy, N., and Nobles, P. (1984). Sexual and Aggression Involvement of the Vomeronasal in Male System ' Mice : J. Neurosci.

Croy, I., Nordin, S., and Hummel, T. (2014). Olfactory disorders and quality of life-an updated review. Chem. Senses *39*, 185–194.

Cuschieri, A., and Bannister, L.H. (1975). The development of the olfactory mucosa in the mouse: electron microscopy. J. Anat. *119*, 471–498.

Cygnar, K.D., and Zhao, H. (2009). Phosphodiesterase 1C is dispensable for rapid response termination of olfactory sensory neurons. Nat. Neurosci. *12*, 454–462.

Desjardins, C., Maruniak, J.A., and Bronson, F.H. (1973). Social rank in house mice: Differentiation revealed by ultraviolet visualization of urinary marking patterns. Science (80-.). *182*, 939–941.

Dewan, A., Pacifico, R., Zhan, R., Rinberg, D., and Bozza, T. (2013). Non-redundant coding of aversive odours in the main olfactory pathway. Nature *497*, 486–489.

Dewan, A., Cichy, A., Zhang, J., Miguel, K., Feinstein, P., Rinberg, D., and Bozza, T. (2018). Single olfactory receptors set odor detection thresholds. Nat. Commun. *9*, 1–12.

Dey, S., and Matsunami, H. (2011). Calreticulin chaperones regulate functional expression of vomeronasal type 2 pheromone receptors. Proc. Natl. Acad. Sci. U. S. A. *108*, 16651–16656.

Dey, S., Chamero, P., Pru, J.K., Chien, M.S., Ibarra-Soria, X., Spencer, K.R., Logan, D.W., Matsunami, H., Peluso, J.J., and Stowers, L. (2015). Cyclic regulation of sensory perception by a female hormone alters behavior. Cell *161*, 1334–1344.

Dhallan, R.S., Yau, K.-W., Schrader, K.A., and Reed, R.R. (1990). Primary structure and functional expression of a cyclic nucleotide-activated channel from olfactory neurons. Nature *347*, 184–187.

Dibattista, M., Al Koborssy, D., Genovese, F., and Reisert, J. (2021). The functional relevance of olfactory marker protein in the vertebrate olfactory system: a never-ending story. Cell Tissue Res. *383*, 409–427.

DiBenedictis, B.T., Ingraham, K.L., Baum, M.J., and Cherry, J.A. (2012). Disruption of urinary odor preference and lordosis behavior in female mice given lesions of the medial amygdala. Physiol. Behav. *105*, 554–559.

Dietschi, Q., Assens, A., Challet, L., Carleton, A., and Rodriguez, I. (2013). Convergence of FPR-rs3-expressing neurons in the mouse accessory olfactory bulb. Mol. Cell. Neurosci. *56*, 140–147.

Dietschi, Q., Tuberosa, J., Rösingh, L., Loichot, G., Ruedi, M., Carleton, A., and Rodriguez, I. (2017). Evolution of immune chemoreceptors into sensors of the outside world. Proc. Natl. Acad. Sci. U. S. A. *114*, 7397–7402.

Døving, K.B., and Trotier, D. (1998). Structure and function of the vomeronasal organ. J. Exp. Biol. *201*, 2913–2925.

Doyle, W.I., Dinser, J.A., Cansler, H.L., Zhang, X., Dinh, D.D., Browder, N.S., Riddington, I.M., and Meeks, J.P. (2016). Faecal bile acids are natural ligands of the mouse accessory olfactory system. Nat. Commun. *7*.

Dulac, C., and Axel, R. (1995). A novel family of genes encoding putative pheromone receptors in mammals. Cell *83*, 195–206.

Eckstein, E., Pyrski, M., Pinto, S., Freichel, M., Vennekens, R., and Zufall, F. (2020). Cyclic regulation of Trpm4 expression in female vomeronasal neurons driven by ovarian sex hormones. Mol. Cell.

Neurosci. *105*, 103495.

Egnor, S.E.R., and Seagraves, K.M. (2016). The contribution of ultrasonic vocalizations to mouse courtship. Curr. Opin. Neurobiol. *38*, 1–5.

Elg, S., Marmigere, F., Mattsson, J.P., and Ernfors, P. (2007). Cellular subtype distribution and developmental regulation of TRPC channel members in the mouse dorsal root ganglion. J. Comp. Neurol. *503*, 35–46.

Ennis, M., and Holy, T.E. (2015). Anatomy and Neurobiology of the Main and Accessory Olfactory Bulbs. In Handbook of Olfaction and Gustation: Third Edition, R. Doty, ed. (John Wiley & Sons, Inc.), pp. 157–182.

Enomoto, T., Ohmoto, M., Iwata, T., Uno, A., Saitou, M., Yamaguchi, T., Kominami, R., Matsumoto, I., and Hirota, J. (2011). Bcl11b/Ctip2 controls the differentiation of vomeronasal sensory neurons in mice. J. Neurosci. *31*, 10159–10173.

Fang, Y.Y., Yamaguchi, T., Song, S.C., Tritsch, N.X., and Lin, D. (2018). A Hypothalamic Midbrain Pathway Essential for Driving Maternal Behaviors. Neuron *98*, 192-207.e10.

Ferguson, J.N., Aldag, J.M., Insel, T.R., and Young, L.J. (2001). Oxytocin in the medial amygdala is essential for social recognition in the mouse. J. Neurosci. *21*, 8278–8285.

Ferrero, D.M., and Liberles, S.D. (2010). The secret codes of mammalian scents. Wiley Interdiscip. Rev. Syst. Biol. Med. *2*, 23–33.

Ferrero, D.M., Lemon, J.K., Fluegge, D., Pashkovski, S.L., Korzan, W.J., Datta, S.R., Spehr, M., Fendt, M., and Liberles, S.D. (2011). Detection and avoidance of a carnivore odor by prey. Proc. Natl. Acad. Sci. U. S. A. *108*, 11235–11240.

Ferrero, D.M., Moeller, L.M., Osakada, T., Horio, N., Li, Q., Roy, D.S., Cichy, A., Spehr, M., Touhara, K., and Liberles, S.D. (2013). A juvenile mouse pheromone inhibits sexual behaviour through the vomeronasal system. Nature *502*, 368–371.

Fleischer, J. (2021). The Grueneberg ganglion: signal transduction and coding in an olfactory and thermosensory organ involved in the detection of alarm pheromones and predator-secreted kairomones. Cell Tissue Res. *383*, 535–548.

Fleischer, J., Hass, N., Schwarzenbacher, K., Besser, S., and Breer, H. (2006). A novel population of neuronal cells expressing the olfactory marker protein (OMP) in the anterior/dorsal region of the nasal cavity. Histochem. Cell Biol. *125*, 337–349.

Fraser, E.J., and Shah, N.M. (2014). Complex chemosensory control of female reproductive behaviors. PLoS One *9*, 5–10.

Fülle, H.J., Vassar, R., Foster, D.C., Yang, R.B., Axel, R., and Garbers, D.L. (1995). A receptor guanylyl cyclase expressed specifically in olfactory sensory neurons. Proc. Natl. Acad. Sci. U. S. A. *92*, 3571–3575.

Fuss, S.H., Omura, M., and Mombaerts, P. (2005). The Grueneberg ganglion of the mouse projects axons to glomeruli in the olfactory bulb. Eur. J. Neurosci. *22*, 2649–2654.

Gandelman, R., and Vom Saal, F.S. (1975). Pup-killing in mice: The effects of gonadectomy and testosterone administration. Physiol. Behav. *15*, 647–651.

Gao, J.L., Chen, H., Filie, J.D., Kozak, C.A., and Murphy, P.M. (1998). Differential expansion of the N-formylpeptide receptor gene cluster in human and mouse. Genomics *51*, 270–276.

Gigante, C.M., Dibattista, M., Dong, F.N., Zheng, X., Yue, S., Young, S.G., Reisert, J., Zheng, Y., and Zhao, H. (2017). Lamin B1 is required for mature neuron-specific gene expression during olfactory sensory neuron differentiation. Nat. Commun. *8*, 1–13.

Gilad, Y., Wiebe, V., Przeworski, M., Lancet, D., and Pääbo, S. (2004). Loss of olfactory receptor

genes coincides with the acquisition of full trichromatic vision in primates. PLoS Biol. *2*, 120–125.

Green, W.W., Uytingco, C.R., Ukhanov, K., Kolb, Z., Moretta, J., McIntyre, J.C., and Martens, J.R. (2018). Peripheral gene therapeutic rescue of an olfactory ciliopathy restores sensory input, axonal pathfinding, and odor-guided behavior. J. Neurosci. *38*, 7462–7475.

Grosmaitre, X., Santarelli, L.C., Tan, J., Luo, M., and Ma, M. (2007). Dual functions of mammalian olfactory sensory neurons as odor detectors and mechanical sensors. Nat. Neurosci. *10*, 348–354.

Grüneberg, H. (1973). A ganglion probably belonging to the N. terminalis system in the nasal mucosa of the mouse. Z. Anat. Entwicklungsgesch. *140*, 39–52.

Grus, W.E., Shi, P., Zhang, Y.P., and Zhang, J. (2005). Dramatic variation of the vomeronasal pheromone receptor gene repertoire among five orders of placental and marsupial mammals. Proc. Natl. Acad. Sci. U. S. A. *102*, 5767–5772.

Gubernick, D.J., Winslow, J.T., Jensen, P., Jeanotte, L., and Bowen, J. (1995). Oxytocin Changes in Males over the Reproductive Cycle in the Monogamous, Biparental California Mouse, Peromyscus californicus. Horm. Behav. *29*, 59–73.

Gutiérrez-Castellanos, N., Pardo-Bellver, C., Martínez-García, F., and Lanuza, E. (2014). The vomeronasal cortex - afferent and efferent projections of the posteromedial cortical nucleus of the amygdala in mice. Eur. J. Neurosci. *39*, 141–158.

Haberly, L.B., and Price, J.L. (1977). The axonal projection patterns of the mitral and tufted cells of the olfactory bulb in the rat. Brain Res. *129*, 152–157.

Haga-Yamanaka, S., Ma, L., He, J., Qiu, Q., Lavis, L.D., Looger, L.L., and Yu, C.R. (2014). Integrated action of pheromone signals in promoting courtship behavior in male mice. Elife *3*, e03025.

Haga, S., Hattori, T., Sato, T., Sato, K., Matsuda, S., Kobayakawa, R., Sakano, H., Yoshihara, Y., Kikusui, T., and Touhara, K. (2010). The male mouse pheromone ESP1 enhances female sexual receptive behaviour through a specific vomeronasal receptor. Nature *466*, 118–122.

Hamada, N., Negishi, Y., Mizuno, M., Miya, F., Hattori, A., Okamoto, N., Kato, M., Tsunoda, T., Yamasaki, M., Kanemura, Y., et al. (2017). Role of a heterotrimeric G-protein, Gi2, in the corticogenesis: possible involvement in periventricular nodular heterotopia and intellectual disability. J. Neurochem. *140*, 82–95.

Hasen, N.S., and Gammie, S.C. (2009). Trpc2 gene impacts on maternal aggression, accessory olfactory bulb anatomy and brain activity. Genes, Brain Behav. *8*, 639–649.

Hashikawa, K., Hashikawa, Y., Tremblay, R., Zhang, J., Feng, J.E., Sabol, A., Piper, W.T., Lee, H., Rudy, B., and Lin, D. (2017). Esr1+ cells in the ventromedial hypothalamus control female aggression. Nat. Neurosci. *20*, 1580–1590.

Hashikawa, K., Hashikawa, Y., Lischinsky, J., and Lin, D. (2018). The Neural Mechanisms of Sexually Dimorphic Aggressive Behaviors. Trends Genet. *34*, 755–776.

Hastie, N.D., Held, W.A., and Toole, J.J. (1979). Multiple genes coding for the androgen-regulated major urinary proteins of the mouse. Cell *17*, 449–457.

Hattori, T., Osakada, T., Masaoka, T., Ooyama, R., Horio, N., Mogi, K., Nagasawa, M., Haga-Yamanaka, S., Touhara, K., and Kikusui, T. (2017). Exocrine Gland-Secreting Peptide 1 Is a Key Chemosensory Signal Responsible for the Bruce Effect in Mice. Curr. Biol. *27*, 3197-3201.e3.

He, J., Ma, L., Kim, S., Nakai, J., and Yu, C.R. (2008). Encoding Gender and Individual Information in the Mouse Vomeronasal Organ. Science (80-.). *320*, 535–538.

Hellier, V., Brock, O., Candlish, M., Desroziers, E., Aoki, M., Mayer, C., Piet, R., Herbison, A., Colledge, W.H., Prévot, V., et al. (2018). Female sexual behavior in mice is controlled by kisspeptin neurons. Nat. Commun. *9*, 1–13.

Hendrickson, R.C., Krauthamer, S., Essenberg, J.M., and Holy, T.E. (2008). Inhibition shapes sex selectivity in the mouse accessory olfactory bulb. J. Neurosci. *28*, 12523–12534.

Herrada, G., and Dulac, C. (1997). A novel family of putative pheromone receptors in mammals with a topographically organized and sexually dimorphic distribution. Cell *90*, 763–773.

Holy, T.E. (2000). Responses of Vomeronasal Neurons to Natural Stimuli. Science (80-.). *289*, 1569–1572.

Hong, W., Kim, D.W., and Anderson, D.J. (2014). Antagonistic control of social versus repetitive self-grooming behaviors by separable amygdala neuronal subsets. Cell *158*, 1348–1361.

Hu, J., Zhong, C., Ding, C., Chi, Q., Walz, A., Mombaerts, P., Matsunami, H., and Luo, M. (2007). Detection of Near-Atmospheric Concentrations of CO2 by an Olfactory Subsystem in the Mouse. Science (80-.). *317*, 953–957.

Hull, E.M., and Dominguez, J.M. (2019). Neuroendocrine regulation of male sexual behavior. Compr. Physiol. *9*, 1383–1410.

Hurst, J.L., and Beynon, R.J. (2004). Scent wars: The chemobiology of competitive signalling in mice. BioEssays *26*, 1288–1298.

Hurst, J.L., Robertson, D.H.L., Tolladay, U., and Beynon, R.J. (1998). Proteins in urine scent marks of male house mice extend the longevity of olfactory signals. Anim. Behav. *55*, 1289–1297.

Hurst, J.L., Payne, C.E., Nevison, C.M., Marie, A.D., Humphries, R.E., Robertson, D.H.L., Cavaggioni, A., and Beynon, R.J. (2001). Individual recognition in mice mediated by major urinary proteins. Nature *414*, 631–634.

Ibarra-Soria, X., Levitin, M.O., Saraiva, L.R., and Logan, D.W. (2014). The Olfactory Transcriptomes of Mice. PLoS Genet. *10*.

Imai, T., Suzuki, M., and Sakano, H. (2006). Odorant Receptor-Derived cAMP Signals Direct Axonal Targeting. Science (80-.). *314*, 657–661.

Inbar, T., Davis, R., and Bergan, J.F. (2021). A sex-specific feedback projection from aromatase-expressing neurons in the medial amygdala to the accessory olfactory bulb. J. Comp. Neurol. cne.25236.

Inoue, S., Yang, R., Tantry, A., Tessier-Lavigne, M., Ding, J.B., Shah Correspondence, N.M., Davis, C.-H., Yang, T., Knoedler, J.R., Wei, Y., et al. (2019). Periodic Remodeling in a Neural Circuit Governs Timing of Female Sexual Behavior Article Periodic Remodeling in a Neural Circuit Governs Timing of Female Sexual Behavior. Cell *179*, 1–16.

Ishii, K.K., and Touhara, K. (2019). Neural circuits regulating sexual behaviors via the olfactory system in mice. Neurosci. Res. *140*, 59–76.

Ishii, T., and Mombaerts, P. (2008). Expression of Nonclassical Class I Major Histocompatibility Genes Defines a Tripartite Organization of the Mouse Vomeronasal System. J. Neurosci. *28*, 2332–2341.

Ishii, K.K., Osakada, T., Mori, H., Miyasaka, N., Yoshihara, Y., Miyamichi, K., and Touhara, K. (2017). A Labeled-Line Neural Circuit for Pheromone-Mediated Sexual Behaviors in Mice. Neuron *95*, 123-137.e8.

Ishii, T., Hirota, J., and Mombaerts, P. (2003). Combinatorial coexpression of neural and immune multigene families in mouse vomeronasal sensory neurons. Curr. Biol. *13*, 394–400.

Isogai, Y., Si, S., Pont-Lezica, L., Tan, T., Kapoor, V., Murthy, V.N., and Dulac, C. (2011). Molecular organization of vomeronasal chemoreception. Nature *478*, 241–245.

Isogai, Y., Wu, Z., Love, M.I., Ahn, M.H.-Y., Bambah-Mukku, D., Hua, V., Farrell, K., and Dulac, C. (2018). Multisensory Logic of Infant-Directed Aggression by Males. Cell *175*, 1827-1841.e17.

Jakupovic, J., Kang, N., and Baum, M.J. (2008). Effect of bilateral accessory olfactory bulb lesions on volatile urinary odor discrimination and investigation as well as mating behavior in male mice. Physiol. Behav. *93*, 467–473.

Jean, A., Bonnet, P., Liere, P., Mhaouty-Kodja, S., and Hardin-Pouzet, H. (2017). Revisiting medial preoptic area plasticity induced in male mice by sexual experience. Sci. Rep. *7*, 1–13.

Jia, C., and Halpern, M. (1996). Subclasses of vomeronasal receptor neurons: differential expression of G proteins (Giα2 and Goα) and segregated projections to the accessory olfactory bulb. Brain Res. *719*, 117–128.

Jia, C., and Halpern, M. (1997). Segregated populations of mitral/tufted cells in the accessory olfactory bulb. Neuroreport *8*, 1887–1890.

Johnson, C.S., Hong, W., and Micevych, P.E. (2021). Posterodorsal medial amygdala regulation of female social behavior: GABA vs Glutamate projections. J. Neurosci. JN-RM-1103-21.

Jones, D.T., and Reed, R.R. (1989). G olf : an Olfactory Neuron Specific-G Protein Involved in Odorant Signal Transduction. Science (80-.). *244*, 790–795.

De Jong, T.R., Beiderbeck, D.I., and Neumann, I.D. (2014). Measuring virgin female aggression in the Female Intruder Test (FIT): Effects of oxytocin, estrous cycle, and anxiety. PLoS One *9*.

Juilfs, D.M., Fülle, H.J., Zhao, A.Z., Houslay, M.D., Garbers, D.L., and Beavo, J.A. (1997). A subset of olfactory neurons that selectively express cGMP-stimulated phosphodiesterase (PDE2) and guanylyl cyclase-D define a unique olfactory signal transduction pathway. Proc. Natl. Acad. Sci. U. S. A. *94*, 3388–3395.

Juntti, S.A., Tollkuhn, J., Wu, M. V., Fraser, E.J., Soderborg, T., Tan, S., Honda, S.I., Harada, N., and Shah, N.M. (2010). The androgen receptor governs the execution, but not programming, of male sexual and territorial behaviors. Neuron *66*, 260–272.

Kang, N.N., Kim, H., Jae, Y.G., Lee, N.H., Ku, C.R., Margolis, F., Lee, E.J., Bahk, Y.Y., Kim, M.S., and Koo, J.H. (2015). Olfactory marker protein expression is an indicator of olfactory receptor-associated events in non-olfactory tissues. PLoS One *10*, 1–21.

Karlson, P., and Lüscher, M. (1959). 'Pheromones': a New Term for a Class of Biologically Active Substances. Nature *183*, 55–56.

Katada, S., Hirokawa, T., Oka, Y., Suwa, M., and Touhara, K. (2005). Structural basis for a broad but selective ligand spectrum of a mouse olfactory receptor: Mapping the odorant-binding site. J. Neurosci. *25*, 1806–1815.

Katreddi, R.R., and Forni, P.E. (2021). Mechanisms underlying pre- and postnatal development of the vomeronasal organ. Cell. Mol. Life Sci.

Kaur, A.W., Ackels, T., Kuo, T.H., Cichy, A., Dey, S., Hays, C., Kateri, M., Logan, D.W., Marton, T.F., Spehr, M., et al. (2014). Murine pheromone proteins constitute a context-dependent combinatorial code governing multiple social behaviors. Cell *157*, 676–688.

Kavaliers, M. (1995). Discrimination by female mice between the odours of parasitized and non-parasitized males. Proc. R. Soc. London. *261*, 31–35.

Kavaliers, M., and Choleris, E. (2001). Antipredator responses and defensive behavior: Ecological and ethological approaches for the neurosciences. Neurosci. Biobehav. Rev. *25*, 577–586.

Kavaliers, M., Choleris, E., and Pfaff, D.W. (2005). Genes, odours and the recognition of parasitized individuals by rodents. Trends Parasitol. *21*, 423–429.

Keller, A. (2007). Getting that first scent of life while we're in the womb. Nature *445*, 593–593.

Keller, M., Pierman, S., Douhard, Q., Baum, M.J., and Bakker, J. (2006). The vomeronasal organ is required for the expression of lordosis behaviour, but not sex discrimination in female mice. Eur. J.

Neurosci. *23*, 521–530.

Keller, M., Pawluski, J.L., Brock, O., Douhard, Q., and Bakker, J. (2010). The α-fetoprotein knock-out mouse model suggests that parental behavior is sexually differentiated under the influence of prenatal estradiol. Horm. Behav. *57*, 434–440.

Kelliher, K.R., Spehr, M., Li, X.H., Zufall, F., and Leinders-Zufall, T. (2006). Pheromonal recognition memory induced by TRPC2-independent vomeronasal sensing. Eur. J. Neurosci. *23*, 3385–3390.

Keshavarzi, S., Sullivan, R.K.P., Ianno, D.J., and Sah, P. (2014). Functional Properties and Projections of Neurons in the Medial Amygdala. J. Neurosci. *34*, 8699–8715.

Kim, S., Ma, L., and Yu, C.R. (2011). Requirement of calcium-activated chloride channels in the activation of mouse vomeronasal neurons. Nat. Commun. *2*, 365–367.

Kim, S., Ma, L., Jensen, K.L., Kim, M.M., Bond, C.T., Adelman, J.P., and Yu, C.R. (2012). Paradoxical contribution of SK3 and GIRK channels to the activation of mouse vomeronasal organ. Nat. Neurosci. *15*, 1236–1244.

Kim, S.S., Ma, L., Unruh, J., McKinney, S., and Yu, C.R. (2015). Intracellular chloride concentration of the mouse vomeronasal neuron. BMC Neurosci. *16*, 4–9.

Kimchi, T., Xu, J., and Dulac, C. (2007). A functional circuit underlying male sexual behaviour in the female mouse brain. Nature *448*, 1009–1014.

Kimoto, H., Sato, K., Nodari, F., Haga, S., Holy, T.E., and Touhara, K. (2007). Sex- and Strain-Specific Expression and Vomeronasal Activity of Mouse ESP Family Peptides. Curr. Biol. *17*, 1879–1884.

Kleine, B., Freudenberg, M.A., and Galanos, C. (1985). Excretion of radioactivity in faeces and urine of rats injected with 3H, 14C-lipopolysaccharide. Br. J. Exp. Pathol. *66*, 303–308.

Kobayakawa, K., Kobayakawa, R., Matsumoto, H., Oka, Y., Imai, T., Ikawa, M., Okabe, M., Ikeda, T., Itohara, S., Kikusui, T., et al. (2007). Innate versus learned odour processing in the mouse olfactory bulb. Nature *450*, 503–508.

Kohl, J., Babayan, B.M., Rubinstein, N.D., Autry, A.E., Marin-Rodriguez, B., Kapoor, V., Miyamishi, K., Zweifel, L.S., Luo, L., Uchida, N., et al. (2018). Functional circuit architecture underlying parental behaviour. Nature *556*, 326–331.

Koike, K., Yoo, S.-J., Bleymehl, K., Omura, M., Zapiec, B., Pyrski, M., Blum, T., Khan, M., Bai, Z., Leinders-Zufall, T., et al. (2021). Danger perception and stress response through an olfactory sensor for the bacterial metabolite hydrogen sulfide. Neuron *109*, 2469-2484.e7.

Koo, J.H., Saraswati, M., and Margolis, F.L. (2005). Immunolocalization of Bex protein in the mouse brain and olfactory system. J. Comp. Neurol. *487*, 1–14.

Koos, D.S., and Fraser, S.E. (2005). The Grueneberg ganglion projects to the olfactory bulb. Neuroreport *16*, 1929–1932.

Kuhn, M. (2016). Molecular physiology of membrane guanylyl cyclase receptors. Physiol. Rev. *96*, 751–804.

Kunkhyen, T., McCarthy, E.A., Korzan, W.J., Doctor, D., Han, X., Baum, M.J., and Cherry, J.A. (2017). Optogenetic activation of accessory olfactory bulb input to the forebrain differentially modulates investigation of opposite versus same-sex urinary chemosignals and stimulates mating in male mice. ENeuro *4*, 1–16.

Kurzweil, V.C., Getman, M., Green, E.D., and Lane, R.P. (2009). Dynamic evolution of V1R putative pheromone receptors between Mus musculus and Mus spretus. BMC Genomics *10*, 1–11.

Kwak, J., Grigsby, C.C., Rizki, M.M., Preti, G., Köksal, M., Josue, J., Yamazaki, K., and Beauchamp, G.K. (2012). Differential binding between volatile ligands and major urinary proteins due to genetic variation in mice. Physiol. Behav. *107*, 112–120.

Kwon, J.T., Ryu, C., Lee, H., Sheffield, A., Fan, J., Cho, D.H., Bigler, S., Sullivan, H.A., Choe, H.K., Wickersham, I.R., et al. (2021). An amygdala circuit that suppresses social engagement. Nature *593*, 114–118.

Labov, J.B., and Wysocki, C.J. (1989). Vomeronasal organ and social factors affect urine marking by male mice. Physiol. Behav. *45*, 443–447.

Labov, J.B., Huck, U.W., Elwood, R.W., and Brooks, R.J. (1985). Current Problems in the Study of Infanticidal Behavior of Rodents. Q. Rev. Biol. *60*, 1–20.

Lacalle-Bergeron, L., Goterris-Cerisuelo, R., Portolés, T., Beltran, J., Sancho, J.V., Navarro-Moreno, C., and Martinez-Garcia, F. (2021). Novel sampling strategy for alive animal volatolome extraction combined with GC-MS based untargeted metabolomics: Identifying mouse pup pheromones. Talanta *235*, 122786.

Larsson, M.C., Domingos, A.I., Jones, W.D., Chiappe, M.E., Amrein, H., and Vosshall, L.B. (2004). Or83b encodes a broadly expressed odorant receptor essential for Drosophila olfaction. Neuron *43*, 703–714.

Lau, Y.E., and Cherry, J.A. (2000). Distribution of PDE4A and G(o) alpha immunoreactivity in the accessory olfactory system of the mouse. Neuroreport *11*, 27–32.

Leinders-Zufall, T., Rand, M.N., Shepherd, G.M., Greer, C.A., and Zufall, F. (1997). Calcium entry through cyclic nucleotide-gated channels in individual cilia of olfactory receptor cells: Spatiotemporal dynamics. J. Neurosci. *17*, 4136–4148.

Leinders-Zufall, T., Lane, A.P., Puche, A.C., Ma, W., Novotny, M. V., Shipley, M.T., and Zufall, F. (2000). Ultrasensitive pheromone detection by mammalian vomeronasal neurons. Nature *405*, 792–796.

Leinders-Zufall, T., Brennan, P., Widmayer, P., Chandramani S., P., Maul-Pavicic, A., Jäger, M., Li, X.H., Breer, H., Zufall, F., and Boehm, T. (2004). MHC class I peptides as chemosensory signals in the vomeronasal organ. Science (80-.). *306*, 1033–1037.

Leinders-Zufall, T., Cockerham, R.E., Michalakis, S., Biel, M., Garbers, D.L., Reed, R.R., Zufall, F., and Munger, S.D. (2007). Contribution of the receptor guanylyl cyclase GC-D to chemosensory function in the olfactory epithelium. Proc. Natl. Acad. Sci. U. S. A. *104*, 14507–14512.

Leinders-Zufall, T., Ishii, T., Mombaerts, P., Zufall, F., and Boehm, T. (2009). Structural requirements for the activation of vomeronasal sensory neurons by MHC peptides. Nat. Neurosci. *12*, 1551–1558.

Leinders-Zufall, T., Ishii, T., Chamero, P., Hendrix, P., Oboti, L., Schmid, A., Kircher, S., Pyrski, M., Akiyoshi, S., Khan, M., et al. (2014). A family of nonclassical class I MHC genes contributes to ultrasensitive chemodetection by mouse vomeronasal sensory neurons. J. Neurosci. *34*, 5121–5133.

Leinders-Zufall, T., Storch, U., Bleymehl, K., Mederos y Schnitzler, M., Frank, J.A., Konrad, D.B., Trauner, D., Gudermann, T., and Zufall, F. (2018). PhoDAGs Enable Optical Control of Diacylglycerol-Sensitive Transient Receptor Potential Channels. Cell Chem. Biol. *25*, 215-223.e3.

Lepri, J.J., Wysocki, C.J., and Vandenbergh, J.G. (1985). Mouse vomeronasal organ: Effects on chemosignal production and maternal behavior. Physiol. Behav. *35*, 809–814.

Lévai, O., Feistel, T., Breer, H., and Strotmann, J. (2006). Cells in the vomeronasal organ express odorant receptors but project to the accessory olfactory bulb. J. Comp. Neurol. *498*, 476–490.

Leypold, B.G., Yu, C.R., Leinders-Zufall, T., Kim, M.M., Zufall, F., and Axel, R. (2002). Altered sexual and social behaviors in trp2 mutant mice. Proc. Natl. Acad. Sci. *99*, 6376–6381.

Li, Q., and Liberles, S.D. (2015). Aversion and attraction through olfaction. Curr. Biol. *25*, R120–R129.

Li, F., Ponissery-Saidu, S., Yee, K.K., Wang, H., Chen, M.L., Iguchi, N., Zhang, G., Jiang, P., Reisert, J., and Huang, L. (2013). Heterotrimeric G protein subunit Gγ13 is critical to olfaction. J. Neurosci.

33, 7975–7984.

Li, J., Ishii, T., Feinstein, P., and Mombaerts, P. (2004). Odorant receptor gene choice is reset by nuclear transfer from mouse olfactory sensory neurons. Nature *428*, 393–399.

Li, Y., Mathis, A., Grewe, B.F., Osterhout, J.A., Ahanonu, B., Schnitzer, M.J., Murthy, V.N., and Dulac, C. (2017). Neuronal Representation of Social Information in the Medial Amygdala of Awake Behaving Mice. Cell *171*, 1176-1190.e17.

Liberles, S.D., and Buck, L.B. (2006). A second class of chemosensory receptors in the olfactory epithelium. Nature *442*, 645–650.

Liberles, S.D., Horowitz, L.F., Kuang, D., Contos, J.J., Wilson, K.L., Siltberg-Liberles, J., Liberles, D.A., and Buck, L.B. (2009). Formyl peptide receptors are candidate chemosensory receptors in the vomeronasal organ. Proc. Natl. Acad. Sci. U. S. A. *106*, 9842–9847.

Liman, E.R., and Buck, L.B. (1994). A second subunit of the olfactory cyclic nucleotide-gated channel confers high sensitivity to cAMP. Neuron *13*, 611–621.

Liman, E.R., Corey, D.P., and Dulac, C. (1999). TRP2: A candidate transduction channel for mammalian pheromone sensory signaling. Proc. Natl. Acad. Sci. *96*, 5791–5796.

Lin, D., Boyle, M.P., Dollar, P., Lee, H., Lein, E.S., Perona, P., and Anderson, D.J. (2011). Functional identification of an aggression locus in the mouse hypothalamus. Nature *470*, 221–227.

Lin, W., Arellano, J., Slotnick, B., and Restrepo, D. (2004). Odors Detected Mice Deficient in Cyclic Nucleotide-Gated Channel Subunit A2 Stimulate the Main Olfactory System. J. Neurosci. *24*, 3703–3710.

Van der Linden, C., Jakob, S., Gupta, P., Dulac, C., and Santoro, S.W. (2018). Sex separation induces differences in the olfactory sensory receptor repertoires of male and female mice. Nat. Commun. *9*, 5081.

Liu, Q., Li, S., Lu, C., Yu, C.R., and Huang, L. (2018). G protein γ subunit Gγ13 is essential for olfactory function and aggressive behavior in mice. Neuroreport *29*, 1333–1339.

Liu, Q., Zhang, Y., Wang, P., Guo, X., Wu, Y., Zhang, J.-X.X., and Huang, L. (2019). Two Preputial Gland-Secreted Pheromones Evoke Sexually Dimorphic Neural Pathways in the Mouse Vomeronasal System. Front. Cell. Neurosci. *13*, 1–21.

Lloyd-Thomas, A., and Keverne, E.B. (1982). Role of the brain and accessory olfactory system in the block to pregnancy in mice. Neuroscience *7*, 907–913.

Loconto, J., Papes, F., Chang, E., Stowers, L., Jones, E.P., Takada, T., Kumánovics, A., Lindahl, K.F., and Dulac, C. (2003). Functional expression of murine V2R pheromone receptors involves selective association with the M10 and M1 families of MHC class Ib molecules. Cell *112*, 607–618.

Logan, D.W., Marton, T.F., and Stowers, L. (2008). Species Specificity in Major Urinary Proteins by Parallel Evolution. PLoS One *3*, e3280.

Lowe, G., and Gold, G.H. (1993). Nonlinear amplification by calcium-dependent chloride channels in olfactory receptor cells. Nature *366*, 283–286.

Lucas, P., Ukhanov, K., Leinders-Zufall, T., and Zufall, F. (2003). A diacylglycerol-gated cation channel in vomeronasal neuron dendrites is impaired in TRPC2 mutant mice: Mechanism of pheromone transduction. Neuron *40*, 551–561.

Luo, M. (2003). Encoding Pheromonal Signals in the Accessory Olfactory Bulb of Behaving Mice. Science (80-.). *299*, 1196–1201.

Ma, M., Grosmaitre, X., Iwema, C.L., Baker, H., Greer, C.A., and Shepherd, G.M. (2003). Olfactory signal transduction in the mouse septal organ. J. Neurosci. *23*, 317–324.

Malnic, B., Hirono, J., Sato, T., and Buck, L.B. (1999). Combinatorial receptor codes for odors. Cell

96, 713–723.

Mamasuew, K., Breer, H., and Fleischer, J. (2008). Grueneberg ganglion neurons respond to cool ambient temperatures. Eur. J. Neurosci. *28*, 1775–1785.

Mamasuew, K., Hofmann, N., Kretzschmann, V., Biel, M., Yang, R.B., Breer, H., and Fleischer, J. (2011). Chemo- and thermosensory responsiveness of Grueneberg ganglion neurons relies on cyclic guanosine monophosphate signaling elements. NeuroSignals *19*, 198–209.

Manning, A., and McGill, T.E. (1974). Neonatal androgen and sexual behavior in female house mice. Horm. Behav. *5*, 19–31.

Marlin, B.J., Mitre, M., D'Amour, J.A., Chao, M. V., and Froemke, R.C. (2015). Oxytocin enables maternal behaviour by balancing cortical inhibition. Nature *520*, 499–504.

Martel, K.L., and Baum, M.J. (2009). Adult Testosterone Treatment But Not Surgical Disruption of Vomeronasal Function Augments Male-Typical Sexual Behavior in Female Mice. J. Neurosci. *29*, 7658–7666.

Martín-Sánchez, A., McLean, L., Beynon, R.J., Hurst, J.L., Ayala, G., Lanuza, E., and Martínez-Garcia, F. (2015). From sexual attraction to maternal aggression: when pheromones change their behavioural significance. Horm. Behav. *68*, 65–76.

Martínez-Ricós, J., Agustín-Pavón, C., Lanuza, E., and Martínez-García, F. (2008). Role of the vomeronasal system in intersexual attraction in female mice. Neuroscience *153*, 383–395.

Martini, S., Silvotti, L., Shirazi, A., Ryba, N.J.P., and Tirindelli, R. (2001). Co-expression of putative pheromone receptors in the sensory neurons of the vomeronasal organ. J. Neurosci. *21*, 843–848.

Maruniak, J.A., Wysocki, C.J., and Taylor, J.A. (1986). Mediation of male mouse urine marking and aggression by the vomeronasal organ. Physiol. Behav. *37*, 655–657.

Matsumoto, T., Honda, S.I., and Harada, N. (2003). Alteration in sex-specific behaviors in male mice lacking the aromatase gene. Neuroendocrinology *77*, 416–424.

Matsunami, H., and Buck, L.B. (1997). A Multigene Family Encoding a Diverse Array of Putative Pheromone Receptors in Mammals. Cell *90*, 775–784.

Matsuo, T., Hattori, T., Asaba, A., Inoue, N., Kanomata, N., Kikusui, T., Kobayakawa, R., and Kobayakawa, K. (2015). Genetic dissection of pheromone processing reveals main olfactory system-mediated social behaviors in mice. Proc. Natl. Acad. Sci. *112*, E311–E320.

Mayer, H.S., Crepeau, M., Duque-Wilckens, N., Torres, L.Y., Trainor, B.C., and Stolzenberg, D.S. (2019). Histone deacetylase inhibitor treatment promotes spontaneous caregiving behaviour in non-aggressive virgin male mice. J. Neuroendocrinol. *31*, 1–13.

McCarthy, E.A., Kunkhyen, T., Korzan, W.J., Naik, A., Maqsudlu, A., Cherry, J.A., and Baum, M.J. (2017a). A comparison of the effects of male pheromone priming and optogenetic inhibition of accessory olfactory bulb forebrain inputs on the sexual behavior of estrous female mice. Horm. Behav. *89*, 104–112.

McCarthy, E.A., Maqsudlu, A., Bass, M., Georghiou, S., Cherry, J.A., and Baum, M.J. (2017b). DREADD-induced silencing of the medial amygdala reduces the preference for male pheromones and the expression of lordosis in estrous female mice. Eur. J. Neurosci. *46*, 2035–2046.

McEwen, D.P., Jenkins, P.M., and Martens, J.R. (2008). Olfactory Cilia: Our Direct Neuronal Connection to the External World. In Current Topics in Developmental Biology, (Elesvier Inc.), pp. 333–370.

Mendoza, A.S. (1993). Morphological studies on the rodent main and accessory olfactory systems: The regio olfactoria and vomeronasal organ. Ann. Anat. *175*, 425–446.

Mennella, J.A., and Moltz, H. (1988). Infanticide in the male rat: The role of the vomeronasal organ.

Physiol. Behav. *42*, 303–306.

Meredith, M., and O'Connell, R.J. (1979). Efferent control of stimulus access to the hamster vomeronasal organ. J. Physiol. *286*, 301–316.

Meyer, M.R., Angele, A., Kremmer, E., Kaupp, U.B., and Müller, F. (2000). A cGMP-signaling pathway in a subset of olfactory sensory neurons. Proc. Natl. Acad. Sci. U. S. A. *97*, 10595–10600.

Micevych, P.E., and Meisel, R.L. (2017). Integrating neural circuits controlling female sexual behavior. Front. Syst. Neurosci. *11*, 1–12.

Michalakis, S., Reisert, J., Geiger, H., Wetzel, C., Zong, X., Bradley, J., Spehr, M., Hüttl, S., Gerstner, A., Pfeifer, A., et al. (2006). Loss of CNGB1 protein leads to olfactory dysfunction and subciliary cyclic nucleotide-gated channel trapping. J. Biol. Chem. *281*, 35156–35166.

Millet, P., Opiekun, M., Martin, T., Beauchamp, G.K., and Kimball, B.A. (2018). Cytokine contributions to alterations of the volatile metabolome induced by inflammation. Brain. Behav. Immun. *69*, 312–320.

Millet, P., Martin, T., Opiekun, M., Beauchamp, G.K., and Kimball, B.A. (2021). Differing Alterations of Odor Volatiles Among Pathogenic Stimuli. Chem. Senses *46*, 1–8.

Moffitt, J.R., Bambah-Mukku, D., Eichhorn, S.W., Vaughn, E., Shekhar, K., Perez, J.D., Rubinstein, N.D., Hao, J., Regev, A., Dulac, C., et al. (2018). Molecular, spatial, and functional single-cell profiling of the hypothalamic preoptic region. Science (80-.). *362*, 1–22.

Mohedano-Moriano, A., Pro-Sistiaga, P., Úbeda-Bañón, I., Crespo, C., Insausti, R., and Martinez-Marcos, A. (2007). Segregated pathways to the vomeronasal amygdala: Differential projections from the anterior and posterior divisions of the accessory olfactory bulb. Eur. J. Neurosci. *25*, 2065–2080.

Mohrhardt, J., Nagel, M., Fleck, D., Ben-Shaul, Y., and Spehr, M. (2018). Signal detection and coding in the accessory olfactory system. Chem. Senses *43*, 667–695.

Mombaerts, P. (2004). Genes and ligands for odorant, vomeronasal and taste receptors. Nat. Rev. Neurosci. *5*, 263–278.

Montani, G., Tonelli, S., Sanghez, V., Ferrari, P.F., Palanza, P., Zimmer, A., and Tirindelli, R. (2013). Aggressive behaviour and physiological responses to pheromones are strongly impaired in mice deficient for the olfactory G-protein γ-subunit Gγ8. J. Physiol. *591*, 3949–3962.

Morrison, E.E., and Costanzo, R.M. (1990). Morphology of the human olfactory epithelium. J. Comp. Neurol. *297*, 1–13.

Moulton, D.G., and Beidler, L.M. (1967). Structure and function in the peripheral olfactory system. Physiol. Rev. *47*, 1–52.

Mugford, R.A., and Nowell, N.W. (1970). Pheromones and their Effect on Aggression in Mice. Nature *226*, 967–968.

Münch, J., Billig, G., Hübner, C.A., Leinders-Zufall, T., Zufall, F., and Jentsch, T.J. (2018). Ca2+-activated Cl- currents in the murine vomeronasal organ enhance neuronal spiking but are dispensable for male-male aggression. J. Biol. Chem. *293*, 10392–10403.

Munger, S.D., Lane, A.P., Zhong, H., Leinders-Zufall, T., Yau, K.W., Zufall, F., and Reed, R.R. (2001). Central role of the CNGA4 channel subunit in Ca2+-calmodulin-dependent odor adaptation. Science (80-.). *294*, 2172–2175.

Munger, S.D., Leinders-Zufall, T., and Zufall, F. (2009). Subsystem Organization of the Mammalian Sense of Smell. Annu. Rev. Physiol. *71*, 115–140.

Munger, S.D., Leinders-Zufall, T., McDougall, L.M., Cockerham, R.E., Schmid, A., Wandernoth, P., Wennemuth, G., Biel, M., Zufall, F., and Kelliher, K.R. (2010). An olfactory subsystem that detects carbon disulfide and mediates food-related social learning. Curr. Biol. *20*, 1438–1444.

Nakahara, T.S., Cardozo, L.M., Ibarra-Soria, X., Bard, A.D., Carvalho, V.M.A., Trintinalia, G.Z., Logan, D.W., and Papes, F. (2016). Detection of pup odors by non-canonical adult vomeronasal neurons expressing an odorant receptor gene is influenced by sex and parenting status. BMC Biol. *14*, 12.

Nakahara, T.S., Camargo, A.P., Magalhães, P.H.M., Souza, M.A.A., Ribeiro, P.G., Martins-Netto, P.H., Carvalho, V.M.A., José, J., and Papes, F. (2020). Peripheral oxytocin injection modulates vomeronasal sensory activity and reduces pup-directed aggression in male mice. Sci. Rep. *10*, 1–13.

Nakamura, T., and Gold, G.H. (1987). A cyclic nucleotide-gated conductance in olfactory receptor cilia. Nature *325*, 442–444.

Nakashima, A., Takeuchi, H., Imai, T., Saito, H., Kiyonari, H., Abe, T., Chen, M., Weinstein, L.S., Yu, C.R., Storm, D.R., et al. (2013). Agonist-Independent GPCR Activity Regulates Anterior-Posterior Targeting of Olfactory Sensory Neurons. Cell *154*, 1314–1325.

Navarro-Moreno, C., Sanchez-Catalan, M.J., Barneo-Muñoz, M., Goterris-Cerisuelo, R., Belles, M., Lanuza, E., Agustin-Pavon, C., and Martinez-Garcia, F. (2020). Pregnancy Changes the Response of the Vomeronasal and Olfactory Systems to Pups in Mice. Front. Cell. Neurosci. *14*, 1–19.

Neuhaus, E.M. (2020). Signal Transduction in Olfactory Neurons. In The Senses: A Comprehensive Reference, (Elsevier (Inc.)), pp. 545–564.

Nodari, F., Hsu, F.F., Fu, X., Holekamp, T.F., Kao, L.F., Turk, J., and Holy, T.E. (2008). Sulfated steroids as natural ligands of mouse pheromone-sensing neurons. J. Neurosci. *28*, 6407–6418.

Norlin, E.M., Gussing, F., and Berghard, A. (2003a). Vomeronasal phenotype and behavioral alterations in Gαi2 mutant mice. Curr. Biol. *13*, 1214–1219.

Norlin, E.M.M., Gussing, F., and Berghard, A. (2003b). Vomeronasal phenotype and behavioral alterations in Gαi2 mutant mice. Curr. Biol. *13*, 1214–1219.

Novotny, M.V. (2003). Pheromones, binding proteins and receptor responses in rodents. Biochem. Soc. Trans. *31*, 117–122.

Numan, M. (1974). Medial preoptic area and maternal behavior in the female rat. J. Comp. Physiol. Psychol. *87*, 746–759.

Numan, M., and Woodside, B. (2010). Maternity: Neural Mechanisms, Motivational Processes, and Physiological Adaptations. Behav. Neurosci. *124*, 715–741.

Oakley, A.E., Clifton, D.K., and Steiner, R.A. (2009). Kisspeptin signaling in the brain. Endocr. Rev. *30*, 713–743.

Oboti, L., Pérez-Gómez, A., Keller, M., Jacobi, E., Birnbaumer, L., Leinders-Zufall, T., Zufall, F., and Chamero, P. (2014). A wide range of pheromone-stimulated sexual and reproductive behaviors in female mice depend on G protein Gαo. BMC Biol. *12*, 31.

Oboti, L., Ibarra-Soria, X., Pérez-Gómez, A., Schmid, A., Pyrski, M., Paschek, N., Kircher, S., Logan, D.W., Leinders-Zufall, T., Zufall, F., et al. (2015). Pregnancy and estrogen enhance neural progenitor-cell proliferation in the vomeronasal sensory epithelium. BMC Biol. *13*, 1–17.

Ogawa, S., Washburn, T.F., Taylor, J., Lubahn, D.B., Korach, K.S., and Pfaff, D.W. (1998). Modifications of testosterone-dependent behaviors by estrogen receptor- α gene disruption in male mice. Endocrinology *139*, 5058–5069.

Ohara, H., Mogi, K., Ichimaru, T., Ohkura, S., Takeuchi, Y., Mori, Y., and Okamura, H. (2014). Effects of exposure to male goat hair extracts on luteinizing hormone secretion and neuronal activation in seasonally anestrous ewes. J. Vet. Med. Sci. *76*, 1329–1337.

Okabe, S., Nagaswa, M., Koto, M., Koshida, N., Kihara, T., Harada, T., Mogi, K., and Kikusui, T. (2013). Pup odor and ultrasonic vocalizations synergistically stimulate maternal attention in mice. Behav. Neurosci. *127*, 432–438.

Omura, M., and Mombaerts, P. (2014). Trpc2-Expressing Sensory Neurons in the Main Olfactory Epithelium of the Mouse. Cell Rep. *8*, 583–595.

Omura, M., and Mombaerts, P. (2015). Trpc2-expressing sensory neurons in the mouse main olfactory epithelium of type B express the soluble guanylate cyclase Gucy1b2. Mol. Cell. Neurosci. *65*, 114–124.

Osakada, T., Ishii, K.K., Mori, H., Eguchi, R., Ferrero, D.M., Yoshihara, Y., Liberles, S.D., Miyamichi, K., and Touhara, K. (2018). Sexual rejection via a vomeronasal receptor-triggered limbic circuit. Nat. Commun. *9*, 1–15.

Pacifico, R., Dewan, A., Cawley, D., Guo, C., and Bozza, T. (2012). An olfactory subsystem that mediates high-sensitivity detection of volatile amines. Cell Rep. *2*, 76–88.

Padilla, S.L., Qiu, J., Soden, M.E., Sanz, E., Nestor, C.C., Barker, F.D., Quintana, A., Zweifel, L.S., Rønnekleiv, O.K., Kelly, M.J., et al. (2016). Agouti-related peptide neural circuits mediate adaptive behaviors in the starved state. Nat. Neurosci. *19*, 734–741.

Pallé, A., Montero, M., Fernández, S., Tezanos, P., de las Heras, J.A., Luskey, V., Birnbaumer, L., Zufall, F., Chamero, P., and Trejo, J.L. (2020). Gαi2+ vomeronasal neurons govern the initial outcome of an acute social competition. Sci. Rep. *10*, 894.

Pankevich, D.E. (2004). Olfactory Sex Discrimination Persists, Whereas the Preference for Urinary Odorants from Estrous Females Disappears in Male Mice after Vomeronasal Organ Removal. J. Neurosci. *24*, 9451–9457.

Pankevich, D.E., Cherry, J.A., and Baum, M.J. (2006). Effect of vomeronasal organ removal from male mice on their preference for and neural Fos responses to female urinary odors. Behav. Neurosci. *120*, 925–936.

Papes, F., Logan, D.W., and Stowers, L. (2010). The Vomeronasal Organ Mediates Interspecies Defensive Behaviors through Detection of Protein Pheromone Homologs. Cell *141*, 692–703.

Paredes, R.G. (2009). Evaluating the neurobiology of sexual reward. ILAR J. *50*, 15–27.

Parmigiani, S., Brain, P.F., Mainardi, D., and Brunoni, V. (1988). Different patterns of biting attack employed by lactating female mice (Mus domesticus) in encounters with male and female conspecific intruders. J. Comp. Psychol. *102*, 287–293.

Pedersen, P., Stewart, W., Greer, C., and Shepherd, G. (1983). Evidence for olfactory function in utero. Science (80-.). *221*, 478–480.

Pérez-Gómez, A., Bleymehl, K., Stein, B., Pyrski, M., Birnbaumer, L., Munger, S.D., Leinders-Zufall, T., Zufall, F., and Chamero, P. (2015). Innate predator odor aversion driven by parallel olfactory subsystems that converge in the ventromedial hypothalamus. Curr. Biol. *25*, 1340–1346.

Pinching, A.J., and Powell, T.P. (1971). The neuron types of the glomerular layer of the olfactory bulb. J. Cell Sci. *9*, 305–345.

Del Punta, K., Rothman, A., Rodriguez, I., and Mombaerts, P. (2000). Sequence diversity and genomic organization of vomeronasal receptor genes in the mouse. Genome Res. *10*, 1958–1967.

Del Punta, K., Leinders-Zufall, T., Rodriguez, I., Jukam, D., Wysocki, C.J., Ogawa, S., Zufall, F., and Mombaerts, P. (2002). Deficient pheromone responses in mice lacking a cluster of vomeronasal receptor genes. Nature *419*, 70–74.

Raam, T., and Hong, W. (2021). Organization of neural circuits underlying social behavior: A consideration of the medial amygdala. Curr. Opin. Neurobiol. *68*, 124–136.

Renier, N., Adams, E.L., Kirst, C., Wu, Z., Azevedo, R., Kohl, J., Autry, A.E., Kadiri, L., Umadevi Venkataraju, K., Zhou, Y., et al. (2016). Mapping of Brain Activity by Automated Volume Analysis of Immediate Early Genes. Cell *165*, 1789–1802.

Ressler, K.J., Sullivan, S.L., and Buck, L.B. (1994). Information coding in the olfactory system: Evidence for a stereotyped and highly organized epitope map in the olfactory bulb. Cell *79*, 1245–1255.

Reynolds, E. (1971). Urination as a Social Response in Mice. Nature *234*, 481–483.

Ribeiro, A.C., Musatov, S., Shteyler, A., Simanduyev, S., Arrieta-Cruz, I., Ogawa, S., and Pfaff, D.W. (2012). siRNA silencing of estrogen receptor-α expression specifically in medial preoptic area neurons abolishes maternal care in female mice. Proc. Natl. Acad. Sci. U. S. A. *109*, 16324–16329.

Rich, T.J., and Hurst, J.L. (1999). The competing countermarks hypothesis: reliable assessment of competitive ability by potential mates. Anim. Behav. *58*, 1027–1037.

Risold, P.Y., and Swanson, L.W. (1997). Chemoarchitecture of the rat lateral septal nucleus. Brain Res. Rev. *24*, 91–113.

Rivas, F. V., Chervonsky, A. V., and Medzhitov, R. (2014). ART and immunology. Trends Immunol. *35*, 451.

Rivière, S., Challet, L., Fluegge, D., Spehr, M., and Rodriguez, I. (2009). Formyl peptide receptor-like proteins are a novel family of vomeronasal chemosensors. Nature *459*, 574–577.

Roberts, S.A., Simpson, D.M., Armstrong, S.D., Davidson, A.J., Robertson, D.H., McLean, L., Beynon, R.J., and Hurst, J.L. (2010). Darcin: a male pheromone that stimulates female memory and sexual attraction to an individual male's odour. BMC Biol. *8*, 75.

Rodolfo-Masera, T. (1943). Su l'ésistenza di un particolare organo olfattivo nel setoo nasale delà cavia e di altri rodotori. Arch. Ital. Di Anat. e Di Embriol. *48*, 157–212.

Rodriguez, I., Feinstein, P., and Mombaerts, P. (1999). Variable patterns of axonal projections of sensory neurons in the mouse vomeronasal system. Cell *97*, 199–208.

Rodriguez, I., Del Punta, K., Rothman, A., Ishii, T., and Mombaerts, P. (2002). Multiple new and isolated families within the mouse superfamily of V1r vomeronasal receptors. Nat. Neurosci. *5*, 134–140.

Root, C.M., Denny, C.A., Hen, R., and Axel, R. (2014). The participation of cortical amygdala in innate, odour-driven behaviour. Nature *515*, 269–273.

Roppolo, D., Ribaud, V., Jungo, V.P., Lüscher, C., and Rodriguez, I. (2006). Projection of the Grüneberg ganglion to the mouse olfactory bulb. Eur. J. Neurosci. *23*, 2887–2894.

Roppolo, D., Vollery, S., Kan, C. Da, Lüscher, C., Broillet, M.C., and Rodriguez, I. (2007). Gene cluster lock after pheromone receptor gene choice. EMBO J. *26*, 3423–3430.

Rosenson, L.M., and Asheroff, A.K. (1975). Maternal aggression in CD-1 mice: Influence of the hormonal condition of the intruder. Behav. Biol. *15*, 219–224.

Rottman, S.J., and Snowdown, C.T. (1972). Demonstration and analysis of an alarm pheromone in mice. J. Comp. Physiol. Psychol. *81*, 483–490.

Rudolph, U., Srinivasan, Y., Brabet, P., Boulay, G., Birnbaumer, L., Finegold, M.J., Rich, S.S., Harriman, G.R., and Bradley, A. (1995). Ulcerative colitis and adenocarcinoma of the colon in Gαi2-deficient mice. Nat. Genet. *10*, 143–150.

Rünnenburger, K., Breer, H., and Boekhoff, I. (2002). Selective G protein βγ-subunit compositions mediate phospholipase C activation in the vomeronasal organ. Eur. J. Cell Biol. *81*, 539–547.

Ryba, N.J.P., and Tirindelli, R. (1995). A novel GTP-binding protein γ-subunit, Gγ8, is expressed during neurogenesis in the olfactory and vomeronasal neuroepithelia. J. Biol. Chem. *270*, 6757–6767.

Ryba, N.J.P., and Tirindelli, R. (1997). A new multigene family of putative pheromone receptors. Neuron *19*, 371–379.

Vom Saal, F.S. (1985). Time-contingent change in infanticide and parental behavior induced by ejaculation in male mice. Physiol. Behav. *34*, 7–15.

Vom Saal, F.S., and Howard, L.S. (1982). The regulation of infanticide and parental behavior: Implications for reproductive success in male mice. Science (80-.). *215*, 1270–1272.

Saito, H., Nishizumi, H., Suzuki, S., Matsumoto, H., Ieki, N., Abe, T., Kiyonari, H., Morita, M., Yokota, H., Hirayama, N., et al. (2017). photoactivation of single glomerular species responsive to fox odour TMT. Nat. Commun. *8*, 1–10.

Sam, M., Vora, S., Malnic, B., Ma, W., Novotny, M. V., and Buck, L.B. (2001). Odorants may arouse instinctive behaviours. Nature *412*, 142–142.

Samuelsen, C.L., and Meredith, M. (2009). The vomeronasal organ is required for the male mouse medial amygdala response to chemical-communication signals, as assessed by immediate early gene expression. Neuroscience *164*, 1468–1476.

Sano, K., Tsuda, M.C., Musatov, S., Sakamoto, T., and Ogawa, S. (2013). Differential effects of site-specific knockdown of estrogen receptor α in the medial amygdala, medial pre-optic area, and ventromedial nucleus of the hypothalamus on sexual and aggressive behavior of male mice. Eur. J. Neurosci. *37*, 1308–1319.

Sassoè-Pognetto, M., Cantino, D., Panzanelli, P., Di Cantogno, L.V., Giustetto, M., Margolis, F.L., De Biasi, S., and Fasolo, A. (1993). Presynaptic colocalization of carnosine and glutamate in olfactory neurones. Neuroreport *5*, 7–10.

Sathyanesan, A., Feijoo, A.A., Mehta, S.T., Nimarko, A.F., and Lin, W. (2013). Expression profile of G-protein βγ subunit gene transcripts in the mouse olfactory sensory epithelia. Front. Cell. Neurosci. *7*, 1–19.

Sato, K., Hamasaki, Y., Fukui, K., Ito, K., Miyamichi, K., Minami, M., and Amano, T. (2020). Amygdalohippocampal area neurons that project to the preoptic area mediate infant-directed attack in male mice. J. Neurosci. *40*, 3981–3994.

Schindelin, J., Arganda-Carreras, I., Frise, E., Kaynig, V., Longair, M., Pietzsch, T., Preibisch, S., Rueden, C., Saalfeld, S., Schmid, B., et al. (2012). Fiji: an open-source platform for biological-image analysis. Nat. Methods *9*, 676–682.

Schmid, A., Pyrski, M., Biel, M., Leinders-Zufall, T., and Zufall, F. (2010). Grueneberg ganglion neurons are finely tuned cold sensors. J. Neurosci. *30*, 7563–7568.

Schneider, N.Y., Fletcher, T.P., Shaw, G., and Renfree, M.B. (2012). Goα expression in the vomeronasal organ and olfactory bulb of the tammar wallaby. Chem. Senses *37*, 567–577.

Scholz, P., Mohrhardt, J., Jansen, F., Kalbe, B., Haering, C., Klasen, K., Hatt, H., and Osterloh, S. (2016). Identification of a novel Gnao-mediated alternate olfactory signaling pathway in murine OSNs. Front. Cell. Neurosci. *10*, 1–11.

Schwende, F.J., Wiesler, D., Jorgenson, J.W., Carmack, M., and Novotny, M. (1986). Urinary volatile constituents of the house mouse, Mus musculus, and their endocrine dependency. J. Chem. Ecol. *12*, 277–296.

Seegal, R.F., and Denenberg, V.H. (1974). Maternal experience prevents pup-killing in mice induced by peripheral anosmia. Physiol. Behav. *13*, 339–341.

Serizawa, S., Miyamichi, K., and Sakano, H. (2004). One neuron-one receptor rule in the mouse olfactory system. Trends Genet. *20*, 648–653.

Sharrow, S.D., Vaughn, J.L., Žídek, L., Novotny, M. V., and Stone, M.J. (2009). Pheromone binding by polymorphic mouse major urinary proteins. Protein Sci. *11*, 2247–2256.

Shepherd, G.M., Hines, M.L., Migliore, M., Chen, W.R., and Greer, C.A. (2020). Predicting brain organization with a computational model: 50-year perspective on lateral inhibition and oscillatory

gating by dendrodendritic synapses. J. Neurophysiol. *124*, 375–387.

Shi, P., and Zhang, J. (2007). Comparative genomic analysis identifies an evolutionary shift of vomeronasal receptor gene repertoires in the vertebrate transition from water to land. Genome Res. *17*, 166–174.

Silva, L., and Antunes, A. (2017). Vomeronasal Receptors in Vertebrates and the Evolution of Pheromone Detection. Annu. Rev. Anim. Biosci. *5*, 353–370.

Silva, B.A., Mattucci, C., Krzywkowski, P., Murana, E., Illarionova, A., Grinevich, V., Canteras, N.S., Ragozzino, D., and Gross, C.T. (2013). Independent hypothalamic circuits for social and predator fear. Nat. Neurosci. *16*, 1731–1733.

Silvotti, L., Moiani, A., Gatti, R., and Tirindelli, R. (2007). Combinatorial co-expression of pheromone receptors, V2Rs. J. Neurochem. *103*, 1753–1763.

Silvotti, L., Cavalca, E., Gatti, R., Percudani, R., and Tirindelli, R. (2011). A Recent Class of Chemosensory Neurons Developed in Mouse and Rat. PLoS One *6*, e24462.

Simerly, R.B. (2002). Wired for Reproduction: Organization and Development of Sexually Dimorphic Circuits in the Mammalian Forebrain. Annu. Rev. Neurosci. *25*, 507–536.

Simerly, R.B., Swanson, L.W., Handa, R.J., and Gorski, R.A. (1985). Influence of perinatal androgen on the sexually dimorphic distribution of tyrosine hydroxylase-immunoreactive cells and fibers in the anteroventral periventricular nucleus of the rat. Neuroendocrinology *40*, 501–510.

Smrcka, A. V. (2008). G protein βγ subunits: Central mediators of G protein-coupled receptor signaling. Cell. Mol. Life Sci. *65*, 2191–2214.

Song, C., and Leonard, B.E. (2005). The olfactory bulbectomised rat as a model of depression. Neurosci. Biobehav. Rev. *29*, 627–647.

Spehr, J., Hagendorf, S., Weiss, J., Spehr, M., Leinders-Zufall, T., and Zufall, F. (2009). Ca2+-Calmodulin Feedback Mediates Sensory Adaptation and Inhibits Pheromone-Sensitive Ion Channels in the Vomeronasal Organ. J. Neurosci. *29*, 2125–2135.

Spehr, M., Hatt, H., and Wetzel, C.H. (2002). Arachidonic acid plays a role in rat vomeronasal signal transduction. J. Neurosci. *22*, 8429–8437.

Stanić, D., Dubois, S., Chua, H.K., Tonge, B., Rinehart, N., Horne, M.K., and Boon, W.C. (2014). Characterization of Aromatase Expression in the Adult Male and Female Mouse Brain. I. Coexistence with Oestrogen Receptors α and β, and Androgen Receptors. PLoS One *9*, e90451.

Stein, B., Alonso, M.T., Zufall, F., Leinders-Zufall, T., and Chamero, P. (2016). Functional Overexpression of Vomeronasal Receptors Using a Herpes Simplex Virus Type 1 (HSV-1)-Derived Amplicon. PLoS One *11*, e0156092.

Stephan, A.B., Shum, E.Y., Hirsh, S., Cygnar, K.D., Reisert, J., and Zhao, H. (2009). ANO2 is the cilial calcium-activated chloride channel that may mediate olfactory amplification. Proc. Natl. Acad. Sci. U. S. A. *106*, 11776–11781.

Stolzenberg, D.S., and Rissman, E.F. (2011). Oestrogen-Independent, Experience-Induced Maternal Behaviour in Female Mice. J. Neuroendocrinol. *23*, 345–354.

Storan, M.J., and Key, B. (2006). Septal organ of Grüneberg is part of the olfactory system. J. Comp. Neurol. *494*, 834–844.

Stowers, L., Holy, T.E., Meister, M., Dulac, C., and Koentges, G. (2002). Loss of sex discrimination and male-male aggression in mice deficient for TRP2. Science *295*, 1493–1500.

Suárez, R., Fernández-Aburto, P., Manger, P.R., and Mpodozis, J. (2011). Deterioration of the Gαo vomeronasal pathway in sexually dimorphic mammals. PLoS One *6*, 1–6.

Tachikawa, K.S., Yoshihara, Y., and Kuroda, K.O. (2013). Behavioral Transition from Attack to

Parenting in Male Mice: A Crucial Role of the Vomeronasal System. J. Neurosci. *33*, 5120–5126.

Takahashi, L.K. (2014). Olfactory systems and neural circuits that modulate predator odor fear. Front. Behav. Neurosci. *8*, 1–13.

Takami, S., and Graziadei, P.P.C. (1991). Light microscopic golgi study of mitral/tufted cells in the accessory olfactory bulb of the adult rat. J. Comp. Neurol. *311*, 65–83.

Takeuchi, H., Inokuchi, K., Aoki, M., Suto, F., Tsuboi, A., Matsuda, I., Suzuki, M., Aiba, A., Serizawa, S., Yoshihara, Y., et al. (2010). Sequential arrival and graded secretion of Sema3F by olfactory neuron axons specify map topography at the bulb. Cell *141*, 1056–1067.

Tan, S., and Stowers, L. (2020). Bespoke behavior: mechanisms that modulate pheromone-triggered behavior. Curr. Opin. Neurobiol. *64*, 143–150.

Tanaka, M., Treloar, H., Kalb, R.G., Greer, C.A., and Strittmatter, S.M. (1999). Go protein-dependent survival of primary accessory olfactory neurons. Proc. Natl. Acad. Sci. U. S. A. *96*, 14106–14111.

Taniguchi, K., Saito, S., and Taniguchi, K. (2011). Phylogenic outline of the olfactory system in vertebrates. J. Vet. Med. Sci. *73*, 139–147.

Thom, M.D., Stockley, P., Jury, F., Ollier, W.E.R., Beynon, R.J., and Hurst, J.L. (2008). The Direct Assessment of Genetic Heterozygosity through Scent in the Mouse. Curr. Biol. *18*, 619–623.

Thompson, M.L., and Edwards, D.A. (1971). Experiential and strain determinants of the estrogen-progesterone induction of sexual receptivity in spayed female mice. Horm. Behav. *2*, 299–305.

Tian, H., and Ma, M. (2004). Molecular organization of the olfactory septal organ. J. Neurosci. *24*, 8383–8390.

Tinbergen, N. (1963). On aims and methods of Ethology. Z. Tierpsychol. *20*, 410–433.

Tirindelli, R. (2021). Coding of pheromones by vomeronasal receptors. Cell Tissue Res. *383*, 367–386.

Tirindelli, R., Dibattista, M., Pifferi, S., and Menini, A. (2009). From Pheromones to Behavior. Physiol. Rev. *89*, 921–956.

Trivers, R.L. (1972). Parental investment and sexual selection. *13*, 136–179.

Trotier, D., and Døving, K.B. (1998). "Anatomical Description of a New Organ in the Nose of Domesticated Animals" by Ludvig Jacobson (1813). Chem. Senses *23*, 743–754.

Trouillet, A.C., Keller, M., Weiss, J., Leinders-Zufall, T., Birnbaumer, L., Zufall, F., and Chamero, P. (2019). Central role of G protein Gαi2 and Gαi2 + vomeronasal neurons in balancing territorial and infant-directed aggression of male mice. Proc. Natl. Acad. Sci. *116*, 5135–5143.

Trouillet, A.C., Moussu, C., Poissenot, K., Keller, M., Birnbaumer, L., Leinders-Zufall, T., Zufall, F., and Chamero, P. (2021). Sensory Detection by the Vomeronasal Organ Modulates Experience-Dependent Social Behaviors in Female Mice. Front. Cell. Neurosci. *15*, 638800.

Tsitoura, C., Malinowski, S.T., Mohrhardt, J., Degen, R., DiBenedictis, B.T., Gao, Y., Watznauer, K., Gerhold, K., Nagel, M., Weber, M., et al. (2020). Synchronous Infra-Slow Oscillations Organize Ensembles of Accessory Olfactory Bulb Projection Neurons into Distinct Microcircuits. J. Neurosci. *40*, 4203–4218.

Tsuneoka, Y., Maruyama, T., Yoshida, S., Nishimori, K., Kato, T., Numan, M., and Kuroda, K.O. (2013). Functional, anatomical, and neurochemical differentiation of medial preoptic area subregions in relation to maternal behavior in the mouse. J. Comp. Neurol. *521*, 1633–1663.

Tsuneoka, Y., Tokita, K., Yoshihara, C., Amano, T., Esposito, G., Huang, A.J., Yu, L.M., Odaka, Y., Shinozuka, K., McHugh, T.J., et al. (2015). Distinct preoptic-BST nuclei dissociate paternal and infanticidal behavior in mice. EMBO J. *34*, 2652–2670.

Tsuneoka, Y., Yoshida, S., Takase, K., Oda, S., Kuroda, M., and Funato, H. (2017). Neurotransmitters and neuropeptides in gonadal steroid receptor-expressing cells in medial preoptic area subregions of the male mouse. Sci. Rep. *7*, 1–16.

Tsunoda, M., Miyamichi, K., Eguchi, R., Sakuma, Y., Yoshihara, Y., Kikusui, T., Kuwahara, M., and Touhara, K. (2018). Identification of an Intra- and Inter-specific Tear Protein Signal in Rodents. Curr. Biol. *28*, 1213-1223.e6.

Turaga, D., and Holy, T.E. (2012). Organization of Vomeronasal Sensory Coding Revealed by Fast Volumetric Calcium Imaging. J. Neurosci. *32*, 1612–1621.

Uchida, N., Poo, C., and Haddad, R. (2014). Coding and transformations in the olfactory system. Annu. Rev. Neurosci. *37*, 363–385.

Unger, E.K., Burke, K.J., Yang, C.F., Bender, K.J., Fuller, P.M., and Shah, N.M. (2015). Medial amygdalar aromatase neurons regulate aggression in both sexes. Cell Rep. *10*, 453–462.

Ustyugova, I. V., Zhi, L., Abramowitz, J., Birnbaumer, L., and Wu, M.X. (2012). IEX-1 deficiency protects against colonic cancer. Mol. Cancer Res. *10*, 760–767.

Vandenbergh, J.G. (1973). Effects of central and peripheral anosmia on reproduction of female mice. Physiol. Behav. *10*, 257–261.

Vassar, R., Chao, S.K., Sitcheran, R., Nun˜ez, J.M., Vosshall, L.B., and Axel, R. (1994). Topographic organization of sensory projections to the olfactory bulb. Cell *79*, 981–991.

Wachowiak, M., and Shipley, M.T. (2006). Coding and synaptic processing of sensory information in the glomerular layer of the olfactory bulb. Semin. Cell Dev. Biol. *17*, 411–423.

Wagner, S., Gresser, A.L., Torello, A.T., and Dulac, C. (2006). A Multireceptor Genetic Approach Uncovers an Ordered Integration of VNO Sensory Inputs in the Accessory Olfactory Bulb. Neuron *50*, 697–709.

Walz, A., Rodriguez, I., and Mombaerts, P. (2002). Aberrant Sensory Innervation of the Olfactory Bulb in Neuropilin-2 Mutant Mice. J. Neurosci. *22*, 4025–4035.

Walz, A., Feinstein, P., Khan, M., and Mombaerts, P. (2007). Axonal wiring of guanylate cyclase-D-expressing olfactory neurons is dependent on neuropilin 2 and semaphorin 3F. Development *134*, 4063–4072.

Wang, Z., and Storm, D.R. (2011). Maternal behavior is impaired in female mice lacking type 3 adenylyl cyclase. Neuropsychopharmacology *36*, 772–781.

Wang, Z.G., and Ye, R.D. (2002). Characterization of two new members of the formyl peptide receptor gene family from 129S6 mice. Gene *299*, 57–63.

Wang, F., Nemes, A., Mendelsohn, M., and Axel, R. (1998). Odorant receptors govern the formation of a precise topographic map. Cell *93*, 47–60.

Wang, L., Chen, I.Z., and Lin, D. (2015). Collateral Pathways from the Ventromedial Hypothalamus Mediate Defensive Behaviors. Neuron *85*, 1344–1358.

Wei, D., Talwar, V., and Lin, D. (2021). Neural circuits of social behaviors: Innate yet flexible. Neuron *109*, 1600–1620.

Wei, Y.-C., Wang, S.-R., Jiao, Z.-L., Zhang, W., Lin, J.-K., Li, X.-Y., Li, S.-S., Zhang, X., and Xu, X.-H. (2018). Medial preoptic area in mice is capable of mediating sexually dimorphic behaviors regardless of gender. Nat. Commun. *9*, 279.

Weiss, J., Pyrski, M., Jacobi, E., Bufe, B., Willnecker, V., Schick, B., Zizzari, P., Gossage, S.J., Greer, C.A., Leinders-Zufall, T., et al. (2011). Loss-of-function mutations in sodium channel Na v 1.7 cause anosmia. Nature *472*, 186–192.

Wekesa, K.S., and Anholt, R.R.H. (1999). Differential expression of G proteins in the mouse olfactory

system. Brain Res. *837*, 117–126.

Wong, L.C., Wang, L., D'Amour, J.A., Yumita, T., Chen, G., Yamaguchi, T., Chang, B.C., Bernstein, H., You, X., Feng, J.E., et al. (2016). Effective Modulation of Male Aggression through Lateral Septum to Medial Hypothalamus Projection. Curr. Biol. *26*, 593–604.

Wong, S.T., Trinh, K., Hacker, B., Chan, G.C.K., Lowe, G., Gaggar, A., Xia, Z., Gold, G.H., and Storm, D.R. (2000). Disruption of the type III adenylyl cyclase gene leads to peripheral and behavioral anosmia in transgenic mice. Neuron *27*, 487–497.

Wong, W.M., Cao, J., Zhang, X., Doyle, W.I., Mercado, L.L., Gautron, L., and Meeks, J.P. (2020). Physiology-forward identification of bile acid–sensitive vomeronasal receptors. Sci. Adv. *6*, eaaz6868.

Wu, M. V., Manoli, D.S., Fraser, E.J., Coats, J.K., Tollkuhn, J., Honda, S.I., Harada, N., and Shah, N.M. (2009). Estrogen Masculinizes Neural Pathways and Sex-Specific Behaviors. Cell *139*, 61–72.

Wu, Z., Autry, A.E., Bergan, J.F., Watabe-Uchida, M., and Dulac, C.G. (2014). Galanin neurons in the medial preoptic area govern parental behaviour. Nature *509*, 325–330.

Wyatt, T.D. (2013). Pheromones and Animal Behavior (Cambridge: Cambridge University Press).

Wyatt, T.D. (2014). Proteins and peptides as pheromone signals and chemical signatures. Anim. Behav. *97*, 273–280.

Wyatt, T.D. (2017). Pheromones. Curr. Biol. *27*, R739–R743.

Wysocki, C.J., and Lepri, J.J. (1991). Consequences of removing the vomeronasal organ. J. Steroid Biochem. Mol. Biol. *39*, 661–669.

Wysocki, C.J., Nyby, J., Whitney, G., Beauchamp, G.K., and Katz, Y. (1982). The vomeronasal organ: Primary role in mouse chemosensory gender recognition. Physiol. Behav. *29*, 315–327.

Yang, C., and Delay, R.J. (2010). Calcium-activated chloride current amplifies the response to urine in mouse vomeronasal sensory neurons. J. Gen. Physiol. *135*, 3–13.

Yang, C.F., Chiang, M.C., Gray, D.C., Prabhakaran, M., Alvarado, M., Juntti, S.A., Unger, E.K., Wells, J.A., and Shah, N.M. (2013). Sexually dimorphic neurons in the ventromedial hypothalamus govern mating in both sexes and aggression in males. Cell *153*, 896–909.

Yang, H., Shi, P., Zhang, Y.P., and Zhang, J. (2005). Composition and evolution of the V2r vomeronasal receptor gene repertoire in mice and rats. Genomics *86*, 306–315.

Yao, S., Bergan, J., Lanjuin, A., and Dulac, C. (2017). Oxytocin signaling in the medial amygdala is required for sex discrimination of social cues. Elife *6*, 1–31.

Yildirim, E., and Birnbaumer, L. (2007). TRPC2: Molecular biology and functional importance. Handb. Exp. Pharmacol. *179*, 53–75.

Yonekura, J., and Yokoi, M. (2008). Conditional genetic labeling of mitral cells of the mouse accessory olfactory bulb to visualize the organization of their apical dendritic tufts. Mol. Cell. Neurosci. *37*, 708–718.

Young, J.M., and Trask, B.J. (2007). V2R gene families degenerated in primates, dog and cow, but expanded in opossum. Trends Genet. *23*, 212–215.

Young, J.M., Massa, H.F., Hsu, L., and Trask, B.J. (2010). Extreme variability among mammalian V1R gene families. Genome Res. *20*, 10–18.

Yu, C.R. (2015). TRICK or TRP? What Trpc2−/− mice tell us about vomeronasal organ mediated innate behaviors. Front. Neurosci. *9*, 1–7.

Zapiec, B., and Mombaerts, P. (2020). The Zonal Organization of Odorant Receptor Gene Choice in the Main Olfactory Epithelium of the Mouse. Cell Rep. *30*, 4220-4234.e5.

Zhang, X., and Firestein, S. (2002). The olfactory receptor gene superfamily of the mouse. Nat. Neurosci. *5*, 124–133.

Zhang, J., Pacifico, R., Cawley, D., Feinstein, P., and Bozza, T. (2013). Ultrasensitive detection of amines by a trace amine-associated receptor. J. Neurosci. *33*, 3228–3239.

Zhang, P., Yang, C., and Delay, R.J. (2008). Urine stimulation activates BK channels in mouse vomeronasal neurons. J. Neurophysiol. *100*, 1824–1834.

Zhang, P., Yang, C., and Delay, R.J. (2010). Odors activate dual pathways, a TRPC2 and a AA-dependent pathway, in mouse vomeronasal neurons. Am. J. Physiol. Physiol. *298*, C1253–C1264.

Zhang, S.X., Lutas, A., Yang, S., Diaz, A., Fluhr, H., Nagel, G., Gao, S., and Andermann, M.L. (2021). Hypothalamic dopamine neurons motivate mating through persistent cAMP signalling. Nature *597*, 245–249.

Anne-Charlotte Trouillet

Rôle des mécanismes de signalisation olfactive impliquant $G\alpha_{i2}$ dans le contrôle des comportements socio-sexuels.

Résumé

Chez la plupart des mammifères, le système olfactif régule les comportements socio-sexuels via la détection d'informations chimiques. Les neurones sensoriels du système olfactif détectent ces signaux par l'intermédiaire de récepteurs couplés aux protéines G, chacun étant exprimé par un seul ensemble de neurones. Les signaux olfactifs pertinents pour la communication sociale sont principalement détectés par l'organe voméronasal, dans lequel au moins deux populations de cellules réceptrices (les VSNs) détectent les phéromones par l'intermédiaire de deux familles de récepteurs couplés aux protéines G, les V1Rs et les V2Rs. Il a été proposé que la liaison d'un ligand à son récepteur, V1R ou V2R, active une protéine G correspondante, respectivement Gαi2 et Gαo. Les neurones exprimant la protéine Gαo détectent des peptides et des protéines modulant plusieurs comportements sociaux. Des études génétiques et comportementales sur la souris indiquent également un rôle potentiel des neurones exprimant Gαi2 comme transducteurs de l'information olfactive et modulateurs de la physiologie et des comportements sexuels. Cependant, la contribution exacte de cette voie de signalisation reste largement méconnue. Par conséquent, l'objectif principal de ce projet est de déterminer comment les comportements socio-sexuels sont contrôlés par le système olfactif, en particulier par les neurones de l'organe voméronasal exprimant V1R-Gαi2.

Pour répondre à cette question, nous avons utilisé le système Cre-lox pour ainsi générer une souris dans laquelle la délétion du gène codant pour Gαi2 est limitée aux neurones sensoriels olfactifs. Tout d'abord, nous avons évalué le rôle fonctionnel de Gαi2 dans le processus de transduction du signal via des techniques d'imagerie calcique sur cellules vivantes. Nous avons ainsi établi que Gαi2 est nécessaire pour la détection des petites molécules organiques et des stéroïdes sulfatés. Ensuite, nous avons étudié le rôle des VSNs exprimant Gαi2/V1Rs dans l'expression des comportements reproducteurs et sociaux. Nous avons testé les comportements sexuels, parentaux et agressifs de souris mâles et femelles déficientes pour Gαi2 et identifié les régions du cerveau transformant l'information olfactive en décision comportementale. Nous avons observé une influence des VSNs exprimant Gαi2 en fonction du sexe avec des effets spécifiques pour chaque comportement. Nous avons constaté que la délétion de Gαi2 dans les VSNs joue un rôle central dans le comportement agressif des mâles en augmentant l'agression territoriale et en réduisant l'agression dirigée vers les nouveau-nés. Cependant, l'agressivité des femelles reste inchangée en l'absence de Gαi2. Le comportement parental est également affecté par la délétion de Gαi2 de façon différente chez chaque sexe, augmenté chez les mâles et inhibé chez les femelles. De plus, l'expérience sociale modifie l'implication de la signalisation voméronasale Gαi2 dans le comportement sexuel des femelles, alors que chez les mâles, la délétion de Gαi2 n'a aucun effet sur le comportement sexuel. Enfin, nous avons identifié un nouveau rôle pour les VSNs exprimant Gαi2 dans les comportements d'aversion médiés par les signaux de prédateurs et de congénères malades.

Toutes les espèces intègrent continuellement des informations environnementales et adaptent leurs réponses en conséquence. Ce projet vise à mettre en lumière les mécanismes neuronaux qui sous-tendent le traitement des signaux chimiques olfactifs, afin de comprendre comment les entrées olfactives périphériques interagissent avec les centres neuronaux qui contrôlent les réponses comportementales. La compréhension de ces mécanismes a une large portée et peut conduire à de nouvelles perspectives dans la compréhension des troubles du comportement et le développement de nouvelles stratégies d'élevage chez les animaux domestiques.

Abstract

In most mammals, the olfactory system drives socio-sexual behaviors through the detection of chemosensory information. Sensory neurons of the olfactory system detect these signals through dedicated G protein-coupled receptors, each expressed by a single ensemble of neurons. Chemosignals relevant for social communication are mainly sensed by the vomeronasal organ in which at least two populations of receptor cells detect pheromones through two families of G-protein-coupled receptors, V1Rs and V2Rs. The binding of ligands to the receptor (V1R or V2R) has been proposed to activate the corresponding G protein, Gαi2 and Gαo, respectively. Gαo-expressing neurons have been shown to detect peptides and proteins modulating several social behaviors. Genetic and behavioral studies on mice also point to a potential role of Gαi2-expressing neurons as transducers of the olfactory information controlling reproductive physiology and behaviors. However, the exact contribution of this signaling pathway remains elusive. Therefore, the main goal of this project is to determine how socio-sexual behaviors are controlled by the olfactory system, particularly by the V1R-Gαi2-expressing neurons of the vomeronasal organ.

To address this point, we used the Cre-lox system to generate a conditional knockout mouse in which the deletion of Gαi2 gene is restricted to olfactory sensory neurons. First, we evaluated the functional role of Gαi2 in the process of VSNs signal transduction using live-cell calcium imaging experiments. We first established that Gαi2 is necessary for the detection of small organic molecules and sulfated steroids in V1Rs-expressing VSNs. Second, we investigated the role of Gαi2/V1Rs-expressing VSNs in displaying reproductive and social behaviors. We tested sexual, parental, and aggressive behaviors of male and female mice deficient for Gαi2 and identified brain regions transforming the olfactory information into a behavioral decision. We observed an influence of Gαi2-expressing VSNs in a sex-dependent manner with distinctive traits for each behavior. We found that the deletion of Gαi2 in VSNs played a central role in male aggressive behavior by increasing territorial aggression and reducing infant-directed aggression. However, female aggression remained unaltered in the absence of Gαi2. Parenting was also differentially affected by Gαi2 deletion in each sex, activated in males and inhibited in females. Further, social experience changed the implication of Gαi2 vomeronasal signaling in female sexual behavior, while in males, Gαi2-deletion had no effect on sexual behavior before or after experience. Last, we identified a new role of Gαi2-expressing VSNs in avoidance behaviors mediated by predators and sick-conspecifics aversive olfactory cues.

All species continuously integrate environmental information and adapt their responses accordingly. This project aims to shed light on neural mechanisms underlying the processing of olfactory chemosignals in order to understand how peripheral olfactory inputs interact with neural centers controlling the behavioral responses. Understanding these mechanisms is of broad relevance and may lead to new insights in the comprehension of behavioral disorders and the development of new breeding strategies in domestic animals.